

**Historical Land Use/Land Cover Classification and its Change Detection Mapping Using Different Remotely Sensed Data from LANDSAT (MSS, TM and ETM+) and Terra (ASTER) Sensors**

**A Case Study of the Euphrates River Basin in Syria with Focus on Agricultural Irrigation Projects**

**Dissertation**

Zur Erlangung des akademischen Grades doctor rerum naturalium

(Dr. rer. nat.)

Dipl.-Geogr. Wafi Al-Fares



**Historical Land Use/Land Cover Classification and its Change Detection Mapping Using Different Remotely Sensed Data from LANDSAT (MSS, TM and ETM+) and Terra (ASTER) Sensors**

**A Case Study of the Euphrates River Basin in Syria with Focus on Agricultural Irrigation Projects**

**Dissertation**

Zur Erlangung des akademischen Grades doctor rerum naturalium

(Dr. rer. nat.)

Vorgelegt dem Rat der Chemisch-Geowissenschaftlichen Fakultät der Friedrich-Schiller-Universität Jena

Von: Dipl.-Geogr. Wafi Al-Fares

geboren am 24.01.1979 in Murik-Hama-Syria

Gutachter:

1. Prof. Dr. Christiane Schmullius

2. PD Dr. Sören Hese

Tag der öffentlichen Verteidigung: 08.02.2012

To my parents, my country, my brothers and sisters, my wife, my children  
and my friends

### **Acknowledgements**

My great thanks go to my parents (Marwan and Wafaa), for mentoring me, and for providing me with the moral and financial support to obtain a university degree. In addition my thanks also go to Syria, my country of origin, the Higher Education Ministry and the University of Teshreen in Latakia for the financial support to pursue my education in Germany.

I cannot forget to thank my host country Germany, which has given me the opportunity to harness the advantages of its rich scientific environment, and to explore the possibilities awarded by my research area (Cartography and Remote Sensing).

I would also like to thank my supervisor Prof. Dr. Christiane Schmulius, and, of course, Dr. Sören Hese.

I would like to express my gratitude to the numerous people who have played a part in the successful completion of this work.

I thank all my colleagues at the Institute of Geography and the Department of Remote Sensing at the Friedrich Schiller University in Jena.

Last but not least, I want to express my gratitude to my lovely wife, Nourah Al-Kasem, for her continuing support and perseverance during this period in my life. Particular recognition is needed of her encouragement and belief in me, which has helped me to keep pushing hard and continuing with my studies until the end. To my three beautiful children, Mohammad Marwan, Jawad and Yaman, I want to express special thanks for their love.

## Abstract

The work described in this dissertation was performed under the supervision of Prof. Dr. Christiane Schmullius and Dr. Sören Hese at the Institute of Geography, Department of Remote Sensing at the University of Jena in Germany (Friedrich-Schiller-Universität Jena) from 2007 to 2011.

This thesis deals spatially and regionally with the natural boundaries of the Euphrates River Basin (ERB) in Syria. Scientifically, the research covers the application of remote sensing science (optical remote sensing: LANDSAT-MSS, TM, and ETM+; and TERRA: ASTER); and methodologically, in Land Use/Land Cover (LULC) classification and mapping, automatically and/or semi-automatically; in LULC-change detection; and finally in the mapping of historical irrigation and agricultural projects for the extraction of differing crop types and the estimation of their areas. With regard to time, the work is based on the years 1975, 1987, 2005 and 2007.

The remote sensing-based available data used are: LANDSAT-MSS data (eight scenes) acquired in June 1975; LANDSAT-TM data (16 scenes) acquired in May 1987 and in August 1987 (eight scenes for the extraction of the winter crops and eight scenes for extraction of the summer crops); LANDSAT-TM data (16 scenes) acquired in May 2007 and in August 2007 (eight scenes for extraction of the winter crops and eight scenes for extraction of the summer crops); and finally TERRA-ASTER data acquired in May and August 2005 (for extraction of the winter and summer crops). These have been combined with LANDSAT-ETM+ data (14 scenes) for two reasons; firstly to obtain complete spatial coverage of the study area, and secondly, to increase the spectral resolution of the ASTER-data. The LANDSAT-data was received from NASA-GLCF, while the TERRA-ASTER-data was obtained from the General Organization of Remote Sensing (GORS) in Syria.

Initially, preprocessing of the satellite data (geometric- and radiometric- processing, image enhancement, best bands composite selection, transformation, mosaicing and finally subsetting) was carried out. Then, the Land Use/Land Cover Classification System (LCCS) of the Food and Agriculture Organization (FAO) was chosen. The following steps were followed in LULC- classification and change detection mapping: visual interpretation in addition to digital image processing techniques; pixel-based classification methods; unsupervised classification: ISODATA-method; and supervised classification and multistage supervised approaches using the algorithms: Maximum Likelihood Classifier (MLC), Neural Network classifier (NN) and Support Vector Machines (SVM). These were trialed on a test area to determine the optimized classification approach/algorithm for application on the whole study area (ERB) based on the available imagery. Pre- and post- classification change detection methods (comparison approaches) were used to detect changes in land use/land cover-classes (for the years 1975, 1987 and 2007) in the study area.

Classification accuracy has been improved by adopting historical statistical and ancillary data for the year 1975. For the 1987 coverages, the ground truth points from the International Centre for Agriculture Research in Dry Areas (ICARDA) in Aleppo were adopted. For the other coverage years, 2005 and 2007, ground truth points were used that had been collected through two campaigns in Syria and through the GORS project in the Euphrates River Basin in Syria, which was completed between 2005 and 2010. Therefore, the accuracy of the results presented in this study is only as true as the quality and accuracy of the data used.

The remote sensing methods show a high potential in mapping historical and present land use/land cover classes and its changes over time. Significant results are also possible for agricultural crop classification in relatively large regional areas (the ERB in Syria is almost 50,335 km<sup>2</sup>).

LULC-maps have been obtained automatically depending upon the satellite remotely-sensed imagery and digital image processing available. Interpretation for the years 1975, 1987, 2005 and 2007 has been achieved by using digital image interpretation software (ERDAS v. 9.1, ENVI v. 4.3 and later 4.6, and ArcGIS 9.3).

The results of the different applied classification methods and algorithms were obtained keeping in mind the accuracies dependent on historical, statistical, ancillary, and ground truth data using the *kappa coefficient and error matrix*. Based on these accuracy measurements, the most successful approaches were the multi stage classification and algorithm (Maximum Likelihood-MLC).

Change trends in the study area and period was characterized by land-intensive agricultural expansion. The rapid, more labor- and capital- intensive growth in the agricultural sector was enabled by the introduction of fertilizer, improved access to rural roads and markets, and the expansion of the government irrigation projects. Results from land cover change analysis, carried out from the post-classification approach, show that the cultivated land increased from 1,123,268 ha in 1975 to 1,783,286 ha in 2007 on account of a decrease in the natural vegetation area and an increase in bare areas. This approach shows obvious and detailed results. Pre-classification approach results were generalized but very effective in relation to the estimation of the occurred change on the cultivated areas, especially when these areas were vegetated and not fallow. The total change in the whole study area (5,062,082 ha, 100 %) between 1975 and 2007 was about 600,967 ha (11.93 %), in which 238,646 ha (4.74 %) was changed from natural vegetated areas to bare areas and 362,321 ha (7.19 %) changed from bare areas to cultivated areas (especially to irrigated agriculture). Areas recording no change equaled about 4,461,115 ha (88.62 %).

Irrigated areas increased 148 % in the past 32 years from 249,681 ha in 1975 to 596,612 ha in 2007.

These statistics were taken from the maps of the general LULC- classes based on LANDSAT-MSS-data acquired in June 1975, LANDSAT-TM-data in May 1987 and 2007, and ASTER-data, May 2005. The products of the post-classification change detection method were also used. The data mentioned above were also used to map the historical development of the irrigation projects in the ERB. Winter crops maps (especially wheat, barley and sugar beet) were mapped based on LANDSAT-TM-data acquired in May 1987 and 2007, in addition to the ASTER data acquired in May 2005. The summer crops (especially cotton, maize and watermelon) were mapped based on LANDSAT-TM-data from August 1987 and 2007, in addition to ASTER data from August 2005.



## Zusammenfassung

Das grundsätzliche Ziel der vorliegenden Arbeit ist es, einen Beitrag zur Verbesserung der fernerkundungsgestützten Kartierung landwirtschaftlicher Nutzflächen unter Verwendung von LANDSAT-MSS-, TM- und ETM+-Daten sowie TERRA-ASTER-Daten im syrischen Teil des semiariden bis ariden Euphrat-Tals zu leisten. Das Euphrat-Tal erstreckt sich im Nordosten Syriens von der türkischen ( $36^{\circ}49' \text{ N}$ ,  $38^{\circ}02' \text{ E}$ ) bis zur irakischen Grenze ( $34^{\circ}29' \text{ N}$ ,  $40^{\circ}56' \text{ E}$ ), wobei die landwirtschaftlich genutzte Fläche entlang des Flusslaufes etwa  $50\,335 \text{ km}^2$  umfasst. Anfang der 1970er Jahre wurde im Rahmen eines staatlichen Programms begonnen, das Wasser des Euphrat für Bewässerungszwecke zu nutzen, um Flächen für eine agrarwirtschaftliche Nutzung zu erschließen. Diese Bewässerungsprojekte, die während der letzten vier Jahrzehnte stattfanden, haben maßgeblich zu Landbedeckungs- und Landnutzungsveränderungen (LULC) beigetragen.

Diese Arbeit zielt auf vier Schwerpunkte ab: eine LULC-Klassifizierung, eine LULC-Änderungskartierung, die Kartierung der Bewässerungsflächen und die Klassifizierung der angebauten landwirtschaftlichen Pflanzen im Euphrat-Tal. Es wurden vier LULC-Klassifikationsprodukte (vgl. C6.A.1) für die Jahre 1975, 1987, 2005 und 2007 abgeleitet. Darüber hinaus wurden zwei LULC-Veränderungskartierungen für die Zeitspannen von 1975-2007 und 1987-2007 durchgeführt. Zudem wurden vier thematische Karten hergestellt, welche die Lage und flächenmäßige Ausdehnung der Bewässerungsgebiete (vgl. C5.A.2) zu den diskreten Zeitpunkten 1975, 1987, 2005 und 2007 darstellen und somit die Entwicklung der letzten 37 Jahre dokumentieren. Schließlich wurden sechs detaillierte Klassifikationsprodukte (vgl. C5.A.3) zur landwirtschaftlichen Nutzung während der Hauptanbauphasen im Winter (Mai-Daten) und Sommer (August-Daten) der Jahre 1987, 2005 und 2007 erstellt.

Um diese Ziele zu erreichen, wurden acht im Juni 1975 aufgenommene LANDSAT-MSS-Szenen sowie insgesamt 32 LANDSAT-TM-Szenen für die Monate Mai 1987, August 1987, Mai 2007 und August 2007 ausgewählt. Außerdem wurden 16 korrigierte LANDSAT-ETM+/SLC-OFF-Szenen (filling of SLC-OFF data gaps using multi-temporal remotely sensed data / SLC-Gaps Filling Process - see Schultz, 2011), die im Mai und August 2005 aufgenommen wurden, mit TERRA-ASTER-Daten aus denselben Monaten verschnitten, um die spektrale Auflösung von drei auf sechs spektrale Bänder zu erhöhen.

Fernerkundungstechniken wurden genehmigt und angewendet auf der Fernerkundungsdaten (vgl. C4.A) von 1975, 1987, 2005 und 2007 für die vier Hauptschwerpunkte (LULC-Klassifizierung, LULC-Änderungserkennung, Bewässerungskartierung und bewässerte Landwirtschaft Klassifizierung). Da nicht auf Methoden zurückgegriffen werden konnte, deren Übertragbarkeit auf die Gegebenheiten des Untersuchungsgebietes hätte vorausgesetzt werden können, mussten neue Techniken entwickelt und validiert werden, die kompatibel mit den verwendeten Daten und auf die Ziele der Arbeit und die Privatsphäre der Studiengebietsumfeld zugeschnitten sind. Viele der in dieser Arbeit verwendeten Vorgehensweisen (vgl. C4.A) wurden schon früher entwickelt. In einigen Fällen wurden Methoden kombiniert oder modifiziert.

Aufgrund sinkender Kosten, sowohl für Fernerkundungsdaten als auch für Software zu deren Bearbeitung – bestimmte Fernerkundungsprodukte sind inzwischen kostenlos verfügbar –, bietet sich Forschern in zunehmendem Maße die Möglichkeit, Methoden der Fernerkundung zu nutzen, aber die Prozessierung und Interpretation der Daten ist noch immer zeitaufwändig, und die sind nicht passend für alle Gebiete der Erde an demselben Niveau der Genauigkeit. In dieser Studie wird gezeigt, dass die geometrische, atmosphärische und radiometrische Korrektur (vgl. C5.B) in Abhängigkeit von der konkreten Szene, dem jeweiligen Sensor und dem Aufnahmezeitpunkt nicht in jedem Fall notwendig ist. Die geometrische Korrektur, im Besonderen die Georeferenzierung, war leicht durchzuführen, wobei sehr hohe Genauigkeiten erreicht wurden. Für relativ alte Daten (MSS-1975) konnte keine Atmosphärenkorrektur durchgeführt werden, da die notwendigen Wetterparameter nicht vorlagen. Die radiometrische Korrektur konnte wiederum an allen Datensätzen

durchgeführt werden, was aber nicht bedeutet, dass immer zufriedenstellende Ergebnisse erreicht wurden. Wenn weder die Rohdaten noch die radiometrisch und/oder atmosphärisch korrigierten Daten als geeignet für die Mosaikierung eingeschätzt wurden, dann wurden die Szenen getrennt prozessiert und klassifiziert. ATCOR-2 wurde für die atmosphärische Korrektur verwendet, währenddessen iMAD bei der radiometrischen Korrektur zur Anwendung kam. Beide Algorithmen können mit geringem Zeitaufwand und ohne zusätzliche Inputparameter angewendet werden und liefern bessere Ergebnisse als Methoden wie MFF und 6S, die zudem eine größere Anzahl an Eingabegrößen benötigen (Chavez, 1996).

Die aus den Ergebnissen der Klassifikation entstandenen Karten wurden in einem einheitlichen Bezugssystem dargestellt. Sämtliche Daten wurden unter Bezugnahme auf den internationalen Ellipsoiden WGS84 und das Datum WGS84 auf die UTM-Zone 37 N projiziert.

Die geometrische Korrektur, die Georeferenzierung und die geometrische Registrierung bilden die Grundlage für die Mosaikierung mehrerer Szenen (vgl. C5.B.5) sowie für das Verschneiden von Daten unterschiedlicher Sensoren. ASTER-Daten wurden mit LANDSAT-ETM+-Daten fusioniert (vgl. C5.B.4), um Veränderungen der Landnutzung zu kartieren (vgl. C5.L).

Eine genaue Mosaikierung ist sehr wichtig für die weitere Datenverarbeitung (z.B. Klassifikation, Veränderungskartierung, usw.). Bei der Anwendung entsprechender Algorithmen gelang es nicht immer, im Farbverlauf kontinuierliche Datensätze zu erzeugen. Aufgrund dieser diskontinuierlichen Farbverläufe würde es zu verschiedenartigen Repräsentationen von LULC-Eigenschaften innerhalb einer zusammengesetzten Szene kommen. In diesen Fällen wurde die MAD-Technik angewendet, um eine radiometrische Konsistenz der Szene zu erhalten. Dieses Verfahren ist eine leicht handhabbare, nutzerfreundliche Kalibrierungstechnik, welche keine Kalibrierung mittels Gain- und Offset-Koeffizienten erfordert. Diese Technik hat den Vorteil, dass Szenen auch dann verglichen werden können, wenn Werte nicht verfügbar oder fehlerhaft sind.

Die Klassifikation folgte konsequent dem hierarchischen Klassifikationsschema (LCCS) der FAO. Dieser Ansatz definiert und bestimmt die LULC-Klassen, die bei der Klassifikation berücksichtigt werden. Die Klassen wurden folglich vor dem Starten der verwendeten automatisierten überwachten Klassifikationsverfahren festgelegt.

Die Klassifikation beruhte auf dem traditionellen pixelbasierten Ansatz. Die Klassifikationsergebnisse werden stets in Form von thematischen Karten präsentiert. Für die aus den verschiedenen verwendeten Ansätze und Algorithmen hervorgehenden Klassifikationsergebnisse wurde jeweils eine Genauigkeitsanalyse durchgeführt.

Innerhalb dieser Studie wurden mehrere automatisierte Klassifikationsansätze (one-step und multi-stage classification), und mehrere Algorithmen, namentlich MLC, NN und SVM, getestet, um eine möglichst optimale Methode für das Erreichen der Zielstellung zu finden. Die besten Ergebnisse wurden bei der Anwendung des Multi-Stage-Klassifikationsansatzes in Verbindung mit dem MLC-Algorithmus erzielt (vgl. C5.G).

Die Klassifikation von Daten mit geringer räumlicher und spektraler Auflösung, d.h. von LANDSAT-MSS-Daten, erlaubte es lediglich, auf einem, fünf Klassen umfassenden Klassifikationslevel thematische Karten für das gesamte Gebiet des syrischen Euphrat-Tals zu erstellen, welche u.a. die räumliche Verteilung von bewässerten Gebieten wiedergeben. Darüber hinaus war es nicht möglich, mit diesen Daten zufriedenstellende Ergebnisse auf einem höheren Klassifikationslevel zu erzielen. LANDSAT-TM-Daten erlaubten eine genauere Klassifikation auf dem höheren Klassifikationslevel, aber waren im Vergleich zu den miteinander verschnittenen LANDSAT-ETM+- und ASTER-Szenen weniger gut für die Ausweisung von Klassen geeignet, welche die landwirtschaftliche Nutzung mit einer höheren inhaltlichen Tiefe repräsentieren. Schließlich erwiesen sich die (nicht verschnittenen) ASTER-Daten mit einer niedrigen spektralen Auflösung von nur drei Bändern trotz einer höheren geometrischen Auflösung von 15 m als weniger zweckmäßig als die

LANDSAT-TM-Daten. Bei der Klassifikation der miteinander verschnittenen LANDSAT-ETM+- und ASTER-Daten wurden die besten Ergebnisse erzielt. Im Allgemeinen gelang die Klassifikation landwirtschaftlicher Nutzflächen vor allem auf den großen, von staatlicher Seite geplanten Bewässerungsarealen mit einer hohen Genauigkeit (z.B. dem 21 000 ha umfassenden Gebiet bei Ost-Maskana), wo einzelne bepflanzte Felder vergleichsweise groß und die Heterogenität der LULC-Eigenschaften gering waren. Dieser Zustand änderte sich, wie aus den LANDSAT-TM-Daten von 2007 zu ersehen ist. Die Felder wurden kleiner und die Heterogenität angebauter Pflanzen wuchs. Akzeptable Klassifikationsergebnisse wurden in Gebieten erzielt, die sowohl durch Privatpersonen als auch von staatlicher Seite bewirtschaftet werden (z.B. West-Maskana), wobei die Größe der in Privateigentum befindlichen Felder beträchtlich variiert. Demgegenüber wurden für die sehr alten Anbauflächen, die sich unmittelbar an den Uferbereichen des Euphrat befinden, wo die einzelnen Felder sehr klein sind und auf kleinem Raum eine Vielzahl von Feldfrüchten angebaut wird, inakzeptable Klassifikationsgenauigkeiten ermittelt. Für diese Gebiete würden Fernerkundungsdaten mit einer höheren räumlichen und spektralen Auflösung benötigt (z.B. IKONOS).

Die Klassifikation der natürlichen Vegetation außerhalb der Bewässerungsgebiete in den ariden und semiariden Regionen Syriens, im Besonderen innerhalb der fünften landwirtschaftlichen Stabilisierungszone, wurde durch die Dominanz und Variabilität der Bodenreflektanz erschwert (Huet et al., 1994). Dies gilt auch für die Feldfrüchte und Bäume (wegen den verhältnismäßig großen Abständen zwischen einzelnen Bäumen im Vergleich zur räumlichen und spektralen Auflösung der verwendeten Fernerkundungsdaten), die teilweise in der dritten und vierten landwirtschaftlichen Stabilisierungszone angebaut wurden.

Im Rahmen dieser Arbeit wurden zwei Ansätze der Veränderungskartierung auf nahezu alle landwirtschaftlich genutzten Gebiete in der ariden bis semiariden Umgebung des syrischen Euphrat-Tals angewendet, um die Eignung dieser Methoden zu prüfen. Der Ansatz einer der Klassifikation vorausgehenden Veränderungskartierung (pre-classification change detection) basiert auf den Grauwertdifferenzen zweier Szenen und erwies sich als sehr effektiv für die Erfassung neu entstandener landwirtschaftlicher Nutzflächen (neuer Bewässerungsprojekte) in der Zeitspanne zwischen 1975 und 2007. Der Post-Klassifikationsansatz (post-classification change detection) führte zur Definition, Erfassung und Kartierung von 21 Änderungsklassen. Allerdings resultierte diese Herangehensweise in einer geringeren Genauigkeit (83 %) im Vergleich zur erstgenannten Methode (86 %), was zum einen auf die Abhängigkeit der letztgenannten Methode von der Qualität der Klassifizierung und zum anderen auf eine wesentlich größere Anzahl von ausgewiesenen Veränderungsklassen (bei der ersten Methode wurden nur 3 Veränderungsklassen ausgewiesen) zurückzuführen ist. Dennoch widerspricht dieses Ergebnis der Annahme, dass die Post-Klassifikationsmethode der genaueste Ansatz für die Veränderungskartierung sei (Mas, 1999). Die zwei Ansätze und aus denen gewonnene hervorgehende Ergebnisse waren leicht zu interpretieren.

Aus dem Prä-Klassifikationsansatz (vgl. C6.C.1) konnten drei Haupttrends der Landnutzungs- und Landbedeckungsveränderung abgeleitet werden: Der erste Trend – keine Veränderung – ist mit einem Anteil von 88,62 % der dominierende. Ein zweiter Trend wird in der Veränderung einiger Flächen (4,74 %) von vormals natürlicher Vegetation zu vegetationslosen Arealen sichtbar. Dieser Trend dürfte hauptsächlich auf klimatische Fluktuationen, vor allem variable Niederschlagssummen, zurückzuführen sein, die großen interannuellen Schwankungen unterliegen. Zusätzlich muss ein anthropogener Einfluss, der sich u.a. in der Überweidung einiger Flächen niederschlägt, in Betracht gezogen werden. Innerhalb des Untersuchungsgebietes befindet sich der größte Teil der natürlichen Vegetation in der fünften landwirtschaftlichen Stabilisierungszone, in der natürliche Graslandschaften anzutreffen sind. Der dritte Veränderungstrend besteht in dem flächenmäßigen Rückgang von vegetationslosen Gebieten (7,19 %), eine Beobachtung, die wie in den meisten entwickelten Ländern, auf eine landwirtschaftliche Inwertsetzung von Flächen zurückzuführen ist. Diese Ergebnisse werden durch die Resultate bestätigt, die aus der Veränderungskartierung mit der Post-Klassifikationsmethode hervorgingen (vgl. C6.C.2). Der starke Rückgang von Flächen mit

natürlichem Vegetationsbestand, die im Jahr 1987 noch 304 983 ha ausmachten (68,33 % sind betroffen), ist hauptsächlich auf deren Umwandlung in agrarwirtschaftlich genutzte Flächen (42,95 %) oder auf den kompletten Verlust der Vegetationsdecke (24 %) zurückzuführen. Insgesamt konnte im betrachteten Zeitraum ein Verlust an vegetationsbestandenen Flächen von 43,22 % detektiert werden, wobei 17,86 % auf landwirtschaftliche Nutzflächen entfallen. Durch die Errichtung neuer agrarwirtschaftlicher Nutzflächen kommt es trotz des Verschwindens einiger Anbauflächen zu einem flächenmäßigen Zuwachs dieser Landnutzungsform um 35,49 %. Insgesamt gesehen konnte auch eine leichte Zunahme vegetationsloser Flächen um 0,23 % festgestellt werden, obwohl von der zum ersten Aufnahmezeitpunkt noch 263 863 ha umfassende Fläche 2007 13,89 % anderweitig genutzt wurden. Dabei wurden 10,01 % der ursprünglich vegetationslosen Gebiete in landwirtschaftliche Flächen umgewandelt.

Einschränkungen in der Aussagekraft dieser Studie entstehen in der Hauptsache aus der sehr niedrigen geometrischen Auflösung von  $60 \times 60$  m und der niedrigen spektralen Auflösung von lediglich vier Bändern bei den LANDSAT-MSS-Daten von 1975. Die korrigierten LANDSAT-ETM+/SLC-OFF-Daten von 2005, die mit den ASTER-Daten verschnitten wurden, um deren spektrale Auflösung von drei auf sechs Bänder zu erhöhen, wurden - nach der Verwendung einer Korrektur-Methode aus USGS - erhalten. waren demgegenüber verhältnismäßig genau aufgrund der verwendeten Korrekturmethode der USGS. Die Zeitlücke zwischen der Akquirierung der Fernerkundungsdaten in den Jahren 1975 sowie 1987 und den Geländearbeiten 2007 und 2009 bedeutet ebenfalls gewisse Einschränkungen für die Aussagekraft der Untersuchungen, zumal die Beschaffung von empirischen Daten aus dem Gelände, im Besonderen von Ground-Control-Points, schwierig war. Einige der gesammelten Ground-Control-Points sind deshalb für einige Zwecke nur bedingt geeignet. Zudem waren einige Standorte in dem großen Untersuchungsgebiet während der Geländearbeiten nicht zugänglich.

## **Motivation**

There are many motives that led me to write this thesis under the abridged title: Historical Land Use/Land Cover Classification and its Change Detection Mapping Using Different Remotely Sensed Data: A Case Study of the Euphrates River Basin in Syria. Foremost are the representation and mapping changes which occurred during the time period between 1975 and 2007 in data and remote sensing techniques or so-called remote sensing. This includes data from the artificial sensors LANDSAT-, MSS/TM/ETM+ and TERRA-ASTER.

These developments required me to specialize and to study towards a doctorate degree in the field of cartography, made possible by a grant from the Ministry of Higher Education in Syria. The science of remote sensing and its requisites of techniques, software and algorithms which fall under the so-called processing or analysis of real and satellite-images automatically in digital format, is a very modern science compared with medicine, engineering, geography, etc. For my research and my specialist field of cartography, my interest lies in the possibility of remote sensing science to provide significant data and results in the study of land use dynamics and the nature of land cover. Thematic maps of the Euphrates River Basin represent the reality of land use and natural cover, and provide an ability to detect real change in the region over the time period of my research, more than 30 years. This data is characterized also by its spatial comprehensiveness, allowing me to develop thematic maps of the study region, which extends over an area of almost 50,335 km<sup>2</sup>. The combination between the remote sensing data, computers and algorithms which have been created in the field of image processing for general and remotely sensed data, shortens the time, effort and cost of research. This combination allows a shift from traditional cartography to automatic cartography or so-called digital computer cartography, a continuous, automated form of science depending significantly on the rules, basics and equations of classical cartography.

An important factor in my decision to study the data of the artificial sensors LANDSAT and TERRA-ASTER is the free, affordable and easy access provided. This data is characterized by good spectral accuracy that allows the ability to discriminate and separate between the different manifestations of the Earth. Spatial resolution is good, and appropriate for mapping land use and natural cover. The most important point in these data sets however, is the temporal and historical comprehensiveness, which provide information spanning more than 30 years. Finally, the spatial coverage is relatively large for each scenario with the LANDSAT-data slightly larger than that of ASTER.

The Euphrates River Basin is one of the most important regions and territories in Syria. It contains a diversity of natural resources and has been developed over millennia for agricultural and irrigation purposes. My selection of the area for this period of research was based on my personal knowledge and interest; the Euphrates River Basin was the subject of my study and research for my Diploma thesis.

Only a few old and general studies have been presented on this territory of the Euphrates, and the use of remote sensing technique in such studies has not been well developed. Therefore, this thesis is an attempt to readdress the balance of knowledge in this area and to test the effectiveness of remote sensing in the development of thematic maps, especially regarding the spread of strategic crops such as wheat, barley, sugar beet, cotton and corn in the arid and semi-arid territory of the Euphrates.

## Table Of Contents

<b>Acknowledgements</b> .....	<b>I</b>
<b>Abstract</b> .....	<b>II</b>
<b>Zusammenfassung</b> .....	<b>IV</b>
<b>Motivation</b> .....	<b>VIII</b>
<b>Table of contents</b> .....	<b>IX</b>
<b>List of figures</b> .....	<b>XII</b>
<b>List of tables</b> .....	<b>XVI</b>
<b>Abbreviations</b> .....	<b>XVII</b>

<b>Chapter 1-Introduction</b> .....	<b>1</b>
<b>A. Problem statement and research question</b> .....	<b>1</b>
<b>B. Significance of the study</b> .....	<b>5</b>
<b>C. Research objectives</b> .....	<b>5</b>
<b>D. Research hypotheses</b> .....	<b>6</b>
<b>E. Organization of the thesis</b> .....	<b>6</b>
<b>Chapter 2-Theoretical background and literature review / state of the art</b> .....	<b>7</b>
<b>A. Remote sensing concept</b> .....	<b>7</b>
<b>B. Remote sensing application in Syria</b> .....	<b>12</b>
<b>C. Land use / land cover mapping</b> .....	<b>14</b>
1. Distinction between land use and land cover .....	15
2. The classification process .....	15
3. Classification schemes.....	18
4. The general classification techniques and methods.....	19
4.1. Training sample-based categories.....	21
4.2. Parametrical-based categories .....	23
4.3. Pixel information-based categories .....	23
4.4. Land cover class output-based categories .....	27
4.5. Spatial information-based categories .....	28
4.6. Combinative-based classifiers .....	29
5. Remote sensing application for land use/land cover mapping .....	29
6. Issues in the classification of remote sensing data .....	32
<b>D. Land use / land cover change detection mapping</b> .....	<b>34</b>
1. Change detection techniques .....	35
2. Comparison between the change detection techniques .....	39
3. Change detection using remote sensing .....	40
4. Change detection in arid and semi-arid environment .....	41
<b>E. Remote sensing for irrigated agriculture</b> .....	<b>43</b>
1. Remote sensing approaches for vegetation studies .....	46
2. Remotely sensed vegetation indices .....	48

3. Crop discrimination from satellite-based images .....	49
4. Crop area estimation from satellite-based images .....	51
<b>F. Status of the accuracy assessment methods .....</b>	<b>53</b>
<b><i>Chapter 3-Overview of study area .....</i></b>	<b><i>57</i></b>
<b>A. Syria .....</b>	<b>57</b>
<b>B. Euphrates River Basin (ERB) .....</b>	<b>64</b>
<b>C. Irrigation projects on the Euphrates River .....</b>	<b>65</b>
<b>D. Climate .....</b>	<b>68</b>
<b>E. Morphological structure .....</b>	<b>70</b>
<b>F. Soils .....</b>	<b>71</b>
<b>G. Hydrology .....</b>	<b>71</b>
<b>H. Vegetation and land use / land cover .....</b>	<b>73</b>
<b><i>Chapter 4-Data and tools .....</i></b>	<b><i>77</i></b>
<b>A. Satellite data .....</b>	<b>77</b>
1. LANDSAT (MSS, TM, and ETM+) sensors .....	79
2. TERRA-ASTER .....	81
3. SRTM .....	83
<b>B. Reference and complementary data .....</b>	<b>84</b>
1. Field reference data .....	85
2. Maps .....	85
3. Statistics .....	86
4. Ancillary data .....	86
<b><i>Chapter 5-Research methodology .....</i></b>	<b><i>87</i></b>
<b>A. Extraction of the study area .....</b>	<b>89</b>
<b>B. Pre-processing of the satellite data .....</b>	<b>89</b>
1. Geometric data processing .....	90
2. Atmospheric correction.....	94
3. Radiometric processing / calibration .....	99
4. Data fusion .....	102
5. Mosaicing, subsetting and masking .....	103
<b>C. Design of land use / land cover classification system .....</b>	<b>105</b>
<b>D. Field work .....</b>	<b>107</b>
<b>E. The possibility of spectral separation between crops .....</b>	<b>110</b>
1. The phenological case of the different crops .....	115
2. The size of the agricultural holdings and methods of water supply.....	116
3. Selection of the most appropriate time for satellite imaging .....	117
4. Selection of the most appropriate satellite imaging band composites .....	118
<b>F. Training samples: Selection, analysis and evaluation .....</b>	<b>119</b>
<b>G. Choice and evaluation of the optimized method of automated classification .....</b>	<b>125</b>

1. The test area .....	125
1.1. Unsupervised classification .....	126
1.2. Supervised classification .....	128
1.2.1. The Multi Stage Classification Approach (MSCA) .....	128
1.2.2. Maximum Likelihood Classifier (MLC) .....	132
1.2.3. Neural Network (NN) .....	134
1.2.4. Support Vector Machine (SVM) .....	136
2. Results and evaluation.....	138
<b>H. General classes classification .....</b>	<b>143</b>
<b>I. Irrigated areas mapping .....</b>	<b>145</b>
<b>J. Crops classification .....</b>	<b>148</b>
<b>K. Post-classification processing .....</b>	<b>156</b>
<b>L. Automated change detection mapping .....</b>	<b>157</b>
1. Pre-classification approach between MSS-June-1975 and TM-August-2007.....	157
2. Post-classification approach between TM-May-1987 and TM-May-2007.....	158
<b>M. Accuracy assessment .....</b>	<b>159</b>
<b><i>Chapter 6-Results, analysis and discussions .....</i></b>	<b><i>164</i></b>
<b>A. LULC-classification .....</b>	<b>164</b>
1. The broad major LULC-features .....	164
2. Temporal development mapping of the irrigated areas.....	170
3. Distinguishing, classification and area measurement of strategic crops .....	172
<b>B. Accuracy assessment comparisons .....</b>	<b>180</b>
<b>C. LULC-change detection mapping .....</b>	<b>181</b>
1. Pre-classification results .....	181
2. Post-classification results .....	183
<b><i>Chapter 7-Summary, concluding remarks and recommendations .....</i></b>	<b><i>188</i></b>
<b>A. Summary .....</b>	<b>188</b>
<b>B. Concluding remarks .....</b>	<b>190</b>
<b>C. Recommendations/outlook .....</b>	<b>192</b>
<b><i>References .....</i></b>	<b><i>194</i></b>



## List Of Figures

Fig. 2.1:	Electromagnetic remote sensing of Earth resources.....	7
Fig. 2.2:	Schematic of satellite operation, specifically the LANDSAT satellite and the Thematic Mapper (TM) sensor .....	9
Fig. 2.3:	The primary spectral regions of the electromagnetic spectrum that are of interest in Earth remote sensing applications .....	10
Fig. 2.4:	Atmospheric transmission spectra showing windows available for Earth observation .....	10
Fig. 2.5:	Idealized reflectance plots for different land cover types .....	11
Fig. 2.6:	A model for pattern recognition in remote sensing .....	16
Fig. 2.7:	The classification process .....	17
Fig. 2.8:	Major approaches for image segmentation/classification .....	20
Fig. 2.9:	The principal idea of the supervised classification approach for multi-spectral remote sensing .....	22
Fig. 2.10:	The general concept of the object-based classification (e-cognition classification model) .....	26
Fig. 2.11:	The difference between hard and soft classification .....	27
Fig. 2.12:	The relationship between a satellite sensor array's grid and features in the landscape .....	34
Fig. 2.13:	A framework for classifying change detection methods .....	35
Fig. 2.14:	The typical spectral response curve for vegetation that shows the characteristic bands that differentiate vegetation spectrally .....	47
Fig. 2.15:	Hypothetical crop calendar for an area in the Midwestern United States .....	48
Fig. 2.16:	Schematic relation of pixel size, numbers of classes and estimated accuracy dependent on the classification level .....	56
Fig. 3.1:	Present-day Syrian borders, the 14-governorates administrative divisions, Agro-Climatic Zones and the Euphrates River Basin study area .....	57
Fig. 3.2:	Present-day Syrian borders, general geomorphological characteristics and the Euphrates River Basin study area .....	60
Fig. 3.3:	Irrigated areas distribution by basins in Syria .....	61
Fig. 3.4:	Land use / land cover distribution in Syria, 2009 .....	62
Fig. 3.5:	Study area and irrigation projects in Syria .....	67
Fig. 3.6:	Precipitation of the Euphrates-Tigris basin .....	69
Fig. 3.7:	The temperature averages of the Euphrates-Tigris basin .....	69
Fig. 3.8:	The evaporation averages of the Euphrates-Tigris basin .....	69
Fig. 3.9:	The topography of the Euphrates-Tigris basin .....	70
Fig. 3.10:	Euphrates River; monthly mean discharges (m <sup>3</sup> /s) for the period 1925-2005 .....	72
Fig. 3.11:	Mean annual discharge of the Euphrates River (m <sup>3</sup> /s) for the period 1975-2005.....	72
Fig. 3.12:	LULC- spatial distribution in the Euphrates-Tigris basin .....	74
Fig. 3.13:	Approximate spatial LULC-distribution in ERB and Syria .....	74
Fig. 4.1:	An overview of general characteristics of the used satellite dataset in the study.....	78
Fig. 4.2:	The used imagery spatial coverage of the sensors : MSS (June, 1975), TM (May And August 1987 and 2007) and ETM+/SLC-Off/corrected (May and August 2005) .....	81
Fig. 4.3:	Comparison of the spectral coverage between LANDSAT-sensors (MSS, TM, and ETM+) and ASTER-sensor .....	82
Fig. 4.4:	The used imagery spatial coverage of the sensors: ASTER (May and August, 2005 and ETM+/SLC-Off/corrected (May and August, 2005) .....	83
Fig. 4.5:	The used imagery spatial coverage of the sensor SRTM .....	84
Fig. 5.1:	The general conceptual workflow chart of the thesis .....	88
Fig. 5.2:	The reposition of pixels from their original locations (Input matrix) in the data	

	array into a specified reference grid (Output matrix) .....	91
Fig. 5.3:	The geometric correction results of two ASTER-scenes (including the radiometric corrections) .....	93
Fig. 5.4:	The distribution of the 14-GCPs used for registration of the tow data set (MSS-June 1975 and TM August 2007), image-to-image concept .....	94
Fig. 5.5:	Simplified model of the atmospheric effects on the reflection on a target object .....	95
Fig. 5.6:	ATCOR-2 and its central sub-modules .....	97
Fig. 5.7:	The general concept of atmospheric correction using ATCOR-2 .....	98
Fig. 5.8:	Histogram comparison of the LANDSAT-TM-Band-1 before and after the atmospheric correction .....	98
Fig. 5.9:	Radiometric normalization between the two data sets, which will be used for change detection .....	101
Fig. 5.10:	iMAD results for the two data sets (MSS-1975 and TM-2007) .....	101
Fig. 5.11:	Fusion and Mosaic concepts for the LANDSAT-ETM+ and TERRA-ASTER data sets, acquired in May and August 2005 .....	103
Fig. 5.12:	Two mosaic-results of the data set LANDSAT-TM August 2007 .....	105
Fig. 5.13:	Overview of the Land Cover Classification System (LCCS), its two major phases and the classifiers .....	106
Fig. 5.14:	Description of the resulting 14 class for the Four Regions sub-study-area .....	107
Fig. 5.15:	Excursion –GPS Points 2007 and another GPS-measurements from ICARDA and GORS .....	108
Fig. 5.16:	The followed methodology for collecting the ground truth data during the field work in 2007 .....	109
Fig. 5.17:	The followed methodology for collecting the results during the office-work .....	110
Fig. 5.18:	The followed concept in spectral measurements using FieldSpecPro by GORS .....	111
Fig. 5.19:	The distribution of the training fields that are used in the spectral measurements .....	111
Fig. 5.20:	Spectral reflectance measurements for wheat at different growth stages .....	112
Fig. 5.21:	Spectral reflectance values of irrigated wheat during its growth stages in Arraqqah using the ASTER-bands .....	112
Fig. 5.22:	Spectral reflectance values of ASTER-bands during the different growth stages of the irrigated wheat .....	113
Fig. 5.23:	NDVI-values of major winter crops during growth stages in Arraqqah Provence in Syria .....	113
Fig. 5.24:	The relationship between the spectral reflectance and the different growth stages of the three essential summer crops by the first three bands of ASTER .....	114
Fig. 5.25:	The relationship between the spectral reflectance and the different growth stages of cotton by the third spectral band of ASTER .....	114
Fig. 5.26:	Temporal and spectral separability of cotton, corn, and watermelon by the third spectral band of ASTER .....	115
Fig. 5.27:	The spectral response of cotton, corn and watermelon during the suggested date to recognize these crops in the spectral range (350-2500) Nanometer .....	115
Fig. 5.28:	Schematic diagrams of the spatial characteristics of the irrigated agricultural areas in the study area .....	117
Fig. 5.29:	The small and very small crops fields on the Euphrates River banks near Deir Azzour in July 2009 .....	121
Fig. 5.30:	Spectral class signatures (band means) related to ASTER-data (three spectral bands, 15 m) .....	124
Fig. 5.31:	Spectral class signatures (band means) related to fused ASTER-data with LANDSAT-ETM+- data (six spectral bands, 15 m) .....	124
Fig. 5.32:	The spatial extent of the four administrative regions (Athawra, Al-Jurnia, Ain Eysa and Menbij) .....	126

Fig. 5.33:	Integrating the ISODATA-clustering with the supervised classification algorithms in a so-called hybrid-procedure .....	127
Fig. 5.34:	Illustration of the application of multi stage classification approach (chain-steps), using MLC-algorithm on the LANDSAT-TM-data of May 2007 with spatial resolution of 30 m .....	129
Fig. 5.35:	The flow-chart of the applied multi stage classification approach in this study .....	130
Fig. 5.36:	Combination of the 14-classes illustrated in the previous figure, using ArcGIS-software to sum the individual thematic results and LCCS-software to prepare the legend .....	131
Fig. 5.37:	Maximum Likelihood Classifier (MLC) concept .....	133
Fig. 5.38:	The Neural Network Classification Model .....	136
Fig. 5.39:	Geometric explanation for the linear classification of SVM .....	137
Fig. 5.40:	LULC-classes that generated from the LCCS-software (version-2) for the Four-Regions study area .....	138
Fig. 5.41:	The produced thematic maps from LANDSAT-MSS data using various supervised classification approaches and algorithms for the testing area .....	139
Fig. 5.42:	The produced thematic maps from LANDSAT-TM-data using various supervised classification approaches and algorithms for the testing area .....	139
Fig. 5.43:	The produced thematic maps from ASTER- and LANDSAT-ETM+-data using various supervised classification approaches and algorithms for the testing area .....	140
Fig. 5.44:	The produced thematic map from ASTER-data with only the first three spectral bands , and the resulted map after fusing the previous three bands with the 4, 5 and 7 spectral bands of LANDSAT-ETM+-data .....	140
Fig. 5.45:	The comparison between the areas of various LULC-classes which generated from the supervised classification of remotely sensed data, with the statistical records in the Menbij region, 2007 .....	141
Fig. 5.46:	Illustration of the accuracy assessment values presented in Ttable 14 visually .....	143
Fig. 5.47:	The distances between the rain-fed olive trees in the study area .....	143
Fig. 5.48:	LANDSAT-MSS June 1975 imagery subsetting based on the spatial extent of ERB ..	145
Fig. 5.49:	LANDSAT-MSS data June 1975 classification results for each subsetted image and mosaicing of all results in one thematic map .....	145
Fig. 5.50:	The spatial distribution of the 16-projects in the ERB (ca. 230,000 ha) which generated from the detailed irrigation projects and the remotely sensed data .....	146
Fig. 5.51:	Irrigation mapping in the ERB based on the traditional supervised classification approach .....	147
Fig. 5.52:	The general concept steps adapted to classify the various agricultural classes, especially the major strategic winter and summer crops .....	149
Fig. 5.53:	The followed concept to classify the major winter crops based on both the previous general classes classification and the generated spatial distribution of the irrigated areas .....	149
Fig. 5.54:	The followed concept to classify the major summer crops based on both the previous winter crops classification and the generated spatial distribution of the irrigated area .....	150
Fig. 5.55:	The integration of the remotely sensed data with the construction scheme of the 21,000 ha project .....	151
Fig. 5.56:	The followed concept to collect training samples for the area/s with no truth-data or with insufficient reference data .....	153
Fig. 5.57:	General classes classification, irrigation mapping and agriculture classification methods performed based on the spatial extent of each irrigation projects .....	154
Fig. 5.58:	The general classes classification, irrigation mapping and agriculture classification results produced based on spatial extent of irrigation-projects .....	155

---

Fig. 5.59:	Illustration of the individual 16-project-based classification results (permanent and winter crops classification results for 1987) .....	156
Fig. 5.60:	Pre-classification change detection mapping concept performed for the two remotely sensed data sets (MSS-June 1975 and TM August 2007) .....	157
Fig. 5.61:	Flow chart of the post-classification change detection mapping approach for the two remotely sensed datasets (TM May 1987 and TM May 2007) .....	158
Fig. 5.62:	The general accuracy assessment steps applied on the resulted thematic map/s from the classification process .....	159
Fig. 5.63:	Explanation of the error matrix approach .....	160
Fig. 5.64:	The major spatial levels of collecting the statistical information about various LULC-features .....	162
Fig. 5.65:	The major structural levels of collecting the statistical information about various LULC-features .....	163
Fig. 6.1:	Illustrated overview of the LULC-occupations rate over several years .....	165
Fig. 6.2:	The spatial distributions classification of the five major LULC-categories in the ERB for the data of LANDSAT-MSS acquired in June 1975 .....	167
Fig. 6.3:	The spatial distributions classification of the five major LULC-categories in the ERB for the data of LANDSAT-TM acquired in May 1987 .....	168
Fig. 6.4:	The spatial distributions classification of the five major LULC-categories in the ERB for the data of TERRA-ASTER fused with LANDSAT-ETM+/SLC-Off/corrected acquired in May 2005 .....	169
Fig. 6.5:	The spatial distributions classification of the five major LULC-categories in the ERB for the data of LANDSAT-TM acquired in May 2007 .....	170
Fig. 6.6:	The final irrigation mapping thematic maps that explain the temporal development of the spatial distribution expansion of the irrigated areas during the last three decades using various remotely sensed data .....	171
Fig. 6.7:	The classification of the major permanent, winter and summer irrigated crops within the irrigation projects in the ERB for the data of LANDSAT-TM acquired in May and August 1987 .....	174
Fig. 6.8:	The classification of the major permanent, winter and summer irrigated crops within the irrigation projects in the ERB for the data of TERRA-ASTER and LANDSAT-ETM+ acquired in May and August 2005 .....	176
Fig. 6.9:	The classification of the major permanent, winter and summer irrigated crops within the irrigation projects in the ERB for the data of LANDSAT-TM acquired in May and August 2007 .....	177
Fig. 6.10:	Statistics of occurred changes in percentage and hectare that resulted from applying the pre classification approach using the data of LANDSAT-MSS from June 1975 and the data of LANDSAT-TM from August 2007 .....	182
Fig. 6.11:	The three wide major LULC-changes that resulted from applying the pre classification change detection approach for the period 1975-2007 .....	182
Fig. 6.12:	Statistics of occurred changes in percentage that resulted from applying the post classification approach using the data of LANDSAT-TM from May 1987 and the data of LANDSAT-TM from May 2007 .....	184
Fig. 6.13:	Statistics of occurred changes in hectare that resulted from applying the post classification approach using the data of LANDSAT-TM from May 1987 and the data of LANDSAT-TM from May 2007 .....	185
Fig. 6.14:	The 21-detailed LULC-changes that resulted from applying the post-classification change detection approach for the period 1987-2007 .....	186

## List Of Tables

Table 2.1:	Types of land cover and associated types of land use .....	15
Table 3.1:	The distribution of the rainfall averages in the Syrian territories .....	59
Table 3.2:	The expected difference between the supply and demand on water in Syria in the period from 1989 to 2010 (Million m <sup>3</sup> ) .....	61
Table 3.3:	General statistical information on the ERB .....	65
Table 3.4:	The water needs of the countries located along the Euphrates River .....	66
Table 3.5:	Reclamation and irrigation projects on the Euphrates River .....	66
Table 4.1:	General information about the two satellites (LANDSAT and TERRA-ASTER) .....	78
Table 4.2:	General information about the sensors-data used in the study .....	78
Table 5.1:	The selected GCPs coordinates used for registration of the tow data set (MSS June 1975 and TM August 2007), image-to-image concept .....	94
Table 5.2:	Weather data from the Arraqah climatic station .....	98
Table 5.3:	Variations, source and date used training samples in the supervised classification process .....	122
Table 5.4:	The spectral separability of the training samples related to ASTER-data (three spectral bands, 15 m) .....	123
Table 5.5:	The spectral separability of the training samples related to fused ASTER-data with LANDSAT-ETM+- data (six spectral bands, 15 m) .....	124
Table 5.6:	The final resulted overall accuracy values of applying various classification approaches and algorithms on various remotely sensed data .....	142
Table 5.7:	The statistical information about each farm of the 21,000 ha project for 1987 .....	152
Table 5.8:	The remotely sensed data classification based statistical results for the 21,000 hairrigation project for the years 1975, 1987, 2005 and 2007 .....	155
Table 5.9:	The classification accuracy assessment for the resulted thematic map representing the spatial distribution of the permanent and the winter agricultural classes in the 21,000 ha project .....	161
Table 6.1:	Overview of the LULC-occupations rate over several years .....	164
Table 6.2:	The areas rates of the three wide existing general classes based on the irrigated areas level .....	171
Table 6.3:	The areas rates of the three wide existing general classes and the various agriculture features based on the irrigated areas level .....	171
Table 6.4:	The areas rates of the three wide existing general classes and the various agriculture features based on the individual 16-irrigated projects level .....	178
Table 6.5:	The final overall accuracy of classification results of the general classes, the irrigated areas and the agricultural features (permanent, winter and summer), using various remote sensing data (LANDSAT: MSS and TM; and TERRA: ASTER fused with LANDSAT: ETM+) for various years (1975, 1987, 2005 and 2007) .....	180
Table 6.6:	Accuracy assessment of pre-classification change detection approach results .....	183
Table 6.7:	LULC-change matrix (%) in the study area for 1987 and 2007 .....	184
Table 6.8:	LULC-change matrix (ha) in the study area for 1987 and 2007 .....	185
Table 6.9:	Accuracy assessment of post-classification change detection approach results .....	187

**Abbreviations**

ACSAD	Arab Center for the Studies of Arid Zones and Dry Lands
AQUASTATE	FAO's global information system on water and agriculture
ASTER	Advanced Spaceborne Thermal Emission and Reflection Radiometer
ASZs	Agricultural Settlement Zones
AVHRR	Advanced Very High Resolution Radiometer
CBS	Central Bureau of Statistics
CWANA	Central and West Asia and North Africa (project)
EMS	Electro Magnetic Spectrum
ERB	Euphrates River Basin
ETM+	Enhanced Thematic Mapper
FAO	Food and Agriculture Organization
GIS	Geographical Information System
GDP	Gross Domestic Product
GORS	General Organization of Remote Sensing
GPS	Global Positioning System
ICARDA	International Centre for Agriculture Research in Dry Areas
IFAD	International Fund for Agricultural Development
LANDSAT	LAND SATellite
LULC	Land use/land cover
MAAR	Syrian Ministry of Agriculture and Agrarian Reform
MLC	Maximum Likelihood Classifier
MODIS	Moderate Resolution Imaging Spectroradiometer
MSS	Multispectral Scanner System
NDVI	Normalized Difference Vegetation Index
NNC	Neural Network Classifier
NOAA	National Oceanic and Atmospheric Administration
RMS	Root Mean Square
ROWA	Regional Office for West Asia
SAR	Synthetic Aperture Radar
SVMC	Support Vector Machine Classifier
SWIR	Short Wave Infra-Red
TIR	Thermal Infra-Red
TM	Thematic Mapper
UNEP	United Nations Environment Program
VI <sub>s</sub>	Vegetation Indices
VNIR	Visible Near Infra-Red

ck	cubic kilometer
ha	hectar
km	kilo meter
km <sup>2</sup>	square kilometer
m	meter
m <sup>2</sup>	square meter

## ***Chapter 1: Introduction***

### **A. Problem statement and research questions**

Syria, with a total area of 185,180,000 km<sup>2</sup>, has arable land estimated at 6.22 million hectares, or 33 % of the total area of the country. The cultivated land is estimated at 5.66 million ha, which is 94.07 % of the cultivable area. Of this area, 4.27 million ha consists of annual crops and 0.67 million ha consists of permanent crops. About 62.41 % of the cultivated area is located in the three northern governorates (Aleppo, Arraqa and Al-Hasakah), representing only 33 % of the total area of the country. The area of steppe and pastures is about 8.23 million ha, or 44 %; non arable land about 3.68 million ha, or 20 %; and forests quasi 0.57 million ha, or 3 % of the total area of Syria (Central Bureau of Statistics: CBS, 2009). The total populations were 23.02 million in 2009 (as registered by the Department of Civil Status), while the number of permanent residents, excluding those who live outside Syria, were 19.88 million. Some 46.48 % of the population lives in rural areas. Actual population growth was 2.5 % for the period 2000-2005. Agriculture employs around 16.79 % of the total labor force, accounting for nearly 20 % of Gross Domestic Product (GDP), compared to 39 % in 1963. In 2004, the average population density was about 96 inhabitants/km<sup>2</sup> (CBS, 2009). Almost 55 % of Syria is dry steppe or quasi-desert, suitable only for grazing sheep and goats. Rain-based farming of cereals, food and feed legumes is the backbone of agriculture in Syria. Irrigated land makes up about 23.91 % of cultivated land, which is about 7 % of the total area of the country (Kangarani, 2006; CBS, 2008).

Syria's climate is Mediterranean (arid and semi-arid) with a continental influence consisting of cool, rainy winters and warm dry summers, with relatively short spring and autumn seasons. Large regions of Syria have a high variability in daily temperatures. The greatest difference in daily temperature can reach a 32 °C in the inside and about 13 °C in the coastal region. The common annual precipitation in the country is 252 millimeters (long-term average). Syria has limited water resources, since 55.1 % of the total area receives precipitation of less than 200 mm per annum. The region is located in the fifth settlement zone (agro climatic zone) (see Fig. 3.1), which consists of rangelands and desert areas covering 1,208 million ha, representing 55.1% of the total area of the country. This zone includes 86 % of the pastoral land not suitable for rain-fed cultivation (Akkad, 2001; Al-Fares, 2007; FAO-AQUASTAT, 2009).

As outlined by this introduction, agriculture has traditionally been the foundation of the economy (46.48 % of the population was described as rural in 2009, with 16.79 % of the population employed in the agricultural sector and 20 % of Syria's GDP attributed to this industry). The agricultural sector has been influenced over the past 40 years by several factors. First, a growing population (4.565 million in 1960, compared to 19.88 million in 2009) with a slight increase in acreage. Secondly, the natural climatic conditions in Syria are not conducive to agricultural stability, due to heavy precipitation. Since the output of agriculture (both plant and animal) is heavily dependent on precipitation (only about 23.91 % of the cropped area is irrigated), the large variation in the quantities and timing of precipitation can be a reason for a large changes in areas planted, yields and production. Thirdly, over 90 % of the total Syrian territory (arable lands) needs sustainable irrigation, even in areas which receive large quantities of precipitation, since most of the rain falls during the winter rather than in the growing season. In addition, the discharge periods of Syria's rivers in March and May are late for winter crops and early for summer crops. The stream of the rivers varies significantly every year. Years of low stream make irrigation and agriculture difficult. These factors have led to a focus on large scale irrigation projects such as dam construction as a basis for economic and social development. The irrigable arable lands estimated in the ERB are 1,040,000 ha (ACSAD, 2001). Syria has its own plans for irrigation development within the Euphrates basin. These involve using water from the Euphrates to irrigate six major regions: the Maskana-Aleppo-Basin (155,000 ha), the Arrasafa-Basin (25,000 ha), the Al-Balikh-Basin

(185,000 ha), the Euphrates-Floodplain (170,000 ha), the Al-Mayadin-Plain (40,000 ha), and the lower Al-Khabour-Basin (70,000 ha) (see Fig. 3.4). This is a total of 645,000 ha (Beaumont, 1996). Until now, only ca. 225,000 ha has been irrigated. Some 63 % of the irrigated areas in Syria are located in the Euphrates River Basin, according to the World Bank (CBS, 2009).

Syria has limited water resources. There are 16 main rivers and tributaries in the country, of which six are main international rivers. The most important is the Euphrates, which is Syria's largest river, originating in Turkey and flowing to Iraq. Its total length is 2,880 km, of which 610 km are in Syria. The Euphrates River Basin has a surface area of 444,000 km<sup>2</sup>, (17 %, or 75,480 km<sup>2</sup> in Syria) and its actual annual volume is 35.9 million cubic kilometers (ACSAD, 2001; Kangarani, 2006). Total actual renewable water resources in Syria are estimated at 16.797 million ck/year. The natural average surface runoff to the Syrian Arab Republic from international rivers is estimated at 28.515 million ck/year. The actual external renewable surface water resources are at 17.335 million ck/year, which includes 15.750 million ck of water entering the Euphrates, as unilaterally proposed by Turkey. The Euphrates River provides more than 80 % of the total Syrian water resource (Kangarani, 2006; Radwan, 2006; FAO, 2009; CBS, 2009) and is the country's biggest source of irrigation water. Early in the 1960s, Syria, due to the need to expand the agricultural areas and to reduce the rain fed based agriculture areas, and the need for electricity, started utilizing the Euphrates water in irrigation and hydropower, with construction beginning on the Attabqa Dam in 1973 (it was completed in 1978) (FAO, 2009).

Most regional crop estimate frameworks in Syria are based on knowledge from local experts (e.g., extension officers, farmers, grain traders etc.). These frameworks have developed depending heavily on the expertise of the various officials. Estimates were often based on historical regional, state and national level statistics, which were, and still are, collated by the Central Bureau of Statistics (CBS) via an agricultural census/survey at the province/Muhafazah (statistical local area) scale. Lack of detailed province scale information further emphasizes the need for alternative accurate and objective crop area estimates to assist agro-industry decision-making at the regional scale.

Earth Remote Sensing can be defined as the detection, measurement and analysis of electromagnetic energy reflected, emitted or diffracted by an Earth surface feature without being in physical contact with it (Lillesand et al., 2008). This broad definition includes aerial imaging in the ultraviolet, visible and infrared (near, mid and far) reflective part of the spectrum, as well as thermal imaging and active technologies like radar, and moreover, geo-electric and geo-magnetic measurements. The use of remote sensing is essential in recording a variety of information about the Earth's surface and the atmosphere. This form of data gathering is an important tool in numerous sciences such as meteorology, environmental research and cartography. To make full use of the information potential of remote sensing, data must be processed, interpreted and evaluated systematically.

The used techniques for interpretation of remotely sensed data are based on many compatible disciplines including: remote sensing; pattern recognition; artificial intelligence; computer vision; image processing; and statistical analysis. The progress in automated analysis of remotely sensed data is optimistic by the growing volumes of data, the great developments in computer science (software and hardware) that processes these data, as well as the high cost and effort involved in ground surveying. The new generation of remote sensing sensors provides superior spatial and spectral resolution data, leading to the use of remotely sensed products and further underlining the need for more automated and simplified forms of processing, interpretation, and analysis. Earth Observation Remote Sensing has led to the development of human perspectives and increased greatly our understanding of the planet (Steffen & Tyson, 2001). Beginning with data from the successful CORONA missions in 1960 and the start of the LANDSAT-program in the early 1970's, remotely sensed data are now globally available and deliver an exceptional amount of information about the Earth surface and the biosphere, thereby offering an enormous potential of information for monitoring (Jensen, 2007; Campbell, 2002).



A mainly central application of remote sensing is the production of LULC-maps from satellite imagery. Compared to more conventional mapping approaches such as terrestrial survey and basic aerial photo interpretation, LULC-mapping using remote sensing imagery has the competitive advantages of low cost, repetitive large area coverage. Earth Observation Systems (EOS) have the potential to offer spatially-distributed and multi-temporal information on LULC and its environmental state over extended areas. Furthermore, satellite systems offer near-real time information, which is particularly important for natural hazards and disaster management, as one example. Overall the conduction of LULC-information from remote sensing imagery is a significant application, concerning the support of multilateral environmental agreements, decision-making and monitoring systems. Its future use promises to be rewarding, judging by recent and rapid developments in sensor technology. Mainly remarkable in this view aspect is the superior spatial and spectral resolution of the imagery captured by new satellite sensors. As well as existing sensors such as LANDSAT-TM and SPOT-HRV, a number of new remote sensing sensors with up to 1 m spatial resolution are already in operation.

The quality of the agricultural information systems in Syria and the cropped areas estimate range from timely and reliable to virtually non-existent. Estimates are based on past trends (e.g., ground survey or census), and are sometimes adjusted by subjective judgment, rather than on objective information. There exists an established need for the nations of the world to better manage the planet's agricultural production, with improved seasonal information on crop prospects for important producing regions. This need, coupled with the state of technical development and the conceptual processing of remote sensing, has brought into focus the possibility of applying remote sensing and related technology, to the task of developing a technical concept for agricultural monitoring (Erb, 1980). The reliance on remote sensing techniques and using its data in Earth Observing Studies has many important advantages for these studies in comparison to other old and classical approaches. These remotely sensed data are objective, well-timed, recurrent and thus they could be able to present results (e.g., classification results) with a higher accuracy. During the last four decades, satellite- obtained information in the agriculture sector, using low spatial resolution images to high spatial resolution images, was helpful in the decision-making processes of governments. Agricultural production is highly dynamic and depends on complicated interactions of prices, weather, soils and technology all over the world. This production has an influence on the global food market. For the purposes of agricultural studies, there is the need for accurate data at a specific time. Here, because the meaningful forces (e.g., economic, food, policy and environmental impacts) of major strategic crops, it is significant to know the local distribution and the acreage of these types of crops. For these reasons, remote sensing, either alone or in combination with ground surveys (important for training samples gathering, classification use and ground truth points used for accurating the classification results), has been used in crop acreage assessment (Erb, 1980; Allen, 1990; Hanuschak et al., 2001; You et al., 2004; Carfagna & Javier Gallego, 2005; Wardlow & Stephen, 2008).

The use of remote sensing data and its applications for distinguishing between types of agricultural crop and interior crop characteristics was widely researched during the last four decades (Cloutis et al., 1996; Metternicht et al., 2000; Senay et al., 2000; Thenkabail et al., 2000; Van Niel & McVicar, 2000; Van Niel & McVicar, 2004 a; Blaes et al., 2005; Wardlow et al., 2007; Ozdogan, 2010). The well improved tendencies involving particular types of crop, maturity, levels of the nutrient, and their reflectance values within the spectral bands and in correlation to the vegetation indices (VIs), are becoming more accurate and are helpful when the availability of ground truth data is limited (Senay et al., 2000). The majority of the presented efforts in mapping that were highlighted above have focused on the classification of LULC-features associated with natural systems (e.g., forest, grassland, and shrub land) and have a tendency to generalize/simplify the areas of cropland into a single or limited number of thematic classes.

Techniques of satellite remote sensing have a fundamental role in irrigation management. Some applications of satellite remote sensing techniques for irrigation management are: crop acreage; crop condition; crop yield; and performance of irrigation canal system. These techniques were applied effectively in monitoring irrigated lands in many areas around the world under a variety of climatic conditions. It offers a synoptic and a suitable temporal coverage of agricultural lands in several spectral regions. Its archived data offers comparison of imagery among dates, and yielding change over time. Up to now, there are many studies that have used remotely sensed imagery, mainly at high spatial resolutions such as LANDSAT, to observe and classify irrigated agriculture. The early studies focused on determining the ability of remotely sensed data to classify, map and update irrigated land acreage. This was mainly used in the US and India (Draeger, 1976; Heller & Johnson, 1979; Thiruvengadachari, 1981; Kolm & Case, 1984; Thelin & Heimes, 1987; Rundquist et al., 1989). Some new studies have improved and tested new classification methods particularly appropriated for mapping irrigated lands (Eckhardt et al., 1990; Ram & Kolarkar, 1993; Pax-Lenney et al., 1996; Abuzar et al., 2001; Martinez-Beltran & Calera-Belmonte, 2001, Ozdogan et al., 2006; Ozdogan & Gutman, 2008; Pervez et al., 2008; Dheeravath et al., 2010).

To monitor the changes in our surrounding Earth environment and to manage the natural resources of the Earth, researchers have presented many models and strategies, especially during the last few decades. The major element in structuring these models is how LULC-features change over the time dimension. Land use and land cover change has become a central component in current strategies for managing natural resources and monitoring environmental changes. Remote sensing satellite images have proven their ability in change detection studies. So-called *Change Detection Methods* have been applied to multi-temporal images, in order that variations and changes in the state (especially spectral) and spatial distribution of features and phenomena can be recognized, mapped and interpreted (Singh, 1989; Coppin et al., 2004). This method includes procedures, which can identify and evaluate changes without past or present detailed knowledge of the land surface (Rogan et al., 2002). This information should offer land managers a better understanding of relations and interactions between the anthropogenic and natural phenomena. This should be able to offer an efficient distribution and management of available natural resources. The deep understanding and consideration of all other issues on the reflected EMR-signal, within and between multi temporal remotely sensed data, will offer the basis for successful change detection studies (Lu et al., 2004).

The research problem is that Syria, in general, and the Euphrates River Basin in particular, like other developing countries, rely very heavily on traditional statistical methods to monitor and study changes in the natural cover and land use over time. This is in order to obtain and compare statistical data and figures, and allows these data to act as a basis and reference to the decision makers in the development of national plans, including agricultural policy. Based on this collected data, with regard to the agriculture sector for example, decisions must be made on the abolition of creative projects, the development of new irrigation schemes, asset-sufficiency, and whether food should be imported or if local production covers the needs of the population. Many other procedures and policies rely on the accuracy of statistical information and data for their success. The statistical methods used in Syria give unreliable results, because of their complete dependence on the human element. There is a need for the application of other methods that produce more accurate data, and which may be less expensive and require less effort. The inability to represent the distribution and prevalence of various agricultural crops spatially increases the size of the problem and is a negative factor in statistical data collection in Syria.

One challenge for researchers lies in the need to find scientific tools and methods with a suitable methodology, which can be applied to the study area. Remote sensing can contribute a greater role to the understanding of this problem by providing accurate mapping data about land uses, including crop utilization over multiple time periods. Remote sensing also results in a realistic depiction of land use, by providing a spatial dimension.

Many kinds of data supply, especially spatial data on the dynamics of LULC, are poor and thus insufficient. Nevertheless, extended knowledge on the state and changes of LULC is needed in order to support the implementation of sustainable strategies of regional development. Spatial information is the basis for various planning tasks. This information could be obtained by application of the remote sensing techniques.

This monograph discusses four basic themes in the study area: the mapping of land use and natural cover; development mapping of irrigated areas; the mapping of the distribution of irrigated agricultural crops, especially strategic crops; and mapping, monitoring and study of the changes in land use and natural landscape during the last 30 years. The questions this research poses and answers are:

Which automatic classification technique or approach is the best for the study area?

How can land use/land cover be mapped using different data from remote sensing instruments in arid and semi-arid regions?

How can remote sensing be applied to the mapping and monitoring of the spatial expand in the irrigated projects constructed in the Euphrates River Basin in Syria?

How can remote sensing be applied to the mapping of irrigated agricultural crops in arid and semi-arid regions?

Can mapping and monitoring aid understanding of land use/land cover changes over time by using the remote sensing concept in arid and semi-arid regions?

## **B. Significance of the study**

The importance of this research stems from the location of the study, the Euphrates River Basin. This basin is one of the most important areas and territories in Syria, containing the important elements of life: stability, food and water. The basin contains more than 80 % of the total water resources of the country. It is the food basket of Syria, and is made up of three provinces: Aleppo, Arraqa and Deir Azzour. These agricultural provinces contain 34 % of the total population of Syria, 38.4 % of the total area of Syria and 37.4 % of the total arable land. Some 40.2 % of the country's total irrigated areas are found in these three provinces and almost half of the population that live there work in the agriculture sector. The equivalent of 37.67 % of the total acreage is planted with wheat, 51.27 % of the area in barley, 92.50 % in yellow corn (maize), 58.79 % cotton, 49.63 % sugar beet and 49.92 % watermelon.

## **C. Research objectives**

The major component in the development of LCLU-maps is satellite imagery. The objective of this work is the use of high resolution remote sensing data (LANDSAT: MSS, TM and ETM+; TERRA: ASTER) for the mapping of land use/land cover, land use/land cover change, and irrigated agricultural crops. The research objectives for this study are:

- Understanding the spatial and temporal distribution of the interested study area surface features;
- Determination of the major dominant LULC in the area using LANDSAT: MSS, TM and ETM+-, and TERRA:ASTER satellite imagery from 1975, 1987, 2005 and 2007;
- The temporal development mapping of irrigated areas;
- The creation of one classification method to provide a sufficiently accurate discrimination of the main irrigated crops types in the study area; and
- To determine and analyze the dynamics of change of LULC-classes (trend, nature, rate, location and magnitude of land use land cover change).

#### **D. Research hypotheses**

The rural environments have unique spectral characteristics and the application of remote sensing provides a unique opportunity to study these requirements. The process of integration between remote sensing data (in the case studies: LANDSAT and ASTER), and developments in Computer Science (hardware and software) and mathematics (algorithms) allows for the mapping of the historical and current land use and natural land cover, thus ensuring access to the true spatial dimension of each type of land use. These technologies also allow the study and analysis of the changes in land use and natural cover over time, and the comparison of the current status of the region with how it was 30 years ago.

#### **E. Organization of the thesis**

This study is organized into seven chapters including this *Introductory Chapter*, which provides a statement of intent and sets out research questions, study objectives and study hypotheses. *Chapter 2* covers the necessary basics for understanding remote sensing in accordance to the current state of the art applications in use in Syria. Here, the classification process and various classification algorithms used, including unsupervised and supervised, parametric and non-parametric, pixel and object classification techniques, are discussed in detail in addition to the application of remote sensing in land use/land cover classification. This second chapter also reviews the literature on the current state of knowledge on regional scale crop area estimate approaches. This includes crop area estimates using remotely sensed data, the importance of temporal and spatial resolution, and the ability of satellite imagery to discriminate among crops.

The *third chapter* describes the study area of the Euphrates River Basin, Syria. In this chapter the location, irrigation projects, climate, morphology, soil, hydrology, land use/land cover and human impacts are discussed. *Chapter 4* describes the common resources that were available for this study, including satellite data, maps, field reference data, statistics and another ancillary data. *Chapter 5* discusses the pre-processing techniques applied to the satellite images in order to obtain data with low calibration errors as a prerequisite for interpretation and comparison. Emphasis was placed on the geometric and radiometric accuracy of the processed data. In addition, research methodology, image processing, image classification and accuracy assessment are outlined in this chapter. In *Chapter 6*, results, analysis and thematic interpretations are discussed. The overall summary, general conclusions and recommendations of the research study are provided in *Chapter 7*.

## Chapter 2: Theoretical background and state of the art

This chapter provides a short overview of the principles of remote sensing outlines current studies focused on the Euphrates River Basin (ERB) and presents a survey of the literature available on the topics that the thesis covers. Within the confines of this study, remote sensing is defined as the measurement of emitted or reflected electromagnetic radiation, or spectral behaviors, from a target object by a multispectral satellite sensor. This thesis contains four main sections: land use/land cover classification, the mapping of irrigated areas, irrigated agriculture mapping (especially crops classification), and land use/land cover change detection mapping. A great number of papers have been published on the above four topics. In this section a small range is given, based on significance and likeness to this thesis, with the goal of providing no wide-ranging survey, but of giving an experience of the techniques, applications and performances found in the literature.

### A. Remote sensing concept

A broad definition of remote sensing would include vision, astronomy, space-probes, most of medical imaging, nondestructive testing, sonar, observation of the Earth from a distance, in addition to many other fields (Schott, 2007). For purposes of this text, discussion has been limited to Earth observation from space. "Remote sensing is the science and art of obtaining information about an object, area or phenomenon through the analysis of data acquired by a device that is not in contact with the object, area or phenomenon under investigation. Using various sensors, we remotely collect data that may be analyzed to obtain information about the objects, areas or phenomena being investigated. The remotely collected data can be of many forms, including variations in force distributions, or electromagnetic energy distributions" (Lillesand et al., 2008). Fig. 2.1 illustrates schematically the generalized processes and elements involved in the electromagnetic remote sensing of Earth resources (Lillesand et al., 2008).

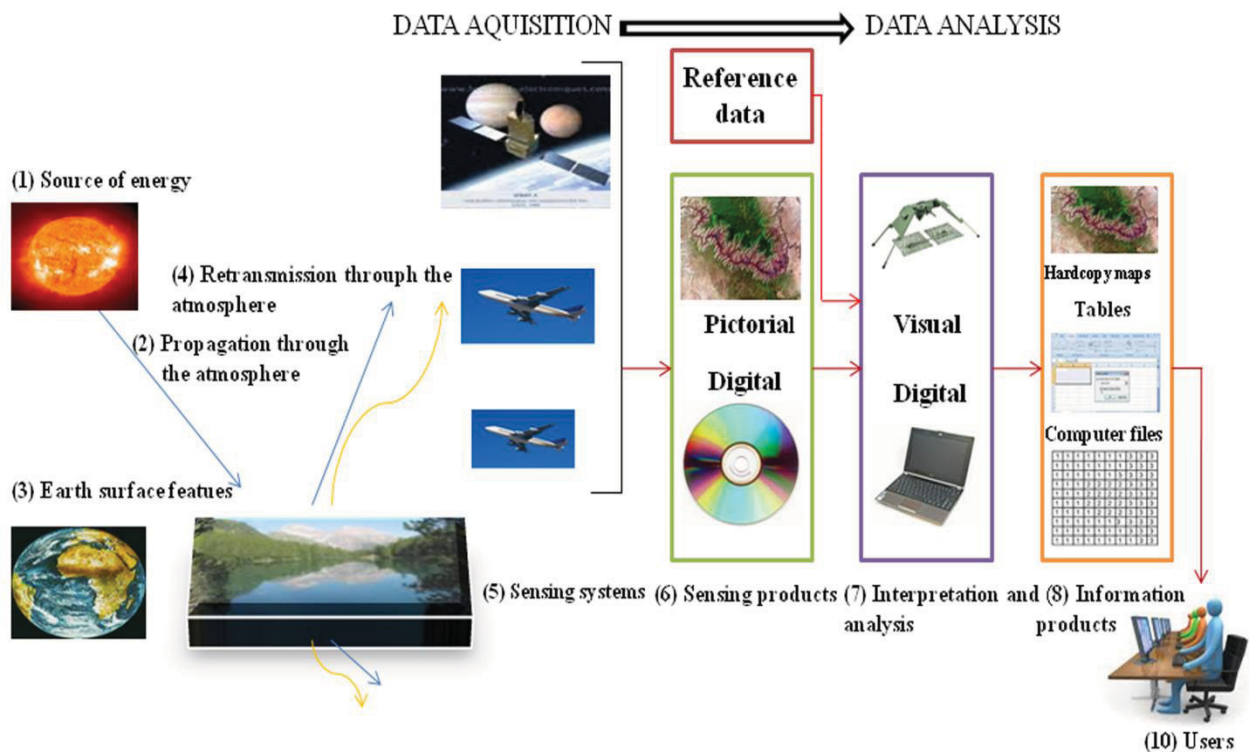


Fig. 2.1: Electromagnetic remote sensing of Earth resources (Source: Modified from Lillesand et al., 2008)

The translation of the former schematic view into text is given in the following essential relevant components (De Jong et al., 2007; Lillesand et al., 2008):

1. The source of the electromagnetic energy: all materials with a temperature above 0 Kelvin have the ability to produce electromagnetic energy. Other materials or objects on or near the Earth's surface are able to replicate or disperse incident EM-radiation emitted by an energy source (e.g., artificial sources such as microwave radiation, or natural sources like sun radiation).
2. The path through the atmosphere: before energy source radiation (e.g., solar) reaches the Earth's surface, it will be affected by the atmosphere. In addition, the atmosphere will impact reflected solar radiation or emitted radiation by an object at the Earth's surface before an airborne (aircraft) or space borne (satellite) sensor detects it (Van der Meer & De Jong, 2001). "The changes of the radiation can vary with wavelength, condition of the atmosphere and the solar zenith angle" (Slater, 1980 cited in De Jong et al., 2007). The most significant processes here are scattering (Herman et al., 1993) and absorption (LaRocca, 1993).
3. The interaction with the object: transmission, absorption and emission transmission are the three essential processes of the EM-radiation when it hits an object at the Earth's surface. Here, the characteristics and properties of target object, especially those of a physical nature, determine the mutual significance of these processes.
4. The signaling of the energy via a sensor: a sensor is a satellite-borne engine. It is constructed to be able to measure the electromagnetic energy radiating from *Earth- and its surrounded Atmosphere- features*. There are two major types of sensors: 1) inactive sensors: they have not a built-in source of energy to radiate the atmosphere and/or the Earth surface. Thus, they use an external source of raw radiation (e.g., the light reflected from the sun, or when an object of interest due to its physical properties - is able to emit an energy). 2) active sensors: they have their private artificial source of energy to radiate the objects of interest. They have to be used for those objects that do not have the ability to emit either energy or radiation. Examples are RADAR (RADio Detection And Ranging), and LIDAR (LIght Detection And Ranging). Radiation can be recorded in an analogue form (by aerial photograph), or it can be stored in a digital array, as a set of signal values on a magnetic device CD-Rom or DVD (used by most remote sensing systems at present) (De Jong et al., 2007).
5. Transmission, receiving and preprocessing of the recorded radiance: the recorded energy by the receiver on the sensor has to be transformed in electronic form to a receiving and processing station where the data is processed into an image (digital and/or hardcopy). Preprocessing operations are required to correct the sensor- and platform-specific radiometric and geometric distortions of data. Each of these preprocessing operations will vary depending on the specific sensor and platform used to obtain the data and the conditions during acquisition of the data (De Jong et al., 2007).
6. Interpretation and analysis of the remote sensing data: the exceptional benefit of digital recordings is that many manipulations can be carried out according to an extended set of algorithms and techniques of digital image processing and pattern recognition by using one of the different software packages for image analysis. Techniques of remote sensing offer us in general three major types of information (De Jong et al., 2007): 1) the classification of separate pixel(s) or separate object(s) (group of alike pixels) in a remote sensing image to their really class(es) in the real world (e.g., producing a thematic LULC-map); 2) the quantity calculation of some objects components in regard to temporal and spatial dimensions (e.g., measuring a forest biomass amount); and 3) the observation of the spatial activities within the various types of LULC included in (1) or the quantity object characteristics included in (2) throughout a time period (e.g., change detection mapping). In summary, there are four major united characteristics in remote sensing techniques and components,

and in objects of interest. Based on these characteristics, information about the Earth's surface features can be carried out De Jong et al. (2007): "a) spectral characteristics (wavelength or frequency, reflective or emissive properties); b) spatial characteristics (viewing angle of the sensor, shape and size of the object, position, site, distribution and texture); c) temporal characteristics (changes in time and position); and d) polarization characteristics (object effects in relation to the polarization conditions of the transmitter and receiver)".

7. Creation of the final product: the resulting output based on the remotely sensed data can be in different forms, and frequently results in information that can be used as input for further analysis and studies (e.g., in GIS) (De Jong et al., 2007).

Imagery of remote sensing are recorded digitally using detectors and receivers located on sensors on board the satellites (McVicar & Jupp, 1998). Digital techniques of remote sensing convert the various elements of the electromagnetic energy (color, light, heat, etc.) to a digital type. Spatially, the data is composed of separate picture elements, or pixels, and radiometrically, it is quantized into separate brightness levels (ERDAS, 1999). An example of operation a satellite is explained in Fig. 2.2. The satellites vary in altitude above the Earth's surface from those which orbit the planet at approximately 700 km, to those which are geostationary above the equator at 36,000 km (McVicar & Jupp, 1998).

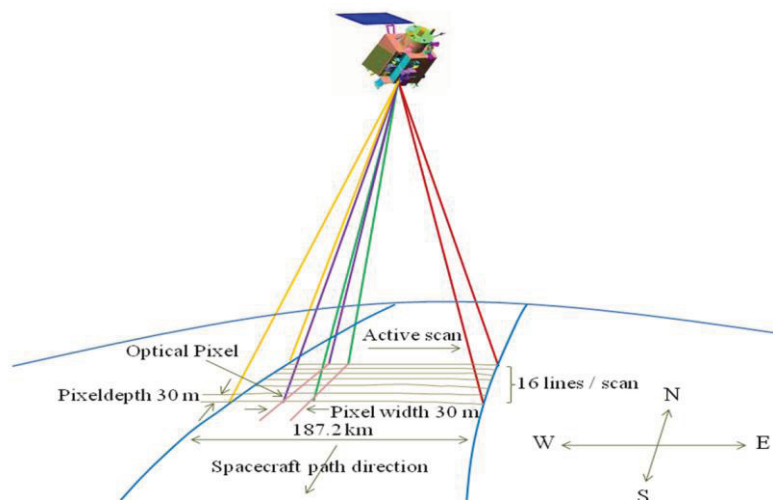


Fig. 2.2: Schematic of satellite operations, specifically the LANDSAT satellite and the Thematic Mapper (TM) sensor (Source: Modified from Harrison & Jupp, 1989)

Key to the consideration of remotely sensed imagery is the coverage, resolution and density of its spectral, spatial and temporal characteristics. *Spectral coverage* describes which part of the EMS (Fig. 2.3) is being used (e.g., visible, infra-red, thermal, etc.). *Spectral resolution* indicates to the spectral bandwidths in which the sensor collects information. *Spectral density* indicates to the number of spectral bands in an exacting part of the EMS (e.g., the LANDSAT-MSS has only four bands, while the TERRA-ASTER has 14 bands, etc.). *Spatial coverage* is the area enclosed by the image, while *spatial resolution* indicates to the smallest pixel or picture element recorded. *Temporal coverage* is the acquiring period over which the data is obtainable (e.g., LANDSAT-Sensors have a temporal coverage of 41 years). *Temporal resolution* relates to the time that the data is obtainable over. It is generally low by most remote sensing systems. *Temporal density* refers to the repeat properties of the satellite. A good repeating in gathering the data would, for some applications, offer more availability of cloud free data (McVicar & Jupp, 1998). *Radiometric resolution* indicates to the active range or number of potential data file values in each spectral band (the number of bits into which the recorded energy/data is divided). For example, the total *intensity* of the energy for 8-bit data is measured from 0 to the maximum amount of 256 brightness values. Where 0 stands for no energy return, 255 is the maximum return of each pixel (ERDAS, 1999).

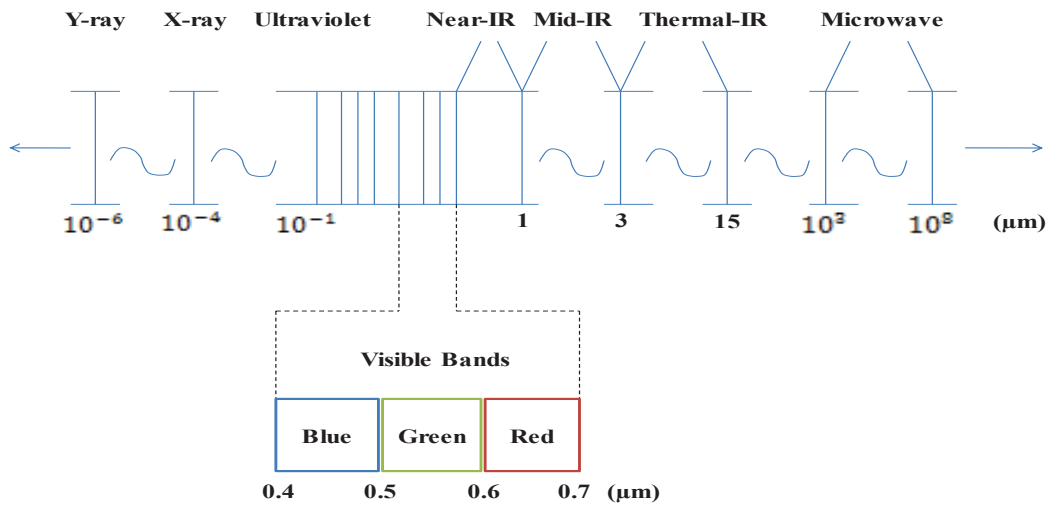


Fig. 2.3: The primary spectral regions of the electromagnetic spectrum that are of interest in Earth remote sensing applications (Source: Modified from Tso & Mather, 2009)

No remote sensing of the Earth’s surface is possible without active *atmospheric windows* (Fig. 2.4). These transmission bands allow light to pass through the atmosphere of the Earth with little or no interaction at different wavelengths of the EMS. This refers to the spectral coverage in which radiation reaching satellite sensors carry information about the Earth’s surface conditions (McVic-ar & Jupp, 1998). This information includes: vegetation stress; surface temperature; atmospheric water content; and a mass of other characteristics that the human eye cannot see or recognize (Schott, 2007).

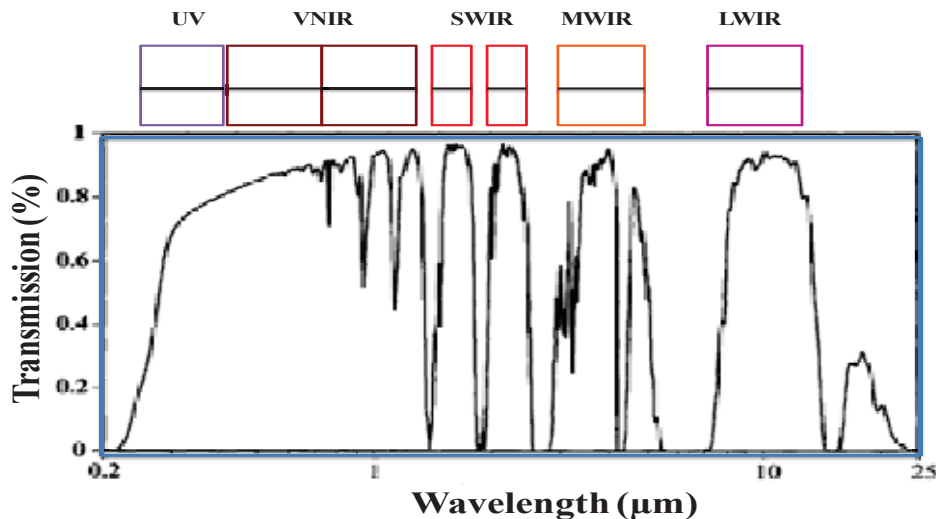


Fig. 2.4: Atmospheric transmission spectra showing windows available for Earth observations (Source: Modified from Schott, 2007)

A multispectral sensor (e.g., LANDSAT-MSS) acquires multiple images of the same target Earth surface feature (e.g., water, soil, bare area, agricultural crops, etc.) at different wavelengths (spectral bands). Each band measures single spectral characteristics about the target (e.g., the fourth near infra-red band of MSS is responsible for detection and recoding the spectral response of the natural vegetation). A spectral band is a data set recorded by the sensor with information from separate parts of the electromagnetic spectrum (Richards, 1986). One foundation of remote sensing is



that LULC-features have different spectral properties and responses (McVicar & Jupp, 1998). Analysts generate spectral signatures based upon the detected electromagnetic energy's measurement and place in the electromagnetic spectrum. A spectral signature contains statistics that define the spectral characteristic of a target feature or training samples. Image interpreters detect the value of these statistics by quantitatively comparing the relation between studied class signatures and the used spectral bands. Spectral signatures are made more sophisticated by superior ground-truth points/measurements and accuracy assessment analysis. By utilizing the sophisticated spectral signatures in multispectral classification and thematic mapping, the interpreter generates new data for analysis (ERDAS, 1999). Fig. 2.5 shows idealized spectral reflectance plots for two types of vegetation, soils and water types, respectively.

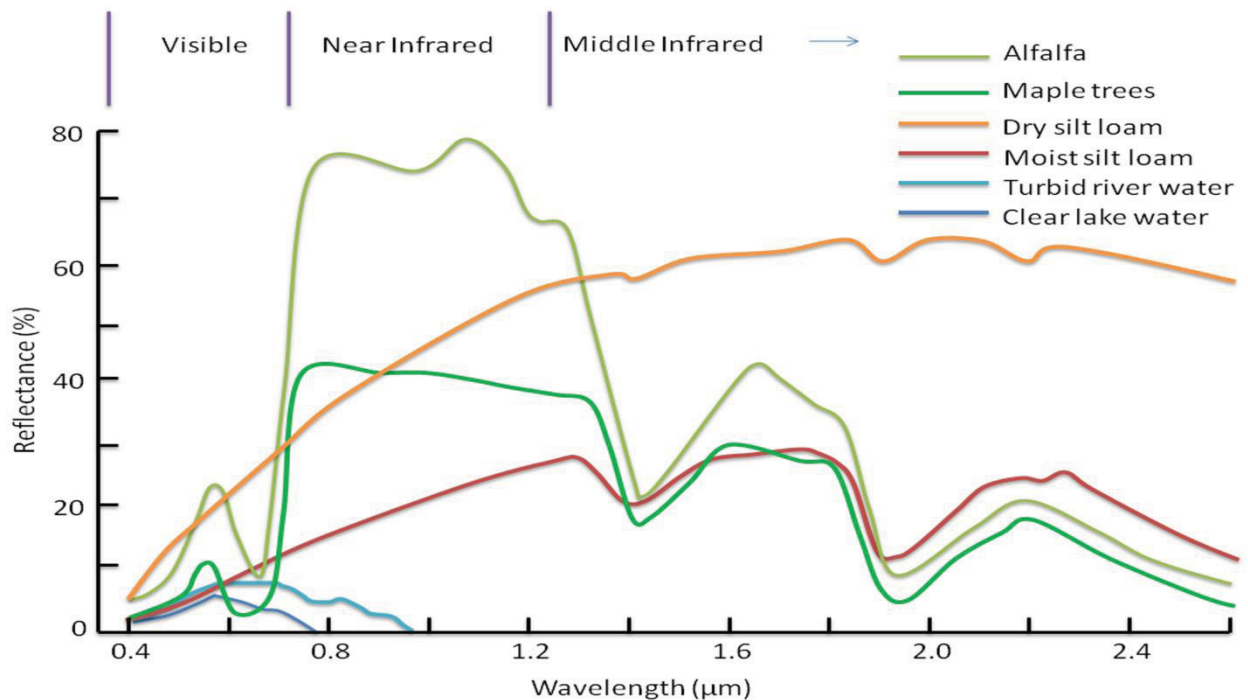


Fig. 2.5: Idealized reflectance plots for different land cover types (Source: Modified from Harrison & Jupp, 1989)

Remote sensing lets us overcome the classical problem of “not being able to see the forest for the trees” in traditional Earth observation approaches (e.g., ground surface studies). These classical approaches can be rendered incomplete by providing too much detail on too few samples or by only having data from a very limited location. The ability of remote sensing techniques on *the synoptic perspective* lets us “see the individual trees in the forest”. The use of this perspective offers a wide view of broad-scale environments with various features, tendencies and relationships. In turn, this leads to the interpolation or extrapolation of parametric values from extensively studied ground sites (ground truth sites). The temporal perspective offered by remote sensing techniques from minutes up to decades over large areas, provides the ability to “see through the clouds” in atmospheric windows where this would generally be impossible (Schott, 2007).

The most broadly used *optical systems* in the period from 1972 to 2000 were the LANDSAT-TM and MSS, the SPOT-HRV and the NOAA-AVHRR instruments. Examples of other optical remote sensing systems include the Chinese-Brazilian remote sensing system, the TERRA spacecraft, the European ENVISAT, the Indian IRS series and several Japanese experimental projects. *High resolution systems* (4m in multispectral mode, one meter or less in panchromatic mode) are for example the Quick-Bird satellite, IKONOS, and Rapid-Eye. *Radar systems* are also becoming more numerous: Canada’s RADARSAT-1, and 2, the German TERRA-SAR-X, the European Advanced Synthetic Aperture Radar (ASAR) positioned on ENVISAT, and the Italian COSMO-SkyMed-X-band system. Significant interest is also being shown in the application of *hyper spectral systems*.

In comparison to multispectral sensors, a hyper spectral sensor collects data in a large number of very narrow wavelengths. NASA's Earth Observer-I, launched in 2000, was the first orbiting spacecraft to carry a hyper spectral imager-Hyperion. The Hyperion instrument collects data over a narrow swath in 220 bands of 10  $\mu\text{m}$  width. Other examples are DAIS instrument, the Compact Airborne Spectrographic Imager (CASI), and NASA's AVIRIS. Another class of satellites systems is the *small sat*, developed using off-the-shelf mechanisms. The leader in this new technical field is Surrey Satellite Technology Limited, which has constructed the DMC or Disaster Monitoring Constellation of small satellites, which were purchased by several governments, including Algeria, Nigeria, China and the United Kingdom. The imaging sensor carried by these satellites is similar to LANDSAT's TM in the visible and near-infrared spectral bands (Tso & Mather, 2009). More details about the working of the main types of sensor carried by the different remote sensing platforms presented in textbooks such (e.g., Mather, 2004; Lillesand et al., 2008).

## **B. Remote sensing application in Syria**

The application of remote sensing in Syria is similar to the situation which exists in other developing countries. Remote sensing technology has been in place for more than two decades but has lacked the expected effectiveness of such technology as used in the countries of the developed world. The General Organization for Remote Sensing (GORS) was established by the Syrian Arab Republic (SAR) in 1986 and is today the most important and highest scientific body in the country competent to conduct remote sensing. It carries out many scientific projects and studies based on the application of remote sensing in the Syrian territories, and has utilized these skills even outside the country's borders (e.g., in Sudan). All of these studies have been addressed to the government's institutions and ministries, and thus the basics and the details of remote sensing techniques has remained almost entirely within the confines of GORS and the researchers who work within this organization.

Access to remote sensing technology has been limited to those interested in studying this science further. Until 2001, for example, the remote sensing module was taught in geography departments at Syrian universities for only one semester (two hours per week). Greater access to this technology is needed, including an upgrade of the facilities and training available in this subject throughout Syrian universities.

In addition to GORS, there are two other scientific authorities who have published studies based on the use of remote sensing technology: the Arab Centre for the Studies of Arid Zones and Dry Lands (ACSAD) and the International Centre for Agriculture Research in Dry Areas (ICARDA). Unfortunately, these two bodies have refused to cooperate with university and graduate students, requiring several levels of approvals before any research is distributed for academic purposes. The other related international institutions in Syria are the Food and Agriculture Organization (FAO) and the United Nations Development Program (UNDP), which work in co-operation with national institutions mentioned above.

A vital component of the research required for this thesis was a project undertaken by GORS in the provinces of Arraqqqa, Deir Azzour and Al-Hasakah. "The Survey of Natural Resources in the Eastern Regions of Syria in Cooperation with the Ministry of Agriculture and Agrarian Reform" was initiated in 2004 and was undertaken over a period of five years. Data was remotely collected from ASTER, IRES, SPOT and an Algerian satellite. The project included:

- A tour of the provinces in question to choose the appropriate areas from which to take spectrometry readings on a variety of crops for the purpose of spectral profile/characterization, during which different stages of growth were to be distinguished spectrally using satellite images;
- Field testing of the devices to be used in the study (Spectrometer/FieldSpecPro and GPSs);

- The characterization of agricultural crops and land use during May 2005, consistent with the presence of winter crops, and during August 2005, consistent with the presence of summer crops. Some 1,050 sites were identified for the purposes of the study;
- Spectrometry readings on strategic crops (wheat, barley, lentils, sugar beet, cotton, watermelon and maize). These readings were conducted on average once every two weeks through the stages of crop growth;
- Input of field survey data and spectrometry readings to databases through electronic forms prepared for this purpose; and
- The creation of spectral signatures for each crop under study. Analysis of these spectral signatures led to the identification of the optimal time to request satellite images to be used in the estimation of the areas of winter and summer crops.

The project's objectives were: a study and cost estimate on crop area and yield for various strategic crops in Syria compared with traditional methods, and the production of maps of winter and summer crops, allowing the calculation of the level of agriculture in the regions. Many other studies focused on the Euphrates River Basin have proved essential during the development of this thesis.

One of the aims of the project of [Beaumont \(1996\)](#) was to evaluate the effectiveness of satellite data for approximation agricultural changes within the upper part of the Euphrates basin and to calculate the area of irrigated agriculture. Two satellite images (LANDSAT-MSS) taken in the mid-1980s of two catchments was used. It is maintained that the satellite data offer more details and gives insights into the agriculture of the region which was not available from any other prior source.

The paper from [Hirata et al. \(2001\)](#) focused on the vegetation classification in the Abd Al- Aziz mountain region in north-eastern Syria using geo-coded bands (2, 3, and 4) of LANDSAT-5-TM images to analyze the vegetation distribution in this highly diverse rangeland. The average classification accuracy was 85%. This shows that a 30\*30 m spatial resolution of LANDSAT-TM images had the ability to classify natural vegetation at six sub-divided community levels.

[Zaitchik et al. \(2002\)](#) used two LANDSAT-TM images from September 1990 and 2000, jointly with created digital elevation data from the ASTER sensor and the statistical tools of landscape ecology, to measure changes within the irrigation projects in the Al-Khabour-watershed. This analysis provides a description of the changing nature of agriculture. By joining this remotely sensed data with biophysical information on climate and hydrology, it is also possible to assess the hydrologic impact of various water extraction and diversion schemes.

The activities of ICARDA cover a wide range of countries of the Middle East and North Africa. Research on the agricultural systems in Syria was carried out at the Yale Center for Earth Observation (CEO) in 2004. Time-series analysis of satellite data and ground truth studies were utilized to observe and evaluate changes in agricultural land use over the past 30 or more years. The research plan was used to expand these time-series data throughout historical and archaeological studies, and to relate land use changes to socio-economic methods. The major objectives were to classify the present classes and spatial geographic distribution of agricultural systems, and to map their development and evaluate their sustainability. The six agricultural systems were: river and wadi; rain-fed steppe; irrigated steppe; canal-fed steppe; mountain/hill; and coastal ([ICARDA, CEO, 2004](#)).

[De Pauw et al. \(2004\)](#) published a paper on the land use and land cover in Syria during the period 1989/1990. The research was based on an interpretation of the data (LANDSAT-5-TM) and field checking. The approach to map land cover/land use was based on manual interpretation of hard-copy images. The main product was a LULC-map of Syria for the base years 1989/1990. For this LULC-map, a local and a posteriori classification system was selected, incorporating elements of both land cover and land use. The map legend consists of two main classes: homogeneous units,

which can be considered relatively pure (80-90%), and mixed units, which are complexes of homogeneous units. Twenty-four homogeneous classes were differentiated on the basis of the following major categories: (i) bare areas with or without sparse cover; (ii) cultivated areas; (iii) forests and other wooded areas; (iv) rangelands; (v) urbanized areas; and (vi) water bodies. In addition, 43 mixed classes were distinguished. Overall, the research confirmed that there is a good agreement between the derived land use estimates based on the remote sensing interpretation and between statistics derived from the Food and Agriculture Organization of the United Nations database (FAOSTAT).

[De Pauw \(2005\)](#) used remote sensing data with validation through expert knowledge and ground truth to map the agricultural regions in Syria. This satellite imagery (LANDSAT) was used in conjunction with secondary information (including geological, soil, landform and climate maps) to delineate boundaries.

[Celis et al. \(2007 a\)](#) used the Normalized Difference Vegetation Index (NDVI) calculated from spectral data obtained from the AVHRR-sensor on board the National Oceanic and Atmospheric Administration satellite NOAA-12 to research the year 1990, and the period April 1992 to March 1993 using an established classification scheme that employed a hierarchical decision tree to identify LCLU-types in the Central and West Asia and North Africa region (CWANA). LCLU-types relevant for CWANA were selected on the basis of expert opinion, field surveys, and analysis of thematic maps and LANDSAT-satellite imagery. To assign a pixel to a particular LCLU-type, the decision tree used “sliding thresholds” for the annual minimum, maximum and mean, which varied by agro-climatic zones. NDVI-thresholds were then fine-tuned, based on a careful analysis of climate station data and land use maps from different agro-climatic zones.

The researchers monitoring land degradation and conducting LCLU-change mapping in the CWANA-region used remote sensing as a highly valuable tool to understand the highly complex issues of land change and degradation. AVHRR-imagery was used for delineating “hot spots” of LULC-change. The main advantage of the “hot spots” approach is that it allowed zooming into “target areas” for more detailed observations, through ground-based characterization and monitoring assisted by high-resolution satellite information, such as LANDSAT. Some 612 10-daily composites of 8-km (AVHRR) reflectance data, covering the period from January 1982 until December 2000, were used. The NDVI was calculated and aggregated into monthly NDVI-composites in order to reduce the effects of cloud cover. The following kinds of change were allocated to each pixel: noise, stable LULC, stable LULC-mosaic, and change pattern. Seventeen stable classes were recognized, as well as 66 change patterns, which were regrouped into 22 change classes and four change trends (“intensification of agriculture”; “intensification of natural vegetation”; “retrenchment of agriculture”; and “retrenchment of natural vegetation”) ([Celis et al., 2007 b](#)).

The study from [Udelhoven & Hill \(2009\)](#) focused on long-term variations (1982 to 2004) in the Syrian rangelands using the “Mediterranean Extended Daily One Km AVHRR-Data Set” (MEDOKADS) and the 8-km Global Inventory Modeling and Mapping Studies (GIMMS) data set. In agreement with other studies it was found that the NDVI was a suitable proxy for land surface response to precipitation variability even at low vegetation coverage. The inter-calibration of existing AVHRR-data with new data from the recent generation of moderate resolution narrow band satellite systems such as Spot (VEGETATION or MODIS) is a promising source of data for future LULC change monitoring that was already realized in the GIMMS-data set.

### **C. Land use-land cover mapping**

During the past decade, after improvements in remote sensing data and computing resources in addition to the promise of the advanced classification algorithms, the mapping of LULC features became easier, potentially in a digitally form ([DeFries & Belward, 2000](#)). During this period, mapping of LULC features has developed through many efforts at state ([Eve & Merchant, 1998](#);

Craig, 2001), regional (DeFries & Townshend, 1994; DeFries et al., 1998; Bosard et al., 2000; Vogelmann et al., 2001; Homer et al., 2004), and global (Hansen et al., 2000; Loveland et al., 2000; Friedl et al., 2002; Bartholome & Belward, 2005) levels.

### 1. Distinction between land cover (LC) and land use (LU)

There is separation between land use and land cover, but they have a clear joined aspects in the real world (Meyer, 1995). Land use indicates to "man's activities on land which are directly related to the land" (Clawson & Stewart, 1965). Land cover, in contrast, describes "the vegetation and artificial constructions covering the land surface" (Burley, 1961). To explain these definitions: a land cover expression is "grassland", while "rangeland" or "tennis court" indicates the use of grass cover. "Recreation area" is a land use expression that may apply to different land cover types, such as a beach, park or woodlands.

Land use indicates to what are the human activities in the land, while land cover indicates to what natural features covering the surface of the Earth (Jensen, 2007). Land use influences land cover and changes in land cover influences land use. A change in either however is not necessarily the result of the other (Riebsame et al., 1994). Land cover is changed mainly by human use (Allen & Barnes, 1985; Turner et al., 1990; Turner et al., 1995), but natural occurrences such as weather, flooding, fire, climate fluctuations and ecosystem dynamics may also instigate modifications upon land cover (Meyer, 1995). Land use and land cover are not identical although they are interrelated (Briassoulis, 2000). The difference is schematically depicted in Table 2.1.

Table 2.1: Types of land cover and associated types of land use (Source: Modified from Briassoulis, 2000)

Types of land cover	Types of land use
Forest	Natural forest-Timber production-Recreation
Grassland	Natural area-Pastures-Recreation-Mixed use: Pastures and recreation
Agricultural land	Cropland: Annual crops-Orchards-Mixed uses
Built-up land	City-Village-Archaeological site-Industrial area-Transportation-Mixed uses

### 2. The classification process

The most commonly considered technical, methodological and experience fundamentals to produce an accurate classified thematic map from a remotely sensed image, are: the remotely sensed data have a suitable temporal, spectral and spatial resolution in regard to the characteristics of the study area of interest. Furthermore, the obtainability of supplementary data would give the data of remote sensing more accuracy in representing the real world in thematic maps (classification process), especially those ground control points; the ability to create an appropriate classification procedure, and the skills and experiences of those employed for analysis (Lu & Weng, 2007).

Classification of satellite images is one of the most commonly applied techniques used in remote sensing data processing. "Classification involves performing a transformation from the numerical spectral measurements into a set of meaningful classes or labels, which can describe a landscape. Classification effects a transformation from a physical measurement into a cartographic or thematic description of the Earth's surface, for examples into terms such as forest, built-up area, water bodies, etc. As such, classification can be viewed as a signal inversion process" (Wilkinson, 2000).

During the 15-year phase studied, there has been progress in three main aspects of remote sensing data classification. These are: 1) the advancement of mechanism of the classification techniques:

the training or learning strategy; and methods applied to class separation based on statistical or other estimators and class separability indexes; 2) the advancement of innovative systems-level approaches that supplement the original classifier algorithms; and 3) the utilization of various types of data or auxiliary information, both numerical and categorical, in a classification process (Wilkinson, 2005).

While Earth surface features have their own characteristic and spectral reaction in different spectral bands of the electromagnetic spectrum, they can be recognized, identified and delineated in multispectral remote sensing. Therefore, the multispectral approach is the heart of the application of remote sensing in LULC-classification. By interpreting an image in several spectral wavelengths, we can improve the utilized remotely sensed data's ability to distinguish the various LULC-features. For example, water and vegetation reflect light nearly equally in visible bands, but these features are almost always separable in near-infrared bands.

In general, techniques of machine learning and pattern recognition execute the classification. Fig. 2.6. shows that a *pattern* is a vector of features that describing an object. This pattern consists of measurements on a set of *features*. The feature of a natural pattern is a set of  $n$ - radiance measurements acquired in the various spectral bands for each pixel. It can be considered as the axes of a  $k$ -dimensional space, named the *feature space* (Tso & Mather, 2009). The classifier or the decision maker allocates the measurement vector to one of a set of classes based on a suitable decision rule (Swain & David, 1978; Lillesand et al., 2008). In the case of multispectral or hyper spectral imagery for example, the set of spectral reflectance measured in the different spectral wavelengths can be regarded as a *signature*. In addition, simple pixel values (e.g., spectral reflectance), spatial and/or temporal image information can be used (Lillesand et al., 2008). Spatially, one can use texture analysis considered in the subsequent classification process (Haralick et al., 1973; Soares et al., 1997). Temporally, one derives some temporal information, such as multi-temporal mean and variance, which can be integrated in the following image investigation (Bruzzone et al., 2004 b). Classification of remotely sensed data can be executed using: a single image dataset; multi-temporal data (multiple images); image data with supplementary information (e.g., digital elevation measurements or models); or expert of study area based knowledge.

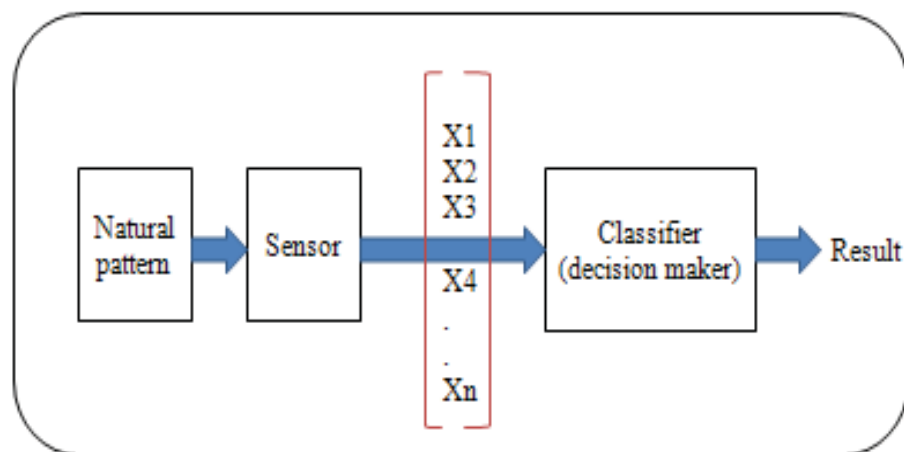


Fig. 2.6: A model for pattern recognition in remote sensing (Source: Modified from Swain & David, 1978)

In general, classification of LULC-features using remote sensing data consists of numerous phases (Robinove, 1981; Mather, 2004; Schowengerdt, 2007), as shown in Fig. 2.7:

- *Identifying*: the number and the name of classes that represents the real-world features which have defining priority;
- *Feature extraction*: data are frequently highly correlated between spectral bands. This high correlation might be inappropriate for classification of LULC-features and may reduce

classification accuracy. Optionally, one can apply the spatial (e.g., smoothing filter) or spectral (e.g., bands subset, such PCT, to reduce the data dimensionality) transformation of the multispectral data with the aim to: 1) differentiate between valuable information and noise or non-information; and 2) reducing the dimensionality of the data to shorten the computing time needed by the classifier, and thus to raise the effectiveness of statistical estimators in a statistical classifier;

- *Training*: the term “training” is the choosing of the pixels to train/prepare the classifier to identify the preferred *themes*, or *classes*, and the selection of decision boundaries. Here, the drawing of boundaries around geographically located pixels has to be homogeneous, or acceptably heterogeneous. This phase can be carried out either supervised or unsupervised by the user; and
- *Labeling*: this is the process of allocating different pixels to their most likely class based on the application of the feature space decision boundaries. This process of labeling can be supervised or unsupervised. If a pixel is not spectrally alike to any of the available classes, then it can be assigned to an unknown class. There are two kinds of relationships between the object and the class label: one-to-one (producing a *hard classification*); or one-to-many (producing a *fuzzy classification*). The object may be a single pixel or a group of neighboring pixels forming a geographical unit (e.g., an agricultural field). As a result, a thematic map is produced, presenting every pixel with a class label. The end result is a transformation of the digital image data into descriptive labels that classify different Earth surface objects or conditions.

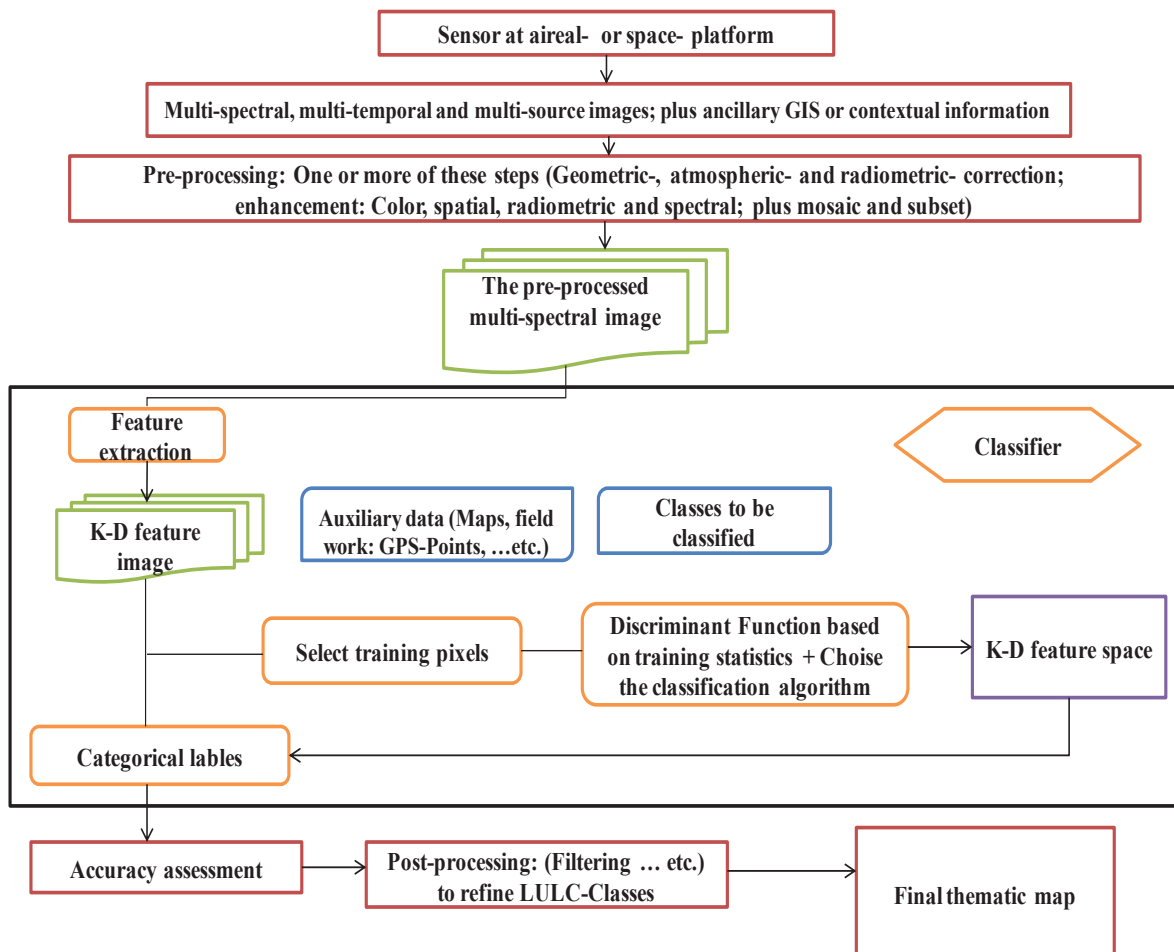


Fig. 2.7: The classification process (Source: Modified from Townshend & Justice, 1986; Tutz, 2000; Wilkinson, 2005; Schowengerdt, 2007)

### 3. Classification schemes

"If a reputable classification system already exists, it is foolish to develop an entirely new system that will probably only be used by ourselves" (Jensen, 2005).

Before creating any (LULC) thematic map, a classification system should be selected. Throughout the world there are no typical LULC-classification systems, thus many countries have their own differing systems. Various LULC-classification systems are designed particularly for use with remotely sensed data. Many of these are comparable to other classification systems (or integrate aspects thereof) to maintain coherence and allow for data integration. Classification systems come in two basic formats, *hierarchical* and *non-hierarchical* (Di Gregorio, 2005). A hierarchical construction is often implemented within a classification system. It has the advantages of a harmonized structure and different levels of class detail. This level can then be adapted to the required scale of the mapping product (Foti et al, 1994).

There are two general approaches to classify the remotely sensed data, namely a *superior* or an *inferior*. The *superior* approach based on the consideration that the classes are absolutes of the LULC-features in the real world. The user determines the classes of interest before obtaining any data. Then, the user has to understand the complete probable combination and mixtures of rational rule between the various classes (Di Gregorio, 2005). "The major benefit is that classes are standardized, free of the area and the means used. The weakness, however, is that this method is inflexible, as some of the field training sites may not be easily assignable to one of the pre-defined classes. *A posteriori* classification varies primarily by its direct method and its autonomy from predetermined designs. The approach is based upon definition of classes after clustering likeness or unlikeness of the ground truth sites gathered. The advantage of this kind of classification is its flexibility and adaptability in comparison to the inherent inflexibility of the *a priori* classification. The *a posteriori* approach involves a minimum of generalization. This kind of classification fits the collected field observations in a specific area. At the same time, however, because an *a posteriori* classification depends on the specific area described and is adaptable to local conditions, it is impossible to define standardized classes. Clustering of samples to define the classes can only be done after data collection, and the significance of individual criteria in an individual area may be limited when used in another place or in ecologically extremely different zones" (Di Gregorio, 2005).

Anderson et al. (1976) defined 10 standards for saying that the applied system for classification of LULC-features is improved and successful: 1) the accuracy percentage of 85 % has to be obtained; 2) the similarity in accuracy percentages for different classes is necessary; 3) the possibility to obtain a classification results from one analyst, which have to be reproducible if another user used the same data and methods. This reproducibility must be available not only for various users but also over several times; 4) the applicability for large areas has to be satisfied; 5) the ability to use the categorization of LULC-features as an alternative for activity; 6) the effectiveness of the application of the classification system with multi-temporal remotely sensed data; 7) the system has the ability to integrate the subcategories that can be achieved from a ground survey; 8) the system of classification must satisfy that the resulting classes must be conformable with larger scale maps or enhanced remote sensor data; 9) the ability to compare a future LULC data; and 10) it is important - if possible - to recognize the multiple uses of land.

There is the often realizable fact that no single classification could be applied with all kinds of images and scales. There are many Land Use/Land Cover Classification Systems (LULCCS). Anderson et al. (1976) developed a hierarchical LULC-classification system for use with remote sensor data. It has been implemented by the USGS for 1:250.000 and 1:100.000 scales LULC-mapping of the United States. Other classification schemes existing for use with remotely sensed data are mostly modifications of the Anderson et al. (1976) one. The CoORDinated INformation on the Environment (CORINE) land cover classification scheme with three levels from the European



Environment Agency (EEA) is an example of a hierarchical classifier, constructed for European countries by using LANDSAT-TM/ETM+ data with focusing on agricultural and area of the forests. The first level distinguishes five general LULC-features: 1) artificial surfaces; 2) agricultural areas; 3) forest and semi-natural areas; 4) wetlands; and 5) water bodies. The second level is more detailed with 15 classes. It is designed for scales between 1:500,000 and 1:1000,000. The third level includes 44 classes. It is designed for scales of 1:100,000. The land cover classification system of the FAO of the United Nations (UN), as part of the IGBP-land use and cover change LUC initiative AFRICOVER, developed a highly flexible scheme of several environmental layers including: soil; lithology; climate; plant physiology; ...etc., with the major goal of creating an environmental database. The IGBP-DIS Cover global (1km) data set is based on the NOAA-AVHRR (Africover, 2003).

There are many certified country-based classification system around the world, but they are, unfortunately, not trustworthy when we want to apply it in other countries with different characteristics to that one, for which the classification system was originally constructed. Thus, there are up to now no systems certified in all countries (i.e. Worldwide) for the classification of remotely sensed data, in spite of the advantages that could be presented by depending on a single classification system. The detailed reasons for that were explained by Di Gregorio (2005). They are the three general standards: purpose, steadiness and causal.

#### 4. The general classification techniques

To gain higher accuracy values in the classification of remotely sensed data, and thereby obtain higher quality in derived thematic map(s), is possible using advanced classification algorithms. The recent literature (e.g., Gong & Howarth, 1992; Kontoes et al., 1993; Foody, 1996 and 1998; Miguel-Ayanz & Biging, 1997; Aplin et al., 1999 a; Stuckens et al., 2000; Franklin et al., 2002; Pal & Mather, 2003; Gallego, 2004) recommended several major standards for increasing the classification accuracy: 1) new technical development of sensors; 2) sufficient availability and a wide spectrum of variability of remote sensing data; 3) finding new superior methods that can offer a better use of spectral information; 4) developing techniques for fusion of the different sources of information, and for integration GIS-data with the other sources of information; 5) giving more attention to the use of knowledge-based classification techniques and other more powerful machine learning algorithms; and 6) the permanent technical development of computer power to have a constant performance. This led to changing from conventional statistical techniques to those advanced but complex techniques and algorithms that are more sophisticated (Jain et al., 2000; Richards, 2005).

The general concept of pattern classification applied to a specific problem depends on: *the data*; *the model* of the data; and *the information* that one is supposed to get from the data (Bezdek, 1981). The data could be: qualitative; quantitative; numerical; pictorial; textual; linguistic; or any combination of them. For example, pictorial data records information about the object represented in the image. "The model used must be such that it transforms the data and makes them compatible with the search and matching strategies to be used. Each search and matching strategy corresponds to a different pattern classification methodology. This is the reason for the use of different concepts to pattern classification (e.g., mathematical or statistical, heuristic, and structural etc.)" (Tou & Gonzalez, 1974).

Researchers have presented various approaches for image classification, which can be divided into three general groups (Fig. 2.8) (Pal & Pal, 1993).

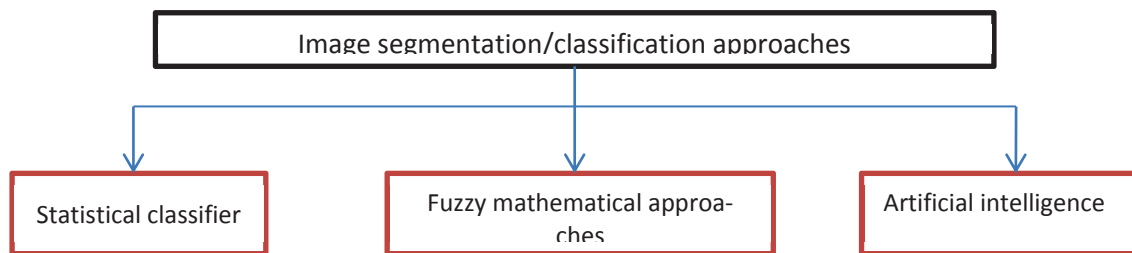


Fig. 2.8: Major approaches for image segmentation/classification (Source: Modified after Pal & Pal, 1993)

*Statistical classifiers*: these are ideally suitable for data that have information with an assumed theoretical model based distribution within each of the classes. The representative algorithms for this group are: MLC; PPC; k-NNC and MDC. Corresponding literature for these algorithms can be found in (Swain & Davis, 1978; McLachlan, 1992; Ripley, 1996; Hastie et al., 2001). *Fuzzy mathematical approaches*: Zadeh, (1965) presented the concept of fuzzy sets in which unclear knowledge can be used to delineate a result. *Artificial intelligence (AI)*: here, supervised classification approaches were developed from the starting of the 1970s, with the well-known “Arch Concept Learning” problem presented by Winston (1975). These methods based on the learning from descriptions of a constructive pattern, and therefore gave up the value-attribute based model that was used in other methods. AI-type models were constructed based on semantic networks and on predicate logic.

Liu & Mason (2009) summarized the classification approaches in seven categories: unsupervised classification; supervised classification; hybrid classification; single pass classification; iterative classification; image scanning classification; and feature space partition. In most cases, image classification approaches included: supervised and unsupervised; parametric and nonparametric; hard and soft (fuzzy) classification; per-pixel, sub-pixel, object-oriented and per-field; spectral classifiers, contextual classifiers and spectral-contextual classifiers; or combinative approaches of multiple classifiers (Lu & Weng, 2007). This last division was adopted in this chapter. This previously mentioned article presents: present practices; remotely sensed data classification troubles and scenarios. It highlighted the main advanced classification approaches, in addition to those techniques that can improve the at-end classification accuracy.

Although there are many developed classification approaches, which approach is more appropriate for objects of interest in a selected study area is not totally understood (Schowengerdt, 2007). Selection of an appropriate classifier needs consideration of many issues, such as: classification accuracy; algorithm performance; computational resources (DeFries & Chan, 2000); and effective separation of the classes (Flygare, 1997). Also, there are other issues that could be considered to select a classifier. They are: the spatial resolution; utilization of supplementary data; the used classification scheme; the available and selected digital image processing software; and the skill of the user (Lu & Weng, 2007). A comparative study of various classifiers is often carried out to determine the best classification result for a definite study area (Zhuang et al., 1995; Atkinson et al., 1997; Cortijo & De La Blanca, 1997; Flygare, 1997; Michelson et al., 2000; Hubert-Moy et al., 2001; Keuchel et al., 2003; Pal & Mather, 2003; Erbek et al., 2004; Lu et al., 2004; Olthof et al., 2004; Pal & Mather, 2004; South et al., 2004). According to many studies and cases, contextual-based classifiers, per-field approaches, and machine-learning approaches give more classification accuracy than, for example, MLC, although some exchanges presented in: classification accuracy; time consumption, and computing resources have to be considered (Lu & Weng, 2007).

Modifications of image classification techniques increase classification accuracy. Therefore, in contrast to classifiers which join a variation of the same classifier, other techniques are based on

the joining of different algorithms (multiple classifier systems) (Benediktsson & Kanellopoulos, 1999; Jeon & Landgrebe, 1999; Steele, 2000; Liu et al., 2004 a; Fauvel et al., 2006 a and b).

The next sub-chapter will review the fundamental ideas of classification techniques applied in remote sensing. Classification techniques, grouped using these criteria (training samples, parameters, pixel information, definitive decision and spatial information), and their advantages and disadvantages will be discussed in detail. A detailed explanation for all supervised classifier approaches is beyond the scope of this dissertation. Interested readers can be referred to several references. A general introduction to pattern recognition and classification is given in the textbooks by Duda et al. (2000); and Bishop (1995 and 2006), and in the review paper by Jain et al. (2000). A detailed introduction in the context of remote sensing is given by Richards and Jia (2003), and a general overview by Richards (2005).

#### 4.1. Training sample based categories

*Unsupervised classification:* when insufficient ground reference information is available (e.g., field work measurements such as representative training samples) about the characteristics of specific classes for classification processes, an unsupervised classification technique is used to identify natural homogeneous groups (clusters) within the remotely sensed data.

Unsupervised classification approaches are based on non-parametric statistical approaches, such as Iterative Self-Organizing Data Analysis Technique (ISODATA) (Tou & Gonzalez, 1974), K-means-clustering (Johnson & Wichern, 1988) algorithms, and the advanced unsupervised neural classification method Self-Organizing feature Mapping (SOM) (Kohonen, 1989). The details of other clustering algorithms can be found in Jain and Dubes (1988); and Mather (2004). In this approach, the image processing software groups pixels that have similar properties (in feature space and in adequate representative spectrally-separable clusters for the ground surface features), based on the statistics of the radiometric value/digital number of each pixel. Then the analyst evaluates the classified map with field survey data, aerial photographs and other reference data, and labels these clusters (spectral classes) with its equivalent in the real world to information classes, without having a prior knowledge of the classes. Generally, some clusters must be subdivided or combined to make this equivalence. Results of an unsupervised classification can be used to define the training samples, which are a main input in the supervised classification, or the labeled cluster map can be just accepted as the final map (Duda et al., 2000; Richards & Jia, 2003; Jensen, 2005; Lu & Weng, 2007; Schowengerdt, 2007).

A general problem of algorithms used in unsupervised classification is that data can include clusters with different shapes and sizes. Providing an applicable definition of clusters and the selection of a sufficient guide for likeness are complex (Jain et al., 2000). Although this approach is automated and seems complicated and powerful, the results are generally lower than those attained by using supervised approaches, where the most real-world features are complex in their nature, and therefore may not be easily spectrally separable. The assumption formed of the unsupervised approach that the pixels belonging to a specific class will have similar spectral response and that all classes are separable from each other in spectral feature space, is not easy to realize in practice. The approach also depends upon the analyst's skill in determining suitable parameter values, and in integrating the clusters with information classes. Finally, the analyst cannot impact the identity and coverage of the resulting categories. Accordingly, the classification accuracy based on unsupervised classification methods is inadequate (Jain et al., 2000). Computational complexity is high and there is little fitness for very high resolution data.

The advantage of unsupervised approaches is that it requires no prior-knowledge. On the other hand, its disadvantage is that it does not provide any final membership decision. Also, class memberships (e.g., class labels) and other knowledge about the image source do not influence the clustering algorithm, only the interpretation of the final clusters (Jain et al., 2000). Finally, unsuper-

vised classification is used particularly if reliable training samples for supervised classification inaccessible or are too expensive to obtain (Richards & Jia, 2003).

*Supervised classification:* supervised approaches, as seen in Fig. 2.9, are based upon training sites, and can assure the former but not the latter; unsupervised approaches can assure the latter but not the former (Tso & Mather, 2009).

Each image is characterized by  $n$ -observations (the values in  $n$ -data bands). Supervised image classification is an approach in which the analyst delineates the training samples (vectors in an  $n$ -dimensional feature space) on the image which are representative of each interested LULC-class (Mather, 2004). A basic step in supervised classification and mapping is the design of a realistic classification scheme, which satisfies a clear definition of separable discrete informational LULC-categories within the available data (Cingolani et al., 2004). Training sites/samples can be created from fieldwork, aerial photography and other existing maps based on analyst knowledge (e.g., thematic, Google Earth), and are then used as reference information (Skidmore, 1989; Wilkinson, 2000; Jensen, 2005; Lillesand et al., 2008). Visual interpretation is used to locate the training samples position on the image (Mather, 2004). These training samples have to be homogeneous spectrally to represent specific LULC-classes. A supervised algorithm, after the training samples stage, uses the distribution of the training samples for each class to assess density functions in the feature space statistically and to divide the space into class regions (Fukunaga, 1990). In other words, the used image's processing software recognizes the spectral signature of each training site based on its statistics (Leica Geosystems, 2005), and then classifies the images in different LULC-classes according to the applied classification algorithm (Jensen, 2005). Here, the information required from the training data differs from one algorithm to another. To get the assessment of the accuracy of supervised classification, two parts are available to determine the accuracy: partly by the quality of the ground truth data; and partly by how well the set of ground truth pixels are representative of the full image.

The most general and used supervised approaches are: The Maximum Likelihood Classifier (MLC) and the Minimum Distance Classifier (MDC). The advanced supervised classification algorithms are: The Artificial Neural Network (ANN), the Decision Tree Classifier (DTC), the Nearest Neighbor Classifier (NNC) and the Support Vector Machines classifier (SVM).

The supervised approach is more popular but requires more detailed *a priori* knowledge of the study area and analyst expertise, to identify suitable training sites and the resultant spectra for classification (ERDAS, 1999). The characteristics of the training sites selected by the analyst have a great impact on the dependability and the functioning of a supervised classification process. This approach has a more subjective impact on the analyst during the defining of the LULC-categories characteristics and its representative training samples. Supervised classification approaches need more user-data-software interaction, especially in the collection of training data.

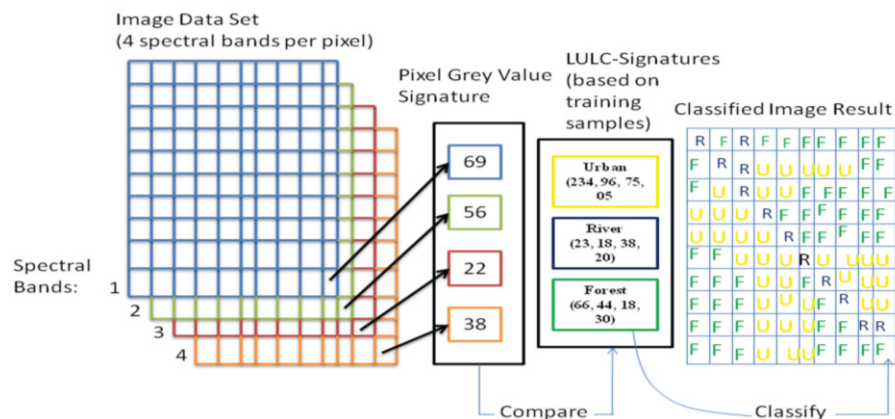


Fig. 2.9: The principal idea of the supervised classification approach for multi-spectral remote sensing (Source: Modified from Eastman, 2006)

## 4.2. Parametrical based categories

*Parametric classifiers:* these are also called single-stage classifiers, where an observation gives the label of one of a determined number of classes in a single step (Swain & Hauska, 1977).

Parametric classification methods use a predetermined parameterized model (usually the Gaussian normal distribution) of the classes in the spectral feature space. Its assumption is based on the premise that a normally distributed dataset presents and that the statistical parameters (e.g., mean-vector, and covariance-matrix) produced from the training samples are representative. The working of statistical classification algorithms will consequently be based on how acceptably the data agree with the predetermined model. If the data used meet with the requirements of this model, these classification methods would give higher classification accuracy than nonparametric methods. The Maximum Likelihood Classifier (MLC) is the most famous and important model for parametric methods, due to its strength and its easy availability in almost any image-processing software.

The advantage of parametric classifiers in comparison to non-parametric classifiers is the theoretical evaluation of classifier error from the assumed distributions (Schowengerdt, 2007). Nevertheless, this assumed normal spectral distribution is often not true, especially in complex landscapes. Also, inadequate, non-representative, or multi-mode distributed training samples can introduce more uncertainty to the image classification process. Another disadvantage is the difficulty in integrating spectral data with auxiliary data. As Swain and Hauska (1977) found, the statistical approach has two essential disadvantages, which are: 1) classification used only one probable combination of features; and 2) because the testing of each sample against all classes, this leads to a rather high degree of ineffectiveness.

*Non-parametric classifiers:* where the purpose of the training stage for a classifier is to define distinction surfaces that split the multidimensional feature space into zones matching to various thematic classes, the simplest structure of classifier is that based on non-parametric methods, because these classifiers are probability distribution free (no assumption of a normal distribution for the dataset is required), and they make no assumptions about the statistical estimates form of the density functions (Fukunaga, 1990). Therefore, non-parametric classifiers are often considered as robust because they could work satisfactorily for a broad range of class distributions, as long as the class signatures are plausibly separate. Non-parametric classifiers are consequently mainly appropriate for the integration of non-spectral data (ancillary data) into a classification process. Broad categories of non-parametric spectral classifiers exist, including statistical methods (e.g., the parallel-piped or box classifier, the minimum distance classifier), and non-statistical methods (e.g., the neural network, support vector machines, decision tree classifiers and expert systems). Various prior studies have showed that non-parametric classifiers may offer more improved classification results than parametric classifiers especially in complex landscapes (Paola & Schowengerdt, 1995 a; Foody, 2002).

## 4.3. Pixel information-based categories

*Per-pixel classifiers:* most classification approaches are based on per-pixel information, where each pixel is classified into one category and the LULC-classes are mutually exclusive. Various statistical methods can be used for pixel-based classification (see: Löffler, 1994; Hildebrandt, 1996; Richards & Jia, 2003; Mather, 2004; Lillesand et al., 2008; Albertz, 2009). The automated classification of distinct pixels can be based on their spectral characteristics (spectral classification), or texture characteristics (texture analysis). The spectral signature of each distinct pixel matches the reflected radiation energy of the imaged segment of the Earth's surface. The recording of the radiation spectrum can be done in several bands. Merging these various spectral bands creates an n-dimensional feature space, where each pixel, depending on its spectral values, can be

denoted. Alike pixels correspond as the one same thematic class, thereby resulting point clusters. The delineation of these clusters in feature space is the goal of multi-spectral classifiers. However, the resulting signature in these classifiers ignores the influence of the neighboring mixed pixels (one pixel covers an area with more than one type of land cover). The mixed pixels result from the technical geometry of the sensor and data storage in grid format. They arise by geometric resolution in this relation: the lower the spatial resolution, the higher the ratio of mixed pixel is the pixel. For this reason, the grid-cell-based close of separate information (LULC) can only be approximated to be correct. Another reason for mixing is because of the sensor blooming effects from neighboring pixels that impact the range of the pixel (Townshend et al., 2000). Finally, if the used spectral bands of a multispectral image are mis-registered, mixing occurs even without reassembling resampling for geometric registration (Billingsley, 1982; Townshend et al., 1992; Schowengerdt, 2007). This fact was recognized early in the analysis of LANDSAT-MSS-data (Horwitz et al., 1971; Nalepka & Hyde, 1972; Salvato, 1973).

*Sub-pixel classifiers:* these have been developed to give a more suitable representation and accurate area estimation of LULC than per-pixel approaches, mainly when coarse spatial resolution data are used (Foody & Cox, 1994; Binaghi et al., 1999; Ricotta & Avena, 1999; Woodcock & Gopal, 2000).

All natural (heterogeneity landscapes) and most man-made surfaces are inhomogeneous at some level of spatial resolution, therefore the remotely sensed data has its limitations (especially in medium and coarse spatial resolution data). Thus, signature mixing does not go away if one changes to higher-resolution imagery. The mixed pixels are a major problem, impacting the successful use of remotely sensed data in per-pixel classification approaches (Fisher, 1997; Cracknell, 1998). The development of hyper-spectral sensors has encouraged renewed interest in techniques for approximating pixel mixture mechanism and its components, based on the traditional spectroscopy techniques (Adams et al., 1995). A fuzzy representation, in which each location is collected from various and biased memberships of all candidate classes, can participate in solving the pixel mixing problem. Different techniques have been used to develop soft classification algorithms, including: fuzzy-set theory; Dempster-Shafer theory; certainty factor (Bloch, 1996); softening the output of a hard classification from MLC (Schowengerdt, 1996); IMAGINE's sub-pixel classifier (Huguenin et al., 1997); and neural networks (Foody, 1999 a; Kulkarni & Lulla, 1999; Mannan & Ray, 2003). The fuzzy-set technique (Foody, 1996 and 1998; Maselli et al., 1996; Mannan et al., 1998; Zhang & Kirby, 1999; Zhang & Foody, 2001; Shalan et al., 2003), and Spectral Mixture Analysis (SMA) classification (Adams et al., 1995; Roberts et al., 1998 b; Rashed et al., 2001; Lu et al., 2003 b) are the superior methods that frequently used to solve the problem of the mixture between pixels. SMA, for example, is helpful for improving classification accuracy accordingly to (Adams et al., 1995; Roberts et al., 1998 a; Shimabukuro et al., 1998; Lu et al., 2003 b), and is mainly significant for improving area estimation of LULC-classes based on coarse spatial resolution data.

However, one major drawback of sub-pixel classification is the difficulty in evaluating accuracy (Lu & Weng, 2007).

*Object-oriented classifiers:* segmentation methods have been in use since about 1970. They were developed primarily in the topic of image processing for particular applications in: medicine; pattern recognition; neuron-informatics (scene analysis); computer aided vision (computer vision); and communications engineering.

It is true that the pixel-based approaches have specific robust advantages and remain broadly used, but these too have general disadvantages: 1) it might be difficult to pinpoint a definite assignment of the pixels on the plot-level to a single LULC-class because of the pixel values variations, where the changeability in spectral response and reflectance ratio within an object (e.g., agricultural parcel) can be influenced by parcel-internal variations (e.g., soil moisture and heterogeneities or plant disease). 2) the spectral properties of neighboring pixels may be a mixture between two or more

classes (e.g., two different agriculture parcels). Applying the object-based image segmentation can average each pixel value to separate each LULC-object. Therefore, the mixed pixels are eliminated (Smith & Fuller, 2001). 3) the target-object is significantly larger than the pixel size (Carleer et al., 2005). 4) the spatial extent of each pixel and LULC-feature of interest do not always correspond (Aplin & Smith, 2008). Classifications that rely on the spatial scale of the objects of interest more than on the coverage/dimension of image pixels, may lead to a reduction of this problem (Flanders et al., 2003; Hay & Castilla, 2006; Platt & Rapoza, 2008).

In object-based approaches, bordering pixels with similar characteristics (spectral, texture, form) are aggregated into pixel-groups (regions, segments, image-primitives, image-objects) (Haralick & Shapiro, 1985; Haralick & Shapiro, 1992; Haberäcker, 1995; Baatz et al., 2004; Hay & Castilla, 2006; Lee & Warner, 2006; Aplin & Smith, 2008). Segment information (mean spectral value, texture, shape and neighborhood relationships) can be derived using an object-based approach, isolating the ground surfaces features imaged on an image into a number of spatially continuous, non-overlapping regions which are homogeneous. This is then used instead of the pixels during the classification process (Pal & Pal, 1993).

Gorte (1999) determined the following requirements for successful object-based approaches: 1) high spatial resolution; and 2) powerful hardware with extensive memory.

The well applied techniques to segment remotely sensed data could be classified into *pixel-*, *edge-* and *region-* based methods and their combinations. Pixel-based segmentation approaches start by grouping the pixels using image histogram thresholding or clustering in the multiple-band feature space. This can be considered as unsupervised classification rather than segmentation (Haralick & Shapiro, 1985; Pal & Pal, 1993). Edge-based segmentation approaches use edge detection algorithms (e.g., Sobel-filter) to find the edges of the different neighboring regions in an image. One disadvantage is that there are often gaps in the edges, so that the segmentation cannot be accomplished with these approaches alone (Haralick & Shapiro, 1985; Pekkarinen, 2002).

The difference between an *object-based* and *object-oriented* classification is the data type. The object-based approach utilizes the segments of an image to stabilize or to get a better classification, such as in the land cover map of UK produced from Smith and Fuller (2001); and Fuller et al. (2002). The object-oriented classification, however, can be considered as a multi-level data procedure to extract information from the illustrated reality in complex, hierarchical data models (Egenhofer & Frank, 1989; Molenaar & Richardson, 1994). The complete procedure consists of: 1. classification; 2. classes-generalization; 3. association; and 4. aggregation.

The availability of the eCognition software gives the object-based classification of remotely sensed data more fame. It uses a region-growing model at various scale levels from coarse to fine, using spectral and spatial information (Campbell, 2002). The segmentation techniques implemented by the eCognition software were carried out and tested in a number of studies (e.g., Tufte, 2003; Hay et al., 2003). The hierarchical association of the network of image objects with different scales, which can be created after multi-resolution segmentation with eCognition, can be used to classify objects at one level based on the classification of their sub-objects or super-objects (Fig. 2.10) (Mitri & Gitas, 2004).

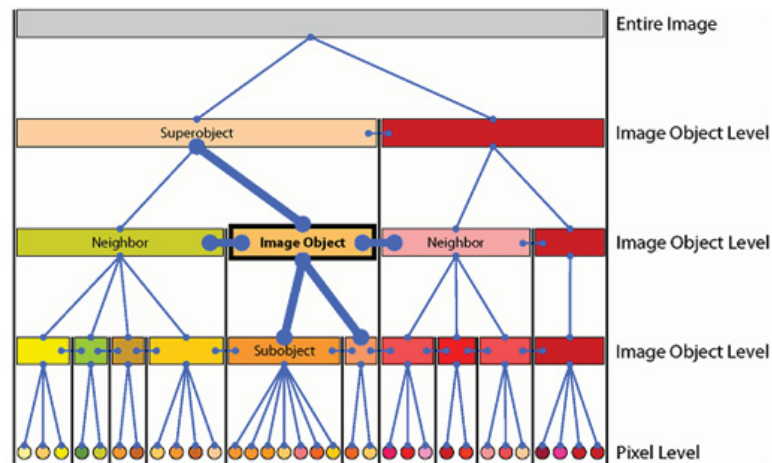


Fig. 2.10: The general concept of the object-based classification (e-cognition classification model) (Source: Adapted from Definiens, 2004)

Despite the possibility of misclassifying specific pixels, object-based classification has these advantages: 1) thematic maps produced could be more identifiable and directly usable by users (Benz et al., 2004; Wu et al., 2007); 2) the object-based information can be joined with other spatial data under Geographical Information System (GIS) environments (Geneletti & Gorte, 2003; Benz et al., 2004; Walter, 2004); 3) reducing the inter-class spectral variation and noise generally deletes the so-called salt-and-pepper effects that are classic in pixel-based classification; and 4) the availability of more classification accuracy than pixel-based, because of the complementary use of large object information sets (spectral, spatial, textural, and contextual) (Lobo, 1996; Aplin et al., 1999 b; Guo et al., 2007; Platt & Rapoza, 2008). This approach shows higher accuracy (~ 8 %) than the MLC, although the MLC-algorithm still had a surprisingly high accuracy of about 85 % (Mather, 2004).

More studies have presented the advantages of object-based classification in comparison to pixel-based classification. Also, there are other studies that refer to its potential limitations (Hay & Castilla, 2008; Kampouraki et al., 2008). In the object-based classification approaches, two kinds of uncertainty are discussed: 1) characteristic uncertainty (uncertainty about the thematic class to which objects or image primitives belong); and 2) spatial uncertainty (e.g., uncertainty about the location of object boundaries (Cheng et al., 2001). Both kinds are strongly correlated (Brown, 1998; Zhang & Stuart, 2001). For example, the letter from Liu and Xia (2010) reviewed the advantages and disadvantages of an object-based approach application in remote sensing image classification in comparison to a pixel-based approach. Two kinds of errors often arise in image segmentation including: over-segmentation; and under-segmentation (Möller et al., 2007; Kampouraki et al., 2008). These errors may influence the next classification process in two ways: 1) under-segmentation could result in image objects that extend among more than one class and so establish classification errors since all pixels in each neighboring mixed image object have to be allocated to the same class. (Wang et al., 2004) also indicate that there is the risk of integrating pixels from various classes into one object primitive, resulting in mixed-object and misclassifications; and 2) LULC-features extracted from missegmented image objects, resulted from over-segmentation or under-segmentation errors, are not representative for real ground surface characteristics (e.g., shape and area), so they may reduce the classification accuracy if not selected correctly (Song et al., 2005 a). For that reason, the final performance of object-based classification is determined by both its advantages and disadvantages (Liu & Xia, 2010).

*Per-field classifiers:* the per-field/per-parcel classifier is constructed to deal with the problem of environmental heterogeneity and it was applied successfully in improving classification accuracy



(Aplin et al., 1999 a and b; Aplin & Atkinson, 2001; Dean & Smith, 2003; Lloyd et al., 2004). This classifier equalizes out the noise by using land parcels (called *fields*) as separate units (Pedley & Curran, 1991; Lobo et al., 1996; Aplin et al., 1999 a and b; Dean & Smith, 2003). GIS provides the basis for implementing per-field classification by integration of the both vector and raster data (Harris & Ventura, 1995; Janssen & Molenaar, 1995; Dean & Smith, 2003). The vector data are used to subdivide an image into parcels, and classification is then carried out based on the parcels, thus avoiding within-class spectral variations. The image data will be pixel-based classified, using either a supervised- (see: Aplin et al., 1999 b) or unsupervised- (see: Hoffmann, 2001) approach. However, per-field classifiers are often, according to (Janssen & Molenaar, 1995), affected by such factors as: 1) the spectral and spatial characteristics of remote sensing data; 2) the size and shape of the fields; 3) the definition of field boundaries; and 4) the LULC-classes chosen.

It is difficult to treat the dichotomy between vector and raster data types. Also, an update of existing GIS-data sets is not possible by this approach (Hoffmann, 2001). Therefore, the per-field classification approach is not broadly used. Here, an alternate approach is to use an object-based classification (Thomas et al., 2003; Benz et al., 2004; Gitas et al., 2004; Walter, 2004), which requires no GIS-vector data.

The basis for a successful application of a per-field classification is the satisfaction of a geometrically accurate vector data set with a matching date. If this data must be produced by visual interpretation or manual adjustment of existing spatial data, the time required increases considerably, and this approach loses its advantages (Hoffmann, 2001).

#### 4.4. Land cover class output-based categories

A class definition always contains uncertainties and can never be absolute. Therefore, *hard* or sharp (crisp) and *soft* or vague (fuzzy) classification methods differ.

*Hard classification*: most classification algorithms produce a “probability” function for the allocation of a class label to each pixel. A hard classification is created by selecting that class label with the greatest probability of being accurate (*Winner-Take-All*), where the feature space decision boundaries for a hard classification are well-defined (Fig. 2.11). Even if the probability values are reserved, multiple labels at each pixel must be allowed for. The probability values represent the virtual proportions of each real ground surface category within the spatially- and spectrally-integrated multispectral vector of the pixel in the default feature space (Schowengerdt, 2007).

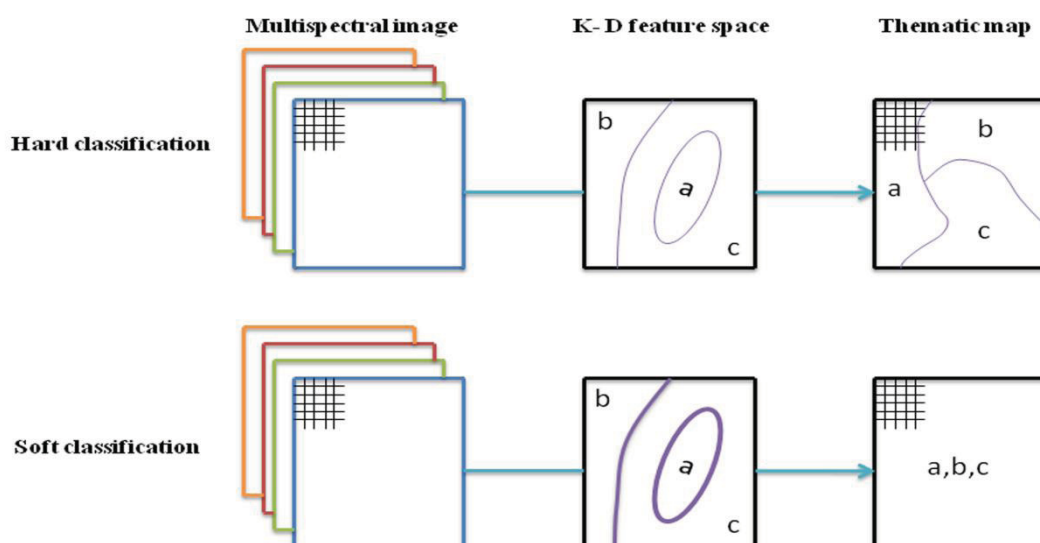


Fig. 2.11: The difference between hard- and soft- classification (Source: Modified from Schowengerdt, 2007)

*Soft (fuzzy) classification:* while there are limitations in the ability of classical hard classification approaches in solving the mixed pixels problem (Liu et al., 2010), soft classification approaches have a greater ability for solving this problem, where they can label one class as true and all others as false through employing the fuzzy logic concept. Fuzzy terms can be expressed in relation to probabilities and how they use fuzzy-logic-based algorithms (fuzzy classification). These algorithms can divide a pixel which has a membership of more than one LULC-class into all its real components (for example, they could divide a pixel existing on a parcel that has more than one land cover use, to 70 % agriculture, 25 % pasture and 5 % urban). Softness allows for a level of heterogeneity and thus allows a more realistic representation of the real ground surface features on the produced thematic map (Foody, 1999 a). Fuzzy classification algorithms are based originally on fuzzy-set-theory introduced in 1965 by Zadeh (cited in: Cheng, 2002; Ricotta, 2004). It takes uncertainty into account by allowing biased membership to a class. Each elementary in the remotely sensed image can be assigned in a membership function based on a range of values from 0 to 1. If the elementary has the value of 0 then this means that this elementary has no membership to a specific class, and it has a certain membership when its value equal to 1. These values refer to the possibility, not to the probability, hence, the values for all classes located in one pixel need not sum to 1. Another approach to control uncertainty is irregular classification, where image primitives can be allocated to three probable values for each class: not a member; maybe a member; or certainly a member (Ahlqvist et al., 2000).

Implementation found that fuzzy-logic-algorithms came into being mostly as an extension of existing algorithms, such as the supervised fuzzy maximum likelihood (Paola & Schowengerdt, 1995 a; Palubinskas et al., 1995; Ricotta, 2004) and unsupervised fuzzy k-means, in NNC (Baatz et al., 2004). Also, artificial neural networks (Paola & Schowengerdt, 1995 b), segmentation approaches using the eCognition software (Baatz et al., 2004), can be jointed with fuzzy-logic-algorithms. Soft classifications can also be created by *softening* the output of hard classifiers (Woodcock & Gopal, 2000).

#### 4.5. Spatial information-based categories

This category is divided into: *spectral classifiers*, *contextual classifiers* and *spectral-contextual classifiers*.

*Contextual classifiers:* as we know, classical supervised and unsupervised classifiers are pixel-specific classifiers, in that they rely on the spectral characteristics of each pixel in assignment to matched ground features, as independent from other pixels. To overcome the broadly existing problem of within-class spectral variations, in addition to object-based and per-field classifiers, contextual classifiers exist which apply within-image but pixel-external spatial information to improve the remotely sensed data classification (Wharton, 1982; Gong & Howarth, 1992; Kartikeyan et al., 1994; Flygare, 1997; Sharma & Sarkar, 1998; Keuchel et al., 2003; Magnussen et al., 2004). The basic idea is that separate bordered pixels construct a related and correlated context of pixels, which can be considered in the classification process. For example, when an image pixel is located in the center of a homogeneous area that represents an agricultural field (e.g., sugar beet), then the surrounded pixels have high probability of being of the same land use class (sugar beet). Based on this simple idea, spatial classifiers attempt to automate the visual human spatial interpretation by applying it in digital image processing. Context is then used to describe the spatial relationship between it with the adjacent pixels, and it covers the spatial area between a pixel or group of pixels and the surrounding areas (Jensen, 2005). Using of spatial information or some of them, such as: pixel proximity; repetition; directionality; location; image texture; feature size; shape; etc., can assist in identifying the ground surface features.

Contextual classifiers are also referred to as smoothing techniques, which can improve the classification results (Flygare, 1997; Stuckens et al., 2000; Hubert-Moy et al., 2001; Magnussen et al.,

2004). Smoothing techniques used in contextual classifiers include: markov random fields; spatial statistics; fuzzy logic; segmentation; or neural networks (Binaghi et al., 1999; Cortijo & De La Blanca, 1997; Kartikeyan et al., 1998; Keuchel et al., 2003; Magnussen et al., 2004). There are two types of smoothing: 1) pre-classification-smoothing classifiers that integrate the contextual information as additional non-spectral bands, in the classification process using the general spectral classifiers; and 2) post-classification-smoothing classification which is carried out on the previously-classified image. The Markov random field-based contextual classifiers, such as iterated conditional modes, are the most often used techniques in contextual classification, where they have been proven to improve classification results (Cortijo & De La Blanca, 1997; Magnussen et al., 2004).

The advantages of contextual classifiers will usually result in increases in the classification accuracy rates (Swain et al., 1981; Jung & Swain, 1996). However, they need much more computational time than spectral classification classifiers and require a more complex decision process (Lillesand et al., 2008). Finally, the development of spatial classification approaches and the useful use of spatial and jointed spectral-spatial image classification methods are still relatively limited, compared to spectral classification methods, where the produced spatial resolution of most existing remote sensing satellite sensors is insufficient. Recently launched high resolution satellites should give a boost in efficiency to the technical basis for spatial classification algorithms (Lu & Weng, 2007).

#### **4.6. Combinative-based classifiers**

The general concept of the *combinative classifiers* is the integration of several classifiers into one new enhanced classifier, with the aim of improving the classification process and increasing its accuracy. This approach was developed based on the knowledge of the merits and limitations of various classifiers (Franklin et al., 2003; Tso & Mather, 2009). Some studies that have proven the preference of the combinative classifiers are: (Giacinto & Roli, 1997; Roli et al., 1997; Benediktsson & Kanellopoulos, 1999; Warrender & Augusteihn, 1999; Steele, 2000; Huang & Lees, 2004). One common example is the use of the unsupervised classification cluster analysis, followed by the supervised classification maximum likelihood classifier, since by clustering, spectrally similar classes are identified, which in continuity will lead to supervised classifying (Richards & Jia, 2003). A crucial step in applying these approaches is to develop appropriate rules to join the classification results from different classifiers. Some previously investigated different techniques, such as: a production rule; a sum rule; stacked regression methods; majority voting; and thresholds have been investigated as ways to join multiple classification results (Steele, 2000; Liu et al., 2004 a).

### **5. Remote sensing applications in land use/land cover mapping**

The broad utilization of remote sensing is to extract and represent LULC-information from multi-spectral imagery as thematic maps, data and GIS-layers. Remote sensing provides a cost-effective method to acquire present and dependable LULC-information because of its availability and frequency of update (Donnay et al., 2001).

Research proves that remote sensing can be considered as a useful tool for studying arid and semi-arid ecosystems (Tucker et al., 1983; Justice & Hiernaux, 1986; Townshend & Justice, 1986; Tucker, 1986; Maselli et al., 1993; Bastin et al., 1995; Hobbs, 1995; Schmidt & Karnieli, 2000; Kheiry, 2003; Suliman, 2003).

In comparison to the more classical classification methodologies such as basic aerial photo interpretation, LULC-mapping using satellite imagery has four distinct advantages: 1) LULC-classes

can be mapped faster and often with lower costs; 2) fast and inexpensive updating of LULC-map products is possible, where the satellite imagery are captured for the same geographic area at a high repeat ratio; 3) remotely sensed data are captured in digital forms and can thus be easily jointed with other types of ground feature information through such techniques as GIS; and 4) the large economies of scale offered by digital satellite image processing make it fairly low-cost to map large areas, meaning it is easier and more cost effective to produce large amounts of map products.

Many issues may impact the success of the classification process, for instance: the complexity of the landscape in a study area; selected or accessible remotely sensed data; approaches used for image-processing and classification (Lu & Weng, 2007). Therefore, it is a confrontation task to classify remotely sensed data into a thematic map. Many prior studies and some books are particularly concerned with image classification (Landgrebe, 2003; Tso & Mather, 2009). Although the number of studies and published papers has greatly increased during recent decades, remotely sensed data analysis is not a new research topic. Richards (2005) pronounced that the classification of remotely sensed data had "its genesis in the signal processing methods of the 1950s and 1960s and their extension to handling image data". The research by Wilkinson (2005) of published papers on classification applications between 1989 and 2003 is worthy of mention as: 1) it illustrates that the mean classification accuracy stayed at nearly 80 % during his period of research; 2) it is noteworthy that the accuracy does not show an improving tendency; 3) the presented analysis of this fact in the articles is not exhaustive enough; 4) it however provides an interesting standard against with to compare this thesis' results; and 5) he demonstrates that resulted accuracy does not depend on the number of features (input spectral bands) used, nor on the pixel spatial resolution of the number of classes, and the area of the studied site (the author hypothesizes that the advantage obtained from the higher spatial resolution is equalized by the lower spectral resolution). Much promoted neural-network based algorithms do not show any considerable advantage, nor disadvantage, compared to other methods.

Although the optical remote sensing systems such as LANDSAT-MSS/TM/ETM+, ASTER, and SPOT have limitations in obtaining cloud-free imagery and the resulted difficulties in performing spectral classification for specific categories of land features (Ulaby et al., 1982), they have proven an efficient device for LULC-mapping (Gong & Howarth, 1990; Ji, 2000). Kanellopoulos et al. 1992 conducted a 20 class classification test on SPOT High-Resolution Visible (HRV) images, and the end-result was proven to be satisfactory. Muchoney et al. (2000) evaluated an artificial neural net (fuzzy ARTMAP), the MLC classifier and a DT in a study of vegetation and land cover mapping in Central America. Liu et al. (2002) too reached better classification results using ANN than using MLC for a land cover classification based on a medium resolution multispectral remotely sensed data and an auxiliary GIS-data layer. A good number of studies conformed that ANN classifications created in higher accuracy than MLC. Erbek et al. (2004) and De Colstoun et al. (2003) applied a decision tree on multi-temporal images from the ETM+ to distinguish between 11 features of land cover. The overall accuracy was clearly enhanced by using classifier ensemble techniques, as boosting. Mehner et al. (2004) explain the application of a multi-layer perception network to IKONOS-data, in which a classification performance of 80% was achieved. Pal (2005) presented the classification results created from applying the random forest and support vector machines (SVMs) on ETM+ data in the United Kingdom with seven land cover classes. The paper from Berberoglu et al. (2007) aimed to evaluate the usefulness of integrating texture measures into MLC and ANN classifications in a Mediterranean environment, using LANDSAT-TM-imagery. The best classification accuracies were reached by using the ANN classifier. The dealing with the measures of texture characteristics were most effectively with the ANN rather than the MLC classifier. Kandrika and Roy (2008) presented a study based on using a temporal data set available from a moderate resolution sensor (AWiFS) aboard IRS-P6 for deriving LULC-classes. The use of a decision tree classification algorithm was able to exploit the temporal differences to distinguish between the land cover classes by asset of their spectral behaviors in temporal domain, where the

overall kappa was at 0.8651. [Yuan et al. \(2009\)](#) explained and applying an automated two-module ANN classification system, i.e. an unsupervised SOM network module and a supervised MLP neural network module, using LANDSAT-TM. After an evaluation of the performance of MLC, DA, and ANN in image classification, ANN classifications have the advantages in image accuracy overall and for single land cover classes ([Heinl et al., 2009](#)).

LULC-Classification using the three VNIR- and six SWIR- bands of ASTER-data has been discussed in the past 10 years. The most commonly used approach is separating the ASTER-data into two sets of images, i.e. 15 m and 30 m spatial resolution, where each have three and six spectral bands, respectively. For each set, support vector machine (SVM)-based algorithms ([Zhu & Blumberg, 2002](#)) or segmentation algorithms ([Marcal et al., 2005](#)) were applied for processing of classification. An approach based on *wavelet fusion* was proposed by [Bagan et al. \(2004\)](#). Other studies based on the Principal Component Analysis (PCA) were used to the nine VNIR and SWIR spectral bands. From the earlier obtained principal components, a supervised MLC algorithm was implemented ([Gomez et al., 2005](#)). However, most of the approaches referred to have not adopted thermal band data (TIR) in classification processing. In a study by [Al-Khateeb \(2008\)](#), TIR was used as a method to merge with other bands using wavelet transform, and compared with other usual methods, like Principle Component Analysis Analyses (PCA). It was observed that after applying the wavelet transform, the classification accuracy was better. ASTER-data can be used to perform LULC-classification effectively and accurately, but the general problem of the difference in spatial resolutions needs to be solved, namely, the different spatial resolutions of the Visible Near-InfraRed (VNIR), ShortWave InfraRed (SWIR), and Thermal InfraRed (TIR) spectral bands must be transformed to the same spatial resolution ([Bagan et al., 2008](#)). [Jianwen and Bagan \(2005\)](#) used ASTER-data and the Kohonen's Self-Organized neural network feature Map (KSOM) to LULC-classification. It classified 7 % more accurately than MLC. Also, the study showed that the quality of ASTER-data was good for LULC classification. [Yüksel et al. \(2008\)](#) used ASTER-data and converted it into Top Of Atmosphere reflectance data (TOA) to generate LULC-maps according to the CORINE-Land cover project, using supervised and the knowledge-based expert classification systems to get a better accuracy of the classified image. In the study from [Bagan et al. \(2008\)](#), a LULC-classification methodology was developed using a composites of ASTER VNIR, SWIR and TIR spectral bands. This methodology was created based on the wavelet fusion and the SOM neural network methods. It compared the classification accuracies of different combinations of ASTER multi-band data. SOM classification accuracy was increased from 83 % to 93 % by this fusion. Also, the increasing in band numbers had the benefit that the classification accuracy increased. The final results were: using the all 14 bands performed the highest classification accuracy; the narrowly accuracy value to the above mentioned highest one was obtained when the three VNIR-bands, three SWIR-bands and two TIR-bands were used; and a like trends were too obtained using the MLC classifier, but the classification accuracies of MLC over all band composites were significantly lower than those obtained using the SOM classifier.

These optical remotely sensed data can be integrated with recordings from remote sensing active systems such as the microwave sensors (e.g., Synthetic Aperture Radar SAR), which has the ability to acquire remotely sensed imagery under various weather condition during both day and night ([Curlander & McDonough, 1991](#); [Won et al., 1999](#); [Goetz et al., 2000](#); [Haack et al., 2000](#)). Studies ([Haack & Slonecker, 1994](#); [Solberg et al., 1994](#); [Huang et al., 2007](#)) using SAR and optical sensor data have confirmed clear enhancement in classification accuracies contrary to an optical sensor alone. [Huang et al. \(2007\)](#) presented the promise of combining radar data (RADARSAT) with optical data (LANDSAT-ETM+) to improve automatic LULC-classification using the Maximum Likelihood Classifier (MLC) for the study area of St. Louis, Missouri in the United States of America. [Watanachaturaporn et al. \(2008\)](#) used the SVM classifier to execute multisource classification. An IRS-1C-LISS-III image, NDVI image and DEM were used to produce a LULC-classification for a study area in the Himalayas. The accuracy of SVM-based multisource classifi-

cation was compared with other nonparametric algorithms, i.e. a Decision Tree Classifier (DTC), a Back Propagation Neural Network (BPNN) classifier and Radial Basis Function Neural Network (RBFNET) classifiers. The results confirm that using the SVM based classifier for integrated multisource data offers a significant increasing in accuracy.

The main research goal of the study from [Shimoni et al. \(2009\)](#) was to examine the complementarity and fusion of different frequencies (L- and P-band), polar-metric-SAR (PolSAR) and polar-metric-interferometric (PolInSAR) data for LULC-classification. The SVM algorithm was found to be a more suitable classifier in this research than NN.

[Xu and Gong, \(2007\)](#) evaluated the potential of the Earth Observing-1 (EO-1) Hyperion hyperspectral (HS) data with that of the EO-1 Advanced Land Imager (ALI) multispectral (MS) data for distinguishing various LULC-classes in Fremont, California.

In addition to the progress achieved by the referenced studies, the use of object- or segment-based classification techniques is another new development in the environment of remote sensing image classification. This approach has achieved generally better success with the narrow bands and high spatial resolution data such as IKONOS, SPOT-5, or QUICKBIRD ([Willhauck, 2000](#)). In several of the followed studies (e.g., [Lobo, 1996](#); [Tso & Mather, 1999](#); [Aplin et al., 1999 b](#); [Smith & Fuller, 2001](#); [Fuller et al., 2002](#); [Geneletti & Gorte, 2003](#); [Benz et al., 2004](#); [Carleer et al., 2005](#); [Marcal et al., 2005](#); [Platt & Rapoza, 2008](#)) segment-based classifications were more accurate than conventional pixel-based classifications. A few researchers used general statistical classifiers (e.g., [Geneletti & Gorte, 2003](#)), while other segment-based classifications based on non-parametric algorithms: [Liyod et al. \(2004\)](#) used ANN, while [Lalilberte et al. \(2007\)](#) applied a DTC. In other studies were based on SVMs, such as ([Marcal et al., 2005](#); [Bruzzone & Carlin, 2006](#); [Van der Linden et al., 2007](#)). [Hay et al. \(2003\)](#) used IKONOS-data to extract image objects for a landscape with two major LULC-features, i.e. forestry and agriculture. [Matinfar et al. \(2007\)](#) compared between pixel-based and object-oriented classification methods using LANDSAT-7 ETM+ imagery. After evaluation of the accuracy, it was demonstrated that: object-oriented image analyses achieve higher overall accuracy; and an increased accuracy rate for individual producers and users for each classified land cover class.

[Robin et al. \(2008\)](#) presented a new method for a sub-pixel land cover classification using both high-resolution structural data and coarse-resolution temporal data. The linear mixture model was used for pixel disaggregation. [Liu et al. \(2010\)](#) presented a new soft classification approach to improve the performance of classification process for remote-sensing applications. It used the Mixed-Label Analysis (MLA). Classification accuracy achieved by MLA was evaluated with other usual techniques such as linear spectral mixture models, MLC, MD, and ANN. MLA had an overall accuracy of 91.6 %. ANN, ML, and the MD methods had an overall accuracy of 88.7 %, 85.3 % and 83.7 % respectively.

## 6. Issues in the classification of remote sensing data and uncertainty

To obtain a successful thematic map with high classification accuracy, we have to understand the relationships between the classification steps find the weakest relations in the image-processing chain and then improve them ([Friedl et al., 2001](#); [Dungan, 2002](#)). Many issues impact the accuracy of classification, such as: scale; dates; the number of used image spectral bands; the needed number of classes that have to be classified; and their reflectance properties ([McCloy & Bøcher, 2007](#)).

Usually, classical spectral classifiers are limited by the spectral resolution of the used remotely sensed image, which cannot represent the whole range of variations captured in the training data or to separate them in the classification process. Also, as the size of area to be classified increases, accuracy typically decreases ([Carlotto, 1998](#)). Two essential issues are responsible for this misclassification: 1) the “noise” contained in a satellite image, such as temporal and spatial variations

of the same LULC-classes, atmospheric affects, mechanical sensor effects, mixed spectral information contained in some pixels, etc. This leads to the differing of the spectral response of an individual LULC-class from its real response (complex spectral response problem). Another issue related to the spectral response is that some different LULC-classes have very similar spectral reflectance curves (puzzling pixel problem); and 2) the insufficient spatial resolution of imaging sensors (scale issue/spatial resolution). A remotely sensed image is an extraction of the real world (scene) and the objects which represent the scene (Ferro & Warner, 2002). The relationship between the scene and the image is largely controlled by the scale of acquire or transform, which is determined by the spatial resolution of sensor, estimated by its Instantaneous Field Of View (IFOV) and GSI, where it cannot get any information about objects of interest - founding on the ground areas - smaller than the IFOV (Zhang, 2003). Therefore, the limitation of a sensor in recording the spatial characteristics is based on the IFOV (Atkinson & Aplin, 2004). Therefore, it is responsible for the quantity and type of information that can be obtained from digital imagery (Schowengerdt, 2007; Lillesand et al., 2008). To recognize and classify a specific object (informational class), the used imagery elements/pixels have to be smaller than the object but larger than its individual elements (objects at the next finest level in the hierarchy of scales) (Curran, 1988; Ferro & Warner, 2002). However, it is complex to determine a single suitable spatial resolution (Atkinson & Aplin, 2004). Some spatial resolution determining approaches are: the Average Local Variance (ALV) (Woodcock & Strahler, 1987), and the semi-variogram (Curran, 1988). The LULC-classes spatial arrangement in the real world (the landscape structure) impacts on the spatial resolution. Smith et al. (2002) studied the impact of LULC-heterogeneity and parcel-size factors on classification accuracy and came to the result that increased heterogeneity and smaller parcel sizes led to lower accuracies. Therefore, more complex arrangement landscapes need higher spatial resolution data (Chen et al., 2004 a). Many studies have evaluated the influence of spatial scale on classification accuracy (e.g., Markham & Townshend, 1981; Irons et al., 1985; Marceau et al., 1994 a and b; Raptis et al., 2003; Ju et al., 2005; McCloy & Bøcher, 2007). These showed that a single best scale cannot exactly represent all classes in a complex scene, due to the different sizes, shapes and internal variation of the parcels for various LULC-classes. Consequently, latest study has highlighted the development of multi-scale classification tools (Ju et al., 2005).

*Training area size* can influence the classification accuracy, where there is a positive relationship between it and the classification accuracy for various classifiers (Zhuang et al., 1994; Foody & Arora, 1997; Foody, 1999 b; Foody & Mathur, 2004 b).

*The Problem of Class Definitions* is a major problem in LULC-classification in that by definition, the classes to be classified are based on different subjective human concepts in understanding that are not exactly related to the physical signals detected and recorded by satellite sensors (Wilkinson, 2005).

*Field-work* and gathering ground truth data is often a subjective man-based discipline that is dependent on field analysts and which method is used to collect the truth-data. No analyst, gathering method or measurement tools can assure that the reference data are 100 % accurate. Also, there is the uncertainty when the field-work occurred in a time and the achievement of the classified image carried out in another time period. This gives the result that the reference data generally represents only a “relative truth” that will negatively influence the classification accuracy (Langford & Bell, 1997).

The paper from Lechner et al. (2009) studied the impact of plot area and its extent on classification accuracy. In this paper, the impact of grid position, object size and shape on classification accuracy was simulated. It was found that classification error was lowest when the scale and the location of the object and the raster grid matched.

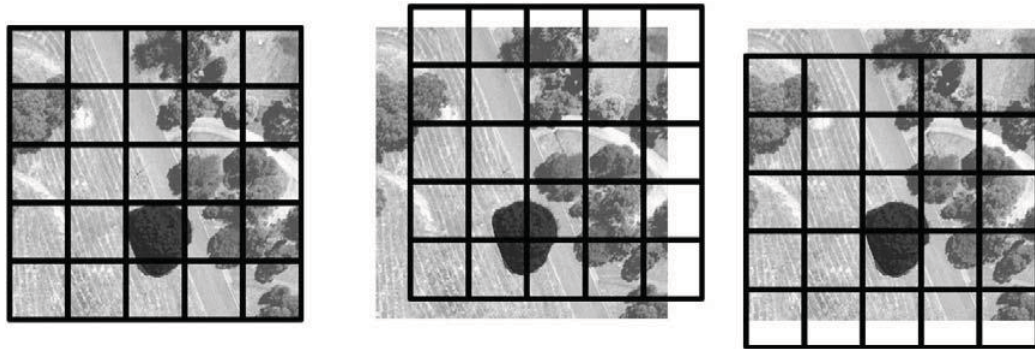


Figure 2.12: The relationship between a satellite sensor array's grid and features in the landscape (Source: Adapted from Lechner et al. 2009)

Most of the applied atmospheric calibration approaches have clear residual inaccuracies that impact negatively on the classification process (Schott, 2007), where the used algorithms may cause radiometric errors (Lu & Weng, 2007). In the same way, geometric rectification or image registration between multisource data could give uncertainty in the position (Lu & Weng, 2007). Friedl et al. (2001) summarized three main sources of errors: Image acquisition process errors, data-processing technique errors, and spatial resolution introduced by the satellite sensor and the scale of ecological processes in the real world. Dungan (2002) defined five kinds of uncertainties in remotely sensed data: positional; support; parametric; structural (model); and variables.

#### D. Land use/land cover change detection mapping

Change detection analysis is important in monitoring and managing the natural resources of the Earth. It gives statistical analysis of the occurred spatial distribution of the LULC-changes of interest (Singh, 1989). Some of its applications are: Monitoring shifting agriculture, estimation of deforestation, estimation of desertification, changes in vegetation phenology, seasonal changes in paddock production, damage evaluation, crop stress detection, disaster monitoring, and other environmental changes (Vitousek, 1994; Lambin & Ehrlich, 1997; Houghton et al., 1999; Lunetta et al., 2002; Achard et al., 2002; Gutman et al., 2004; Jingan et al., 2005). Natural change can have a wide impact on natural resources, such as a shift in the vegetation cover, a change in the physical and chemical soil components, alterations in plant and animal inhabitants, and effects on hydrological externalities (Turner et al., 1994; Lambin et al., 1999; Aylward, 2000). Therefore, in relation to land use/land cover and natural resource and ecosystem management, there is an important need for timely, permanent, and truthful monitoring of changes occurring (Lu et al., 2003 a; Coppin et al., 2004). However, the problems challenging the change detection process are: where is the change?, how much?, when did it occur?, and how great is its impact on the ecosystem? (Lambin & Linderman, 2006). Changes can occur either suddenly or gradually (Lu et al., 2004; Coppin et al., 2004; Lambin & Linderman, 2006; Bontemps et al., 2008). Here, the remote sensing techniques take on an increasing importance in natural resource monitoring programs and in answering the above questions (Coppin et al., 2004; Gross et al., 2006; Kennedy et al., 2009; Wiens et al., 2009).

In the case of LULC-changes, two kinds of change can be classified from previously published literature: conversion and modification (Riebsame et al., 1994; Turner et al., 1995; Lambin et al., 2003). LULC-conversion is the change from one cover category to another (e.g., the complete replacement of an agricultural parcel by man-made buildings), while LULC-modification is the modifications of structure or function without a complete change from one category to another (e.g., changes in productivity, biomass, or phenology) (Skole et al., 1994).

Driving forces can be simply defined as causes or factors responsible for LULC-change (Braimoh, 2004). An exact understanding of the *drivers* or *determinants* or *driving forces* of change is not



always possible (Briassoulis, 2000). The major aspects were summarized according to Bürgi et al. (2004) as: 1) human-related driving forces: a. socio-economic driving forces are fixed in the economy and to a smaller degree in demographics; b. political driving forces are expressed in policies and political programmers; c. technological driving forces contain modernism, such as the fabrication of the automobile (especially over the 20th century); and d. cultural driving forces imprint the landscape (e.g., through traditional agricultural practices). And 2) bio-physical driving forces: a. site factors (e.g., climate, topography, or soil conditions); and b. natural disturbances profoundly modify the existing LULC-pattern as they impact on the bio-physical conditions within the impacted area.

## 1. Change detection techniques

There are numerous change detection approaches applied on remotely sensed data, as a result of increasing versatility in processing digital data and increasing computing power (Pacifici et al., 2007). Generally applied approaches are: image differencing; and image rationing (Singh, 1989; Muchoney & Haack, 1994). Some of the proposed supervised and unsupervised approaches in the literature are: write function memory insertion; image algebra; multiple-date composite; post-classification comparison; image differencing; image rationing; change vector analysis; etc. (Nelson, 1983; Singh, 1989; Fung, 1990; Townshend et al., 1992; Muchoney & Haack, 1994; Townshend & Justice, 1995; Wiemker, 1997; Carlotto, 1997; Bruzzone & Serpico, 1997; MacLeod & Congalton, 1998; Nielsen et al., 1998; Mas, 1999; Xiaomei & Ronqing, 1999; Sohl et al., 2004; Lu et al., 2004; Jensen, 2005). Expert systems and neural networks were too used in change detection (e.g., Dai & Khorram, 1999; Chan et al., 2001; Seto & Liu, 2003). These approaches use multi-date imagery from multi- and hyper-spectral sensors, so that alterations, in feature or phenomena, be accurately recognized, measured and if needed observed (Civco et al., 2002; Coppin et al., 2004; Jensen, 2007), each of which could be spatially, spectrally, or temporally controlled (Lu et al., 2003 a). It is not the purpose of this chapter to exhaust the inventory or give an evaluation of each approach. However, a general framework will be provided that could be useful to classify the various techniques of change detection. Fig. 2.13 illustrates how the various frequently used techniques are located in this framework (Lam, 2008). Detailed discussion about this can be found in: (Lu et al., 2004; Jensen, 2005 and 2007).

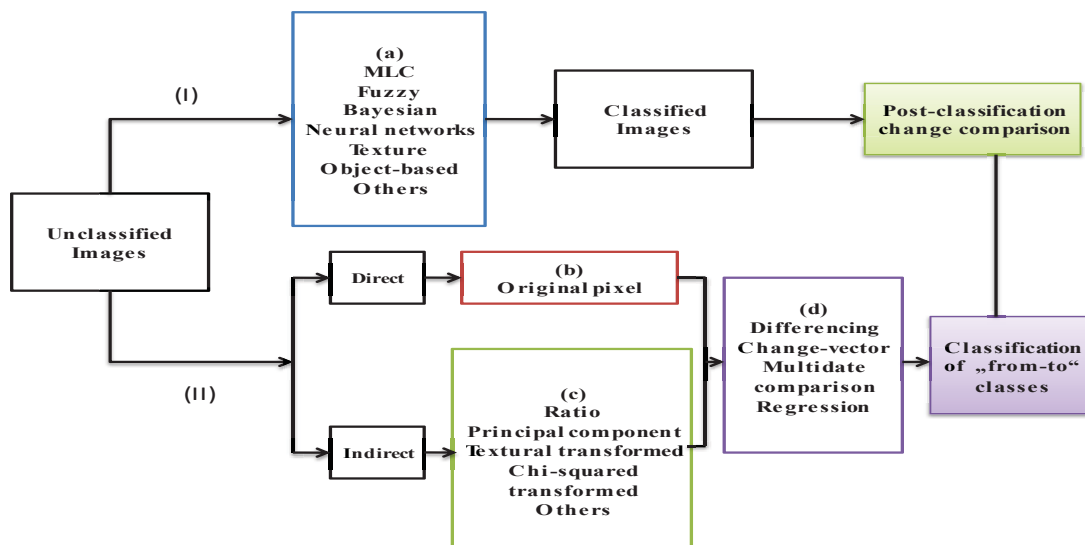


Fig. 2.13: A framework for classifying change detection methods (Source: Modified from Lam, 2008)

There are a mass of change detection techniques. These techniques can be classified into two general categories: post-classification comparison techniques; and enhancement change detection

techniques (Nelson, 1983). Coppin and Bauer (1996) summarized 11 various techniques documented in the literature by 1995: 1) mono-temporal change delineation; 2) delta or post-classification comparison; 3) multidimensional temporal feature space analysis; 4) composite analysis; 5) image differencing; 6) image rationing; 7) multi-temporal linear data transformation; 8) change vector analysis; 9) image regression; 10) multi-temporal biomass index; and 11) background subtraction. Chan et al. (2001) collected them in: 1) change enhancement methods; and 2) “from-to” change information extraction methods. In Civco (2002), the author identifies four main categories: 1) traditional post-classification; 2) cross-correlation analysis (Koeln & Bissonnette, 2000); 3) neural Networks; and 4) image segmentation based classification. Deer (1998) suggested a three level categorization system: 1) pixel level: indicates to numerical values of each spectral band in an image, or simple computations between equivalent spectral bands (e.g., image differencing or rationing); 2) the feature level: is a higher level of processing, which includes transforming the spectral or spatial characteristics of the image (e.g., PCA, texture analysis or VIs). These transformed features may have real-world value (e.g. VIs in the radiometric field, or lines/edges in the spatial field), or may not (e.g. PC in the radiometric field); and 3) the object: is the highest level of processing (Blaschke, 2005). Finally, Pacifici et al. (2007) categorized two main approaches of change detection in: Unsupervised and supervised.

Returning to Fig. 2.13, change detection techniques can be separated into two general groups, depending on whether the technique needs classification before or after change detection process.

1) techniques which first detect change and then assign classes (e.g., image differencing or PCA)-Unsupervised Approach- Pre-classification method.

Many unsupervised change detection approaches deal with the multispectral images in order to produce an additional image. The most essential basis for these algorithms is the determining of the finest global threshold in the histogram of the so-called generated difference image, where the classifying of change and unchange classes is made on the importance of the resulting spectral change vectors by applying of empirical or theoretical well-founded global threshold strategies. The best global threshold depends on the statistical irregularity of the two images, which are often unknown (Melgani & Bazi, 2006; Pacifici et al., 2007). For this category, Pacifici et al. (2007) reviewed the published techniques in the past decade: the *Image Differencing* (ID), *Normalized Difference Vegetation Index* (NDVI), *Change Vector Analysis* (CVA), *Principal Component Analysis* (PCA), *Image Rationing* (IR), *Expectation Maximization* (EM) (Bruzzone & Fernández-Prieto, 2000), *Markov Random Field* (MRF) (Bruzzone & Fernández-Prieto, 2000), *Object-Level Change Detection* (OLCD) (Hazel, 2001), *Reduced Parzen Estimation* (RPE) (Bruzzone & Fernández-Pireto, 2002), *Maximum a Posteriori Probability* (MPP) decision criterion (Kasetkasem & Varshney, 2002), *Multivariate Alteration Detection* (MAD also called *Iteratively Reweighted MAD* (IR-MAD)) (Nielsen et al., 1998; Nielsen, 2007), MAD and the combined MAF/MAD (*Maximum Autocorrelation Factor*) transformations, and *Genetic Algorithm* (GA) (Celik, 2010). Image differencing, change vector method and multi-date comparison methods (Fig. 2.13 Box d) can be applied *directly* on the raw values of image pixels, or *indirectly* on manipulated values from the spectral bands (e.g., band ratios, principal components, chi-squared transformed, and texture transformed) (Fig. 2.13 Boxes b and c).

The above techniques generally do not aim to identify clearly what types of LULC-changes have taken place in an area (e.g., which vegetated areas have been urbanized). They are suitable for applications such as detection of burned areas, or detection of deforestation. However, they are not useful when it is necessary to define the types of changes that have occurred in the studied area, for example, in: observing the shifting in cultivation; urban growth; or where it is required to know all the types of changes that occurred in investigated area.

Only the CVA-technique allocates the various types of occurred changes. However, it does not clearly identify the typologies of changes, because it is not supervised (Pacifici et al., 2007).

Decisions are needed regarding: 1) selecting the raw to used spectral bands as input (e.g., DN, radiance reflectance, vegetation indices); 2) selecting the kind to applied classification method and classifier (e.g., supervised, neural-net); and 3) selecting the kind to used error assessment method (Lunetta, 1999).

Advantages: 1) pre-classification is not necessary, therefore, avoiding the tiring in classification process at the starting; 2) it is regarded as simple and rapid, and can be applied on a great number of images; and 3) the ease in fine-tuning to detect the specific interested changes, and they are, in general, likely to have a higher ability to find slight changes (Lambin & Ehrlich, 1997; Woodcock et al., 2001; Foody, 2002; Chen et al., 2003; Lunetta et al., 2004; Yuan et al., 2005).

Disadvantages: 1) the detection of image changes, especially if focused on agricultural areas, may be affected by troubles with phenology and cropping. Such troubles could be worsened by inadequate image accessibility and poor quality in moderate zones, and the problems in adjusting poor images (Blaschke, 2005); 2) furthermore, these techniques are corrupted by: changes in illumination at two times, changes in atmospheric conditions, and in technical sensor calibration. These make complex a direct evaluation between raw imagery obtained at different times where additional processing steps are required (e.g., radiometric calibration) (Pacifci et al., 2007); and 3) there remains the problem of defining the threshold value at which the change between the two images is measured. Also, it is clear that using unsupervised methods is obligatory in many remote-sensing applications, when appropriate ground truth information is not always available (Bruzzone & Fernández-Prieto, 2002).

The study from Im and Jensen (2005) presented a change detection method depended on the Neighborhood Correlation Image (NCI) logic. This logic take advantages of that the same geographic area (e.g., a 3\*3 pixel window) on images with two different acquired dates will tend to be highly correlated if little change has occurred, and uncorrelated if change occurs. Melgani and Bazi (2006) proposed an unsupervised change detection approach based on the fusion of an ensemble of different threshold algorithms through a Markov Random Field (MRF) framework. Liu et al. (2008) used spatial-temporal Markov Random Fields (MRF) models to combine spatial-temporal information with spectral information for multi-temporal classification. The goal was to reduce the influences of classification errors on change detection. Mura et al. (2008) proposed an unsupervised technique for change detection in very high geometrical resolution images, which is based on the integrating of morphological filters with a Change Vector Analysis (CVA) method. Malpica and Alonso (2008) publicized a new method in field of unsupervised change detection methods. It based on jointly analyzing the spectral channels of multi-temporal images in the original feature space with no training data. This method is tested with two SPOT-5-satellite images pan-sharpened to a resolution of 2.5 m. Celik and Kai-Kuang (2010) developed an unsupervised change-detection algorithm by conducting probabilistic Bayesian inference to perform unsupervised thresholds over sub-band difference images created at the various scales and directional sub-bands using the DT-CWT for representation.

2) techniques which first assign classes and then detect change (post-classification comparison) Supervised Approach Post classification methods.

In order to overcome the limitations of the first technique, one can use techniques based on a supervised classification of multi-temporal images: *Direct Multi-data Classification* (DMC), *Neural networks* (NNs) (Bishop, 1995), *Knowledge-Based Systems* (KBS), *Support Vector Machines* (SVMs) (Vapnik, 1998; Melgani & Bruzzone, 2004; Bruzzone & Carlin, 2006), *Post-Classification Comparison* (PCC) (Del Frate et al., 2004 and 2005; Colwell & Weber, 1981).

The fame of the above techniques may be because they can be freely applied on available created single date classifications, where they are based on separate single-date classifications whose results are later compared (Weismiller et al., 1977) with the result of the second independently classified image (Lunetta, 1999). This simple technique includes: 1) producing the classified image

based on the classification process; and 2) assessment the occurred changes based on the principle of identifying the areas of change as pixel per pixel differences in class membership (Castelli et al., 1999).

Advantages: 1) the ability to clearly identify the kinds of occurred LULC-conversions; 2) the robustness to the various atmospheric and light conditions at the two recording times (Bruzzone & Fernández-Pireto, 2000); 3) where the two datasets/imagery are separately classified, so it is not needed to normalize these data (Singh, 1989); 4) it is more flexible than those used the comparison of multi-temporal raw data; 5) it allows one to make change detection also by using different sensors and/or multi-source data at two times; and 6) the possibility in entering several modifications on the used classifier in classification process (e.g., contextual information as using the texture of an image, or a priori likelihoods from historical sources to weight class allocation) would increase the change detection mapping accuracy (Pacifiçi et al., 2007). Also, the new image classification algorithms, other than the traditional MLC, can be used to increase both accuracy and effectiveness.

Disadvantages: 1) requires more human supervision for classifying the images; 2) despite its potential, this category is not relevant to quick change detection, because user supervision is required to pre-classify the images; 3) limitations also include cost in terms of money and implementation time, and generated errors from classification of imagery (Singh, 1989; Castelli, 1999), where the generation of a suitable training set has the two drawbacks, i.e. the difficulty and the high cost (Bruzzone & Fernández-Pireto, 2000); and 4) finally, the accuracy of the change thematic map will be equal to the accuracies of each individual classification for each date (Lambin & Stralher, 1994).

In addition to all of the above, there are more powerful alternatives, called *cascade-classification* approaches (Swain, 1978), which use all the information integrated in the image series to try and to make the use of the temporal correlation between used imagery. Diverse schemes of cascade classification were proposed, for example: bayesian methods (Serpico & Melgani, 2000); neural networks (Bruzzone et al., 1999; Melgani et al., 2003); and multi-classifier approaches (e.g., Bruzzone et al., 2004 a). Despite of the globally rising importance of knowledge-based classification systems that are based on fuzzy rules, fuzzy cascade multi-temporal methods are mentioned rarely in the literature compared to other multi-temporal approaches (Feitosa et al., 2009). Feitosa et al. (2009) proposed a new fuzzy cascade multi-temporal classification method based on fuzzy Markov chains. This method varies from past fuzzy multi-temporal approaches in that: the method requires no knowledge about the true class at an earlier date; and also, as an alternative, it uses the characteristics of the image object being classified at the earlier date. This method joins the fuzzy, non-temporal, and classification of a geographical region at two points in time to give a single united result.

The most general use of many of the above mentioned techniques has been applied to mapping change in coarse to medium spatial resolution satellite data, and they have worked successfully in the high-resolution field (Pacifiçi et al., 2007). In the last decade, some researchers have confirmed that it is possible to use the object-oriented image segmentation based change detection as an alternative to pixel-by-pixel based change detection. It compares the homogeneous polygons/objects found in two images acquired at two different dates (Niemeyer & Canty, 2001 and 2003; Walter, 2004). But, it has the drawback that the required algorithms for high-resolution image processing are more complex (Malpica & Alonso, 2008). A lot of present studies focus on the application of object-based approaches to for temporal studies (Walter, 2004; Zhou et al., 2008). For example, Im et al. (2008) compared between different pixel- and object-based change detection methods. The conclusion was that the advanced object-based approaches were superior. Object-based change detection has also been applied to different ecological interests, such as urban growth (Zhou et al., 2008) and shrub-land infringement (Laliberte et al., 2004; Benfield et al., 2007; Stow et al., 2008).

## 2. Comparison between change detection techniques

All digital change detection techniques are influenced by spatial, spectral, temporal and thematic limitations, which would consequently influence the qualitative and quantitative approximations of the change. Even in the same natural environment, various techniques might produce different change thematic maps. As a result, it is very significant to select the more appropriate technique. [Singh \(1989\)](#); and [Coppin and Bauer \(1996\)](#) both presented excellent and complete summaries of approaches and techniques of digital change detection. Not all these techniques are suitable to all regions, or all kinds of imagery ([Nordberg & Evertson, 2003](#)): each has its own merits and limitations, and thus no single technique is best and appropriate to all cases ([Berberoglu & Akin, 2009](#)). In practice, various techniques are often compared to discover the most accrued change detection results for a particular application ([Lu et al., 2004](#)). Considerations that have to be taken before choosing the change detection technique are: the characteristics of the area to be studied, the remotely sensed data used, pre-processing needs, and the processing/computing capability of existing systems, in addition to time and budget ([Coppin & Bauer, 1996](#); [Jensen, 2007](#)).

It will be of immense use when researchers can develop capable and reliable change detection techniques which are automated, simple to use, and germane to various LULC as observed by different sensors at various scales, times and places ([Lam, 2008](#)). [Bruzzone & Fernández-Prieto \(2002\)](#) proposed a new automatic method for unsupervised change detection techniques, which presented a number of significant advantages in comparison to the conventional unsupervised techniques. [Im et al. \(2008\)](#) introduced an automated dual change detection method using a threshold-based calibration model in his study.

According to the research by [Coppin and Bauer \(1996\)](#), image differencing seems to present generally better results than other change detection techniques. This monitoring technique, based on multispectral satellite data, has confirmed capability as a way to detect, identify and map changes. It may be the most widely applied method for a range of geographical environments ([Singh, 1989](#)). The approach is based on deduction one date of images from a second date that was exactly recorded to the first. Image differencing and CVA include the transformation of input spectral bands into temporal change vectors, with the previous being a band-by-band temporal deducting, and the latter needing derivation of scale and angle of spectral change. Post-classification approaches use the input spectral bands directly in classification ([Lunetta, 1999](#)). Although difference and CVA imagery represent direct information of spectral change over time, they include no reference to place within the original input data domain. In contrast, post-classification approaches use input spectral bands directly, and so include this reference information. Consequently, natural changeability in initial and final (e.g., T1 and T2, respectively) LULC-classes are directly included into the change classification approach ([Lunetta, 1999](#)).

A multi-date Tasseled Cap (TC) transformation is scene-independent and has been revealed to be successful for change detecting ([Collins & Woodcock, 1996](#)).

[Civco et al. \(2002\)](#) provided a comparison between the following five LULC-change detection techniques: post-classification; cross correlation analysis; neural networks; knowledge-based expert systems; and image segmentation/object-oriented classification. Nine LULC-classes were selected for analysis. It was observed that there were merits to each of the five techniques studied, and that, at the point of their study, no single technique could perform change analysis.

The most important advantages of the NDVI-based change detection technique presented by [Lunetta et al. \(2006\)](#) were: a) satisfying a powerful results; b) needs a small time in computation; c) offers the automatically in presenting the data processing procedures; d) it has potential to illustrate the product of annual change alarm; and e) the ability to deliver a product rapidly.

[Yamamoto et al. \(2001\)](#); [Bruzzone and Fernández-Prieto \(2002\)](#); and [Lam \(2008\)](#) summarized the intrinsic difficulties of change detection when they listed the existing techniques into a framework,

and then disputed that the approach based on texture had potential for rapid change detection. Lam (2008) hypothesized that the integration of both textural and spectral indices could improve some of the existing change detection problems. 1) the texture measures (e.g., fractals, lacunarity, wavelets, and spatial autocorrelation statistics) could be applied directly to pre-classified images, so less human supervision would be required because there is no need in the classification process; and 2) while the spatial/texture techniques quantified the spatial differences across the image rather than comparing the values of brightness using the method of a pixel by pixel, they were more probable to expose main changes rather than false changes that arise because the noise, clouds or illumination dissimilarity.

Shaoqing and Lu (2008) discussed in their paper the three main change detection techniques: 1) image differencing; 2) image rationing; and 3) post-classification. The first is a simple idea, easy to understand and easy to apply. It is beneficial to information extraction, in which the value of the object and surroundings value is smaller (e.g., the beach zone, the ditch of estuaries). The main limitation is that it cannot show which category is changed. The second is applicable during change detection of a city. Its limitation is that it cannot show which category is changed. The third technique can provide information about changing property, but it is limited in that accuracy depends on the accuracy of its classification.

Berberoglu and Akin (2009) verified that, for LANDSAT-TM images based change detection of LULC in Mediterranean area, the CVA method could be advantageous for definite land covers. The conclusions of their research can be summarized as follows: 1) image differencing was simple, direct and analysis of the results was easy. However, the approach overrated the changes; 2) rationing was incapable to delineate changes well in complex areas like the Mediterranean environment. In comparison to other change detection methods, CVA offered the lowest accuracy with an inadequate information about the occurred change; 3) the image regression technique was responsive to changes in reflectance. In addition, the production of accurate results was dependent on band selection. Determining the most fit linear function was generally time intense. It offered a lower accuracy than CVA, though it is a reflective and sensitive technique; and 4) CVA disadvantages were: the most computationally; the most time-consuming technique (including atmospheric and radiometric normalization). CVA advantages: the most precise one for detecting and classifying changes using bands 3 and 4 of LANDSAT-TM imagery; the capability of using any number of bands in change detection; and the most accurate of all the tested techniques.

### 3. Change detection using remote sensing

Change detection mapping is one of the most essential remote sensing applications, as it can define both the quantitative and qualitative changes in a study area (Lunetta, 1999; Jensen et al., 1993; Ridd & Liu, 1998; Lunetta & Elvidge, 2000). Change detection based on remotely sensed data is the process of detecting, recognizing and locating differences in the components of an area (object or phenomenon) through monitoring, comparison between two classified data sets - *post-classification change detection approaches*, and by examination and understanding the physical change indicators (changes in radiance values) based on radiometry measurements between sets of multi-temporal and geo-referenced satellite images at different dates - *pre-classification change detection approaches* (Singh, 1989; Wang, 1993; Lu et al., 2003; Nordberg & Evertson, 2003; Ramachandra & Kumar, 2004; Lunetta et al., 2006; Alberga, 2009). If possible, change detection techniques should be applied on remotely sensed data that have the following characteristics: obtained via the same sensor; including the same of (spatial resolution, viewing geometry, spectral bands, and radiometric resolution); and obtained at the same time of day (i.e., this will remove errors caused by the different angles of the sun) (Lunetta, 1999; Jensen, 2005; Lillesand et al., 2008). However, this supposition is often not explored before correcting imagery for atmospheric affects, sun elevation, and also various sensor conditions (calibration) (Lunetta, 1999).

Lu et al. (2004) grouped the extraction of LULC changes based on remote sensing data in the two broad groups: 1) finding of detailed “from-to” change information; and 2) finding of simple binary change information (e.g., change versus no change). The aims of remote sensing change detection are to: a) identify the geographic location of change; b) identify the kind of change if possible (e.g., from agriculture to urban); and c) quantify the amount of change (e.g., 500 ha).

There are many sources of uncertainty using remotely sensed data for change detection mapping, for examples see (Congalton & Green, 1993; Foody, 2002; Sohl et al., 2004; Comber et al., 2004; Jensen, 2005). Hence, the next issues have to be considered for more accuracy: 1) noise: the dates of the two compared images should be nearly similar to avoid seasonal dissimilarity in vegetation, soil moisture, sun-angle and other responses (non-real land cover change). However, despite using the same date, specific atmospheric conditions, which differ from year to year, can impact the ability to delineate real changes (e.g., cloud cover or precipitation). Therefore, atmospheric correction must be applied to each image before processing; 2) pre-processing steps applied on the imagery might add errors; 3) additional care is needed to guarantee no pixel mis-registration between the two images (registration noise) and no geometrical distortion; 4) the applied algorithm in order to convert pixel values from analog to digital scale must be considered; 5) a large amount of data should be processed for detecting only a few change areas; and 6) the spectral bands of several types of satellite sensors do not always match in center wavelength and band width (Yamamoto et al., 2001; Bruzzone & Fernández-Prieto, 2002; Lam, 2008). There are some major complexities that have the influencing on change detection from remote sensing data. These arise from: the need to previous information about the nature of changed areas; the need to a reference data; and the skills of the interpreter and his experience (Singh, 1989; Townshend et al., 1992; Bruzzone & Serpico, 1997). Despite these limitations, remotely sensed based change detection is highly successful for studying the dynamics of LULC (Lunetta, 1999). Change detection mapping errors are often temporally correlated (Van Oort, 2007). Three different patterns are generally reported in measurement of change detection accuracy: 1) single date error patterns (Woodcock et al., 2001; Chen et al., 2003; Lunetta et al., 2004; Stehman, 2005; Yuan et al., 2005); 2) binary change/ no change error patterns; and 3) the full change error patterns which are only very rarely reported. The paper from Van Oort, 2007 discussed the relation between these patterns.

#### 4. Change detection in arid- and semi-arid- environments

Approximately 50 % of the total surface areas of the world are arid and/or semi-arid regions (Meadows & Hoffman, 2002). Arid and semi-arid areas feature irregular, low precipitation, dry ecosystems, and have a limited sustained economical potential (Adam et al., 1978). In relation to the ratio of total annual precipitation and potential evaporate-transpiration (P/ETP), arid and semi-arid ecosystems have the values of 0.05 to 0.65, respectively. This ratio gives only a simple evaluating of aridity or humidity of climate, and does not have a strong relation with agricultural or grazing potential. In response, the Length of Growing Period (LGP) concept was improved and applied in FAO studies on agro-ecological zones. This model gives better information on the potential and suitability of region for diverse land uses and/or land covers. The LGP begins when precipitation rises above half of the potential evaporate-transpiration (ETP) and ends after the date when precipitation falls to under half of the ETP. Areas with an LGP of less than one day are described as hyper-arid (true desert), less than 75 days are arid, 75 to less than 120 days are dry semi-arid, and 120 to less than 180 days are described as moist semi-arid. Taken together, these areas are denominated as dry-lands (FAO, 1993 a). These arid and semi-arid ecosystems are very unstable and liable to drought cycles during periods of precipitation shortage, which in turn, leads to deteriorating natural vegetation cover, which may quickly recover during periods of good precipitation. Despite their isolation and little numbers of human population, these areas frequently provide a variety of economic activities, such as public and commercial forage, mining operations and tourism. Because of the sensitive nature of these areas, it may only require a small amount of tur-

bulence to cause clear changes within the environment (Okin et al., 2001). As a result, remote sensing is quickly becoming an essential tool to use in the study of these areas (Zhou et al., 1998).

The deficit of information concerning to land cover and its dynamics, especially in developing countries which are almost all located in arid and semi-arid environments, can be attributed to a number of factors: 1) lack in state support for mapping agencies and related research institutions; 2) expensive software and hardware; 3) inadequate finance for data buy; and 4) resistance to the modern digital mapping from classical cartography school followers. Fortunately, the growing availability of low-cost data and the accessibility of gratis data such as that offered by the Global Land Cover Facility (GLCF), the steady decreases in the costs of hardware and software and the increase in knowledge about the superior applications of remote sensing technology provides the necessary force for LULC-change assessment in the developing world (Geneletti & Gorte, 2003).

In addition to the previously-discussed factors, there is a variety of other problems that confuse the detection of variations in the reflected EMR: 1) low irregular precipitation and high potential ETP allows only spatially-limited low vegetation cover by the available moisture. As a result, the greater part of the area-averaged reflectance of a pixel is for the soil substrate (Smith et al., 1990 a and b). Associated problems in these regions include the low organic components of the soils, which therefore tend to be bright. These issues join to negate, or reduce, the vegetation signal present within an individual pixel (Huete et al., 1985; Huete & Jackson, 1987; Qi et al., 1994). 2) the variability of soils (light, dark, etc.), and their spectral responses, over the ecosystem of the study area and over the resulting image also cause problems to the detection of vegetation. Huete and Jackson (1987) found that NDVI-values were undervalued in regions of light soils and overvalued for regions with dark soils. This detected weakness (especially in the arid and semi-arid regions) in one of the most frequent and broadly used vegetation indices encouraged a vast amount of research that accounted for corrected soil noise (Baret & Guyot, 1991; Bannari et al., 1995).

Existing remote sensing algorithms allow the application of LULC-change detection in moderate areas of the world (Berberoglu & Akin, 2009). However these algorithms are less able to be applied in the Mediterranean environment because: 1) the high temporal variability of the spectral responses of major land covers causes large inter-class spectral variability; 2) the complex mixed spatial frequency of the landscape; and 3) the similar reflectance responses of major land covers makes spectral separation hard (e.g., the bright toned, often calcareous soil can have alike reflectance responses to urban areas and alike near-infrared reflectance to a crop canopy) (Berberoglu et al., 2000). Therefore, the observation of land cover change is complicated in Mediterranean environments (Berberoglu & Akin, 2009).

Before mapping LULC-change detection using optical sensors data in arid and/or semi-arid areas, we have to answer this question: at which scale is green vegetation detectable and how can we best distinguish it? Siegel and Goetz (1977) demonstrated that major changes in the reflectance characteristics need a vegetation cover of more than 10 %, and that a vegetation signal has a tendency to be more significant than the soil signal when vegetation coverage is more than 30 %. Hill (2000) argued that this does not mean that vegetation coverage of less than 30 % is not detectable by remote sensing, but affirms that ratio based vegetation indices do not offer the best approximation. Vegetation approximation under the spectral un-mixing concept offers better approximation of the true vegetation coverage (Hurcom & Harrison, 1998; Hill, 2000).

A number of change detection studies, such as (Ram & Kolarkar, 1993; Ray, 1995; Kwarteng & Chavez, 1998; Ram & Chauhan, 2009) rely on the clear difference between agricultural fields or urban areas, and the neighboring arid environment, in order to detect LULC-change. However, for example, the detection of vegetative change (within the same LULC-category) within arid areas is significantly more difficult. Image differencing, especially the vegetation index differencing, is one of the most familiar vegetation change detection approaches, because of its simplicity (Singh, 1989; Lu et al, 2003). Pilon et al. (1988) favored the use of the visible red spectral band information to detect changes for their semi-arid study area. Chavez and Mackinnon (1994) established



that the red band differencing process presented improved information about vegetation change rather than NDVI in an arid environment. [Lyon et al. \(1998\)](#) accomplished that the NDVI-vegetation index differencing technique achieved the best when comparing several vegetation indices for change detection.

[Adeniyi and Omojola \(1999\)](#), in their LULC-evaluation of the Sokoto Rima Basin in North Western Nigeria based on archival remote sensing and GIS techniques, used aerial photographs, LANDSAT-MSS, SPOT-XS Panchromatic image transparency and topographic map sheets to study changes in two dams (Sokoto and Guroyo) between 1962 and 1986. [Serrano et al. \(2000\)](#) compared different techniques developed to create a homogeneous time series of LANDSAT images from 1984-2007 for the Middle Ebro Valley in Spain. [Mahmood and Easson \(2006\)](#) explored the capability of using ASTER imagery integrated with LANDSAT-7-ETM+ imagery of southwestern Bangladesh to detect equivalent measurements for change detection studies. The used methods were regression with Discrete Fourier Transform (DFT) and the cross-calibration method using digital number ratios. [French et al. \(2008\)](#) demonstrated and confirmed a method using ASTER-imagery obtained between 2001 and 2003) over the Jornada Experimental Range, to map the LULC-changes in a semi-arid area in southern New Mexico, USA. The results emphasize the importance of multispectral thermal infrared data that contains observations at wavelengths within 8-9.5  $\mu\text{m}$ . [Alphan et al. \(2009\)](#) assessed land cover changes in Kahramanmaraş in Turkey and its environs by using multi-temporal LANDSAT- and ASTER- imagery taken in 1989, 2000 and 2004. [Ram and Chauhan \(2009\)](#) prepared a LULC-change map of Jhunjhunun canton of arid Rajasthan in India based on LANDSAT-2-MSS from 1975 and IRS-LISS-III data from 2005. [Alberga \(2009\)](#) proposed a technique for probable change detectors in multi-sensor configurations, based on similarity measures that did not rely totally on radiometric values. A chain of such measures was used for automatic change detection of optical and SAR-images and an evaluation of their functioning were carried out to detect the limits of their applicability and their understanding to the occurred changes.

## **E. Remote sensing for irrigated agriculture**

Exact information on irrigation spatial coverage is the foundation of many sides of the knowledge of the Earth's systems and global change research. These contain: modeling of water exchange between the land surface and atmosphere ([Boucher et al., 2004](#); [Gordon et al., 2005](#); [Ozdogan et al., 2006](#)); investigation of the influence of climate change and variability on irrigation water requirements/supply ([Alcamo et al., 2003](#); [Rosenzweig et al., 2004](#); [Vörösmarty et al., 2000](#)); and managing of water resources that influence global food security ([Vörösmarty et al., 2005](#)). Agriculture is certainly the main water-use sector, accounting for about 70 % of all water reserved globally from rivers and aquifers for agricultural, domestic and industrial purposes ([FAO, 2009](#)). [Ozdogan and Gutman \(2008\)](#) defined irrigation as "agricultural area that receives full or partial application of water to the soil to offset periods of precipitation shortfalls under dry land conditions". The remote sensing techniques offer a unique approach to the gathering of various data across place and time, facilitating the application of various methods to obtain irrigated area statistics ([Thinkabail et al., 2008](#)). In addition, time-series remotely sensed data allow the dynamics of irrigated agriculture to be clearly researched, as differing from other land uses (mapping) ([Thinkabail et al., 2008](#)).

To date, a number of researchers have used remote sensing to observe irrigated agriculture ([Ozdogan, 2010](#)). Initial efforts focused on applying remote sensing in mapping and to update irrigated land areas mostly in the US and India ([Draeger, 1976](#); [Heller & Johnson, 1979](#); [Thiruvengadachari, 1981](#); [Kolm & Case, 1984](#); [Thelin & Heimes, 1987](#); [Rundquist et al., 1989](#)). More recently, studies on classification irrigated areas were carried out based on advanced classification algorithms ([Eckhardt et al., 1990](#); [Ram & Kolarkar, 1993](#); [Pax-Lenney et al., 1996](#); [Abuzar et al., 2001](#); [Martinez-Beltran & Calera-Belmonte, 2001](#)). These researchers concluded

that irrigation monitoring and mapping using remote sensing were at an advanced phase of improvement (Ozdogan et al., 2006) and that multi-temporal data were more effective rather than single-date data in determining individual irrigated crop classes (Thiruvengadachari, 1981; Rundquist et al., 1989; Abuzar et al., 2001). Spatial resolution of used remotely sensed data for irrigation mapping was seen as vital to obtaining sufficient spatial details about the irrigated fields (Pax-Lenney & Woodcock, 1997), as was the potential of vegetation indices (e.g., NDVI) in classification irrigated fields, if suitable time-series are obtainable. This latter fact was proved in several studies (Kolm & Case, 1984; Eckhardt et al., 1990; Pax-Lenney et al., 1996; Abuzar et al., 2001; Martinez-Beltran & Calera-Belmonte, 2001).

Spatial resolution impacts the calculated irrigated areas (Thinkabail et al., 2008). Ozdogan and Woodcock (2006) argued that with coarser spatial resolution, calculated irrigated areas were higher, because of the use of the full pixel area as actual area instead of irrigated area fraction. The difference lies in the fact that individual pixels contain more feature types. Ozdogan and Woodcock also demonstrated that the LANDSAT 30 m was insufficient to estimate the real spatial extent of cultivated areas in parts of China, while a spatial resolution of 500 m was sufficient for the USA (Thinkabail et al., 2008). Thinkabail et al. (2008) had reported a comparison study within the GIAM-project, since irrigated areas have been estimated for specific areas of the Earth at 30 m (Velpuri et al., 2007) and 500 m (Dheeravath et al., 2010) spatial resolution. Thinkabail et al. (2008) had given low indications in the relationship between irrigated areas and spatial resolution of the imagery: a) "[the] finer the resolution, [the] greater is the area when irrigated areas are in fragments". This is because in lower-resolution pixels, fragmented portions will not be calculated sufficiently and/or may lose out completely, resulting in the under-estimation of irrigated areas; and b) "[the] finer the resolution, [the] lesser is the area in contiguous areas". This is because in neighboring areas higher spatial resolution imagery will isolate small parts like settlements, roads and leaved lands. These parts are subtracted out of the total area of high resolution imagery. However, in lower resolution, these small parts are summed into larger irrigated areas in the pixel, resulting in the over-estimating of irrigated areas.

Agriculture resources are one of the most significant renewable and dynamic natural resources. Forecasting and estimating crop production information is a major practiced activity in most countries of the world, used in supervising crop production, grain storage, transportation and determining grain prices. Also, crop production data are an important tool that was using from governments around the world to design countrywide farm programs and to establish import and export policies. The timely and objective agricultural statistical numbers are the bases for the management of agricultural policy and the food security. In well-organized countries, crop area quotes are usually offered a few months after harvest, as providing trustworthy statistics before harvest is a major challenge (Bauer, 1975; Ozdogan & Woodcock, 2006). Agricultural survey is the traditional method for estimating cultivated areas, but it has the tendency to be based on samples that are often inadequate in space and time (FAO, 1993 b; USDA, 2004).

The analysis and mapping of both the spatial coverage and temporal change of cropland using remotely sensed data is significant for agricultural sciences (Rahman et al., 2005). It has become an effective tool for approximation cropland area and crop production in many parts of the world (Hill et al., 1980; Pax-Lenney et al., 1996; Panigrahy & Chakraborty, 1998; Froelking et al., 1999; Ares et al., 2001; Pinter et al., 2003; Xiao et al., 2003; Foody et al., 2006). Remote sensing technology has the ability to much improve the quality (availability, timeliness and accuracy) of national and world crop production data, which could have large economic and social benefits (Bauer, 1975). Since the launch of LANDSAT-1 in 1972, the specific application of remote sensing techniques for agriculture has been used for: a) Detection; b) Identification; c) Measurement; and d) Monitoring of agricultural phenomena and estimation of crop acreage, pest detection (Penuelas et al., 1995), crop stress (Jurgens, 1997), water stress (Moran et al., 1994), soil properties or soil inventory (Yang & Anderson, 1996), predicting crop yield, nutrient detection (Blackmer et al.,

1996), vegetation change, crop vigor, crop density, crop maturity, growth rates, effects of fertilizers, water quality, irrigation requirement, and location of canals (Asati & Asati, 2007). It has been proved that remote sensing is economical, complete, simple and fast, but derived approximates are not without weaknesses.

Remote sensing is an ideal technique for application in agriculture, because of the essential characteristics of the features of this industry: a) the large spatial extent of the agricultural activities makes the traditional field survey or census long and generally expensive; b) the per-unit-area economic productivity from agriculture is not as important in comparison with other industries; c) the major characteristic of most of the crops is that they are non-permanent annual plants. They have diverse growth and development stages in diverse seasons. Agricultural activities have clear phenological regularities, and so the intra-annual change may be very extreme; and d) agriculture is basically a human activity, where timely and accurate monitoring information is needed for effective management. Remote sensing technology responds to these needs through its speed, accuracy, economy, timing, dynamics and repetitive monitoring capability. Significant developments in remote sensing technology, including high spatial resolution data, the hyper-spectral data, quantitative inversion algorithms, etc., have advantaged the application of this method for agricultural purposes (Chen et al., 2008).

However, Van Niel and McVicar (2000) outlined five limitations of remote sensing in agriculture: data availability, length of the recording period, limited mapping capability, requirement of expertise and computer facilities, and cost. Some of the satellite systems' limitations were carefully presented by Zhang et al. (2002) and contained: "a) The revisit-cycle may not allow a specific event to be captured; b) The limited extent of the area of interest; c) The cost of the data; d) Poor spatial resolution; and e) The time taken to access imagery from the supplier".

Successful application of remote sensing in agriculture requires clear differences in the spectral reflectance of vegetation categories, and an appropriate sensor spatial, spectral, and temporal resolution to detect the differences (Lamb & Brown, 2001). The foundation of this applied field of remote sensing for agriculture was the work done by Colwell (1965) on small-grain cereal crops and their infection using a color infrared film (also known as *camouflage detection film*). Application of the visible and near-infrared portions of the EMS for remote sensing has its roots in the innovative works by (Gates et al., 1965; Allen et al., 1969; Gausman et al., 1969; Woolley, 1971; Allen et al., 1973; Gausman, 1973 and 1974; Gausman et al., 1971 and 1974; Gausman, 1977), who has contributed a great deal to the basic theory relating the morphological properties of crop plants to their optical properties. Natural and cultivated classes, with high resolution spectral signatures, were presented as basis of information about normal plant growth and conditions caused by nutrient deficiency, pests, and abiotic stresses (Gausman & Allen, 1973; Gausman & Hart, 1974; Gausman et al., 1975, 1976, and 1981; Peynado et al., 1980). Research on plant canopy construction, solar lighting conditions and soil reflectance has improved remote sensing as an instrument for study and its relevance to agronomic problems (Suits, 1972; Tucker, 1977; Bauer et al., 1986; Liang, 2004). A review on the development of remote sensing for agricultural purposes was published in a set of articles in *Photogrammetric Engineering and Remote Sensing* (Volume 69). Another review on the application of remote sensing for dry-land crops was presented by Hatfield et al. (2004).

The successful use of optical remote sensing has shown that it is already the most widely applied data-gathering method in agriculture. Sensors like SPOT, ASTER, with LANDSAT/TM & ETM+ will further enhance the assimilation of such technology (USGS, 2009). MODIS, with its relatively low spatial resolution (250 m x 250 m pixel size), has reported the most success in agricultural applications because of its high temporal resolution and its availability (Chen et al., 2008). High-resolution commercial satellites, such as IKONOS & Quick-Bird, have an advantage in their temporal resolution (1-3 days) (Moran, 2000). Microwave imaging sensors such as RADARSAT also play an important role. Within the past years, researchers have explored the usefulness of ENVI-

SAT-ASAR dual polar-metric data for environmental mapping of agricultural areas (Lohmann et al., 2008). Multispectral sensors have drawbacks in their ability to give exact approximations of biophysical and yield information about agricultural crops (Thenkabail et al., 2002), and on crop class or species identification (Asner et al., 2000). To overcome these drawbacks, there has been an increasing interest in the narrow-waveband hyper-spectral sensors which can normally acquire data in hundreds, or even thousands of spectral bands. These hyper-spectral sensors such as Hyperion on NASA's Observing-1 Platform have all played a role in the advancing application of remote sensing for agriculture (Mather, 2004). This satellite with 220 spectral bands (0.4-2.5  $\mu\text{m}$ ), a 30 m spatial resolution and a 7.5 km by 100 km spatial coverage land area per image, has allowed researchers to develop new vegetation indices, for example, Bannari et al. (2008) who developed several spectral chlorophyll indices.

Some new advanced satellites with advantages in terms of revisit periods, and spatial and spectral resolution, such as VENUS and HypSIRI, will launch in the next five years. For instance, the new micro satellite VENUS, will carry a sole super spectral space camera and will have an advanced plasma-thruster mechanism for momentum. The hyper-spectral satellite HypSIRI is proposed to be launched sometime around 2013 and will carry a TIR scanner and a hyper-spectral imager that will cover UV, VIS, SWIR and TIR ranges. The TIR-range will have eight bands between 3.9 and 12.7  $\mu\text{m}$  with 45 m spatial resolution. Its data will offer practical information in the investigation of surface temperature, geology, surface morphology, natural resources, drought, soil and vegetation. However, for processing so many spectral bands, it requires the use of advanced digital image processing software and algorithms to decrease the dimensionality of the data to a manageable level. These sensors are: costly to buy; costly to operate; large; and need a full-sized aircraft to board the instrument (except for the handheld sensors) (Deguise et al., 1998; Jensen, 2007). Where the growth and management of agricultural crops are influenced by local climate conditions (Atkinson & Curran, 1995), cloud cover can have an influence on the satellite remote sensing possibility. Airborne platforms sensors present more flexibility rather than satellite platforms and have solved some of these problems, i.e.: they can operate under clouds; and have a higher spatial resolution (Lamb & Brown, 2001). However, the cost and the difficulty in geometric correction of the images is still a source of interest, and work is being conducted on sinking the cost of the sensors (Everitt et al., 1995). Remote-control helicopters have been used to produce maps of crop status (Sugiura et al., 2005), and model aircraft have also been used as platforms for remotely sensed crop biomass and nitrogen status studies (Hunt et al., 2005). In addition, a high-altitude unmanned aerial vehicle was used to observe crop maturity and weeds in a coffee farms (Herwitz et al., 2004). However, these systems are expensive. For further reference, Pinter et al. (2003) presented the geographical extent of the agricultural research remote sensing programs.

### 1. Remote sensing approaches for vegetation studies

The optical characteristics of vegetation and different leaves were explained in detail by (Lambers et al., 1998; Ustin et al., 1999; Kumar et al., 2001). In general the reflectance of vegetation in the visible wavelengths (0.43-0.66  $\mu\text{m}$ ) is small and reflection in near infrared (0.7-1.1  $\mu\text{m}$ ) is large (Fig. 2.5). The life cycle in crop plants includes the three major phases: a vegetative stage, reproductive phase and a grain-filling stage. Three features of leaves have an important impact on their reflectance characteristics: pigmentation (e.g., chlorophyll a and b), physiological structure and water content. *Pigments* absorb the energy of the visible wavelengths, where the highest level of absorption from chlorophyll a is located at 430 nm and 480 nm, while for chlorophyll b it is at 450 nm and 650 nm. For example, the bandwidth of the LANDSAT-TM is too wide to detect these thin absorption bands (Bidwell, 1974; Lambers et al., 1998). The reflectance response of *vegetation canopy* is affected by: the vegetated and non-vegetated areas spatial distribution, vegetation classes, leaf area index, distribution of the leaf angle, and bio-chemical and physical vegetation

conditions. The *water content* of the leaves and water in the atmosphere decrease overall leaf reflectance and causes some thin absorption features (water absorption bands) (Irons et al., 1989).

The spectral response of vegetation changes permanently during the growing season and with alterations in moisture content. Appropriate information about these changes assists in the determining of the best time period for field work and in determining biophysical features to be measured. Fig. 2.14 illustrates a simplified spectral reaction curve for vegetation from 400 to 2.500 nm. The relationship between the irradiation absorption and the irradiation reflection illustrated in this figure changes with wavelength. The biophysical controls (pigment, cell structure and water) of the irradiation to plant interaction are also affected by differing wavelengths (Swain & Davis, 1978; McCoy, 2005).

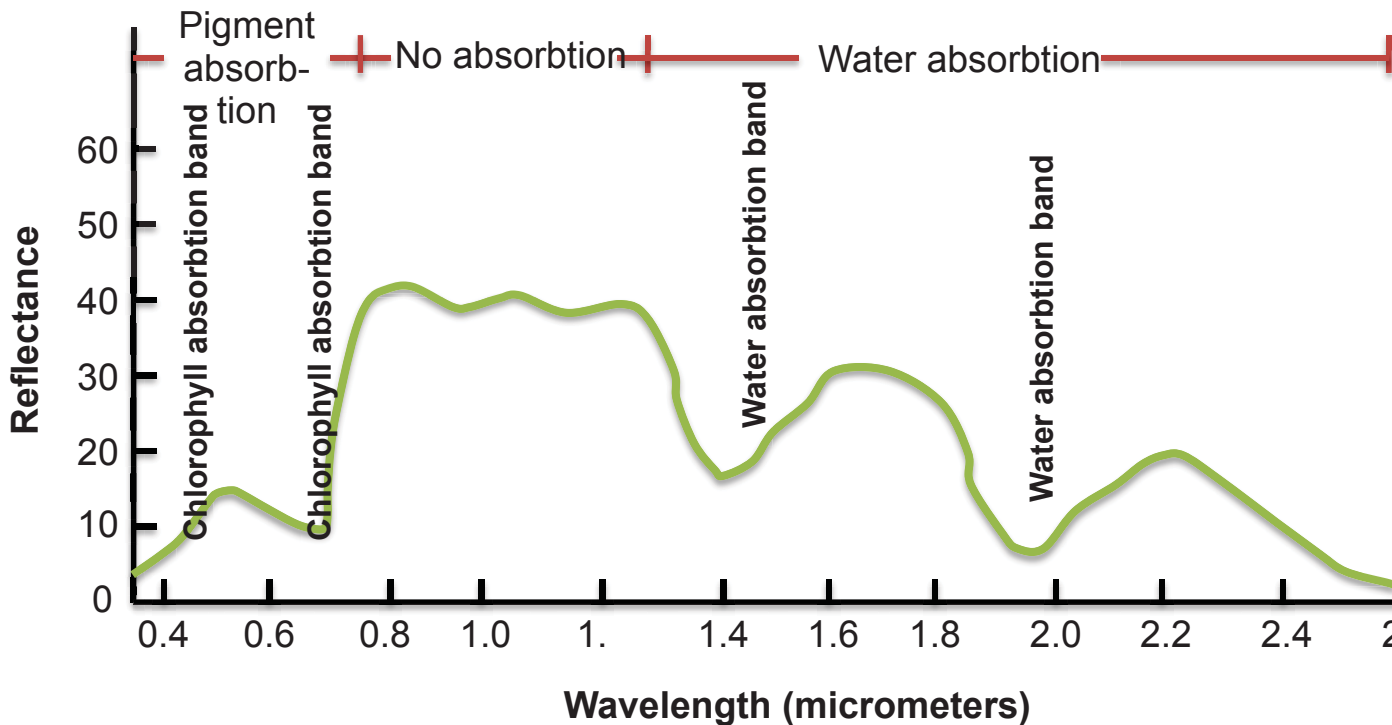


Fig. 2.14: The typical spectral response curve for vegetation showing the characteristic bands that differentiate vegetation spectrally (Source: Modified from Hoffer & Johannsen, 1969)

Factors controlling the spectral responses of the vegetation and its reflectance measurements include many natural and technical parameters, such as: atmosphere conditions (e.g., the quantity of occurring sunrays and the proportion of water vapor, change reflectance from plant canopies (Lord et al., 1985 a; Gao & Goetz, 1992); soil background (it has a large effect especially during the very early growth stages, where the density of plant shoots and leaves are low (Huete et al., 1984; Elvidge & Lyon, 1985; Huete, 1988; Mickelson et al., 1998); wind (it influences the formation of canopies and leaf opening angle, and thus, reflectance (Lord et al., 1985 b); viewing angle (the ratio of off-nadir to nadir radiance increases or decreases as the view zenith angle increases based on view azimuth angle (Pinter et al., 1987; Ranson et al., 1985; Galvao et al., 2004); the altitude of the sensor from plant canopies; and the amount of light.

There is an important relationship between the available images for an individual study area and the plant growth stages, where the growth stage determines which images are suitable for separation between the crops spectrally. Therefore, learning the phenological details about the crops of interest to an individual study area may be required. These phenological details refer to the natural vegetation calendar or a crop calendar. Data for these calendars can be obtained from: literature of previous ecological studies; meeting with qualified field-oriented ecologists; in state or regional bureaus engaged with natural resource management in the region; or from field-work based obser-

vation and measurements (e.g., Spectrometer measurements). In Syria, these can be obtained from the Agriculture Ministry. Fig. 2.15 illustrates a supposed example of a crop calendar for a hypothetical area. The time in which corn and soybean fields are most different phenologically is in October, during harvest. If those crops proved to be spectrally separable, then October imagery would be appropriate for digital classification.

	JAN	FEB	MAR	APR	MAY	JUN	JUL	AUG	SEP	OCT	NOV	DEC
Corn	Stubble			Planting	Increasing ground cover		Tasseling	Maturing	Harvest		Stubble	
Pasture	Dormant grasses				Full cover green color		Stays green in wet year Turning brown in dry year				Dormant grasses	
Soybeans			Stubble		Planting	Increasing ground cover			Harvest		Stubble	

Fig. 2.15: Hypothetical crop calendar for an area in the Midwestern United States (Source: Modified from Jensen, 2007)

Single-date captured remotely sensed data would be inadequate for primarily vegetated areas described by large temporal changeability and typical spatial patterns of highly frequent land cover changes between vegetation canopies. Multi-date remote sensing would be able to cover this problem: when specific data might not be suitable to separate individual LULC-classes, the use of another acquisition date might prove more appropriate for classification. Therefore, the use of the total multi-temporal information gives us a better separation between several classes, and consequently, more classification accuracy (see Fig. 5.23). Crop phenology understanding is very important in crop monitoring and classification (Chen et al., 2008). This fact is established by the results of a number of studies (Brisco & Brown, 1995; Guerschman et al., 2003; Blaes et al., 2005).

## 2. Remotely sensed vegetation indices

The mathematical combinations of the visible and near infrared spectral bands allow us to separate naked soil surfaces or water bodies from vegetation. These combinations can be called spectral *Vegetation Indices (VIs)* (Crist & Cicone, 1984; Huete & Jackson, 1987), which provide us with insight into the spatial patterns of vegetation cover or canopy formations. Vegetation indices are "a dimensionless, radiometric measure that indicates relative abundance and activity of green vegetation" (Jensen, 2007). Their functionality is based on highlighting the spectral role of green vegetation in images, while obliterating the role of soil background, sun angle and atmosphere by joining several spectral bands in visible and near infrared portions of the EMS. Vegetation indices were improved on the basis of simple arithmetical principles (e.g., added, divided or multiplied) between the reflectance at given wavelengths in an intended method to harvest a single value that suggests the amount or activity of vegetation in a pixel and to improve the vegetation signal of pixels and spectral measurements (Araus et al., 2001; Campbell, 2002). The newly generated values of these indices are more highly correlated to plant parameters (e.g., leaf area index, biomass or vegetative cover) rather than the unprocessed reflectance values (Wanjura & Hatfield, 1986). The narrow spectral bands are also more capable than wide spectral bands in exactly defining physiological changes at certain wavelengths, which increase the efficiency of the spectral indices

(Gitelson et al., 2005). A variety of VIs has been developed during the past 40 years. Hatfield et al. (2004) reviewed the progress in VIs and their using to crop canopies. The original finding of VIs goes back to Jordan (1969), who linked the ratio of NIR-800 nm to red-675 nm reflectance (NIR/RED) to LAI. As a modification, Tucker (1979) proposed a Difference Vegetative Index (DVI) as NIR-RED. These spectral vegetation indices include among others: the Normalized Difference Vegetation Index (NDVI) (Tucker, 1986; Hurcom & Harrison, 1998); the Soil Adjusted Vegetation Index (SAVI) (Huete, 1988); the Tasseled Cap Greenness (TCG) (Crist & Cicone, 1984; De Jong, 1994); the Ratio Vegetation Index (RVI); Physiological Reflectance Index (PRI); Water Index (WI); and Simple Ratio (SR). A lot of the current VIs are based on wide spectral bands strongly linked with LANDSAT. Thresholding a VI is a simple dual choice to classify the ground surface features as vegetated or non-vegetated. Any advanced within-vegetated areas classification requires further exhaustive information about the vegetation characteristics, where the life of any variety of vegetation in an individual area is controlled by the biophysical environment and the ecological conditions (Jensen, 2005).

The calculation of NDVI can be very practical in the making of a LULC-classification. It is the most commonly used (Ahmadi & Mollazade, 2009).

### 3. Crop discrimination from satellite-based images

The most frequently practiced utilization of remote sensing for agriculture is the identification of crop types and then classification (Van Niel & McVicar, 2000), where crop discrimination is a critical and difficult first step for most agricultural observing activities. The capability of remotely sensed data to identify crop class makes it promising to classify and estimate each crop area, and so calculate the relevant statistics automatically that can used as inputs to crop production forecasting models (Blaes et al., 2005). The application of remote sensing for discrimination between agricultural crop classes and internal crop characteristics has been widely studied throughout the past decade (Metternicht et al., 2000; Senay et al., 2000; Thenkabail et al., 2000; Van Niel & McVicar, 2004 b; Blaes et al., 2005; Brooks et al., 2006; Lucas et al., 2007; Wardlow & Stephen, 2008; Satalino et al., 2009). Most of these researchers have focused on increasing classification accuracy through the development of several techniques and methods. In contrast, only small studies have been presented on determining the best time(s) to obtain images in order to distinguish different crops (Van Niel & McVicar, 2004 a).

The temporal information dimension in used remotely sensed data is the most useful factor in natural vegetation and agricultural applications for identifying crop types (Smith & Ramey, 1982; Badhwar, 1984; Hall & Badhwar, 1987; Price et al., 1997; Wardlow et al., 2007). This is because agricultural features have great (within-class and within-season) spectral flexibility, that is based on several complex natural and biophysical factors (e.g., crop type/s, soil, water and geographical location). The observation and understanding of these various spectral responses of crops, and comparison with the physical characteristics of remotely sensed data recorded in various dates in the year (building a crop-specific temporal record), would give us the appropriate date(s) during the growing stages in which the crops of interest are spectrally separable. Also, by observing the physical derived spectral indices from remotely sensed data that are sensitive to natural vegetation cover over time, it is possible to discriminate crops (Van Niel & McVicar, 2000; Ozdogan, 2010).

Discrimination of crops using remote sensing imagery is generally achieved with supervised or unsupervised classification algorithms (Jensen, 2007). Recently, nonparametric algorithms, expert knowledge and ancillary data have been used in the process of cropland classification, improving the overall classification accuracy. One example of this is the establishment of neural networks for crop type identification, which is the most important development in information extraction from remotely sensed data in the last 15 years (Del Frate et al., 2003). Multi-sensor data fusion and classification of time series data are being applied in cropland classification more and more (Chen et

al., 2008). Multi-temporal imagery has been found to clearly obtain better results than those attained by mono-temporal remotely sensed data (Brisco & Brown, 1995; Guerschman et al., 2003). The most simple method of distinguishing crops is the classification of images into large-scale classification categories including all agricultural features (Level 1 in LULC-classification) (Campbell, 2002). From this level of classification, agricultural features can be classified into cropping and non-cropping regions.

The interaction between crop field scale and pixel size is a significant factor, especially in heterogeneous cropping areas. For instance, large pixel dimensions allow an increasing chance of recording mixed reflectance values. This resulted mixed spectral response is confused by traditional local agricultural management practices, such as found in most areas of the Euphrates River Basin, where crops are sometimes planted in almost 30 m strips (see Fig. 5.29). This is alternated with un-cropped areas (bare soil, stubble, dirt roads, etc.) of similar size to the cropped strips. So, pixels that are not entirely homogeneous (e.g., solely forest, vegetation, wheat crop, etc.), have mean reflectance values (composite spectral response that might match neither feature's spectral response) as a result of more than one feature within the pixel area. Such pixels are known as mixels and are an ever-present problem in cropland classification, reducing their discriminating power (Chen et al., 2008). Spectral Mixture Analysis techniques (SMA) have been developed and used to solve the mixel-problem in remotely sensed data (Tompkins et al., 1997; Broge & Mortensen, 2002; Doraiswamy et al., 2005; Fitzgerald et al., 2005; Theau et al., 2005). Confusion between natural vegetation and cropland is also another major source of error in crop classification using low spatial and/or spectral resolution remotely sensed data. Sometimes this is also true of high-resolution imagery. This type of confusion is especially common in areas with very complicated traditional local agricultural management practices, which are controlled by natural topography or from land ownership (Loveland et al., 1999). An additional factor to the quantity of this confusion type is the seasonal variation in the NDVI signals caused by seasonal difference in illumination geometry, which imitates a phenological cycle (Spanner et al., 1990; McIver & Friedl, 2002).

In order to support the capability of remotely sensed data to discriminate between the various crops, researchers have investigated many alternatives which have to do with: The sensor-type (e.g., optical or microwave); number of images (e.g., single-date or multi-date); timing of the imagery; digital processing techniques; or ancillary and spatial data integrating in the classification process (Van Niel & McVicar, 2000).

Abou El-Magd and Tanton (2002) presented a multi stage MLC method and showed increases from 85 % to 94 % in accuracy of crop classification based on six bands of 30 m resolution LANDSAT-7-ETM+ data. At each stage, only a subset of the classes was classified. The results from individual stages were combined to produce a final crop maps. The case study from Van Niel and McVicar (2004 a) was tasked to: 1) conclude temporal periods for maximum overall and individual crop separation; and 2) evaluate simple techniques for harvesting the best single-date results to improve overall accuracy. Seventeen single-date classifications of four major summer crops (rice, maize, sorghum and soybeans) were evaluated for a single growing season at the Coleambally irrigation area in Australia using LANDSAT-ETM+ data. Per-pixel classifications were applied using MLC and were then joined with field borders to apply per-field classifications based on the greater part crop class within each field. Multi-date classifications were achieved by: 1) merging diverse numbers of spectral bands for each date into a single image stack previous to classification (two-date, and three-date-termed standard multi-date classification); and 2) obtaining maximum accuracy single-crop classes from diverse dates and merging them during the post-classification process (termed iterative multi-date classification). Mart'inez-Casasnovas et al. (2005) presented a method that made available long term cropping categories to be classified using time-series remotely sensed data and supervised classification techniques. The method was used to map the multi-year cropping categories in the Flumen irrigation region (33,000 ha) in the Ebro Valley in northeast Spain. A seven year time series (1993, 1994, 1996, 1997, 1998, 1999 and



2000) of crop maps derived from LANDSAT-5-TM and LANDSAT-7-ETM+ images were used to produce the yearly crop maps, from which to get the multi-year cropping categories. [Blaes et al. \(2005\)](#) used 15 ERS and RADARSAT/SAR- and three optical images to determine agricultural crop classes based on devoted per-parcel classification and photo interpretation schemes. A hierarchical classification strategy was applied in order to take into account the spectral signatures variability within each crop type. [Brooks et al. \(2006\)](#) studied the potentials of multi-temporal (different parts of the agricultural growing season in the years 2004 and 2005), and multi-sensor (LANDSAT-5-TM, TERRA-MODIS and TERRA-ASTER) remotely sensed data to discriminate crop classes (corn, soybeans, wheat, alfalfa and grasses), in the 14,600 ha Upper Tiffin watershed in southeastern Michigan. The overall accuracy was 68.0 %. It was compared with two classifications techniques: the objected-oriented method with e-Cognition and a pixel-based method with ERDAS-Imagine. Both methods were found to have almost identical accuracy. The objective of the research from [Wardlow and Stephen \(2008\)](#) was to assess the applicability of time-series MODIS-250m-NDVI data for large-area crop-related LULC-mapping over the U.S. Central Great Plains. A hierarchical/graded crop classification approach, that used a decision tree classifier to multi-temporal NDVI data gathered over the growing season, was experienced for the state of Kansas. This approach created a series of four maps that increasingly classified: 1) crop/non-crop; 2) general crop classes (alfalfa, summer crops, winter wheat and fallow); 3) specific summer crop classes (corn, sorghum and soybeans); and 4) irrigated/non-irrigated crops. The general classification accuracy was at 84 %. In the study from [Conrad et al. \(2010\)](#), a multi-sensor model using 2.5m-SPOT, and bi-temporal 15–30m-ASTER data, was designed to support classifications of wheat, rice and cotton rotations in the irrigation system of Khorezm, Uzbekistan. The model consisted of two steps: a) the marking out of field borders using very high resolution satellite data; and b) the classification of multi-temporal medium resolution satellite data for discriminating crops and crop rotations within each field area. An overall accuracy of 80 % proved the success of the selected per-field classification rule base.

#### 4. Crop area estimation from satellite-based images

Crop area measurement and survey are very common practices in agriculture. Photo-interpretation of images can give better information than statistical analysis to evaluate an amount, or area, for a thematic category ([Ozdogan & Woodcock, 2006](#)). Remotely sensed data plays a significant role in bringing precise and opportune information on the location and area of specific crop types, which has important economic, food, policy and environmental consequences ([Deaton & Laroque, 1992](#); [Nelson, 2002](#); [Ozdogan, 2010](#)). Usually, crop area estimation has been achieved with very costly and hard statistically-based ground surveys that do not determine either the area or the geographical distribution of individual crops. To overcome or decrease these drawbacks, remote sensing, either alone or in combination with ground surveys, were used in crop area estimation ([Allen, 1990](#); [Hanuschak et al., 2001](#); [Carfagna & Javier Gallego, 2005](#); [Wardlow & Stephen, 2008](#)). Obtaining full efficiency of remote sensing for crop area estimation depends on the landscape characteristics, especially field size compared with the image resolution, where a suitable resolution for a specific landscape is realized when the most image pixels are pure. However, when this relationship is not realized, for example when using MODIS- or MERIS images especially for landscapes with small fields, then sub-pixel classification techniques (e.g., pixel un-mixing) can be used ([GEO, 2010](#)). Remote sensing has not been widely used for crop area estimation, due to the tradeoff between spatial detail (the scale of the remote sensing data) and area coverage for each image. In addition, there is the relationship between the spatial resolution of the remotely sensed data and the agricultural field sizes. Agricultural fields in most countries in the world are rather small, requiring medium to high spatial resolution data. However, increases in spatial resolution provide a decrease in the temporal availability which in turn lowers the chance of clouds-free coverage. Even if the clouds-free suitable spatial resolution data were obtainable, the increased num-

ber of datasets makes the cost high, and the high spatial resolution sensor covers only small geographical areas at a time. This leads to an additional problem, the need for atmospheric corrections in automated image digital processing and classification, as the required images are often gained at diverse times during the growing cycle of a crop. Medium spatial resolution data (e.g., LANDSAT) may be too coarse in countries with very small cultivated fields (e.g., China), but high spatial resolution is more appropriate for use in countries with large cultivated fields, such as the U.S. (Ozdogan & Woodcock, 2006). In contrast, lower spatial resolution data (e.g., MODIS) offer wide temporal and geographical coverage at continental and global scales, but need detailed spatial information. The fact that not each pixel in an image represents only single crop type can introduce uncertainty into area estimates because of the mixture (Van Niel & McVicar, 2000; Ozdogan & Woodcock, 2006). Where cultivated areas are smaller than the spatial resolution of the image, here, both cultivated and uncultivated areas (e.g., roads, houses, irrigation channels) are integrated in a pixel classified as agriculture or cropland. In agricultural situations, the amount of uncultivated area has been reported to vary from 10 to 40 % (Crapper, 1980; Okomato & Fukuhara, 1996; Gonzales-Alonso et al., 1998; Fang, 1998; Froking et al., 1999). To relatively solve this mixed pixel problem which occurs especially in high temporal resolution data at low spatial resolution, some contributors have developed techniques that use the concept of *temporal un-mixing* (Adams et al., 1986). It is similar to the traditional *spectral un-mixing* technique, where pure end-members are distinguished by their spectral response. Temporal un-mixing uses end-members defined by their single temporal response to improve the fractional area of each end-member based on its part to the mixed temporal reaction observed by the sensor (Ozdogan, 2010). Finally, previous crop class identification steps also influence crop area measurement from remotely sensed data (Van Niel & McVicar, 2000).

There are two generally used area estimation methods with remote sensing (Ozdogan & Woodcock, 2006). The first method calculates portions/fractions of a thematic category of interest for each pixel (Quarmby et al., 1992; Hansen et al., 2002). The essential drawback here is the accuracy assessment of fractions of the thematic field. However, area estimation by this method is becoming more common (Hansen et al., 2002; Liu & Wu, 2005). A second method is based on generating the thematic map through image classification and then multiplying the area of the pixels with their number in a specific class. The drawback here is the classification accuracy of the thematic map (Ozdogan & Woodcock, 2006).

The first version of the Digital Global Map of Irrigated Areas (DGMIA) was published in 1999. It contained a raster map with a spatial resolution of  $0.5^\circ$  by  $0.5^\circ$  containing the fraction of the area that was ready for irrigation around 1995, the so-called irrigation density (FAO, 2009). Within the GIAM-project, irrigated areas were predicted for individual regions of the World at 500 m (Dheeravath et al., 2007; Thinkabail et al., 2008). Ozdogan et al. (2006) estimated changes in summer irrigated crops areas and related water use from remotely sensed data and secondary data in semi-arid southeastern Turkey, where usually rain-fed agricultural lands are fast being changed into irrigated fields using of water from the Euphrates-Tigris Rivers. An image classification methodology depended on thresholding of LANDSAT-NDVI data from the peak summer period shows that the sum area of summer irrigated crops has enlarged threefold (from 35,000 ha to over 100,000 ha) in the Harran Plain between 1993 and 2002. Bayraktar and Bülent (2007) successfully achieved the irrigation of a total of 23,085 ha irrigateable land in central Diyarbakir and Ergani in Turkey using one ASTER-image. Ozdogan and Gutman (2008) presented a dry land irrigation mapping methodology that based on remotely sensed inputs from the MODIS sensor. Pervez et al. (2008) mapped irrigated areas of the conterminous USA using three sources of data: 1) county irrigation statistics from the USDA-NASS; 2) LULC-information from the 2001 National Land Cover Database (NLCD); and 3) satellite imagery from the MODIS sensor. The study from Lu et al. (2008) pointed out that high temporal-resolution MODIS data can improve the observation of irrigation in a large area and assist local mapping applications. In addition, it is free of cost, suita-

ble and simple to receive and analyze MODIS data. [Dheeravath et al. \(2010\)](#) established a complete method for the approximation of irrigated areas using MODIS-500 m over an eight day time series in India from 2001 to 2003. The irrigated areas were extracted with an overall accuracy of 88 %.

For several countries in the world which produce big amounts of wheat were important to approximate their total production at suitable time using a dependable method. Thus, the Large Area Crop Inventory Program (LACIE) was found ([MacDonald & Hall, 1980](#); [Los et al., 2002](#)). In the work from [Ozdogan and Woodcock \(2006\)](#), the resolution confidence of errors in approximation of cultivated areas was investigated using cases from six agriculturally different regions around the world. The major question behind this study was: how much is the ability to approximate cultivated area using remotely sensed data with various resolutions in relation to impact of the size and spatial pattern of agricultural fields in different geographic regions? A following question: how much is the influence of the overall proportion of a landscape under cultivation on the accuracy of area estimates with remote sensing?. [Liu et al. \(2005\)](#) used LANDSAT TM/ETM+ data with the spatial resolution of 30 m to recreate spatial and temporal characteristics of cropland across China for the time period of 1990–2000. [Hereher \(2009\)](#) estimated the agricultural land area of Egypt in 2005 using four images from MODIS-data (the wide swath of this sensor was 2,330 km). [Potgieter et al. \(2010\)](#) investigated the question of "How early and with what accuracy?" crop area estimates can be concluded using multi-temporal MODIS Enhanced Vegetation Index (EVI) imagery. The study was carried out for two shires in Queensland, Australia for the 2003 and 2004 seasons, and focused on obtaining total winter crop area estimates (including wheat, barley and chickpea).

## **F. Status of the accuracy assessment methods**

A classification process is not finished until its accuracy is measured ([Lillesand et al., 2008](#)). The assessment of the classification algorithm, change detection approach and the related end-results, which is generally a thematic map, is an important part of the digital remotely sensed data interpretation chain and LULC-classification approach. Assessment approaches can be based on a qualitative estimation using expert knowledge, or based on a quantitative estimation using statistical methods and previous data. These methods can be costly or cheap, brief or long in time, elegant and professional. The purpose of quantitative accuracy evaluation is the detection and measurement of map errors, where it compares an area on an end-product map versus result-based reference information of the same area ([Campbell, 2002](#); [Lu & Weng, 2007](#)). These reference data can be gathered from field work, or the interpretation of previous large scale thematic maps and aerial photographs, or the visual interpretation of imagery. Then, the reference classes can be compared to the result of the classification, and the percentages of correctly against wrongly classified pixels that were calculated for each class can be determined ([Foody & Mathur, 2006](#)).

There is no optimized method to measure the absolute accuracy of end-results derived from remotely sensed data, because one cannot achieve such an evaluation without knowing 100 % of ground truth. However, in contrast, if we do have absolute information of ground truth in the study area, what is the meaning of the classification? Therefore, we can only obtain a relative accuracy, that gives us a base from which to accept or refuse the end-results (e.g., classification, change detection, etc.) based on specific criteria at a specific confidence level ([Liu & Mason, 2009](#)). Accuracy assessment based on *error matrix* is the most frequently used method for evaluating per-pixel classification in addition to the possibility of use for object-based classification (e.g., [Wang et al., 2004](#)). Also, recently, fuzzy methods have been used for evaluating fuzzy classification results. The error matrix (also called confusion matrix or contingency table), describes the total part to which degree the created image classification matches with the reality (e.g., the reality represented by the ground truth points that is assumed to be correct). Thus a variance between the resulted map from automated classification and reference information is a classification error ([Congalton & Green, 1999](#); [Foody, 2002](#)). The accuracy formats allow the derivation of the most

general evaluation measurements: 1) overall accuracy; 2) producer accuracy; and 3) user accuracy. A detailed overview was presented by (Congalton & Green, 1999; Foody, 2002). In order to correctly produce an error matrix, one must respect the following issues: 1) reference data gathering; 2) classification scheme; 3) sampling method; 4) spatial autocorrelation; and 5) sample size and sample unit (Congalton & Plourde, 2002).

The overall accuracy value, derived from error matrix, includes a ratio that can be consolidated to likelihood conformity between the two data sets. Cohen (1960) improved the *Cohen's Kappa coefficient* as a measure of conformity/agreement which is used to likelihood conformity. It is frequently applied for an assessment of maps from diverse areas. Congalton (1991) recommended the application of the Kappa coefficient as an appropriate measure of the accuracy of a classification as a way of correlating the uncertainty of the results. It measures the variance between the real agreement in the error matrix (see Fig. 5.63) (e.g., the conformity between the remotely sensed data classification and the reference data as showed by the main diagonal/transverse) and the likelihood conformity which is showed by row and column totals. Kappa analysis is documented as a robust method for evaluating a single error matrix and for comparing the divergences between various error matrices (Congalton, 1991; Smits et al., 1999; Foody, 2004 b), and it takes into account the entire error matrix rather than the diagonal elements only. The assessment of the Kappa coefficient is the lag between the two values, i.e. -1 and +1. A positive value is likely containing a positive correlation between the image and reference data that were used for classification. A value of zero shows no harmony in classification, while a value of 1 pointed to an ideal conformity between the classification method output and the reference data.

*Modified Kappa coefficient and Tau coefficient* were founded to be as superior measures tools of classification accurateness (Foody, 1992; Ma & Redmond, 1995). The *Kappa Index of Agreement (KIA)* is not as well-known as the overall accuracy (percentage correct) as a tool with which to measure classification accurateness in applications of remote sensing techniques, but it is also used by many researchers (e.g., Dikshit & Roy, 1996; Cingolani et al., 2004). Næsset (1996) explains the application of a weighted Kappa coefficient to estimate the classification accurateness when all errors are not similarly important (e.g., if there are informational classes which are more strongly related to each other than others). Finally, accuracy assessment based on a normalized error matrix was carried out, which is observed as an improved contribution compared to the classical error matrix (Congalton, 1991; Hardin & Shumway, 1997; Stehman, 2004).

Many researchers, among them: Congalton (1991); Janssen and Van der Wel (1994); Smits et al. (1999); Foody (2002); and Foody and Mathur (2006), have presented evaluation reviews for classification accuracy assessment, discussing the state of accuracy assessment of image classification and other important topics. For example, Congalton and Green (1999) methodically reviewed the idea of fundamental accuracy assessment and some superior issues included in fuzzy-logic and multilayer assessments, and clarified standards and practical considerations in modeling and achieving accuracy assessment of remote-sensing data. The traditional error matrix approach is not suitable for assessing the soft classification results that have been presented to reduce the mixed pixel problem using fuzzy logic. Hence, various novel methods, such as a modal/qualified entropy/selective and shared information (Finn, 1993; Maselli et al., 1994), fuzzy-set methods (Gopal & Woodcock, 1994; Binaghi et al., 1999; Woodcock & Gopal, 2000), symmetric index of information nearness (Foody, 1996), Renyi generalized entropy function (Ricotta & Avena, 2002), and parametric generalization of Morisita's index (Ricotta, 2004), were developed. On the other hand, a critical problem in evaluating fuzzy classifications is the complexity of gathering reference data. Therefore, more research is needed to find a suitable method for assessing fuzzy classification results.

A classification accuracy assessment process in general consists of three basic mechanisms: design of sampling model; design of response; and methods that used for estimation and analysis (Stehman & Czaplewski, 1998). Choosing an appropriate sampling model is a significant stage

(Congalton, 1991), and it has been argued that the sampling design stage is not always suitable and an alternative is required (Foody & Mathur, 2006). The major components of a sampling model/strategy contain: units/shapes of sampling (pixels or polygons); plan of sampling; and range of sample in size and number (Müller et al., 1998). Achievable sampling designs contain random, stratified random, systematic, double and cluster sampling. It is dependent on the distribution of the class areas, thus this generally carried out after classification. A full explanation of sampling methods can be found in previous literature such as (Stehman & Czaplewski, 1998; Congalton & Green, 1999). By applying random sampling, each sample (e.g., pixel) has the same chance to be chosen. However, random sampling may lead to difficulties if the chosen samples are situated in inaccessible areas (e.g., very dense natural forests). Also, absolute random sampling could represent the classes of low coverage that fail to be represented in the sample, thus stratified random sampling, with prior knowledge about the areas, is often used in order to guarantee that samples from all classes are included in the accuracy assessment (e.g., Congalton, 1991; Congalton & Green, 1999; Helmer et al., 2002; Qiu & Jensen, 2004). To overcome the problem of an area's inaccessibility by random sampling, some researchers use cluster sampling, related to the selected samples in earlier known areas. This positively helps to reduce the field access cost. However, this will negatively cause a biased (influenced and subjective one) testing sample and an overestimation of the classification accuracy (Arora & Mathur, 2001). Cluster sampling and too systematic sampling, which chooses samples with an equivalent distance over the study area to be tested, can create spatially auto-correlated data. Finally, these methods do not guarantee that every entity in the population has an equivalent possibility to be included in the sample, thus disturbing the requirements for deductive statistics (Næsset, 1996; Brogaard & Ólafsdóttir, 1997; Arora & Mathur, 2001).

There are two commonly conventional methods to obtain reference data: 1) use field-collected data. This is important for fast and temporally changing LULC-classes (e.g., crops), where the field data should be gathered at the same time with image acquisition; and 2) image-collected data. This uses spectral signatures and limited field knowledge, especially for slow changing LULC-classes (e.g., rivers), where a user can manually select training samples of different classes using a multispectral image. These two methods are often integrated and used in combination as a hybrid approach (Liu & Mason, 2009).

There are three ground data collecting ability scenarios: 1) no ground data may be acquired. This may be the situation when no approval can be attained from state establishments to visit the country (e.g., North Korea), or by a crisis (e.g., large areas of Somalia). As an alternative, samples collected from a high resolution images or areal-photo-interpretation can be combined with image classification on medium resolution. A sampling strategy (random, systematic or stratified) should be used to select reference data from the high resolution images. However, accuracy is limited and needs to be confirmed from experience in other areas with similar landscape characteristics (GEO, 2010); 2) an inadequate quantity of ground data can be acquired. This is the situation when state or local establishments do not create major hindrances to the gathering of ground data, but do not show interest in the research (e.g., Syria). In this situation, the efficiency of ground data is limited, although accuracy is more likely than in the first scenario; and 3) ground survey is possible. This occurs when state establishments are interested in the research subject and in the applications of remote sensing. Under this scenario, it is possible to collect sufficient samples of ground data. High accuracy can in this situation be reached.

Before applying the assessment process to get the classification accuracy, one requires to determine the causes of errors (Congalton & Green, 1993; Powell et al., 2004). The measured accuracy of a classified remotely sensed data depends on many factors. In addition to the classification method itself, there are other causes of errors, such as location errors resulting from the geometric registration, interpretation errors, and reduced superiority of training or test samples. These all have an impact on classification accuracy. Many studies have shown that factors such as the sam-

ple size (number of samples), structure and nature of the sampling strategy used, can have a large influence on image classification accuracy (Foody & Mathur, 2006). The sample size decides the confidence-intervals of the accuracy approximations (Næsset, 1996; Brogaard & Ólafsdóttir, 1997). If confident/sure approximations of the classification accuracies for single classes are necessary, the sample size has to be larger than that for a similarly confident approximation of the overall accuracy. Bigger samples than for a regular estimation of the overall accuracy are also required in order to sufficiently represent the uncertainty between all couples of classes in the error matrix (Congalton, 1991). The sample size is limited by the cost of determining the truth values for a large number of testing samples (Congalton, 1991; Langford & Bell, 1997). Accuracy assessment is also influenced by sample numbers for each class, where as the sample numbers increase, thus the accuracy assessment will be more trustworthy (Richards & Jia, 2003). Sometimes, the measured accuracy is influenced by whether the interpreters are assigning the reference data to the generated classes from classification process separately (blindly), or whether they know the classification result to be evaluated and can be impacted by it. This can lead to a clear increase in the overall accuracy value (Langford & Bell, 1997). It is better to eliminate areas close to class borders (mixed pixels) from the accuracy assessment by selecting testing samples in the center of homogeneous classes on the image, where errors in these areas may be due to mis-registration between the classified image and reference data (Langford & Bell, 1997; Hill, 1999; Schlerf et al., 2003). Most guidance on training set design advises the use of a great number of complete pure pixels (Foody & Mathur, 2006). Foody and Mathur (2006) provided a method based on mixed spectral responses, using small training samples having mixed/assorted pixels for accurate hard image classification.

Where a classification be more in depth/detailed (having more informational classes which are classified more exactly), the possible satisfied information of the resulting map increases, but the chance for classification errors thus increases (Campbell, 2002; Laba et al., 2002). Fig. 2.16 a shows the increasing in classes number against the increasing level of classification detail with respect to the needed pixel size. Fig. 2.16 b shows a like relationship but with a graphic demonstration of the predictable error increasing by rising the classification level with respect to the sub-pixel analysis of LANDSAT-TM/ETM+ data.

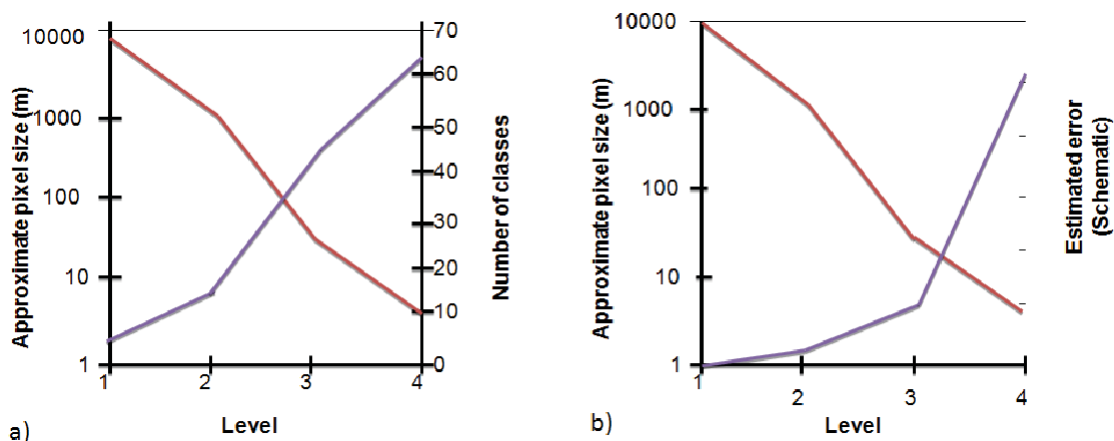


Fig. 2.16: Schematic relation of pixel size, numbers of classes and estimated accuracy dependent on the classification level (Source: Modified from Schmidt, 2003)

The accuracy of an approach to approximate the variability of cropland is influenced by sets of issues, such as the data used, scale, crop type, etc (Chen et al., 2008). However, agricultural land use has, as a special characteristic, frequent changes in surface reflectance response in time with the growth of a crop, requiring recordings from remotely sensed data to cover the essential phenological phases of the cropping system. This makes the accuracy assessment process more difficult (Thenkabail et al., 2000).

### Chapter 3: Overview of study area

#### A. Syria

Present-day Syria (Fig. 3.1) forms only a small part of antique geographical Syria. Until the twentieth century, when western forces started to create the irregular outlines of the modern countries of Syria, Lebanon, Jordan, and Palestine, the entire settled territory at the eastern ending part of the Mediterranean Sea was named Syria, a name came from the ancient Greeks to the land connection that links the three continents of Asia, Africa, and Europe. Historians and political scientists mostly use the expression “Greater Syria” to indicate this region in the pre-state time. Historically, Greater Syria seldom ruled itself, mainly because of its susceptible location between the Mediterranean Sea and the desert. As a district between commonly powerful empires on the north, east, and south, Syria was frequently an arena for the political fates of dynasties and empires (Kangarani, 2006).

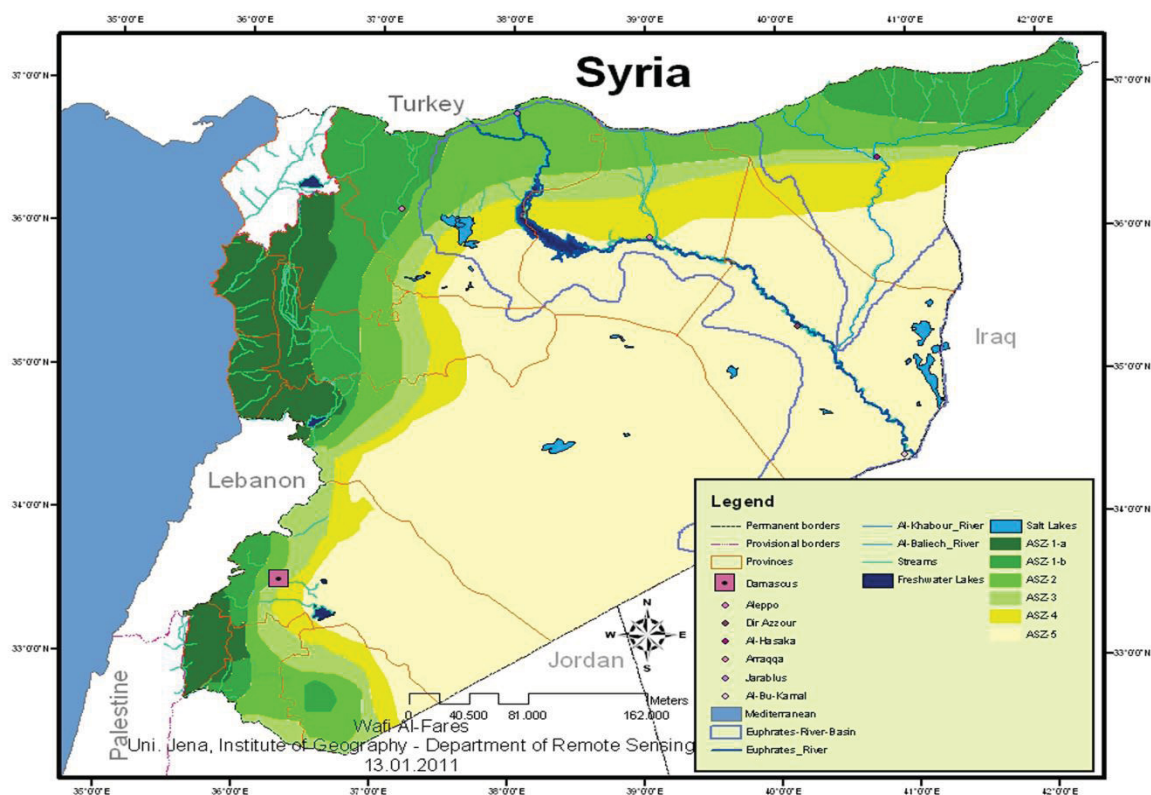


Fig. 3.1: Present-day Syrian borders, the 14-governorates administrative divisions, Agro-climatic Zones, and the Euphrates River Basin study area

The Syrian Arab Republic (SAR), with a total area of 185,180,000 km<sup>2</sup> (ca. 18.5 million hectares), is located on the eastern coastline of the Mediterranean Sea, and is surrounded in the north by Turkey, in the east and southeast by Iraq, in the south by Jordan, in the southwest by Palestine, and in the west by Lebanon and the Mediterranean Sea. As administrative organization, Syria has 14 Mohafazats (governorates), one of which is the capital Damascus (FAO, 2009). The coordinates of its geographic position are 32° to 37° N and 35° to 42° E (Miski & Shawaf, 2003). The total population is 19.88 million, of which 46.48 % is rural. Actual population growth was 2.5 % for the period 2000-2005. Over the half of the inhabitants are under 15 years old. The standard number of family members is greater than six. About half of the people live in the main cities, while the other half lives in the countryside (Miski & Shawaf, 2003). The average population density was about 96 inhabitants/km<sup>2</sup> in 2004 (CBS, 2009). In 2009, agriculture employed around 16.79 % of the total

labor force, and accounted for nearly 20 % of GDP (compared to 39 % in 1963) and 60 % of all non-oil exports.

Syria can be classified into four main climate regions: Mediterranean climate, Mediterranean influence steppe, desert and mountain. Each of these classifications appears again in two variants (Wirth, 1971; Akkad, 2001; FAO, 2009). The two major seasons in Syria are identified by significant differences in precipitation and temperature. Summers are warm to hot and almost rainless; winters are rainy, mild to cool, and relatively moist. In between, spring and autumn appear often as only short transitional seasons. Overall, the winter in Syria can be described as more oceanic, while the summer has a more continent basic character. The most welcoming and nice climate in Syria is found near the shoreline. Precipitation increases with rising elevation in the mountains close to the shoreline, and snow is common in winter. Annual precipitation along the coastal mountain series from 750 to 1,000 mm. Moving inland from the coast, the climate becomes drier and less mild. Syria's flat terrain areas have an average temperature close to 35° C in summer and 12° C in winter, and the precipitation changes over these flat areas from 250 to 500 mm in the year. Winter in the north can be cold, with temperatures frequently falling under freezing. In the dry steppe and open desert countryside east of the mountains, a clear continental climate exists, with high summer temperatures and rather cold winters, with many nights of frost. This region, which covers approximately 60 % of the country, has an average annual precipitation less than 250 mm. During spring and autumn, "KHAMASIN" wind, which are hot and dusty, blowing from the east and southeast. Thus, temperatures can be raised up to 43° and 49° C. The temperature values in Syria meet the definitions of the Mediterranean climate: the coldest month of almost all the weather stations has an average temperature of more than 5° C, the hottest of 25° C. Therefore the climate of Syria is under the threshold of the corresponding unit systems: warm-temperate (coldest month > 2° C), hot summer (July > 23° C), subtropical (January > 6° C), Mediterranean (January > 5° C). The majority of Syria has relatively high daily variations between the maximum and the minimum temperatures. This variation sometimes reaches 23° C in the interior areas and about 13° C in the coastal areas. The coldest months of the year are December and January, while the hottest months are July and August. The temperature often falls under 0° C, but rarely under -10° C, in the winter season in all areas excluding the coastal areas (with the exception of north Aleppo and north Al-Hasaka). In summer, the temperature may rise frequently up to 45° C in places such as Al-Badia and Al-Hasaka (Akkad, 2001). Areas that have an elevation higher than 1500 m above the sea level, receive a snowy precipitation during the winter season. Areas with an elevation of 800-1500 m receive the both (rain and snow). Other areas with a lower elevation receive more rain and rarely snow, not including desert areas that receive insufficient rain. Precipitation falls constantly or at intervals. Frequent thunderstorms come with the intense showers do happen during winter. The greatness of such showers reaches in some areas 75 mm in 24 hours. The dense precipitation areas are the mountainous and coastal areas. These are followed by the northern region (i.e., north Aleppo, Kamishly and Malikiéh) (Akkad, 2001). The regular annual precipitation over the country is 252 mm giving 46.6 km<sup>3</sup>. Precipitation becomes less and less when moving from west to east and from north to south. Total annual precipitation varies from 100 to 150 mm in the north-west, 150 to 200 mm from the south towards the central and east-central areas, 300 to 600 mm in the plains and alongside the slopes/foothills in the west, and 800 to 1000 mm along the coast, increasing to 1400 mm in the mountains (Al-Fares, 2007; FAO, 2009). Table 3.1 shows the distribution of the precipitation averages in the Syrian territories (Al-Fares, 2007), where only 25 % of its area receives more than 500 mm/year precipitation, 25 % of the area receives 250-500 mm/year, and 50 % of the area receives less than 250 mm/year (Miski & Shawaf, 2003; Al-Fares, 2007).



**Table 3.1:** The distribution of the precipitation averages in the Syrian territories (Source: Modified from Al-Ashram, 2001)

Area/km <sup>2</sup>	Percentage to the total area of Syria/%	Annual rainfall average/mm	Area/km <sup>2</sup>	Percentage to the total area of Syria/%	Area/km <sup>2</sup>
9,250	5	More than 1000	74,000	40	100-250
37,000	20	500-1000	18,500	10	Less than 100
4,600	25	250-500			

"The relative humidity is high during winter and low in summer, of course, desert and semi-desert areas are those with the least relative humidity. For example, in winter the relative humidity varies from 60 to 80 % in the interior region and from 60-70 % in the coastal region. During summer, the rate of humidity in the interior region varies from 20 to 50 %, and in the coastal region from 70-80 %. During winter, the prevailing winds in the eastern part of the country are easterly and in both the northern and northwestern parts, the winds are northerly. Other parts of the country are subject to westerly and southwesterly winds. During summer the prevailing winds in the northeastern part of the country are northerly, and the remaining parts of the country are subject to westerly and southwesterly winds" (Akkad, 2001).

Most of the country is flat (Fig. 3.2), but a mountainous region is found towards the boundary of Lebanon. The east is desert, the west coast. The coastline is 183 km long and borders the Mediterranean. Syria has two mountain ranges alongside the shoreline, with a cleft in between, which is an extension of the Red Sea rift (Miski & Shawaf, 2003). The country has the four next physiographic regions: 1) the coastal region between the mountains and the sea; 2) the mountains and the highlands expanding from north to south alongside the Mediterranean shoreline; 3) the plains or central, situated east of the highlands and including the plains of Damascus, Homs, Hama, Aleppo, Hassakeh and Dara; and 4) the Badia and the desert plains in the southeastern part of the country, neighboring Jordan and Iraq (FAO, 2009). Behind the narrow Mediterranean coastal plain, the Jabal Al-Nusayriyah range rises to about 1,500 m, then falls suddenly to the Al-Aasi (Orontes) River Valley to the east. In the southwest of the country are the Anti-Lebanon Mountains, with a higher range which forms a boundary between Syria and the neighboring Lebanon. It rises to 2,814 m at Jabal Al-Sheikh (Mount Haramon) on the Lebanese border. This series of mountains decreases into a hilly area in the southwest, known as the Golan Heights (captured by Israel in 1967). The only other main area of highland is the Jabal Al-Duruz, southeast of Damascus on the Jordanian boundary. East of these mountain series, the land gradients softly northeast towards the Euphrates (Al-Furat) River Valley, which flows crossways/diagonally from Turkey in the north to Iraq in the east. This plateau includes the main towns and cities of Syria. The Orontes (Al-Aasi) spring from the Anti-Lebanese mounts in the south and passes the three governorates (Homs, Hama, and Idlib) in the west to Turkey in the north. It is the second longest river in Syria after Euphrates. In the wide east area of Syria are the open arid and semi-arid grass-covered plains. The stony Syrian Desert (Al-Hamad) locates in the southeastern corner of Syria (FAO, 2009).

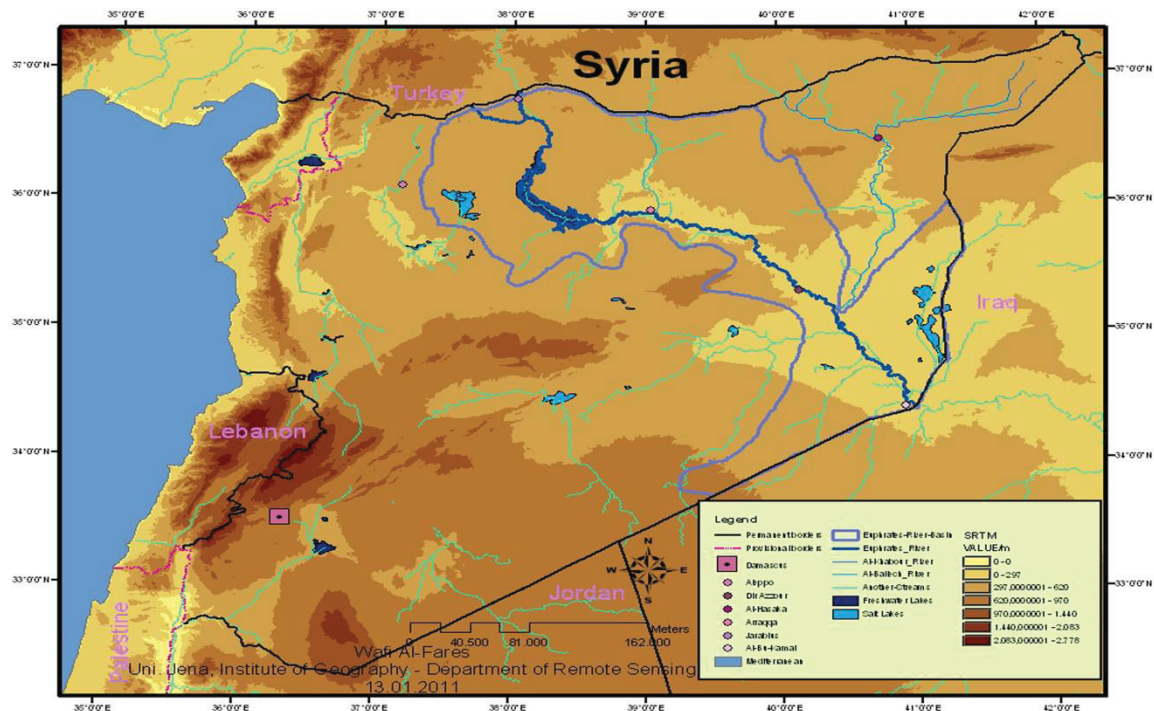


Fig. 3.2: Present-day Syrian borders, general geomorphologic characteristics, and the Euphrates River Basin study area

The soils of Syria have, despite their differences, many common characteristics: the humus content is very low, but the carbonate content is very high. The pH-value varies with minor variations around eight. In their spatial differentiation, the soils of Syria are primarily determined by four factors; parent rock, climate, soil history and human impact (after German to English translation and modification from Wirth, 1971). One of the best, most productive soils of Syria is the deep and heavy Grumusole. This is a bright red to dark reddish calcareous soil, which is found mainly in the arable plains of Homs and Hama, east of Idlib, and north of Aleppo to the Syrian-Turkish border. Here in winter, wheat is the preferred agricultural crop, while cotton, watermelons and sugar beets are grown in summer. The similar deep and loose arable soils of the northeastern Syrian plains are comparable to the Grumusols. For agriculture, these soils are perhaps better suited than the Grumusole in western Syria because of the amount of swell-able or shrinking clay minerals which are lower, dry-out less quickly and can therefore be easier processed. More favorable are the basalt soils of Jabal Al-Hass and Jabal Chbeit in northern Syria. However, the best soils in Syria include the Pleistocene and Holocene fine-grained river and sea deposits of intra-Syrian basins and sinks. Irrigation on these soils provides high yields in sugar beets, hemp and cotton (after German to English translation and modification from Wirth, 1971). Based on soil type, Syria (18,518,000 ha) is classified into the following: Red Mediterranean soils (850,000 ha); reddish dark brown soils (2,217,000 ha); yellowish brown soils (4,782,000 ha); desert soils (4,244,000 ha); gypsum soils (5,528,000 ha); and other soils (897,000 ha) (Akkad, 2001).

Water is an insufficient resource in Syria as it is all over the Middle East (Kangarani, 2006). Rapid increases in population have made it essential to enlarge the area of irrigated land to improve the agricultural inputs and meet the food requirements of the increasing population (DIWU, 1993). Seven main hydrographic basins can be identified (Fig. 3.3): Al-Jazeera; Aleppo (Quaick and Al-Jabboul sub-basins); Al-Badia (Palmyra, Khanaser, Al-Zelf, Wadi Al-Miah, Al-Rrasafa, Al-Talf, and Assabe' biar sub-basins); Horan or Al-Yarmouk; Damascus; Al-Aasi-Orontes; and Al-Sahel. Precipitation and snowfall represent the main water supply for the basins, excluding the Al-Jazeera and Al-Aasi-Orontes, where the major sources of which are situated in the bordering countries.

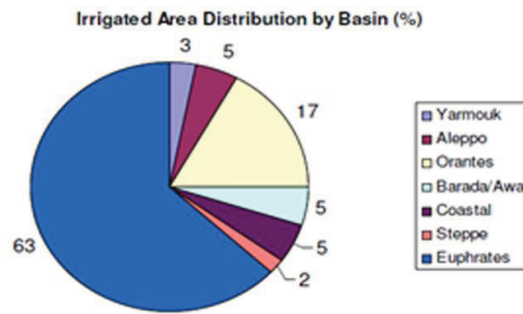


Fig. 3.3: Irrigated areas distribution by basins in Syria (Source: Adapted from: World Bank Report, 2001)

Syria has 16 major rivers and tributaries, where six are major international rivers (FAO, 2009). Some of them are: the largest and the most important river in Syria is the Euphrates (Al-Furat), which originates in Turkey and flows to Iraq; the Afrin in the north-western region of Syria, which stems from Turkey, traverses Syria and runs back to Turkey; the Orontes (Al-Aasi) in the western region of Syria, which stems from Lebanon and streams into Turkey; the Al-Yarmouk in the south-western region of Syria, which stems from sources in Syria and Jordan. It forms the boundary between these two countries before streaming into the Jordan River; in the south Al-Kabier Al-Janoubi with, which stems from sources in Syria and Lebanon. It forms the boundary between them before streaming to the Mediterranean Sea; and the Tigris (Dijla), which forms the boundary between Syria and Turkey in the great north-eastern part of the country. 17.97 km<sup>3</sup>/year is the real regenerable resource of water. About 28.51 km<sup>3</sup>/year is the natural water resources (surface runoff) to Syria from rivers that spring from the border countries. 17.33 km<sup>3</sup>/year is the real regenerable surface resources of water. These involve: the Euphrates with 15.75 km<sup>3</sup>/year; the Orontes (Al-Aasi) with 0.33 km<sup>3</sup>/year; and the Tigris (Dijlah) with 1.25 km<sup>3</sup>/year (FAO, 2009). Table 3.2 clarifies the gap between supply and demand of water in Syria (Al-Fares, 2007).

Table 3.2: The expected difference between the supply and demand on the water in Syria in the period from 1989 to 2010/Million m<sup>3</sup> (Source: Modified from Al-Mansour, 2000)

Sub-basin name	Water resources average (above surface + underground)	Water needs for (drinking+agriculture+industry)		Deficit	
		1989	2010	1989	2010
Al-Aasi (Orontes)	2,717	17,100	2,921	+1,007	-204
Al-Sahel (Coast)	2,335	415	1,116	+1,920	+1,219
Barada and Al-Aawaj (Damascus)	850	981	1,530	-131	-680
Al-Yarmouk (Daraa)	447	195	366	+252	+81
Al-Badia (Homs)	354	45	122	+309	+232
Aleppo	649	661	944	-12	-295
Tigris and Al-Khabour (Al-Hasaka)	2,388	1,213	2,116	+1,175	+272
The sum	9,740	5,220	9,115	+4,520	+625
	7,792			+2,572	-1,323
Euphrates	25+X1	3,060	8,812	According to Syria's share of Euphrates water	
Tigris	X2	-	1,500	According to Syria's share of Tigris water	
Total	9,765+X	8,280	19,427	9,765*0.8+X=19,427 X 2010=11,651	

Syria has 166 dams with an overall real storage of 19.7 km<sup>3</sup>. The biggest one is on the Euphrates. It is the Dam of Al-Tabqa near Arraqqqa city. Behind it is the biggest lake in Syria. It is the Al-Asad Lake with an actual storage of 14.1 km<sup>3</sup> and a surface area of 674 km<sup>2</sup>. Syria's famous dams which have a medium surface area and thus a medium storage capacity are: the Arrastan (228 million m<sup>3</sup>); the Qattinah (200 million m<sup>3</sup>); the Mouhardeh (67 million m<sup>3</sup>) and the Tal-Dau (15 million m<sup>3</sup>). The third type of dams are those dams with a small surface area and thus a small storage capacity (about 20 million m<sup>3</sup>). The important and the largest of which is Dam of Daraa with an actual storage of (15 million m<sup>3</sup>). The greater part of these dams is constructed near Homs and Hama. Other lakes are Lake Al-Jabboul near Aleppo with a surface area of about 239 km<sup>2</sup>, and Lake Qattienah near Homs (FAO, 2009). In 2004, the total area prepared for irrigation was expected at 1,439,100 ha, about 16 % of arable land, which is about 6 % of the total area of Syria (Miski & Shawaf, 2003). Irrigated areas are not spread regularly across Syria and the majority is concentrated in the Mohafazat (Governances) of: Al-Hasakeh (33.1 %); Arraqqqa (13.6 %); Aleppo (13.1 %); Hama (10.6 %); and Deir Azzour (10.1 %) (CBS, 2006). Irrigation water is largely pumped from wells, while the rest is river and spring water (Miski & Shawaf, 2003). About 73.9 % of the water resources in Syria are used in irrigation, 20 % is used in industry and 4 % in households (Miski & Shawaf, 2003). The main sources of the total irrigation water (22,491.00 m<sup>3</sup>) in Syria are: surface water (16,477,000 m<sup>3</sup>); renewable underground (2,321,000 m<sup>3</sup>); and springs (3,693,000 m<sup>3</sup>) (Akkad, 2001).

"Much of the agriculture is concentrated in the ancient "Fertile Crescent" which extends in an arc from the inner rim of the coastal mountains, through northern Syria and down the Euphrates valley into Iraq. The main crops are: cotton, wheat, barley, rice, olives, millet, sugar-beet and tobacco" (Murdoch et al., 2005). Dry farming of cereals, food and feed legumes is the backbone of agriculture in Syria. Moreover, based on land use, Syria is categorized into four major groups (Fig. 3.4) as follows: 1) cultivable land (6.22 million ha). The cultivated land is estimated at 5.66 million ha or 94.07 % of the cultivable land. Of this area, 4.27 million ha involves annual crops, and 0.67 million ha involves permanent crops. About 62.41 % of the cultivated area is situated in the three northern governorates (Aleppo, Arraqqqa and Al-Hasaka), representing only 33 % of the total area of Syria. The total agricultural crop production records for 1997 were: 4.318 million tons of grain, 2.249 million tons of agricultural raw products for industry, 2.118 million tons of fruits, 1.920 million tons of vegetables, and 183,000 tons of pulses. These statistical records represent a quadrupled increase in agricultural products during the two later decades; 2) uncultivable land (3.68 million ha); 3) pasture, steppe and desert land (8.23 million ha), which is only appropriate for grass growing and it is used as pastures during the years of enough precipitation for grazing sheep and goats. The Al-Badia once offered the most important feed needs for five million sheep, but now only provides 20-25 % of this. The Al-Badia offers two thirds of all red meat production in Syria and one third of all milk; and 4) forests (0.57 million ha) (Akkad, 2001; Miski & Shawaf, 2003; Kangarani, 2006; CBS, 2009).

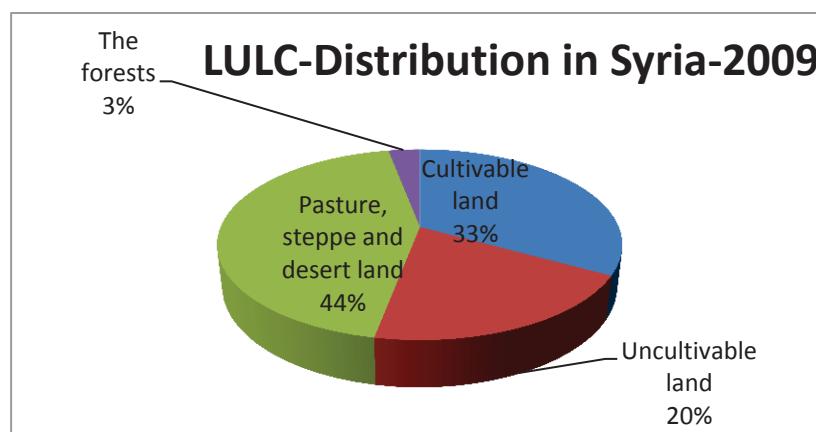


Fig. 3.4: Land use/land cover distribution in Syria in 2009 (Source: Modified from: CBS, 2009)

The total area of rain-fed land (3,636,000 ha) is divided into five Agricultural Settlement Zones (ASZ) (Fig. 3.1). The borders are generally delineated on the basis of the precipitation amounts. These zones are: "a) first agro-climatic zone: with average annual precipitation greater than 350 mm, the total area of this zone (2.071 million ha), represents 13 % of the total area of the country and includes around 28 % of the total cultivated land and 60 % of pastoral land. It is subdivided into two sub-zones: 1) a sub-zone with precipitation greater than 600 mm, where rain-fed crops are grown without any risk; and 2) a sub-zone with precipitation between 350 and 600 mm, where only two seasons out of three are secured. This zone can be mainly cultivated with wheat, legumes and summer crops; b) second agro-climatic zone: with average annual precipitation between 250-350 mm, two out of three seasons are secured in this zone. Its total area (2.473 million ha), represents 15 % of the total country's area and includes 30 % of the total cultivated land. The actual cultivated area in this zone in 1998 was 1.358 million ha, out of which 143,000 ha were planted with fruit trees and 1.215 million ha with field crops (mainly barley, wheat, legumes and summer crops); c) third Agro-climatic Zone: with an average annual precipitation greater than 250 mm in more than half of the seasons. The total area of the zone is 1,306 million ha, representing 7 % of Syria's total area. The actual cultivated area in 1998 (830,000 ha) was planted with field crops (maize, lentils and chickpeas); d) fourth Agro-climatic Zone: with an average annual precipitation between 200 and 250 mm in more than half of the seasons. The area under this zone is about 1.833 million ha, representing 10 % of the total country's area. The actual cultivated area in 1998 reached 592,000 ha, out of which 7,000 ha were planted with trees and 585,000 ha were planted with field crops (maize, wheat, barley, lentils and chickpeas); and e) fifth Settlement Zone: with an average annual precipitation of less than 200 mm in more than half of the seasons". Here locate the Syrian Desert and the marginal-lands. The total area of this zone is 10.208 million ha, i.e., 55 % of Syrian's territory. This zone is only suitable for grazing, were 86 % of the Syrian's pastures located here. In general, there is a mechanism to determine types of crops to be plants in each year for each ASZ (Akkad, 2001).

Syria can be divided into five major agricultural regions, i.e.: 1) the southern region which covers about 15.7 % of the total area of Syria and contains Damascus, Daraa, Assuweida, and Al-Qunaytirah. It is well-known for production of the fruit, especially apricots, apples and grapes, but it also produces crops such as chickpeas and tomatoes, besides raising livestock. Between 1998 and 1999, the region's involvement to national production was: 36 % of chickpeas, 51 % of apples, 31 % of grapes and 62 % of apricots; 2) the central region accounts for about 27.6 % of the total area and includes Hama and Homs. It produces largely sugar beets, dried onion, potato and almonds. Between 1998 and 1999, the region's involvement to the national production was 57 % for sugar beets, 53 % for dried onions, 31 % for potatoes, and 14 % for irrigated wheat; 3) the coastal region on the Mediterranean sea contains the cities of Lattakia and Tartous. Although this region is relatively small (2.3 % of the total area), its involvement to the national agricultural production was 98 % of citrus, 42 % of olives, 55 % of tomatoes and 56 % of tobacco; 4) the northern region covers 12.6 % of the country's total area and contains the cities of Aleppo and Idleb. Its major involvements to the national agricultural production are lentils with 55 %, chickpeas 51 %, olives 56 % and pistachios 69 %. Local farmers breed about 20 % of the total Syrian sheep population; and 5) the eastern region is the largest in the country, including 41.8 % of the total area, and contributes to production of cereals and cotton. In order to enhance productivity several irrigation networks were built in this region, especially on the Euphrates and Al-Khabour rivers; and a number of wells were constructed. Farms have a tendency to focus on irrigated wheat which adds 64 % to the national production, while rain-fed wheat contributes 38 %, cotton 63 % and lentils 29 % (CBS, 2003; FAO, 2009).

Syria with its entire territories of 18.5 million ha, has 5.66 million ha cultivated areas. 1,439,100 ha, or 25.42 % of these cultivated areas are irrigated (Miski & Shawaf, 2003). The area stability of these irrigated lands relies essentially on the actual Syrian's share from water of the rivers that spring from border countries. 349,820 ha from the total irrigated lands locate within the irrigation projects of the government. 272,859 ha or 78 % of these irrigation projects receive the water from drainage. The ownership of irrigated parcels in Syria is in general small in comparison to the rain-fed holdings size, and change from region to another. Almost 75 % of Syrian's farmer have about 10 ha of agricultural holdings (irrigated and/or rain-fed). However, each household has only about 3.5 ha of irrigated land (FAO, 2009).

The irrigation water resources were in general (1993): from groundwater with 62 % (pumped from the wells); and from surface water with 39.8 % (gravity-fed or pumped from the rivers and lakes). The irrigated systems are: the traditional practiced one is the flooding for irrigation of cereals; the furrow irrigation for vegetables; the basin irrigation for trees; and sprinkler irrigation with about 30,000 ha (FAO, 1993 b; MAAR, 1993 b; UNDP/FAO, 1994).

There is a broad variant in cropping samples in the irrigated areas, based on the water resources existing and the agro-climatologic circumstances. Strategic crops such as wheat and cotton are concerted in the northern and eastern region of Syria. More than 50 % of the wheat and cotton producing offers from the Al-Hasakeh governorate, in the north-eastern region of Syria (MAAR, 1993 a). The production of winter vegetables is located mainly in the coastal region, while summer vegetables are located mainly in the inside plains, especially in the central and southern areas. In 2004, of the total area prepared for irrigation of 1,439,100 ha, about 0.89 million ha were used for annual crops, where the cropping amount/intensity for annual crops achieving 121 %, leading to a total cropped area of annual crops of about 1.08 million ha (CBS, 2008).

The vegetation throughout Syria, from the rainy mountains to the Mediterranean semi-desert, has been greatly changed by human intervention and seriously degraded (after German to English translation and modification from Wirth, 1971). Syria has no less than four major floral regions: mediterranean (western Syria); the Euro Siberian (mountains of the northwest); the Irano-Turanian (intra- and east Syria); and finally the Saharo's-Indian (south Syria). The surviving vegetation includes oak maquis on the narrow coastal plain and foothills, remnant coniferous forests on the slopes of the Jabal Al-Nusayriyah and along the Anti-Lebanon range, and subalpine and alpine communities above 2,000 m in the southern mountains. The floral elements in the steppes of central, north and east Syria are made up of *Pistacia atlantica*, *Artemisia herba-alba*, *stipa barbata*, *Poa sinaica*. In the southern desert steppe and Euphrates Valley, Date palm, *Haloxylon salicornicum* and *Populus euphratica* can be found among the mainly Irano-Turanian vegetation (after German to English translation and modification from Wirth, 1971). The main landscapes and leading vegetation categories in Syria were lately summarized by Evans (1994); and Murdoch et al. (2005).

## **B. The Euphrates River Basin (ERB)**

The name of this river comes from Old Persian and means "good to cross over". The geographical coordinates of the Euphrates River Basin are 36°49'N, 38°02'E at the Turkish border and 34°29'N, 40°56'E at the Iraqi border. The ERB (Fig. 3.1) includes the majority of the three governorates of Halab/Aleppo, Arraqqa and Deir Azzour. The variation in altitude (Fig. 3.2) is from ca. 520 m at the Turkish border to ca. 185 m at the Iraqi border. The Euphrates goes up in the mountains of eastern Turkey, and the sink has high mountains to the north and west and wide plains to the south and east. Two-thirds of river's course flows throughout the highlands of eastern Anatolia in Turkey and the valleys of the Syrian and Iraqi flat terrain before down-warding into the arid plain of Mesopotamia. The Euphrates has its sources in the eastern highlands of eastern Turkey, between Lake Van and the Black Sea, and is created by two major tributaries, the Murat and the Kara-su. It enters the Syrian territory at Karkamish, down-tributary from the Turkish town of Birecik. It is

then joined by its major tributaries, the Al-Balikh and Al-Khabour, which too begin in Turkey, and streams southeast across the Syrian flat terrain before inflowing Iraqi terrain near Qusaybah. The Euphrates watershed includes five countries (Table 3.3): Turkey, Iraq, Syria, Saudi Arabia and Jordan. Of its total area of 350,000 km<sup>2</sup>, 28 % (98,000 km<sup>2</sup>) lies in Turkey, 17 % (59,500 km<sup>2</sup>) in the Syrian Arab Republic, 40 % (140,000 km<sup>2</sup>) in Iraq, 15 % (52,500 km<sup>2</sup>) in Saudi Arabia, and just 0.03 % (105 km<sup>2</sup>) in Jordan (Kattan, 2008). The Saudi Arabian Euphrates dries in summer and there are no permanent rivers. The water requirements of Saudi Arabia and Jordan is a small proportion of watershed. The Euphrates River, at 3,000km in length, is the longest river in south western Asia, divided between Turkey (1,230 km), the Syrian Arab Republic (710 km) and Iraq (1,060 km). Some 62 % of the catchment part that generates contributions to the river is located in Turkey and 38 % in Syria. Its real annual volume is 35.9 billion cubic meters (Kibaroglu, 2002; Kangarani, 2006; FAO, 2009). For almost its total length, the river streams in a valley changeable in width from 2 to 12 km, and with the valley base some 80-250 m less than the neighboring plains. In several places, the river splits into two or more canals, constructing several atolls/islands, several of which support dense thickets. There are also meanders, oxbow lakes, gravel pits and silted old water courses covered in reed-beds. Much of the river bank contains low alluvial cliffs. The water level was previously some 3-4 m higher in spring than in autumn due to the snow-melt in the Turkish highlands, but with the production of several large dams in Turkey during the previous decade, this yearly flood is now greatly decreased.

The Euphrates River has a number of main tributaries where the Syrian government has carried out numerous projects. These flows are: 1) The Al-Khabour River (460km), which rises in the Raas Al-ain region in Syria and flows into the Euphrates; 2) The Assajour River, which originates in Turkey and flows through Syria for a length of 48 km; its annual runoff is 100 million m<sup>3</sup>; and 3) The Al-Balikh River, which rises near the Syrian villages of Aain Al-Arous and Tal-Abiad and flows through 105 km within Syria before joining the Euphrates. Its annual runoff is 150 million m<sup>3</sup>.

Table 3.3: General statistical information on the ERB (Source: Modified from: Kattan, 2008; FAO, 2009)

Country-Name	Basin-Area/km <sup>2</sup>	Length/km	Catchment-Area/%
Turkey	98,000	1,230	62
Syria	59,500	710	38
Iraq	140,000	1,060	0
Saudi Arabia	52,500	0	0
Jordan	105	0	0
Total	350,000	3,000	100

### C. Irrigation projects in the ERB

Since the 1970s, attention was given to drainage and irrigation rehabilitation, largely in the Euphrates Valley, where irrigation using water pumped from the river was improved quickly since the 1950s. Significant development was made in renovating large irrigated areas which fell out of cultivation because of water-logging and salinity, especially in the lower and middle parts of the Euphrates Valley (DIWU, 1993).

Table 3.4 explains the water requirements in the three major ERB countries. The available level of irrigated agricultural projects in Syria on the Euphrates is 194,000 ha (although according to other sources, it is about 250,000 ha). Over the coming decade, some further 542,275 ha will be irrigated, thus in the future, some 636, 275 ha will be irrigated in Syria with water from the Euphrates. The future water demand, including steam water, equals 13.263 billion m<sup>3</sup>. If we deduct from the returning water 2,463 billion m<sup>3</sup>, one obtains net 10.8 billion m<sup>3</sup>, representing the water needs of Syria from the Euphrates. This amount represents 34 % of current flow.

In 1987, Syria and Turkey signed a water agreement over the Euphrates River, determining the water flows on the Syrian-Turkish border at 500 m<sup>3</sup>/second. In 1990 a similar deal was agreed to between Syria and Iraq, dividing the Euphrates into the proportions of 42 % for Syria and 58 % for Iraq, thus allowing the current water situation for Syria of not more than  $15.7 \times 0.42 = 6.627$  billion m<sup>3</sup>/pa Euphrates water. The 15.7 billion m<sup>3</sup>/pa corresponds to the amount of water that flows from Turkey towards Syria, as a result of the temporary agreement of 1987. Research sources expect that the 6.627 billion m<sup>3</sup>/pa Euphrates water are sufficient only for the irrigation of 308,000 ha instead of the planned 640,000 ha. According to others, a deficit of one billion m<sup>3</sup> in Syria will give a proportion of withering from 26,000 ha of agricultural land and transform it into unusable land. This would lead to at least a total of 110,000 ha from 640,000 ha, that could be converted to unusable lands (Al-Fares, 2007).

Table 3.4: The water needs in the countries located on the Euphrates River (Source: Al-Samman, 1991)

	Turkey	Syria	Iraq	Total
The executed agricultural facilities/in ha	300,000	194,000	1,200,000	1,694,000
The futuristic facilities/ha	1,146,300	542,275	752,400	2,840,975
The total agricultural land/ha	1,446,300	636,275	1,952,400	4,024,975
The total amount of the waters' needs in future (irrigation + evaporation)/billion m <sup>3</sup> /pa	17.40	13.26	25.10	55.76
The returning water/billion m <sup>3</sup> /pa	1.70	2.47	5.10	9.26
Net consumption (average)/billion m <sup>3</sup> /pa	15.70	10.80	20.00	46.50
Ratio of the net consumption to amount of the river flow/%	50 %	34 %	64 %	148 %

The Syrian needs from the Euphrates in 2000 were 11 billion m<sup>3</sup> water, as agreed to by most sources, Turkey's requirements were 15.7 billion m<sup>3</sup>/pa, and Iraq's usage was 13 billion m<sup>3</sup>/pa. Thus, the minimum requirement for water of the Euphrates for the three countries is equivalent to the equation:  $11 + 15.7 + 13 = 39.7$  billion m<sup>3</sup>/pa. If we consider that the average annual income of the Euphrates River does not exceed 27 billion m<sup>3</sup>/pa, it follows that a water deficit of more than 10 billion m<sup>3</sup>/pa exists, this, if Turkey agrees to reduce its share from 15.7 billion m<sup>3</sup>/pa to 12 billion m<sup>3</sup>/pa, and after Iraq has reduce its share from 20 to 13 billion m<sup>3</sup>/pa. The required amount of water from the Euphrates in the three riparian countries of Syria, Turkey and Iraq exceed the income of the river water to more than one-half. With this mind, the total area which can be irrigated from the Euphrates in the riparian countries cannot exceed 2.5 million ha, despite measuring 4 million ha in total, according to official statistics.

Syria too has its individual strategies for irrigation expansion within the Euphrates Basin (Table 3.5, Fig. 3.5). These include using waters from the Euphrates to irrigate six major regions: the Maskana-Aleppo Basin (155,000 ha); the Arrusafa Basin (25,000 ha); the Al-Balikh Basin (185,000 ha), the Euphrates floodplain (170,000 ha); the Al-Mayadin plain (40,000 ha); and the lower Al-Khabour Basin (70,000 ha). This is a total of 645,000 ha. The water need for such land, assuming a water application rate of about  $10,000 \text{ m}^3 \text{ ha}^{-1} \text{ yr}^{-1}$ , would be  $6,450 \times 10,000 = 64,500,000 \text{ m}^3$ , or about 16 % of the unregulated stream of the Euphrates where it enters Syria from Turkey (Beaumont, 1996).

Table 3.5: Reclamation and irrigation projects on the Euphrates River (Source: the Syrian Ministry of Irrigation, 2005)

Project name	The area, which have to irrigated/1000 ha	The current investment status
<b>1. The Al-Balikh Basin</b>	<b>141</b>	
1.1. The pioneering project (Arraed)	19.9	Under investment
1.2. Beer Al-Hishm project	10	Under investment
1.3. Reclamation project of the part (1-B)	10	Under investment



1.4. Remaining sections of the Al-Balikh Basin	101.1	Under construction
<b>2. The Euphrates Basin</b>	<b>152</b>	
2.1. The Middle Euphrates project	27	Under investment
2.2. The Lower Euphrates project	125	Under construction
<b>3. The Lower Al-Balikh Basin</b>	<b>70</b>	Under construction
<b>4. The Arrusafa Basin</b>	<b>25</b>	Under construction
<b>5. The Al-Mayadin Basin</b>	<b>40</b>	Under construction
<b>6. The Maskana Basin</b>	<b>166</b>	
6.1. The 17000-ha project and the state farm	21	Under investment
6.2. The Maskana-west project	20	Under investment
6.3. The Maskana-east project	17.8	Under investment
6.4. The rest of the Maskana Basin	107.2	Under construction
<b>The total</b>	<b>594</b>	-

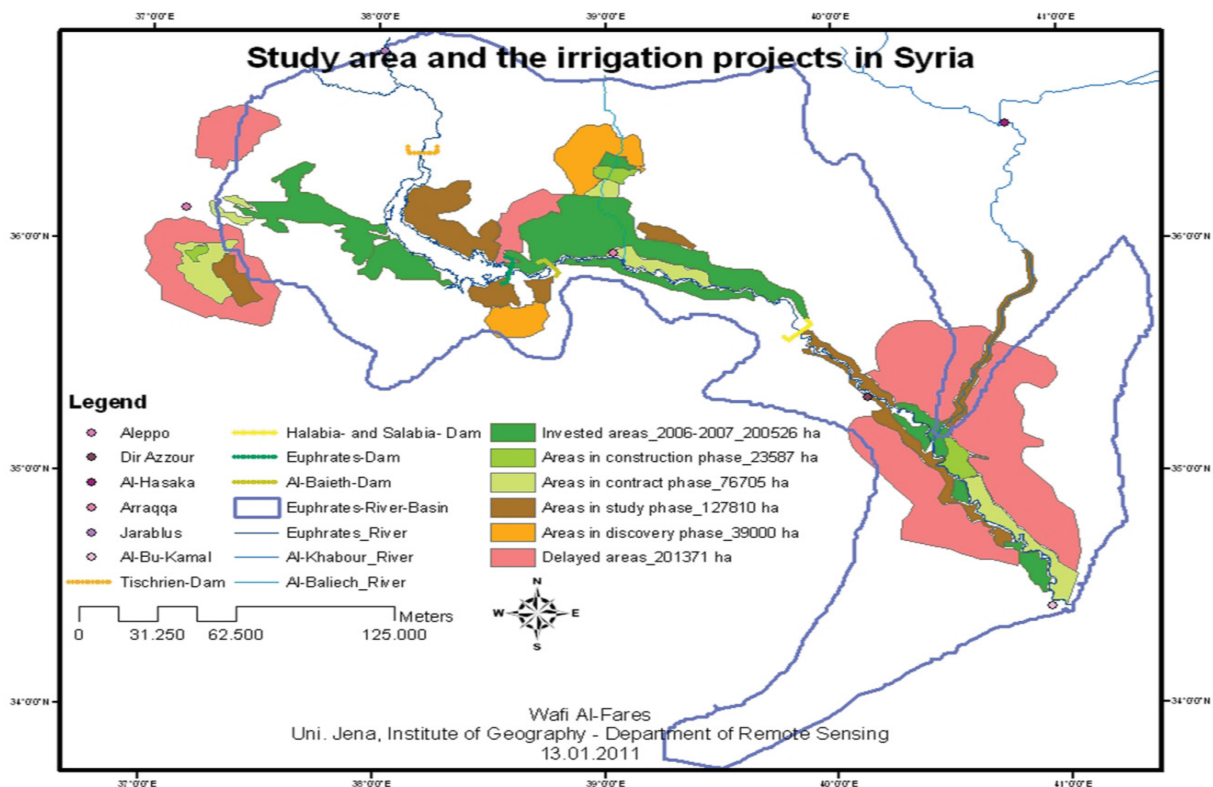


Fig. 3.5: Study area and the irrigation projects in Syria (Source: MAAR, 2008)

There are three big and major dams on Euphrates, which are: the Attabqa Dam, constructed between 1968 and 1975, has an actual water storage of 14.1 km<sup>3</sup>, and it produces electricity of 860 mw based on hydropower; the al-Baath Dam with the essential purpose of regulation the water quantity of Euphrates; and the Tishreen Dam with the essential purpose of producing the hydro-power based electricity, start of working was in 1991, has an actual water storage of 1.9 km<sup>3</sup>, and it produces electricity of 630 mw. The Lake Al-Asad behind the Attabqa Dam were constructed to increase the irrigated lands in ERB in Syria to be around 640,000 ha. Until 1997 about 240,000 ha were irrigated based on the storage water of Lake Al-Asad (Bagis, 1997).

In Euphrates one can recognize two major systems which practice to supply the water for the agricultural sector: 1) from surface water of the Euphrates and its tributaries (flooding, furrow, and canals); and 2) from groundwater (water extraction from wells) (Zaitchik et al., 2002). The mostly practiced irrigation system in ERB is the floodplain irrigation, were since thousands of years, human worked in agriculture along the Euphrates (Hillel, 1994 cited in Zaitchik et al., 2002). Close to the Euphrates planted crops in these floodplains benefit from flooding of the Euphrates using

small gravity-driven diversions and levee breaks. Far to Euphrates planted crops obtain the water using low-power diesel and electric pumps (Zaitchik et al., 2002).

The practiced drainage systems in ERB have two general types, i.e. surface (open) and sub-surface (covered) systems. As an example, about 62 % of the irrigated lands in the province of the Arraqa is drained. Almost 24 % of these drained lands was supplied with water using power-based irrigation methods (e.g., diesel, electricity). The open surface drainage system has the disadvantage that it leads to salinization in irrigated soils. This system was installed on about 90 % of the actual irrigated areas. For instance, soils about 60,000 ha of irrigated areas in the year of 1993 has been affected by salinization. Also, about 5,000 ha have to be totally new reclaimed due to water logging and salinization of the soils. The covered drainage system was installed on only a small area. Near Arraqa, about 10,000 ha essentially situated within the second Euphrates terrace were brought under irrigation in 1970. The land was sited for a modern irrigation project, with a soil survey carried out in 1980. Severe salinization with more than 16 ds/m of the soil paste extract was found in around 24 % of the project area as a consequence of lacking and inappropriate drainage system. The major reason for soil salinization was the planting of a new rice crop. Soil salinization is the major problem within the irrigated areas in the ERB, where about 3,000-5,000 ha of irrigated land have to be totally new reclaimed yearly (FAO, 1993 b).

#### **D. Climate**

"Most areas in the ERB have a sub-tropical Mediterranean climate with wet winters and dry summers. In the mountainous headwater areas, freezing temperatures prevail in winter and much of the precipitation falls in the form of snow. As the snow melts in spring the rivers rise, augmented by seasonal precipitation which reaches its maximum between March and May. In southeastern Turkey as well as in the north of the Syria and Iraq, the climate is characterized by rainy winters and dry warm summers. Average annual precipitation in the ERB is estimated at 335 mm, although it varies all along the basin area" (Hillel, 1994 cited in Kibaroglu, 2002). The yearly precipitation in the Mesopotamian plain is seldom above 200 mm, while it attains 1,045 mm in other parts in the basin. The summer season is very hot and dry with midday temperatures reach 50° C and daytime relative humidity about 15 %. These climatic conditions demonstrate that the Euphrates streams within arid and semi-arid areas inside Syria with increasing aridity downstream (Hillel, 1994 cited in Kibaroglu, 2002). The yearly standard temperature of the whole ERB is 18° C. It is about 5° C in January, although it can decline to -11° C in the coldest areas in the basin. This yearly standard temperature in July reaches 31° C, although it can raise to 37° C in the hottest areas (Hillel, 1994 cited in Kibaroglu, 2002; FAO, 2009). In the Syrian part of ERB, the winter season is usually cool (5-10° C) and rainy, and the summer is warm (30-45° C) and almost totally devoid of precipitation. The average annual air temperature increases from north to south, and differs between 18° C in Jarablous and 20° C in Al-Bou-Kamal, where the dryness becomes more emphasized. The average monthly precipitation increases - from October to May - from south at Al-Bou-Kamal with 5-30 mm to north at Jarablous with 20-60 mm. The average annual precipitation increases over the year from south at Al-Bou-Kamal with about 130 mm, over Dir Azzour with about 160 mm, to the north at Jarablous with about 350 mm. The average yearly precipitation value over the whole ERB in Syria is around 240 mm. The average yearly value of the relative air humidity differs between 56 % (Jarablous) and 47 % (Dir Azzour), and declines to less than 44 % (Al-Bou-Kamal), the lowest recorded value in Syria. The highest values of average monthly relative humidity (60-70) % are commonly observed during the coolest time period (i.e., December to January), while the lowest 25-30 % happen in the warmest months (i.e., July and August). The potential evapo-transpiration value commonly goes above the precipitation and varies from 1,300-2,600 mm, with an average yearly value about 2100 mm (Kattan, 2008). Fig. 3.6; Fig. 3.7; and Fig. 3.8 illustrate the geographical distributions and the values of the precipitation, temperature and evaporation.

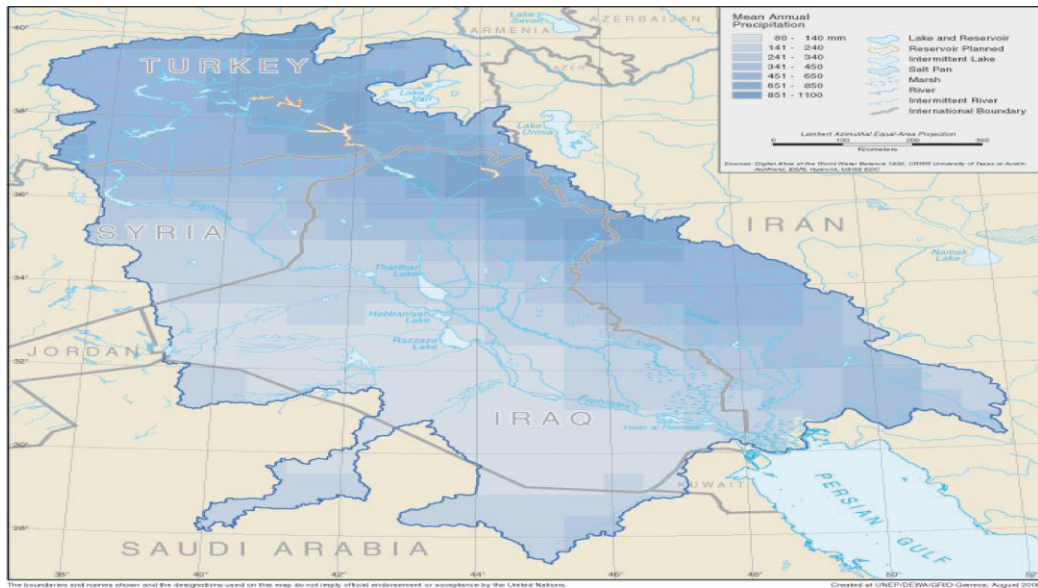


Fig. 3.6: Precipitation in the Euphrates-Tigris Basin (Source: <http://www.grid.unep.ch/product/map/index>)

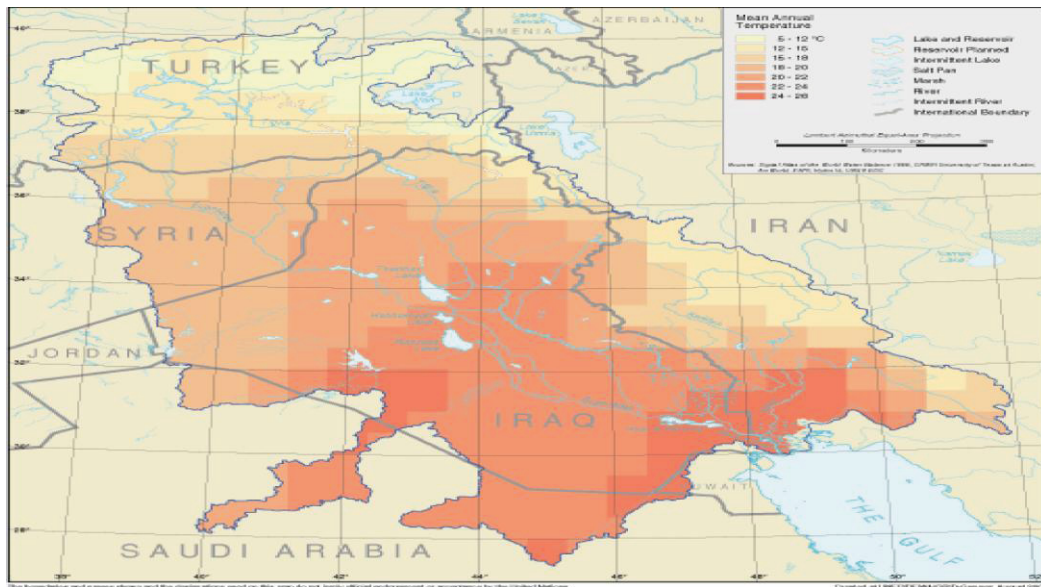


Fig. 3.7: The temperature averages of the Euphrates-Tigris Basin (Source: <http://www.grid.unep.ch/product/map/index>)

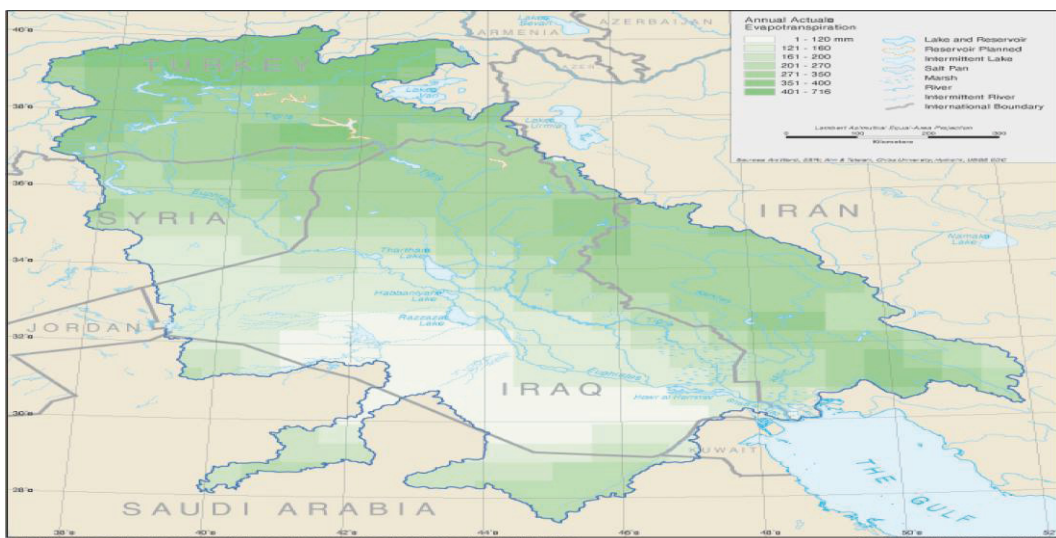


Fig. 3.8: The evaporation averages of the Euphrates-Tigris Basin (Source: <http://www.grid.unep.ch/product/map/index>)

The ERB in Syria is located in two general climatic zones: 1) Mediterranean-influenced steppe climate: in dry and drought years, precipitation is often not enough for growing winter wheat, thus crop failures threaten. In January, average temperatures of about 5° C make frosts of -5° to -10° C possible. There are two variants: a) west-Syrian's steppe climate (stations: Hama, Aleppo, Menbij and Daraa). This variation is to some extent DI > normal expression < the Mediterranean-influenced Syrian steppe climate. In the sequence of shape changes between the heavily stained oceanic climates of the west and the highly colored continental climates of the east, the west-Syrians steppe climate adapts all its manifestations without a break; and b) East-Syrian's steppe climate. This is located out of the range of this study of the ERB. 2) desert climate: the desert climate in Syria is at the continental end of the so called west-east-sequence. The number of months during which one can expect precipitation is three to four, similar to the steppe climate. At these times, the precipitation amount is line with the average per month-precipitation, but it falls heavily. Under these conditions, it is usually not economical to cultivate crops without additional irrigation. On the whole, however, the Syrian Desert climate is characterized by dry air and clear visibility. It has two variants: a) the Syrian Desert climate (stations: Damascus, Qariateine. Dir-Azzour, Arraqa and Palmyra): with annual precipitation between 120 and 220 mm, crops are only able to thrive in pronounced wet years or through soil and relief of preferred sites. Opportunistic cultivation of this kind can only be operated by sedentary settlements. Supplementary irrigation fields must provide alternative nutrition and merit bases to cater for the possibility of drought years. However, the likelihood of rain in winter and spring is usually enough to leave a good pasture for the herds of the Bedouin and semi-nomads; and b) full Syrian Desert climate (stations: Attanf and Al-Bou-Kamal): precipitation has remained at an average of less than 120 mm per year for many years. Apart from irrigation areas which provide the base for crop cultivation, the availability for pasture is very sparse. The area of the Syrian Desert is therefore an empty space, usually avoided even by full-nomads (after German to English translation and modification from Wirth, 1971).

### E. Morphological structure

The major topographical characteristic of ERB territories is the simplicity (Fig. 3.9). There are some of little height hills, essentially areas surrounds the Lake Al-Asad. The average height of ERB territories is 350 m in the north at Jarablous and 180 m in the south at Al-Bou-Kamal. Euphrates's "base valley" located downstream below 200 m. Its path-slope is about ( $0.25 \text{ m/km}^{-1}$ ) (Kattan, 2008).

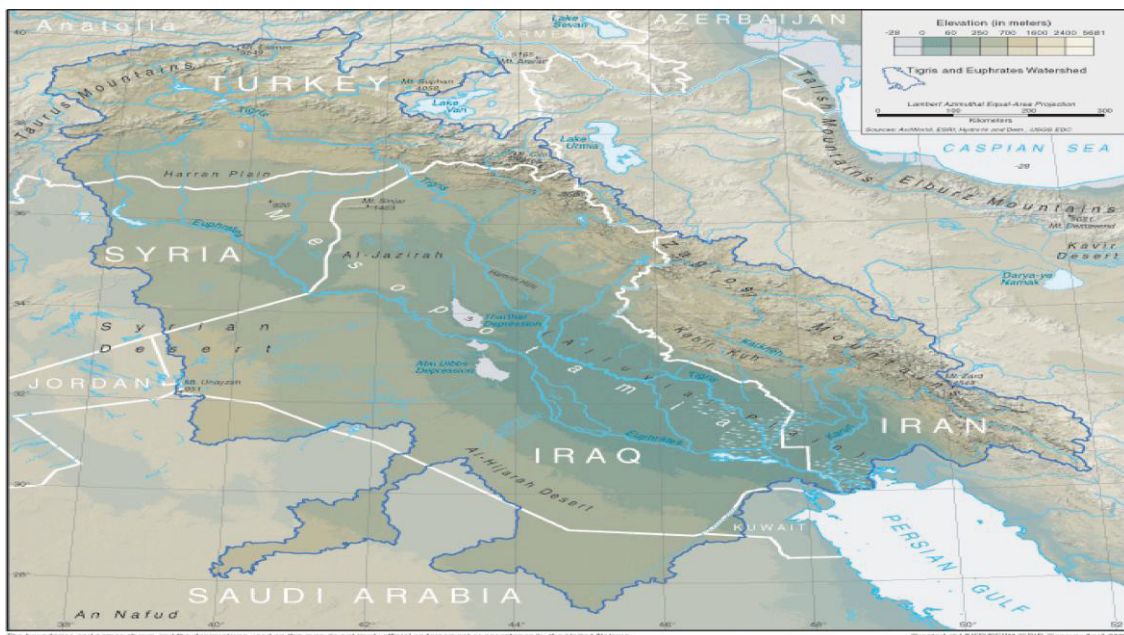


Fig. 3.9: The topography of the Euphrates-Tigris Basin (Source: <http://www.grid.unep.ch/product/map/index>)

Euphrates has a length of about 675 km in Syria. It across Syria within a low geological formation. The major geological components return to the three geological times: Paleogene (argillaceous limestone); Neogene (gypsum, silty clays, sandstone, siltstone, clays, and pebbles); and Quaternary (pebbles, gravels, loams, and sandy loams) (Ponikarov, 1967). The alluvial aquifer, composed mainly of gravels and boulders at the base and bigger alluvial sediments (i.e., loams and sandy loams) at the top, is the mainly significant water bearing system in the basin (Gersar-Scet, 1977; Kattan, 2008).

## F. Soils

Soil is found on either side of the Euphrates in Syria which despite having copious irrigation, offers unfavorable growing conditions, and thus reduce crop yield. The humus is low in the arid east, where mostly raw soils are found on soft, low resistive source rock. The soil debris, the plaster floors, and dust and loose soils of the Syrian desert steppe and desert are heavily climate conditioned. This may represent an almost insurmountable obstacle for agricultural use in the northeast of Aleppo, especially for trees and vines. Soils with a high salt or gypsum content are not suitable for agricultural use. Fortunately, the Miocene gypsum and anhydrite of the lower Fars in Syria is found only in a large area in the desert steppe. The salt or salt surfaces of Sabchat Al-Jabboul, which today is the dry-end lake Syria, are also not so significant (after German to English translation and modification from Wirth, 1971). Gypsiferous crust soils covers a wide parts of ERB territories. The breakdown of irrigation water canals because flowing of the water within canals material due to soil salinization. The second major reason for salinization is over-pumping. After salinization due to the aforementioned reasons, the soil will be exposed. As a result, ERB soils have to be carefully irrigated (FAO, 1993 a).

## G. Hydrology

The Euphrates River has a relatively regular watery regime/system, described by two months of very high rate stream in April and May, and a phase of eight dry months from July to February (Fig. 3.10). The yearly stream differs significantly from year to year (Fig. 3.11), as well as very low stream records between July 1957 and January 1963, during which time the average flow decreased to only 83 % of the long-term average. Euphrates's discharge rate is from 200 to 300 m<sup>3</sup>/sec. It begins to increase during early spring, i.e. in February. Then, becomes it more abundant in March during the melting of snow in the high mountains in Turkey. The peak of discharge is in April and May with 2,000 m<sup>3</sup>/sec and sometimes more. Because snow melts on peaks of mountains and because the high rates of precipitation in April and May, the maximum flooding will be happening from mid-April to early May. Starting from July, the discharge begins to decrease. The bottom of discharge is either in September or in October. In April and May, discharge during the two months records for 42 % of the yearly full amount. Minimum streams happen from August through October and add only 8.5 % of the whole discharge (Beaumont et al., 1988; Shahin, 1989).

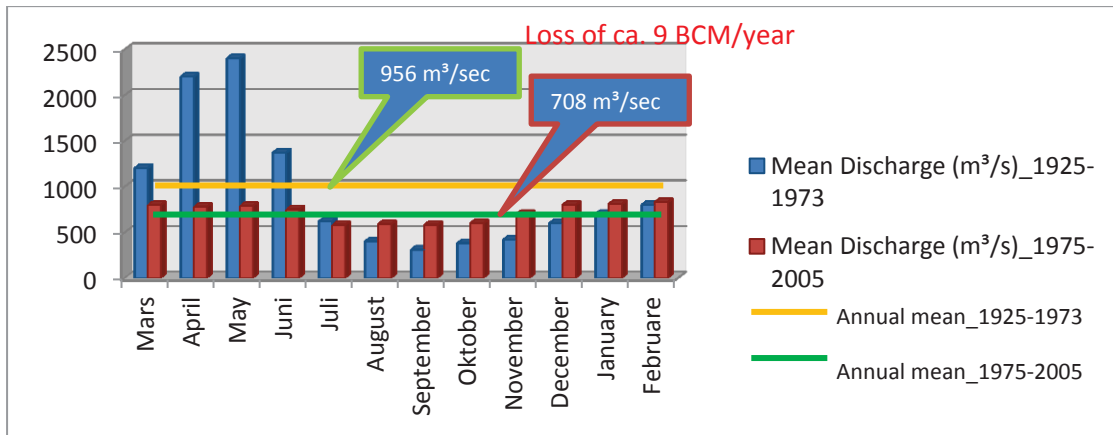


Fig. 3.10: Euphrates River monthly mean discharges (m³/s) for the period 1925-2005 (Source: Adapted from DIWU, 2009)

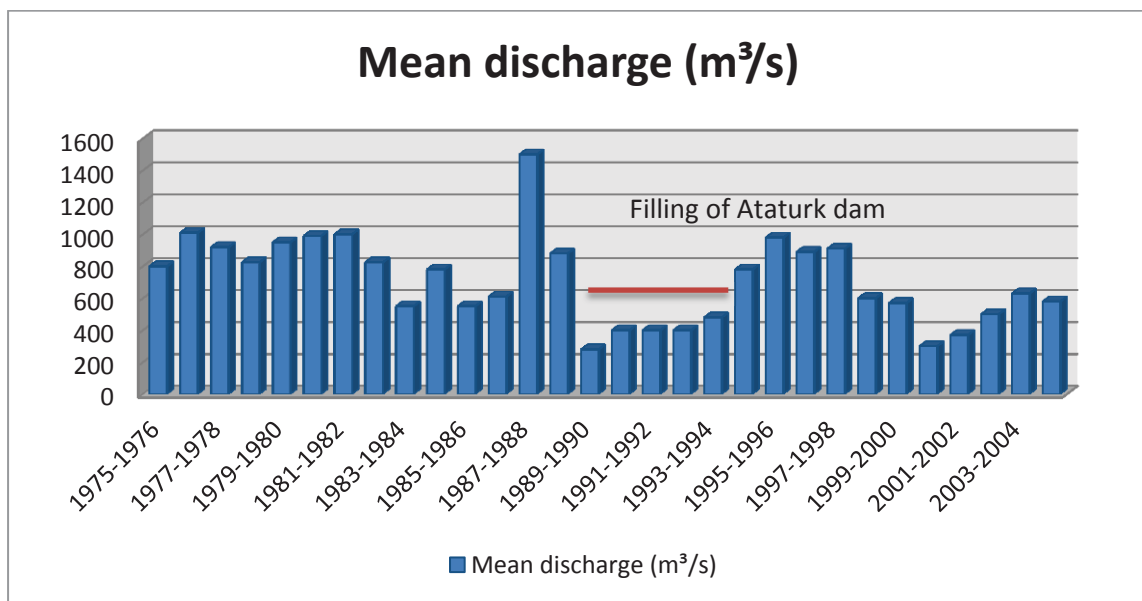


Fig. 3.11: Mean annual discharge of the Euphrates River (m³/s) for the period 1975-2005 (Source: Adapted from DIWU, 2009)

Only about 12 % of the ERB hydrous-network, that supplies the Euphrates River with water, located in the Syrian's territories which cover almost 1/3 of Syria. The other major 88 % hydrous-network is formed in Turkey. Euphrates has three main tributaries: Assajour; Al-Balikh; and Al-Khabour. There is no estimation about contribution of the precipitation above the Turkish territories in stream of these three tributaries. In general, this contribution supplies the Euphrates with about 95 % of its actual flow (Beaumont, 1996). The rest of the riparian countries add very little water (FAO, 2009). No other tributaries stream into the Euphrates after the Al-Khaour, excluding in Iraq, where some of the Tigris' waters are added. The observed average yearly stream across the Turkish/Syrian boundary is 29.8 billion m³ (29.8 km³). The natural stream of the river can be given as 33.4 bcm (33.4 x 10<sup>9</sup> m³) annually (Beaumont et al., 1988; Shahin, 1989), 30.0 km³ from Syria to Iraq (FAO, 2009).

"One of the problems in the Euphrates system has been the variability of flow from year to year. Long-term records on the upper Euphrates before the construction of major dams (1937-1964) have revealed that minimum discharge fell to 16.871 MCM/y (1961), while a maximum value of 43.457 MCM/y was recorded in 1963. Such large variations in discharge have made it difficult to plan irrigation schedules efficiently in the lower part of the basin when no water storage capacity has been available" (Beaumont, 1996).

Starting from the middle of the 20 century, the Euphrates had no longer its own natural hydrological system due to the building of artificial dams (20 in Turkey) and a station that use the hydro-power to produce the electricity (17 in Turkey). In Syria, only three smaller dams (Tishreen, Euphrates/or Attabqa and Al-Baath) were constructed, with the plan to stop the main flooding and to produce the electrical power (Kattan, 2008). Syria started the using of the water of the Euphrates for irrigation and for hydropower in the early 1960s. The Attabqa Dam with its large lake (length 75 km) was constructed on the Euphrates in 1973, largely with the assistance of the then Soviet Union. The purpose of this main dam was to meet the Syrian's water and energy needs. The Al-Baath Dam, finished in 1986, was the second Syrian dam on the Euphrates River. But, the hydro-power capacity of the Al-Baath Dam was not of the same amount as the Attabqa Dam. The Al-Baath Dam had a limited capacity for electricity generation and provided relatively little water for irrigation. The Tishreen Dam, the third Syrian dam on the Euphrates essentially planned for hydropower, is still under building (Korkutan, 2001; FAO, 2009).

"The average monthly discharge at the Syrian-Turkish border ranges between 450 and 886  $\text{m}^3/\text{s}^{-1}$ , with several peaks during winter and summer periods, and obviously lower registries 250 – 875  $\text{m}^3/\text{s}^{-1}$  at the Syrian-Iraqi border (Al-Bou-Kamal). Similar temporal patterns in river discharge can be observed for the upstream stations of Jarablous and the Tishreen Dam. Downstream of the Euphrates Dam, the river discharge trends have a different evolution, and thus the temporal discharge patterns at the monitored stations (Al-Baath Dam and Al-Bou-Kamal) are similar and generally identical to the outflow discharge from the Euphrates Dam" (Kattan, 2008). The average monthly discharge of the Euphrates River at the Jarablous station previous to the 1960s was about 735  $\text{m}^3/\text{s}^{-1}$  (UNDP-FAO, 1966). During the previous few decades, the river discharge was managed and controlled by Turkey, through an agreement that fixed the minimum monthly river discharge for both Syria and Iraq at about 500  $\text{m}^3/\text{s}^{-1}$ ). On several occasions in recent years, low water levels in the Lake Al-Asad reservoir behind the Attabqa Dam were restricted the hydro-power output (with an installed capacity of 800 MW) and irrigation development. In the 1970s Syria had planned to reclaim 640,000 ha or more in the Euphrates Basin. In 1989, 80 % of the natural run-off of the Euphrates River was developed by closing the Ataturk Dam, the biggest dam in Turkey, with a gross reservoir storage volume of  $48.7 \times 10^9 \text{ m}^3$  (effective volume:  $19.3 \times 10^9 \text{ m}^3$ ).

## H. Vegetation and land use - land cover

Fig. 3.12 illustrate the broad general LULC-features in the whole Euphrates-Tigris Basin, while Fig. 3.13 provide general information about the LULC-activities in the ERB and Syria.

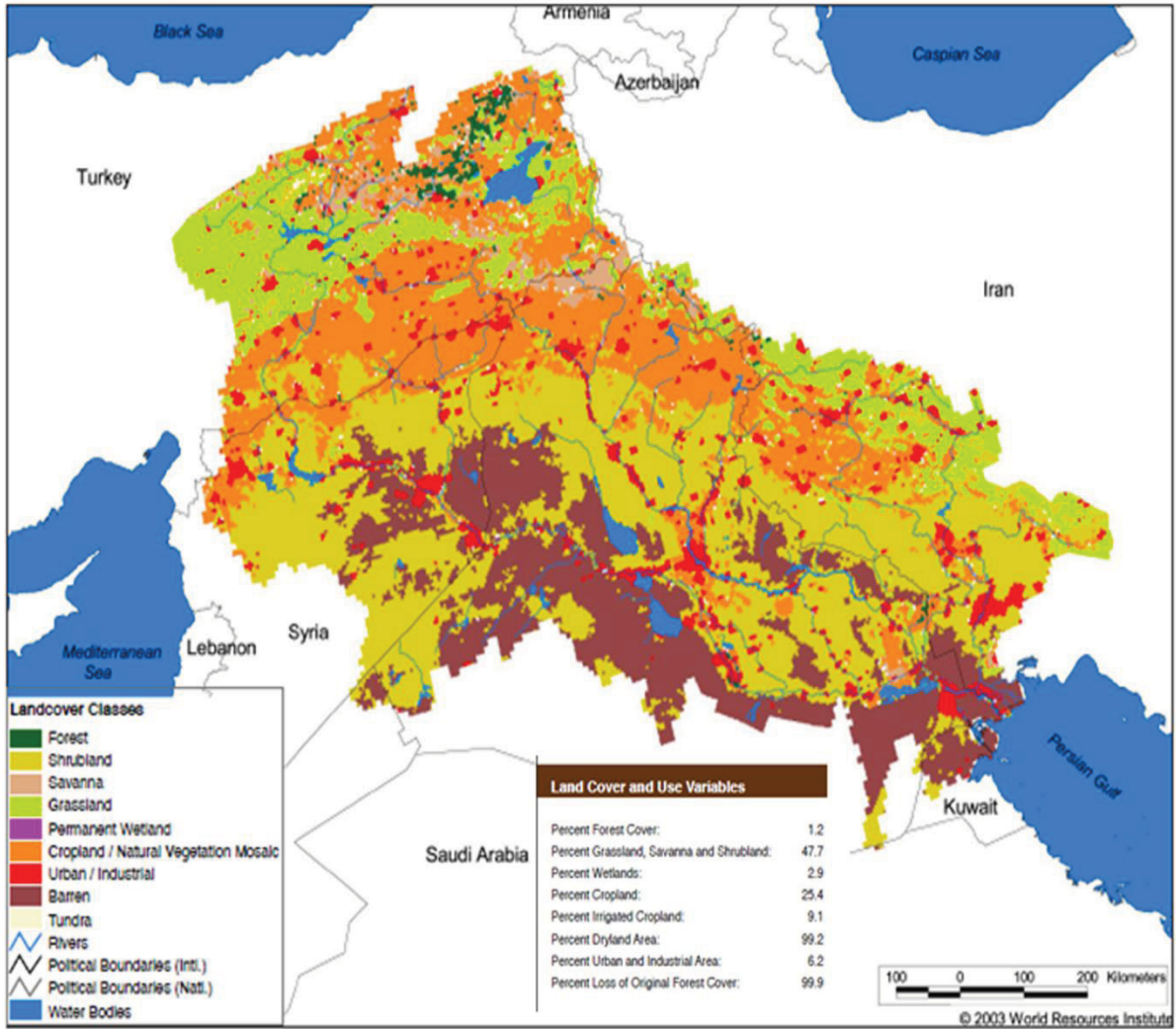


Fig. 3.12: LULC- spatial distribution in the Euphrates-Tigris Basin (Source: [http://earthtrends.wri.org/pdf\\_library/maps/watersheds/eu28.pdf](http://earthtrends.wri.org/pdf_library/maps/watersheds/eu28.pdf))

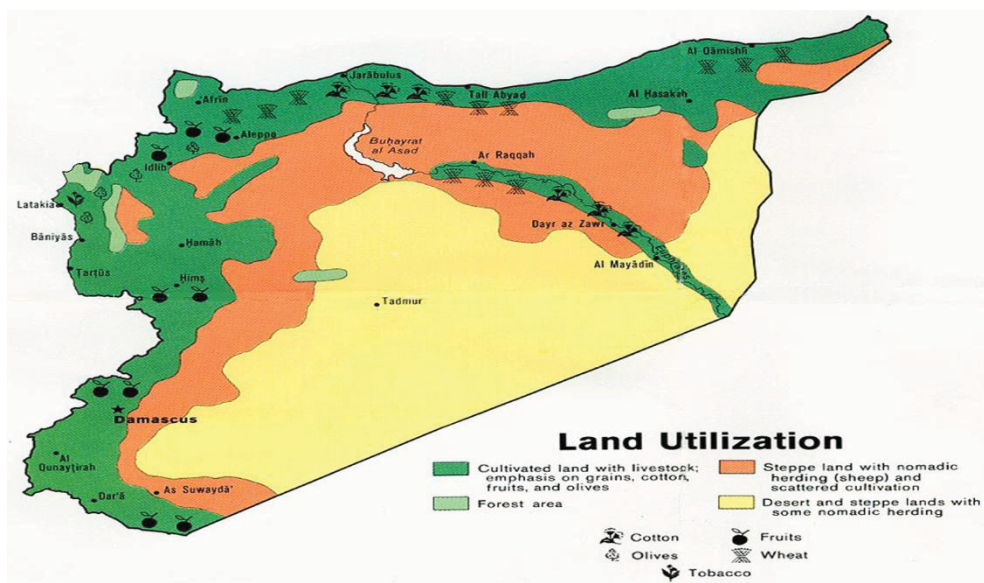


Fig. 3.13: Approximate spatial LULC-distribution in the ERB and Syria (Source: [http://images.nationmaster.com/images/motw/middle\\_east\\_and\\_asia/syria\\_land\\_1979.jpg](http://images.nationmaster.com/images/motw/middle_east_and_asia/syria_land_1979.jpg))



The natural vegetation of the Euphrates River Basin includes riverine thickets of *Populus euphratica*, *Tamarix articulata*, *Salix* sp., *Glyzyriza glabra*, *Lycium barbarum*, and reed-beds of *Phragmites* sp. and *Typha* sp. The river banks are intensively cultivated: There are vast areas of irrigated cotton and cereals, as well as orchards and plantations of *Populus* and *Pinus halepensis*. The heavily cultivated steppe of the Al-Jazirah region lies to the east and the Syrian Desert to the southwest (Murdoch et al.; 2005). For instance, an old and random *Pistacia atlantica* trees found in Jabal Abd Al-Aziz region. For decades, no young growth has been recorded because the destruction of the undergrowth has significantly deteriorated the micro-climate and the soil surface is now largely eroded. It is predicted that it will take only a few more decades in many parts of Syria before all of the few remaining tree ruins die and the last remnants of former high forests will disappear. This is due in the main because of thousands of years of human cultural activity. The desert steppe in the ERB was originally densely vegetated featuring tall grasses over 50cm in height, with species such as *Stipa*, *Agropyrum*, and *Festuca* species dominating. This grassland likely contained sparse groves or woods of pistachios. In addition, it is thought the steppe was home to junipers such as *Juniperus excelsa*, *Kreuzdorn Rhamnus Palaestinae*, *Prunus*, *Pirus*, *Crataegus* and *Amygdalus*. Occasional old pistachio trees of up to 5 m in height can still be found on many desert heights (e.g., Jabal Al-Bilaas, 500 m above sea level, near Deir Azzour). They have been however, decimated at alarming rates by the firewood needs of the camping nomads in winter. This wood steppe is traditionally the habitat of sheep and camel nomads. The nomads have largely destroyed the original vegetation over the centuries. The establishment of additional water supplies from deep wells and the transport of water by truck have also had disastrous consequences on this fragile ecosystem. The steppe is also home to a variation of groundwater and riparian natural vegetation, on the floodplains and low terraces of the rivers which are not in use for agricultural purposes. In this region, this vegetation consists mainly of Euphratpappeln (*Populus euphratica*) and pastures (*Salix acmophyll*), with an understory of tamarisk (*Tamarix tigrensis*) (after German to English translation and modification from Wirth, 1971).

For the human activities of land use in the ERB, we differentiate between two geographical-historical regions: 1) the Young-settled (Arraqa- and Deir Azzour- provinces) dominant winter cereals (wheat and barley) on dryland and cotton on irrigated ground almost to the level of monoculture. These represent the major growing crops in Syria. Much of the harvesting of these proportional sparsely populated areas goes to market or is readied for export. Tillage and harvest are increasingly mechanized; and 2) the Old-settled (Aleppo Province) shows, in contrast a much larger variety of crops. Wheat and cotton are also cultivated in large parts of the fields in this region but not to the point of monoculture, as there are competitors with many other crops. Less demanding summer plants can grow well here, even without additional irrigation. Permanent crops, such as tree groves and vineyards, as well as intensive, irrigated vegetable crops are found almost exclusively in these old-settled areas. Only a relatively small portion of the harvest is exported. Here, too, is found a juxtaposition of rain- and irrigated- crops; both are cultivated to a much greater extent with more traditional tools than in the Young-settled areas (after German to English translation and modification from Wirth, 1971).

Cultivation of olive trees, which has a long tradition in Syria (oil presses such as Ugarit were already in use around 2000 BC), is located almost exclusively in the Old-settlement (particularly north-west of Aleppo). Vineyards are located throughout this region, either on pure dry land or at the edge of the irrigation areas. All other fruit trees are found only in small areas. The cultivation of pistachios is focused primarily on the perimeter of Aleppo (after German to English translation and modification from Wirth, 1971).

Field-irrigation is used in almost all of the agricultural areas of the ERB. In the areas with more than 400 to 500 mm average annual precipitation, only intensive crops which need a high water demand are irrigated, e.g. vegetables, sugar beets, potatoes and peanuts. The irrigated land here (particularly in the west and northwest of Aleppo Province) is embedded with little natural contrast to a rain-floor, and both winter and summer crops flourish. In the areas with about 200-400 mm

average annual precipitation (particularly the north, south and east of Aleppo Province, and the northern parts of the provinces of Deir Azzour and Arraqqqa) only winter crops can be grown without additional irrigation. In drought years however, this does not provide sufficient income. During the summer months, the irrigation fields are lush green islands, raised above the dry yellow and brown rain-fed land. Between the two there is a clear division of function: in analogy, the drying fields of wheat and barley were appointed/ordered, while the irrigated areas in the old-settled areas had intensive cultivation of vegetables, a variety of summer fruits and fruit trees. The focus of irrigation in the dry steppe areas of northern Syria has been the use of groundwater pump wells. Here, the irrigation area is more scattered in an island-way over the rain-hall/floor. Finally, in the Syrian desert-steppe, where in years with little or average precipitation no winter grain grows, the irrigated floors are no longer being reserved for the cultivation of special crops. Instead, the self-sufficiency of the local resident population of grain must now take place on irrigated land. In the Deir Azzour Province, for example, 90 % of the land use areas are irrigated (after German to English translation and modification from Wirth, 1971).

The human impacts and changes in the Euphrates River Basin have clearly increased over the track of the 20<sup>th</sup> century, and the average of change in this first decade of the 21<sup>st</sup> century is especially significant. Major land degradation processes in Syria include salinization in irrigated areas, water erosion in mountain regions and wind erosion in the steppe area. Salinization is the main land degradation process in irrigated agriculture, with about 45 % of this area affected by different degrees of soil salinization (e.g., the Arraed project near Arraqqqa). However, assessment of the salinity grade and type needs efficient surveys and sampling. Water erosion degrades about 6 % of the country. Wind erosion is the more serious degradation type. If the steppe area where wind erosion has its greatest impact is measured, around 25 % of the total area is influenced by wind erosion. For instance, in the lower fields region of the Al-Khabour Basin there was a drop in the total dynamic irrigated area between September 1990 and September 2000, from 7,167-6,222 hectares. Also, building of the huge dams on Euphrates in Turkey led to a decrease in its actual flow. In the regions of Halabiya-Zalabiya, Ashumaytiyah and Al-Mayadin in Dir Azzour governorate there are three major risks: farmers change floodplain wetlands to cultivated land to be planting with agricultural types; they using the natural swamp plants as feed for their herds in extreme ways; and their disturbance is very high per km<sup>2</sup>. Other two overall important risks are: using the riverine woody plants for heating; and the uncontrolled hunting of aquatic birds (Murdoch et al., 2005). Finally, in an environment where agricultural production is not possible with no irrigation, changes in the machineries of water diversion and withdrawal have led to a changed allocation of human settlement in the landscape. As one technique to be used in LULC-studies, remote sensing techniques offers a better understanding of LULC dynamics and its changes of activities over the time, where this technique determines and draws the spatial distribution of various LULC-features and thus quantify their areas (Zaitchik et al., 2002).

## **Chapter 4: Data**

One decides what information and data is needed to achieve the purpose of a study. The data collection is, however, often controlled by what is obtainable or what the financial map will allow, rather than what is actually needed. During the searching process, one may find other undecided data sources or types that are useful to the achievement of the research. Data and information for the LULC-component is available from the local, county and state administrations. Moreover, administrative divisions, libraries, universities and private companies can offer data. For instance, the Syrian's Central Bureau for Statistics (CBS) offers a periodical demographic data. Processing time and resources require attention, depending on the amount of data collected and organized. Enough data is essential to guarantee accuracy and answerability. At sensor type choosing stage, in relation to rapid sensor development and various sensor configuration (spectral resolution, spatial resolution, temporal resolution, radiometric characteristics, etc.), one has to consider the broad range of application sectors in an attempt to give potentials that meet actual obligations, as it is impossible to find a specific sensor type to satisfy the all specific needs of all cases.

Here, to optimize the choice of the remotely sensed data, we have to determine the purpose of the research and which dataset can realize the two criterions of being cost effective and providing the relevant information in relation to the research purpose. Finally, at these basic stages of choosing and preparing the dataset, it is also significant to consider the relationship between the used dataset and the required mapping scale (Liu & Mason, 2009).

Despite the fact that some gaps exist, there are sufficient data capable of mapping traits of natural environment and land uses.

The purpose of the current study is to set maps of land uses and the natural coverage of the basin area of the Euphrates River. The satellite images suggest basic inputs for a comprehensive study of this area, which is also reliant on other data and information to achieve targets, such as topographic maps and statistical records published by the Ministry of Agriculture, which are associated with land use at village level and at that of the administrative district, the governorate and agricultural areas. Lastly, the study cannot be fulfilled without reliance on field observations.

### **A. Satellite data**

In general, sensors gather the electromagnetic spectrum of the sun radiation. The EMS has a range from the shortest wavelengths to the longest one and it includes the whole variety of the sun radiation (radiant energies, wave frequencies). It is divided into seven ranges: Radio; microwave; infrared; visible; ultraviolet; x-ray; and gamma ray radiation (NASA, 2005). Satellite data are characterized basically by four major and important types of resolutions: spatial resolution; spectral resolution; temporal resolution; and radiometric resolution (see C2.A).

LANDSAT and ASTER general characteristics (Fig. 4.1, Table 4.1, Table 4.2) are: Medium spatial resolution, medium area coverage, moderate revisit capability and multispectral bands characteristic. The scale of the area coverage (imagery) of the LANDSAT satellite and the ASTER sensor makes them mainly suitable for LULC-studies for extended areas, such as regions, countries and continents. The largest part of Earth observation satellites that have a medium resolution are in a sun-synchronous orbit (Van der Meer et al., 2002). The LANDSAT data archive at the USGS/EROS Center-holds an unequaled 36-year record of the Earth's surface and is available at no cost to users via the Internet (Woodcock et al., 2008). The Earth Science Data Interface (ESDI) has a data archive with a global coverage, free for download or for very low managing and delivery costs to large numbers of countries around the world. The data-archive includes: orthorectified LANDSAT-imagery from the three Sensors (MSS, TM, and ETM+); composite MODIS-imagery; and remotely sensed data based derived products (e.g., vegetation cover imagery, and

NDVI). The owner of this archive is NASA and it hosted at the University of Maryland in the USA (<http://glcf.umd.edu/index.shtml>). The Earth Observing System Data Gateway (EOS) provides a big archive of land, water and atmosphere data products. Also, the source of these data comes from NASA in USA (<http://edcimswww.cr.usgs.gov/pub/imswelcome/>). There are also a valuable and gratis remotely sensed data or with an inexpensive shipping costs. Well-known remotely sensed data such as AVHRR, MODIS and ASTER can also be obtained.

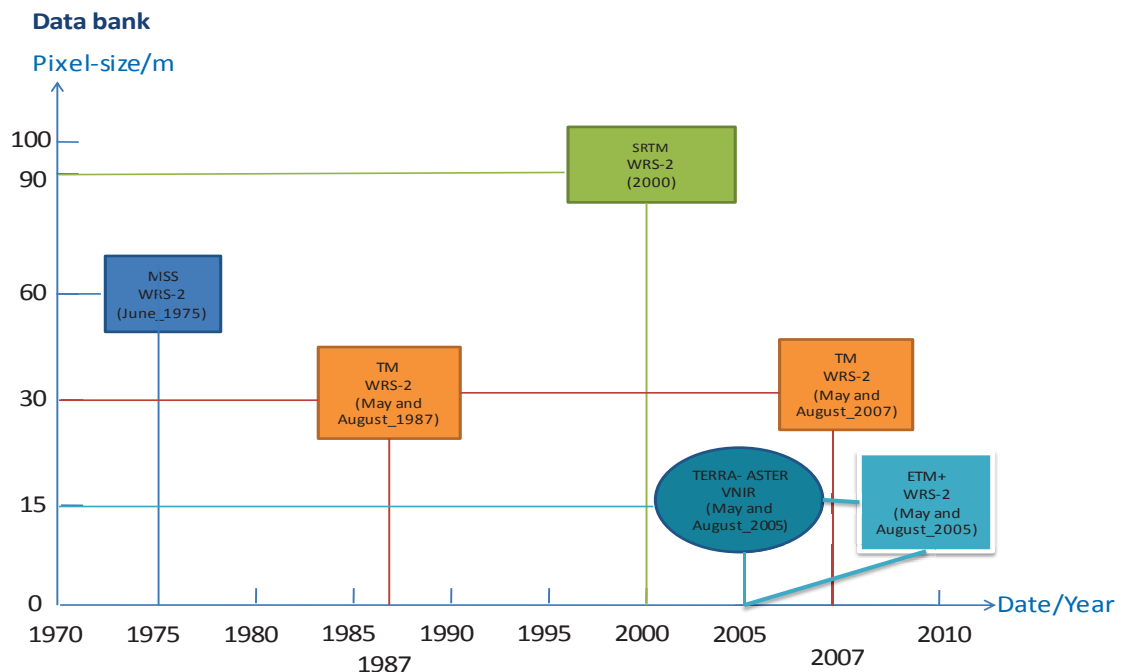


Fig. 4.1: An overview on the general characteristics of the used satellite dataset in the study

Table 4.1: General information about the two satellites LANDSAT and TERRA-ASTER (Source: Adapted from: Schowengerdt, 2007; Chander et al., 2009)

Satellite	Launch dates	Decommission	Altitude/km	Indination/degrees °	Period/min.	Temporal resolution/days	Crossing time (a.m.)
LANDSAT-1	23.07.1972	07.01.1978	920	99.20	103.34	18	9:30
LANDSAT-2	22.01.1975	25.02.1982	920	99.20	103.34	18	9:30
LANDSAT-3	05.03.1978	31.03.1983	920	99.20	103.34	18	9:30
LANDSAT-4	16.07.1982	30.06.2001	705	98.20	98.20	16	9:45
LANDSAT-5	01.03.1984	Operational	705	98.20	98.20	16	9:45
LANDSAT-6	05.10.1993	Did not achieve orbit					
LANDSAT-7	15.04.1999	Operational	705	98.20	98.20	16	10:00
TERRA-ASTER	18.12.1999	Operational	705			16	10:30

Table 4.2: General information about the sensors-data used in the study (Source: Adapted from: Van der Meer et al., 2002; Schowengerdt, 2007; Liu & Mason, 2009)

Platform	Sensor	Spatial Resolution/m	Spectral Bands	Spectral Range/ $\mu$ m	Swath width/km	Pointing Capability/degrees °	Mapping scales/m
LANDSAT (1-5)	MSS- Multi-spectral	60	1-4	0.5-1.1	185×185	No	1/160,000
LANDSAT (1-3)	RBV- Return Beam Vidicon	25	1	0.505-0.750	185×185	No	1/50,000

<b>LANDSAT (4-5)</b>	TM-Multispectral	30	1-5, and 7	0.45-2.35	185×185	No	1/60,000
	TM-Thermal	120	6	10.40-12.50	185×185	No	
<b>LANDSAT (7)</b>	ETM+ /Multispectral	30	1-5, and 7	0.450-2.35	185×185	No	1/60,000
	ETM+ / Thermal	60	6-1, 6-2	10.40-12.50	185×185	No	1/120,000
	ETM+ / Pan-chromatic	15	8	0.52-0.90	185×185	No	1/30,000
<b>TERRA-ASTER</b>	VNIR	15	1-3N	0.52-0.86	60×60	±24	1/30,000
	Stereoscopic	15	3B	0.76-0.86	60×60	±24	1/30,000
	SWIR	30	4-9	1.600-2.430	60×60	±8.55	1/60,000
	TIR	90	10-14	8.125-11.65	60×60	±8.55	1/180,000
<b>SRTM</b>	C- and X- bands	90			1 degree latitude*1 degree longitude		1/180,000

### 1. LANDSAT (MSS, TM and ETM+) Sensors

[Lauer et al. \(1997\)](#) provides a short history of the LANDSAT-program and its noted successes. The development of the LANDSAT-program originated from global efforts to improve our knowledge of Earth, and it is perhaps the most successful satellite remote sensing program devoted to land monitoring. The first Earth Resources Technology Satellite (ERTS-1) was launched to space on 23 July 1972 in cooperation between the National Aeronautics and Space Administration (NASA) and other USA-federal agencies. It was later renamed LANDSAT-1. This launch is seen as the birth of the present age of Earthly satellite remote sensing. LANDSAT-1 was a Nimbus-type platform which held a sensor box and data-relay tools. ERTS-2 was launched to the space on 22 January 1975. It was too renamed to LANDSAT-2. Other four LANDSATs (3, 4, 5 and 7) were launched in 1978, 1982, 1984 and 1999 respectively. Each successive launch has included improved sensor and communication capabilities. This has had a huge influence in several application fields ([Lauer et al, 1997](#)). In comparison to the military satellite systems, the civilian LANDSAT-family of satellites has supplied civilization with over 34 years of consistent, medium spatial resolution, multispectral images of the world. Due to the long historical record of the LANDSAT-program, no other remotely sensed data sets allow us to study the nature of the Earth and the human activities and impacts so effectively ([Green, 2006; Williams et al., 2006](#)). This continuous record was realized because of good luck and superb engineering rather than careful management oversight ([Williams et al., 2006](#)). The LANDSAT World Wide Reference (WWR) system catalogs the Earth's landmasses into 57,784 scenes, each 185 km wide and 170 km long ([USGS, 2009](#)).

The famous family of LANDSAT-satellites (LANDSAT-1, 2, 3, 4, 5, 6 and 7) and sensors (MSS, TM, ETM and ETM+) can be divided to three common types based on the characteristics of their sensors and platforms: 1) LANDSAT (1, 2 and 3), that have the sensor type of MSS and the camera type of Return Beam Vidicon (RBV). The platform was like a Nimbus (cloud). MSS has the spatial resolution of 79 m (frequently, prepared to be 60 m as pixel size). Its spectral resolution is not large enough for some studies (e.g., crops classification), where it has four spectral bands only. These bands located within the four spectral portions (wavelengths) with a four typical band-naming: blue (MSS-4), green (MSS-5), red (MSS-6) (the visible spectral portion); and the Near-Infra-Red (NIR) (MSS-7). Only the third LANDSAT hold a MSS sensor that has five spectral bands, were the fifth one was a thermal infrared (10.4 to 12.6)  $\mu\text{m}$  ([Markham & Barker, 1983 cited in Chander et al., 2009](#)). This standard is no longer used; instead the MSS-bands are referred to the

bands 1,2,3 and 4 respectively, consistent with the TM and ETM+ sensors; 2) LANDSAT (4 and 5), which carried the TM sensor, in addition to the MSS. This second generation offered a clear enhancement in remote sensing through the supplement of a more advanced sensor, enhanced gaining and transmission of data, and more rapid data processing at a highly automated processing capability. The MSS-sensor was kept to provide continuity with the previous LANDSAT-missions, but TM-data rapidly became the main source of information used from these satellites because of its enhanced spatial, spectral, radiometric and geometric characteristics in comparison to MSS-data. Finally, the gaining was limited to real-time download only, since there were no onboard recorders on these sensors (Chander et al., 2009); and 3) LANDSAT (6 and 7), consisting of LANDSAT-6 which carried the Enhanced Thematic Mapper (ETM) sensor and failed on launch, and LANDSAT-7, with its Enhanced Thematic Mapper Plus (ETM+) sensor. LANDSAT-7 also had a 378 gigabit Solid State Recorder (SSR) that could store 42 minutes (about 100 scenes) of sensor data and 29 hours of housekeeping telemetry concurrently (L-7 Science Data User's Handbook). No MSS-sensors were included on either satellite. The following TM-bands list describes the most appropriate applications of each of the seven spectral bands (ERDAS, 1999): Band 1: it has the mapping ability of many features (coastal water regions, types of forests, civilizing features, and soil and vegetation mapping); Band 2: it has the distinguishing ability between healthy and unhealthy vegetation, where it is equivalent to the spectral reflectance of healthy vegetation within the green spectral portion of this band. It has too the ability to distinguish between the various cultural features; Band 3: it has the spectral separation ability between various plant types. It has also the ability to draw civilizing features, soil and geological borders; Band 4: especially responsive to the presented vegetation biomass in an image, where it has the ability to quantify sum of the biomass. It used often for classification of agricultural crops. It is useful for highlighting the contact between soil and crop and between land and water; Band 5: it has the ability to determine whether the natural and the agricultural plants and crops suffer from drought or not, and whether they are healthy or not, where this band is sensitive to the amount of water in plants and thus it can quantify the portion of water. It used also to distinguish between clouds, snow and ice; Band 6: it has the ability to detect the stress in the natural vegetation and in the agricultural crops. It used also to determine intensity of the heat for these plants. Other use for this band in agriculture is for insecticide. Some other uses of the sixth spectral band are: thermal pollution activity determination; and geothermal activity locating; and Band 7: it has the ability distinguish between types of the geologic deposits. It used also to draw of soil borders. Also, it is useful for quantifying the moisture content in both soil and vegetation.

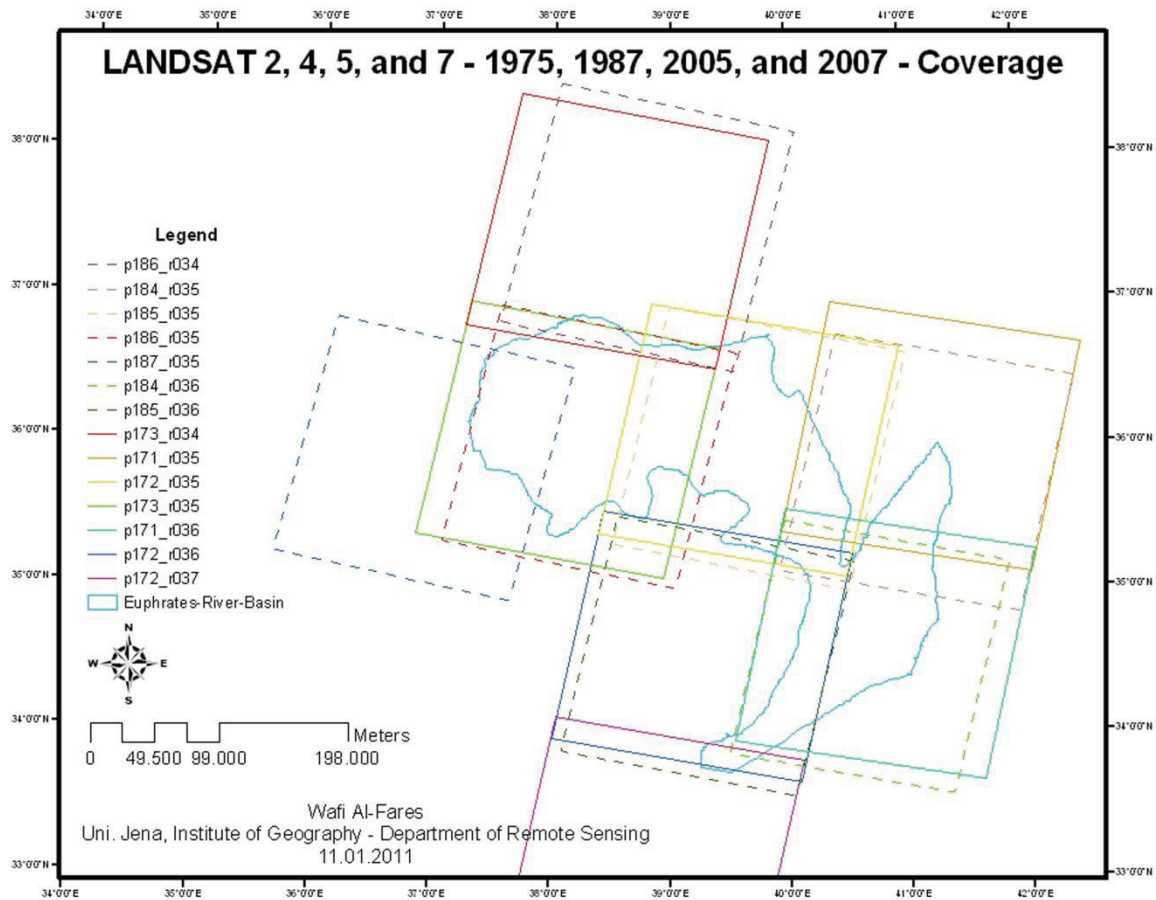


Fig. 4.2: The used imagery spatial coverage of the sensors: MSS (June, 1975), TM (May and August, 1987 and 2007), and ETM+/SLC-Off/corrected (May and August, 2005)

## 2. TERRA-ASTER

In 1999, after the cooperation between NASA and the Japan's Ministry of Economy Trade and Industry (METI), the Advanced Space-borne Thermal Emission and reflection Radiometer (ASTER) was launched into the space. It was held on board the NASA-TERRA satellite. The ASTER-sensor represents the next generation in remote sensing, following the older LANDSAT-TM. It acquires high spatial resolution data in 14 spectral bands, ranging from visible to thermal infrared portions. This sensor contains three separate instrument subsystems that operate in different spectral portions and have their own telescope(s). The subsystems are: 1) the Visible and Near Infra-Red (VNIR): operates within three spectral bands at visible and NIR wavelengths of 0.52-0.86  $\mu\text{m}$ , with a spatial resolution of 15 m. It is especially useful for topographic interpretation because of its along-track stereo coverage with 15 m spatial resolution. Also, it is useful in assessing vegetation and iron-oxide minerals in surface soils and rocks; 2) the Short-Wave Infra-Red (SWIR): operates within six spectral bands in the NIR region of 1.600-2.430  $\mu\text{m}$ , through a single-nadir pointing telescope that offers a spatial resolution of 30 m. These six bands were selected mainly for the purpose of surface soil and mineral mapping; and 3) the Thermal Infra-Red (TIR): operates within five bands inside the thermal infrared region of 8.125-11.65  $\mu\text{m}$ , using a single, fixed-position, and nadir looking telescope with a spatial resolution of 90 m. This subsystem allows for a more accurate determination of the variable spectral emissivity of the land surface, and hence a more accurate determination of the land surface temperature. The spatial coverage of the ASTER-sensor is at 60 \* 60 km (Yamaguchi et al., 1993; Fujisada, 1994 and 1995; Yamaguchi et al., 1998; Kiffer et al., 2008).

The relatively high spatial (Fig. 4.1) and spectral (Fig. 4.3) resolution of the ASTER-data in comparison to LANDSAT-data can increase the ability of separation between the various ground surface features and decrease the problems of mixed pixels (Yamaguchi et al., 1998). Therefore, ASTER-data are more suitable for LULC-classification (Bagan et al., 2008).

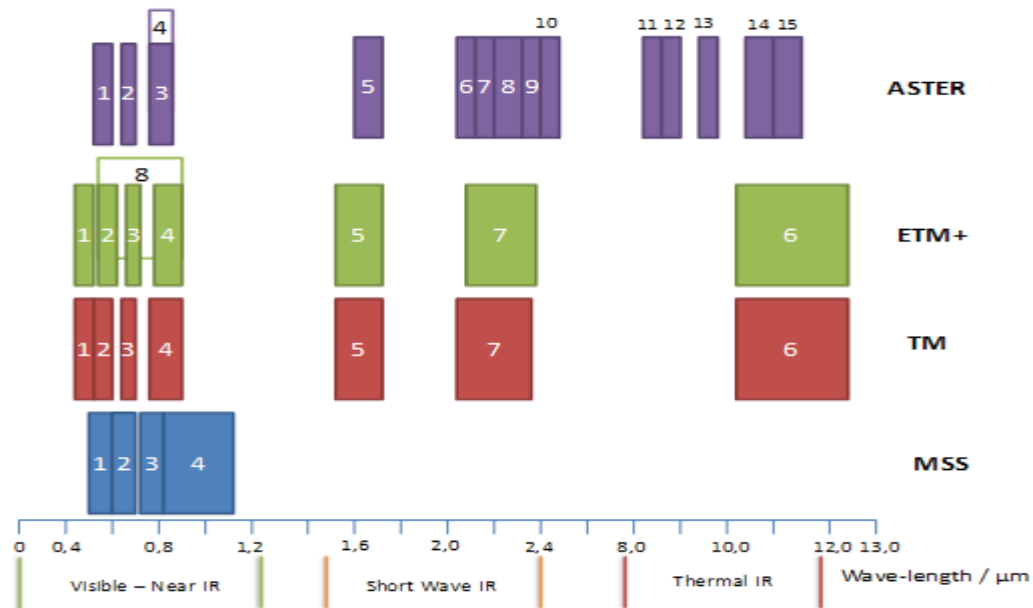


Fig. 4.3: Comparison of the spectral coverage between LANDSAT-sensors (MSS, TM, and ETM+) and the ASTER-sensor

The ASTER-sensor, because it is the only high spatial resolution sensor, is the “zoom lens” for the other carried sensors onboard the TERRA-satellite. TERRA is in a sun-synchronous orbit, 30 minutes behind LANDSAT-ETM+, and it crosses the equator at about 10:30 am local solar time. ASTER can obtain data over the whole globe with an average obligation cycle of 8 % for each track. This offers a gaining of about 650 scenes per day (subject to on-board storage limitations), that are processed to the two products types (Level-1A; of these, about 150 are processed to Level-1B). ASTER-L1A data are officially classified as reconstructed, unprocessed data at full resolution. They contain the image data, the radiometric coefficients, the geometric coefficients and other supplementary data without applying the coefficients to the image data, thus keeping the original data values (raw data). The L1B-data are produced by applying the coefficients for radiometric calibration and geometric resampling. All gained 1A and 1B scenes are transferred to the EOSDIS archive at the EROS Earth Data Center’s EDC Land Processes Distributed Active Archive Center (LP-DAAC), for storage, distribution and processing to higher-level data products. All ASTER-data products are stored in a specific implementation of Hierarchical Data Format called HDF-EOS.

ASTER’s geometric system correction mainly contains the rotation and the coordinate transformation of the line of sight vectors of the detectors to the coordinate system of the Earth. This is done as part of ASTER-Level-1 processing at GDS using supplementary engineering data from the sensor and similar auxiliary data from the spacecraft platform. The geometric correction of ASTER-data has developed in two complex processes of both pre-flight and post-launch calibration (ASTER Users Handbook). Tests have proven that ASTER has excellent radiometric, geometric and spectral functioning (Ono et al., 1996).



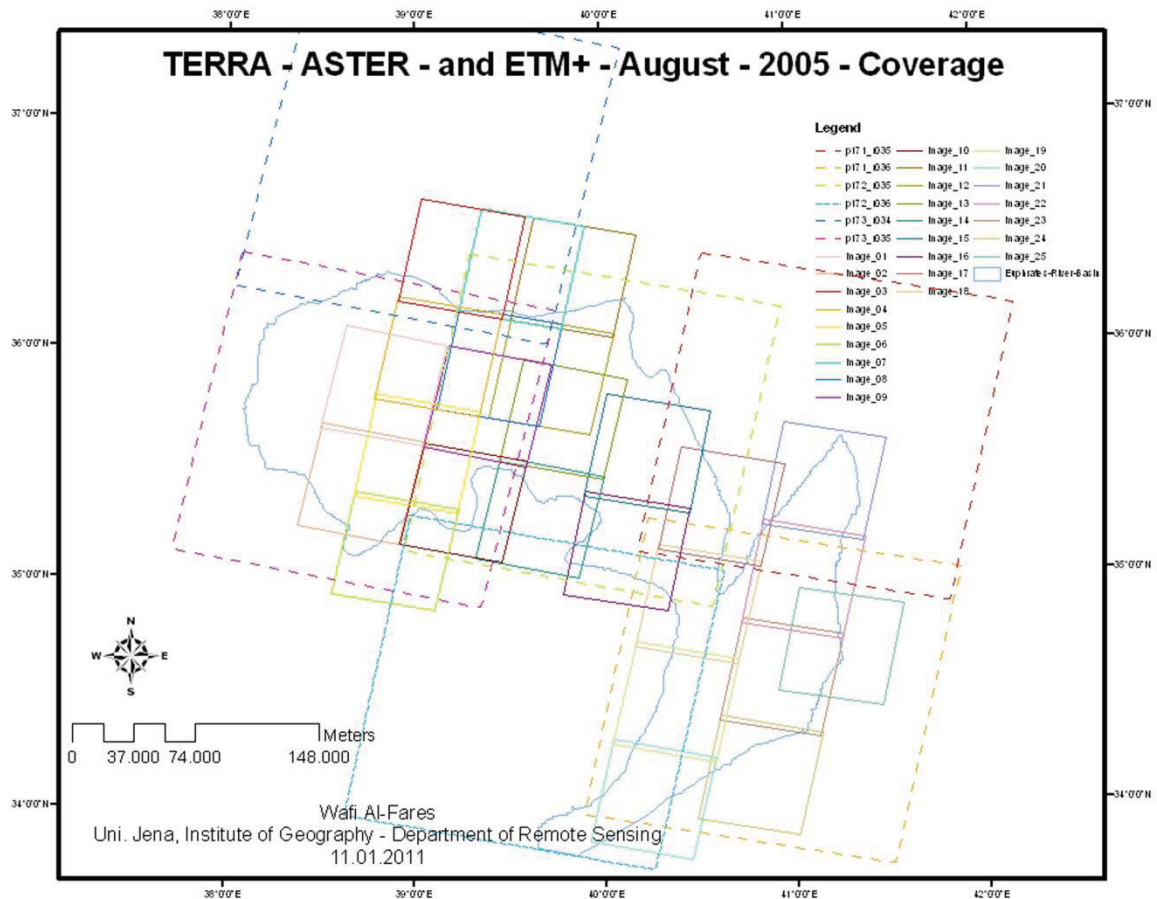


Fig. 4.4: The used imagery spatial coverage of the sensors ASTER (May and August, 2005), and ETM+/SLC-Off/corrected (May and August, 2005)

The main scientific purpose of the ASTER-mission is to gain better knowledge of the local and regional scale processes happening on or near the Earth's surface and lower atmosphere, as well as the relations between the Earth surface and the atmosphere. Special applications are: 1) earth surface climatology; 2) vegetation and ecosystem dynamics; 3) volcano observing; 4) hazard observing; 5) aerosols and clouds; 6) carbon cycling in the marine ecosystem; 7) hydrology; 8) geology and soil; and 9) LULC-change (Yamaguchi et al., 1999).

### 3. SRTM

The Shuttle Radar Topography Mission (SRTM) was started in February 2000. This mission took eleven days and named as STS-99-mission. The mission was ended successfully after an international cooperation. The goal of this mission was to offer a new source for deriving of topographical data digitally, especially the height element/z, where the traditional methods were based on digitizing the contours lines from the topographic maps. After achieving the goal of the mission, we had become the Digital Elevation Models (DEM). This product was until 2009 the most complete archive of digital topographical data, which covers a near-global scale from 56° S to 60° N with a high spatial resolution. To realize the above mentioned goal, the mission included a specially modified RADAR-system, which was based basically on the model used in the 1994 Shuttle, the older Space-borne Imaging Radar (C and X) bands Synthetic Aperture Radar (SIR-C/X-SAR). The system was carried on board of the Endeavour Space Shuttle. The technique used to generate topographic data digitally from the space with representation of the elevation element (z), is the Interferometric Synthetic Aperture Radar (ISAR). The SRTM mission was supplied with two radar

antennas. "One antenna was placed in the Shuttle's payload bay, the other, a critical change from the SIR-C/X-SAR allowing single-pass interferometry, on the end of a 60 m mast that extended from the payload bay as soon as the Shuttle was in space" (Nikolakopoulos et al., 2006; Farr et al., 2007).

"The elevation models were set into tiles, each covering one degree of latitude and one degree of longitude, named according to their south western corners. It follows that "n45e006" stretches from 45° N 6° E to 46° N 7° E and "s45w006" from 45° S 6° W to 44° S 5° W. The resolution of the cells of the source data is one arc second. The one arc second 30 m data have only been released over United States territory; for the rest of the world, only three-arc-second 90 m data are available" (Nikolakopoulos et al., 2006; Farr et al., 2007).

The second realized DEM-product was presented from ASTER-sensor in 2009. Thus, it can charge the digital topographic database with new and different source. It named as Global Digital Elevation Model (GDEM).

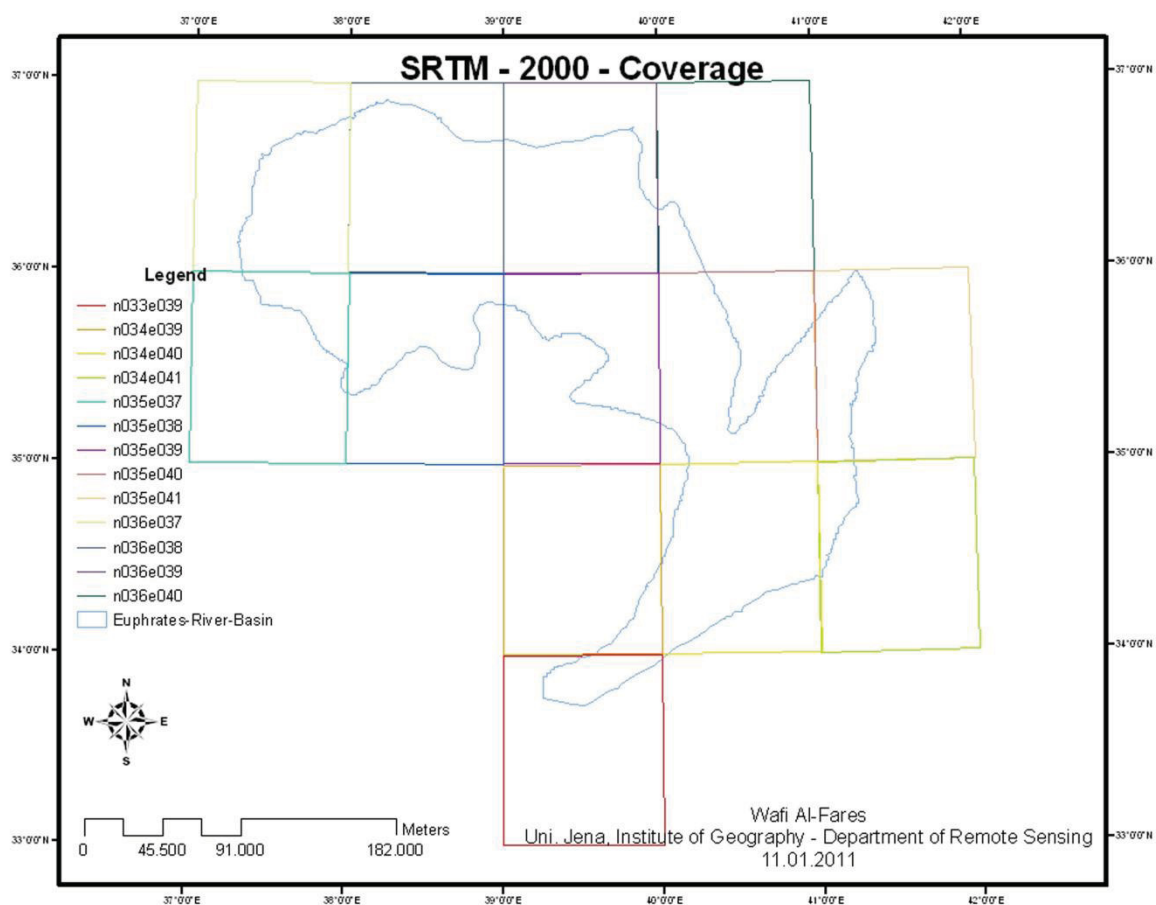


Fig. 4.5: The used imagery spatial coverage of the sensor SRTM

## B. Reference- and complementary- data

Reference and complementary data can be obtained from information sources other than the imagery data itself, such as field observations and measurements, aerial photograph interpretation, thematic maps and other archival materials. The expression "ground truth" can be substituted by the more appropriate expression "reference information", which is seen to be "more inclusive than "ground" and less absolute than "truth" ". Generally, no study should be carried out without study area visits, but it is often possible to select training and testing samples for accuracy assessment

from high resolution aerial photographs or from a suitable thematic maps showing LULC-categories (McCoy, 2005), in addition to topographic maps and Google Earth data. On the other hand, social science can help to confirm and analyze remotely sensed observations (e.g., validating remote observations versus data gathered on the ground). For example, it is possible to determine a number of land use activities (classes) during classification remote sensing imagery based on a few social behaviors (McCoy, 2005). One of the interesting example presented by Lesschen et al. (2005) presents other data sources such as questionnaires (often used by sociologists). It is particularly helpful to obtain management-related data (e.g., agricultural crop cycles) and can also give insight into the main factors of LULC-change.

### 1. Field reference data

One of the mainly and important steps in any remotely sensed based study is gathering the thematic data (attribute data, such as qualitative breaks by vegetation cover density: Low, medium, high), and measurements (e.g., a quantitative differentiation of vegetation cover density by break points: < 10 %, 11-40 %, > 40 %), or observations (e.g., determination which category of the legend is more suitable to a surface feature) of the phenomenon of interest in the field. This is also the most difficult step, because it is a very time-consuming, often boring task which entails difficulties such as what want the researcher measuring and observing, where it is important to determine that before the field work, and then it is important to choose the method to be applied in the field to gather the required data (McCoy, 2005). Ground truthing is important for remote sensing to properly identify objects, provide precise image registration and verify results. Before beginning to gather reference data in the field, two steps must have been completed: 1) study goals must be obviously determined; and 2) a classification scheme for all LULC-classes must have been selected (McCoy, 2005).

Spectro-radiometry is a frequently used ground-based reference data source in remote sensing techniques (Yang et al., 2007). Spectro-radiometer can measuring the values of radiance, irradiance, reflectance or transmission of individual targets or objects, by locating the radiometer above the targets of interest, and records these values as digital spectral quantitative records. It used mostly as hand-held cameras (or mounted on a tripod, tower, tractor etc.). After finishing the measuring process, the user compares them to the biological, chemical and physical characteristics of the object. For agriculture, red and NIR portions of the EMS profile utilized particularly to calculate and generate the Vegetation Indices (VI) that are correlated with parameters of canopy structure (e.g., LAI). Spectro-radiometers named also radiometers or InfraRed Thermometers (IRT) (Schowengerdt, 2007).

For the purpose of this study, the major related field-work/s was: The 1987-GPS points (ICARDA); the 2005-GPS points (GORS); the 2007 and 2009 GPS-points obtained from two excursions; Spectrometer-measurements (GORS); and the NDVI-measurements (GORS). (see C5.D).

### 2. Maps

Thematic maps of LULC-types should be a part (especially in the visual interpretation) of the selection of training samples and the gathering of testing sites for accuracy assessment when there is no alternative. Thematic maps are generalized information with two drawbacks, in that they are probably based on unlike designations for classes, plus an unlike minimum unit (cell or pixel) size than that which is being used in a specific study. Therefore, most maps are considered untrustworthy and unacceptable for use as reference data, other than for a general understanding of the area (McCoy, 2005).

Soils and thematic maps are reproduced from previous studies (especially from ICARDA-Aleppo), as well as topographic maps with various scales from 1/25,000 to 1/100,000, which cover the whole study area. These were purchased from the General Organization for Military Survey in

Damascus. Some aerial photos for small areas in the Aleppo-governorate were also obtained from the military survey.

### 3. Statistics

The analysis of spatial distribution of agricultural features were based on: statistical data taken at both village and the administrative district level for the years of 1975, 1987, 2005, and 2007; on previously achieved studies relating to the study area; and on the field observations. Statistical data were checked and proven. They are the basic foundation of Syrian agricultural statistics. These data are collected by agrarian engineers working in counselling units centred in the administrative sectors.

Furthermore, there are general information and agricultural statistical records for the period 1970–2010. These are useful to understand the geographical history of the study area in relation to nature and human activities, and especially the historical development of the irrigation projects in the ERB. Each of these information and statistical records has a periodical annual publication, issued by the CBC in Damascus. The agricultural statistical records are collected on various levels, including village, administrative region, governorate, agricultural stable zones and the whole area of Syria (Fig. 5.63, Fig. 5.64).

Detailed information and statistics for the period 1970–2010 about the agricultural irrigation projects were obtained from IGDEP in the city of Arraqqqa.

### 4. Ancillary data

Ancillary data is used to facilitate a better understanding of LULC-dynamics and the reasons behind them. There are a various obtainable types of ancillary data: digital elevation models; soil map; housing and population density; road network; temperature; and precipitation. These can be integrated, as external inputs to remotely sensed data. into a classification process in various concepts (Lu & Weng, 2007). This integration has the benefit of improving the overall accuracy of produced thematic maps based on classification of remote sensing imagery. The percentage of this improvement based essentially on the used classifier (Heinl et al., 2009).

Climatic data (such as precipitation, temperature, humidity, etc.) was also gathered for the climatic stations that existed in the three major governorates within the ERB: Aleppo, Arraqqqa, and Deir Azzour, during the temporal period of the study. These were obtained from the General Organization for Meteorology in Damascus. These data were useful for radiometric normalization using (iMAD) (see C5.B.3). Ancillary data for the entire water basin of the Euphrates is also included, as well as the agricultural calendar.

## ***Chapter 5: Research methodology***

This chapter gives a review about techniques and methodologies that were applied to answer the presented research questions and to confirm the hypothesis of this thesis. The conceptual workflow chart of the thesis is illustrated with an overview provided in [Fig. 5.1](#). It will be clarified in the text part below.

Tone or color is the basis factor for most methods of digital image analysis. It is represented as a digital number (i.e., brightness value) in each cell of the recorded remote sensing image. The first step before the main image analyses operated is applying a various procedures of preprocessing on the raw digital image. To carry out image classification, many steps have to be considered: choosing of a fit classification system; choosing of training samples; preprocessing of image(s); drawing out the feature; choosing of fit classification approaches; processing the resulted products of classification (post-classification); and accuracy assessment.

Utilization of several variables during the classification process can make the classification accuracy worse because of unlike capabilities in separation between classes of interest ([Price, 2003](#)). Therefore, many potential variables were used in image classification for the study case of this thesis, including spectral signatures, vegetation indices and transformed images (NDVI), multi-temporal images (1975, 1987, 2005 and 2007; April, May, July and August), multi-sensor images and ancillary data (GPS measurements, spectral information, statistical records, Google Earth etc.).

In this thesis, I will try to propose the methodological means which contribute to analysis of various data and information, and to integrate some of these data between each other, if necessary, to extract the information/results from the satellite images, to be presented in the final thematic maps.

*Setting three local levels with multi-temporal levels to process sensory data available for obtaining thematic maps.*

The first local-level: this level was embodied in the four administrative areas' borders (Menbij, Al-Jurnia, Ain Eisa and Athawra), and was accredited to test and compare several algorithms and automated classification methods in order to best determine the optimized algorithm and method of classification. Algorithms such as MLC, NN and SVM were tested in two ways. The first approach relied on a hierarchical shape and involved the extraction of classification outcomes through multiple stages, starting from the wide general level with little details and ending up at low levels subdivided from the previous general one, yet, advantaged with more detailed classes. The second approach classified sensory data through one stage. The used data were: LANDSAT-MSS-June-1975-60m; LANDSAT-ETM+/SLC-Off/corrected and fused with ASTER-May-2005-15m; and LANDSAT-TM-May-2007-30m.

The second local-level: represented in the entire natural borders of the ERB. This level's outcomes were represented in three products. The first product involved setting thematic maps to represent the natural coverage and the wide general land uses distribution (LULC). Five classes counting on classification system were accredited in this study. The used data and dates were: LANDSAT-MSS-June-1975-60m; LANDSAT-TM-April-1987-30m; LANDSAT-ETM+/SLC-Off/corrected-April-2005-15m; and LANDSAT-TM-April-2007-30m). Here, for the automated classification process, one product (map) was obtained for each year (coverage), which represented and illustrated the quality and quantity of the spatial and temporal distribution of the natural coverage and uses of the lands. A quantitative analysis of produced maps was set (statistical data and tables) to compare, explain and analyze these numbers. Comparison was made between recordings extracted from various sensory data, regarding spatial and spectral resolution (positives, negatives, advantages and disadvantages).

The third product involved setting map/s representing the temporal and spatial change of the natural coverage distribution as well as land uses, utilizing the pre-classification change detection ap-

proach. For this, the LANDSAT-MSS-June-1975 and the LANDSAT-TM-August-2007 coverages were used.

Regarding the last two products, temporal and spatial changes were studied and analyzed.

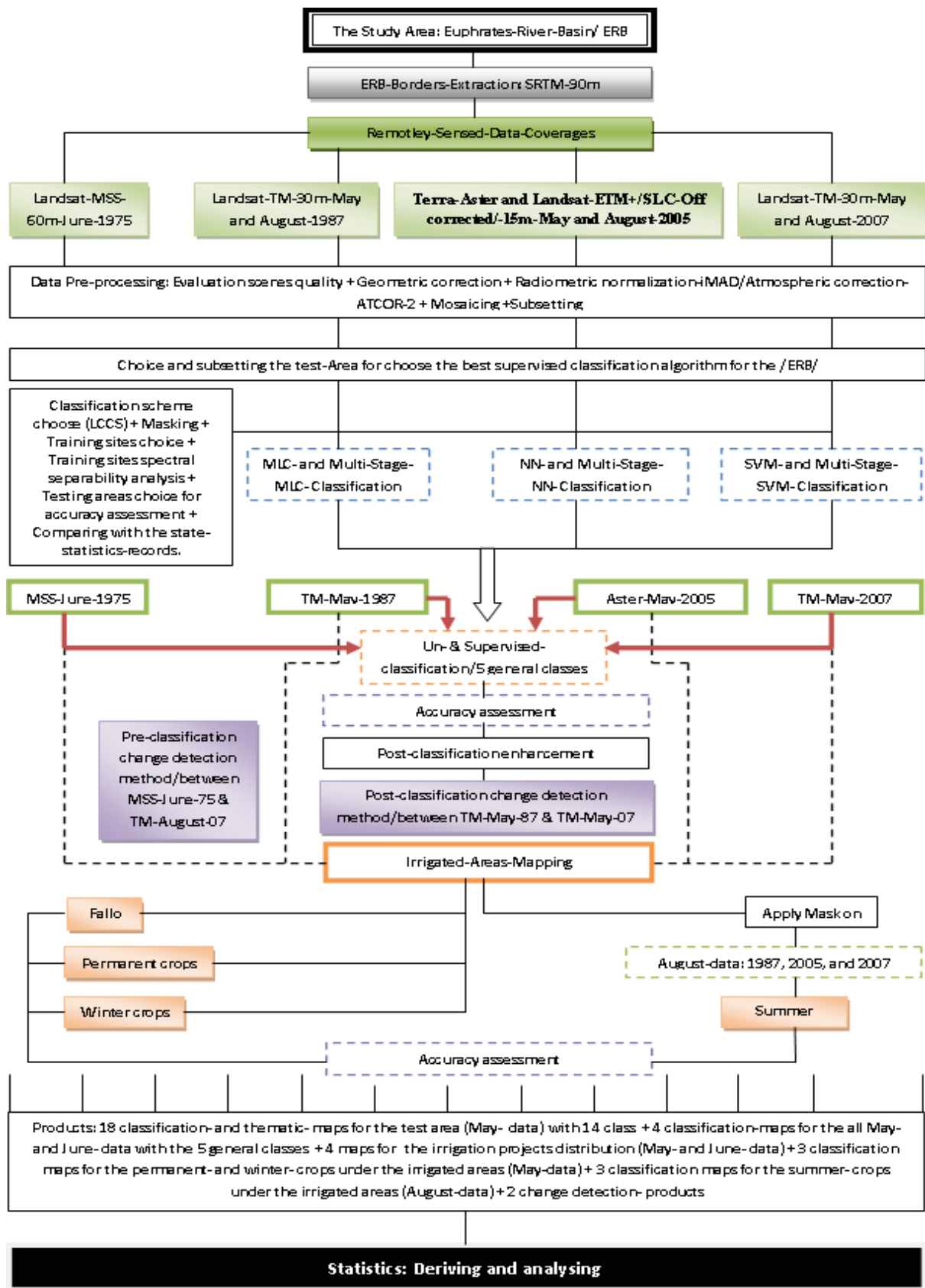


Fig. 5.1: The general conceptual workflow chart of the thesis

The third local-level: represented in distribution of the irrigated agricultural projects within the natural limits of the ERB. The first product involved setting maps of distribution and change of agrarian irrigated areas, temporally and spatially, for the following data and years: LANDSAT-MSS-June-1975-60m; LANDSAT-TM-May-1987-30m; LANDSAT-ETM+/SLC-Off/corrected and fused with ASTER-May-2005-15m; and LANDSAT-TM-May-2007-30m.

As for the second product, this was manifested by setting thematic maps to represent the distribution of winter and summer basic crops in irrigated plantation projects, the types of cultivations and their area. The used data for this purpose was as follows: For the winter crops: LANDSAT-TM-May-1987-30m; LANDSAT-ETM+/SLC-Off/ corrected and fused with ASTER-May-2005-15m; and LANDSAT-TM-May-2007-30m. For the summer crops: LANDSAT-TM-August-1987-30m; LANDSAT-ETM+/SLC-Off/ corrected and fused with ASTER-August-2005-15m; and LANDSAT-TM-August-2007-30m).

The development of irrigated agricultural areas was calculated for the past 40 years.

### **A. Extraction of the study area**

Extraction of the natural aquatic borders of the ERB in Syrian lands through the use of the digital elevation model DEM available from the sensor data SRTM in 90m spatial resolution, in addition to the DEM-data from ASTER in 30m spatial resolution.

Data was imported to the ArcGIS 9.3 program using the following steps: Export raster data (raw-data) to GRID-format; ArcToolBox/Spatial Analyst Tools/Hydrology: (Fill/Flow direction/Flow accumulation/Conditional-Con/Stream to feature/Add one point -.shp file-/Watershed); Conversation Tools: (from raster – Watershed-/Raster to polygon); and Analysis Tools: (Extract/Clip).

Throughout the proposed results, the spatial distribution layer of the natural borders of river-basin was obtained from the SRTM-data. Concerning ASTER-data, there has been an unwillingness to depict the river basin edges because of their higher spatial resolution rather than the SRTM-data. Unfortunately, dealing with this data proved to be exhausting and full of errors. Therefore, a return to the SRTM-data ensued. There has been no accredited map issued by the Ministry of Irrigation that draws the borders of the ERB. The majority of Syria's irrigation projects lie within the natural boundaries of the ERB, except for some projects in the north and the south of the city of Aleppo, where waters have been extracted from the Euphrates River for the past five years. This means that many of these projects are not introduced in this study, as they occurred after the date of the last remote sensing data used (i.e., 2007).

### **B. Pre-processing of the satellite data**

*“A good player never makes more effort than he needs to win” - old Arabic wisdom.*

Remote sensing data may have two common types of distortions (systematic and non-systematic). This is because the method performance of the Earth observation system and the characteristics of Earth's surface (Henderson & Lewis, 1998; Richards & Jia, 2003).

There are a variety of preprocessing procedures that could be applied on satellite data: finding and replacement of damaging lines of pixels; geographical registration of image and geometric rectification; radiometric calibration and atmospheric correction; and correction the topographical effects. As example about textbooks that explained the subject of preprocessing thoroughly are (Toutin, 2004; Jensen, 2007). The most often carried out procedures of preprocessing are geometric correction and atmospheric calibration.

According to Mather (2004), pre-processing procedures used to correct the generated deficiencies of geometric and radiometric formation of a remotely sensed image, and then it used to remove the errors of data. These deficiencies and errors have to be removed or at least manipulated, if it is achievable, before the starting with imagery classification. Which method would be applied, is dependent upon the goal of study. The most availability of preprocessing procedures or programs,

automatic, is for coarse and medium spatial resolution data (e.g., LANDSAT-TM) and for high temporal resolution data (e.g., NOAA-AVHRR).

A good optimization in presentation of an individual object in the dataset of remote sensing data, is a result of a suitable selection of digital image preprocessing procedures. This goodness can be confirmed using a visual interpretation (Liu & Mason, 2009). There are many digital methods to better enhancement of an image. These methods have the benefit of increasing the visual interpretability of used data and thus the thematic information of interest could be easily derived. The common three methods of image-enhancement are: 1) enhancement of contrast ("more of the available range of digital values is used, and the contrast between targets and their backgrounds is increased" (Jensen, 2005)); 2) spatial enhancement (spatial filtering, edge enhancement, and Fourier analysis etc.); and 3) spectral transformation (generating more valuable data or products - e.g., NDVI - based on manipulation - e.g., division - of several spectral bands of data).

Despite the LANDSAT-images being level 1G corrected (Level-1G was corrected from USGS, and this modification consists of the basic corrections of radiometric and geometric distortions. But these corrections are not suitable for each application and thus user have to make additional corrections if the from USGS corrections are not sufficient), they are not good enough accurately registered in form pixel-to-pixel. USGS had pointed to a possible error of up to 250 m (<http://landsat7.usgs.gov/index.php>), and had not atmospherically corrected the data, thus all findings were subsequently re-corrected geometrically for this work (see C5.B.1). Atmospheric effects on the spectral signal were also minimized with a correction method (see C5.B.2). In addition to radiometric normalization (see C5.B.3), the ASTER data were delivered in Level 1A without any corrections.

ETM+-bands 6 and 8, plus TM-band 6, were eliminated from the entire processing and classification. The panchromatic information of band 8 was only used for pan sharpening. The sixth thermal spectral band - with its thermal information - was not used because the two reasons: it has a coarse spatial resolution; and it can recording only the transmitted radiation from objects in contrast to other spectral bands that measure the reflected radiation.

All image processing, classification and preparing the final results were carried out using two programs: ENVI, Version 4.6 and ArcGIS, Version 9.3.

## 1. Geometric data processing

"The more time steps involved for a change analysis, the more effort should be spent on image registration and radiometric adjustment" (Wulder & Franklin, 2003 cited in Schultz, 2011). Consequently, the goodness or badness of method used in the registration of remote sensing data (image/s) will determine the quality/accuracy of the resulting change detection product (Schultz, 2011). Townshend et al. (1992) assumes that the "problems created by misregistration are likely to be greater in the sensing of land surfaces compared with the atmosphere or many ocean properties".

There are several common expressions used to explain geometric correction process (registration, rectification, geo-coding and ortho-rectification) (Schowengerdt, 2007). This process corrects the two different errors types (systemic and nonsystematic) resulting from the two different sources (within the remote sensing system itself, and during the recording of images) (Lo & Yeung, 2002). The various applications of geometric correction on remotely sensed data are: co-registration of images that cover the same area on the Earth but they were obtained from two or more different sensors, or they were obtained at two or more different periods of times, or they were obtained from two or more different sites; and rectifying an image to be accurate to an individual coordinate system (geo-coding) (Liu & Mason, 2009). "Spatial distortion arises from scanner characteristics and their interaction with the airborne platform or satellite orbital geometry and figure of the Earth" (Schowengerdt, 2007). Geometric correction can maximize the usefulness of the remotely



sensed data for information extraction (e.g., thematic maps). To get more details about geometric rectification or image registration and their application on remotely sensed data, there are many textbooks and articles (e.g., Jensen, 2005).

The geometric correction is the first image processing step (pre-classification approach) carried out when the remotely sensed data are not geo-rectified (Liu & Mason, 2009). However, geo-rectification can be carried out as a post-classification approach to reduce the errors and distortions resulting from the geometric correction process. This step is influenced by the approach used to process a remotely sensed image, and therefore depends on the use for which the data is intended, and when the geo-rectification is done (Liu & Mason, 2009). Generally, it is more competent to begin with geo-rectifying the still unprocessed data. Therefore, all products that will result from the raw data will be automatically geo-rectified (Liu & Mason, 2009).

The problems that can occur in pixels of an image that will be rectified to other one (source image) are: the pixels have a different position; different orientation; and different size (Fig. 5.2). With this in mind, resampling methods have been developed to cope with these problems. The methods are based on choosing well-known and matching sites in both images of the selected cartographic projection. Based on these sites, a resampling technique will calculate the relation between their positions in the two images. These positions can be located exactly on an image using the so-called *Ground Control Points (GCPs)*. These points are potential to define a suitable transfer function to be applied between the both images, i.e. rectify and master scenes (McCloy, 1995). There are three components to the process: 1) selection of suitable mathematical distortion model(s); 2) coordinate transformation; and 3) resampling (interpolation). These are also known as *warping* (Wolberg, 1990).

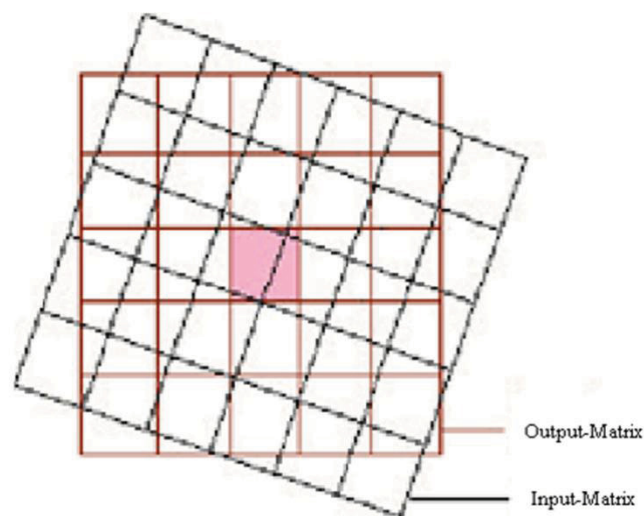


Fig 5.2: Reposition pixels from their original locations (Input matrix) in the data array into a specified reference grid (Output matrix) (Source: Modified from Lillisand et al., 2008)

"Resampling is the process of calculating the data file values for the pixels in the rectified image by the use of data file values in the source image data" (McCloy, 1995). There are three resampling schemes: nearest neighbor (sometimes called *zero-order interpolation*); bilinear interpolation; and cubic convolution. In the nearest neighbor approach, "the data file value of the nearest pixel to the retransformed pixel in the source image is adopted as the data file value for the output rectified pixel" (Liu & Mason, 2009). By comparison with the other two schemes, it has the advantages: that it does not change the digital number value in the data file; it is simple and rapid; and the main drawback is the stair stepped effect. This is used frequently before the process of classification is carried out (Liu & Mason, 2009).

Ground control points (GCPs) are pixels with well-defined positions in an image for which the output map coordinates are previously definite. They must have the following conditions and characteristics: 1) they have to be recognizable with a site both on the image and the real world surface (high contrast); 2) they are accessible in the field; 3) they are consistently located within the study area of interest; 4) there are sufficient of them; 5) they have a small feature size; and 6) they have to be fixed over time. The most frequently used method to select these GCPs is the visual method (Liu & Mason, 2009). If the point features to be GCPs are difficult to be exactly located on an image, it is better to select the ground object features to be a GCP (e.g., intersections of linear features). In an image-to-image registration model, intersections of highways or main roads are frequently used as GCPs. The next mathematical statement determines the minimum number of GCPs to be used:

*Minimum number of GCPs =  $((n1)(n2)) / 2$ , where (n) is the order of polynomial.*

To obtain superior classification results, additional GCPs to the minimum number are commonly used. There is an error measurement technique that can compute the correctness of selected GCPs. It named the *Root Mean Square (RMS)* error, which is the distance between the input (source) position of a GCP in the input-matrix and the re-transformed position for the same GCP in the output-matrix. RMS-error is computed using the next mathematical statement:

$$RMS - Error = \sqrt{(x_r - x_i)^2 + (y_r - y_i)^2}$$

Where:  $x_i, y_i$ : The input source coordinates;  $x_r, y_r$ : The retransformed coordinates.

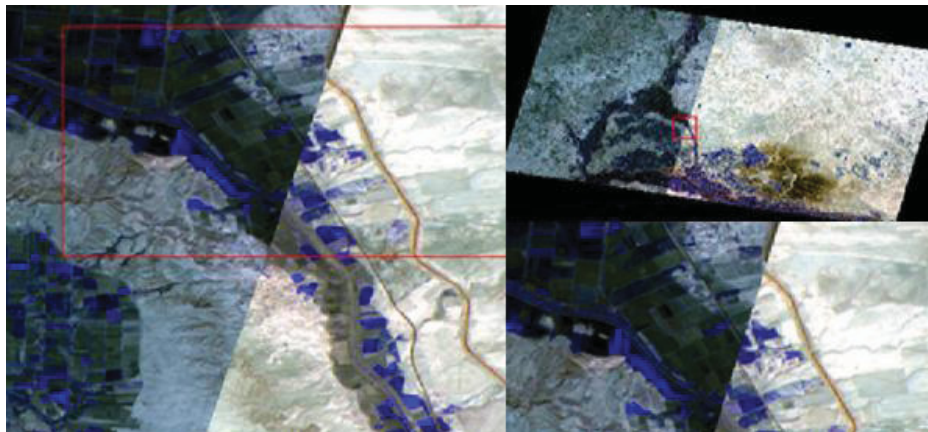
The RMS error will be determined for each GCP. In the next step, the total RMS error will be computed by calculation the all RMS error of all GCPs. In the third step, the RMS error will then be tested for accuracy. If the overall RMS error is not good enough, then those GCPs with high RMS errors must be removed. This previous step will be repeated until the RMS error is good enough.

For comparison and combination based studies that use diverse sources of data and information, like remote sensing imagers obtained from diverse sensors (e.g., MSS, TM, ... etc.), field reference points (e.g., GPS-points), topographical data (e.g., DEM) and other available data for a study area, it is important to transfer all these data into a reference cartographic projection system; the result of which is a generally suitable data basis. The ERB projection parameters are: (Projection: UTM, Ellipsoid/spheroid: WGS84, Datum: WGS84, Units: Meters, Zone: 37 North). The study area is in one UTM-zone (37 N), which was an advantage for this work, since no geometric problems occurred due to changes between two UTM-zones.

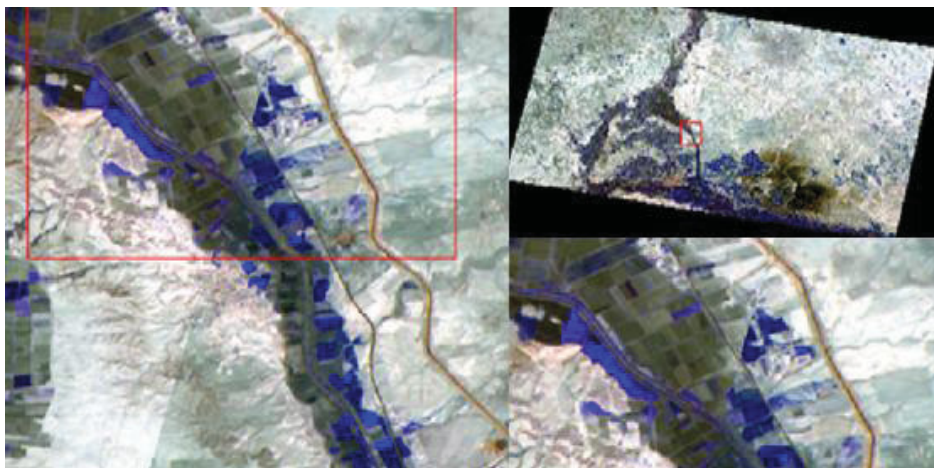
All LANDSAT-data with their different sensors have no spatial deformations among them (i.e., among the images of each sensor). However, during the connection and use of mosaic scenes, which result from gathering individual sensor images together, it was necessary to register the mosaic scenes to each other by accrediting one scene as the master-scene and linking the other scene/s. Regarding the ASTER-data, the majority of images were not geometrically corrected, particularly between close paths. Therefore, a geometric correction was needed, in addition to a spatial registration with ETM+-data which was considered to be the geographical reference. Here, the problem was that ASTER-data had a geographical reference different from the geographical projection system of the ETM+-data, and with a 16\*16 m pixel dimensions. For the purposes of this study, they were re-projected from: Geographic Lat/Lon, Datum: WGS-84, 16\*16 M Pixel Dimensions to UTM, Datum: WGS-84, Zone: 37 North, Units: Meters, 15\*15m pixel dimensions using Rigorous Transformation.

Although the program ENVI can automatically correct the ASTER-data geometrically, these data were geo-referenced using the “Image to Image” concept, and then analyzed on the basis of

LANDSAT-data, prior to fusing the two sensors-data. Fig. 5.3 illustrates the results of the geometric correction for two ASTER-images.



A) Before corrections



B) After corrections

Fig. 5.3: The geometric correction (including the radiometric corrections) results of two ASTER-scenes

The registration of the multispectral images was carried out using ENVI 4.6 software. The three general steps were: 1) locate GCPs in the two images to be corrected using the GCP-editor. The GCPs were interactively selected manually; 2) compute the transformation matrix using the GCP editor and the transformation editor until the RMS error is small enough. A first-order polynomial was sufficient for the transformation; and 3) resample the image data. The nearest neighbor resampling technique was applied for rectifying the multispectral imagery.

For example, the geo-registration for the two remotely sensed data coverages LANDSAT-MSS-June-1975 and LANDSAT-TM-August-2007, was carried out using 14 GCPs (Fig. 5.4) which distributed across the image, especially on the margins (the number was dependent on the size and image spatial resolution of the used remote sensing data set). Table 5.1 lists the GCPs coordinates. It was simple to gather and present good results. The nearest neighbor 1<sup>st</sup> order polynomial correction was also used. According to the criteria presented in the literature of remote sensing, the RMS error per image must be always less than the half of spatial resolution of the image pixels, namely, < 15 meters (0.36) (Townshend et al., 1992; Mather, 2004; Jensen, 2007).

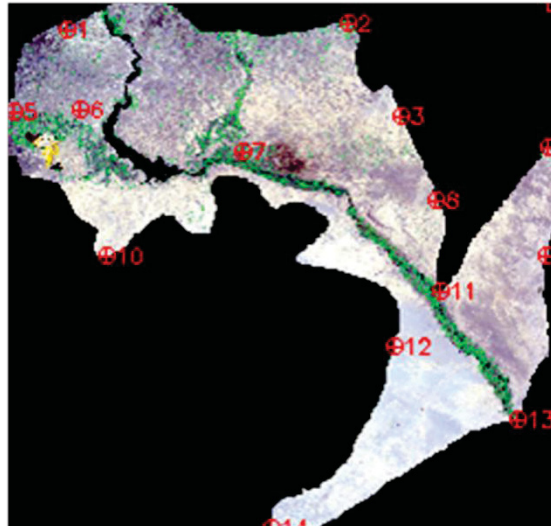


Fig. 5.4: The distribution of the 14-GCPs, used for registration of the tow data set (MSS-June-1975 and TM-August-2007), image-to-image concept

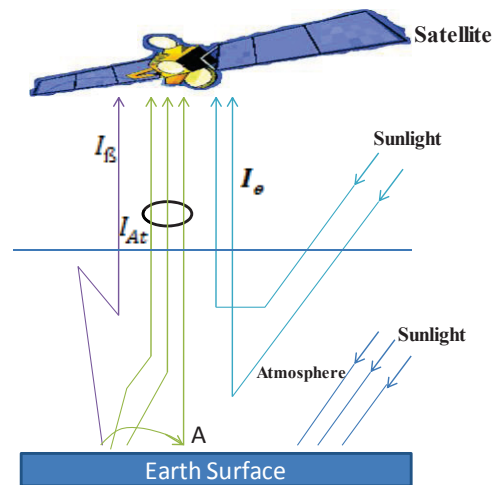
Table 5.1: The selected GCPs coordinates, used for registration the tow data set (MSS-June-1975 and TM-August-2007), image-to-image concept

GCPs	Base (x)	Base (y)	Warp (x)	Warp (y)	Predict (x)	Predict (y)	Error (x)	Error (y)	RMS-Error
1	74.730.000	63.920.000	14.390.000	74.400.000	14.370.695	74.499.013	-19.305.143	0.99013222	0.50213654
2	13.666.000	62.370.000	76.300.000	59.400.000	76.309.792	59.333.543	0.97916066	-0.66456802	0.10258974
3	14.781.000	82.830.000	87.465.000	26.392.500	87.461.775	26.395.139	-0.32248964	0.26385880	0.41667857
4	18.051.000	89.730.000	12.016.000	33.310.000	12.016.498	33.305.137	0.49801720	-0.48629317	0.69606191
5	63.010.000	81.650.000	26.400.000	25.190.000	26.523.039	25.180.724	12.303.943	-0.92761745	0.23569874
6	77.410.000	81.380.000	17.030.000	24.930.000	17.053.866	24.916.530	23.866.399	-13.470.035	0.15429854
7	11.331.000	90.470.000	52.975.000	33.990.000	52.958.665	34.021.619	-16.335.435	31.618.867	0.15214582
8	15.591.000	10.136.000	95.570.000	44.930.000	95.562.622	44.923.377	-0.73775910	-0.66228433	0.99141768
9	18.008.000	11.303.000	11.973.000	56.590.000	11.973.374	56.594.625	0.37395907	0.46254371	0.59480422
10	83.510.000	11.310.000	23.170.000	56.650.000	23.159.195	56.647.066	-10.804.704	-0.29344471	0.20245697
11	15.686.000	12.107.000	96.510.000	64.630.000	96.512.613	64.628.173	0.26131315	-0.18272012	0.31885922
12	14.659.000	13.287.000	86.250.000	76.430.000	86.242.500	76.424.509	-0.74995666	-0.54913877	0.92950975
13	17.364.000	14.886.000	11.329.000	92.410.000	11.329.206	92.409.188	0.20638698	-0.081211834	0.22179032
14	11.962.000	17.240.000	59.270.000	11.595.000	59.275.189	11.595.316	0.51886214	0.31586047	0.60744198
Total RMS Error: 0.367236									

## 2. Atmospheric correction

A literature review describing the atmospheric effect and its correction is provided by (Kaufman, 1989). Electromagnetic energy detected and recorded above the atmosphere by remote sensing sensors (here, those that work in the optical section of the EM spectrum/especially in the visible and near-infrared regions) includes two sources of energy: reflected and/or emitted from the ground surface; and energy scattered within and/or emitted from the atmosphere. The quantity of this electromagnetic energy is dependent on the quantity of exhaustive solar energy (irradiance), which is reduced due to many factors: atmospheric absorption; the reflectance characteristics of the various ground surface features; the differences in path length; the atmospheric conditions; and the wavelengths. Hence, energy recorded by the sensor is a constructed process of: 1) incident en-

ergy (irradiance); 2) target reflectance; 3) atmospherically scattered energy (path radiance); and 4) atmospheric absorption (ERDAS, 1999; Liang, 2004). Fig. 5.5 illustrates this process.



Schematic of the atmospheric influence on the recorded radiation at the sensor. The Sunlight is broken into three components:

$I_e$  : Air light.

$I_g$  : Diffuse lighting. Distracted Radiation and Reflection/Emission.

$I_{At}$  : Direct Reflection/Emission + Reflection/Emission by neighborhood effects.

A: Target

Fig. 5.5: A simplified model of the atmospheric effects on the reflection on a target object (Source: Modified from Kaufman, 1985)

A large amount of optical remote sensing data is affected by the impact of the atmosphere. This impact is called atmosphere effects (Liang, 2004). It includes "molecular and aerosol scattering and absorption by gases, such as water vapor, ozone, oxygen and aerosols" (Liang, 2004). These effects are not measured as "error", because they are a component of the entire recorded signal by a receiver or sensor (Bernstein, 1983). To deal with these effects in optical remote sensing, there is a procedure known as *Atmospheric Correction*. It corrects for surface reflectance from remotely sensed images. However, it is not always simple to remove or enhance these effects. The procedure of atmospheric correction includes: assessment of the parameter of the atmosphere; and regain of the surface reflectance. To correctly regain the surface reflectance based on converting of sensor measurements to actual reflectance values on the ground using radio transfer codes, may need a well knowledge about the atmospheric conditions at the time of image acquisition by a remote sensing sensor (e.g., humidity and temperature).

The assumptions that the reflectance values recorded on the remotely sensed data (optical remote sensing) are equal to the real reflectance of the different features on the ground surface, and that there is representative relation between the recorded values on the images and between the three properties of the ground surface (physical, chemical and biological), is not acceptable unless atmospheric corrections are applied (Liang, 2004). Smith and Milton (1999) had presented the next more radical principle: "to collect remotely sensed data of lasting quantitative value then data must be calibrated to physical units such as reflectance".

It is not always necessary to apply an atmospheric correction technique for each remotely sensed study, since the necessity for that depends on the goals of the analysis and the expected results or products. For clarification, it is very important to be applied when a remotely sensed data of a certain region are to be evaluated over a time period - e.g., over a period of a crop growing - (Liang, 2004). Atmospheric correction is necessary for classifying a multi-sensor (especially when inte-

grated for an image classification) or multi-date imagery. It is moreover, essential for mapping of change detection over a time, since it used to guarantee that gray values of pixels are comparable in both images in a temporal sequence (Liang, 2004), since atmospheric effects are one of the error sources in change detection studies (e.g., Chavez & Mackinnon, 1994; Coppin & Bauer, 1996; Song et al., 2001; Rogan et al., 2002; Coppin et al., 2004). Atmospheric correction is essential for enhancing the results carried out based on remotely sensed data (Elmahboub et al., 2009).

In general, if a single-date image is used in LULC-classification, it may not require atmospheric correction as long as the atmospheric effects are consistent over the whole scene, since their impacts are similarly on the spectral vectors of training and unknown pixel, and their relative positions in spectral space are unaffected. However, if the atmospheric conditions varies largely within the study area (e.g., due to haze, smoke or dust storm), then spatially-dependent correction is needed (Song et al., 2001; Liang, 2004; Schowengerdt, 2007).

A lot of models and techniques were founded to normalize and, if possible, to correct the radiometric distortions of the data and the atmospheric effect related to atmosphere conditions. These include, for example: the simple relative calibration approaches (e.g., the dark-object subtraction); and the complex approaches (e.g., 6S) (Markham & Barker, 1987; Gilabert et al., 1994; Stefan & Itten, 1997; Vermote et al., 1997; Tokola et al., 1999; Heo & Fitz-Hugh, 2000; Song et al., 2001; Du et al., 2002; McGovern et al., 2002; Canty et al., 2004; Hadjimitsis et al., 2004). These methods include: 1) *Invariant-Object Methods* (Moran et al., 1992; Chavez, 1996); 2) *Histogram Matching Methods* (Richter, 1996 a and 1996 b); 3) *Dark-Object Methods* (Chavez, 1988 and 1996; Moran et al., 1992; Kaufman et al., 1997 a and b, and 2000; Liang et al., 1997), which is frequently used; 4) *Contrast Reduction Methods* (Tanre et al., 1988; Tanre & Legrand, 1991); 5) *Cluster Matching Method* (Liang et al., 2001); 6) *The MODTRAN-code* (Berk et al., 1998); and 7) *The Second Simulation of the Satellite Signal in the Solar Spectrum 6S-code* (Vermote et al., 1997).

In the study presented here, the simplified and fast correction approach using the software program *ATCOR-2* (Richter, 2011) was used in an attempt to atmospherically correct the images when needed.

The *ATCOR-2/ Atmospheric CORrection* program was developed by the German Center for Aerospace (DLR/ Deutschen Zentrum für Luft- und Raumfahrt) (see: Richter, 1996 b and 2011; <http://www.op.dlr.de/atcor>). It provides spatially adaptive and fast algorithm. It supports the remote sensing sensors LANDSAT-MSS/TM and SPOT from SPOT-4. It works with a set of functions for atmospheric correction. This set (or catalog) was developed based on MODTRAN-2 and SENSAT-5 code. *ATCOR-2* assumes that the target objects have an isotropic reflection behavior, where the error effect is taken in account by the blooming effect. The program uses the comparative analysis of the measured reflectance of a target object on the sensor with the back-calculated reflection of the same target, which it derived from models. It is also implemented in ERDAS IMAGINE (<http://www.geosystems.de>; <http://www.atcor.de>). The software has been available since 1996/2002, and is a part of other digital image processing software such as ENVI and PCI-Geomatica, or as an independent program.

Some of the advantages of *ATCOR-2* are: 1) short times required for computing process; 2) adequate results in comparison to other simple approaches or models; 3) it is easy to get the required parameters to be input to the program; and 4) it is uncomplicated to set and modify these parameters separately across the study area, especially if this area is large enough to have different radiation effects (Leica Geosystems, 2005). Fig. 5.6 subdivides the module *ATCOR-2* into many sub-modules.

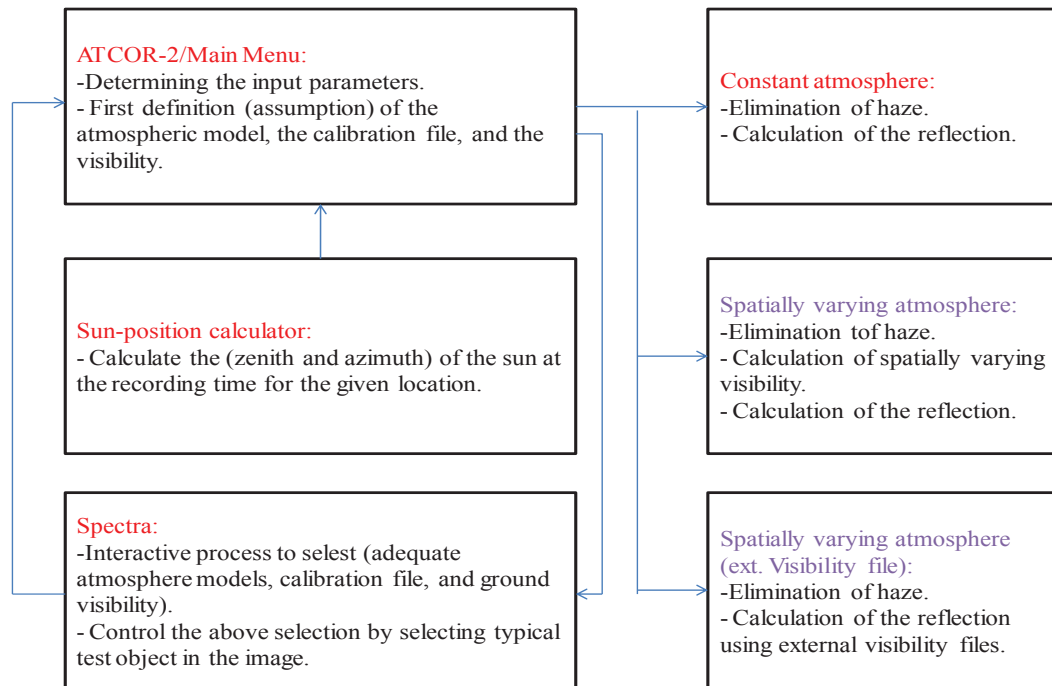


Fig. 5.6: ATCOR-2 and its central sub-modules (Source: Modified from Leica Geosystems, 2005)

The parameters that have to be entered in the ATCOR-2/main menu are: 1) the image has to be corrected, the input-file source location, and the output-file destination after finishing the process of correction; 2) selection of spectral bands to be corrected; 3) determining the sensor specifications (calibration file); 4) determining the atmospheric model (based on meteorological information and the parameters of the applied model); 5) the size of the study area; 6) size of the used filter (to minimize the blooming effect), reflection- and emission- correction factors using the maximal dynamic range of the output-file by rescaling 8 bit; 7) some secondary information (e.g., location coordinates, recording date/time, zenith angle, mean elevation of the study area, air pressure, air temperature, absolute and relative humidity, and visibility); and 8) selection of the suitable atmospheric conditions from constant and spatially varying by comparison with secondary sources (Leica Geosystems, 2005).

The Spectra-module can be used optionally after point 7 as parameter number 8 in the module (main menu), checks whether the selected atmospheric model and the visibility are adequate (and if necessary adjusts the parameters iteratively).

Fig. 5.7 illustrates the major followed steps in atmospheric correction of the data set in this study. The solar zenith/sun elevation ( $61.07^\circ$ ) and the solar azimuth/sun angle ( $126.22^\circ$ ) were calculated using the sun position calculators based on the recording date of the image (e.g., p172r035)/(07.8.2007), scene-center-scan-time (07:50:59 clock), and the Longitude (039 45 10 E) and Latitude (35 10 05 N) of the scene center. The necessary information can be found in the header file of the image data. The used atmospheric type was midlat-summer-rural, where: midlat = radiation region of the mid-latitudes, summer = season, and rural = aerosol type. Table 5.2 provides the used weather information. If the meteorological data are not always obtainable, then the standard atmosphere (dry desert) have to be used, which took into account the atmospheric effects in a good approximation (Richter, ATCOR-2/3 User Guide, 2011).

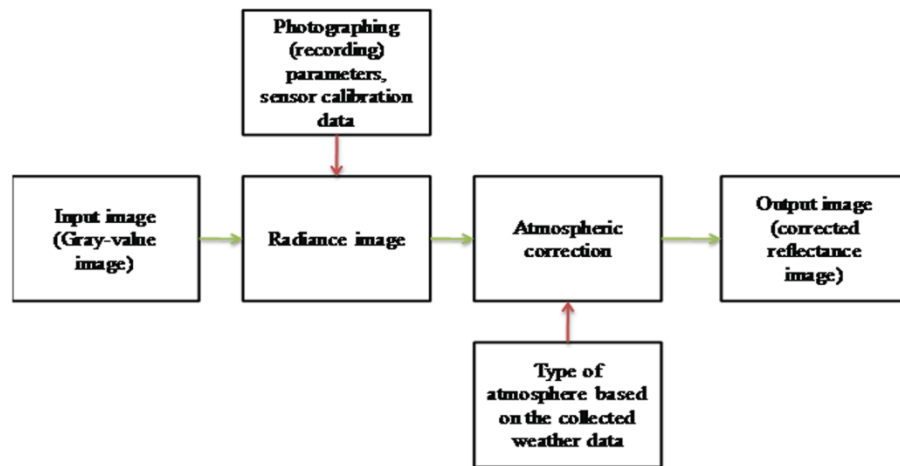


Fig. 5.7: The general concept of atmospheric correction using ATCOR-2

Table 5.2: Weather data from the Arraqah climatic station (Longitude: 039 59 00 E; Latitude: 35 54 00 N; Elevation: 250 Meters), 07.08.2007, 8.20 clock (Source: The General Authority for Meteorology, Damascus, 2008)

Temperature	30.4°C
Relative Humidity	44 %
Visibility	35 km
Air pressure	870.3 hPa
Sun elevation	61.07

The sensor calibration file represents another important input. This file includes the calibration data (correction factors: Bias [c0] and Gain [c1]) of each channel. Bias: Describes the spectral radiation on the sensor for a gray value of zero. Gain: Represents the gradient calibration. The data takes place in the unit of electromagnetic radiation [mW cm<sup>-2</sup> sr<sup>-1</sup> μm<sup>-1</sup>] (Lillesand et al., 2008). ATCOR-2 calculates the reflection on the sensor using these factors in the linear equation:

$L = c0 + c1 * DN$ , where: **L** = calculated radiance on the sensor; **DN** = digital numbers

The new atmospheric corrected image (LANDSAT-TM-p172r035-070807) has new gray-values (e.g., DN<sub>s</sub>-before: 50, 65, 83; DN<sub>s</sub>-after: 41, 45, 65). The corrected histogram band 1 has, in comparison to the raw data, the same trends. It is darker, the individual object-groups are more evident through peak formation in the corrected data (DN-values), and they are, therefore, better to delimit than in the raw data (uncorrected) (Fig. 5.8).

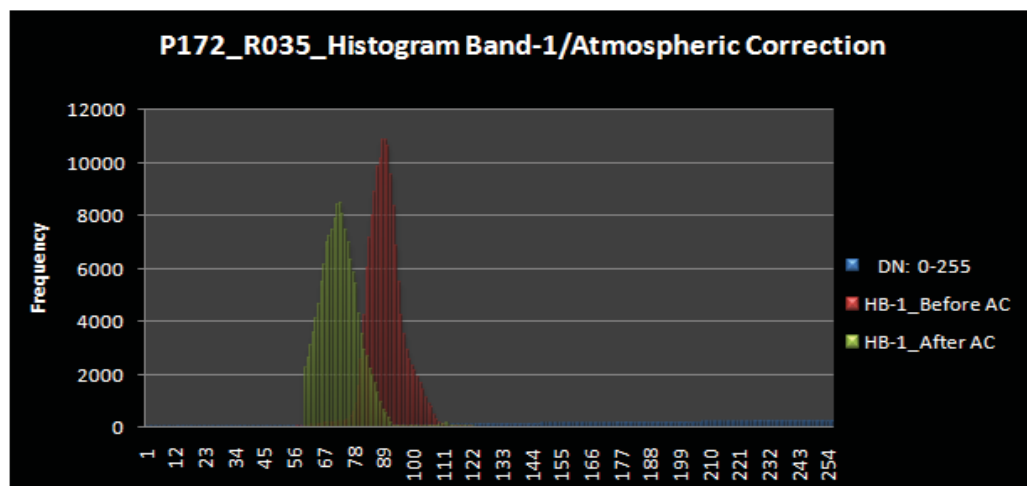


Fig. 5.8: Histogram comparison of the (LANDSAT-TM-Band-1) before and after the atmospheric correction



### 3. Radiometric processing/calibration

The application of the information-extraction algorithms for LULC-classification, change detection and other remotely sensed Earth observation studies can be generally useful when the data are radio-metrically processed (De Jong et al., 2005). On the other hand, if the user select an approach, that is based on products resulting after classification, for mapping the change detection, then radiometric correction is avoidable (Jensen, 2007). It is true when only one image at each compared time (no mosaic) is used in classification, and when each image has the same irradiance conditions (e.g., no haze or dust). However, the using of some change detection approaches (image differencing, change vector analysis), would requires a radiometric normalization. Also, radiometric correction is necessary for some applications (e.g., image mosaicing, generating of vegetation indices over the time) (Yang & Lo, 2000).

The radiometric correction set can correct radiometric distortion, which occurs because of sensor noises and atmospheric effects. Radiometric correction of remotely sensed data is a process of converting the recorded pixels' brightness values (where they are simply numbers, without physical units) to an absolute independent scale of radiance that serves as a more direct link between image and biophysical phenomena, then addressing the errors in pixel values. It is then possible to manipulate these values to maximize their information for studies that are based on the digital processing of remote sensing data (Wulder & Franklin, 2003; Liang, 2004; Richards, 2005; Schowengerdt, 2007; Lillesand et al., 2008).

Schowengerdt (2007) has listed three levels of radiometric calibration. The first converts the sensor DNs to at-sensor radiances. The second transforms the at-sensor radiances to radiances at the Earth's surface. The third transforms it to surface reflectance.

The radiometric correction/adjustment set includes the three mechanisms: 1) calibration of the sensor: it is the process of converting the DNs to at-sensor radiance for inter-sensor data comparison. Gains and offsets are well-known for each remote sensing sensor, and these used to the recorded signals to generate the DNs. This first mechanism is frequently calculated at the satellite ground stations; 2) atmospheric correction (see C5.B.2); and 3) radiometric normalization (absolute and relative). A) absolute radiometric normalization: "for a linear sensor, is performed by ratioiding the digital numbers (DNs) from the sensor, with the value of an accurately known, uniform radiance field at its entrance pupil" (Liang, 2004). In this case, user has to carry out atmospheric corrections, which require atmospheric information at the time of the image acquisition (see C5.B.2). However, when it is difficult to obtain these atmospheric parameters and/or the absolute surface radiance is not necessary, one can change to B) relative radiometric normalization: it is an in-image technique which uses the information contained within the image itself, and used when the full radiometric calibration for remote sensing data is complex. The concept is based on the supposition that it is possible, by application of linear functions, to estimate the at-sensor radiances recorded at two different times and for the same area but under different conditions (Yang & Lo, 2000). This technique has the disadvantages of difficulty and time-consuming, where it has to determine the suitable time-invariant features upon which the normalization is based (Teillet & Fedosejevs, 1995; Schowengerdt, 2007). This method is applied especially in applications based on LULC-classification and post classification change detection (Song et al., 2001).

Several methods (Schott et al., 1988; Hall et al., 1991; Moran et al., 1992; Furby & Campbell, 2001; Du et al., 2002) were developed and proposed to be applied as techniques for the relative radiometric normalization in remote sensing applications. Canty et al. (2004) proposed a method based on MAD, which use the advantage of the invariance properties of MADs. Canty and Nielsen (2008) further improved this approach by introducing an iteratively re-weighting method of the MADs, which executed superior in isolating no-change pixels fit to use for the relative radiometric normalization. The MAD method, after the modifications by Canty et al. (2004); and Schroeder et al. (2006) provides better radiometric normalization than those achieved with manual selected invariant features.

MAD can be used for bi-temporal change detection and for automatic relative radiometric normalization (Nielsen, 2007; Canty & Nielsen, 2008; Canty, 2010). Canty (2010) explained the mathematical background of MADs.

To create a MAD-image, it is necessary to select two multi-spectral images that have alike spatial dimensions (size of the pixels). The two images will be modeled as a casual variable  $G_1$  and  $G_2$ . When each image has, for example, 123 pixels, then these 123 pixels have a 123 times repetition of a mathematical random experiment, where, –here, the accurate value of pixels are not defined or described. If  $G_1$ ,  $G_2$  represent only a specific pixel or an entire image, then it will be illogical for them. What is important here is the properties of the causal variables  $G_1$ ,  $G_2$ . Some suppositions about  $G_1$ ,  $G_2$  can be made by using the metrics of histogram (e.g., empirical variance, mean-based assessment of predictable value). Each image includes an  $N$  spectral bands, with  $G_1$  (also  $G_2$ ) as a random vector (Schultz, 2011).

The  $X^2$  image expresses the representative pixels which may be suitable for the radiometric normalization (Canty, 2009). The  $X^2$  distributions are only the pixels that satisfy the formula:  $/Pr(\text{no change}) > t$ , where  $(t)$  is a decision threshold that is typically 95%/. The radiometric normalization based on these satisfying pixels will be used to perform an orthogonal regression.

The iMADs,  $X^2$ -values can only be calculated for overlapping areas, since the iMAD is designed for applying the automated radiometric normalization of multi-temporal remotely sensed data sets. Adjacent scenes can be normalized by selecting their overlapping area (subsets) and followed by using the created transfer function of the orthogonal regression expressed on an entire image. It is important to cover all LULC-properties in the overlapping region of the two images (master and target), while pixels with an alike spectral behavior from overlapping and non-overlapping regions will be treated according to the regression function (Canty & Nielsen, 2008).

Large water bodies (e.g., sea) affect the iMAD negatively (Canty, 2009). Clouds and their shadows do not affect the normalization superiority, while they are detected as change (Canty & Nielsen, 2008).

Summarized after Canty and Nielsen (2008) and Schultz (2011), the performed radiometric normalization was achieved in the five phases: 1) insert the dual-temporal data set; 2) compute CVs, build MADs and reweighing the spectral information accordingly; 3) repeating until no significantly improvement in correspondence of the CVs; 4) select pixels that have a no-change chance greater than a threshold value  $(t)$ ; and 5) determine the two radiometric normalization coefficients, i.e. slope and intercept, based on the orthogonal regression on selected pixels that have to be performed previously.

The iMAD was applied to the imagery using ENVI 4.6 and IDL 7.06. The source code used was provided by Morton Canty and can be downloaded at “<http://mcanty.homepage.t-online.de/software.html>”. In Canty (2009) the implementation and installation of the software to ENVI 4.6 is presented and explained.

To normalize the radiometry of all the used remote sensing sensor (e.g., LANDSAT-MSS-June-1975 and LANDSAT-TM-August-2007) data sets, a master scene has been selected in each data set to which all other scenes have been adjusted. LANDSAT-MSS scene (p185r035) and LANDSAT-TM scene (p172r035) were selected as master scenes for each data set, as each was in the center of the study area and covered the greater part of it. Atmospheric conditions/illumination were the same overall in each scene (e.g., no dust, no haze, etc.), and they had no cloud cover. All other scenes in each data set were radio-metrically adjusted based on the two master scenes. Regions in the image overlap areas of the bordering scenes were used to calculate regression coefficients, which were applied in a second phase to the complete sub-scene. The overlapping areas were selected to represent the variability of surface across the scenes. Finally, after mosaicking the images of each data set, the TM-Mosaic-Image was chosen as a master scene to normalize the MSS-Mosaic-Image radio-metrically (Fig. 5.9).

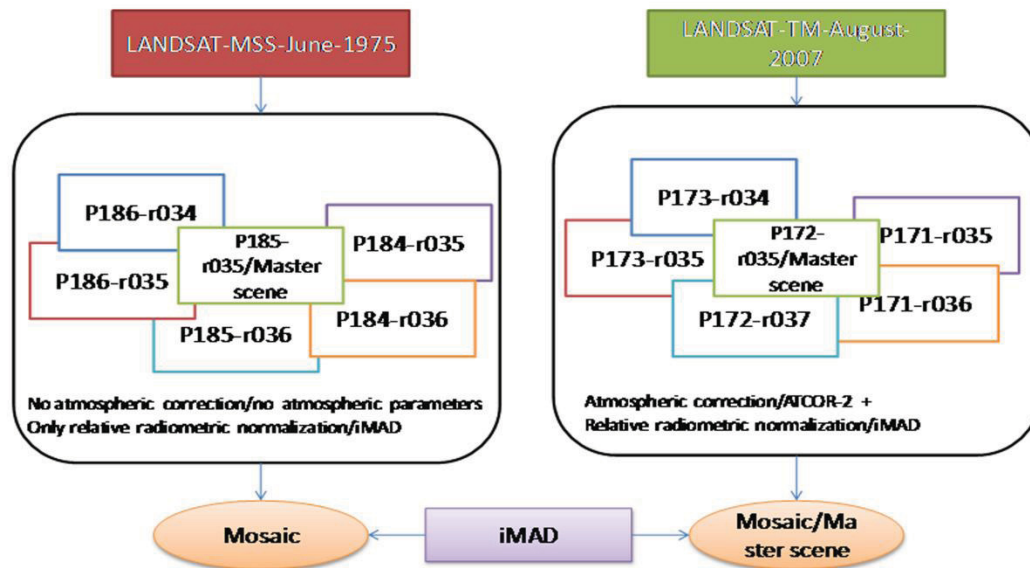
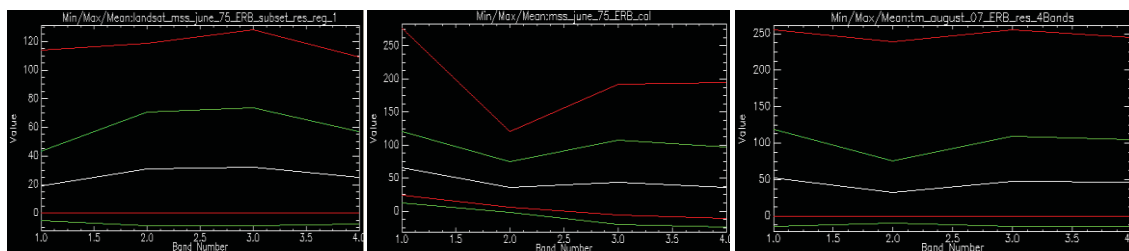


Fig. 5.9: Radiometric normalization between the two data-sets, which were used for change detection

Fig. 5.10 provides the results of the radiometric normalization using iMAD.

MSS-1975-Mosaic/before (iMAD) MSS-1975-Mosaic/after (iMAD) TM-2007-Mosaic/Master scene



Basic Stats	Stdev	Stdev	Stdev
Band 1	24,345611	53,79413	66,910881
Band 2	39,756239	38,173823	42,59285
Band 3	41,205301	63,594957	62,193548
Band 4	31,961721	60,645272	59,189952

Fig. 5.10: iMAD results for the two data sets MSS-1975 and TM-2007. We can notice that the basic statistics (e.g., Stdev) of the radiometric normalized image are more similar to the master scene than the unnormalized image

A radiometric correction process was fulfilled on the mosaic scenes which comprehensively covered the study area. This was achieved by accrediting one of the scenes as a radiometric-reference (master-scene). Then, the other image/s were matched with it radio-metrically, i.e., a transformation process of the radiometric characteristics of the source-scene was conducted on the other images (targets). This resulted in obtaining close and similar radiometric characteristics for all scenes that covered the study area, because all had the same reference/source (i.e., the master-scene). Consequently, the Earth features (e.g., wheat fields) that existed in an individual scene, appeared spectrally (reflectance values/gray values) and radio-metrically, similar to those wheat fields located in each of the other scenes. This degree of similarity was based on the applied radiometric correction method/s and on the nature of the ground surface features that existed in the satellite image.

After finishing the atmospheric correction using ATCOR-2, a radiometric correction process was conducted of the scenes covering the study area (MSS-June-1975 and TM-August-2007) using

iMAD. A radiometric correction was applied upon the two mosaic-scenes, since the TM-data was too basic for use with iMAD.

Concerning the scenes that could not pass the radiometric correction process (for instance, TM-May-2007-data), it was enough to make atmospheric correction using ATCOR-2, followed by an automated classification applied for each image. Finally, the mosaicing-process was applied for the produced thematic maps that resulted from classifying each image. This mosaicing-process was helpful, in that it made it easier to find the final statistical results for the whole study area, and to compare the area with other results from separate data and dates.

#### 4. Data fusion

Image fusion is the process of fusing the lower multi-spectral spatial resolution with the higher panchromatic spatial resolution, to generate a higher multi-spectral resolution data set, which has the advantages of both: the high spatial resolution of the panchromatic image; and the higher spectral resolution of the multi-spectral image. It is one of the spatial enhancement techniques which are able to use the corresponding information that obtained from different imagery about the same terrain features in an effective way. The application of this technique is more for visual observation and interpretation than for quantitative analysis, as it can maximize the differences between different targets (Liu & Mason, 2009).

Fusing panchromatic- and multispectral- data includes two general steps: 1) the geometrically registration the low-resolution multispectral imagery to the high-resolution panchromatic imagery (see C5.B.1); and 2) merging the information contents, spatial and spectral, to produce one data set that have the best characteristics of the two input data sets. Examples of image fusion techniques are: IHS (Intensity-Hue-Saturation); PCS (Principal Component Substitution); HPF (High-Pass Filter); RVS (Regression Variable Substitution); and SVR (Synthetic Variable Ratio). In this study, the Gram Schmidt Spectral Sharpening Algorithm was used.

The merged data were fit for further digital classifications, since the spectral separability for LULC- and crops- classes/six spectral bands of the merged data was better than the spectral separability of the original data. This was because there were only three spectral bands. Therefore, merged images were used for visual interpretation and for features extraction (classification).

Fig. 5.11 explains the concepts followed to generate the final fused and mosaiced data set of the ERB-borders based on TERRA-ASTER & LANDSAT-ETM+ images.

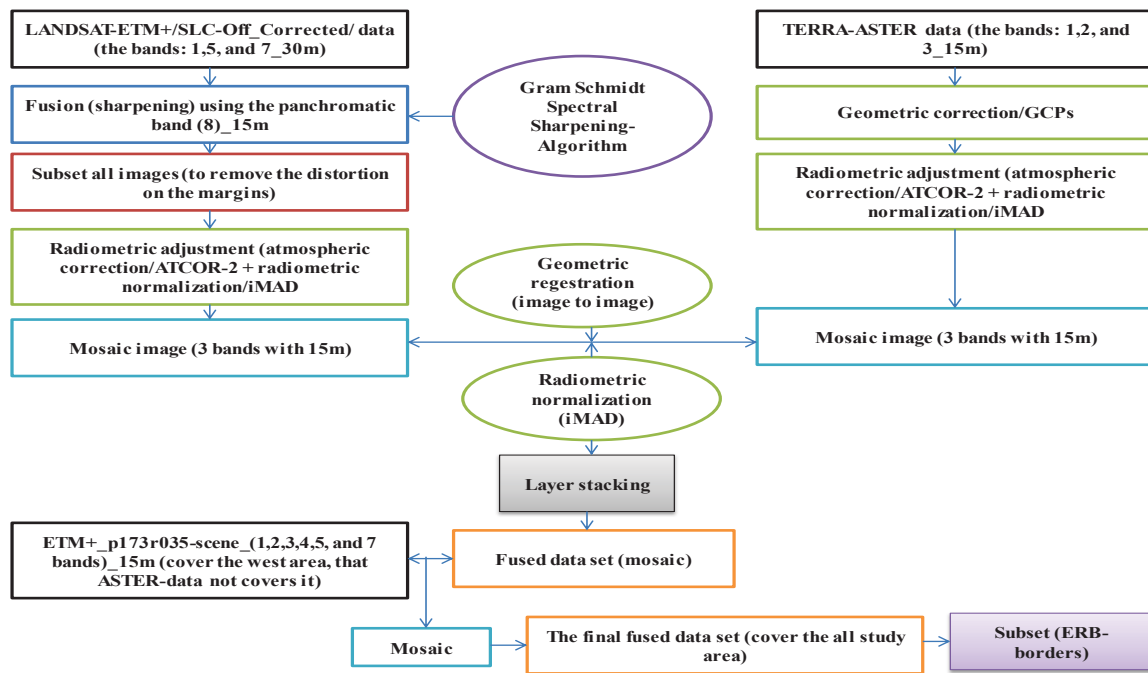


Fig. 5.11: Fusion- and Mosaic- concept for LANDSAT-ETM+ and TERRA-ASTER data set, acquired in May and August 2005

The ASTER data did not cover the entire study area, only the first three bands with a spatial resolution of 15 m. This data was previously tested on the separability among the extracted classes of interest from the study area and compared to the same ASTER data after they were merged with the three spectral bands (1, 5 and 7) of LANDSAT-ETM+. However, these three bands were useless in the classification process due to their low separability when compared with the results of spectral separability that resulted after fusing with the other three bands of ETM+ (see Table 5.4, Table 5.5). Therefore, ETM+-scenes which were corrected SLC-off data were used. This data had similar temporal coverage to the ASTER data. The purpose was to increase the spectral resolution which in turn, increased the spectral separability between classes. These offered classification results with higher accuracy rather than using only the three spectral bands of ASTER data in the classification process.

Because the ASTER data had a spatial resolution of 15 m, and in order to benefit from this to compare results with the results of MSS-60m, and TM-30m, a spatial enhancement of the ETM+-scenes with the spatial resolution of 30 m was required. This was conducted by transforming the data into a 15 m spatial resolution using the ENVI-program and selecting the Schmidt Spectral Sharpening Algorithm.

(Fig. 4.4) shows the spatial distribution of the two remotely sensed data which were used in the fusion and mosaicing process.

## 5. Mosaicing, subsetting and masking

The mosaic-process was applied to data which had similar atmospheric conditions and no radiometric distortion overall, or to those data whose atmospheric and/or radiometric distortions were corrected or normalized using ATCOR-2 and/or iMAD (see C5.B.2 & C5.B.3). For the data which were impossible to correct, a LULC-classification was carried out for each scene and then mosaiced to the results, to determine statistics. These results were in turn compared with those of the other data set (e.g., post-classification change detection) (see C5.L.2). The advantages of the mosaic process were found to be their ease and the speed in digital image processing.

The section C5.B.4 and the two figures (Fig. 5.9 & Fig. 5.11) explain the followed process for two data sets. Fig. 5.12 explains the difference between two generated mosaics and the importance of the pre-processing steps, especially color balancing, radiometric normalization and atmospheric correction.

The masking operation enables researchers to use an image file to choose (mask) definite areas and/or values from a matching raster file, and use those areas and/or values to generate one or more new files. The input mask file and input file must be the same as masking will be performed on the image area that both files have in general through the intersection process. This operation was used too often in the Multi Stage Classification Approach (see C5.G.1.2.1), especially in crops classification (see C5.J). The masking areas were selected by generated class values or were based on NDVI transformation (the masking operation was a processing and not a pre-processing step). All the class values of classes to be masked were set to zero or recoded to zero, then all unwanted zero signed features will be ignored when masking was executed.

The sub-setting operation was used broadly in this study to cut and remove the distorted margins of the LANDSAT-data; to subset only the study area (ERB borders) from each image or from the whole data set mosaic scene; to reduce processing time; and to reduce the geographical local extent that increased the spectral differences of the existing ground surface features. The final subset of the study area was about 50,335 km<sup>2</sup>.

Mosaics for the ASTER-May and August-Data in 2005 were produced, eight paths from left to right (path-1: 4 rows, path-2: 4 rows, path-3: 3 rows, path-4: 3 rows, path-5: 3 rows, path-6: 4 rows, path-7: 5 rows, and path-8: 4 rows).

After the enhancement of the three bands of the ETM+-data (six bands for the scene (p173r035), i.e., the bands (1, 2, 3, 4, 5 and 7) which covered a part of the study area that the ASTER data did not cover), scenes were collected in one mosaic-scene. Here, before mosaicing, subsets were completed for each scene to remove margin deformations. After that, a geographic registration was applied for the ASTER-mosaic-scene with the ETM+-mosaic-scene as master-scene, using the image to image method. Before the last step, the three bands of ASTER data were composited with the three bands of ETM+-data (one layer-stack). The last step created a mosaic for the last scene which resulted from fusing ASTER-bands with ETM+-bands, and for the p173r035-scene of ETM+-data that covered the rest of the study area. The final result was the creation of one compound mosaic scene from both the ASTER- and ETM+-data that was homogeneous: Radiometrically (i.e., no or acceptable spectral appearance of the same features overall in the mosaic-scene); spatially (15 m); and spectrally (six bands).

In order to reduce temporal and effort processing series on the remote sensing scenes which covered more than the spatial distribution of the study area, these scenes were subsetted (either separately or inclusively in one mosaic-scene) to include only the spatial distribution of the ERB borders.

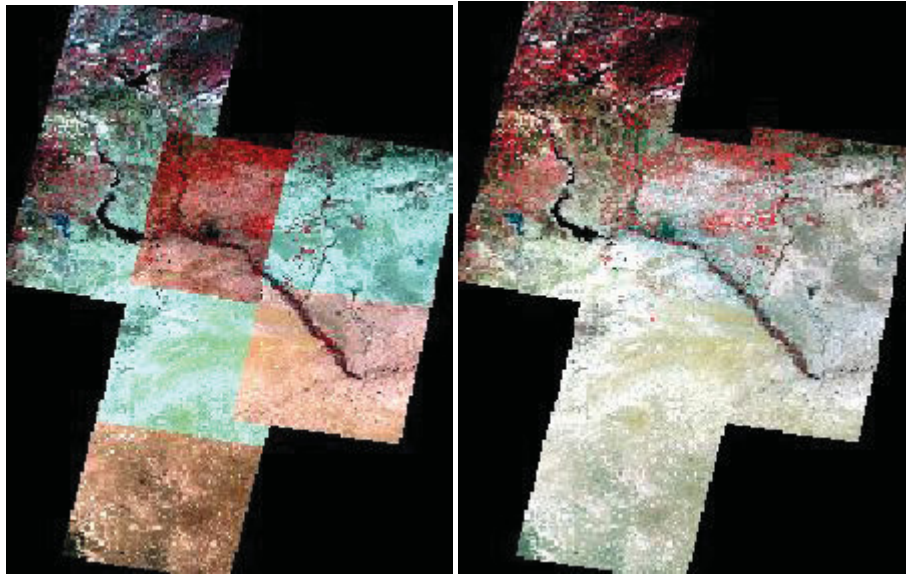


Fig. 5.12: Two mosaic-results of the data set (LANDSAT-TM-August-2007). Left: without any digital pre-processing steps/techniques or corrections; Right: After applying corrections

### C. Design of the LULC- classification system

A LULC-classification process starts with defining a classification system. A successful LULC-classification requires a suitable classification system and an adequate number of training sites. Its design is related to: the needs of the user; the spatial resolution of used remote sensing data; the capability with the prior studies; the used algorithms for image-processing and classification; and the time limitations. A system of LULC classification categorizes the all definable LULC-features into classes in the system. A good system should have three characteristics (informatively, exhaustively and separability) (Landgrebe, 2003; Jensen, 2007). A system is exhaustive when each feature in the real world has a label. Also, a good system structure can be located at any point on the map/ground into one and only one LULC-category.

An a priori hierarchical structure system for the LULC-classification for the study area was build. This system was adopted to increase the flexibility of classification procedures and to take different conditions into account. Furthermore, the LULC-classification system used the "diagnostic criteria and their hierarchical arrangement to form a class (*map-ability function*), that had the ability to define a clear boundary between two classes. Hence, diagnostic criteria should be hierarchically arranged in order to assure a high degree of geographical accuracy at the highest levels of the classification. These prerequisites can only be accomplished if the classification has the possibility of generating a high number of classes with clear boundary definitions" (Di Gregorio, 2005).

The *Land Cover Classification System (LCCS)* was designed with two main phases (see Fig. 5.13): A) an initial *Dichotomous Phase*, in which eight major land cover types were defined: (1) Cultivated and Managed Terrestrial Areas; (2) Natural and Semi-Natural Terrestrial Vegetation; (3) Cultivated Aquatic or Regularly Flooded Areas; (4) Natural and Semi-Natural Aquatic or Regularly Flooded Vegetation; (5) Artificial Surfaces and Associated Areas; (6) Bare Areas; (7) Artificial Water bodies, Snow and Ice; and (8) Natural Water-bodies, Snow and Ice (Di Gregorio, 2005).

Five major classes were classified: 1, 2, 5, 6 and 8, since the classes 3, 4 and 7 did not exist in the study area ERB. A dichotomous key was applied at the major level of classification to identify the major land cover classes (see Fig. 5.13). Three classifiers were used in the dichotomous phase, i.e.: *Presence of Vegetation*; *Edaphic Condition*; and *Artificiality of Cover*. "These three classifiers were hierarchically arranged, although independent of this arrangement, the same eight major land

cover types would be keyed out. The hierarchical arrangement is thus not important in this phase, but was a guiding principle in the subsequent Modular-Hierarchical Phase" (Di Gregorio, 2005).

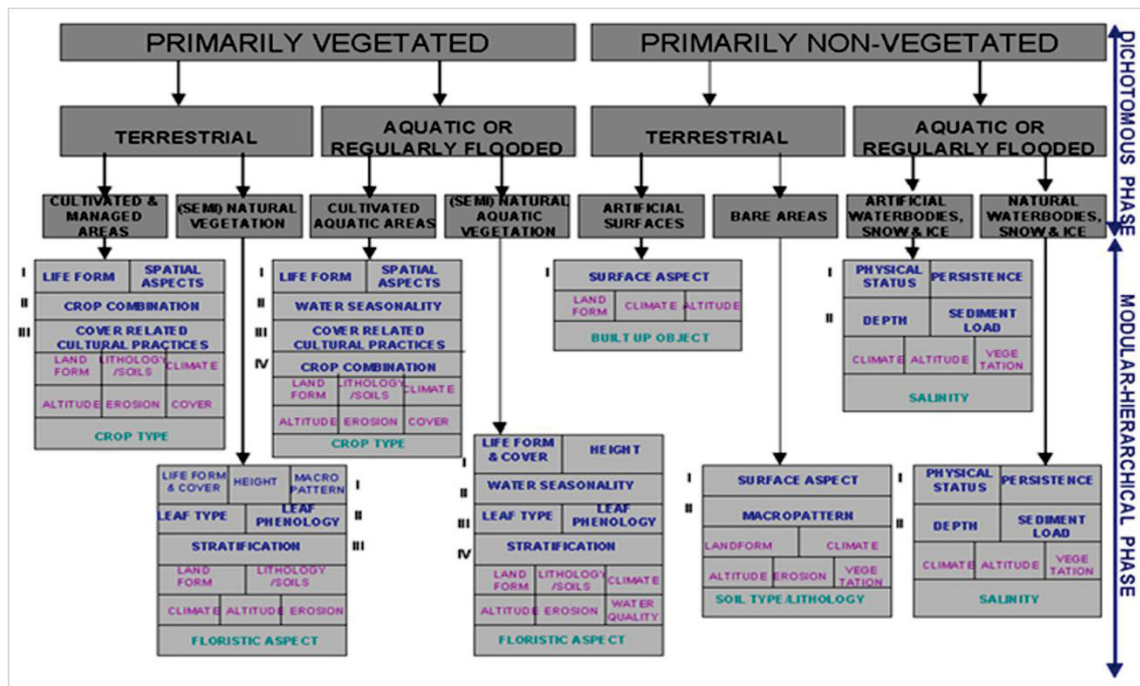


Fig. 5.13: Overview of the Land Cover Classification System (LCCS), its two major phases and the classifiers (Source: Adapted from Di Gregorio, 2005)

This was followed by a subsequent so-called: "B) *Modular-Hierarchical Phase*, in which land cover classes were created by the combination of sets of pre-defined classifiers. These classifiers were tailored to each of the eight major land cover types. The tailoring of classifiers in the second phase allowed the use of the most appropriate classifiers to define land cover classes derived from the major land cover types and at the same time, reduced the likelihood of impractical combinations of classifiers" (Di Gregorio, 2005).

The classifiers of the pure land cover can be joined with so-called *attributes* for additional description. There are two kinds of these attributes, which form separate levels in the classification: (Di Gregorio, 2005): "(1) *Environmental Attributes*: these attributes (e.g., climate, landform, altitude, soils, lithology and erosion) influence land cover but are not inherent features of it and should not be confused with "pure" land cover classifiers. These attributes can be combined in any user-defined order; and (2) *Specific Technical Attributes*: these attributes refer to the technical discipline. For Semi- Natural Vegetation, the *Floristic Aspect* can be added (the method on how this information was collected as well as a list of species); for Cultivated Areas, the *Crop Type* can be added either according to broad categories commonly used in statistics or by crop species; and for bare soil, the *Soil Type* according to the FAO/UNESCO Revised Soil Legend can be added. These attributes can be added freely to the pure land cover class without any conditions".

The LCCS is a wide-ranging, standardized *a priori* classification system, designed to meet specific user requirements, and formed for mapping exercises, free from scale factor or means used to map. Any LULC-feature well-known overall around the world can be readily contained. The classification uses a set of diagnostic standards that are independent and that able to allowing a correlation with presented classifications and legends. The advantages of the classifier or parametric approach are manifold. The system created is a highly flexible *a priori* land cover classification in which each land cover class is clearly and systematically defined, thus providing internal consistency. The system is truly hierarchical and applicable at a variety of scales. Re-arrangement of the classes based on re-grouping of the classifiers used facilitates extensive use of the outputs by a wide variety of end-users. Accuracy assessment of the end product can be generated by class or by the indi-



vidual classifiers forming the class. All land covers can be accommodated in this highly flexible system; the classification could therefore serve as a universally applicable reference base for land cover, thus contributing towards data harmonization and standardization (Di Gregorio, 2005).

Included here is the general legend which generated from the LCCS-Software, because it is difficult to read the description of the resulted classes once the legend is integrated with the resulting thematic maps (Fig.5.14).

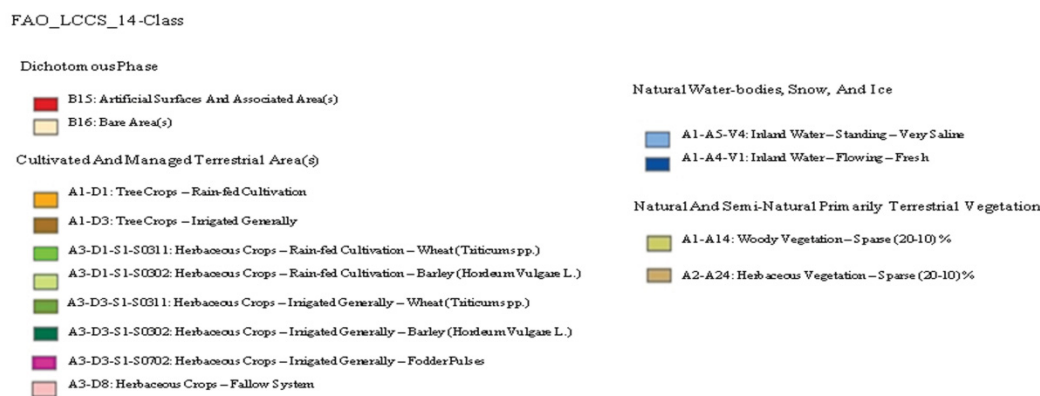


Fig. 5.14: Description of the resulting 14-class for the four 4-Regions sub-study-area (Source: Adapted from: LCCS-Software/Version 2.0)

## D. Field work

The identification of the potential LULC-classes and the thematic content that a classification can or should be included is necessary, where a classification process is a thematic interpretation of the landscape (Jensen, 2007). Such interpretation to be founded, it is necessary to identify and understand factors that control and determine the form of features or phenomena. Therefore, field work and observations are essential if a supervised and/or knowledge based classification method will be used (Richards & Jia, 2003).

Interviewing local farmers provides important understanding of the general characteristics of the LULC in the study area during the past decades. For the purposes of this thesis, interviews were conducted with village leaders and farmers. The main reason for interviewing these people was to find the relationship between the satellite data and the qualitative LULC-history in the surroundings of the villages.

Field work was carried out in June, 2007 (Fig. 5.15), since measurements can be taken (GPS-points) for either winter and/or summer crops. Annually in June in Syria, the wheat and barley are harvested (N.B., most irrigated wheat in east Syria will not be harvested yet), the sugar beet will still be green, cotton and corn will grow without problems. A second campaign was conducted in July 2009 for complementary information and some GPS-measurements based on the knowledge of the farmers. These two field work periods were held to increase the understanding of the patterns of LULC in the study area. Preliminary image classification (unsupervised) and RGB-composite imagery of the study area were printed to show target areas to be surveyed depending on the accessibility of each site. The data were gathered from different sites depending on the differing soil types and irrigation systems in the study area. Random sampling methods were used. Each plot was registered by using GPS-technology (using a GARMIN-Colorado-300 global positioning receiver) to allow for further integration with the spatial data in a geographic information system (GIS) and image classification programs.

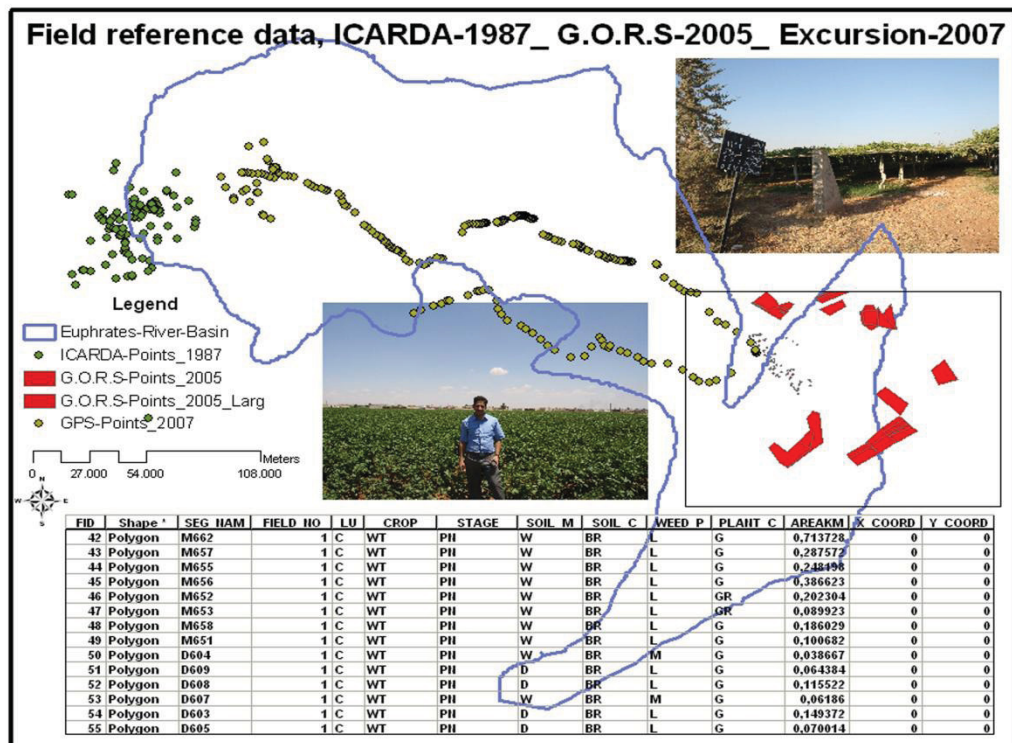


Fig. 5.15: Excursion-GPS-Points-2007 and other GPS-measurements from ICARDA and GORS

Information was gathered based on specific procedures such as: identification of the dominating species of trees, shrubs and herbs; detection of the physical aspects of the soil; conduction of interviews and group discussions with local farmers to extract historical information about the LULC in the study area; and gathering of information about prior LULC activities regarding to types, densities, distributions, and species.

Fig. 5.16 illustrates one example from the study area as explanation of the steps followed during the excursion in 2007 to collect ground truth data (especially for agriculture). The outputs of this first experimental stage were the gathering of the training samples and the testing of sites for automated supervised classification algorithm/s and accuracy. Fig. 5.17 presents the complementary stages of the field-work, which could perhaps be described as “office work”. This was essentially based on the gained output-results of the previous stage and their use as inputs in the automated supervised classification processes chain. The classification process in this work included two types (see C5.M; C6.B); the first using the automated accuracy assessment based on trusted data (e.g., aerial photographs, GPS-measurements, etc.); and the second manually comparing the result-ed readings from remote sensing data with the state statistical records. One cannot separate between these two stages, especially when the desired classification result reaches a very detailed level of information about the LULC-features (e.g., crops mapping). Thus, these stages have been linked and described in the same place here.

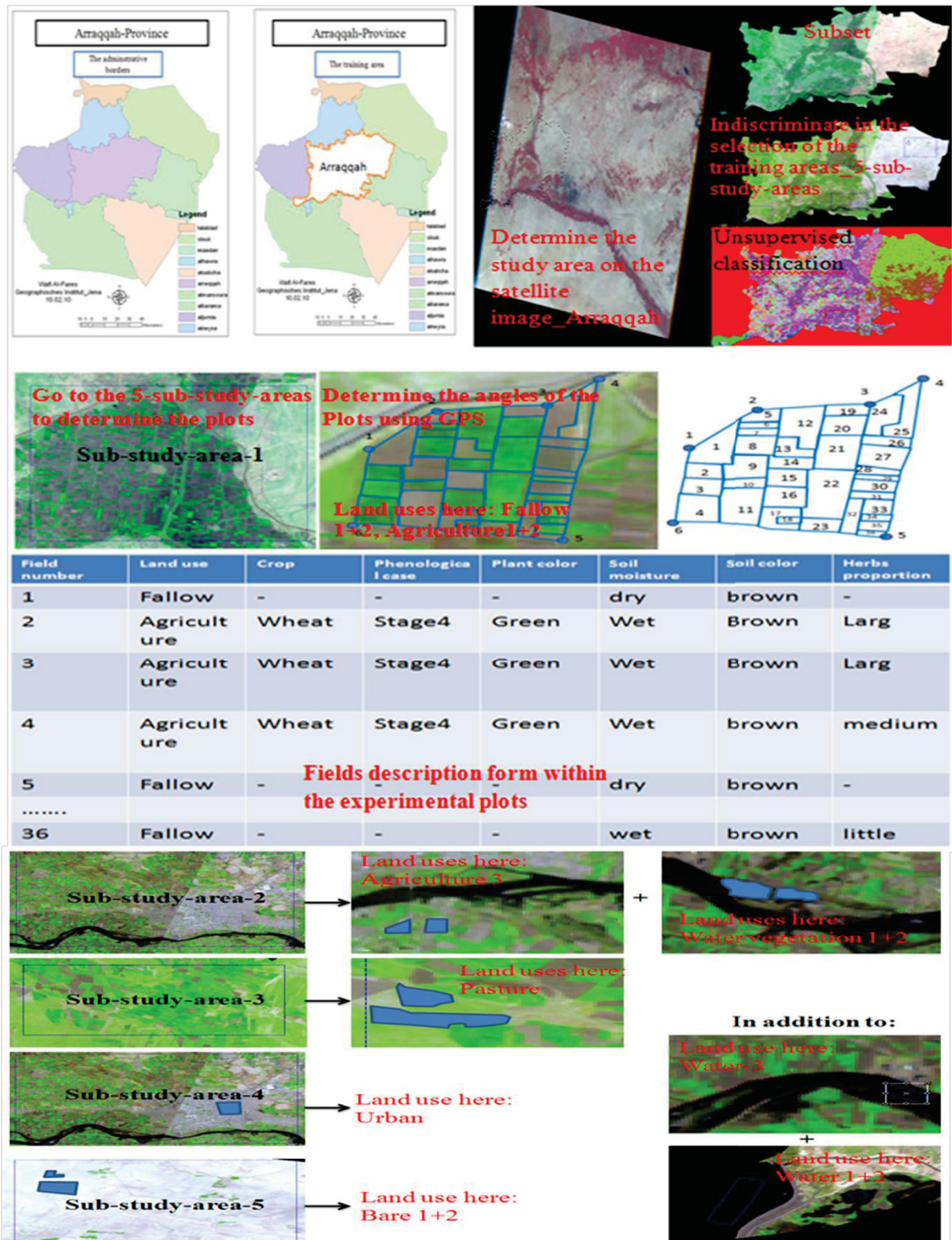


Fig. 5.16: The followed methodology for collecting the ground truth data during the field-work in 2007

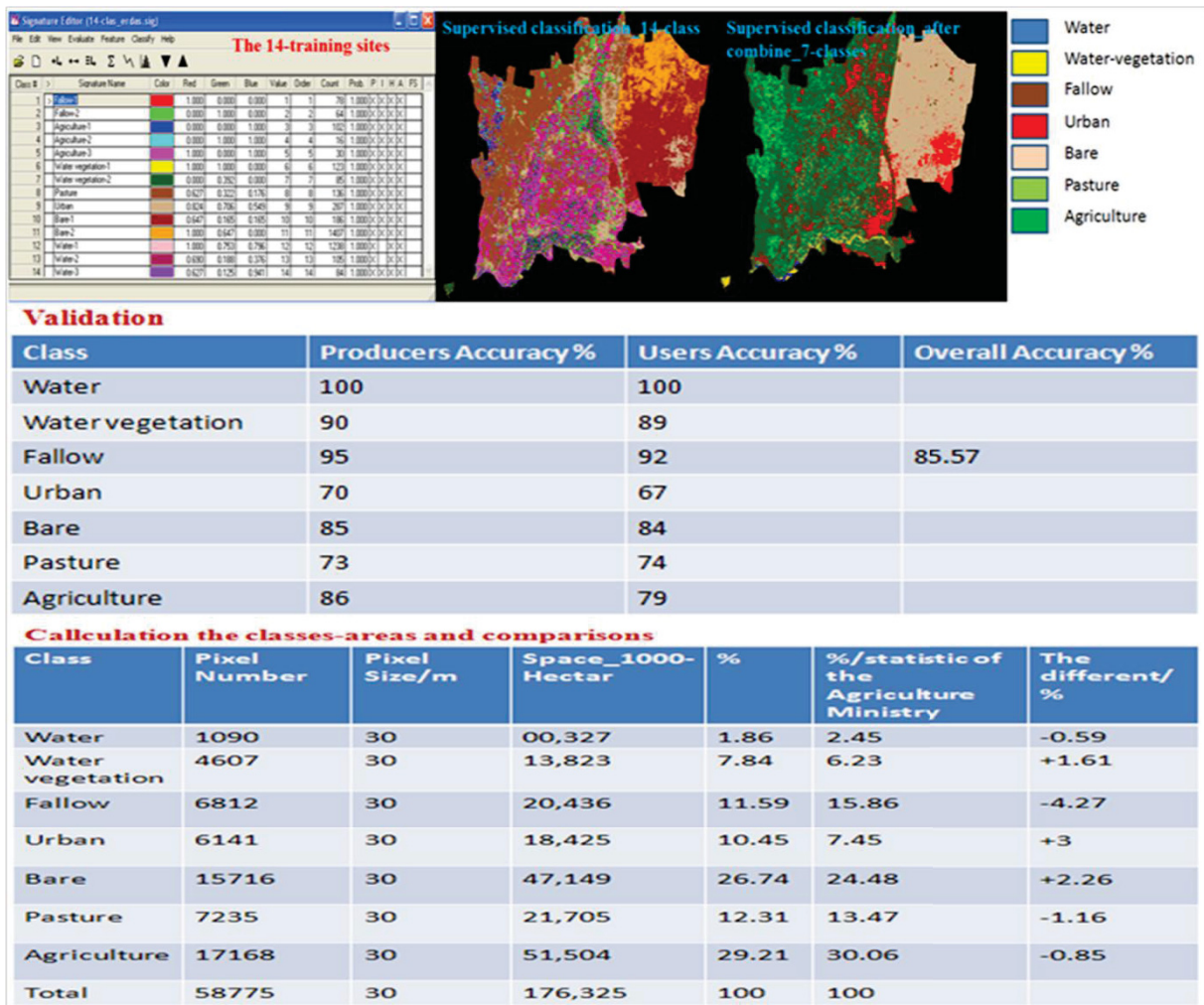


Fig. 5.17: The followed methodology for collecting the results during the “office-work”

### E. The possibility of spectral separation between crops/spectral considerations

Satellite data was procured based on agricultural crop calendars and separability (dependant on crop cover, density, leaf area, leaf structure, crops growth stage, etc.) of the main crops cultivated in the region. By application of remote sensing data in agriculture, the observing of spectral of the crops at one exact stage is more common than those over the entire growing season. Thus, the spectral behavior of plants and the effects of the background surface (soil or water) should be well understood.

The questions related to the spectral characteristics of the used data are: what are the agricultural features that have to be classified? are they spectrally separated from the other associated agricultural features and land cover types (especially the natural plants)? which EMS portion, wavelength, or spectral band are most helpful for spectrally distinguishing and classifying the agricultural features? and what time period of the year is more suitable, in which remote sensing data would be acquired? This based on the fact that the spectral behavior of these agricultural features is unique or more unique during certain times of the year (Hoffer, 1980).

The conceptual method and the final results carried out from the GORS-project (see C2.B) using the spectrometer measurements were used to determine the appropriate date/s, in which is it was possible to separate between the agricultural crops spectrally and then to classify the individual winter and summer crops. This presentation was to confirm the temporal choice of the various remotely sensed data that are used in this study.

A FieldSpecPro spectrometer by GORS was used to collect the radiometric measurements of the major crops in the study area. It had a spectral range of 350-2,500 nanometers, with a spectral interval of 1 nanometer. It offered very sensitive and accurate measurements in the spectral ranges of visible, near infra-red, far infra-red, and thermal, and was equipped with two software-programs. The first, RS3, recorded target reflectance and saved the measurement records. The second, View-SpecPro, processed the recorded data and transformed them to digital-format, for ease of analysis (Fig. 5.18).

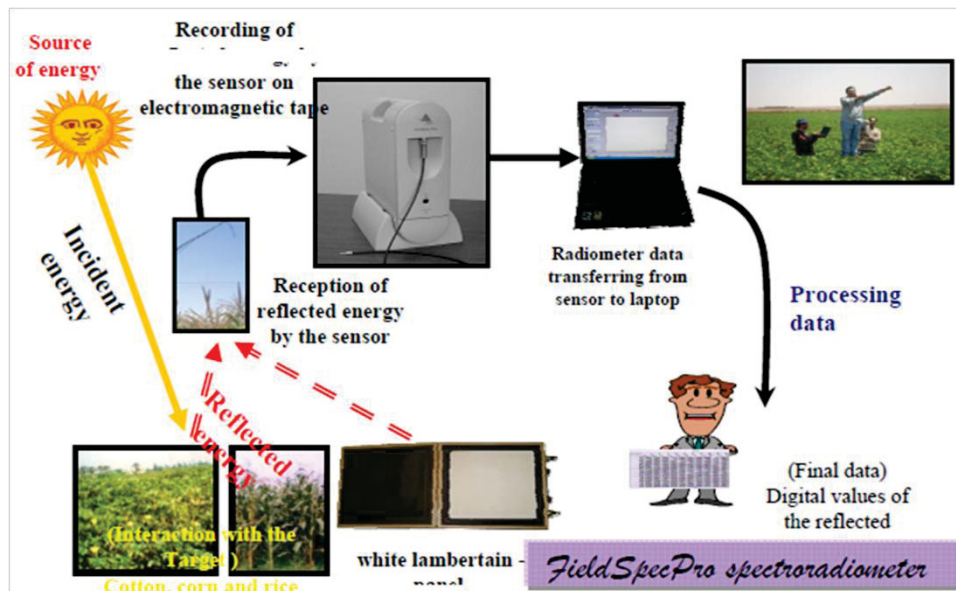


Fig. 5.18: The followed concept in spectral measurements using (FieldSpecPro) by (GORS) (Source: GORS, 2007)

The total radiometric readings numbered 2,669 measurements that represented 103 training-fields of different crops (Fig. 5.19).

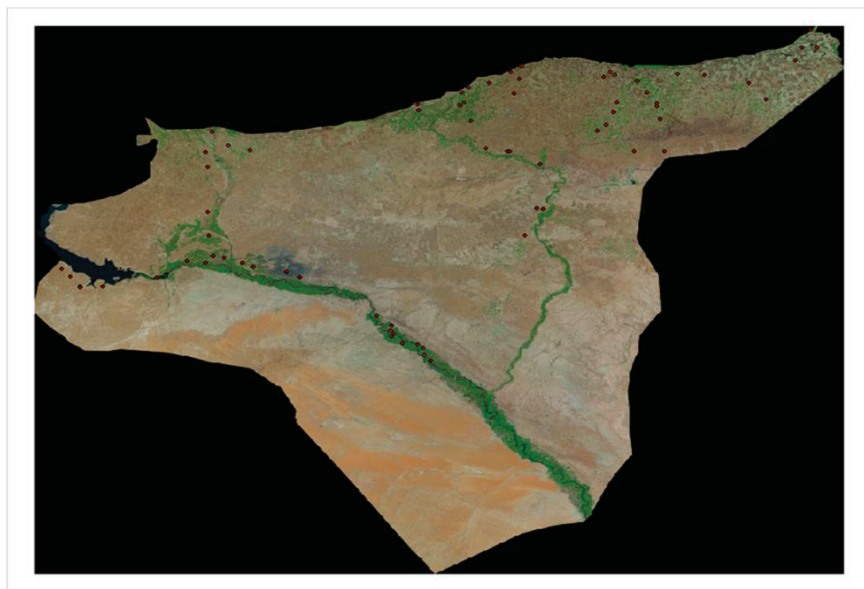


Fig. 5.19: The distribution of the training fields used in the spectral measurements (Source: GORS, 2007)

These displayed the values of the spectral reflectance as spectral signature for each crop, within the wave-lengths from 350-2,500 nm and with a spectral interval of 1 nm for the crops in the study area through their growth stages, allowing for a temporal succession of 15 days between the various readings, from planting and germination until harvest.

The spectral results that represented the winter crops included wheat, barley and sugar beet. For example, the training fields of wheat in Arraqqah Province were made up of 35 fields (Fig. 5.20).

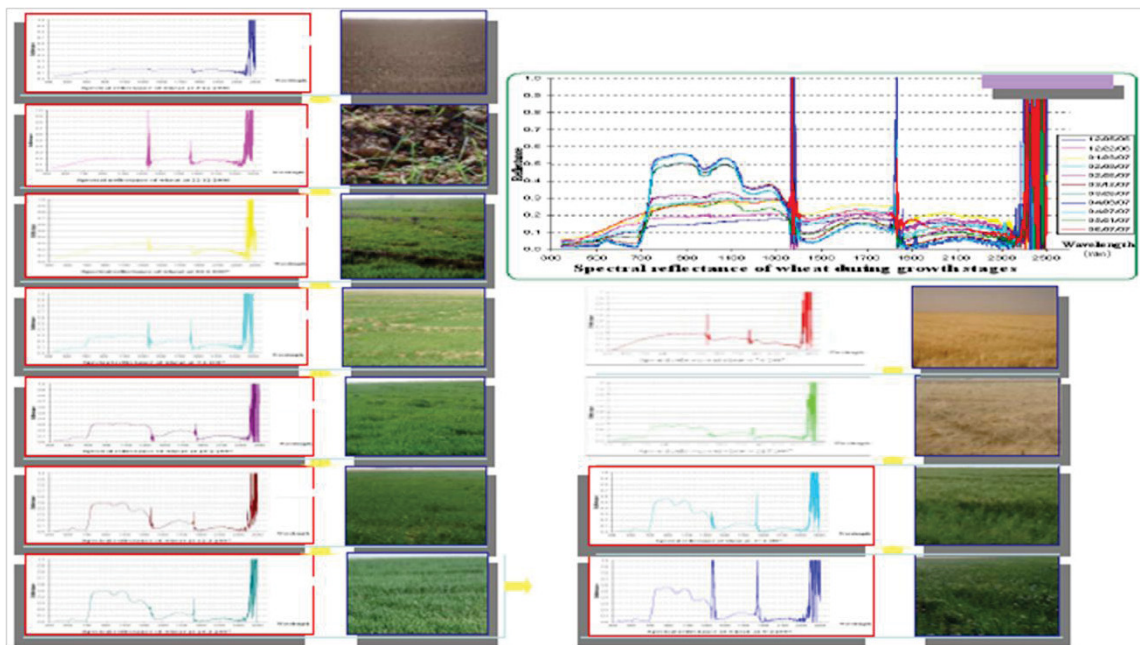


Fig. 5.20: Spectral reflectance measurements for wheat at different growth stages (Source: GORS, 2007)

Fig. 5.21 illustrates the relationship between the spectral responses of the irrigated wheat during 10 different growth stages and the characteristics of the eight bands of ASTER-data. It is clear that the reflectance potential is greatest at the third spectral band among the whole growth stages, with the exception of the time period from 04.12 to 23.01 in the study year, where the reflectance of the soils prevailed.

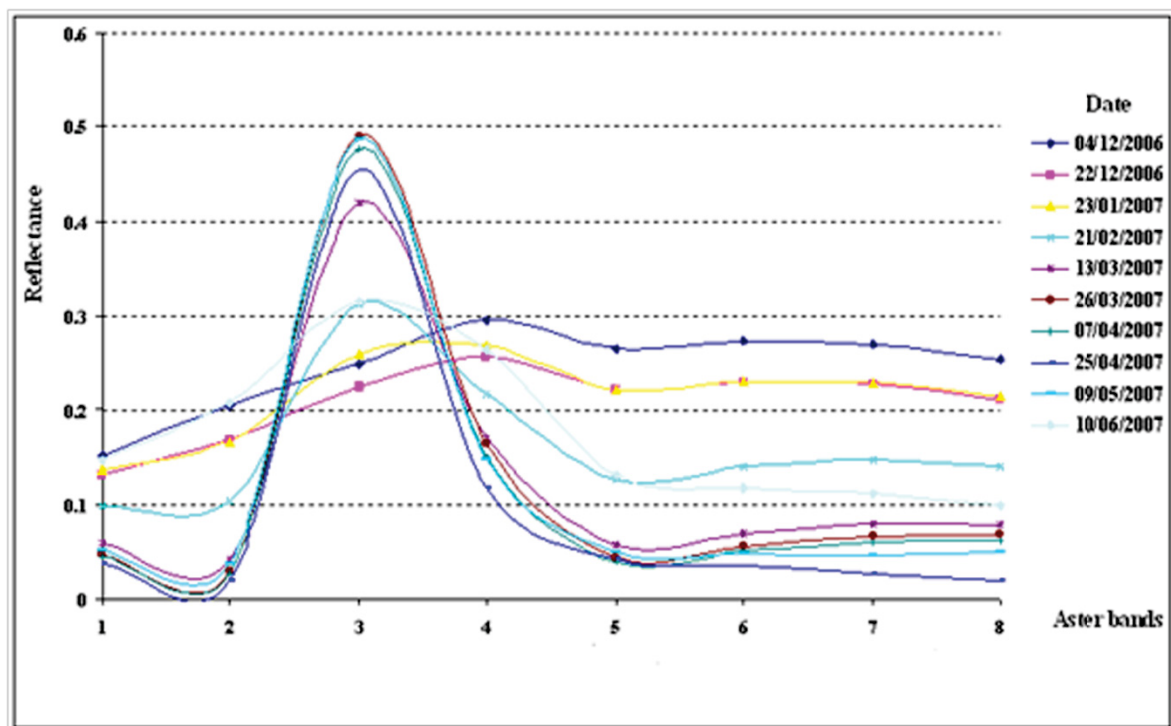


Fig. 5.21: Spectral reflectance values of irrigated wheat during its growth stages in Arraqqah using the ASTER-bands (Source: GORS, 2007)

Fig. 5.22 illustrates the change in the spectral response of the irrigated wheat in relation to the eight spectral ASTER-bands among the 10 various growth stages.

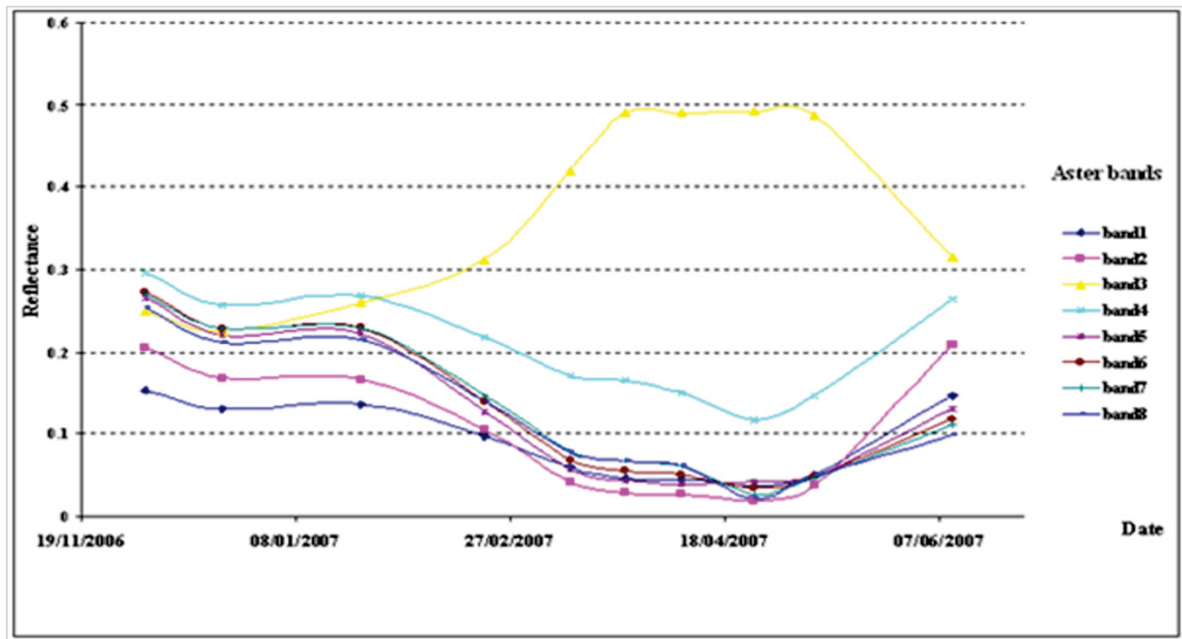


Fig. 5.22: Spectral reflectance values of ASTER-bands during the different growth stages of the irrigated wheat (Source: GORS, 2007)

After analyzing the various spectral responses of the different winter crops in the study area, the appropriate date for separation between the three irrigated major strategic crops (wheat, barley and sugar beet) was determined in the first days of May. In addition, sugar beet was found to have another separation date in mid-June, when the other two crops (wheat and barley) were harvested or had a dry and yellowish appearance (Fig. 5.23).

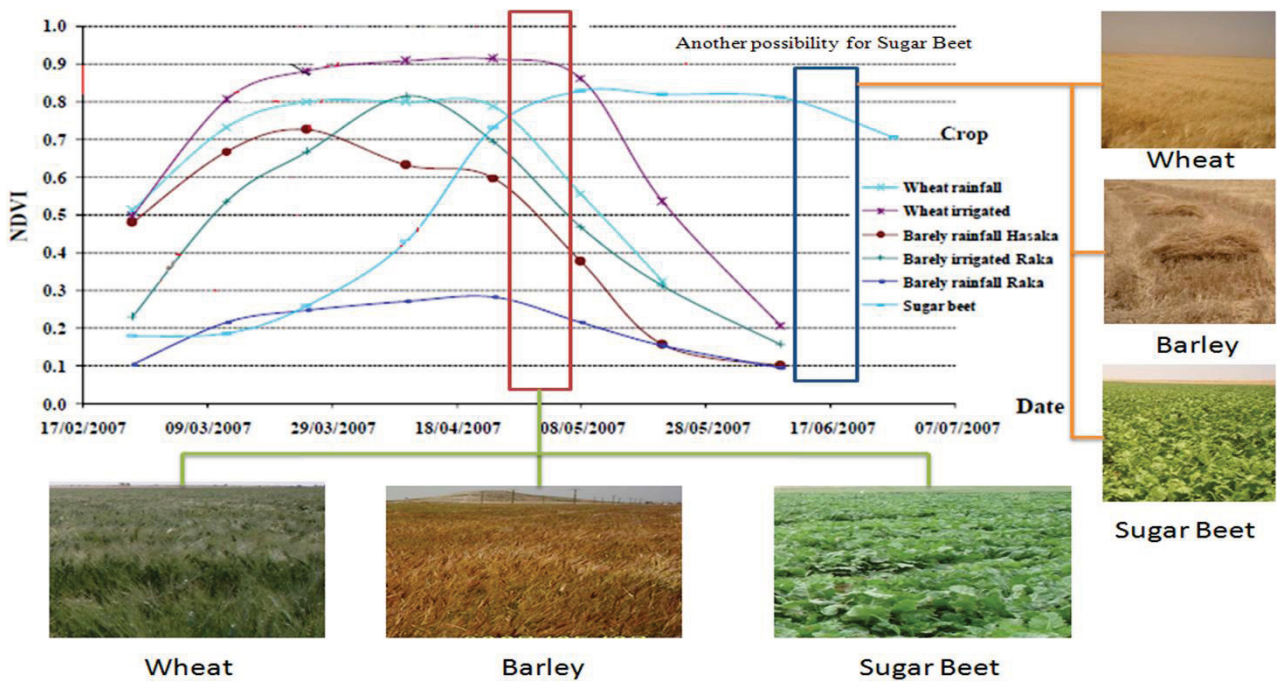


Fig. 5.23: NDVI-values of major winter crops during growth stages in Arraqqah Province in Syria (Source: GORS, 2007)

Secondly, the spectral results that represent the major summer crops included cotton, corn and watermelon. Fig. 5.24 illustrate the spectral response of each crop. The third spectral band of the ASTER-sensor had the greatest sensitivity and potential to detect the spectral characteristics of the three crops of interest, among the various growth stages, using the first three ASTER-bands.

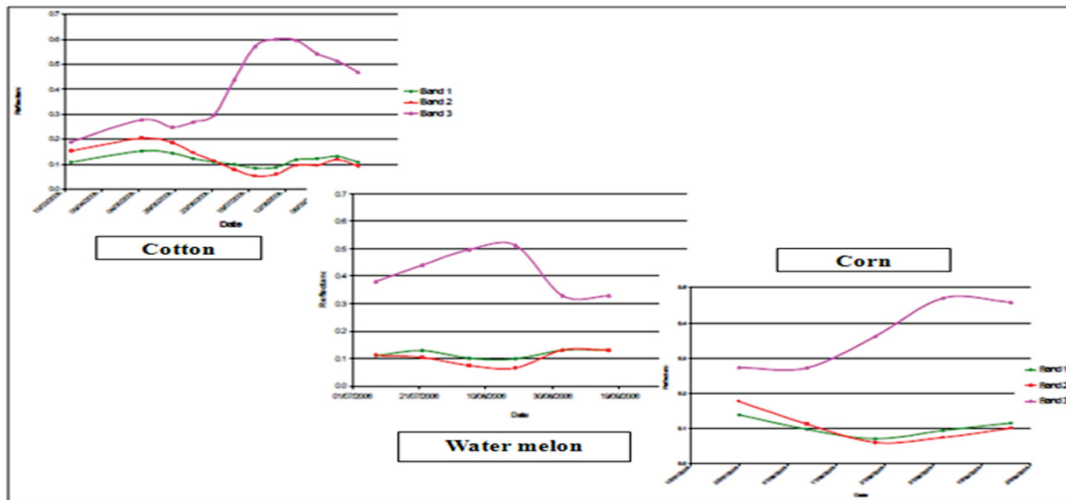


Fig. 5.24: The relationship between the spectral reflectance and the different growth stages of the three essential summer crops by the first three spectral bands of ASTER (Source: GORS, 2007)

Fig. 5.25 represent the effect of the vegetation growth stages on the spectral response of cotton at the third ASTER-band.

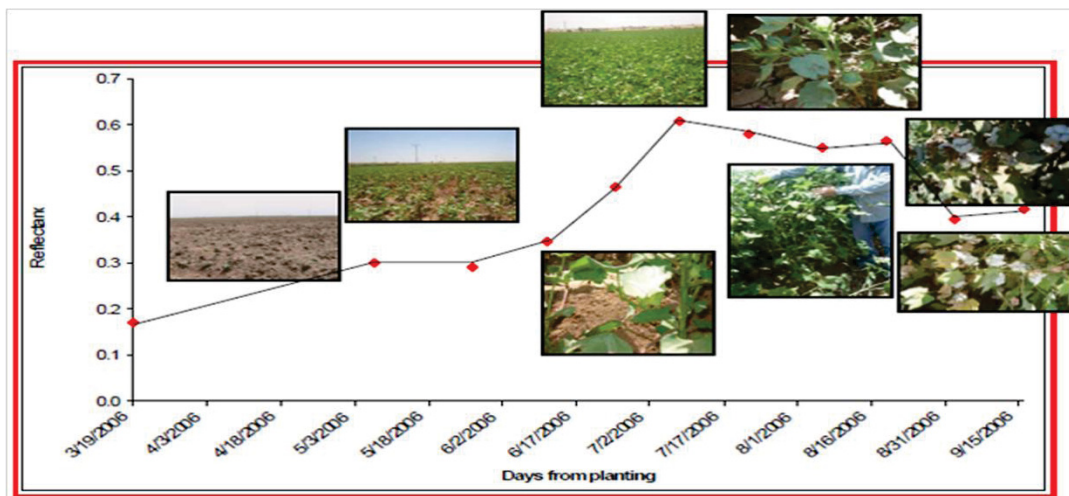


Fig. 5.25: The relationship between the spectral reflectance and the different growth stages of cotton by the third spectral band of ASTER (Source: GORS, 2007)

The suggested date of separation and classification of the three summer crops is the period between 20 July and 20 August (Fig. 5.26). Fig. 5.27 illustrate the different spectral responses of these major crops.



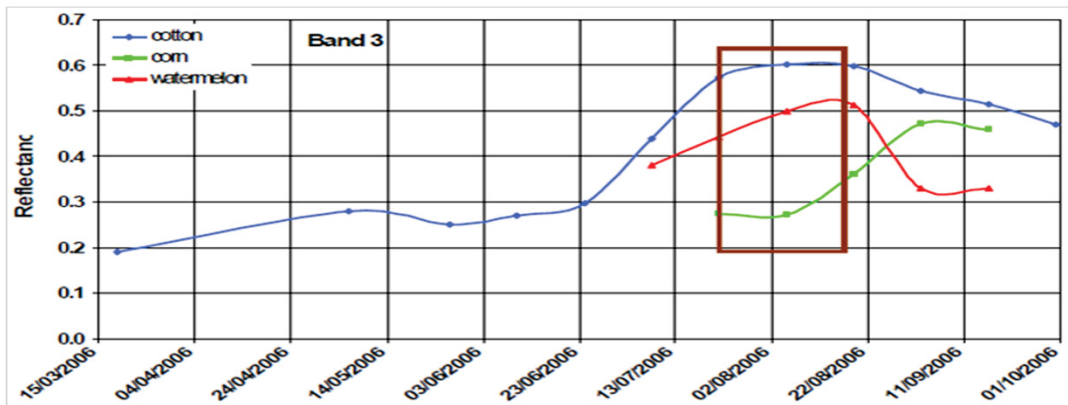


Fig. 5.26: Temporal- and spectral- separability of cotton, corn and watermelon by the third spectral band of ASTER (Source: GORS, 2007)

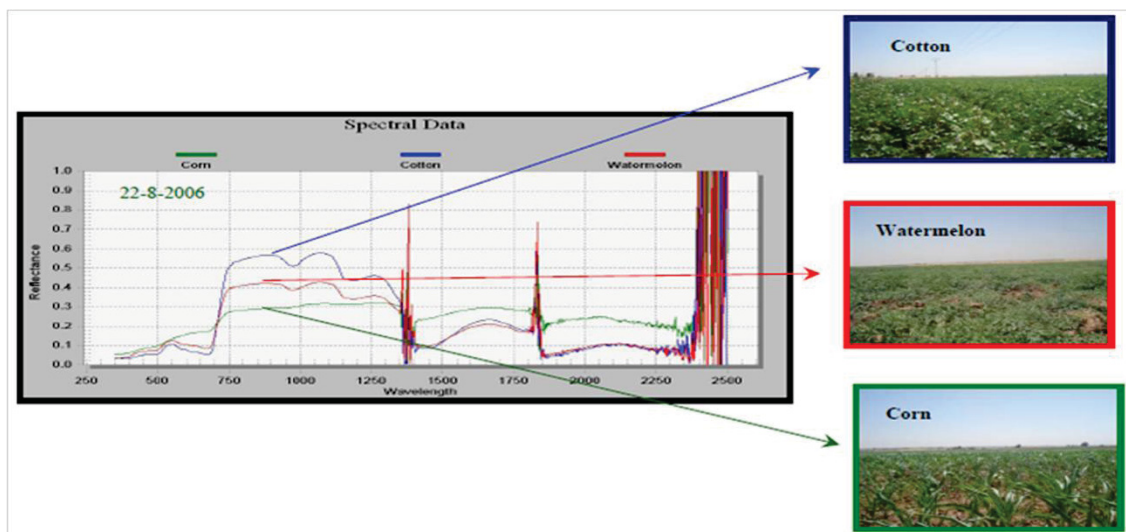


Fig. 5.27: The spectral response of cotton, corn and watermelon during the suggested dates to recognize these summer crops in the spectral range (350-2500) Nanometer (Source: GORS, 2007)

These results are compatible with both ASTER-data and LANDSAT-data, and it is possible to generalize them with other remotely sensed data that operates especially in the visible and the near infra-red spectral ranges (GORS, 2007).

### 1. The phenological case of the different crops/the agricultural calendar

With the use of remote sensing to separate the agricultural crops, the spatial dimension of land uses were obtained but the problem remained of identifying of the crops spectrally, particularly those whose spectral behavior was similar in the date of access to the remotely sensed data (e.g., wheat and barley). To overcome this latter problem, good knowledge of the study area was required in terms of types of crops that were cultivated, growth stages, the dates of propagation and harvest (agricultural calendar), and the type of farming prevailing, whether irrigated crops/plantations, rain-fed, or mixed.

"Agricultural crops have rapid changes in spectral characteristics at various times in the growing season. For example, at the beginning of May, wheat planted in the ERB presents a green canopy of vegetation to the remote sensor, but by late May, the same wheat will be golden brown and nearing maturity. Two weeks later between mid and late June, the crop will have been harvested and one will see only the highly reflective yellow straw. Sometimes, when there has been no tillage or another crop has been planted, many weeds and green vegetation will be mixed in with the straw, which could be observed as grazed pasture or perhaps hay. Therefore, it is very important to

understand the rapid seasonal changes of the crops or other Earth surface features of interest (especially natural vegetation). To this end, crop calendars can be developed for any particular geographic area. Crop calendars describe the general characteristics of the different crops types as a function of the time of year and the geographic location. They can vary from one year to the next, depending on the various conditions such as extreme weather events of that particular year. Finally, crop calendars should be developed more effectively in areas of the world where seasonal changes are distinct" (Hoffer, 1980).

Crop phenology (regular information on the growth cycle of crops) is important in the monitoring and classification of land use, where it can have a significant effect on the accuracies of crop yield and acreage change. It controls the temporal changes observed from remotely sensed data. The integration of space and time represent crop growth in remote sensing. Therefore, crop phenology contributes to the understanding and monitoring (e.g., spectral measurements) of crop type reorganization and area measurement. Different crops (wheat, barley, sugar beet, cotton, corn, etc.) have a clear and unmistakable spectral response exhibit and period of maximum greenness. This information or phenology can be used in the classification process to accurately discriminate vegetation classes (Hoffer, 1980).

Phenological knowledge (beside the spectral measurements) plays a critical role in determining optimal acquisition dates for the selection of the remotely sensed data for agricultural monitoring and classification. For example, wheat can be easily recognized from other crops and vegetation because of its greater Greenup (Greenup is the date of onset of photosynthetic activity), that occurs earlier than for other crops. Crop phenology is generally divided into: "1) vegetative stage: is largely defined by the part of the growth cycle where the crop develops and grows, starting emergence to tasseling; and 2) reproductive stage: starts at anthesis and ends after maturity. For dry-land crops, several transitions are important in terms of management: emergence, tasseling and initiation of senescence" (Chen et al., 2008).

## **2. The size of the agriculture holdings and methods of water supply/spatial considerations/spatial aspects of spectral response patterns**

The questions related to spatial characteristics of the used data are: how much is the size area concerned? is it sufficient to classify only a sample of all the data, or is it necessary to classify the all data for the whole coverage of the study area? what format of results is needed (maps and/or tables)? if the needed format is a map as a final product, then what scale and level of accuracy is needed? what are the spatial characteristics of the agricultural features in comparison to the characteristics of the used remotely sensed data (Hoffer, 1980)? And finally, what are the spatial aspects of the spectral response patterns?

Geographic variability of various categories or crop species of interest is another aspect of spatial variability of spectral signatures. Namely, the same crop species does not have the same spectral response pattern in all geographic locations on any one date. For example, barley may be harvested in east Syria at the beginning of May when it has reached maturity, but has not yet been harvested in west Syria, and perhaps is still immature and green in southern east Syria. Based on the spectral (signature) concept, it is impossible to define a single spectral response pattern that will be applicable for the same crop species in all geographic areas at any one time. Geographic variability of agricultural crops includes another related aspect, since not all crop species are found in all geographic locations. Therefore, knowledge of the location from which remote sensor data was obtained can prove useful in attempting to identify a particular crop species, even though the spectral response pattern of that crop may not be well known at that time of the year because of lack of ground truth data. For example, when data from east Syria is analyzed, it could be concluded that the particular spectral response patterns would be essentially wheat, barley, cotton and corn, and

not, for example, tobacco, which does not grow in the area to a large extent. Instead, tobacco is planted widely in the west near the Mediterranean Sea.

Three methods of water withdrawal at present dominated for irrigation the agriculture features in the Euphrates Basin: A) floodplain irrigation (small holdings, not organized geometrically); B) canal irrigation/farmers (small up to big holdings, semi-organized geometrically); and C) canal irrigation/state (medium up to very big holdings, full organized geometrically) (Fig. 5.28).

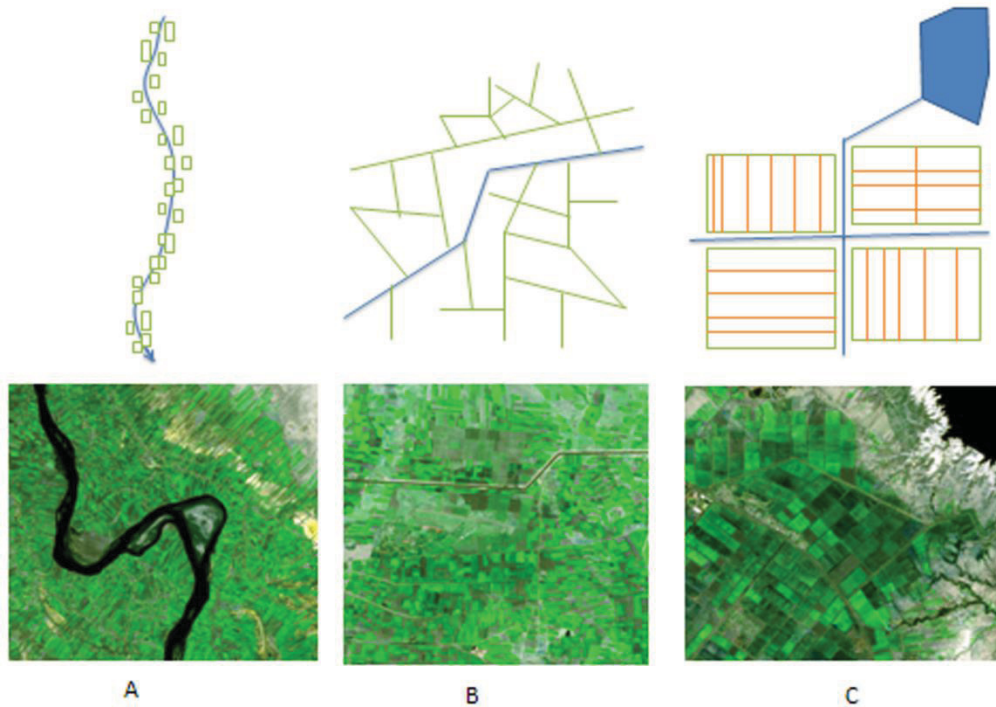


Fig. 5.28: Schematic diagrams of the spatial characteristics of the irrigated agricultural areas in the study area, ERB. A: Floodplain; B: Canal irrigation (Farmers); and C: Canal irrigation (State)

### 3. The choice of the most appropriate time to obtain satellite images/temporal considerations/spatial aspects of spectral response patterns

The questions related to temporal characteristics of the used data are: how much of the remotely sensed data has to be obtained at a certain time? what time or times of the year are more suitable (or required) for obtaining these remotely sensed data? are there particular daytime considerations that have to be involved during the obtaining of data (Hoffer, 1980)? and, what are the spatial aspects of the spectral response patterns?

Image acquisition date selection is essential for successful classification of many vegetation covers, especially agricultural crops (Rundquist et al., 2002).

The study of LULC using remotely sensed data faces the problem of the selection of the date in which the image was captured, i.e., the year and the month. This selection is decisive with regard to the information which researchers receive. Most of the irrigation projects discussed in this study were located within the five agriculturally stable zones in Syria, which receive insufficient precipitation to establish a rain-fed agriculture. Therefore, the majority of cultivated areas are irrigated either in winter or in summer. The agricultural cycle of both winter and summer crops ends in May and August, respectively. This means the spectral differences reach their maximum point of clarity at this time, despite different patterns of land use. For remote sensing based studies, the time of year of the image capture is an important factor, because of the density of vegetation, both natural and cultivated. This depends on many factors, notably the amount of precipitation that changes

from year to year; and human factors, such as the use of fertilizers, which lead to changes in the characteristics of spectral reflectance/response of a specific crop. For example, the spectral response of fertilized wheat will differ from a field of the same crop which is unfertilized. The use of fertilizers where insufficient water exists will lead to early yellowing of the crops.

Generally, worldwide, the best date range for identifying winter wheat is late March through to early May, when the crop is at peak greenness. To identify corn and other summer crops, the best date range is late July to mid-August. The most important and best way to choose an appropriate time for remotely sensed data is to study the growth stages of each type of vegetation and the spectral change in its behavior during the months of growth, through field work and the use of spectral reflectance measurement devices (Spectrometer) (see C5.E). As a result of these measurements, the growth periods of a variety of crops and the differences in their spectral reflections can be determined.

The results of the spectrometry readings taken for the purposes of this study are outlined in C5.E. When comparing the spectral reflectance curves of the studied summer crops (cotton, and corn), it was found that the best spectral region for the separation of crops was the near infrared domain. Under the conditions of the project area, the best period to distinguish these differences was found to be the period between July 20 and August 20. Based on previous results, it was recommended that the satellite imagery for the study area was brought with the same referred date to use in estimating crop area of summer crops. The best spectral range for the separation of winter crops (wheat, barley and sugar beet) was also found to be the near infrared domain. The best period to distinguish these crops was found to be during the month of May (GORS, 2008).

"There are more short-term temporal variations in the spectral responses of agricultural crops and other ground surface features, such as differences in spectral behavior at different times of the day or night. Differences in the angle of the sun cause variations in atmospheric damping. Sometimes, vegetation that is not under moisture stress early in the morning will show severe symptoms of this later in the day" (Hoffer, 1980). "Researchers have also found the problem of temporal definition of a particular cover type of interest, for example, the use of remotely sensed data to classify corn. At what stage of growth do you define a particular agricultural field as being corn?; do you call field (X) a field of corn after it has been planted or after emergence, or when the corn-stems are 15 cm high?; or is it not until the corn covers 25 % of the ground surface?; or indeed 50 %?" (Hoffer, 1980).

#### 4. Choice of the most appropriate bands composite of the satellite images

The optimal selection of spectral bands for classification was broadly discussed in a variety of literature (Mausel et al., 1990; Landgrebe, 2003; Jensen, 2007). There are two general kinds of techniques: 1) graphic analysis (e.g., bar graph spectral plots, co-spectral mean vector plots, two-dimensional feature space plot, and ellipse plots); and 2) statistical methods (e.g., average divergence, transformed divergence, Bhattacharyya distance, Jeffreys-Matusita distance). They were both applied to find an optimal subset of spectral bands (Jensen, 2007).

Generally, it may appear that three spectral bands may be more suitable than two, as more information is offered. Also, data that have a broader radiometry field may provide improved results, since some of the problems related to parametric models are avoided, whose support significantly falls outside of the data domain. However, by using three spectral bands instead of two with broader data domain instead of the standard one, classification and estimation may in fact be much slower.

"Classification accuracy does not increase linearly, or even increase at all, as the number of spectral bands used is increased" (Hoffer, 1980). However, this is not true for the spectral separability of crops or other Earth surface features, which increases steadily as the spectral bands increased.

## F. Training samples: Selection, analysis and evaluation

The most important factor in selecting training sites for supervised classification is that all the variability within classes is representative. Only a few sites will be required in some homogeneous classes, and more sites in classes with high variability. A general concept offered by Jensen (2007), is that in developing training statistics, it is necessary to select a number of pixels in each class that is at least 10 times greater than the number of bands used during the classification process. For example, we need at least 40 training pixels for each class if we used four spectral bands of LANDSAT-MSS data. This is enough to allow good computations of variance–covariance matrices, which are usually carried out with classification software. Related to size of sample sites, it is noted that "as sites grow larger than 10 pixels, there may be no new information added. Therefore, it would be better to have six sites of 10 pixels in each class rather than one training site of 60 pixels" (Schowengerdt, 2007).

In order to classify the remotely sensed data into classes, the classification algorithm needs to be trained to distinguish one class from another. Representative homogeneous class sites are known as *prototypes*, *exemplars* or *training samples*. After the classifier is trained to statistically analyze to "distinguish" the different classes represented by the training sites, the "rules" that were developed during the phase of training are utilized to label all pixels in the image to their "in real world" classes (Schowengerdt, 2007).

A large enough number of training samples and their ability of representativeness are significant for image classifications (Hubert-Moy et al., 2001; Chen & Stow, 2002; Landgrebe, 2003; Mather, 2004). When the biophysical structure of the study area is complex and heterogeneous, selecting enough training samples will be difficult. This problem would be greater if medium or coarse spatial resolution data were used for classification, because a large number of mixed pixels may occur. Therefore, the selection of training samples must consider the three standards: 1) the spatial resolution of the available remote sensing imagery; 2) availability of ground truth data; and 3) the complexity of the biophysical structure in the study area (Lu & Weng, 2007).

Training samples are usually collected from fieldwork/in-situ, fine spatial resolution aerial photographs and satellite images/in-image, recently from Google Earth, etc. Different gathering strategies, such as single pixel, seed and polygon, can be used, but they can influence classification results and accuracy (Chen & Stow 2002).

Care must be taken to collect representative and non-auto-correlated training samples. The problem in spatial autocorrelation occurring in remote sensing data is that pixels in the image should not be considered as fully discrete features independent of their juxtaposition, but rather a set of continuous features influenced by their neighbors (Campbell, 1981). This exists among pixels that are neighboring (e.g., neighboring pixels have a high chance to have alike brightness values), which can cause a decrease in variance between neighboring pixels (Campbell, 1981). This decrease in variance can make large masses of neighboring training pixels less representative of a particular LULC-class in the entire image; in contrast, the use of several single-pixel training samples that are situated spatially separately from each other can result in better classifications than large masses (polygons) of neighboring training pixels (Cambell, 1981; Medhavy et al., 1993). Therefore, if such care is taken, classification results for LULC-types (especially for crop recognition, since they have, generally speaking, a relatively small spatial distributions/fields) can be more effective.

Google Earth (<http://earth.google.com/>) contains ever more wide-ranging coverage of the globe at very high spatial resolution 0.61-4 m, allowing the user to zoom into particular areas to get great detail. Google Earth data were used in this study for: 1) identification and labeling the broadly general classes (e.g., water surfaces) and some sub-classes (e.g., trees, since they change slowly over the time); 2) help in drawing the out-borders of the irrigated projects; and 3) assistance in assessing the classification accuracy (especially for general classes).

Ground-reference data were compiled from ICARDA for the remotely sensed data obtained in the year 1987, from GORS for the remotely sensed data coverage for 2005, and from the two excursions carried out in the years 2007 and 2009. Parts of these ground truth data were used in the generation of training samples and others were used for accuracy assessment at the end of the classification.

Several measures of class separability have been suggested as way to isolate optimal or near-optimal subsets of features for use with classification algorithms. Swain (1978) found three approaches: divergence; Jeffries-Matusita distance; and transformed divergence. The general concept is that the used approach can make a quality measure of the discrimination ratio of a group of spectral features, when achieved over all classes. By comparing between all the achievable combinations of subsets of the spectral features (e.g., which three out of nine available spectral bands), the one that presents the highest quality metric can be used. Only the reduced subset of spectral bands is then used in the overall image classification process.

A potential problem is that if one combination of spectral bands creates classes with a large divergence values for some classes and small values for other classes, and a second creates a small divergence values for all classes, which represents a better overall pair-wise selection of features. This suggests that increasing the pair-wise divergence has a decreasing return (Schott, 2007). Swain (1978) invented the Jeffries-Matusita distance to overcome this problem, but it had the disadvantage of time-consuming computing. A more commonly used heuristic approach is the transformed divergence that has the mathematical statement:

$$Div_{ij}^T = 2 [1 - e(Div_{ij}/8)]$$

"This has the characteristic of exponential saturation of the divergence measure and scales the transformed divergence over the range 0 to 2" (Schott, 2007). Mausel et al. (1990), in assessing separability measures, used the scaling factor of 2000 rather than 2 that gave larger additions for differences between small divergence values (Schott, 2007).

For example, when classifying agricultural crops, it is important to train not only the crop classes of interest but also the other classes of no interest such as urban, bare areas, water, etc. if they occur in the region. Similarly, when we focus on a few existing crops (e.g., wheat, barley, and sugar beet), we also have to classify all other crops (e.g., lentil, cumin, etc.) and list them under "other crops", for example. Failure in the training phase generally results in cases of the untrained classes being commissioned. This means that the analyst must spend considerable time and effort in training the classes of no interest.

Training samples selection also depends on many factors which affect classification results and their accuracy. They are, according to Foody et al. (2006): 1) number of training sites for each category; 2) method of sampling (random or systematic sampling); 3) source of the used data for labeling training sites (ground data, air photographs, etc); and 4) timing of data collection.

Several authors have proven that good separability values between the LULC-features to be classified will improve classification accuracy, because there is no narrow relation between the average transformed divergence for a feature set and the accuracy reached during classification (Gong et al., 1992; Chen et al., 2004 b). The reason is because the separability measures are usually calculated only from the training sites. Therefore, these measures cannot predict the exact classification accuracy for classified LULC-features in the whole image, if the training sites are not fully representative for all spectral ground surface feature variations in the remotely sensed image, including areas of potential edge effects. In general, a specified value of an obtained separability measure can estimate a certain range of possible classification accuracies for the examined training sites (Landgrebe, 2003).

The training sites were chosen in a way to give the broadest possible range that can represent all, or almost all, existing LULC-categories (especially crops) spatially and spectrally. Crop fields

with various planted and fallow areas (on light soil, on dark soil, etc.) were visited. The size of the training areas was chosen to be at least 50\*50 meters, since some studies have concluded that this is a suitable size for training sites in semi-arid areas (Olsson, 1985; Wellens, 1997). Larger training sites were selected, when it was possible, in order to reduce the effect of possible technical geometrical noise in satellite data and GPS-data. Homogeneous agricultural fields smaller than about 100\*100 m were excluded, while they were too small in contrast to LANDSAT-pixels of 30\*30 m. The training site plots were taken in the centre of the homogeneous area. The GPS-measurements were taken twice in the middle of the field in order to obtain a mean value and reduce possible noise related to the GPS-type.

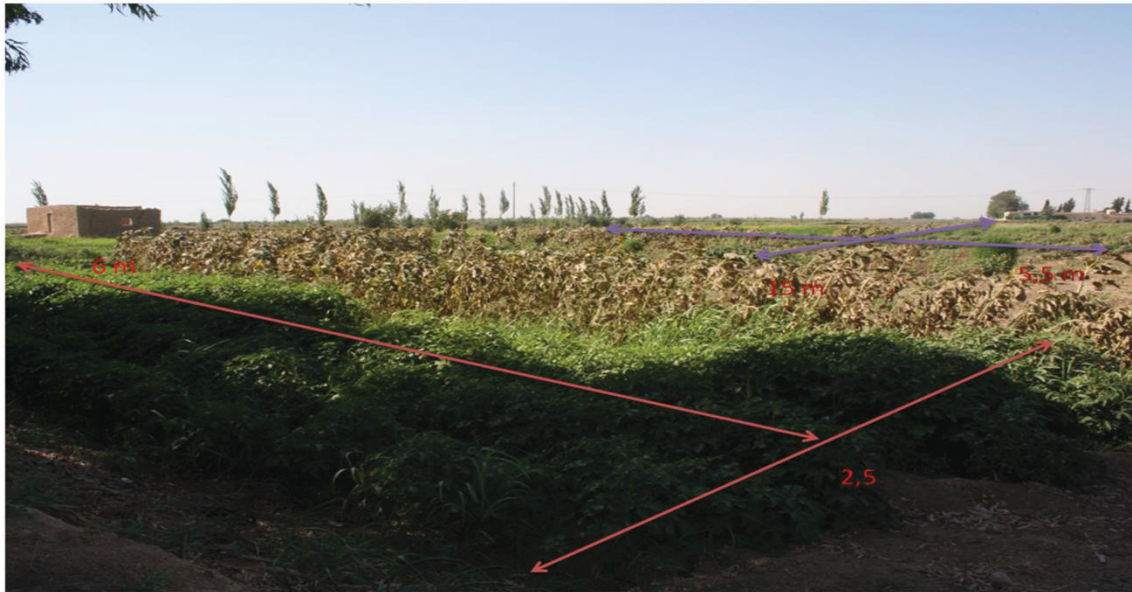


Fig. 5.29: The small and very small crops fields on the Euphrates River banks near Deir Azzour in July 2009

The size of samples also has a great importance, together with distribution, for providing representative training sites. Justice et al. (1981) recommended that the using of a model that takes advantage of using the characteristics of the spatial image to define the size of a training site. The suggested model can approximate the size of any sample quadrant as a function of the pixel size and the predicted geometric accuracy of the images.

$L = P(1 + 2G)$ , Or:  $A = P(1 + 2G)^2$ ; where: (L: length of any side, A: area to be sampled, P: pixel size, and G: geometric accuracy of the image).

Accordingly, using TM or ETM+ images with 1-pixel geometric accuracy, the size of the training site will be 0.81 hectare, the equivalent to a 3\*3 pixel kernel area.

Generally, two procedures were used: 1) ground truth data based approach: here, the agricultural crops to be classified were defined in addition to some of their attributes (e.g., statistical records, agricultural calendar, etc.). Of key interest were the strategic crops, such as the winter crops of wheat, barley, and sugar beet, and the summer crops of cotton and corn. Random GPS-measurements were then taken at the study area and other historical agricultural information was obtained from local farmers in Aleppo in the Upper-Euphrates and in Deir Azzour in the Lower Euphrates Basin. The training sites were analyzed statistically using the two spectral separability measurements (*Jeffries-Matusita* and *Transformed Divergence*) to determine how the used remotely sensed data would be able to distinguish the interested classes (spectrally) on average. According to PCI-Geomatics (2001) and Richards and Jia, (2003), measurements < 1,000 = very bad spectral separability; 1,000 < measurements < 1,900 = limited separability; and measurements >

1,900 = very good spectral separability. The majority of the training sites satisfied the last consideration; and 2) satellite image based approach: this approach in gathering the training sites was based on visual interpretation, using the background of the interpreter about the study area. This approach was used only for gathering the representative training sites for the five general LULC-classes. It was also possible to select the training samples for the agricultural class (trees, especially Poplar) from Google Earth visually by shadows that appear clearly. This method was used to confirm the measurements/or choice based on the statistical records for the year 1987, (see C5.J) for the training sites of some crops. Other remotely sensed images were only used visually without processing. For this purpose, if some fields appear black/burned on an image recorded in August for example, this would indicate it was a wheat field. Sugar beet appeared on the July images as green in contrast to wheat, which once harvested, appeared as burned/black, straw/yellow, or till-aged/light- or dark- brown. Table 5.3 gives an overview about the used training samples in the supervised classification.

Table 5.3: Variations, source, and date used training samples in the supervised classification process

Classes	1975	1987	2005	2007
<b>Cultivated and managed areas</b>	Visual interpretation	Visual interpretation	Visual interpretation	Visual interpretation
Trees		Topographic Maps	Google Earth	Google Earth
Herbaceous (Permanent and winter-crops/Irrigated):	N.C. (Not Classified)	N.C.	N.C.	N.C.
Alfalfa	N.C.	ICARDA-points, statistical records, and detailed schemes	N.C.	N.C.
Vetch	N.C.	ICARDA-points, statistical records, and detailed schemes	N.C.	N.C.
Wheat	N.C.	ICARDA-points, statistical records, and detailed schemes	GORS-points, and visual interpretation for multi-temporal images in this year	Field work, and visual interpretation for multi-temporal images in this year
Barley	N.C.	ICARDA-points, statistical records, and detailed schemes	GORS-points, and visual interpretation for multi-temporal images in this year	Field work, and visual interpretation for multi-temporal images in this year
Sugar beet	N.C.	ICARDA-points, statistical records, and detailed schemes	GORS-points, and visual interpretation for multi-temporal images in this year	Field work, and visual interpretation for multi-temporal images in this year
Other crops	N.C.	ICARDA-points, and visual interpretation	GORS-points, and visual interpretation for multi-temporal images in this year	Field work, and visual interpretation for multi-temporal images in this year
Rain-fed crops	N.C.	Visual interpretation	N.C.	N.C.
Fallow	N.C.	Visual interpretation	Visual interpretation	Visual interpretation
Herbaceous (Summer crops/Irrigated):	N.C.	N.C.	N.C.	N.C.
Cotton	N.C.	ICARDA-points, statistical records, and detailed schemes	GORS-points, and visual interpretation for multi-temporal images in this year	Field work, and visual interpretation for multi-temporal images in this year
Corn	N.C.	ICARDA-points, statistical records, and detailed schemes	GORS-points, and visual interpretation for multi-temporal images in this year	Field work, and visual interpretation for multi-temporal images in this year
Other crops	N.C.	ICARDA-points, and visual interpretation	GORS-points, and visual interpretation for multi-temporal images in this year	Field work, and visual interpretation for multi-temporal images in this year
Fallow	N.C.	Visual interpretation	Visual interpretation	Visual interpretation
<b>Natural Vegetation</b>	Visual interpretation	Visual interpretation	Visual interpretation	Visual interpretation
<b>Artificial Surfaces</b>	Visual interpretation	Visual interpretation	Visual interpretation	Visual interpretation
<b>Bare areas</b>	Visual interpretation	Visual interpretation	Visual interpretation	Visual interpretation
<b>Natural Water-bodies</b>	Visual interpretation	Visual interpretation	Visual interpretation	Visual interpretation



It was impossible to obtain training samples for the study area based on accurate remotely sensed data for 1975 and partially for 1987, as no remote sensing based research had been carried out in this area. This is one disadvantage of using the historical data, where one cannot make any field-work and gather ground truth data. However, there is the essential advantage in the provision of initial information about the study area, with which to compare to the present. It was not necessary to obtain ground truth for the remotely sensed data of LANDSAT-MSS-1975, because classification can only be done in the broad general classes in the study area, as they have poor spectral and spatial resolution. Therefore, it was easy to collect the represented training samples and the accuracy (testing) data, from the remotely sensed data itself using visual interpretation. The ground truth data for LANDSAT-TM-1987 were found by ICARDA, but were insufficient. Attempts were made to increase the potential of these truth data by taking advantage of integrating the remotely sensed data, the historical statistical records and the detailed spatial schemes of the various irrigation projects (see C5.J).

Twenty GPS points were collected for each class of land use and natural coverage. These points were collected along the study area in fields with almost 300 \* 300 m dimensions to ensure the survival of location points in case technology related errors occurred which would affect the accuracy of the measurements. Photographic images were taken for several GPS-points to provide additional descriptive information about land uses, in which reference points exist, such as plants' density, length and phenological cases (when the land use/land cover is agriculture or natural vegetation). As regards to some land use and natural lands such as airports, constructions areas, rivers and lakes, it was easy to find reference points using the satellite images themselves, topographic maps or Google Earth. Hence, the majority of reference points represent the more detailed crops types falling under the more general class of cultivated areas.

Spectral signature generation, analyses and evaluation were processed iteratively. As a result, many signature files were produced due to the two classification approaches (One- and Multi-stage classification), and multi-temporal remotely sensed data (over many months and years) used in the study. Some results of spectral separability based on transformed divergence were presented. The presented training sites here were those used especially in the training study area (see C5.G), and for which the optimized classification algorithms MLC, NN, SVM were chosen.

Table 5.4, Table 5.5, Fig. 5.30, and

Fig. 5.31 illustrate the increase of spectral separability in relation to the spectral bands used, and give an illustrated example of how spectral separability was calculated quantitatively.

Table 5.4: The spectral separability of the training samples related to ASTER-data (3 spectral bands, 15 m)

Pair Separation (least to most)	FW	SW	AS	BA	F	NW	NH	TR	TI	WR	WI	BR	BI	PI
Fresh Water		2000	2000	2000	2000	2000	2000	2000	2000	2000	2000	2000	2000	2000
Saline Water	2000		2000	2000	2000	2000	2000	2000	2000	2000	2000	2000	2000	2000
Artificial Surfaces	2000	2000		2000	2000	1999	2000	2000	2000	2000	2000	2000	2000	2000
Bare Areas	2000	2000	2000		2000	2000	2000	2000	2000	2000	2000	2000	2000	2000
Fallow	1999	2000	1991	1924		2000	1999	2000	1999	2000	2000	1968	2000	2000
Natural Woody	2000	2000	1996	2000	1899		2000	2000	1999	2000	2000	1999	2000	2000
Natural Herbaceous	1978	1999	1984	1963	1054	1847		2000	1999	2000	2000	2000	2000	2000
Trees-Rainfed	1999	2000	1995	1926	0836	1834	0613		2000	2000	2000	2000	2000	2000
Trees-Irrigated	2000	2000	1988	2000	1773	1483	1342	1399		2000	2000	2000	2000	2000
Wheat-Rainfed	2000	2000	1989	2000	1992	1828	1524	1894	1675		2000	2000	1999	1998
Wheat-Irrigated	2000	2000	1976	2000	1975	1793	1669	1848	1383	0718		2000	1999	1979
Barley-Rainfed	2000	2000	1998	2000	2000	1999	1202	1652	1866	1986	1997		2000	2000
Barley-Irrigated	2000	2000	1974	2000	1973	1902	1614	1831	1203	1532	1514	1962		2000
Pastoral-Irrigated	2000	2000	1994	2000	1999	1969	1753	1977	1967	1000	0878	1999	1957	

Table 5.5: The spectral separability of the training samples related to fused ASTER-data with LANDSAT-ETM+- data (6 spectral bands, 15 m)

Pair Separation (least to most)	FW	SW	AS	BA	F	NW	NH	TR	TI	WR	WI	BR	BI	PI
Fresh Water	2000	2000	2000	2000	2000	2000	2000	2000	2000	2000	2000	2000	2000	2000
Saline Water	2000		2000	2000	2000	2000	2000	2000	2000	2000	2000	2000	2000	2000
Artificial Surfaces	2000	2000		2000	2000	2000	2000	2000	2000	2000	2000	2000	2000	2000
Bare Areas	2000	2000	2000		2000	2000	2000	2000	2000	2000	2000	2000	2000	2000
Fallow	2000	2000	2000	2000		2000	2000	2000	2000	2000	2000	2000	2000	2000
Natural Woody	2000	2000	2000	2000	2000		2000	2000	2000	2000	2000	2000	2000	2000
Natural Herbaceous	2000	2000	2000	2000	2000	2000		2000	2000	2000	2000	2000	2000	2000
Trees-Rainfed	2000	2000	2000	2000	1934	2000	2000		2000	2000	2000	2000	2000	2000
Trees-Irrigated	2000	2000	2000	2000	2000	1997	2000	2000		2000	2000	2000	2000	2000
Wheat-Rainfed	2000	2000	2000	2000	2000	2000	1996	2000	2000		1974	2000	2000	2000
Wheat-Irrigated	2000	2000	2000	2000	2000	2000	2000	1985	2000	1776		2000	2000	1989
Barley-Rainfed	2000	2000	2000	2000	2000	2000	1994	2000	2000	2000	2000		2000	2000
Barley-Irrigated	2000	2000	2000	2000	2000	2000	1992	1986	2000	2000	1915	2000		2000
Pastoral-Irrigated	2000	2000	2000	2000	2000	2000	2000	2000	2000	1962	1835	2000	2000	

The resulting training samples for all classes were checked for normal distribution of their digital numbers in the remotely sensed data multispectral bands. Where the training samples' statistical characteristics differed from normal distributions (e.g., bimodal distributions), various classification algorithms and approaches were experimented with to improve the relation of the classes and the characteristics of the study area (geographical, location and its related effects on other sub-characteristics such as climate).

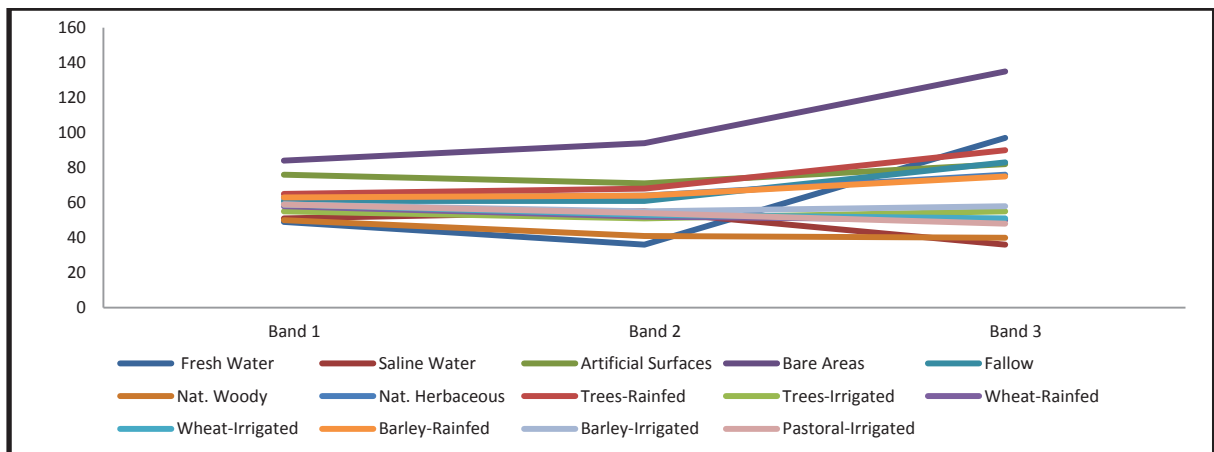


Fig. 5.30: Spectral class signatures (band means) related to ASTER data (3 spectral bands, 15 m)

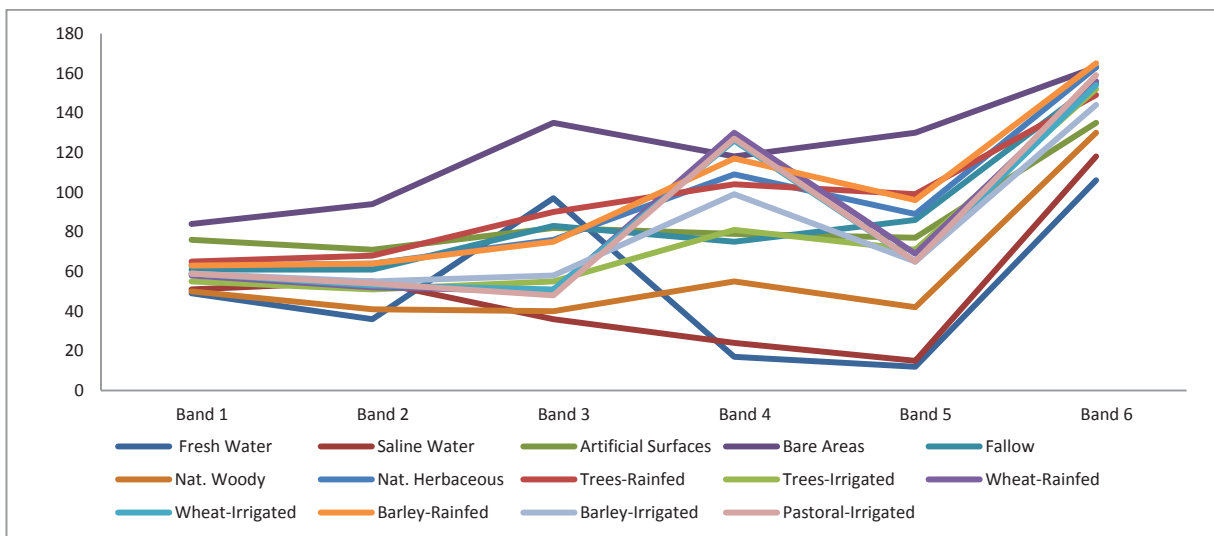


Fig. 5.31: Spectral class signatures (band means) related to fused ASTER data with LANDSAT-ETM+ data (6 spectral bands, 15 m)

The incapability of actual representation of the studied area regarding the accuracy ratio of automated classification and the ROIs-separability ratio among various classes of interest to be classified, can be put down to several reasons, including: the interaction among classes of land uses and the natural coverage distribution; and the lack of concrete borders to separate them. There were two factors affecting and complicating this: The geographical location of the study area; and nature and type of classes of LULC, which was affected generally by the geographical location.

Another important reason is that the selection of the training sites is not completely an objective process, affected by the person who selects and trains the sites. When a researcher selects the training samples, they do so because they consider them fit, appropriate and representative to the LULC in the study area. The training process may not include all areas and classes in a study area (especially within the same class); for instance, there are several kinds of wheat (hard and soft), some are rain-fed and some irrigated, some are located on dark humid soils, while others are on light and less moisture-rich soils, some have organic and chemical fertilizers added, while others grow in different quantities; some wheat-fields may be peppered with natural herbs and plants that grow within the wheat plants, while other fields have homogeneous growth of only wheat plants; and finally, some wheat-fields may be infected with disease. Wherever these differences are related to one class (i.e., wheat) this will make spectral and spatial discrimination between wheat and other crops difficult. Each difference (or more collected differences) leads to various spectral appearances on the satellite image. Therefore, the analyst has to gather training samples that satisfy the entire different spectral responses of the crop especially if there are natural or agricultural crops in the area with a similar spectral response.

## **G. The choice and evaluation of the optimized method of automated classification**

A comparative study of different remotely sensed data classification algorithms is often conducted to find the optimized classification result for a specific study (Lu & Weng, 2007).

Many considerations, such as: spatial resolution of the remotely sensed data (how many meters?); spectral resolution (how many bands?); different sources of data (which sensors?); a classification system (which scheme?); and training samples (which statistical distribution?), must be taken into account when selecting a classification algorithm for use. Each algorithm has its merits and deficits. Therefore, the question of which classification algorithm is more suitable for a specific study in a specific area is not easy to answer. Also, different classification results could be obtained depending on the classifier(s) chosen.

Experiments were conducted on the testing study area to determine the suitable algorithm to use on the entire ERB study area. The supervised classification algorithms tested were: MLC: Maximum Likelihood Classifier, NN: Neural Network, and SVM: Support Vector Machine (Fig. 5.32). Two classification procedures were also applied: 1) one stage classification approach; and 2) multi stage classification approach, to produce land cover maps.

To compare and judge the different classification algorithms results, we have to, as far as possible, exclude the influence of interfering factors. Therefore, while this is a comparative study, a wider choice in the same training samples (size, number, location, etc.) in each studied year and for all remotely sensed data, and for all compared classification algorithms, would be useful. This would not be applicable when using the masking operation used in the multi stage classification approach.

### **1 The test area**

The four administrative areas of Menbij, Ein Eisa, Al-Journia and Athawra were selected as testing areas (sub-study-area) for applying various automated supervised classification approaches and algorithms. These sites were adopted as they contained the majority of natural coverage forms and

land uses which exist among the entire ERB area. These areas were also sited within range of the agricultural stabilization zones in the basin and contained a number of irrigated projects. Finally, the sites were distributed in only one scene of the LANDSAT-data, which satisfied the homogeneity in spectral and radiometric characteristics. The result: this testing area was considered as representative to the whole basin area from the perspective of natural and climatic characteristics, distribution of natural coverage and land uses. Therefore, any outcomes resulting from the sub-study-area could be adopted, generalized and applied to the whole Basin.

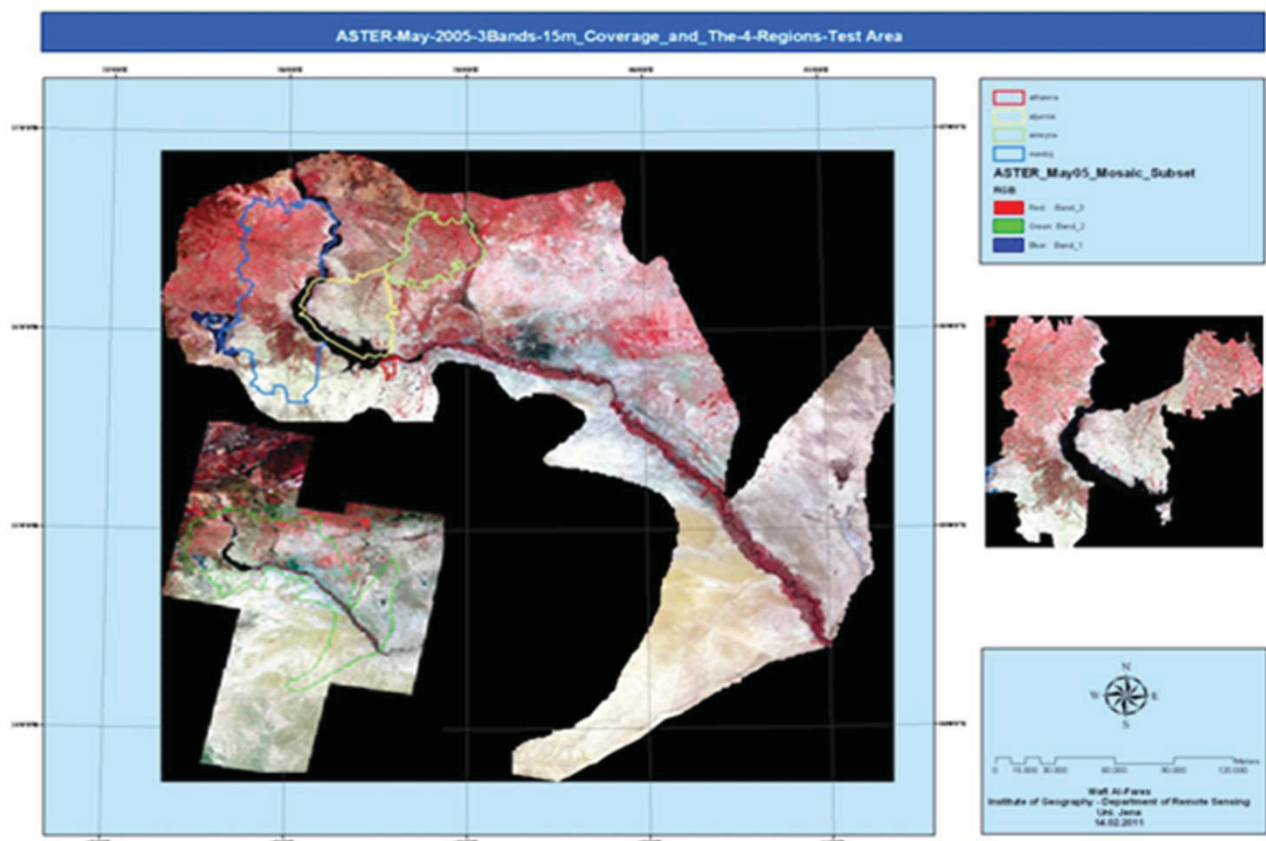


Fig. 5.32: The spatial extent of the four administrative regions (Athawra, Al-Jurnia, Ain Eysa and Menbij)

### 1.1. Unsupervised classification

The migrating means (or ISODATA, or nearest mean) algorithm (Ball & Hall, 1965), is the most commonly used algorithm in unsupervised classification approaches. It frequently executes a complete classification process; recalculates statistics; uses lowest spectral distance method (reducing the value of the function is the average Euclidean distance between each sample point and the matching cluster mean) repeatedly to classify the pixels; and re-specifies the rules of each LULC-class or candidate pixel (iterative processes). Intuitively, the calculated minimized value of the average Euclidean distance is equal to creating sphere-shaped clusters with little difference or dispersity. There is no logical technique for creating clusters that minimize the value of the average Euclidean distance. Therefore, the data will be continuously classified until either a maximum number of iterations have been executed or a maximum percentage of unchanged pixels have been achieved between two iterations (Ball & Hall, 1965; Leica Geosystems, 2005; Jensen, 2005). The process starts with an identified number of random cluster means or the means of existing signatures, and then it processes iteratively, so that those means move to the means of the clusters in the data. "The ISODATA-classifier filters cluster by splitting (if the cluster standard deviation exceeds a predefined value and the number of pixels is twice the threshold for the minimum number of

members) and merging (if either the number of members (pixel) in a cluster is less than a certain threshold or if the centers of two clusters are closer than a certain threshold)" (Leica Geosystems, 2005; Jensen, 2007). There are various forms of this technique, but in all of them at least two factors have to be defined by the analyst: clusters number; and the iterations maximum number (this ensures the method will stop if convergence is not achieved).

This algorithm has several disadvantages. Some of the generated clusters are not important in regard to reality since they represent a mix of different LULC-features or "on the ground" classes. It is also not unusual that several spectral classes build one functional class, and it has to be remerged. Also, there is a causal relationship between the functionality of this algorithm and the ability of the user to identify the number of current spectral classes (Hoffer, 1980). Many of the data characteristics that a photo interpreter would use to identify an individual LULC-feature (such as: shape, size, texture, shadow, association, etc.) are not used in classification of the data that operated based on the computer digitally (Hoffer, 1980).

Methods of unsupervised classification have the ability to define the different classes that could be presented in the study area before the going to the field. Then, the natural objects that are presented in the remotely sensed data can be identified and linked to the resulting spectral classes of classes of interest (crops, land cover classes, etc.) (Hoffer, 1980). For this research, the initial thematic map generated from this approach helped to identify the features and provide the feel of the study area, although the images could not be directly used for other analysis without field-work.

The ISODATA-algorithm has proved useful as an indicator and guide as it provides an idea of the relative stability of each category (McCoy, 2005). The individual data are processed using the unsupervised ISODATA-algorithm to generate a large number of class assortments. These so-called *clusters* are then supposed to represent classes in the image and are utilized to compute statistics of the class signatures. It is helpful to define relatively homogeneous features to be used as training sites in the potential supervised classification approach (Schowengerdt, 2007), where pixels that always arise jointly in the same cluster are strong and are a very homogeneous category (McCoy, 2005).

It was found that the hybrid-procedure integrating ISODATA-clustering with the supervised classification algorithms such as MLC seemed to be the most satisfactory and effective procedure to follow as it simplified the work and produced better results. This was the case mainly in land areas with wild habitat where the fields were small, or where the LULC-categories and spectral classes were complex (Hoffer, 1980). The classification approach is illustrated in Fig. 5.33.

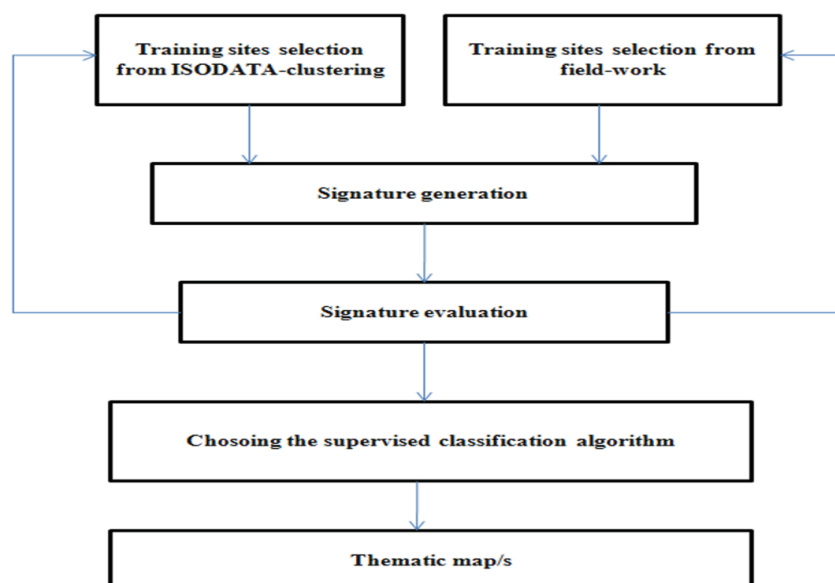


Fig. 5.33: Integrating the ISODATA-clustering with the supervised classification algorithms in a so-called hybrid-procedure

The parameters for the performance of ISODATA-algorithm were given as follows: Number of classes = 25; Maximum iterations = 20; Convergence threshold = 0.98. A thematic raster layer and a signature file (identifiable) were created from the ISODATA-clustering. For example, it was found that water bodies, bare areas, artificial surfaces and fallow ground could be clearly identified using the ISODATA-clustering technique. It gave general information about the spectral mixture between the various LULC-features. Mixtures were between built-up areas and dark color-tones bare areas; dark color-tones bare areas and fallow on dark soils; light color-tones bare areas and fallow on light soils; very dense irrigated trees (especially Poplar) and dark water; and between vine and sugar beet.

## 1.2. Supervised classification

### 1.2.1. The multi stage classification approach

The decision tree classifier is a hierarchically based classification method which compares data with a variety of well-chosen features. The selection of these features is controlled by an estimation of the spectral distributions or separability of the classes (Pal & Mather, 2003). There is no commonly confirmed formula and each decision tree or set of rules must be constructed by a specialist. If a decision tree presents just two outputs at each stage, then it will be named a *Binary Decision Tree Classifier (BDTC)*. This procedure was applied in many cases due to its flexible characteristics. In agriculture applications, the rules of a decision tree are acquired via analyzing the specific attributes (understanding the various spectral responses, the agricultural calendar, etc.) of different crop types (Chen et al., 2008). Fig. 5.34 and Fig. 5.35 illustrate the steps applied in the multi stage classification approach to generating the classification results of the four region study area.

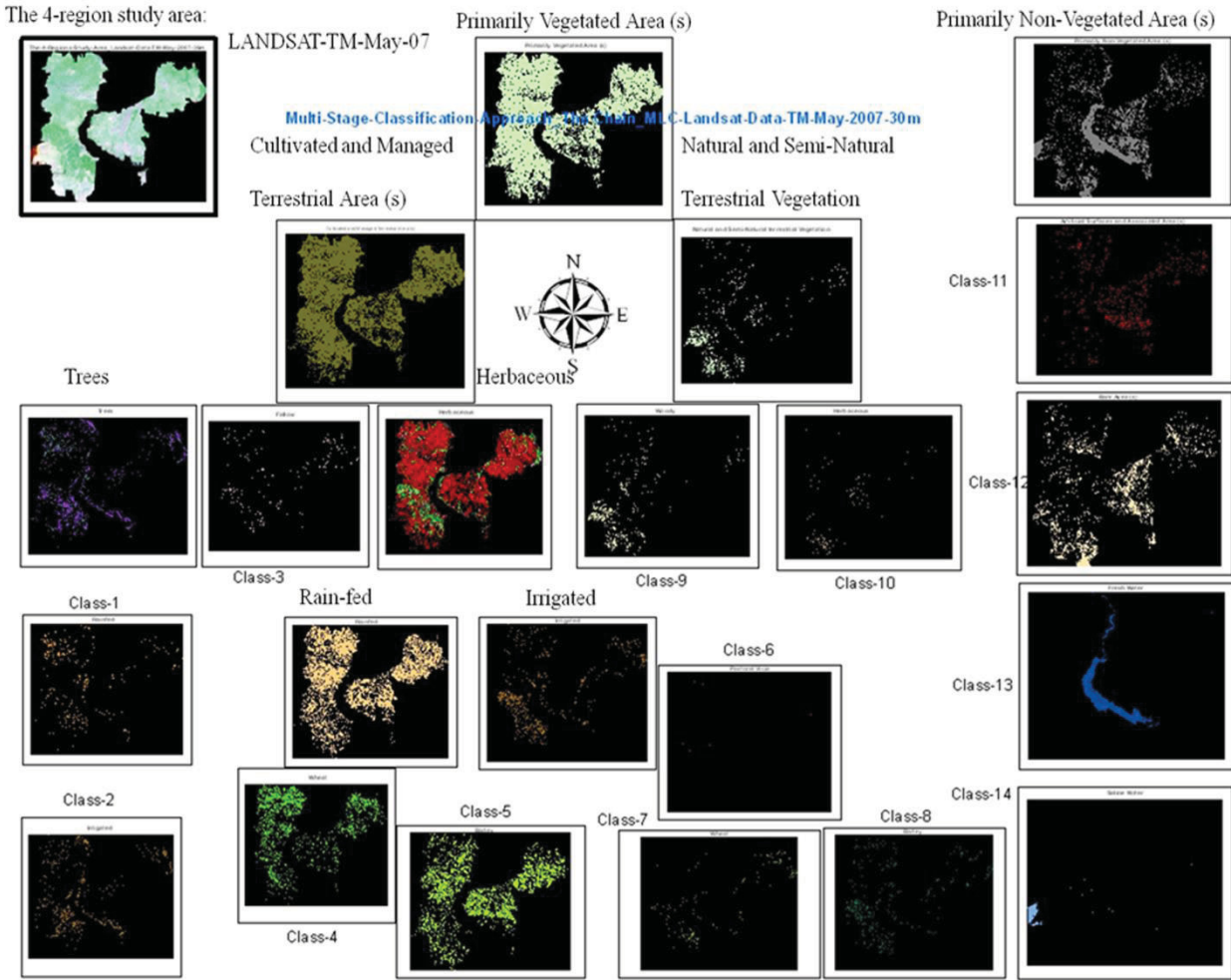


Fig. 5.34: Illustration the application of multi stage classification approach (chain-steps), using MLC-algorithm, on the LANDSAT-TM-data of May 2007 with spatial resolution of 30 m

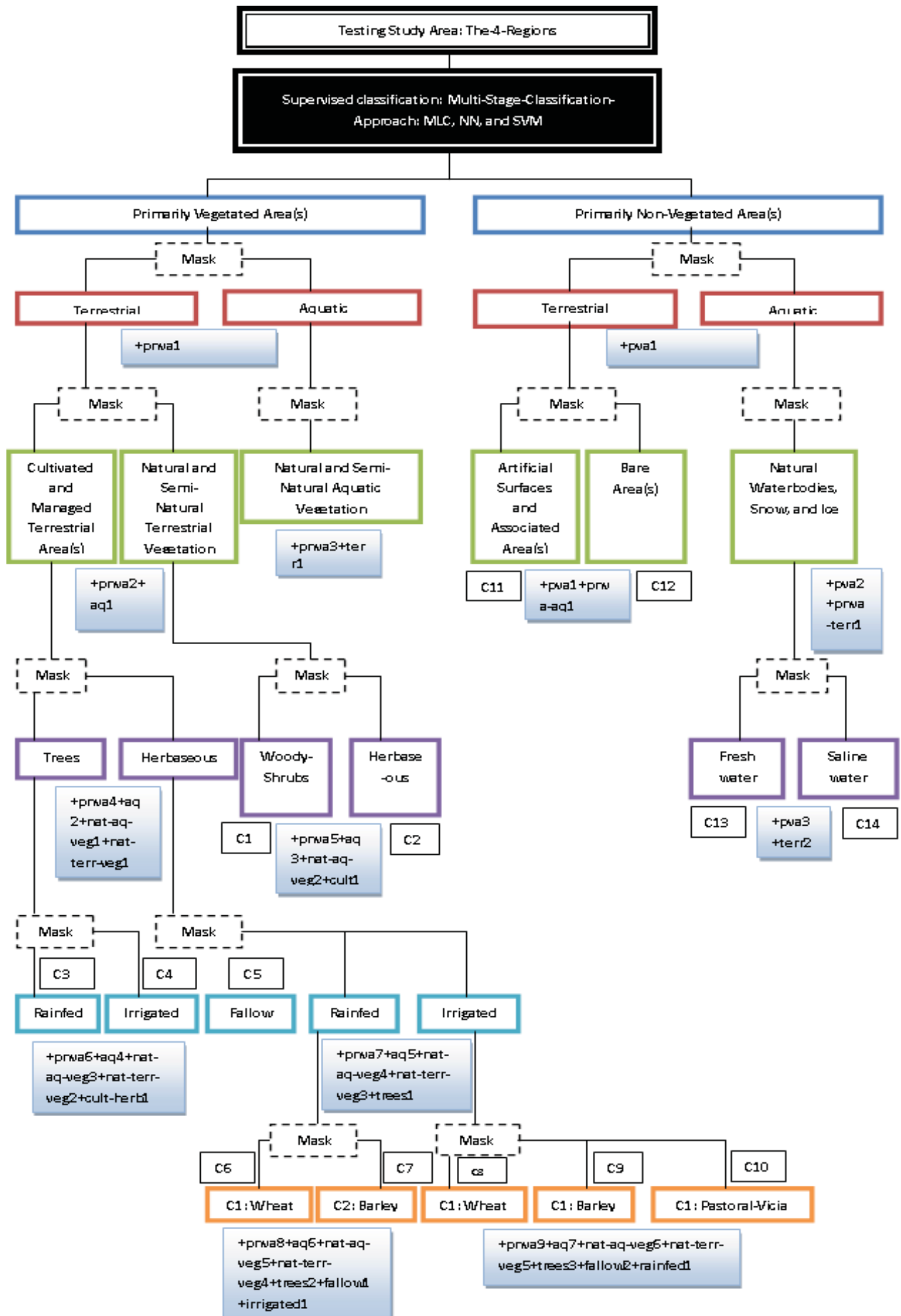


Fig. 5.35: The flow-chart of the applied multi stage classification approach in this study



Training sites and testing areas are fulfilled separately and compared to satellite images for each classification algorithm after applying the masking-process. This is done because, for example, the mask that represents the distribution of the irrigated agriculture (separation and classification of the irrigated agriculture areas and the rain-fed agriculture areas) using the MLC-algorithm covers areas differing from those areas covered by the same mask. This results from using the SVM-algorithm in the classification process.

After finishing the multi stage hierarchal classification, various classes resulting from each stage are collected and fused in one scene that represents the LULC in the study area using ENVI-program (band-math), or the ArcGIS-software (Fig. 5.36).

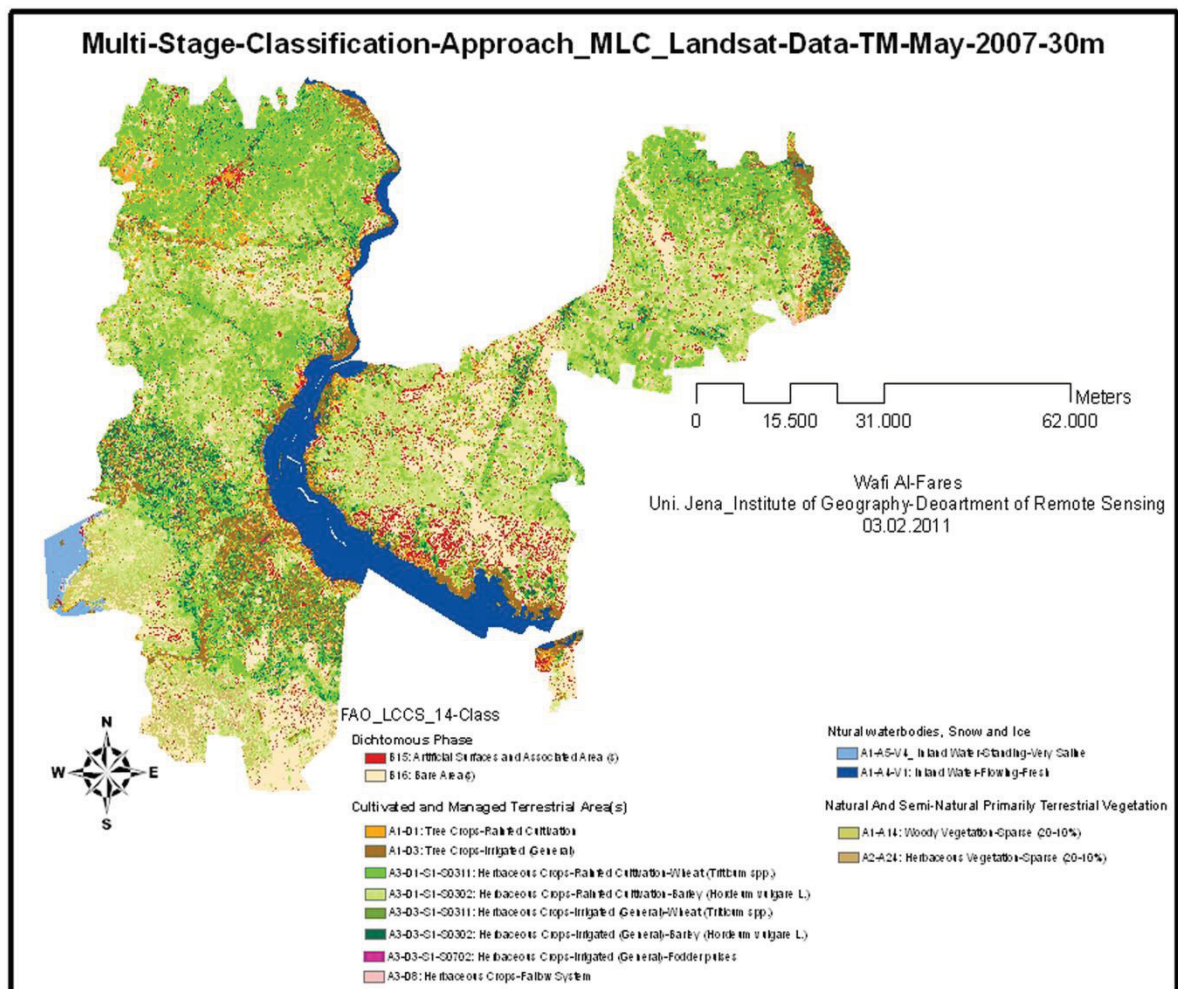


Fig. 5.36: Combine the 14-class illustrated in the previous figure in one thematic map, using ArcGIS-software to sum the individual thematic results, and LCCS-software to prepare the legend

Obtaining 100 %, 90 % or other percentages reflecting accuracy and quality of automated classification (or the semi-automated classification), does not necessarily mean that the percentage completely represents land use distribution or the prevalence of natural coverage on real ground. The accuracy percentage of 100 % obtained from the classification of primarily vegetated areas and non-primarily vegetated areas does not mean that the entire area contains the same percentage of classification. Of the primarily vegetated areas (e.g., 100,000 ha) perhaps 1,000 ha are primarily non-vegetated areas. This error/s in classification would then be repeated in each step or stage of the multi stage classification approach. This means that the primarily vegetated areas class might appear under classification of the components of the second level (i.e., the second terrestrial and aquatic level underlying under the first primarily non-vegetated areas level) within the used classification scheme (i.e., LCCS), although it should have been classified and separated into the first

level. Therefore, the LCCS-principle of classification should be strictly adhered to, that is separation between classes in every level and every stage in classification system. Here the primarily vegetated areas, (for example the 1,000 ha that had been classified incorrectly under the primarily non-vegetated areas class) will during the automated classification process, be automatically fused with classes within the second general level (i.e., primarily non-vegetated areas), thus creating accumulated error/s in the classification process.

Part of the resolution of this problem is to re-classify the wrongly-classified areas when moving to the next stage or level of classification, as long as there are lands representing the wrong classified class within the various levels of the multi stage hierarchical classification approach. When we return to the example of the 1,000 ha, which were classified as non-vegetated areas and consider this at the second level of classification, instead of training sites that represent only the two classes of this level (i.e., terrestrial and aquatic), extra training sites will be selected that represent the 1,000 ha area/s. If this 1,000 ha were completely separated and classified within the second level, it will be appropriate. Otherwise, if a further part of this area, such as 100 ha would appear within the next level, again additional training sites would be trained to represent this class in the classification process.

### 1.2.2. MLC

The *Maximum Likelihood Classifier (MLC)* has been employed since the late 1940s. It found increasing investment in the two fields of: pattern recognition; and remote sensing techniques (Nilsson, 1965). It is offered in almost all remote sensing and image processing software packages, and it is commonly applied as the typical supervised classification approach. It is a widely robust supervised classification algorithm, and it is the primary approach for most multi-spectral remote sensing interpretations at present (Wessel et al., 2004; Jensen, 2005; Lillesand et al., 2008). Its general concept defines the maximum likelihood decision rule, which is the probability that a pixel belongs to an individual class (ERDAS, 1999). This classifier is derived from the *Bayes-rule* in which classes have equivalent priorities. It uses the training data gathered during field-work or on image itself to calculate the mean vector and variance-covariance matrix for each required class. Both means and variances are then employed to assess the probabilities (Jensen, 2005; Leica Geosystems, 2005). This algorithm is based on the supposition that the likelihood degree function for each class is multivariate, and often a *Gaussian distribution* is assumed. A pixel is lastly classified to that class, for which it has the highest probability (Strahler, 1980; Bastin, 1997; Richards & Jia, 2003; Lillesand et al., 2008).

MLC operates (see Fig. 5.37) by using the training-samples-based means and standard deviations of individual spectral bands in order to scheme LULC classes as *centroids* in feature space. These *centroids* are circumscribed by likelihood curves. The likelihood degree function supposes that the representative sample values for each presented class are normally distributed (Bastin, 1997). The so called *Gaussian threshold* can border the class space in feature space, which is the radius (in standard deviation units) of a hyper-ellipsoid around the mean of the class in feature space (PCI Geomatica, 2001). Here, observations which do not locate inside the hyper-ellipsoid of any class are allocated to a *null class* (Strahler, 1980). The necessary number of training samples needed to calculate the statistics of a class for a Gaussian (quadratic) classifier is in addition linked to the square of features number (Fukunaga, 1990). This presents increase in the *Hughes effect*: for a limited number of training samples, the classification accuracy increases in the beginning with the number of features (or difficulty in measurement), but then it attains a maximum and begins to decrease when more features are added. It is generally agreed that the class spectral separability is constantly higher for data with a superior dimensionality (more measurements), but this superior or higher dimensionality impacts and decreases the accuracy of the statistics estimation when the dimensionality becomes too high, and in some cases, this has the result of producing a lower clas-

sification accuracy despite the presented and improved theoretical class separability (Landgrebe, 2003). Enough training samples for each spectral class of interest must be presented to offer logical approximations of the elements of the mean vector and the covariance matrix to be determined. For an (N) dimensional multi-spectral space, at least (N+1) samples are needed, to avoid the covariance matrix being singular.

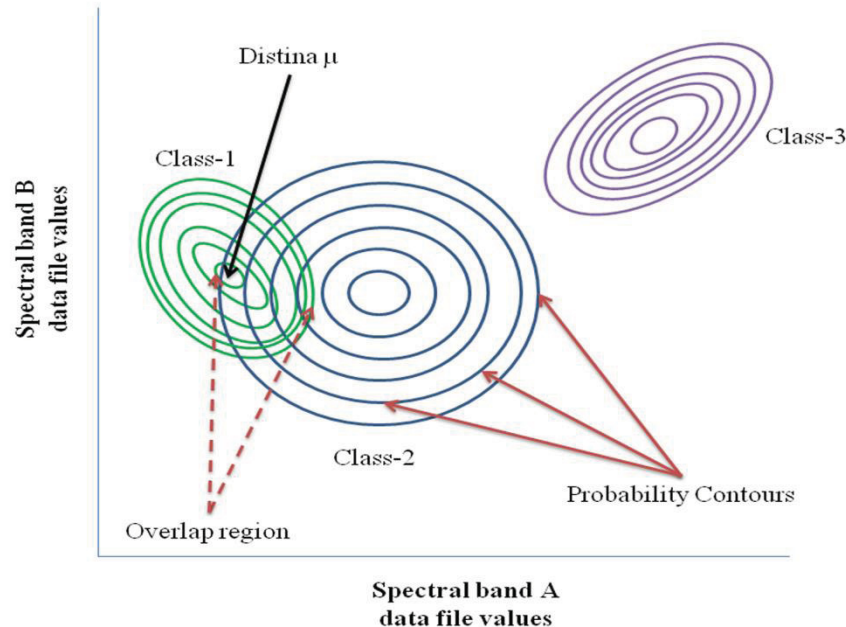


Fig. 5.37: Maximum Likelihood Classifier (MLC) concept (Source: Modified from: ERDAS IMAGINE®, 1999)

The strong advantage of the MLC algorithm is its applying for well-developed probability theory. If it is true that the class likelihood degree functions are Gaussian, then MLC is the best classifier which reduces the overall chance of error (Liu et al., 2002). Benediktsson et al. (1990) noticed that even for data which have not got a normal distribution, the MLC produced a better classification result, although it has also serious known weaknesses under specific situations. Firstly, if the histogram/frequency distribution of the image data does not ensure the normal distribution, the essential supposition of this classifier is violated and presents poor or confusing results. Secondly, the computational cost needed to classify each pixel (data with a large number of spectral bands, or data containing many spectral classes to be distinguished) is at issue. The computing cost increases in conjunction to the square of the applied features channels (Benediktsson et al., 1990). Thirdly, the algorithm works acceptably for relatively low spatial resolution data with a limited number of spectral bands, but it may not be acceptable for the high resolution and/or high dimensionality data sets, which tend to increase the within-class variability. This means that the volume of feature space occupied by each class is extended and increases the risk of class overlap in feature space (Qiu & Jensen, 2004). Fourthly, the relationship between sample size and the number of features impacts the assessments of mean vector and variance-covariance matrix. Furthermore, inadequate ground truth data may present a false assessment of the mean vector and the variance-covariance matrix of population (poor classification results). Fifthly, in case of high correlation between two spectral bands (LANDSAT-data), or when the training samples used for signature generation are not adequately homogeneous, the covariance matrix becomes unstable. This can be overcome through the use of other robust statistical method (e.g., PCA) before proceeding to classification (Hilderbrandt, 1996; Blaschke, 2000; Richards & Jia, 2003; Albertz, 2009). Sixthly, an inherent weakness of MLC is that the subset of features applied in classification is not necessarily to be the optimal selection for all classes (Swain & Hauska, 1977). Finally, when auxiliary data is integrated into a classification process, the assumptions of MLC cannot be confirmed.

There have been a number of researchers who have MLC, such as (Brisco & Brown, 1995; Chust et al., 2004; Huang et al., 2007). MLC can be used with multi-source data with separate scales of measurement (Arora & Mathur, 2001), while a parametric MLC, which is commonly used for pixel-based hard classifications, can be used to segment imagery (e.g., Geneletti & Gorte, 2003) or expand to a fuzzy classification idea (e.g., Schowengerdt, 1996).

### 1.2.3. ANN

Humans are good pattern recognizers. This tenet has given researchers in the field of pattern recognition the basic concept to examine whether computer systems based on a simplified model of the human mind can simulate the real world, and whether better overall accuracies can be given compared to traditional statistical approaches. The *Artificial Neural Networks* (ANN) algorithm is an example of these recently advanced methods. It is designed to simulate human learning processes through organization and strengthening of passage ways between input data and output data. Because of the nonparametric structure of the NN-classifiers and while networks are general-purpose calculating tools that can overcome the complex non-linear problems, the use of NNs for classifying remotely sensed data has developed quickly over the past decade. Researchers have noted that NNs do better than standard statistical classifiers such as MLC (Fischer, 1996; Del Frate et al., 2003; Tso & Mather, 2009). NNs have been increasingly used since the 1990s (Franklin, 1995; Sugumaran, 2001) in field of pattern recognition in general, and in the field of remote sensing analysis and classification in particular. It covers: supervised classification (Benediktsson et al., 1990; Hepner et al., 1990; Heerman & Khazenie, 1992; Foody & Arora, 1997); and unsupervised classification (Baraldi & Parmiggiani, 1995; Schaale & Furrer, 1995; Tso, 1997). A broad-spectrum introduction to neural networks was given by Bishop (1995), while a very good presentation of applying neural network in classification and its relationship to conventional statistical classification was provided by Schürmann (1996). An overview in the context of remote sensing has been described by Benediktsson et al. (1990), and Kavzoglu (2001).

The user-selected parameters affecting the NN-classifier are, according to Kavzoglu (2001): 1) learning parameters: the back-propagation learning algorithm needs from the analyst to offer values of the learning rate and momentum; 2) initial weights: these random settings to the pre-trained network affect the network implementation; 3) number of training iterations: this defines the level of generalization as contrasting to specialization of the solution. If a network is trained using very large number of iterations, it might not work well on the test data. Conversely, if it is not trained well enough, it will not be able to separate the classes; 4) number of hidden layers and units: this controls the ability of the network to learn and generalize; and 5) number of input patterns: some researchers have suggested that classification accuracy is influenced by the number of training patterns.

NNs are based poorly on the data distribution assumptions of examples and on the character of the relationship between inputs and outputs (Paola & Showengerdt, 1995 b). This is an advantage that makes these algorithms smarter than statistical classifiers, mainly in the case when the size of training data is incomplete and sufficient assessment of statistical parameters is hard to achieve (Tso & Mather, 2009). Also, different sources of data can be applied as inputs which are then scaled to a general range (typically values between 0 and 1 like the node output values) before training and classification. According to Paola and Schowengerdt (1995 b), and Qiu and Jensen (2004), ANN-classifiers are strong to noise in the training data and has the ability to generalize. They are error-tolerant and relatively insensitive to background noise.

The drawback of neural networks lies in that they work as a “black box” (Franklin, 1995; Qiu & Jensen, 2004), whilst lacking the ability to give details to further the understanding of the relationship between input and output. Because of their indicative structure and the element of random variations in the results (due to the randomization of the weights of the connection links before

training), functioning prediction and the interpretation of results are not easy. Another drawback is that iterative training needs much more computation time than parametric methods (Paola & Schowengerdt, 1995 b; Landgrebe, 2003). However, when the network is trained, the classification process in this way is rapid (Pal & Pal, 1993). Despite the high cost of training expenses (Foody, 1999; Lillesand et al., 2008), neural networks have no stable rules for the network design and their functionality is influenced by some issues (e.g., the network architecture) (Foody & Arora, 1997), which is dependent on the analyst.

Classification is improved by using hierarchical NN-classifiers and combining the classification results of multiple classifiers by a compromise rule (Lee & Ersoy, 2007). It is established that the use of a collection of neural networks for LULC-classification of multispectral remotely sensed data can give a significant increase in classification accuracy (Canty, 2009). A review and analysis of papers published about ANNs before 1994 can be found in Paola and Schowengerdt (1995 b). Example applications of ANNs in remote sensing image classification for the period between 1994 and 2007 are given in Schowengerdt (2007).

A successful method of classifying remotely sensed data based on different approaches in choosing the networks of ANNs has been referred in many studies (Bagan et al., 2008). E.g., *Multi-Layer Perception MLP* (Benediktsson et al., 1990; Zhang & Scofield, 1994; Foody, 1995; Rumelhart et al., 1996; Foody, 1999; Arora & Mathur, 2001); *ARTMAP* (Carpenter et al., 1997; Borak & Strahler, 1999; Muchoney et al., 2000; Karen et al., 2003; Alilat et al., 2006); *radial basis function* (Bruzzone & Fernandez-Prieto, 1999); and the *SOM-algorithm with Learning Vector Quantization (LVQ)* (Ito & Omatu, 1999; Ji, 2000).

ARTMAP-systems, particularly ART2 and fuzzy-ART, can be practical in executing unsupervised classification on remotely sensed imagery (Tso & Mather, 2009). An example of applying fuzzy-ARTMAP was presented by Carpenter et al. (1997), where the results are compared to those created by the MLC, nearest neighbor and multilayer perceptron approaches. It confirms that it is faster and more constant. The same conclusion is also confirmed by Mannan et al. (1998). Liu et al. (2004 b) presented an ARTMAP-based model called ART Mixture MAP (ART-MMAP) for approximation LULC-fractions within a pixel. Finally, in order to obtain fine results, one might have to try a variety of ART model-based parameters (Tso & Mather, 2009).

The most common NN-classifier in remote sensing is the MLP (the multi-layered feed-forward network) (Tso & Mather, 2009). Excellent reviews about experiments using MLP are presented by Paola and Schowengerdt (1995 b), Atkinson and Tatnall (1997), and Kanellopoulos and Wilkinson (1997). MLP employs the “*generalized delta rule*”. “At the first stage of training a back-propagation network, the training sample vectors (with known classes/target outputs) are used as input for the network and propagated forward to calculate the output values for each output node. The error between the real and preferred output is calculated. In the case where each output node represents one class, the preferred output is a high value (e.g., 0.9) for the node of the correct class, and a low value (e.g., 0.1) for the other nodes. The second training stage features a backward pass from the output nodes through the network, during which the weights are changed according to the learning rate and the error signal passed backwards to each node” (Benediktsson et al., 1990). This process of inputting the training data (Fig. 5.38), estimating the output error and modifying the weights of the connection links is repeated many times (Foody, 2004 a), until some condition is satisfied, and if possible until the network has stabilized in order that the changes in error and weight per cycle have become very small (iterative training). When the network is trained, i.e. suitable weights are found and, all the pixel vectors are fed into the network and classified.

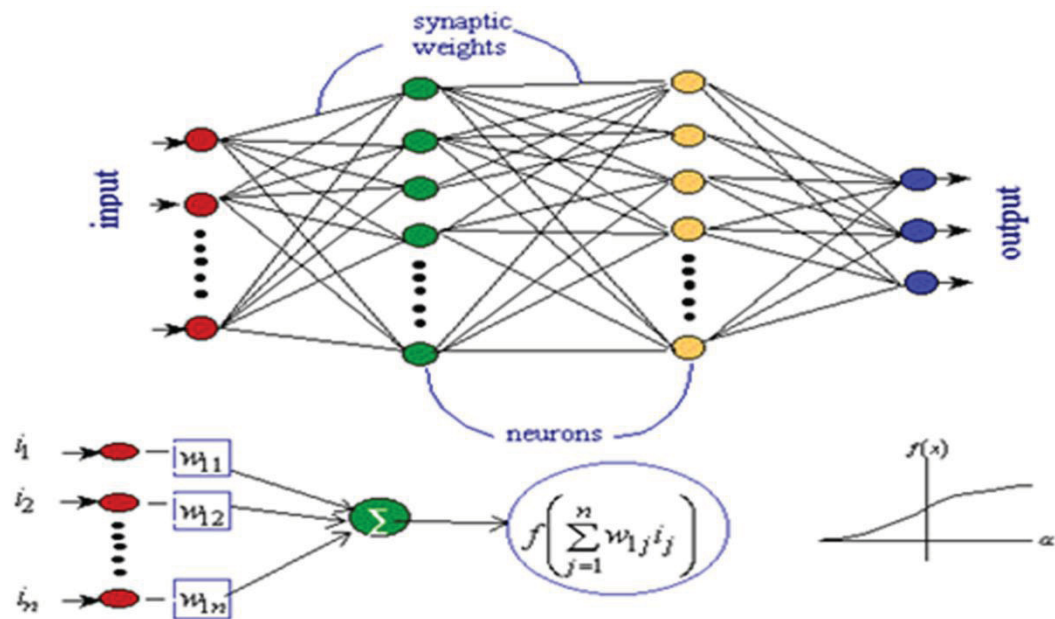


Fig. 5.38: The Neural Network Classification Model (Source: Adapted from: [www.ndt.net/article/v05n07/spanner2/spanner2.htm](http://www.ndt.net/article/v05n07/spanner2/spanner2.htm))

The produced back-propagation neural network utilizes the “*generalized delta rule*” during the learning stage. The network was trained using the same class training samples which were also used in MLC and SVM. The activation type was Logistic; the training threshold contribution was 0.90; the training rate was set to 0.10; the momentum rate to 0.90; the training RMS-exit-criteria was 0.10; the number of hidden layers was 1; and the training cycle (adjustment of weights after forward and backward propagation of values through the network) was repeated for a maximum of 1,000 iterations, or until the maximum normalized total error was less than 0.01, or the maximum individual error was less than 0.001. The last two situations did not occur, so the training was always performed for 1,000 iterations. (“the individual error is the sum of errors in the output values for one sample, meaning the difference between target value and output value of each output node. The normalized total error is calculated as half the sum of the squares of the individual errors, divided by the number of samples”) (PCI Geomatica, 2001). The error plot was then observed to see whether the value for the normalized total error had stabilized before the 1,000th iteration. This was the case for all classifications performed here, although the total error was still between 0.45 and 0.52. In a second step, the training and momentum rates were lowered to 0.05 and 0.20 respectively, for a slower, more stable training with smaller step increases for an enhancement of the network weights (PCI Geomatica, 2001). 1,000 additional iterations were improved with these parameters, resulting in final maximum total errors between 0.39 and 0.46.

#### 1.2.4. SVM

The *Support Vector Machine* (SVM) classification algorithm is based on statistical learning theory as proposed by Vapnik and Chervonenkis (1971). It is discussed in detail by Vapnik (1995 and 1999). The SVM is a newly developed method to train polynomial, radial basis function, or multi-layer perceptron classifiers. Bennet and Cambell (2000) gave a geometric clarification of how the support vector machines functioned (Fig. 5.39). A detailed presentation to the general concept of SVMs is provided by Burges (1998), and Schölkopf and Smola (2002). An overview on the application in remote sensing is given by Gualtieri and Cromp (1998), Chapelle et al. (2002), Huang et al. (2002), Foody and Mathur (2004 a and b), Melgani and Bruzzone (2004), Pal and Mather (2005 and 2006), and Watanachaturaporn et al. (2006).

SVMs were at first presented as a binary classifier (Vapnik, 1998). The idea is based on fixing an *Optimal Separating Hyper-plane* (OSH) to the training samples of two classes, so the pixels from

each tested class are at last on the right side of the hyper-plane. The optimization problem that has to be removed is based on the minimization of structural risk. Its goal is to maximize the borders between the OSH and the nearest neighboring training samples, the so-called support vectors (Vapnik, 1998). Therefore, the model just considers samples nearly from the class boundary and operates well with small training samples, even when high dimensional data sets are used in classification (Melgani & Bruzzone, 2004; Pal & Mather, 2006). Foody and Mathur (2004 b) indicated that a complete description of each class is not necessary for an accurate classification. While only samples close to the hyper-plane are measured, other training data has no influence on the interpretation. However, a larger number of training samples guarantees the employment of sufficient samples (Foody & Mathur, 2004 b).

In contrast to other classification algorithms (e.g., decision tree), the initial output of a SVM does not have the final class label. The outputs include the distances of each pixel to the OSH-plane (rule images). These rule images can then be utilized to verify the final class membership that is based on the *multiclass strategy*. This principle is furthermore known as “winner takes all”, where only one value (the maximum) is used for choosing the membership. Contrary to these two multiclass-methods, other approaches directly identify the SVM as one multiclass problem (Sebald & Bucklew, 2001; Hsu & Lin, 2002). A simultaneous separation of more than two classes presents a more complex optimization problem (Sebald & Bucklew, 2001). Thus, such approaches may be less professional in comparison to conventional multiclass approaches. In Melgani and Bruzzone (2004) a computationally promising hierarchical tree-based SVM was presented as an alternative concept.

SVMs operate very well with high dimensional data (Watanachaturaporn et al., 2004). Their computational cost does not depend on data dimensionality and they require no feature selection. Thus, classification results for multisource data classification from a non-parametric classifier in particular, is probably better than that received from a parametric classifier, since a non-parametric classifier can solve some of the problems of a stacked vector approach (Watanachaturaporn et al., 2008). SVM learning generally requires large memory, a great deal of computation time and small training sets (Su, 2009).

Some of the issues that influence the classification accuracy of SVM-classifiers (Huang et al., 2002) are: Choice of kernel used (linear, polynomial, radial basis function, and sigmoid); and choice of the parameters related to a particular kernel (degree of kernel polynomial, bias in kernel function, gamma in kernel function, penalty parameter, pyramid levels, and classification probability threshold).

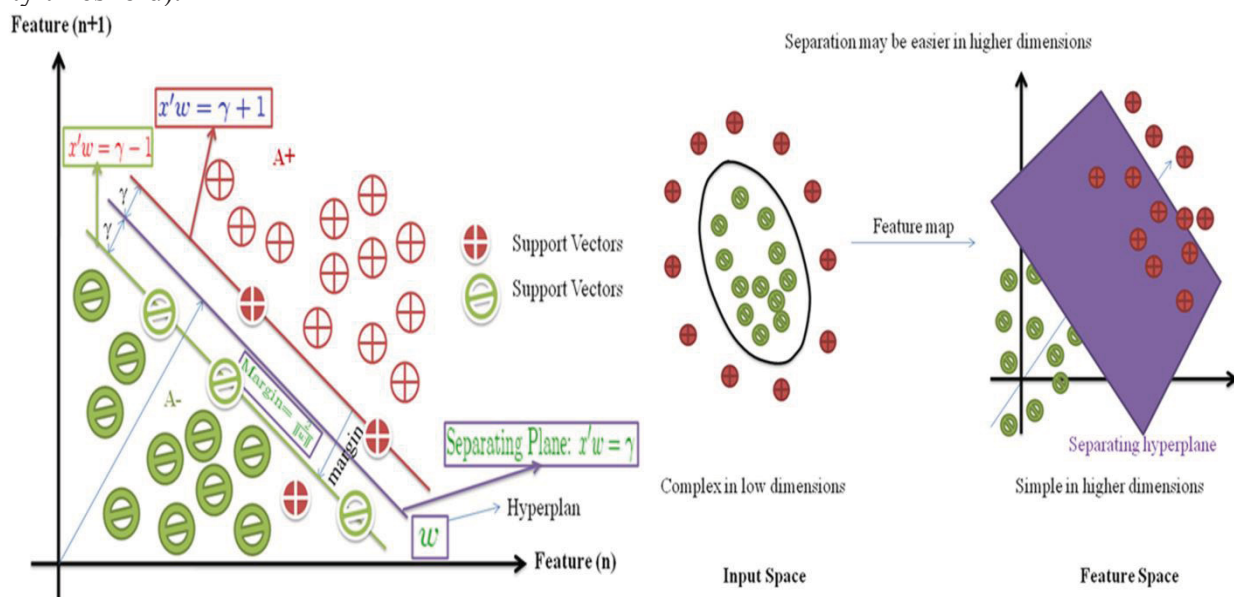


Fig. 5.39: Geometric explanation for the linear classification of SVM (Source: Modified from Vapnik, 1998)

Recent studies have shown that the use of SVMs in remotely sensed data classification might present results with higher accuracy than other classifiers (Tso & Mather, 2009). SVMs have been used for classification of RADAR-data (Fukuda & Hirose, 2001; Lardeux et al., 2006; Shimoni et al., 2009), ASTER-data (Zhu & Blumberg, 2002; Marçal et al., 2005), LANDSAT-TM-data (Keuchel et al., 2003) and hyper-spectral-data (Melgani & Bruzzone, 2004). Only a few studies are known which have used SVMs for classifying multisource or multi-temporal data (Halldorsson et al., 2003; Song et al., 2005 b; Camps-Valls et al., 2006; Fauvel et al., 2006 a).

Foody and Mathur (2004 a and b, and 2006) have examined both the characteristics and the size of training samples in SVMs. The paper from Hernandez et al. (2007) confirmed that applying a classification approach based on SVMs such as the SVDD could be used to provide more accuracy (97.5 %) than a MLC-algorithm (90.0 %). Other significant papers on this topic include: Bruzzone and Marconcini (2009), and Su (2009).

The SVM-options that were used in the study were: Kernel type (polynomial); degree of kernel polynomial (2); bias in kernel function (1,000); gamma in kernel function (0.111); penalty parameter (100,000); pyramid levels (0); and classification probability threshold (0).

## 2. Results and evaluation

This section presents the results (thematic maps) of the comparison study which used the remotely sensed data obtained from LANDSAT: MSS-June-1975 with 60 m spatial resolution and four spectral bands (Fig. 5.41); TM-May-2007/30 m and six bands (Fig. 5.42); and TERRA: ASTER-May-2005/15 m and three bands (Fig. 5.43) fused with additional three spectral bands of LANDSAT: ETM+/SLC-Off-corrected/-May-2005/15 m (Fig. 5.44). Two supervised classification approaches (Multi Stage Classification Approach and One Stage Classification Approach) were adopted, using the three supervised classification algorithms MLC, ANN and SVM. This comparison study was carried out for the selected sub-study-area of the four administrative regions. The LULC-classes generated in relation to the selected testing area based on the LCCS-classification scheme, are described in Fig. 5.40.

<b>Land Cover Classification Legend</b>		
01.02.2011		
<i>List of Land Cover Classifiers Used</i>		
#	Classifier	Classifier Label
<b>Dichotomous Phase</b>		
1	A	Primarily Vegetated Area(s)
2	A1	Primarily Vegetated Terrestrial Area(s)
3	A11	Cultivated and Managed Terrestrial Area(s)
4	A12	Natural And Semi-Natural Primarily Terrestrial Vegetation
5	B	Primarily Non-Vegetated Area(s)
6	B1	Primarily Non-Vegetated Terrestrial Area(s)
7	B15	Artificial Surfaces and Associated Area(s)
8	B16	Bare Area(s)
9	B2	Primarily Non-Vegetated Aquatic or Regularly Flooded Area(s)
10	B28	Natural Waterbodies, Snow and Ice
<b>Cultivated and Managed Terrestrial Area(s)</b>		
11	A1	Tree Crops
12	A3	Herbaceous Crops
13	D1	Rainfed Cultivation
14	D3	Irrigated (General)
15	D8	Fallow System
16	S0302	Barley ( <i>Hordeum vulgare</i> L.)
17	S0311	Wheat ( <i>Triticum</i> spp.)
18	S0702	Fodder pulses
19	S1	Food Crops
<b>Natural And Semi-Natural Primarily Terrestrial Vegetation</b>		
20	A1	Woody Vegetation (Main Layer)
21	A14	Sparse (20-10) - 1% (Main Layer)
22	A2	Herbaceous Vegetation (Main Layer)
<b>Natural Waterbodies, Snow and Ice</b>		
23	A1	Inland Water
24	A4	(Flowing)
25	A5	(Standing)
26	V1	Fresh
27	V4	Very Saline

Fig. 5.40: LULC-classes that generated from the LCCS-software (version-2) for the Four Regions study area



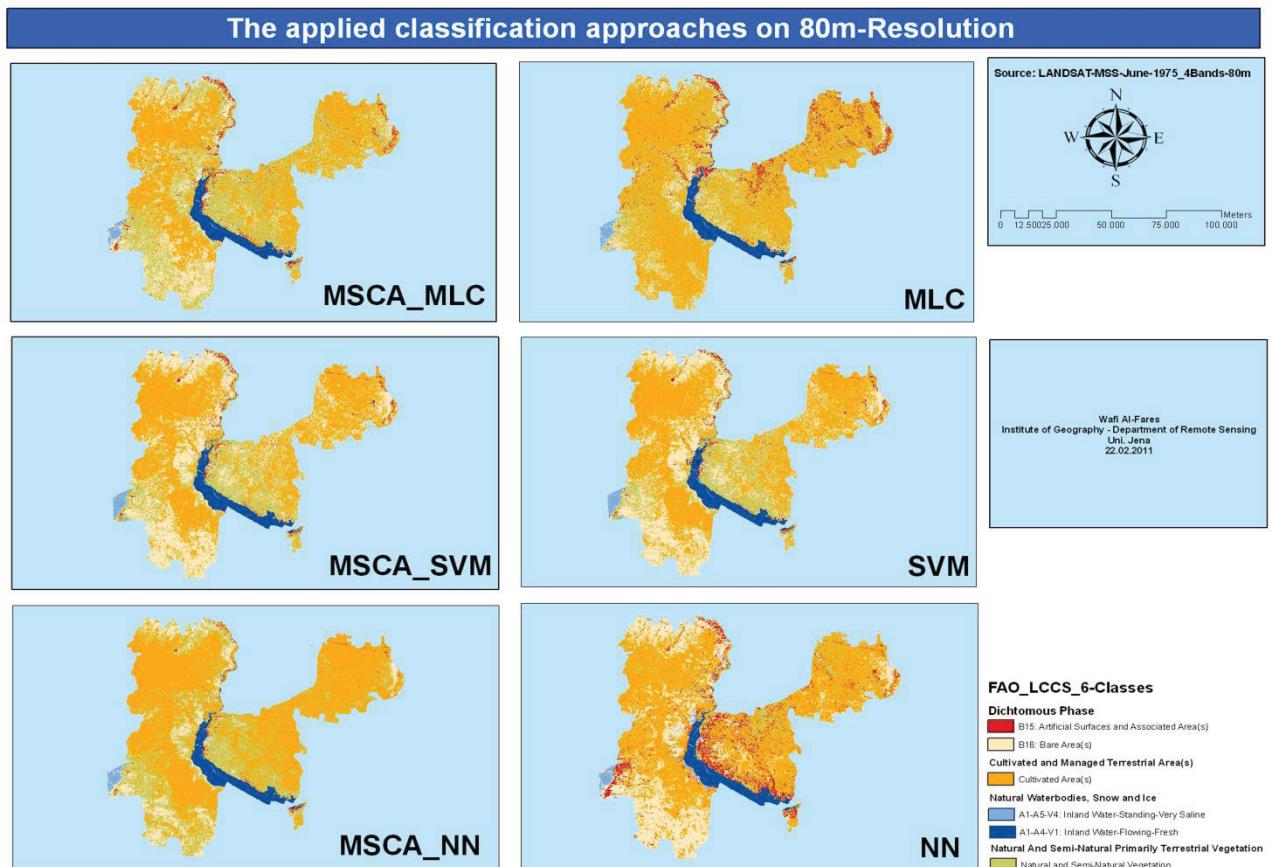


Fig. 5.41: The produced thematic maps from LANDSAT-MSS-data using various supervised classification approaches and algorithms for the testing area

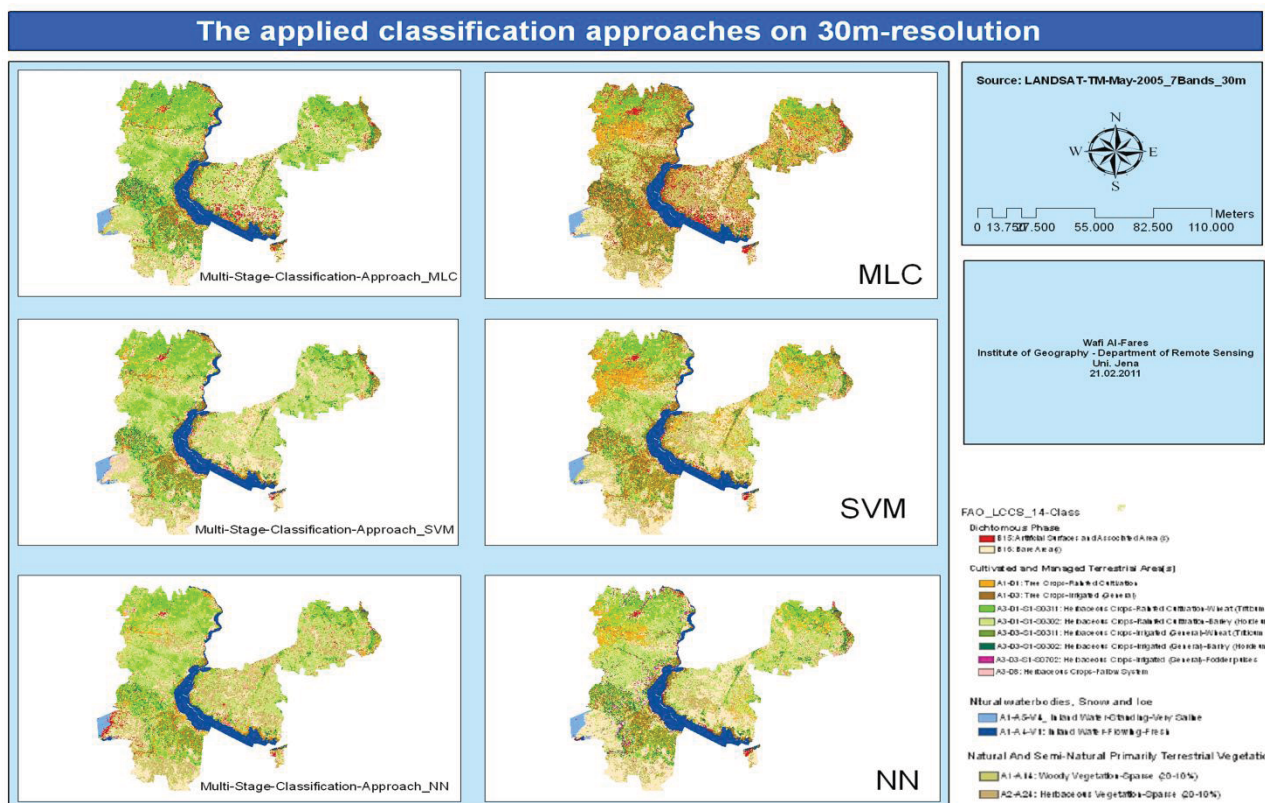


Fig. 5.42: The produced thematic maps from LANDSAT-TM-data using various supervised classification approaches and algorithms for the testing area

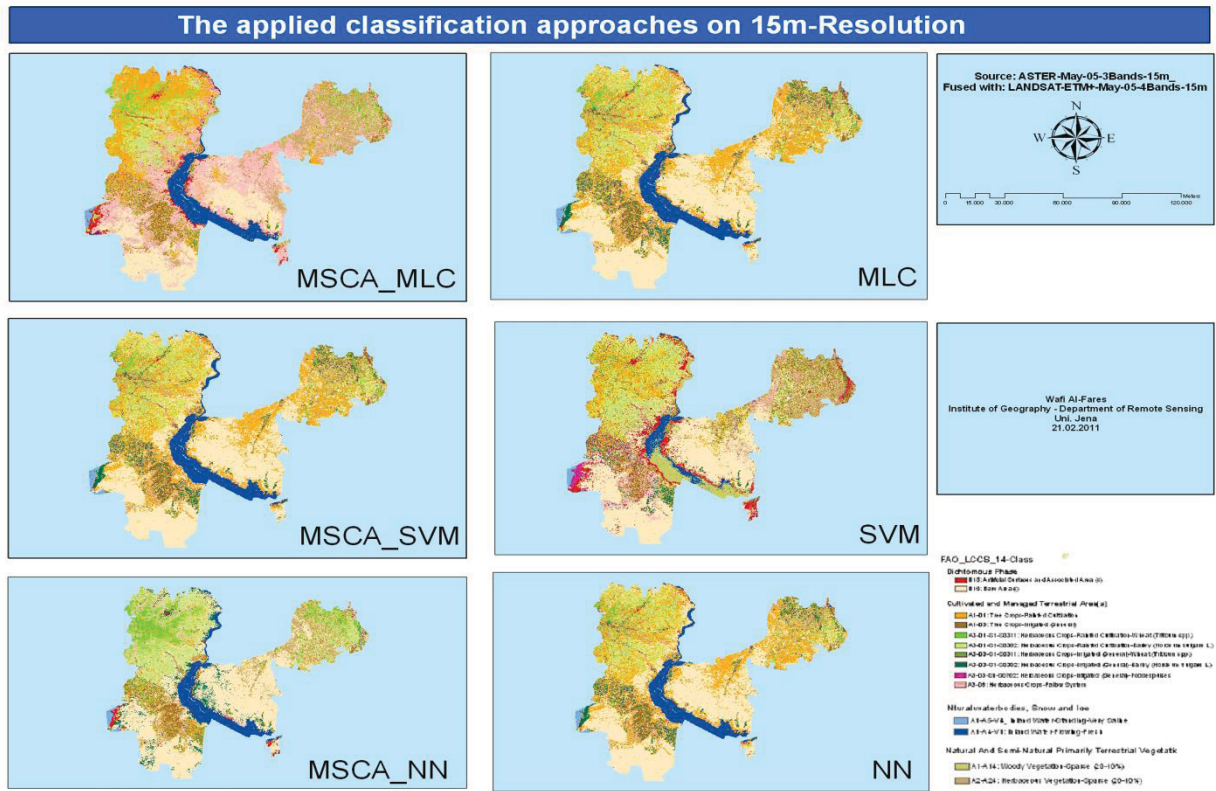


Fig. 5.43: The produced thematic maps from ASTER-data and LANDSAT-ETM+-data using various supervised classification approaches and algorithms for the testing area

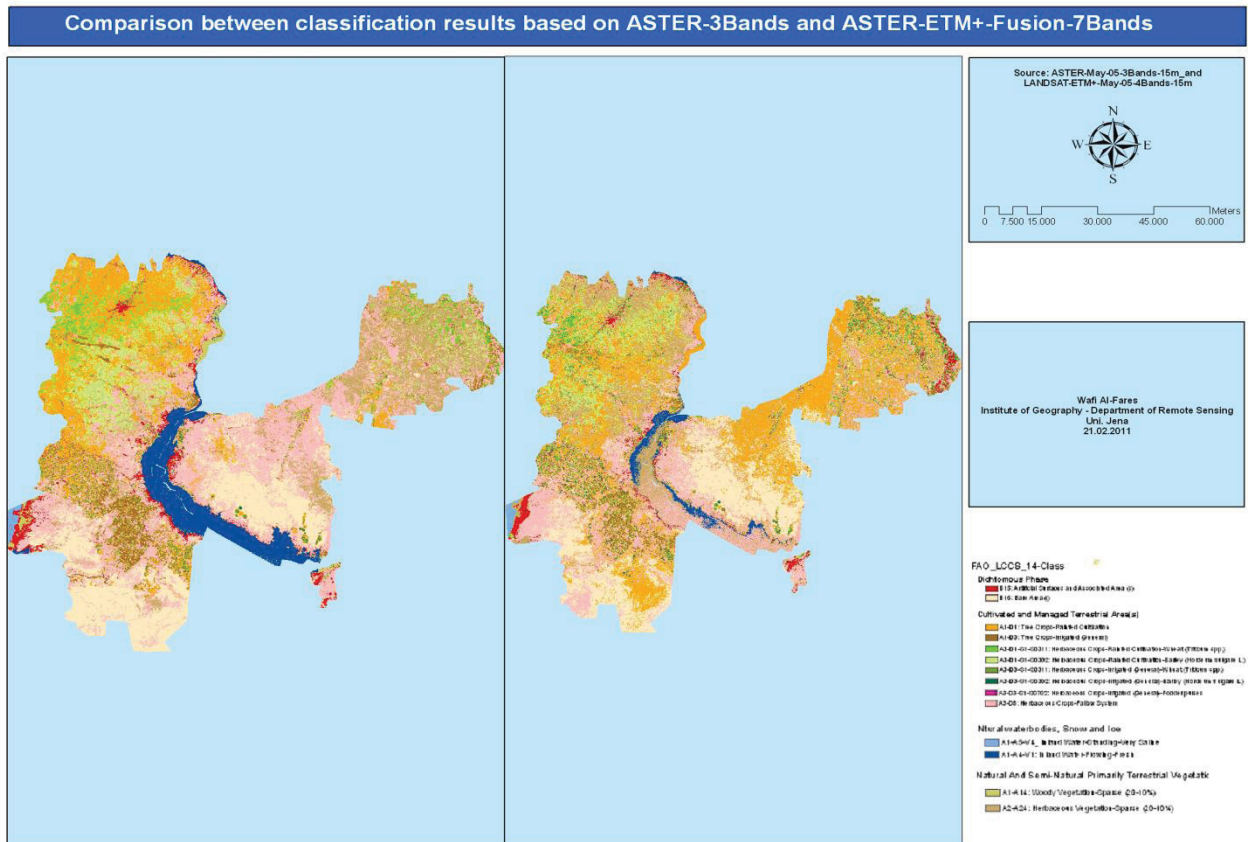


Fig. 5.44: The produced thematic map from ASTER-data with only the first three spectral bands (right), and the resulted map after fusing the previous three bands with the 4, 5, and 7 spectral bands of LANDSAT-ETM+-data (left) using various supervised classification approaches (here, one stage classification approach) and algorithms (here, MLC) for the testing area

An evaluation of the presented results was performed to define and confirm which classification approach and/or classification algorithm was optimized for the sub-study area and for the greater study area of the Euphrates River Basin. Two methods were used in the evaluation process. The first (Fig. 5.45) was qualitative rather than quantitative, more manual, and used non-remotely sensed data (human-based data) as truth-reference for measurement of the accuracy of the produced thematic maps results.

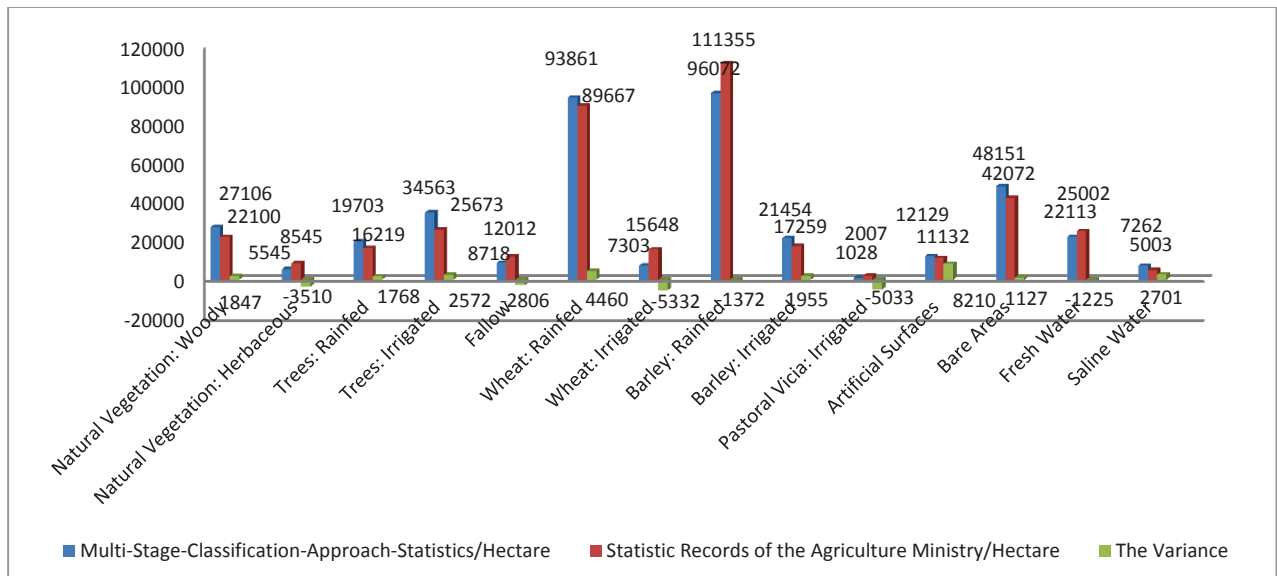


Fig. 5.45: The comparison between the areas of various LULC-classes that generated from the supervised classification of remotely sensed data with the statistical records in the Menbij Region in 2007

The second method (Table 5.6, Fig. 5.46) is quantitative, more automated, and used either non-remotely sensed data (e.g., GPS-measurements) or remotely sensed data as truth-reference/s, based on suitable founded mathematical equations (see C5.M).

This evaluation showed that: 1) the accuracy values range from 49.56 % to 99.02 %; 2) after comparison of each of the three used classification algorithms (MLC, NN, and SVM) with the three different spatial resolutions of remotely sensed data (ASTER-15 m, LANDSAT-TM-30 m, and LANDSAT-MSS-60 m) and various spectral resolution (ASTER-3-bands, TM-6-bands, and MSS-4-bands), for the 12 individual classification levels, it can be concluded that the MLC-algorithm had the highest accuracies in general, followed by SVM and finally, NN. Generally, the accuracy decreased horizontally with the reduction of the spatial resolution at almost each classification level, with the exception of ASTER-data at the more detailed levels. Although these data had the best spatial resolution, there was no corresponding increase in accuracy. Therefore, the higher spectral resolution by LANDSAT-data with coarser spatial resolution was more important than the higher spatial resolution by ASTER-data with coarser spectral resolution. In addition, accuracy decreased vertically with the increase in the information extracted at individual level; 3) after comparison of the final overall accuracy of classification using the multi stage classification approach and the MLC, NN and SVM algorithms (with accuracy values resulting from using one classification approach and the same three algorithms), it was evident that the first approach always showed a higher accuracy among the three classification algorithms. Also here, MLC harvested the higher accuracy in both approaches. The higher accuracy was found by using LANDSAT-MSS-data, while the offered classified classes were too little and wide than those generated from other used remote sensing data; and 4) therefore, the optimized results for the used remote sensing data, the classification approach and classification algorithm were found to be LANDSAT-TM-data (ASTER-data had insufficient spectral resolution, while LANDSAT-MSS-data had insuf-

efficient spatial resolution), the multi stage classification approach and the MLC-classification algorithm.

Table 5.6: The final resulted overall accuracy values of applying various classification approaches and algorithms on various remotely sensed data

	MLC ASTER-15m- May-05	MLC Landsat-TM- 30m- May-07	MLC Landsat-MSS- 60m- June-75	NN ASTER-15m- May-05	NN Landsat-TM- 30m- May-07	NN Landsat-MSS-60m- June-75	SVM ASTER-15m- May-05	SVM Landsat-TM- 30m-May-07	SVM Landsat-MSS-60m- June-75	Average/ Level- based
A/B:	99.02	98.73	92.85	98.58	97.73	91.25	98.92	97.41	93.52	96.44
A1/A2:	97.69	96.31	88.54	96.56	95.58	85.59	96.92	95.89	86.55	93.29
A11/A12:	95.56	94.08	80.21	92.56	90.98	79.55	90.69	87.36	77.56	87.61
A111/A112:	80.56	90.31	-	80.00	90.17	-	81.57	89.41	-	85.33
A1111/A1112:	78.21	89.81	-	76.54	88.44	-	77.66	89.96	-	83.37
A1121/A1122:	57.21	60.88	-	56.58	60.52	-	58.58	61.68	-	59.18
A11211/A11212/ A11213:	58.25	65.22	-	59.85	65.13	-	56.55	66.36	-	61.92
A11221/A11222/ A11223:	65.54	75.02	-	64.59	72.12	-	66.99	75.36	-	69.93
A121/A122:	50.59	57.32	-	49.56	50.36	-	54.55	55.52	-	52.98
B/A:	99.02	98.73	92.85	98.58	98.73	91.25	98.92	99.41	93.52	96.77
B1/B2:	96.69	95.32	89.54	95.56	94.58	85.96	95.92	95.62	87.55	92.92
B11/B12/B211/B 212:	92.69	95.72	90.51	90.31	94.45	88.24	91.54	96.86	92.28	92.45 73.27
Average/Algorithm- based/Multi Stage Classifica- tion Approach	80.91	84.81	89.08	79.96	83.21	86.97	76.18	84.17	88.49	83.75
One Stage Classification Approach	77.32	83.23	88.14	73.25	82.59	84.87	70.24	83.15	86.59	81.04

A: Primarily Vegetated Area(s)	B: Primarily Non-Vegetated Area(s)
<p>A1: Terrestrial Primarily Vegetated Terrestrial Areas</p> <p>A2: Aquatic or Regularly Flooded Areas</p> <p>A11: Cultivated and Managed Terrestrial Area(s)</p> <p>A12: Natural and Semi-Natural Terrestrial Vegetation</p> <p>A111: Trees</p> <p>A112: Herbaceous</p> <p>A1111: Rain-fed</p> <p>A1112: Irrigated</p> <p>A1121: Rain-fed</p> <p>A1122: Irrigated</p> <p>A11211: Fallow or shifting</p> <p>A11212: Crop (1)-wheat</p> <p>A11213: Crop (2)-barley</p> <p>A11221: Crop (1)-wheat</p> <p>A11222: Crop (2)-barley</p> <p>A11223: Crop (3)-pastoral vetch</p> <p>A121: Woody</p> <p>A122: Herbaceous</p>	<p>B1: Terrestrial Primarily Non-Vegetated Areas</p> <p>B2: Aquatic or Regularly Flooded Areas</p> <p>B11: Artificial Surfaces and Associated Areas</p> <p>B12: Bare Areas</p> <p>B211: Natural Water-bodies/Fresh Water</p> <p>B212: Natural Water-bodies/Salt</p>

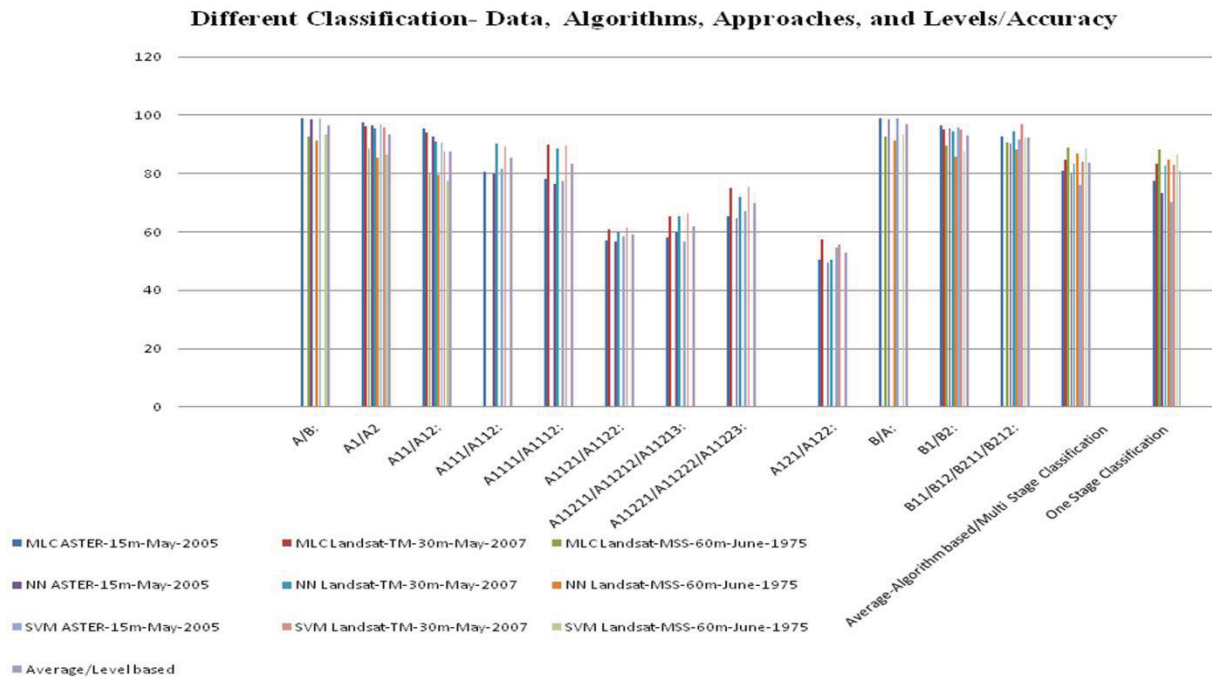


Fig. 5.46: Illustrate the accuracy assessment values presented in Table 5.6 visually

## H. General classes classification

Drought is one of the main characteristics of large areas of the ERB, since variation in lands and natural coverage is partially measured by average precipitation. Geological and geomorphologic characteristics and soil types change depending on the availability of water or the climatic risks affecting the area.

One of the more satisfying results of setting general classification controls representing the natural coverage and land uses of basin areas falling outside the borders of water agrarian projects, is the appearance of planted lands with trees in bare, uncultivated lands as shown in satellite images, particularly, in relatively dry areas with dominated light color soils. This may occur because of the ratio between dimensions of pixel in TM-30 m data, and the distance between planted trees within one field. In the region of Aleppo, pertaining to the widely spread Aleppo-pistachio and olive trees, the distance between every two trees is estimated with 8-10 m (Fig. 5.47), i.e., there will be an approximately 16 trees in each pixel of the TM-data. Because the greater portion of this plantation lies on light soil, and since remotely sensed data are insufficient and unqualified in spatial resolution, it is difficult to detect the distribution of these plantations. It is also complex to represent them through automated classification.



Fig. 5.47: The distances between the rain-fed olive trees in the study area (photo)

However, where there is water availability (prevalence of irrigation projects), all types of cultivations and even gardens appear clearly on the satellite images used in current study.

Time differentiation of termination of the agricultural crop rotation of rain-fed crops existed away from irrigation projects, compared to their counterparts included in irrigation projects. Consequently, it was necessary to have satellite image coverage to be compatible with the precise dates of the agrarian crop rotation of rain-fed crops in April.

The satellite images did not allow discrimination between barley and wheat fields, which were similar in relation to their spatial discrimination (the field areas of each crop) and spectral discrimination (there were no clear differences in spectral reflectance). These two major and strategic crops were planted widely in rain-fed areas based outside the borders of irrigation projects. Yet, the situation was different within the irrigation projects, as barley occupied few of the limited irrigated areas, but was commonly planted. This led to change in the agrarian crop rotation and its spectral behaviour, differentiating it from rain-fed wheat. This in turn led to the possibility of spectral separation between irrigated wheat and barley at the beginning of May, regarding the radio-metric field measurements that proved the possibility of separation (see C5.E.1).

The study area was divided into two almost equal sectors corresponding in the western part with the second, third and fourth agricultural stabilization zones. The eastern part matched the fifth agricultural stabilization zone, which included the pasture Al-Badia and the Syrian Desert. Each of these two general sectors corresponded with distinct areas concerning land use and natural coverage. Applied agrarian legislation was a factor, especially the total prevention of cultivation in the fifth agricultural stabilization zone. These two sectors were almost homogeneous in relation to spectral reflectance on this scale.

The general extracted and classified LULC-classes based on LCCS-scheme (see C5.C) were: Cultivated and managed terrestrial area(s); Natural and semi-natural terrestrial vegetation; Artificial surfaces and associated area(s); Bare area(s); and Natural water-bodies, snow, and ice.

The three period LANDSAT-imageries (MSS-June-1975, TM-May-1987 and TM-May-2007) and the one period ASTER-imagery (ASTER-May-2005 fused with the LANDSAT-ETM+/SLC-Off corrected/-May-2005-data) (see C4.A) were classified using the supervised classification technique MLC to generate the general LULC-classes of the first LCCS-classification scheme.

The concept used to produce the thematic maps of the general classes was divided into two ways: preprocessing steps and the mosaic-process (see C5.B). The classification process was carried out for all defined classes on the one mosaic-image that covered the whole spatial distribution of the study area. This mosaic-image was generated from more than one remote sensing image, in which the temporal, spatial, spectral and radio-metric characteristics of each image were deemed to be compatible with each other, or when it was possible to enhance and/or correct the distortion in these characteristics. The second method was performed when it was impossible to generate a correct and suitable mosaic-image with no, or an acceptable level of, distortion in the above referred characteristics, or when it was possible to generate a more suitable mosaic-image which gave more accuracy in classification. For example, the second method was performed on the LANDSAT-MSS-June-1975 data, where subsetting of each of the seven images using the ERB-borders-vector-file extracted from the SRTM-data was conducted (see C5.A) (Fig. 5.48). The classification procedures were performed for each subsetted image after which mosaicing was carried out on all the individual classification results to produce one final thematic map (Fig. 5.49). The procedures that were performed in the classification were: 1) Creation of the legend including the LULC-classes to be classified based on LCCS-scheme (see C5.C); 2) Selection of the training samples visually from the MSS-data itself; 3) Calculation of the separability values for the selected training samples (see C5.F); 4) Application of the MLC-algorithm that offered the best accuracies (see C5.G.2); and 5) Validation of the classification accuracy using the accuracy assessment methods (see C5.M).

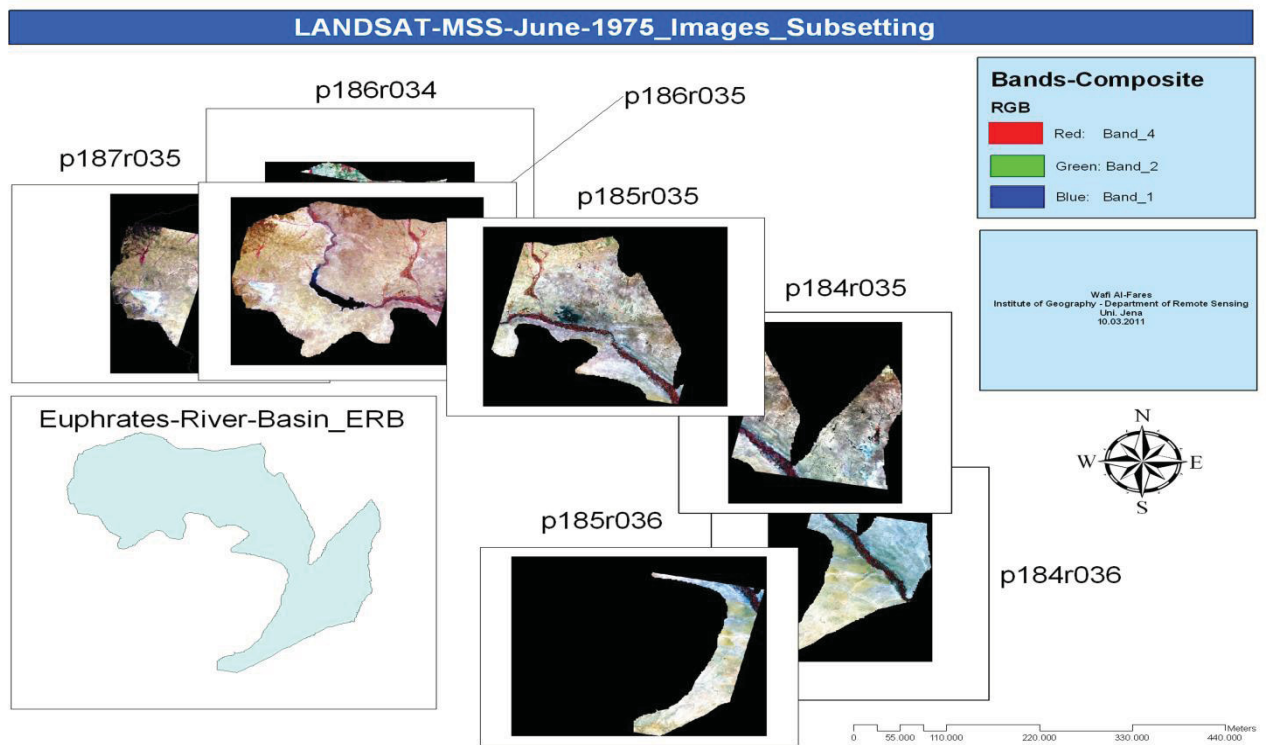


Fig. 5.48: LANDSAT-MSS-June-1975 imagery subsetting based on the spatial extent of the ERB in Syria

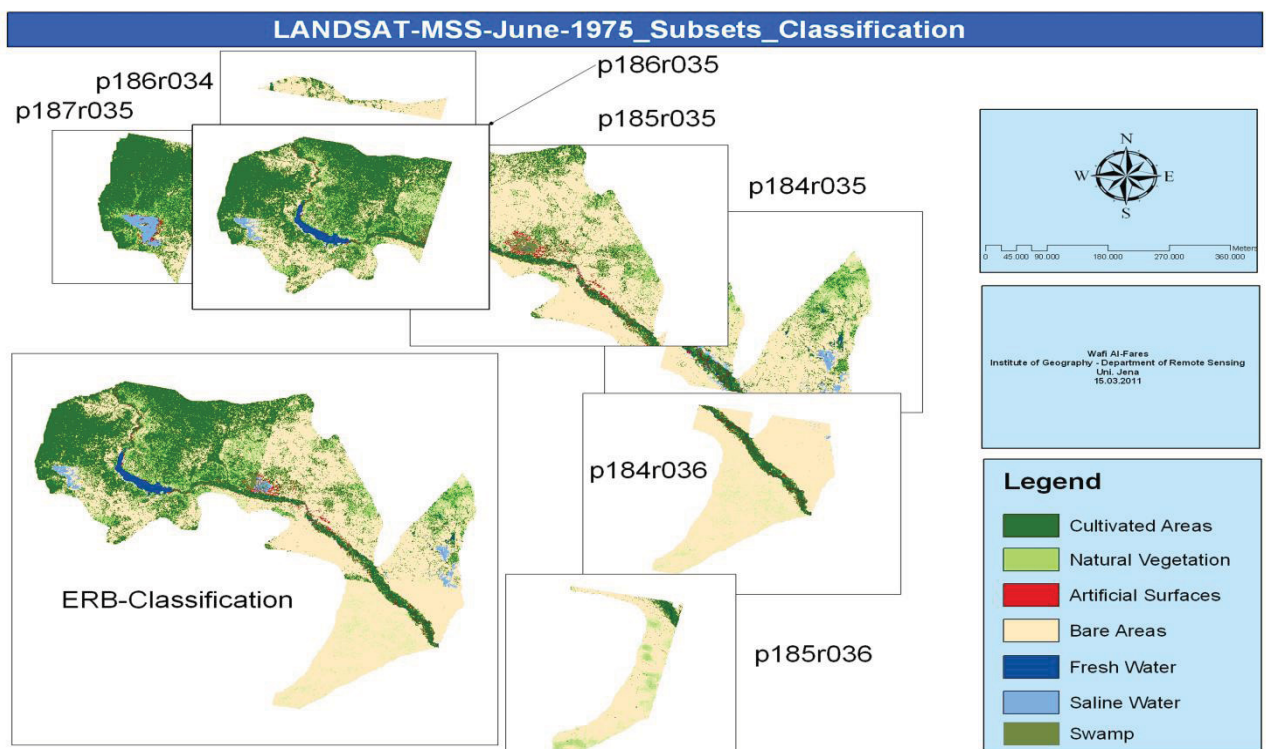


Fig. 5.49: LANDSAT-MSS-data-June-1975 classification results for each subsetting image and the mosaicing of all results in one thematic map

### I. Irrigated areas mapping

As shown in the information obtained from the Syrian Irrigation Ministry, the total reclaimed lands (irrigated areas) in the Euphrates River Basin in the period 1970-2007 comprised some 201,372 ha, distributed in the governorates of Aleppo(72,492 ha), Arraqa (102,512 ha) and Deir Azzour (26,367 ha).

However, the variation in the radiometric characteristics over the various imagery that were used to construct the final mosaic-images and the variation in the spectral, spatial and radiometric characteristics over the various multi-sensor datasets, added their own uncertainties to irrigated area estimates (FAO, 2005).

This section describes the methodology used to locate irrigated areas within the national administrative units in the Euphrates River Basin. Irrigation maps were derived from remotely sensed data (LANDSAT-MSS-June-1975, LANDSAT-TM-May-1987 and 2007, and TERRA-ASTER-May-2005), and from the very detailed schemes of each irrigation project that were obtained from the Syrian Ministry of Irrigation and IGDEP. These schemes represent clearly each project's formative spatial distribution, but with no geographical reference. These schemes were linked with the remotely sensed data available using a hard visual interpretation. The information was also digitized to locate the detailed schemes on the various existed remote sensing data in order to extract the boundaries of the irrigation projects. After the maps were on-screen digitized, the borders of the irrigated areas were evaluated using satellite imagery in many areas. The both shape and size of the digitized areas were followed by an adjusting process where necessary. Finally, it was helpful to use publications such as project reports and the frequently published statistics about the development in the irrigation areas and the agricultural plan over the time.

In general, the following steps were adopted: 1) generation of a vector-file that defined the spatial distribution of the ERB-borders; 2) the register of national irrigation statistics for the ERB in Syria; 3) geospatial information (detailed schemes and various remotely sensed data) used to locate irrigated project areas within the ERB-borders; 4) the production of a detailed vector-based digital map of irrigated project areas in the ERB (Fig. 5.50), to be used as a spatial indicator in combination with the remote sensing data during the agricultural classification within these projects; and 5) fusion of the digital maps of the irrigated areas in the ERB for the years 1975, 1987, 2005 and 2007.

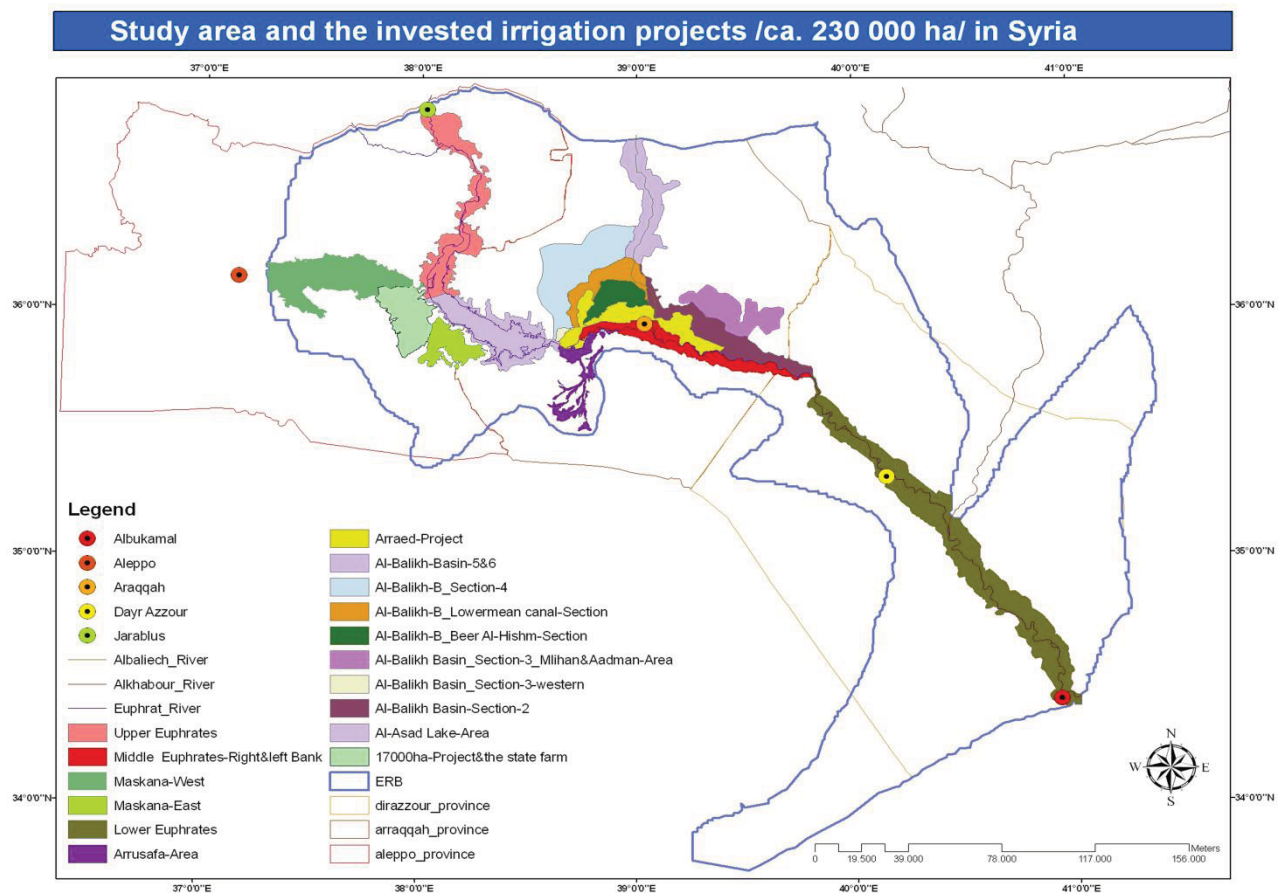


Fig. 5.50: The spatial distribution of the 16-projects in ERB (about 230,000 ha) that generated from the detailed irrigation projects-schemes and the remotely sensed data (as vector-file)



Three methods in mapping the irrigated areas were followed. The first method (Fig. 5.51) was based on the previous general classes classification results (see C5.H), where the class (cultivated areas) represented the irrigated areas, which were actually the agricultural areas (planted and fallow). Then, the irrigated areas vector-file was used to subset and extracts the actual irrigated agriculture within the projects from the ERB-borders. Here, the classification accuracy was equal to the gaining general classes accuracy, which was generally high for wide categories classification. The second method combined the transformed NDVI-values to vector-file (as mask). The drawback here was that NDVI can only detect the planted areas and not the fallow-fields. To overcome this problem, the two major agricultural seasons of winter and summer needed to be classified, where, for example, the non-planted fields during winter would be almost completed planted in summer, especially in areas with an abundance of water. Then, the two winter and summer classification results were added into one thematic map that represented the actual irrigated areas over an individual year. The third method involved the analysis of each of the 16-projects alone. This was more significant for crop classification within the irrigated areas, especially when insufficient truth-references existed. To this end, the use of statistical information was helpful. This method is presented in the next section.

The next task was to define the spatial distribution areas of irrigated agricultural projects within the natural borders of the ERB in the study's reference time period of 1975, 1987, 2005 and 2007 by calculating the values of NDVI and making a mask that covered the spatial prevalence of the projects' areas. This mask was the study area for classification of the irrigated winter and summer crops during the previously mentioned time durations except for in 1975. The remotely sensed data (LANDSAT-MSS) available in that year had a low spatial resolution of 60 m, and for this reason, it was impossible to produce detailed maps of land uses, specifically in those areas included under wide classes (e.g., both wheat and barley are detailed classes that lie under the heading "wide general class", namely, the agrarian lands).

The total cultivated area of the Arraed project was c. 21,000 ha. However, due to bad land reclamation procedures, salinization had resulted in large areas of the project lands. In 2005, the arable land mass was only 2,433 ha.

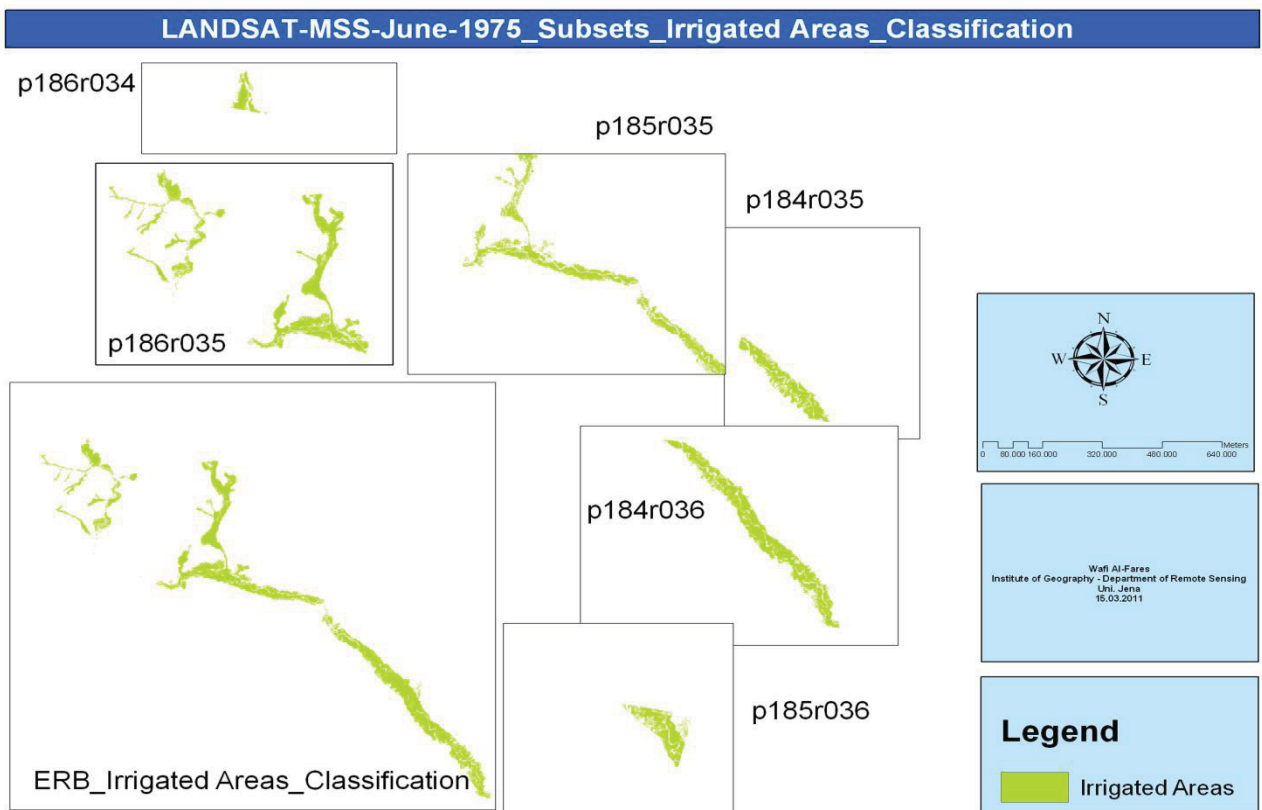


Fig. 5.51: Irrigation mapping in the ERB based on the traditional supervised classification approach (the first method)

## J. Crops classification

Classification of agricultural crops using remote sensing data requires in general, knowledge about crop phenology, climate of the exacting growing season and ground reference information about specific agricultural practices in the drainage basin.

"The development of a regional-scale crop mapping methodology is challenging because it requires remotely sensed data that have large geographic coverage, high temporal resolution, adequate spatial resolution relative to the typical field size, and minimal cost" (Wardlow & Egbert, 2008). Remotely sensed data from customary sources such as the LANDSAT (TM and ETM+) and (AVHRR) proved the usefulness for the classification of LULC-features (Wardlow & Egbert, 2008).

Supervised classification is the most frequently used classification method in agricultural areas (Van Niel & McVicar, 2000).

MSS data are used to set maps concerning the expansion of the agricultural lands and to distinguish them from constructional lands, for example. However, one drawback is that these data are unable to set thematic maps which view the more detailed crops' expansion. Of course, there are always exceptions; for instance, the agricultural cultivated fields planted with different crops are to some extent considered wide spaces, which enables the MSS-data to distinguish them. Yet, this condition was not verified in the ERB, which was characterized by having small agricultural fields, especially those located outside of the borders of the governmental irrigated agrarian projects. These areas were also organized following the agricultural crop rotation policy.

In the third part of this study, carefully timed remotely sensed data were used to map the location and extent of irrigated winter and summer crops for the years 1987, 2005 and 2007.

The commonly implemented crop classification approaches included: unsupervised classification; supervised classification; and decision tree classifier. In the cases where there was less information for a study area, only the characteristics of the image (also, statistical records and the detailed schemes, especially for 1987) were used.

The adopted concept (Fig. 5.52) in agriculture classification was based on the results of the previous two sections (C5.H and C5.I). The first step was to define the classes to be classified, based on the statistical records for the study year/s with no/or insufficient truth-data (e.g., 1987-data). This was followed by selection of the winter related data (Fig. 5.53), and subsetting to remove margin distortions, and to extract only the ERB spatial related areas. The time series of remotely sensed data were first used to generate a LULC-map of the whole ERB-area based on the LCCS-scheme (see C5.H). This process involved the use of one mosaic-image or each individual image, which was then mosaicked into one thematic-mosaic-map. The classification method was based on a MLC-supervised algorithm. The resulting classification had five general classes. The important general class which was used as the basis in irrigated agriculture classification was: cultivated areas: cropped and fallow. Using the derived vector-file which located the detailed spatial distribution of each project, sub-setting was conducted and the cultivated areas which existed only within the irrigation-projects and not within the whole ERB were extracted. Finally, using the unsupervised classification approach as an indicator for additional information about the spectral characteristics of the area, training samples were collected for some general classes (e.g., water), followed with the tested MLC supervised classification approach (see C5.G) to generate the final thematic map of the major winter crops of interest (wheat, barley, and sugar beet), in addition to fallow, which is classified in both seasons.

Trees and shrubs could be classified from either winter remotely sensed data or from data acquired in summer. This information was then combined and a mask constructed that included all the winter-data-based classified LULC-areas which could be planted during the summer-season (fallow, wheat, barley, and other crops). The other classified areas which were almost impossible to be changed during the summer-season of the same year (e.g., trees, permanent crops, etc.) were excluded. Finally, the previously built mask was applied to the summer-related remote sensing data

(Fig. 5.54) for classification of the summer crops of interest (cotton, and corn), in addition to fallow. Before the completion of this task, it was necessary to perform an accuracy assessment for all the produced classification results.

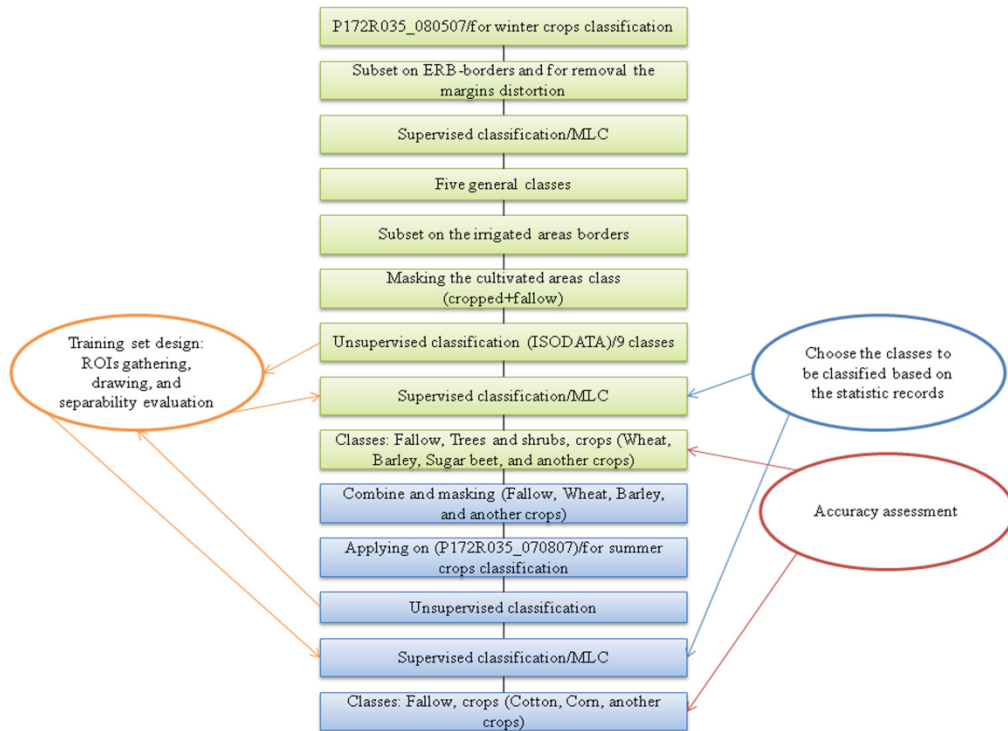


Fig. 5.52: The general concept-steps adapted to classify the various agricultural classes, especially the major strategic winter and summer crops

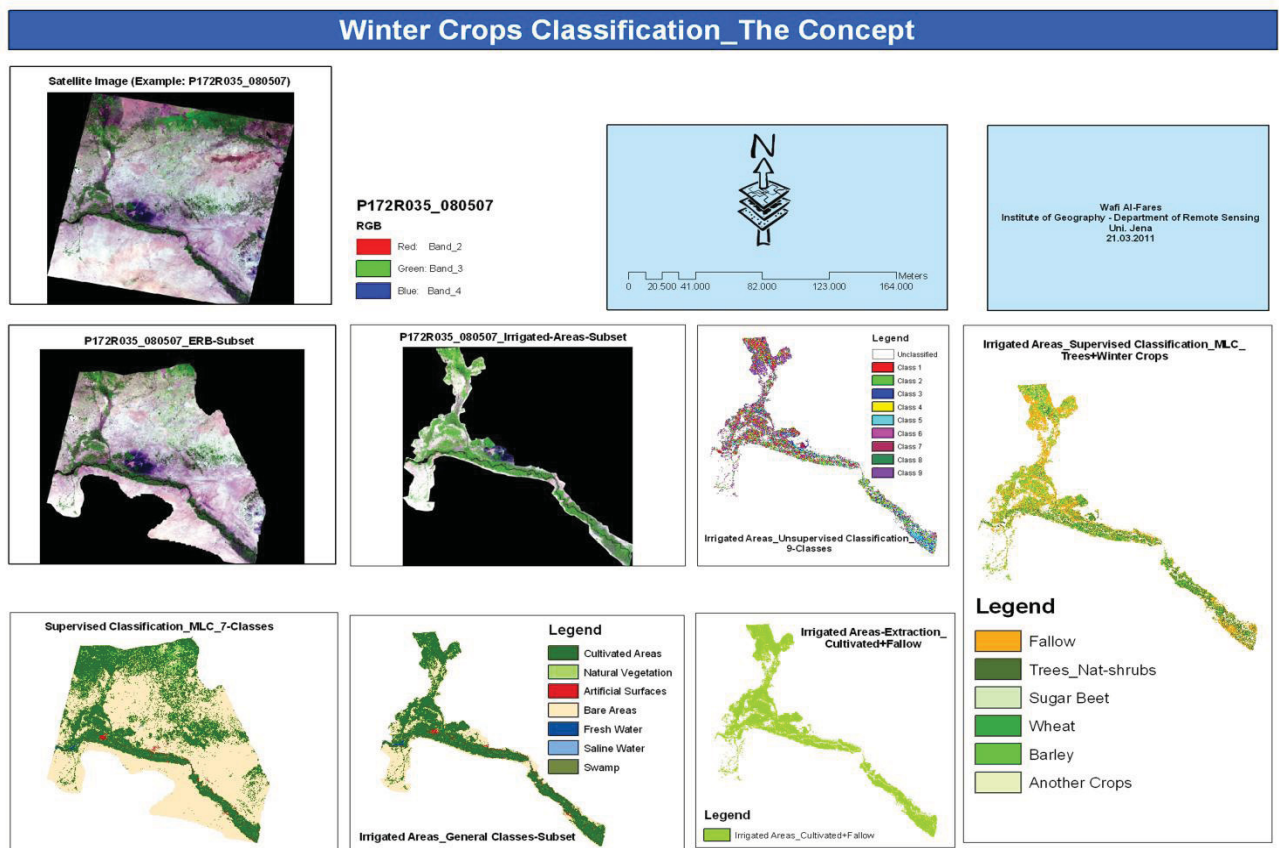


Fig. 5.53: The followed concept to classify the major winter crops based on both the previous general classes classification and the generated spatial distribution of the irrigated areas

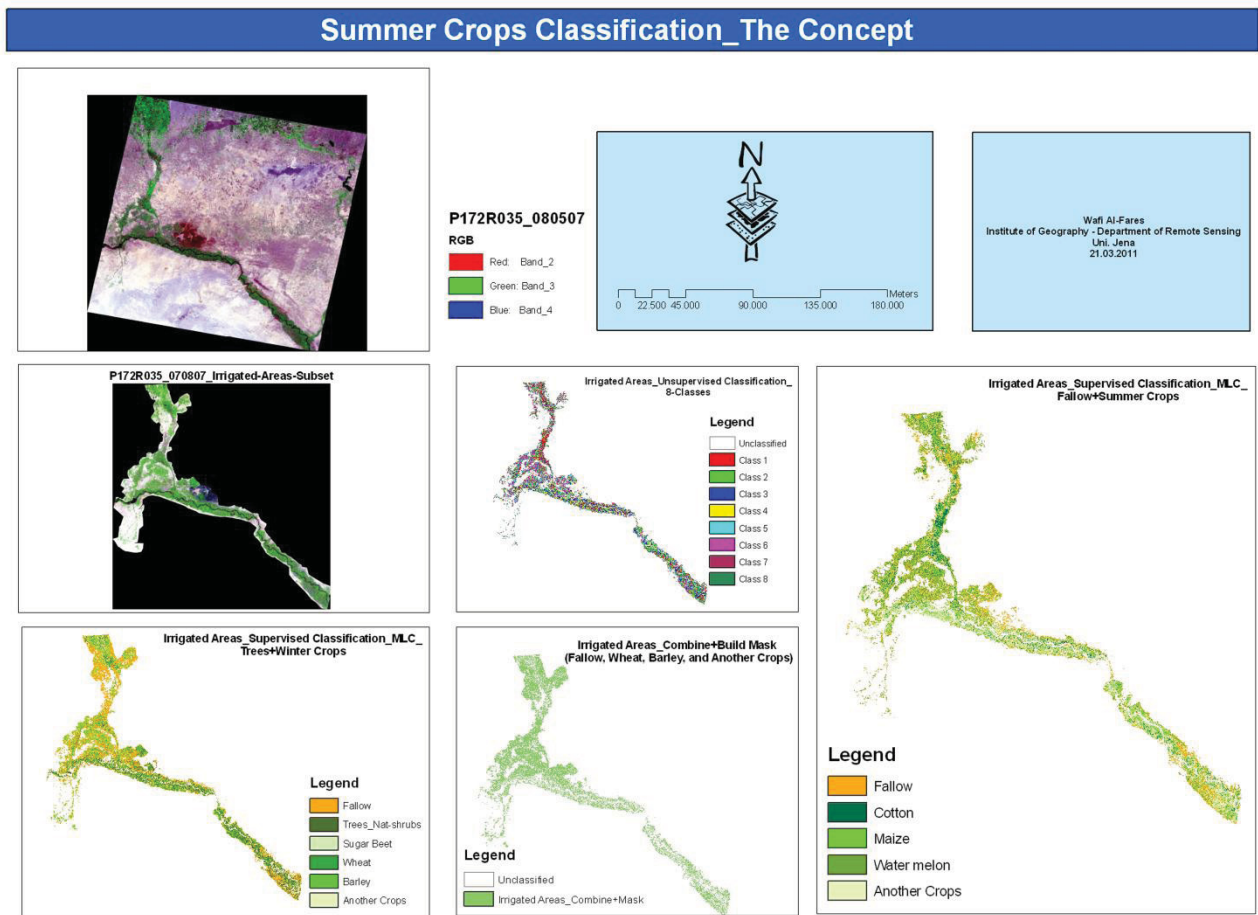


Fig. 5.54: The followed concept to classify the major summer crops based on both the previous winter crops classification and the generated spatial distribution of the irrigated areas

The other method that was adopted to classify the irrigation areas (especially the state projects) and the various permanent, winter, and summer agriculture-categories, was to integrate the remotely sensed data with the non-remotely sensed data (e.g., statistical records and detailed schemes), especially for the LANDSAT-TM-May and August-1987 data. This is explained in the next section.

The most important point involved in these projects was the engineering organization and division of each project into several farms with names and known geographical sites. The cultivated fields were large enough to be easily distinguished by available remotely sensed data. In addition, the geographical distribution of those fields had well known coordinates and detailed charts, and schematics were available for each project with large drawing scales. Because of this, I was able to become familiar with every irrigation project included in the basin and its spatial prevalence on the satellite images. Consequently, I was able to integrate the spatial distribution with the available statistic numbers of each project in several time-durations. This was also compatible with the remotely sensed data about the study area in my possession. These links enabled me to select the training samples used in the supervised classification process and to use them in assessment of the accuracy of the classification. This was, of course, in addition to the remaining referential data previously mentioned.

As for the other basin areas located outside the borders of the irrigation projects, since the required classification level is general and not detailed, it was decided it would be sufficient to count on the remotely sensed data in addition to the thematic, topographic and Google Earth maps and during the selecting process of the training-samples.

Here the problem is that full statistics concerning agrarian activities and types/classes of plantations were available, but only at a governmental and governorates level. This meant that the data did not provide information about what had been previously cultivated. The other problem was that many fields were not planted every year with the same crop. Detailed information about which specific crops had been planted in the training-samples was required. This level of detail was possible for the State-run irrigation projects in the “Organization of Development of the Euphrates Basin”, which has three branches - the Upper-Euphrates in Aleppo, the Mid-Euphrates in Arraqqah and the Lower-Euphrates in Deir Azzour. These areas were well managed, and a detailed agricultural statistics procedure was developed for every project.

One example of a training sample is a 17,000 ha project, which is integrated with a state farm (4,000 ha). Thus, the total area is 21,000 ha. Located within the Upper-Euphrates Basin in Aleppo governorate, the reclamation of the project began in 1979. The land is irrigated by pumping water from Lake Al-Asad.

The temporal developments in the extension of this project were as followed: In 1979 (3,031 ha), 1980 (4,762 ha), 1981 (9,634 ha), 1982 (15,103 ha), 1990 (16,703 ha), 1991 (17,513 ha), 1992 (19,703 ha), 1993 (20,903 ha), and in 2005 (21,325 ha) with 100 % of the irrigation plan.

The first step was to integrate the construction scheme with the remotely sensed data to extract the spatial distribution of the project of interest (Fig. 5.55). This was complicated by the fact the area had no ground truth reference.

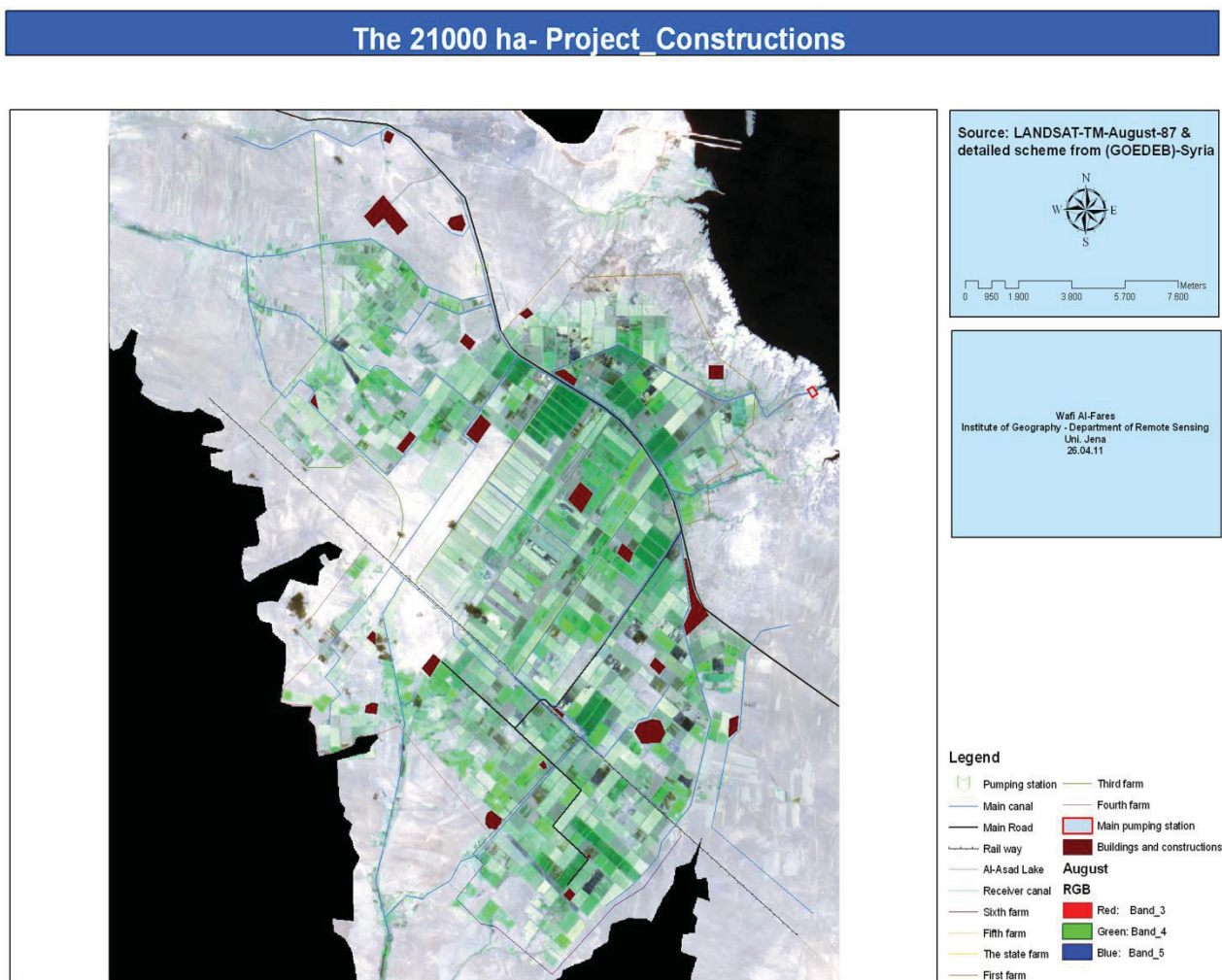


Fig. 5.55: The integration of the remotely sensed data with the construction scheme of the 21,000 ha project

The second step was to define what ratio of agricultural crops existed. This was generated from non-remotely sensed/human-based collected data (Table 5.7).

Table 5.7: The statistical information about each farm of the 21,000 ha project for 1987 (Source: Adapted from: GOEDEB, 1987)

The Farms	State Farm 2937 ha	First Farm 2040 ha	Third Farm 3557 ha	Fourth Farm 2753 ha	Fifth Farm 3293 ha	Sixth Farm 2320 ha	Total/ha
<b>The Crops</b>							<b>1987</b>
<b>Winter</b>							10,146
Wheat	707	562	943	782	974	1073	5,041
Sugar beet	300	130	174	234	231	150	1,219
Barley/Irrigated				127			127
Barley/Rain-fed	965	340	1061	496	463	302	3,618
Vicia beans	53			78	10		141
<b>Fallow</b>							5,359
<b>Summer</b>							3,052
Cotton	400	483	393	401	451	266	2,394
Maize	74	105	155	46	119	159	658
<b>Fallow</b>							12,453
<b>Permanent crops</b>							1,572
Fruit trees	109	53			112		274
Poplar	156	172			203		708
Alfalfa	189	98	42	73	95	93	590

The third step (Fig. 5.56) was to extract the smallest unit/farm in the 21,000 ha project to make the reorganization process of various agricultural features easier. Then, the various record-times/coverages were used in a visual interpretation process to recognize various agricultural features and to define the training samples that represent these features in a supervised classification approach. For example, it was possible to recognize agricultural features such as trees, alfalfa and sugar beet using multi-date remote sensing data and visual interpretation. Based on the agricultural calendar, trees fields appeared as planted areas over the three datasets (May, June and August); alfalfa fields appeared as green areas over the four datasets (April, May, June and August); and sugar beet fields appeared in April data as diverse planted areas in comparison to wheat and barley fields. The June data showed the area was still planted in comparison to other winter crops, especially those that had similar spectral response, such as wheat and barley. These three various appearances of the wheat at first degree and the barley in the June data, confirmed the selection for the training samples from the May data. The region also contained many dairy farms nestled among the irrigation projects with known geographical locations. These farms were planted only with barley, and provided a useful basis for training sites. Circular-irrigation fields also provided a useful source of reference, as the agricultural fields appear in a circle-shape. These fields were planted almost entirely in wheat. To this end, the visual interpretation and unsupervised classification results were able to be compared with the statistical numbers, which provided a background about each farm's planted crop. After all the representative training samples for each agriculture-category (permanent, winter, and summer) were collected, the supervised classification was conducted under the vegetation-mask generated from NDVI-values.

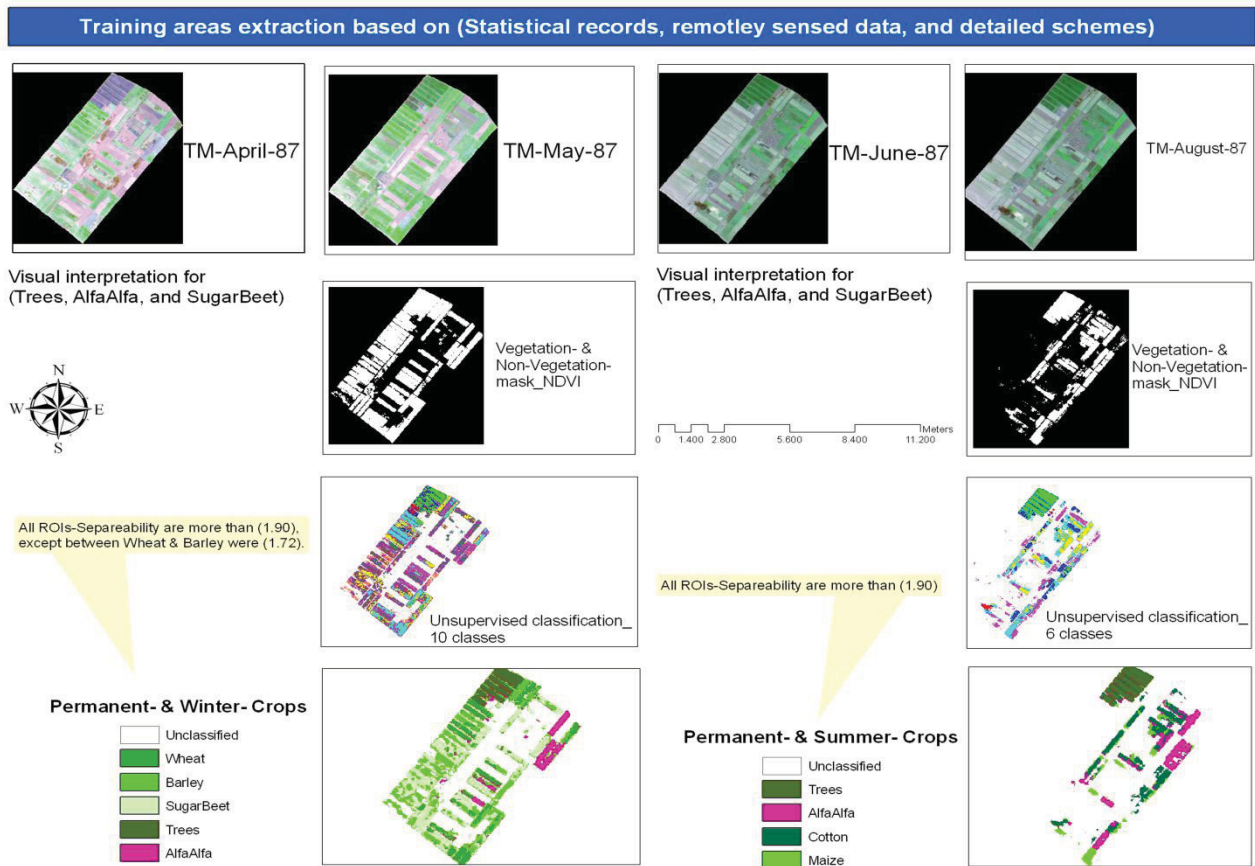


Fig. 5.56: The followed concept to collect training samples for the area/s with no truth-data or with insufficient reference data (the state farm)

This resulted in the collection of several training samples within the irrigation agricultural land projects, which represented the majority of variations in the LULC-categories, especially the agriculture class. Some of training-samples were used in the automated classification process, whereas others were used to evaluate the accuracy of these classifications.

At this point, a query arose over what requirement was needed to link statistical records with spatial records concerning the irrigation projects. This was needed for the training-samples representing the land uses which would be used later in automated classification, despite the availability of other referential GPS-points. There were three reasons for this. Firstly, the GPS-points did not totally cover all the study sites. Points of ICARDA-1987 were all located within Aleppo governorate, but no points existed in the Arraqa and Deir Azzour governorates. The GORS-points for 2005 were all located within Deir Azzour. The only points distributed over the three governorates were those taken in 2007. Secondly, because of the relatively large extension of the study area which lies within various natural regions (climatic: rains, temperature, humidity and soil), there was too much variation in the cultivations and plants along the basin. For instance, points of ICARDA-1987 did not represent poplar tree farms which existed only within the irrigation agriculture projects area in the Arraqa governorate (Al-Asad institution project). Thirdly, the variation in the method of collecting the GPS-points and the training-samples proved of issue, as well as the potential error in measurements of the GPS, relating to technical reasons. It is hypothesized that if one of the points measured a wheat field which neighbored a field of barley, then if the GPS-device was inaccurate enough or the satellite image that received the point was not correctly referenced, then the point may be shown as lying within the closely bordered barley field. Consequently, mistakes could occur in the classification process.

After the collection of sufficient training samples for the existing various LULC-features from the state farm, the entire 21,000 ha project was generalized via the supervised classification method

(Fig. 5.57). Here, the multi stage classification approach was followed with various created masks. At first, both the unsupervised and supervised classification approaches were used to classify the five general classes (see C5.H). Then, the approaches were combined into two more general classes, namely, uncultivated areas and cultivated areas. The subset “cultivated areas” represented the actual planted fields and the fallow and/or drilled lands, and displayed the irrigated area in project-scale. A mask was then created to represent the spatial distribution of this cultivated areas class, and to eliminate the uncultivated areas and their negative spectral influence on the other features of interest. It also reduced the computer processing-time of the data (although the user-data-interaction time was increased because of the greater number of processing-steps). After applying the masking-process and the supervised classification, the three classes were obtained (trees, herbaceous and fallow). The tree class was extracted from the next classification steps. Two masks were then built; the first for the herbaceous class and the second for herbaceous and fallow areas. Under the first mask, a supervised classification was carried out to obtain the permanent and winter crops classification results (alfalfa, wheat, barley, sugar beet and other crops). The second mask for herbaceous and fallow areas, where some of herbaceous areas would be replanted in summer season (e.g., corn after barley), produced the thematic map of summer crops (cotton, corn and other crops) using summer remote sensing data for August.

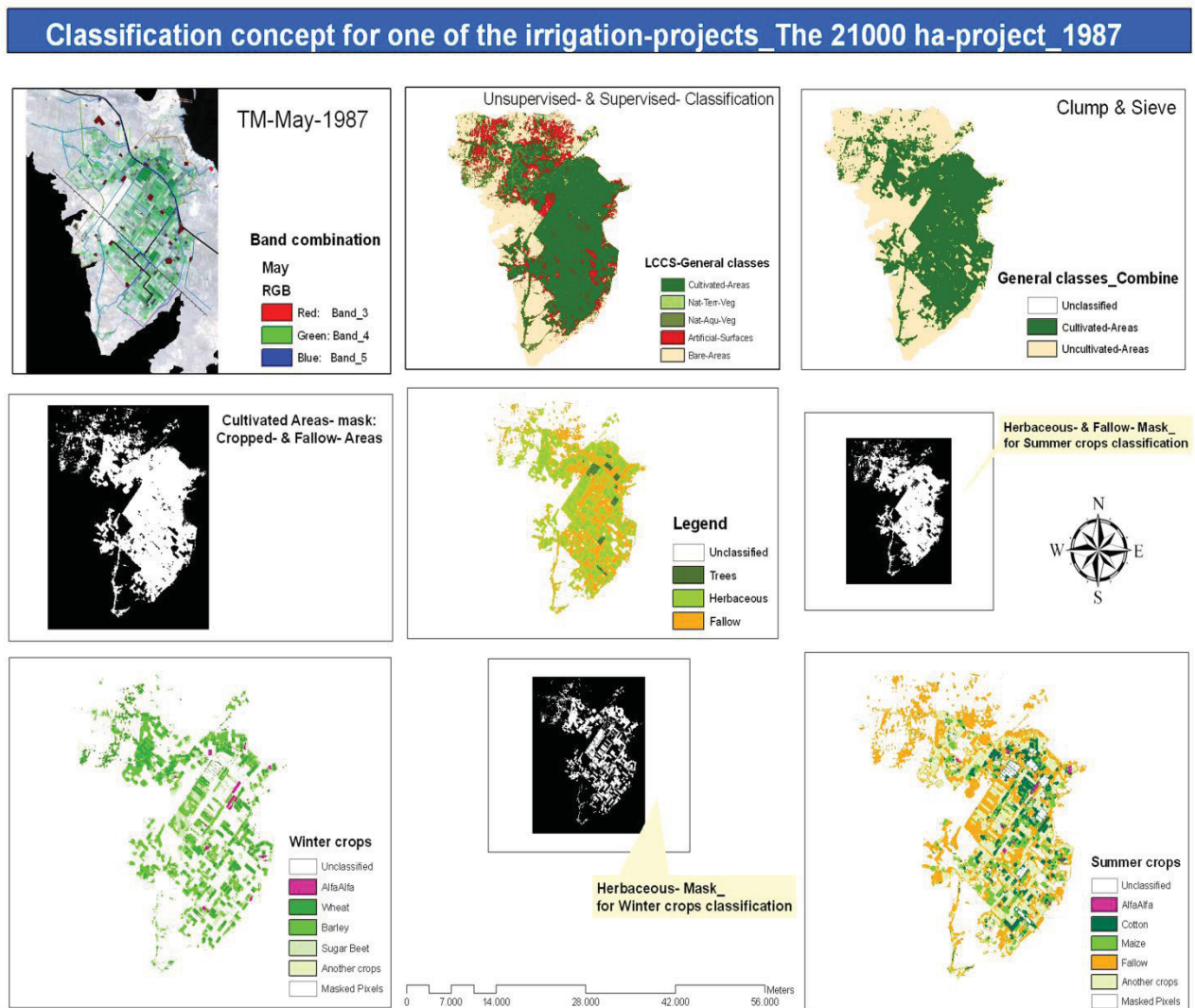


Fig. 5.57: The general classes classification, irrigation mapping, and agriculture classification methods that were performed based on the spatial extent of each irrigation project



The concept in classification adopted above was applied for other study years (Fig. 5.58) to obtain historical remote sensing based statistical numbers (Table 5.8).

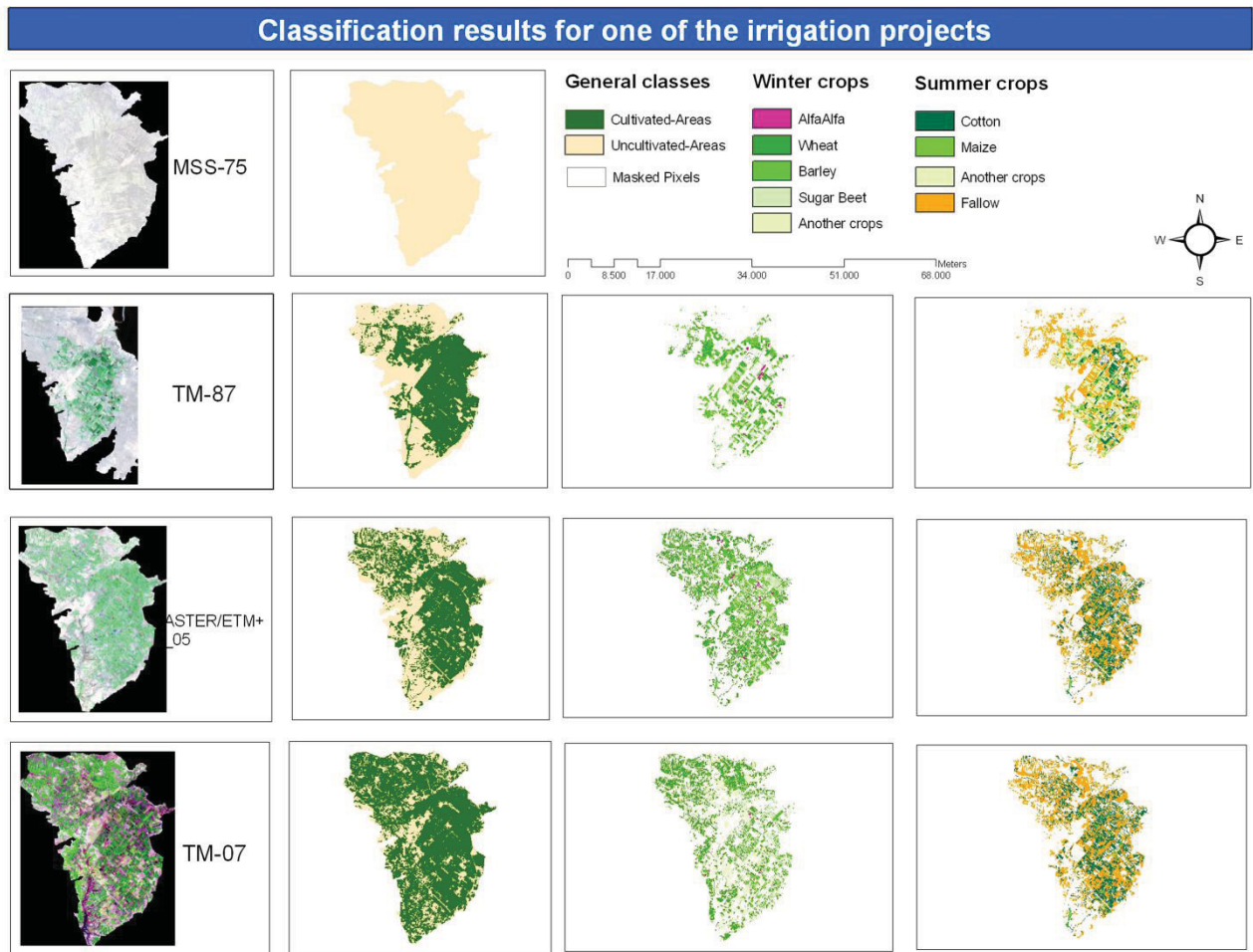


Figure 5.58: The general classes classification, irrigation mapping, and agriculture classification results that were produced based on the spatial extent of each irrigation project

Table 5.8: The remotely sensed data classification based statistical results for the 21,000 ha irrigation project for 1975, 1987, 2005 and 2007

The 21,000 ha- Project _ All Classes	1975	1987	2005	2007
<b>Cultivated Areas</b>		23,834	25,806	34,792
* Trees+Shrubs		648	872	58
* Herbaceous (Winter crops)		12,561	22,377	23,366
AlfaAlfa		275	459	198
Wheat		3,669	11,693	10,560
Barley		5,305	4,150	1,211
Sugar beet		3,454	6,075	2,359
Other crops		62	200	9,038
* Fallow		10,927	2,796	11,970
* Herbaceous (Summer crops)		50,499	24,272	13,303
Cotton		2,950	8,412	2,284
Corn		2,099	463	650
Other crops		8,143	127	10,369
* Fallow		10,063	15,270	22,277
<b>Water</b>	0	0	0	0
<b>Uncultivated Areas</b>	46,324	22,494	20,501	11,489

Finally, all the previously adapted steps and methods were applied and data was added for the other 15 projects to the thematic map/s for the 21,000 ha project (Fig. 5.59).

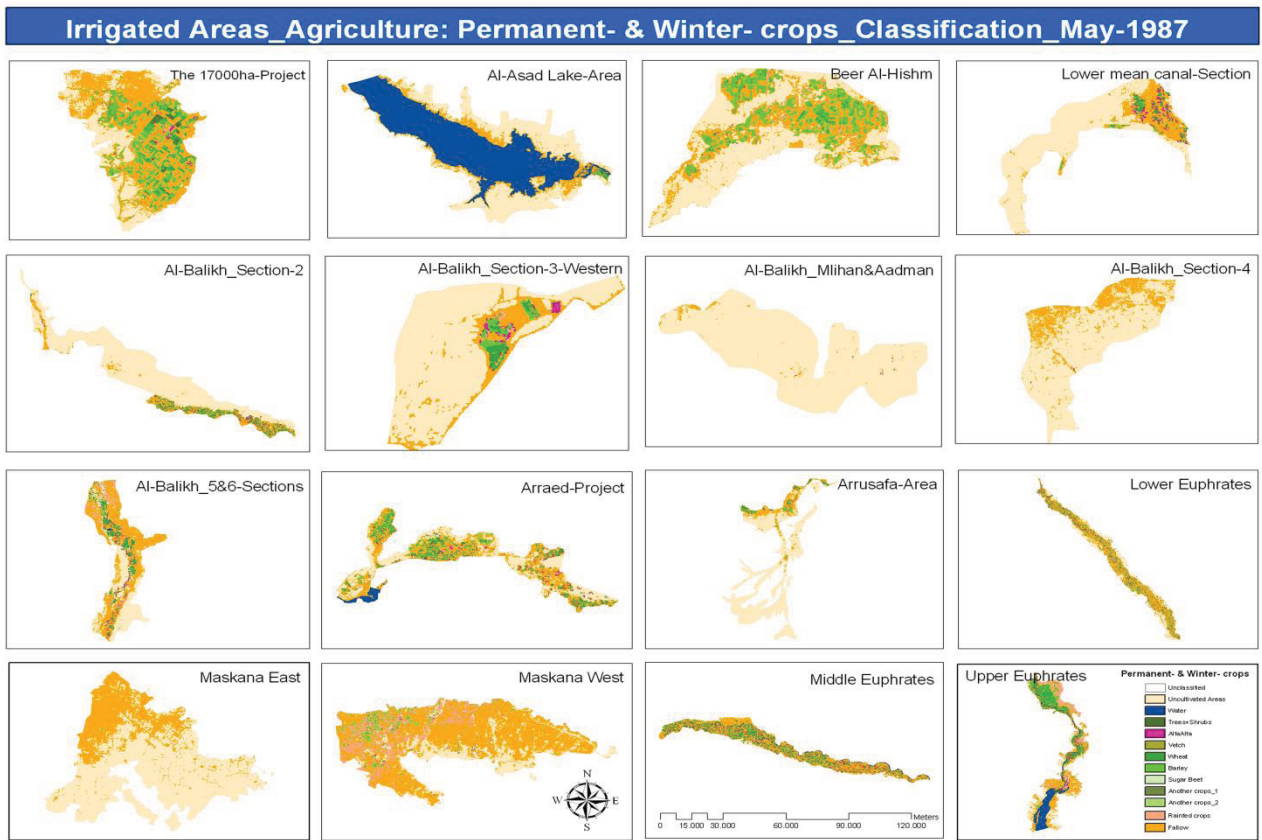


Figure 5.59: Illustration of the individual 16-project-based classification results (permanent and winter crops classification results for 1987)

## K. Post-classification processing

Many researchers have argued that post-classification processing is a vital step to improve the results of classification (Harris & Ventura, 1995; Murai & Omatu, 1997; Stefanov et al., 2001; Lu & Weng, 2004).

Ancillary data are often used to enhance the classification result based on performed expert rules. For example, dense forests are often found in mountain areas in Syria, but food-trees (cultivated plantations) are essentially located in plain areas, with sparse houses and a low population density. Therefore, expert knowledge can be performed based on the relationships between the high factor and the agricultural conditions to separate food trees from forested areas.

Classical pixel-based classification methods often lead to “salt and pepper” effects in final classification results maps, caused by the isolated pixels of some classes within another dominant class. That is due to the complexity of biophysical environments, which potentially decrease the classification accuracy. It is more logical to join these isolated pixels to the dominant class that they are first assigned to. A suitable enhancing filter applied after the classification process on the produced thematic map will not only “clean up” the map and make it visually less noisy, but also increase the classification accuracy.

To improve the classification results, the majority/mode filter in ENVI, v. 4.6 was used as a post-classification procedure. This procedure is a low-pass filter that reduces the created effects and noises from the classification process, where it replaces the isolated pixels by whatever value constitutes the majority in their neighborhood. It could be regarded as a kind of post-classification spatial integration. This filter is simple, where it smoothes a thematic map without any numerical operations (Liu & Mason, 2009).

The classification results (the thematic maps) were filtered using a 3 by 3 majority filter window, followed by a sieve filter. This caused a smoothing of the class boundaries. A small pixels-cluster of an individual class was added to the surrounding area of a larger class, and the boundaries of the LULC-classes were generalized and clearly identified. The sieve filter was used in addition to the majority filter to clean the classification result of further small pixel-clusters that were not eliminated from the majority filter. Clusters with less than 10 pixels were removed by merging them with their largest neighbor.

## L. Automated change detection mapping

### 1. Pre-classification approach

This approach was essential in mapping the increasing changes in the agricultural irrigated areas in the ERB. Data from the LANDSAT-program, MSS and TM spanning the period between 1975 and 2007 were chosen from a similar time of the year in order to allow each LULC-class of interest a similar spectral response and similar illumination conditions. The MSS-data set of six images (Fig. 5.60) were pre-processed (see C5.B) for radiometric normalization using iMAD. The master-scene was p185r035. It was impossible to correct the atmospheric effects because it was difficult to obtain weather parameters for such relatively old dates. However, it was possible to carry out radiometry and atmosphere corrections for the TM-data set of six images. The master-scene for this was p172r035. Each data set was then mosaiced to produce only two mosaic-images, each representing one date. Again, iMAD was applied to the two resulting mosaic-images. The master-scene was chosen as the mosaic-scene produced from the TM-data in 2007, as it was possible to get weather data for the dates, and radiometric normalizations and atmospheric corrections were able to be performed. Finally, the two mosaic-scenes were geometrically registered using the *image to image method*. The MSS-scene was also resampled to the same spatial resolution of 30 m as TM-scene. Finally, the two remote sensing data-scenes were added to the change detection mapping process using the image differencing method. The three major mapped changes over the last 32 years were: natural areas to bare areas, bare areas to cultivated areas, and no change (see C6.C.1).

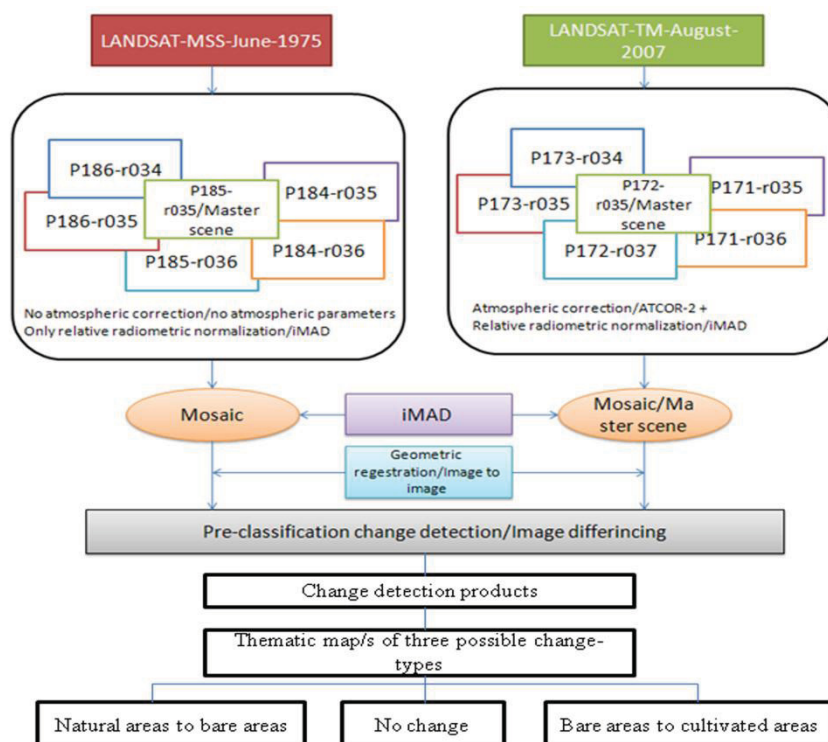


Fig. 5.60: The pre-classification change detection mapping concept that was performed for the two remotely sensed data sets (MSS-June-1975 and TM-August-2007)

## 2. Post-classification approach

The post-classification change detection approach concerned the analysis of the differences between two more or less independently classified images. A comparison of the categorizations was performed using raster-based analysis (ENVI, v. 4.6). The major merit of this approach was that data normalization was not needed because the remote sensing data recorded at two dates were classified separately (Singh, 1989). Disadvantages that reduce the implementation of this approach are: cost; consistency; and error propagation (Lunetta, 1999).

The post-classification change detection approach for the ERB (Fig. 5.61) was based on the two previously supervised classified remote sensing data sets (TM-May-1987 and TM-May-2007) using the MLC-algorithm (see C5.G.1.2.2). The resulted five general classes that provided input in the change detection were: cultivated and managed terrestrial areas; natural and semi-natural terrestrial vegetation; artificial surfaces and associated areas; bare areas; and natural water-bodies (see C5.H). The resulting 1987 and 2007 classification results were used as inputs for classification, then post classification, followed with change detection statistics under the ENVI-program with the version 4.6. This yielded a change image (change matrix), in which 20-types of change between the two dates were potentially possible (see C6.C.2).

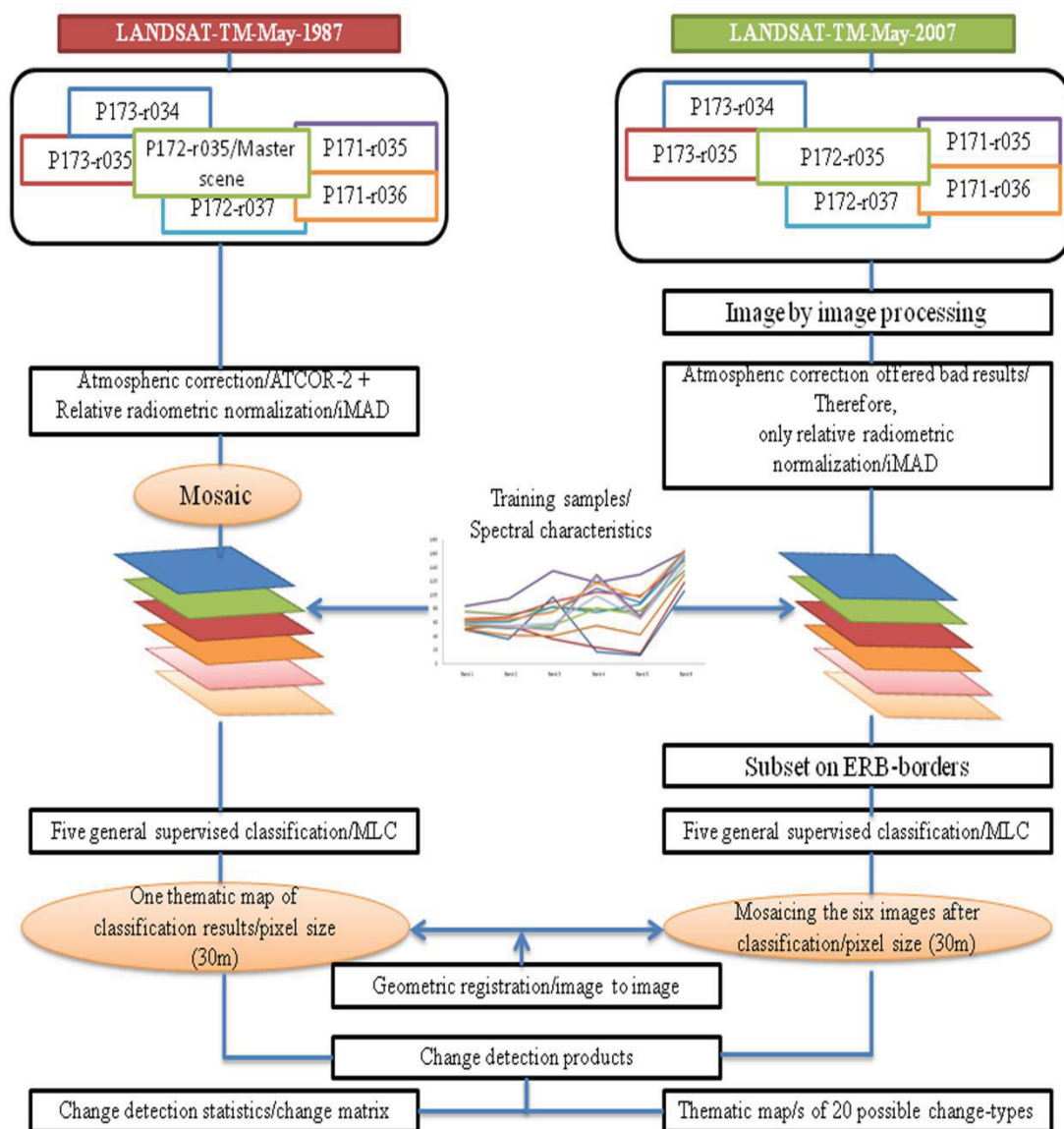


Fig. 5.61: Flow chart of the post-classification change detection mapping approach that was performed for the two remotely sensed datasets (TM-May-1987 and TM-May-2007)

## M. Accuracy assessment

The execution estimation of an applied classification approach is a complex process, involving various criteria. Cihlar et al. (1998) suggested six criteria. These are: "accuracy; reproducibility; robustness; ability to fully use the information content of the data; uniform applicability; and objectiveness". These requirements are difficult to satisfy using only one classification approach. The reason for this relates to the different environmental settings and datasets used. DeFries and Chan (2000) suggested four criteria. These are: classification accuracy; computational resources; stability of the algorithm; and robustness to noise in the training data. In conclusion, accuracy assessment of classification results is, mainly, the most common method for an estimation of classification approach execution. The acceptable accuracy values are relative, determined generally by the users themselves depending on the type of application. Accuracy values that are acceptable for specific application may be unacceptable for others.

Generally, there are no dependable rules for determining the testing samples that are required to evaluate the classification accuracy. However, there are some useful suggestions, including those made by Fitzpatrick-Lins (1981). Another idea, put forward by Congalton and Green (1999), is to use 50 testing samples as minimum for each classified LULC-category. If the study area is larger than 1,000,000 ha, or if there are more than 12 classified categories, then there should be 75-100 samples for each LULC-category. This suggested approach samples small areas thoroughly, while large areas might be under-sampled. Thus, it is suggested that testing sample numbers could be set for variations in size and within-class variability.

Accuracy assessment is a post-classification step. It was accomplished for the purposes of this study using ENVI, v. 4.6, which was used to evaluate the correspondence of the classified LULC-maps to the *true and/or assumed true* geographical reference data (Congalton, 1991). The reference data were: Part of the collected field-data for the years 1987, 2005 and 2007 (see C5.D), where the first part was used as training samples; assumed truth data based on the integration of the remotely sensed data; irrigation projects statistical records and the detailed construction schemes of these projects, which were used to locate the spatial distribution of the various agricultural features in the irrigation projects area for 1987 (see C5.J); thematic maps; visual interpretation based on the remote sensing data itself; and Google Earth. Fig. 5.62 illustrate the major steps that were followed in assessing the various thematic maps that resulted from the classification process.

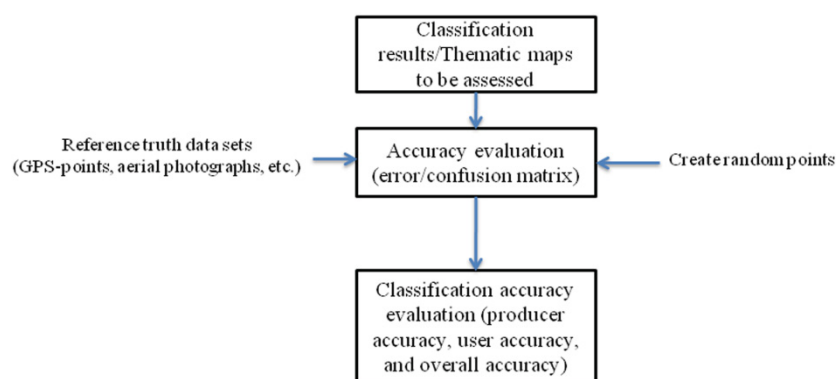


Fig. 5.62: The general accuracy assessment steps that were applied on the resulted thematic map/s from the classification process

Results of classification were presented in form of thematic maps. Using the various truth reference data, accuracy assessments were carried out for all classification results. The reference data/classes were compared with the predicted classes by the adopted classifier/s (and probably enhanced using the post-classification processing). The final evaluation results were reported in the form of error matrices. The overall classification accuracy (percentage correct) was calculated for all classifications, as well as the accuracies of the class-specific user and producer.

Two accuracy assessment methods were performed in this thesis. The first method is *based on the pixel scale* to derive the accuracy of classification in the remotely sensed data, which resulted from the calculation of the error/confusion matrix.

Let, for a ( $l$ -class) classification problem, ( $N$ ) be the total number of reference samples. The corresponding confusion matrix is illustrated in Fig. 5.63. The number of samples that are classified as class  $/oi$  ( $i = 1, 2, \dots, l$ ) and belong to land cover class  $/oj$  ( $j = 1, 2, \dots, l$ ) are described by ( $n_{ij}$ ), for example, ( $n_{11}$ ) denotes the number of samples that belongs to class ( $1$ ) and correctly assigned to class ( $1$ ), whereas ( $n_{21}$ ) defines the samples belonging to class ( $1$ ), but incorrectly classified to class ( $2$ ). The diagonal cells ( $n_{cc}$ ) (the highlighted elements in Fig. 5.63) of the error matrix contain the number of correctly classified samples (Congalton & Green, 1999), while the off-diagonal cells represent the disagreement between the classified image and the ground truth data (Mather, 1999). The overall accuracy is calculated by their sum (the diagonal observations) divided by the total number of samples ( $N$ ) (all observations included in the error matrix):

$$\text{Overall accuracy} = \frac{\sum_{c=1}^L n_{cc}}{N}$$

		Reference truth data			$\Sigma$
		Class 1	Class 2	Class c	
LULC-classification results/thematic maps	Class 1	$n_{11}$	$n_{12}$	$n_{1c}$	$n_{1+}$
	Class 2	$n_{21}$	$n_{22}$	$n_{2c}$	$n_{2+}$
	Class c	$n_{c1}$	$n_{c2}$	$n_{cc}$	$n_{l+}$
$\Sigma$	$n_{+1}$	$n_{+2}$	$n_{+c}$	$N$	

Fig. 5.63: Explanation of the error matrix approach (Source: Modified from: Congalton & Green, 1999)

Generally, the individual LULC-class that accounts for a large rate of the study/testing area, might be classified with a high accuracy using an individual classification algorithm, which creates an alignment in overall accuracy. Therefore, it is necessary to consider the individual class accuracies to avoid the alignment. Class-specific accuracies can be created based on the confusion matrix (i.e., producer and user accuracy). It can be also used to create the corresponding error rates. "An error of omission is to exclude a sample from a class in which it originally belongs (a misclassification error is an omission from the correct class). A commission error on the other hand assigns a sample to a wrong class (a misclassification error is a commission into another class). Consequently, each error is an omission from the correct class and a commission to a wrong class. The producer accuracy, that is a measure of *error of omission*" (Story & Congalton, 1986), for class ( $c$ ) is calculated by dividing the number of correct samples of ( $c$ ) by the total number of reference samples of class ( $c$ ). The resulting percentage producer accuracy indicates the probability that a reference pixel will be correctly classified.

$$\text{Producer accuracy} = \frac{n_{cc}}{n_{+c}}$$

The user accuracy, that is a measure of *error of commission* (Story & Congalton, 1986), describes how many samples that were classified as ( $c$ ) in fact belong to class ( $c$ ). The measurement is resulted from:

$$User\ accuracy = \frac{n_{cc}}{n_{c+}}$$

Finally, multiplying the results of each the previous three accuracies by 100 forms the *percent correctly classified (PCC)* metric.

The second statistic used is the *kappa coefficient (kc)*. It is generally known as a precision measure since it is considered as a measure of agreement in the absence of chance (Cohen, 1960; Lillesand et al., 2008). Conceptually it can be defined as:

$$KC = \frac{Observed\ Accuracy - Chance\ Agreement}{1 - Chance\ Agreement}$$

The kappa statistic is calculated from the confusion matrix by using the following mathematical statement:

$$KC = \frac{n \sum_{i=1}^p x_{ii} - \sum_{i=1}^p x_{io} x_{oi}}{n^2 - \sum_{i=1}^p x_{io} x_{oi}}$$

Where:  $n$  = total number of pixels used for testing the accuracy of a classifier,

$p$  = number of classes,

$\sum x_{ii}$  = sum of diagonal elements of confusion matrix,

$\sum x_{io}$  = sum of row  $i$ ,

$\sum x_{oi}$  = sum of column  $i$ .

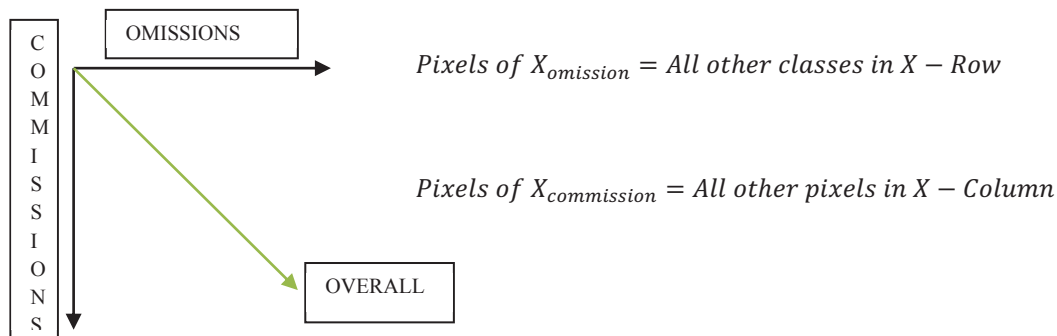
An example is presented to explain the derived classification accuracies for the 21,000 ha project for the year 2007.

**Table 5.9:** The classification accuracy assessment for the resulted thematic map that represents the spatial distribution of the permanent and the winter agricultural classes in the 21,000 ha project

Reference classes (image/ground)	Resulted classified classes from LANDSAT-TM-images							Total/possible	Omissions	Commissions	Mapping Accuracy
	1	2	3	4	5	6	7				
Trees and shrubs (1)	9	1	0	0	0	1	0	11	2/11 = 0.18 *100 = 18%	3/11 = 27%	9/9+2+3 = 64%
Alfalfa (2)	1	7	0	0	1	0	0	9	2/9 = 22%	2/9 = 22%	7/7+2+2 = 63%
Wheat (3)	1	1	17	4	1	0	0	24	7/24 = 29%	5/24 = 20%	17/17+1+5 = 73%
Barley (4)	0	0	4	13	0	0	2	19	6/19 = 31%	6/19 = 31%	13/13+6+6 = 52%
Sugar beet (5)	0	0	1	1	10	0	0	12	2/12 = 16%	2/12 = 16%	10/10+2+2 = 71%
Fallow (6)	1	0	0	0	0	17	0	18	1/18 = 5%	1/18 = 5%	17/17+1+1 = 89%
Other (7)	0	0	0	1	0	0	14	15	1/15 = 6%	2/15 = 13%	14/14+1+2 = 82%
<b>Total</b>	12	9	22	19	12	18	16	108			

Overall LANDSAT-TM Classification Accuracy =  $9 + 7 + 17 + 13 + 10 + 17 + 14 / 108 = 80\%$

$$Mapping\ Accuracy\ for\ any\ Class\ (X) = \frac{Pixels\ of\ X_{Correct}}{Pixels\ of\ X_{Correct} + Pixels\ of\ X_{Omission} + Pixels\ of\ X_{Commission}}$$



$$Kappa\ Coefficient\ (KC) = \frac{108 * 87 - 108 * 108 / 7,569}{108 * 108 - 108 * 108 / 7,569} = \frac{9,396 - 11,664}{7,569 - 11,664} = \frac{-2,268}{-4,095} = 0.55$$

The second method is *based on the state administrative divisions* (e.g., Menbij see C5.D and C5.G.2) and/or *on the state irrigation projects divisions* (e.g., the 21,000 ha project see C5.J), to derive the accuracy of the correspondence between the derived statistical numbers from the automated classification of remote sensing data and those human-based statistical records.

The correspondence degree for a specific season at an administrative-scale was measured by calculating the *Percent Error (PE)*:

$$PE = \frac{Observed_i - Predicted_i}{Observed_i} \times 100$$

PE is calculated as: the percent proportion of the variation between the remotely sensed area estimate (predicted) and the surveyed area estimate (observed) to that of the surveyed area estimate (observed) for each method for each year within a state administration's boundaries.

After finishing the automated classification process, and obtaining the results and evaluations, results were compared with statistical records on the level of the three governorates (Aleppo, Ar-raqqa, and Deir Azzour), on the administrative region level (e.g., Al-Bab) in each governorate, and on the level of the natural borders of agricultural stabilization zones within the borders of the three governorates and their administrative regions. Finally, these statistical records were reported on the level of the irrigation agricultural projects' borders. The next diagrams (Fig. 5.64, Fig. 5.65) show the structure of the statistical process in Syria in general.

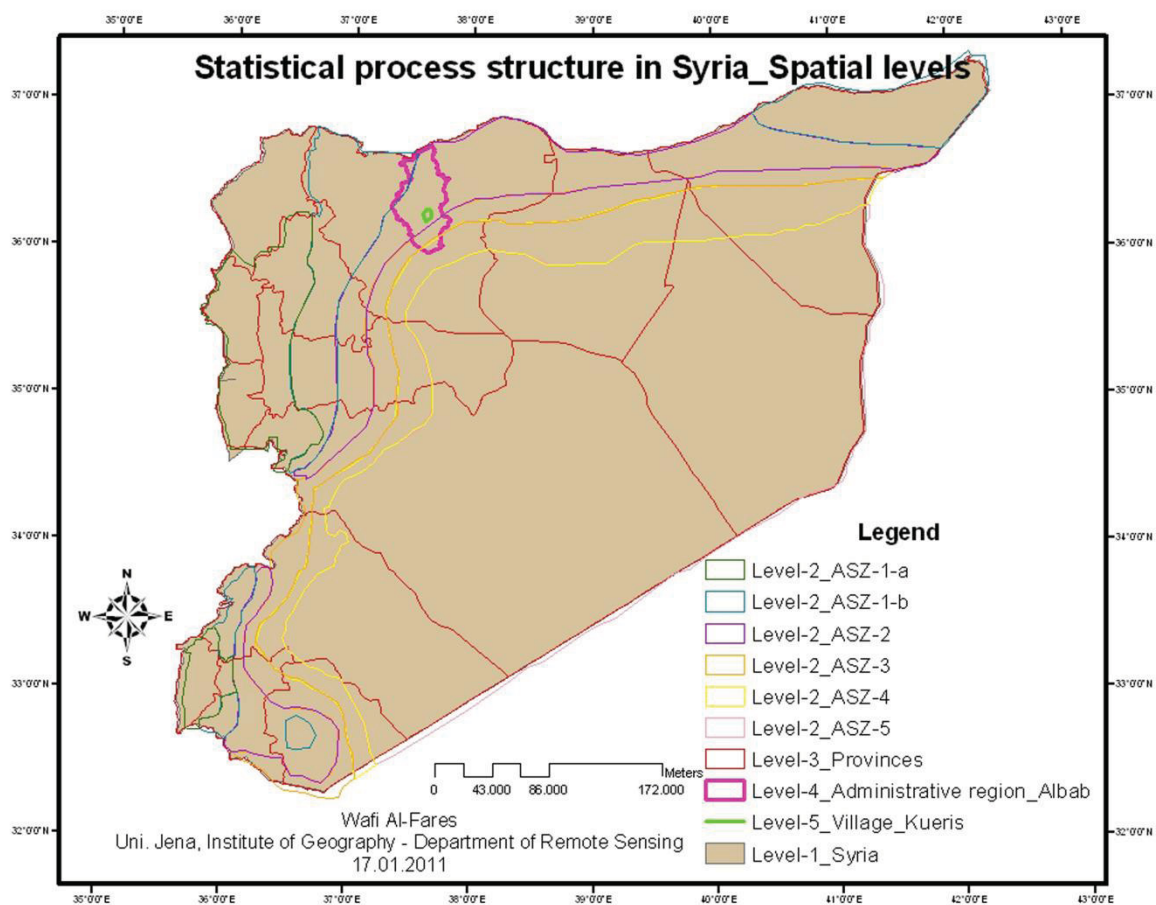


Fig. 5.64: The major spatial levels of collecting the statistical information about various LULC-features (Source: Modified from: CBS, 2008)



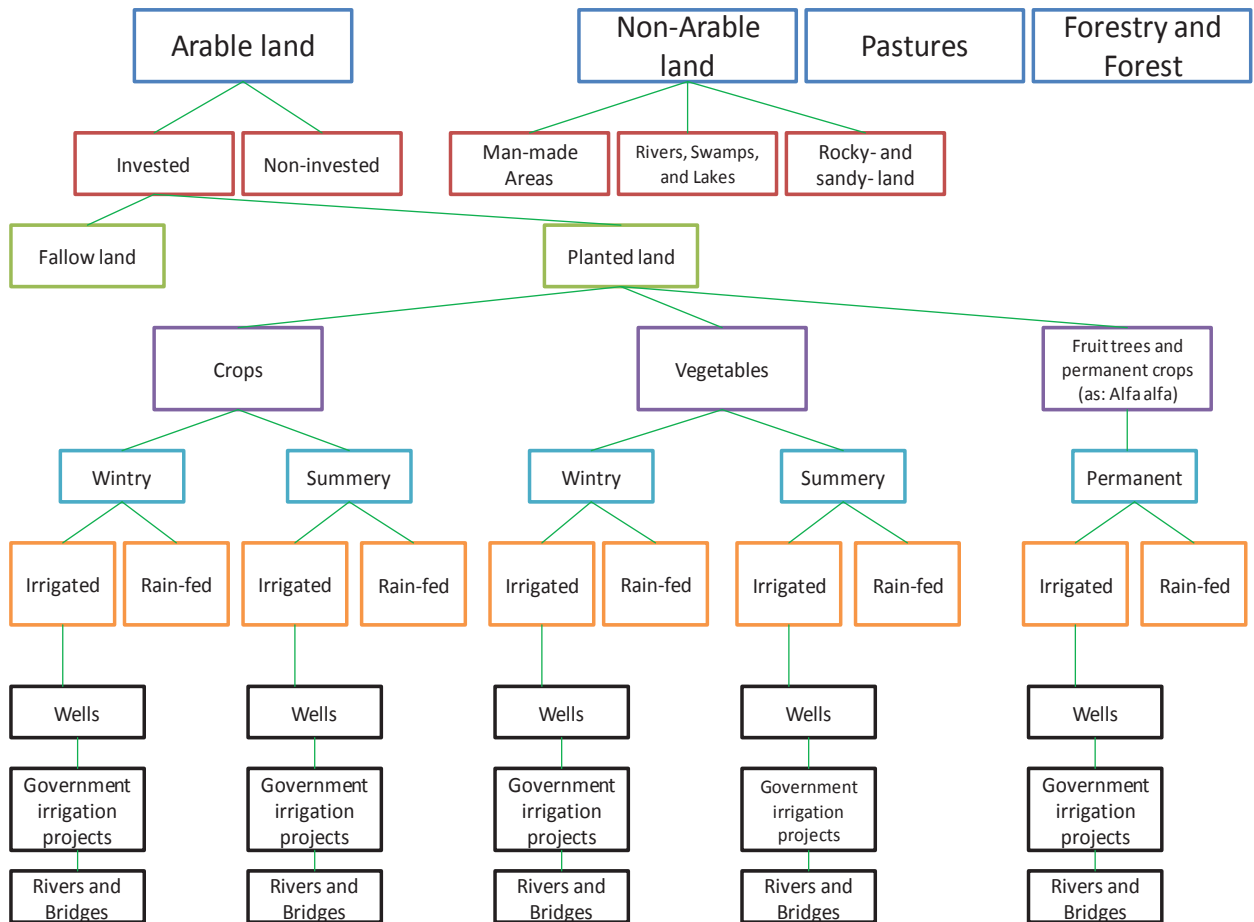


Fig. 5.65: The major structural levels of collecting the statistical information about various LULC-features (Source: Modified from: CBS, 2008)

## Chapter 6: Results, analysis and discussion

This chapter deals essentially with the results of this thesis, that are then followed with analysis and discussions.

This chapter presents the various LULC-features classification results (the wide major classes, the irrigated areas development mapping, and the small detailed agricultural classes), and their accuracies. Factors which influence the classification results are also discussed. Chapter 6 illustrates the various LULC- change detection mapping results (pre-classification approach results and post-classification approach results), and discusses the successes and the limitations of applying the various remotely sensed data used in this study, to satisfy investigation into the objectives of the thesis.

Statistical records do not contain all elements of the irrigation projects. The second step in this research involves employing remotely sensed data to obtain statistical numbers which represent the areas in over past periods. Here, again, emerges the integration between statistical data and remote sensing data in study land uses, distribution of natural coverage and its change across time. In the first step (see C5.J), statistical numbers have been useful in the spatial determination of the spread of the targeted needed classes, and are represented in the automated classification process in order to represent the spectral characteristics of all classes. In addition to the utilization of the total statistical records in evaluation, the accuracy of the classification needs to be determined through comparison of the final results of the automated classification with the results of the traditional human-based survey (i.e., the statistical records). The second step, after obtaining the training-samples from the irrigation projects which have statistical records or by using the available GPS-points as training-samples, is to determine the statistics of the regions which have no governmental statistical data.

### A. LULC-classification

The spatial resolution of LANDSAT 30 m makes LULC-mapping in some situations difficult as compared to other platforms such as IKONOS (4 m), SPOT-5 (2.4 m), and QUICKBIRD (less than 2 m) (Jensen, 2005). Some parts of the ERB have strips of cultivation areas (planted: various crops, non-planted: fallow or drilled), and natural vegetation, that are less than 30 m in width and/or length (see Fig. 5.29), which were not mapped explicitly using the LANDSAT-sensor. This highlights a need to adopt more high-resolution images for this purpose, but unlike other remote sensing platforms (e.g., IKONOS, and ASTER), the LANDSAT-sensor can allow long term monitoring using data from the 1970s up until to present day (Jensen, 2005).

#### 1. The broad major LULC-features

An ERB-map has been created which represents the state of five major LULC-features for the years 1975, 1987, 2005 and 2007. Table 6.1 and Fig. 6.1 provide a statistical overview of the LULC-distributions. The majority is occupied by bare lands, followed by cultivated areas, natural vegetation areas, natural water-bodies, and finally, artificial surfaces. The total area of these major classes is 5,033,537 ha.

Table 6.1: Overview of the LULC-occupations rate in several years

	1975	1987	2005	2007
<b>Cultivated Areas</b>	1,123,268	1,316,117	1,670,625	1,783,286
<b>Natural Vegetation</b>	562,890	710,093	686,718	403,113
<b>Artificial Surfaces</b>	413,204	255,140	18,312	89,772
<b>Bare Areas</b>	2,843,452	2,635,830	2,497,157	2,641,953
<b>Natural Waterbodies</b>	90,723	102,730	160,725	109,580
<b>TOTAL</b>	5,033,537	5,033,537	5,033,537	5,033,537

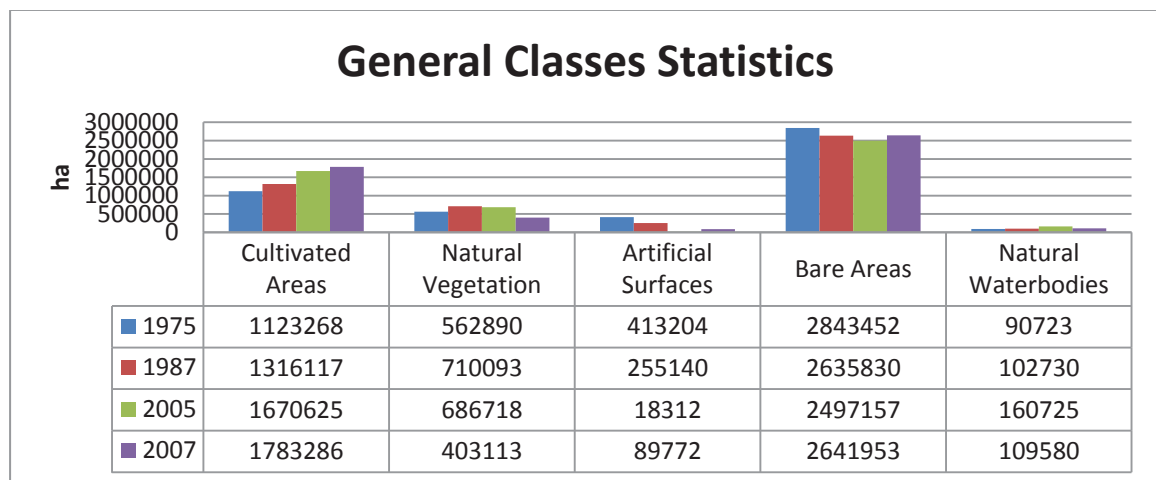


Fig. 6.1: Illustrated overview of the LULC-occupations rate in several years

**Irrigated Aleppo's eastern plains.** These plains are irrigated from the Euphrates River by pumping water from Lake Al-Asad. They extend from the south of Aleppo (near the Tall Addaman town) to the township of Maskana. The southern and southeast borders of the plains are formed by Al-Badia. The marsh of Al-Jabboul that lies east of the city of Assafira separates those irrigated plains from the southern Al-Hass mountain plains which extend to the beginning of the Syrian Desert (Al-Badia). Agriculture in the Al-Hass mountain plains often relies on rain-fed cultivation such as wheat, barley, lentil and cumin, with the omission of cotton. The Al-Badia lands that lie on the borders of the projects of east and west Maskana are protected pastoral lands, and cultivation within them is restricted to secure pastures for animals. The irrigated lands are bordered from north by a large major irrigation canal that transports water from Lake Al-Asad. North of this canal are rain-fed plantations, and in some places, artisan wells upon which the cultivation of vegetables, summer, and winter crops rely in small rates. Here, only one winter crop is planted - either wheat or barley - as ground water is rare and does not cover the need for irrigation of both crops. Recently, cumin has begun to be grown in the area and many farmers have started to cultivate olive trees, which require little water. These rain-fed cultivations extend from the irrigation canal in the south to the Turkish borders in the north.

**A new project, begun in 2007** aims to redirect part of the Euphrates from the basic canal in Arbid Kabeer toward the north, to the Tadif and Al-Bab plains and ending at the village of Bershaia. This project will irrigate nearly five kilometres width of agricultural lands, using the modern technique of irrigation (dropping). In this area, wheat and cotton are largely cultivated, while peanuts and sugar beet are farmed in small spaces. Before the irrigation project, these areas featured bare land, void of planting coverage because of the scarcity of water in summer. The East Aleppo plains end at the city of Maskana and at the pumping station of Babiri. The plains of Maskana-west follow Aleppo administratively. In the winter, wheat, peanuts and sugar beet are cultivated and irrigated barley in low rates. The major cultivated summer crops are cotton, yellow corn, and low rates of vegetables and watermelon.

Therefore, these lands are all agricultural lands depending on rain-fed irrigation systems, with the exception of the recently irrigated plains of Tadif and Al-Bab, which amount to about 6,700 ha. Near Menbij City, there are individual dragging operations by pumps extending about one kilometre or more, which are detectable on the remote sensing data used.

**Al-Badia/the pasture** (the fifth agricultural stabilization zone) is largely classified under the general class of natural vegetation and a lesser part of bare areas. The Syrian Ministry of Agriculture defines this area as one in which precipitation is less than 200 mm per year. Al-Badia is characterized by natural plants, which are either seasonal or permanent, with different densities due to natu-

ral factors such as soil type, water recharge, and the local topography. Human factors, such as the density of the grazing, modern plantations and projects to improve pastures also have an impact.

**Most of the wetlands** and the water surfaces distributed in the study area were characterized by their short-term duration (except the Euphrates River). For instance, the large salty Al-Jabboul lake/marsh, and the marshes of Al-Haraik, Al-Adamy and Maraga are all exposed to seasonal or yearly floods, depending on precipitation amounts. The borders of these areas were represented on the thematic maps according to their expansion in spring season and in a rainy and wet year (LANDSAT-TM-May-1987). This was done to show that the areas may sink underneath waters. As for temporal valley streams, they can be drawn digitally using topographic maps with 1/50,000 scale, for example.

In general, the detection, separation, classification and mapping of **the roads** (especially, the secondary roads) and the small villages, which underlie the general class of artificial surfaces, were classified with low accuracy, using the available remote sensing data. If this is insufficient for other studies about the ERB, topographic maps offer the possibility of digitalization, from which the data can be extracted with very high accuracy. The use of other remotely sensed data with very high spatial resolution (e.g., IKONOS) is also recommended.

The most important problem in the separation and classification of the Earth features in the study area is the classification of the marginal land. The ability to classify these lands is linked to several factors.

*The temporal factor:* some lands were covered with temporary natural vegetation that grew during spring and at the beginning of summer (from March to early May). There were also very small areas covered with seasonal and permanent vegetation. Some of these areas could not be spectrally separated or classified from the surrounding bare areas because their spectral and spatial resolutions were insufficient. Another reason was the dispersion of vegetation that dominated the spectral reflectance of dry soils, particularly those that had light colours. Also, because of the presence of the natural vegetation during the synchronism season with cultivation of winter crops, there emerges the problem of spectral integration/mixing of these vegetation with one or more types of the agricultural crops classes. The presence of these marginal lands in the sensory data of August, led to the disappearance (or semi-disappearance) of the spectral correlation problem between the marginal lands that were covered with the temporarily natural coverage of vegetation during the spring months. Between the lands with agricultural crops this natural coverage almost vanished in August because of the absence of precipitation and domination of drought. However, in contrast, the remotely sensed data taken in August had the problem of spectral correlation of the marginal lands with the spectral characteristics of the fallow lands, especially if they were covered with light soil.

*The spatial factor:* the presence of these lands within the irrigated agricultural projects increased the problem size since more details were required concerning the credited classification system levels, where green areas were classified into several classes/agrarian crops. The presence of marginal land outside the borders of the irrigated areas was a secondary problem with only slight effects (here, a general degree of classification was required, i.e., five classes only, where green areas were classified into only two agricultural lands with all of their crops and classes, and natural vegetation lands).

*The climatic factor:* the rain-element determined prevalence, location and density of the natural vegetation, and as a result, it controlled the spectral behaviours which changed permanently according to time, place, kind of soil and amount of precipitation. Consequently, the spectral behaviour of these natural plants might look similar and correlate with a spectral behaviour of a crop (barley for example). This behaviour is likely to change across time from one year to another, and perhaps even in the same season and location/field, since, the natural plants may correlate with other spectral response of crops other than barley (e.g., wheat).

**LANDSAT-MSS-June-1975 data.** By classifying the study area using several scenes included in one mosaic-scene, it was possible to make classifications for only three classes (i.e., the cultivated areas, uncultivated areas and water areas). There was a mixing between cultivated and uncultivated areas, particularly, in the inactive volcano cones area, which is found to the east of the city of Ar-raqqa, where dark colour soils are interrelated with fallow lands. Also, there were mixing and misclassification concerning water and cultivated areas, particularly in river areas with narrow width and shallow depth. It was possible to integrate the volcano area into the uncultivated areas by manually drawing the borders of the area in the form of vector-shapes. There was also significant mixing between fallow and bare areas, meaning the separation and classification between artificial surfaces and bare areas was impossible.

Each scene was classified separately after sub-setting based on the borders of study area. After that, classification results scenes were collected in one mosaic-scene (Fig. 6.2). Thus, the classification results were better rather than the above mentioned situation, as it was possible to obtain the five needed general classes. These results were improved for several reasons: technically, returning to the used remotely sensed data itself, where, whatever the quality of the present algorithms to correct satellite scenes that contain differences in their radiometric characteristics, they were not accurate 100 % of the time. Hence, using every scene separately ensured the spectral behaviour towards all Earth surfaces features (and the probable variations within each feature alone). The natural reasons for this included: The large size and extension of the study area and its relation with the geographical location that controlled the natural climatic characteristics (especially the precipitation-factor), led to variation in Earth surface features and consequently in their spectral behaviour on satellite images. This in turn provided more details and information within the image but with the decreased possibility of spectral separation between the features of interest (indicating that, spectral separation increases or decreases according to the used sensor and its techniques). One of the negatives reflected by the classifying of each scene alone was the emergence of separating borders between two neighbouring scenes after the mosaicing-process, which meant there was no continuity in representing the prevalence of features and classes naturally and spatially. This problem was limited by use of a “majority-filter”.

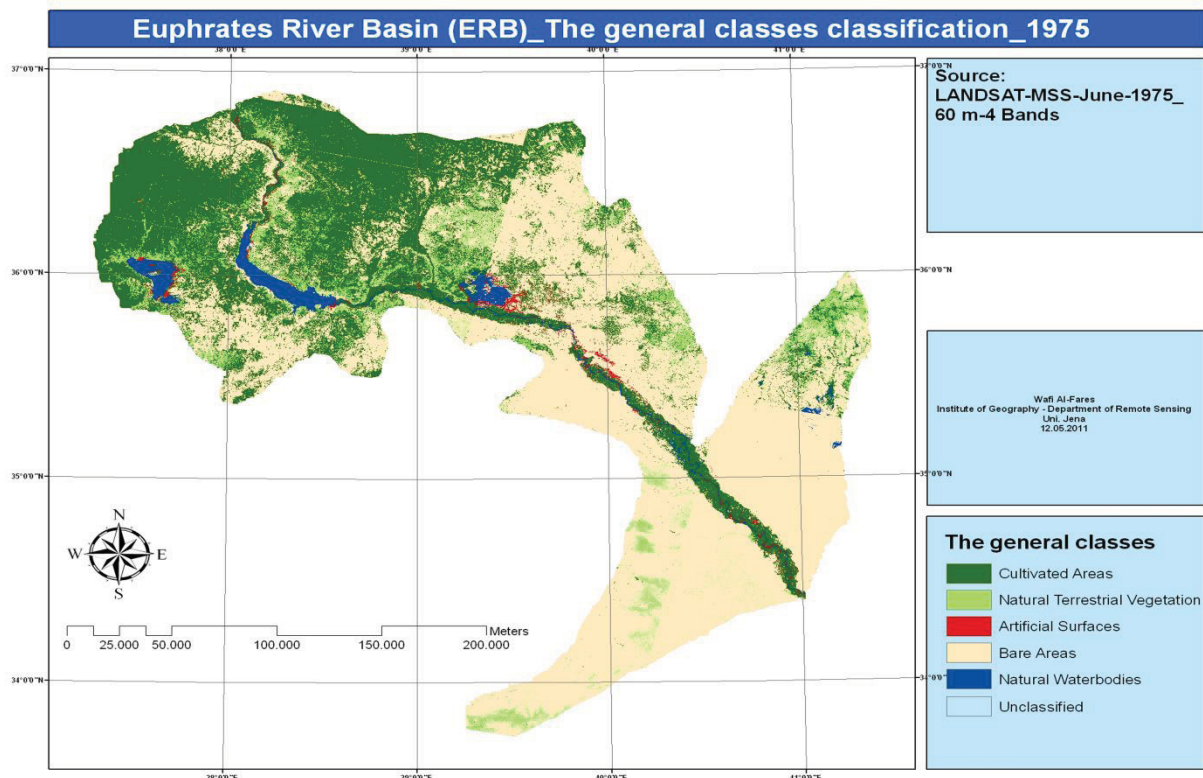


Fig. 6.2: The spatial distributions classification of the five major LULC-categories in the ERB for the data of LANDSAT-MSS acquired in June-1975

**LANDSAT-TM-May-1987 data.** This coverage was one of two coverages (in addition to the LANDSAT-TM-May-2007 coverage) which were used to produce a map of the change detection which has occurred in the past 20 years, through the application of the post-classification change detection approach. During the classification of both coverages into the five basic classes (Fig. 6.3), there was a mistake in classifying some areas of rain-fed cultivations as natural plant lands, because the most rain-fed plantations have a low density vegetal biomass, making them close to that which characterizes natural plants.

There was an increase in ratio of classification (over-classification) of the artificial surfaces specifically in volcano areas and Lake Al-Asad's banks, and also in some bare areas. The reason for this is that as is the case with the MSS-data, the negation or the lack of success ratio of radiometric correction/normalization imbued the radiometric properties of the same land features distributed in the several satellite scenes (i.e., those that construct the mosaic-scene), with similar or at least enough approximate compatible value/s. Thus, to overcome this problem, it was necessary to classify each image alone and then create mosaic-processes of scenes of the automated classification results.

The mixing between the natural vegetation class and the rain-fed based crops areas was lesser than it was in the LANDSAT-TM-May-2007 coverage. Also, the total water area was lesser than it was in the 2007-coverage, because of the recently constructed dams. There were areas located in the five agricultural stabilization zones, that classified in 1987-coverage as cultivated, but were reclassified in 2007-coverage as natural vegetation and/or bare areas. This was related to the prevention of agriculture after 1990 in the fifth agricultural stabilization zone.

There was also (using the all available remote sensing data for this study) a problem in separation and misclassification between fallow and bare areas with dark soils colours.

The ability to separate the inactive volcanoes area from the dark colored fallow fields and classify them, is better rather than with the MSS-data, because the higher spatial and spectral resolution of TM-data.

Another problem detected while using TM-data was correlation between the Euphrates River waters in the shallow and less wide areas because of the number of the training samples concentrating on cultivated lands at the expense of the water areas. However, this problem was overcome by increasing the number of the representative training samples of the water, which were distributed suitably over the whole borders of Euphrates River.

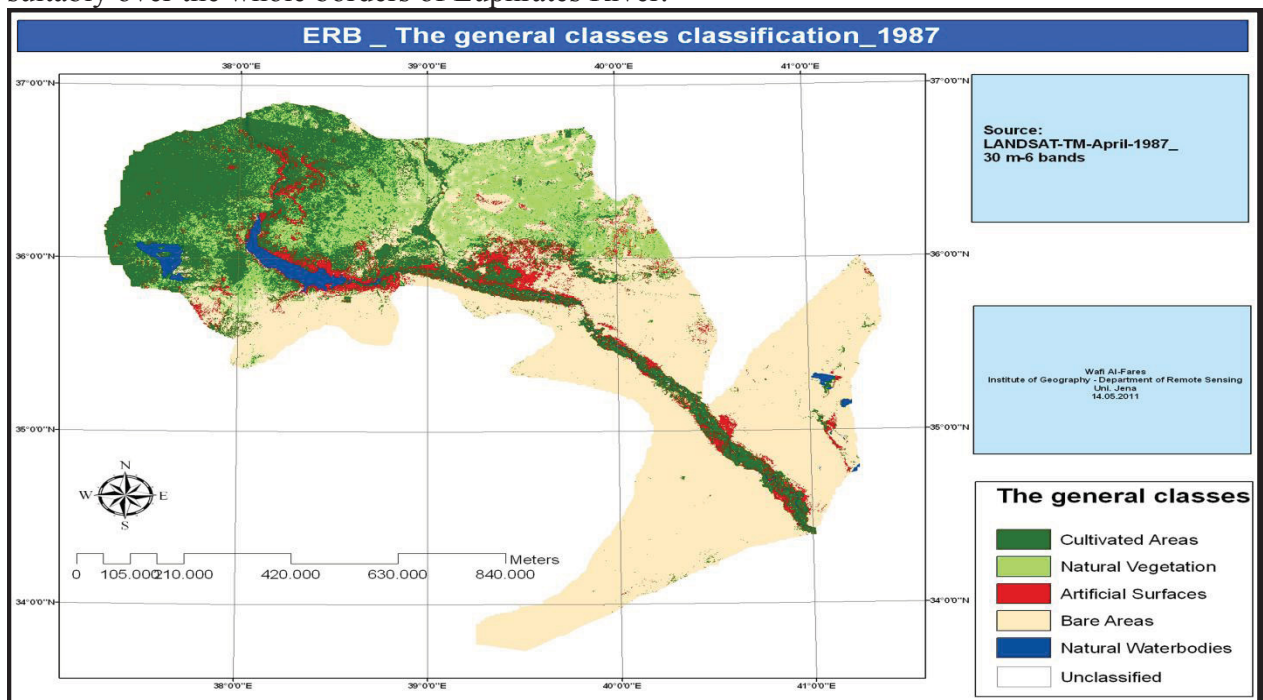


Fig. 6.3: The spatial distributions classification of the five major LULC-categories in the ERB for the data of LANDSAT-TM acquired in May-1987

**TERRA-ASTER-May-2005 data fused with LANDSAT-ETM+-May-2005 data.** These data were found to be optimal in classifying the ERB-study area to the five general LULC-classes (Fig. 6.4), especially for classifying the artificial surfaces which had been classified with poor accuracy using the three other data-coverages. Thus, their outcomes of classification can be considered as a base when more accurate statistical information is required about the distribution of the general classes within the ERB.

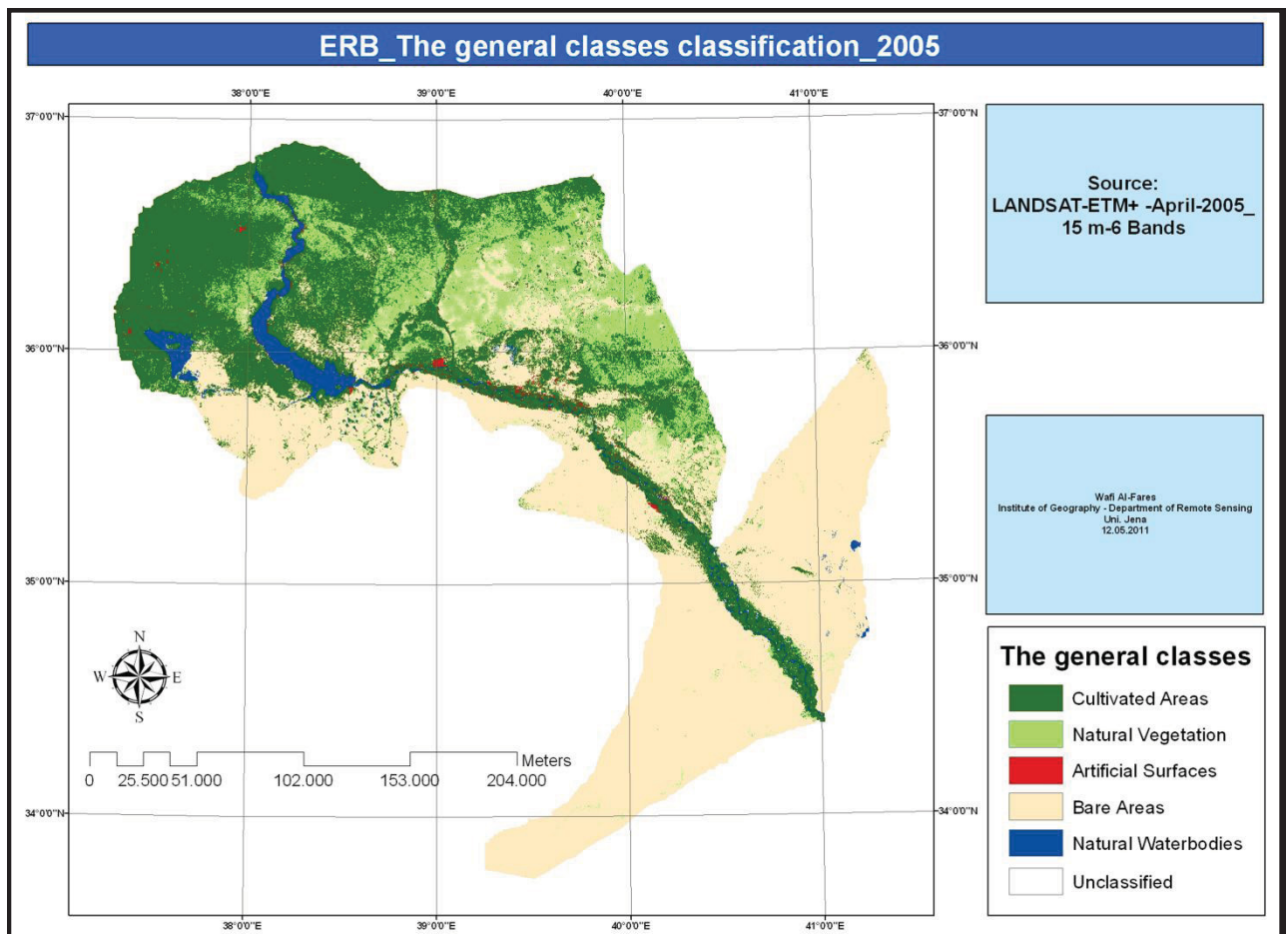


Fig. 6.4: The spatial distributions classification of the five major LULC-categories in the ERB for the data of TERRA-ASTER fused with LANDSAT-ETM+/SLC-Off/corrected acquired in May-2005

**LANDSAT-TM-May-2007 data.** There was a problem in spectral separation between the inactive volcanoes area with dark colour and the fallow lands. Yet, after drawing a large ROI in the volcano area, the spectral separability increased from 1.61 to 1.78. This accentuated the high significance of the process in selecting the training-samples and the bases it included (number of the experimental areas that represented each class, area or total areas of the samples for each class, the shape of the samples whether pixel or polygon, and the geographical spatial distribution of these training samples within the study area).

There was a limited spectral correlation between natural vegetation and the cultivated areas, particularly those lands of rain-fed plantations, because of their similarity in the green vegetation biomass (Fig. 6.5).

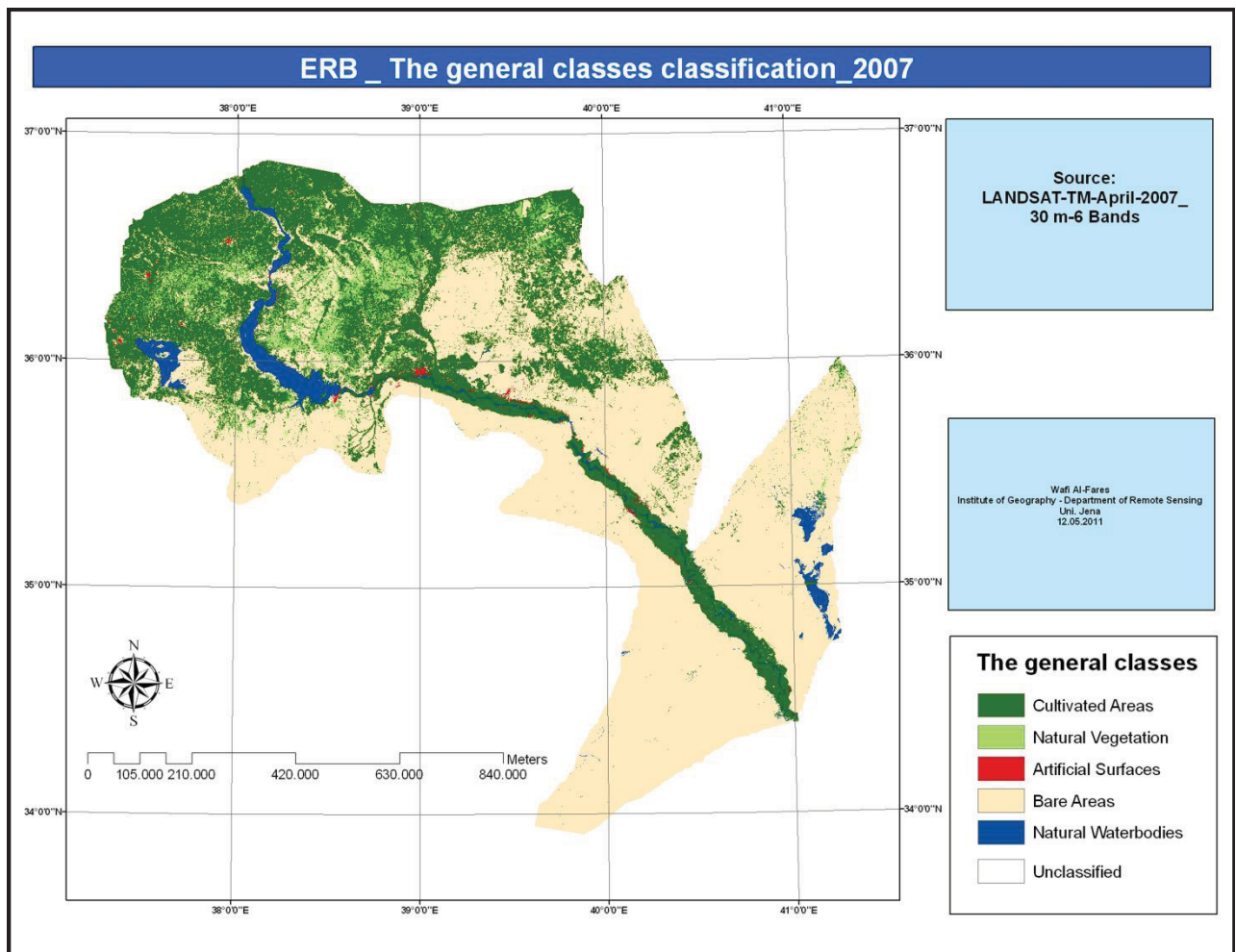


Fig. 6.5: The spatial distributions classification of the five major LULC-categories in the ERB for the data of LANDSAT-TM acquired in May-2007

## 2. The temporal development mapping of the irrigated areas

In Syria, the majority of irrigation projects were devised for two main crops, wheat in winter and cotton in summer. However, since the 1990s other crops have emerged, such as yellow corn, sunflower, peanuts and watermelon. These new species have started to compete with the two main crops, because of their better financial outcomes and the possibility of farming fields for three seasons instead of two.

Fig 6.6 presents the temporal development of the irrigated areas for the years 1975, 1987, 2005, and 2007 using different remotely sensed data.

Table 6.2 presents the statistics of the extension of the irrigated areas over different times. It presents also the areas rates of the other two general classes, i.e., uncultivated areas and water.

Cultivation of sugar beet within the irrigation areas has clearly decreased (Table 6.3), because the high salinity of soil and irrigation water, which make the crop less sweet. At present, this crop is mainly used as animal feed.



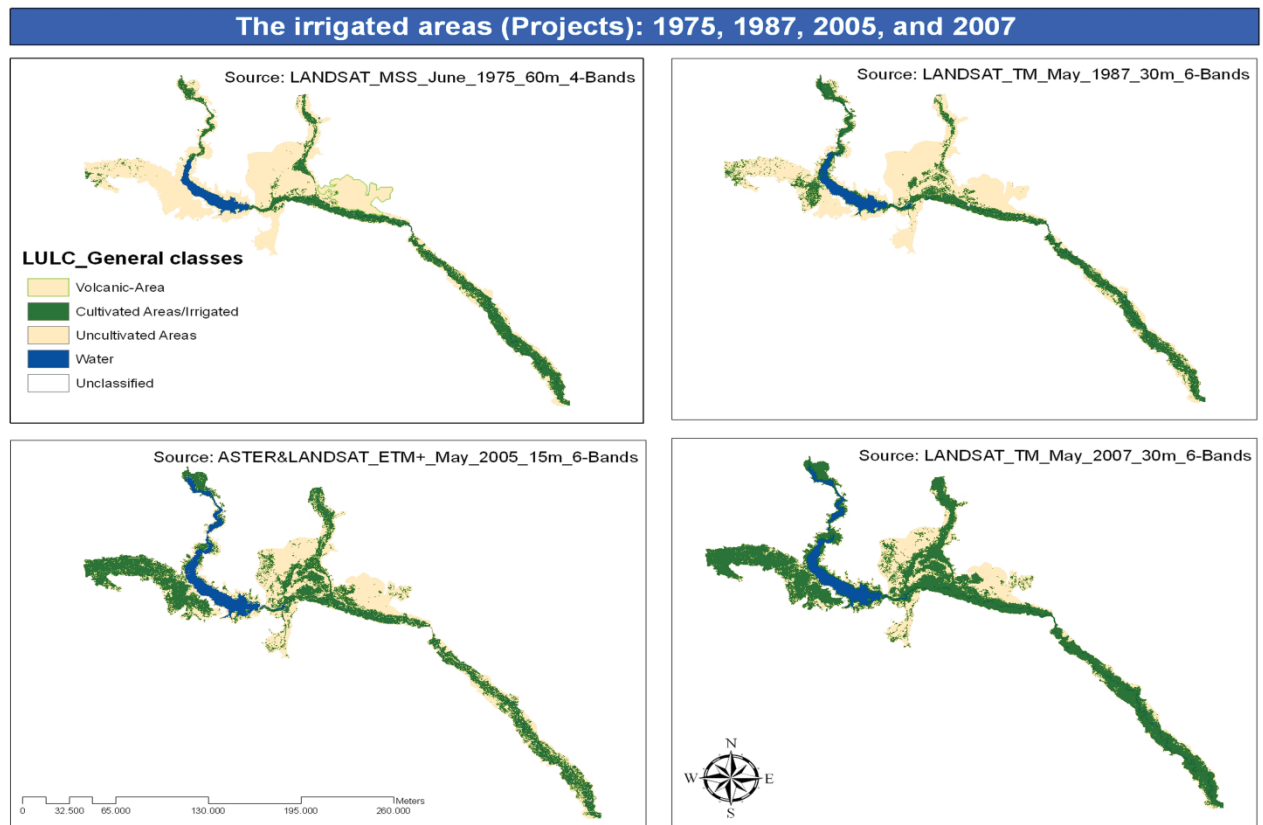


Fig. 6.6: The final irrigation mapping thematic maps, which explain the temporal development of the spatial distribution expansion of the irrigated areas during the last three decades using various remotely sensed data

Table 6.2: The areas rates of the three wide existing general classes based on the irrigated areas level

	1975	1987	2005	2007
<b>Cultivated Areas</b>	249,681	301,517	458,288	596,612
<b>Uncultivated Areas</b>	673,992	607,925	430,129	294,633
<b>Water</b>	52,030	65,980	87,284	84,347

Table 6.3: The areas rates of the three wide existing general classes and the various agriculture features based on the irrigated areas level

		1975	1987	2005	2007
<b>Cultivated Areas</b>		249,681	301,517	458,288	596,612
	Trees + Shrubs		2,137	26,148	27,206
	Herbaceous (permanent- and winter- crops)		163,402	162,211	262,294
	Alfalfa		23,608		
	Vetch		2,328		
	Wheat		53,013	131,881	188,688
	Barley		4,902	19,423	16,299
	Sugar beet		2,349	7,683	1,803
	Rain-fed crops		37,707		
	Other crops		39,495	3,224	55,504
	Fallow		135,978	269,929	307,112
	Herbaceous (summer- crops)		111,968	183,334	126,207
	Cotton		67,881	136,392	37,475
	Corn		33,519	31,198	25,481
	Other crops		10,568	15,744	63,251
	Fallow		189,549	274,954	470,405
	Cropped Total		301,517	371,693	415,707
<b>Uncultivated Areas</b>		673,992	607,925	430,129	294,633
<b>Water</b>		52,030	65,980	87,284	84,347

In Syria, the majority of irrigation projects were devised for two main crops, wheat in winter and cotton in summer. However, since the 1990s other crops have emerged, such as yellow corn, sunflower, peanuts and watermelon. These new species have become competitive with the two main crops because of their better financial outcomes and the possibility of farming fields for three seasons instead of two.

Cultivation of sugar beet within the irrigation areas has clearly decreased (Table 6.3), due to the high salinity of soil and irrigation water, which make the crop less sweet. At present, this crop is mainly used as animal feed.

The agrarian plains directly on the banks of the Euphrates River, specifically, those extending from Arraqqqa to Deir Azzour, are relatively small extended plains in a north-south direction. They are mainly limited between high rocky cliffs (old river terrace) in the south and the Al-Badia/pasture in the north. After passing the pasture Al-Badia, the agrarian lands emerge again in the second, third and fourth agrarian settlement areas. The river plains are characterized by their very small fields and variation of crops even in the one field. Many farmers divide their fields into parts - a section for economic income, one for providing animals with food, and another for vegetables and fruit for domestic use. These plains are crossed by lots of trees and scattered houses. These factors decrease the ability of the used satellite data to discriminate various interrelated land uses, to classify them and map their borders and spatial prevalence.

There are some small areas within the project of west Maskana which were classified as cultivated irrigated lands in 1987, although investment in this project began after this date. These irrigated areas are centred in valleys and seasonal small rivers (e.g., Quieck and Azzahab), while others depend on artisan wells for irrigation.

### 3. Distinguishing, classification and areas measurement of the strategic crops

**LANDSAT-TM-May-1987 data.** The separability and classification of alfalfa during its presence with the winter crops is higher than when it is included with summer crops, since alfalfa mixes spectrally with corn. Hence, the cultivated lands with alfalfa are gathered to the created mask for trees (i.e., fruit, poplar trees, grapevines, and other trees and shrubs located in cities, residence areas, and on the Euphrates River banks).

Some areas which are considered as agriculturally uncultivated, such as the mask created from sensory data taken in May for uncultivated areas, were shown as cultivated lands on satellite images taken in August. Hence, an error in automated classification results due to the masking-process has been made.

The majority of winter and summer cultivation is centred in Deir Azzour governorate (Fig. 6.7); winter vegetable areas are remarkably rare in Arraqqqa; instead while cultivation increases in summer. Sugar beet propagation is focused in Deir Azzour, while in Arraqqqa there is comparatively little. Corn, cotton and sesame are equally distributed throughout the three governorates. Barley is the major crop among rain-fed crops, followed by wheat, lentils, cumin and chickpeas.

The spectral separability between vetch and barley is fair but not good (1.70) because of the interrelation of their planting in some areas, where vetch plant (Thamilip/charged) and barley are both considered forage crops. The separability between irrigated barely and the rest of the rain-fed crops is good to some extent (1.83).

There was difficulty in the separation between the light fallow lands (as the training samples were selecting on purely fallow areas) and the uncultivated areas, including the artificial surfaces within the irrigation areas, to build the mask that represents the cultivated areas, under which the classification was carried out for agriculture features. To overcome this, the merging of training samples of both fallow and cropped areas offered better results in separation.

The differentiation in the spectral response of the winter crops (and the variation within each type) was limited by the early periods of vegetative germination of crops (March), which increased continuously until they reached their peak/s during April and early May, and then began to decline and disappear.

**LANDSAT-TM-August-1987 data** (Fig. 6.7). The problem of spectral correlation and separation between the uncultivated areas and the fallow was raised whether using remotely sensed data of May or August. It was, in general, less effective in August-data, where the separability reached 1.85, and where the most correlation was seen within the artificial surfaces. Here the question was raised “Why are the uncultivated areas again classified since the classification method relies on the hierarchical approach using the mask-process, which separated the uncultivated areas from the cultivated areas (including the fallow) in the previous classification level?”

The answer, previously mentioned (see C5.G.1.2.1), is that the hierarchical approach of classification has its drawbacks that lead to mistakes in the results just like any other approach. Accumulative errors result in those negatives brought by production/extraction of the mask's layer either counting on results of supervised or unsupervised classification, NDVI or others; or where, these credited approaches cannot reach a degree of perfection in spectral separating of the Earth surface features or the other classes of interest. This can also occur if these traditional approaches of classification have the ability to reach a suitable rate in spectral separation and classification. The hierarchical approach was not used in the classification process or in the creation of the masks at each classification level as it costs effort and time. As suggested in Fig. 5.35, the classification process was repeated on the classes which were not classified and completely extracted during the last classification process. The use of this approach was to increase the classification accuracy (the final product that resulted from collecting outcomes of each level and stage of the hierarchical classification), through a decreasing number of features and classes which exist in the study area, either by eliminating some features out of classification process (i.e., insignificant classes in irrigated agricultural projects such as bare areas), or postponing classification to the next stage if spectrally possible. Here, the significance of the accredited methodological approach in building up the used classification system emerged, in the reduction of the number of classes in each stage of classification and the securing of some reduction in the spectral mixture.

One of the positives of the hierarchical principle is to reduce the effect of the geographical location and the natural and climatic properties that affect the spectral behaviour of the studied Earth surface features, specifically, if the study area is within a wide geographic distribution, peppered with large diversion in natural and climatic characteristics. For example, making a mask of the distribution of irrigated plantations gives a natural harmonious area, since all the cultivations here are irrigated and the majority of soils have close colours and close content of humidity, etc. The greater the study area with a geographic and spatial distribution featuring the same or similar natural and climatic characteristics, the more likely homogeneity will be achieved in the spectral response of the Earth surface features contained in the study area. This trait does not exist in the geographical and spatial distribution of the Euphrates River Basin, since, for example, the spectral behaviour of bare areas will be in the dozens.

One of the more significant positives of the masking process was the reduction in the problem of spatial correlation which produces classification errors, as well as separating borders areas and/or the mutual areas between two classes or more (the negative impact increases wherever the spatial resolution decreases and the spectral variation rises). This was most effective when the areas of the class (other crops) were over-classified. Taking into consideration that the mask layer resulted in application of the NDVI has meant a few of the agricultural areas were neglected.

Making automated classification on sensory data after applying the mask (through use of the option: apply mask in ENVI-program) and integrating the mask layer with/or on the satellite scene with spectral bands (layer stacked), will decrease the separability between the spectral signatures

created from the training samples. Consequently, automated classification was conducted directly on sensory data through selecting the option of using mask in the ENVI-program.

The classification of water was more effective when using the remotely sensed data acquired during the summer season (e.g., August).

The reason that the corn was over-classified in some cases, was probably to do with the mixture between the lands that were cultivated previously with wheat during the winter season. This occurred when the wheat residues were not burnt or tilled, and the fields remained covered in yellowish dry residues (straw). In addition, some plants grew naturally after the harvesting of the wheat.

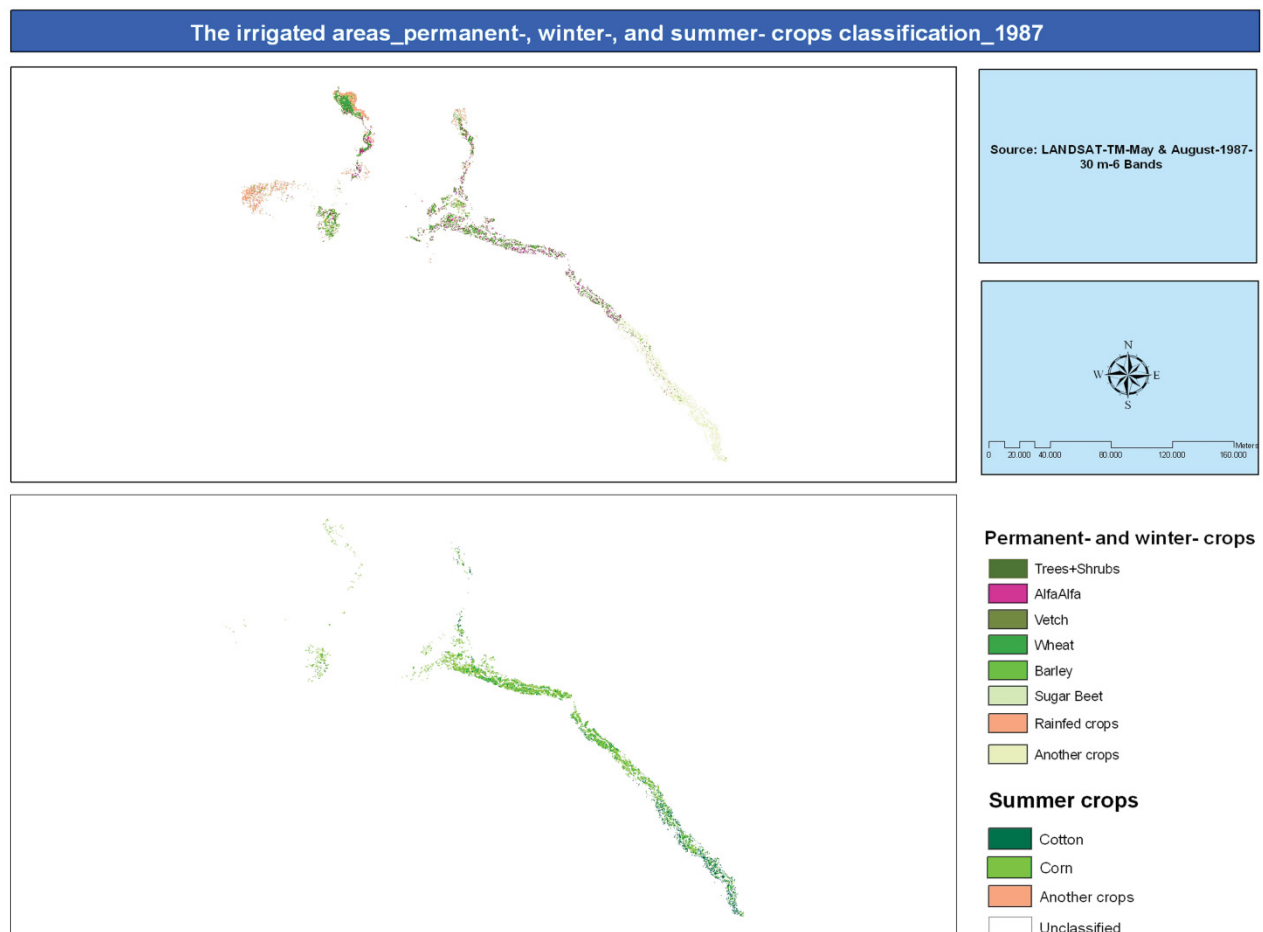


Fig. 6.7: The classification of the major permanent, winter and summer irrigated crops within the irrigation projects in the ERB for the data of LANDSAT-TM acquired in May and August 1987

**TERRA-ASTER-May-2005 data fused with LANDSAT-ETM+-May-2005 data.** There was no negative or positive impact for using thermal spectral and panchromatic bands on the spectral discrimination and the separation between various crops, trees and other surface features in the study area. Therefore, they were dispensed in the automated classification, especially, the panchromatic bands, to decrease the time of classification. Hence, participation of these bands became a negative factor regarding to the time taken required for classification.

An error was also detected in classifying some constructional areas as well as some limited areas from the bare areas considered as fallow lands (Fig. 6.8).

Sugar beet was perfectly classified. Other crops classes were broken in form of lines among fields, either in the shape of trees, shrubs, bushes and fences, or as natural plants and crop residues.

The spectral mixture between wheat and barley was found mostly in the higher areas of the ERB (fortunately, the cultivation of irrigated barley is rare here), while further down the basin in the

Deir Azzour governorate, the spectral separation ratio was reported as good because the majority of irrigated barley is a pastoral barley.

There was no large difference in the spectral separability and discrimination between the various agrarian crops in areas featuring irrigation projects and large, organized fields, either using the TM-data with spectral resolution of six bands and spatial resolution of 30 m, or the ASTER/ETM+-data with the same spectral resolution and a higher spatial resolution of 15 m. There was also no significance in obtaining or using sensory data of larger spatial resolution than 30 m; consequently, the negatives of this were the increases in time, cost and effort. The ASTER-data with the spectral resolution of three bands and a spatial resolution of 15 m were tried on large area fields, and the outcomes of spectral separability and classification were compared with data outcomes of the TM/6-bands/30 m. The result was that the high spatial resolution 15 m could be dispensed with, without lowering the spectral separability among crops.

However, a high spatial resolution data, such as ASTER/ETM+-15m, was found to be beneficial when studying ancient and tiny agrarian areas, such as those centred along the banks of the Euphrates (from the Euphrates Dam near the city of Athawra to the border with Iraq). For this kind of research, it may even be preferable to use even higher spatial resolution while preserving the six spectral bands.

***TERRA-ASTER-August-2005 data fused with LANDSAT-ETM+-August-2005 data.*** The appearance of fruit, poplar and other trees within dwelling areas and their margins were seen in a better and clearer way on satellite images acquired during summer (August) (Fig. 6.8) in contrast to those images acquired in April and May. There was a severe decline in the spectral properties of forest trees that previously existed in multiple places along the banks of Lake Al-Asad and the Euphrates River, in favour of the power and superiority of the spectral reflectance of light soil. This is due to the lowering of moisture and the dryness of the green mass of the forest trees (some are even crusty), in addition to an increase in sunshine levels.

The appearance of fields within the irrigated agriculture projects in very light colours made them look as if they were bare areas, while they were in fact wheat and barley fields seen after harvest (covered by the green mass of ex-crops that remains a very light yellow colour). These fields had been left for grazing purposes or the residue would be collected for use as hay during winter. In summer, these fields appeared after harvesting as a black colour as if they were water surfaces because of the residue left after burning. Here, the importance of the analyst's role in knowing his or her study area is important.

The third appearance the wheat and barley fields after harvesting was in a form in which the dry yellow remains of green mass (straw) of the two crops interacted with several kinds of natural plants that grew in these fields, benefitting from the remaining soil moisture. This occurred when the fields were not tilled. This field shape had a negative impact on summer crops classification, as the growing natural plants have a high vegetarian intensity, high vital mass and similar spectral behaviour as the some of the summer crops' spectral response. These fields were classified as fallow.

The cultivation of trees for agriculture purposes was centred in particular within the irrigation projects (especially poplar trees), in addition to their distribution along the main streets, between the agrarian fields (as separators between the fields or as wind barriers), and along some irrigation canals that were largely within the irrigation projects or reclaimed lands. This also related to the agriculture of forest trees (pine and cypress) in particular on Lake Al-Asad's banks.

Aquatic plants appeared clearly and were distributed more evidently within the August coverage in contrast to May, either in the Euphrates River waters (mosses were seen in shallower locations) or within prevailing swamps stretching out along the river, where the deserted river elbowed. These were seen along the river's bank in an almost continuous linear way. Climatic factors played a fundamental role in this by providing moisture and temperature elements, with the ratio of aquatic

plants increasing in August due to the high number of sun accelerating the growth and density of the plants.

The increase of variation and differentiation in reflectance and in the spectral behaviour of plants (crops and trees) within the coverage period of August was greater than that found in the May data.

Grapevine lands were classified under the orchard class. This was a new type of agriculture cultivation in the study area, which started at the beginning of this present decade in limited areas.

The appearance of some tree-lands (especially, the orchards) on satellite images is unclear, although these areas were irrigated and took on a regular and organized engineering shape. This was because of the disproportion among adapted distances in the cultivation of trees and their spacing from each other, and the available spatial resolution of the used remotely sensed data. They were in most cases classified as fallow or sometimes as a type of crop, although not to tree class.

The problem of classifying poplar trees was represented in that a land plot may be planted with trees of differing ages. Additionally, permanent cutting of part of these trees to be used in the paper, pulp and wood industry led to a mixture in classification from poplar trees to fallow. The problem lay not in how to separate these areas spectrally but in spatial separation resulted in continuous alternation between the two classes within small spatial areas, which allowed some errors to occur in evaluation and the calculation of distribution area. The spatial resolution of the available remotely sensed data did not have the ability to represent this alternation and introduce the spatial boundaries to separate the two classes.

This coverage was found to be the best for separation between the uncultivated areas and the fallow areas.

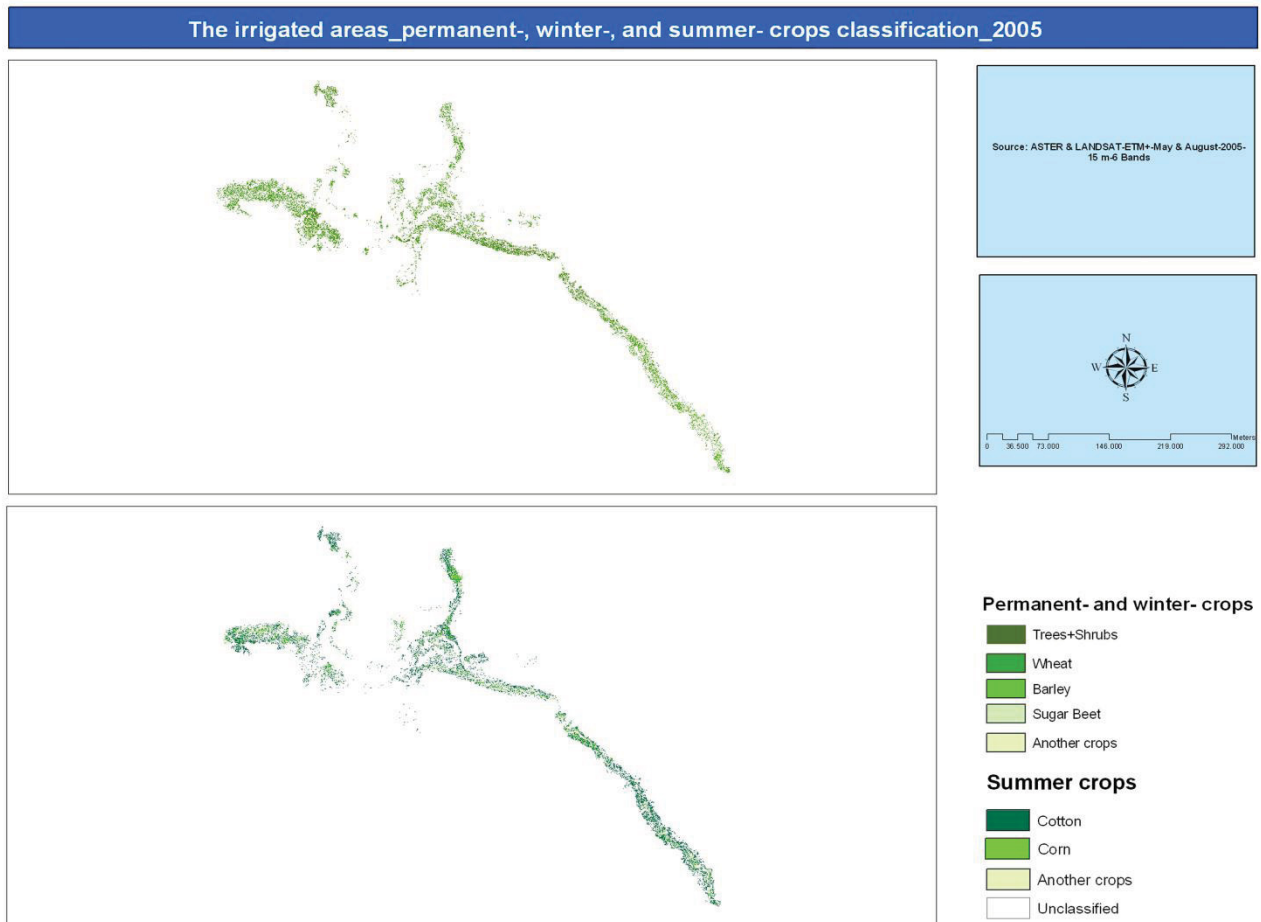


Fig. 6.8: The classification of the major permanent, winter and summer irrigated crops within the irrigation projects in the ERB for the data of TERRA-ASTER and LANDSAT-ETM+ acquired in May and August (2005)

**LANDSAT-TM-August-2007 data.** Sand storms emerged on the August data, which caused great changes in the spectral characteristics of the elements that needed to be classified. This impact was on p172r035 acquired in 07.08.07 along the extended area between Arraqqa and Deir Azzour. It was noticed that in the past years within the irrigation projects (for instance, the previously referenced project of 21,000 hectares), the cultivated areas with specific crops were significantly smaller (Fig.6.9) in contrast to the beginning of these projects' establishment and for long periods, where regular agricultural policies were followed. The reason for this is likely to be that the governmental foundations who established the projects have since transferred management of the projects in favour of the farmers, who are not, in turn, committed to any agrarian policy and rotations accredited by the Ministry of Agriculture. This matter had a critically negative impact on the crops' classification using available data. The spatial resolution became less effective because of the limited area specified for the various crops' cultivation. This was the same negative impact in consideration to the spectral factor, because of the increase in the types of crops seen in this area (possibility of setting two comparative scenes of 1987 and 2007).

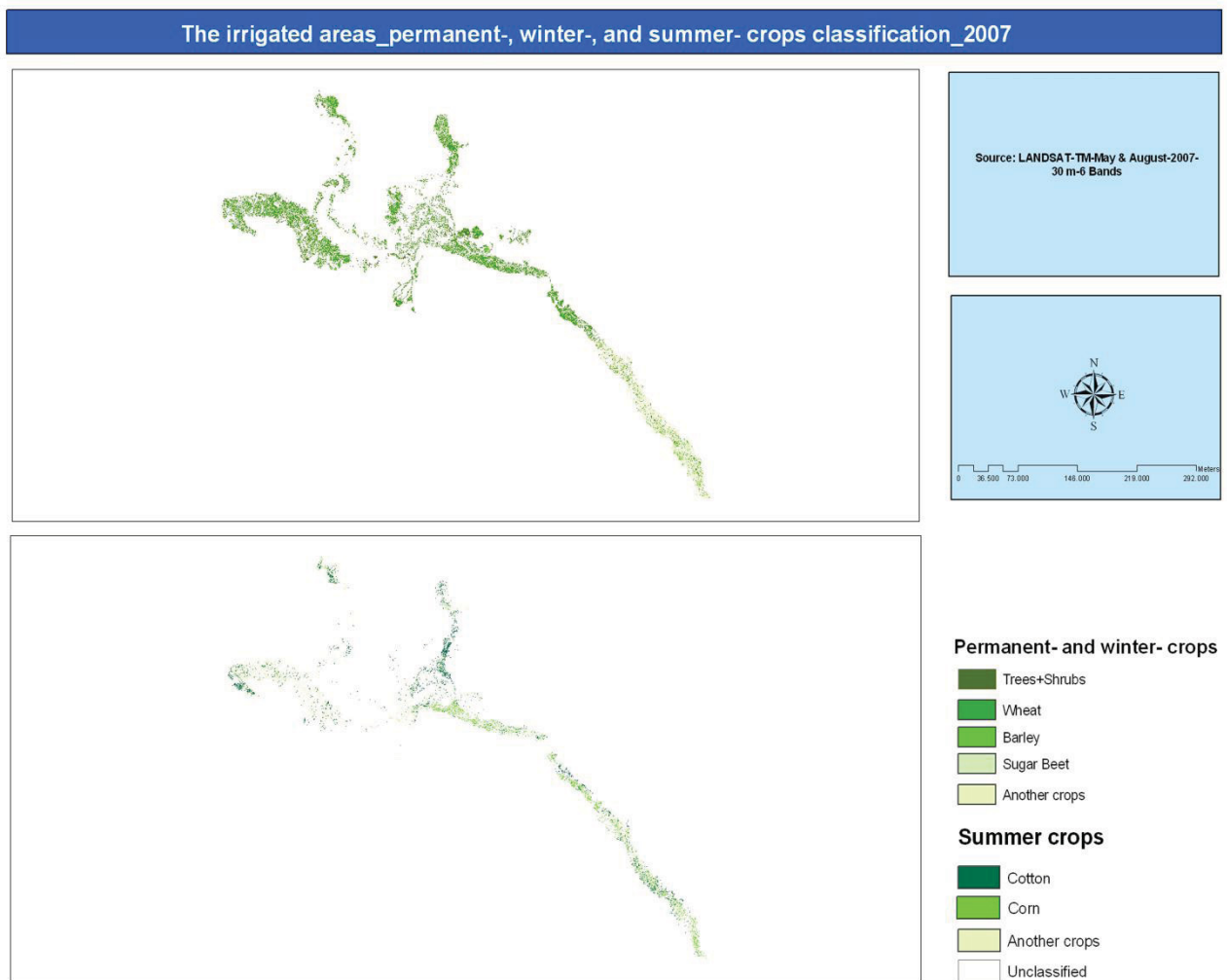


Fig. 6.9: The classification of the major permanent, winter, and summer irrigated crops within the irrigation projects in the ERB for the data of LANDSAT-TM acquired in May and August 2007

Table 6.4 presents the areas rates of the three broad existing classes (cultivated areas, uncultivated areas, and water) and the various agricultural features (permanent-, winter-, and summer- crops) within each adapted irrigation project borders for the time periods 1975, 1987, 2005, and 2007. Finally, this table presents the total area of each above mentioned class within the whole adapted borders of the different irrigation projects for the same four time periods (see too Table 6.2 and Table 6.3).

Table 6.4: The areas rates of the three wide existing general classes and the various agriculture features based on the individual 16-irrigated projects level

	Cultivated Areas/ha	Permanent crops			Winter crops								Summer crops					Uncultivated Areas/h	Water/ha
	Total	Trees+ Shrubs	Alfalfa	T	Wheat	Barley	Sugar Beet	Vetch	Rain-fed-crops	Other crops	T	Fallow	Cotton	Corn	Other crops	T	Fallow	T	T
17000ha-project and the state farm 75	5	n	n	n	n	n	n	n	n	n	n	n	n	n	n	n	n	46325	0
1987	15648	800	767	1567	4359	2310	201	1026	2034	367	10297	3784	3453	311	20	3784	10297		
2005	23479	2565	0	2565	12904	673	8	0	0	2321	15906	5008	3966	1041	1	5008	15906		
2007	26367	4364	0	4364	12877	1033	116	0	0	2172	16198	5805	923	23	4859	5805	16198		
Al-Asad Lake Area 75	3175	n	n	n	n	n	n	n	n	n	n	n	n	n	n	n	n	37845	38124
1987	523	5	47	52	305	0	0	8	1	19	333	138	105	3	30	138	333		
2005	4544	462	0	462	2412	193	25	0	0	3	2633	1449	1167	144	138	1449	2633		
2007	7865	2490	0	2490	3030	513	27	0	0	754	4324	1051	267	118	666	1051	4324		
AL-Balikh Basin Beer Al-Hishm section 75	164	n	n	n	n	n	n	n	n	n	n	n	n	n	n	n	n	24909	0
1987	6518	0	492	492	1306	1204	8	651	1733	2	4904	1122	1010	62	50	1122	4904		
2005	10015	313	0	313	4633	207	124	0	0	82	5046	4656	3748	905	3	4656	5046		
2007	8584	338	0	338	5060	272	39	0	0	74	5445	2801	1365	22	1414	2801	5445		
Al-Balikh Basin Lower mean canal section 75	8174	n	n	n	n	n	n	n	n	n	n	n	n	n	n	n	n	21771	10
1987	2759	0	1	1	1000	35	14	29	163	92	1333	1425	783	567	75	1425	1333		
2005	15067	184	0	184	4949	648	57	0	0	0	5654	9229	7561	1654	14	9229	5654		
2007	11124	643	0	643	4408	132	28	0	0	71	4639	5842	3331	447	2064	5842	4639		
Al-Balikh Basin section-2 75	8924	n	n	n	n	n	n	n	n	n	n	n	n	n	n	n	n	45373	197
1987	16674	34	1165	1199	2955	0	0	0	64	175	3194	12281	5089	1150	42	6281	9194		
2005	14146	1152	0	1152	3927	543	271	0	0	0	4741	8253	6534	1074	645	8253	4741		
2007	17268	1715	0	1715	9754	1287	98	0	0	11	11150	4403	1465	1449	1489	4403	11150		
Al-Balikh Basin section-3-Western 75	0	n	n	n	n	n	n	n	n	n	n	n	n	n	n	n	n	2174	0
1987	252	0	57	57	60	2	0	12	17	0	91	104	95	9	0	104	91		
2005	567	16	0	16	332	29	15	0	0	0	376	175	181	3	0	184	367		
2007	924	32	0	32	532	66	2	0	0	37	637	255	45	0	210	255	637		
Al-Balikh Basin section-3 Mlihan and Aadman area 75	0	n	n	n	n	n	n	n	n	n	n	n	n	n	n	n	n	46599	0
1987	35	0	16	16	0	0	0	0	11	8	19	0	0	0	0	0	19		
2005	2159	17	0	17	1651	197	7	0	0	0	1855	287	285	2	0	287	1855		
2007	3749	617	0	617	3058	42	0	0	0	0	3100	32	32	0	0	32	3100		
Al-Balikh Basin section-4 75	168	n	n	n	n	n	n	n	n	n	n	n	n	n	n	n	n	86564	0
1987	144	0	28	28	5	0	0	0	78	1	84	32	0	0	32	32	84		
2005	6552	51	0	51	3790	88	8	0	0	2	3888	2613	1908	705	0	2613	3888		
2007	13997	800	0	800	10637	1173	121	0	0	117	12048	1149	498	2	649	1149	12048		
Al-Balikh Ba-	15990	n	n	n	n	n	n	n	n	n	n	n	n	n	n	n	n	38897	86



<b>sin_sections-5 and 6 75</b>																			
<b>1987</b>	13040	23	1810	1833	4637	48	549	5	4302	297	9838	1369	594	742	33	1369	9838		
<b>2005</b>	25488	290	0	290	8732	733	139	0	0	10	9614	15584	10918	4654	12	15584	9605		
<b>2007</b>	28909	1436	0	1436	14868	1821	210	0	0	497	17396	10077	6135	334	3608	10077	17396		
<b>Arraed project 75</b>	11735	n	n	n	n	n	n	n	n	n	n	n	n	n	n	n	n	38907	135
<b>1987</b>	20243	186	2808	2994	6156	480	113	278	1397	113	8537	8712	7484	1105	123	8712	8537		
<b>2005</b>	20194	2396	0	2396	6960	1003	1434	0	0	94	9491	8307	7113	888	306	8307	9491		
<b>2007</b>	20505	3355	0	3355	10226	394	107	0	0	614	11341	5809	1553	837	3419	5809	11341		
<b>Arrusafa area 75</b>	2914	n	n	n	n	n	n	n	n	n	n	n	n	n	n	n	n	23958	7
<b>1987</b>	1510	2	344	346	589	2	1	173	86	76	927	237	212	2	23	237	927		
<b>2005</b>	7262	455	0	455	4836	167	70	0	0	0	5073	1734	1543	80	111	1734	5073		
<b>2007</b>	10572	1257	0	1257	7502	268	44	0	0	20	7834	1481	371	111	999	1481	7834		
<b>Lower Euphrates 75</b>	124523	n	n	n	n	n	n	n	n	n	n	n	n	n	n	n	n	63237	3460
<b>1987</b>	109194	29	4812	4841	6599	0	2	0	3	37218	43822	60531	27706	25236	7589	60531	43822		
<b>2005</b>	109384	7303	0	7303	23125	12162	3791	0	0	1?	39078	63003	47166	6613	9224	63003	39078		
<b>2007</b>	119115	3577	0	3577	20016	6347	461	0	0	49234	76058	39480	9750	13901	15829	39480	76058		
<b>Maskana east 75</b>	0	n	n	n	n	n	n	n	n	n	n	n	n	n	n	n	n	28836	0
<b>1987</b>	286	0	0	0	0	5	0	0	18	0	23	263	0	0	263	263	23		
<b>2005</b>	12836	654	0	654	7509	169	0	0	0	59	7737	4445	3331	1114	0	4445	7737		
<b>2007</b>	19816	434	0	434	13523	1085	40	0	0	70	14718	4664	1131	6	3527	4664	14718		
<b>Maskana west 75</b>	0	n	n	n	n	n	n	n	n	n	n	n	n	n	n	n	n	84258	0
<b>1987</b>	18885	15	666	681	476	468	814	6	16077	147	17988	216	190	2	24	216	17988		
<b>2005</b>	56625	504	0	504	26363	1251	70	0	0	618	28302	27819	20434	7371	14	27819	28302		
<b>2007</b>	62205	2500	0	2500	35866	440	335	0	0	510	37151	22554	5763	418	16373	22554	37151		
<b>Middle Euphrates right and left Bank 75</b>	41514	n	n	n	n	n	n	n	n	n	n	n	n	n	n	n	n	6680	2457
<b>1987</b>	44753	153	5810	5963	10930	4	31	21	66	421	11473	27317	19400	4323	3594	27317	11473		
<b>2005</b>	40035	7796	0	7796	12008	731	1630	0	0	0	14369	17870	10154	2906	4810	17870	14369		
<b>2007</b>	33983	1081	0	1081	20205	775	145	0	0	76	21201	11701	1553	7584	2564	11701	21201		
<b>Upper Euphrates 75</b>	25180	n	n	n	n	n	n	n	n	n	n	n	n	n	n	n	n	53618	7602
<b>1987</b>	33488	886	3739	4625	13695	341	607	115	11589	552	26899	1964	1758	6	200	1964	26899		
<b>2005</b>	23107	2004	0	2004	7619	617	26	0	0	32	8294	12809	10308	2032	469	12809	8294		
<b>2007</b>	29834	2322	0	2322	16686	512	22	0	0	1218	18438	9074	3279	232	5563	9074	18438		
<b>Sum 1975</b>	249681	n	n	n	n	n	n	n	n	n	n	n	n	n	n	n	n	673992	52030
<b>Sum 1987</b>	301517	2137	23608	25745	53013	4902	2349	2328	37707	39495	139794	135978	67881	33519	10568	111968	189549	607925	65980
<b>Sum 2005</b>	458288	26148	0	26148	131881	19423	7683	0	0	3224	162211	269929	136392	31198	15744	183334	274954	430129	87284
<b>Sum 2007</b>	596612	27206	0	27206	188688	16299	1803	0	0	55504	262294	307112	37475	25481	63251	126207	470405	294633	84347

## B. Accuracy assessment comparisons

Table 6.5 shows the final comparison between the various accuracies of classification results. There was no classification achieved for the class/es with no accuracy value/s (e.g., alfalfa was included in the coverage of 1987 under broadly cultivated, but later the cultivated alfalfa areas were very small, thus it was included under the class of other crops). In general, the lower accuracies were made using MSS-data, while the higher were found by using ASTER-data fused with ETM+-data. Using TM-data, the accuracies were close. The greatest problems were found while classifying the artificial surfaces, especially by using MSS- and TM-2007- data. The classification accuracy of barley and corn was relatively slight. The details of these classification problems were discussed for each LULC-class and for each used remotely sensed data in C6.A.1, .2, and .3.

Table 6.5: The final overall accuracy of classification results of the general classes, the irrigated areas and the agricultural features (permanent, winter and summer), using various remote sensing data (LANDSAT: MSS and TM; and TERRA: ASTER fused with LANDSAT: ETM+) for the years 1975, 1987, 2005 and 2007)

			MSS- 1975	TM- 1987	ASTER and ETM+ - 2005	TM- 2007
<b>Irrigated Areas</b>			82%	93%	94%	92%
<b>Cultivated Areas</b>			82%	93%	94%	92%
	Trees + Shrubs		-	91%	92%	90%
	Herbaceous (per- manent- and winter- crops)		-	87%	85%	85%
		Alfalfa	-	89%	-	-
		Vetch	-	79%	-	-
		Wheat	-	82%	84%	83%
		Barley	-	71%	74%	73%
		Sugar Beet	-	89%	88%	91%
		Rain-fed crops	-	93%	-	-
		Other crops	-	88%	86%	84%
	Fallow		-	96%	97%	95%
	Herbaceous (sum- mer- crops)		-	89%	87%	86%
		Cotton	-	84%	87%	86%
		Corn	-	74%	78%	76%
		Other crops	-	82%	85%	78%
	Fallow		-	87%	86%	83%
<b>Uncultivated Areas</b>			79%	87%	90%	88%
	Natural Vegetation		60%	67%	73%	63%
	Artificial Surfaces		40%	81%	77%	65%
	Bare Areas		67%	88%	91%	83%
<b>Water</b>			79%	92%	89%	77%

For evaluation of the change detection products, for instance, Macleod and Congalton (1998) proposed an adjusted change detection mapping products method for evaluating their accuracy. This process is based on Congalton (1991) and requires the regular confusion matrices to be applied on bi-temporal resulted change maps. These matrices can represent all combination classes of occurred change. A simplified no-change change matrix was also proposed.

The essential problem for assessing the accuracy of change detection products is the gathering of truth reference data, where the conditions of the initial time period (i.e., 1975) cannot be revisited as the land use has been significantly changed. Therefore, accuracy assessment depended on the remotely sensed data of the final time (i.e., 2007), in addition to ancillary data.

## C. LULC-change detection mapping

This section gives a historical view of the different LULC-features in the study area. It describes the rate of their changes over the last 32 years, in particular the irrigated agricultural lands. The results are essentially presented by maps, statistics/tables and graphs.

### 1. Pre-classification results

Each change detection process analysis/result, whether a pre-classification approach is used (in this section) or a post-classification approach (see C6.C.2), consisted of four major components, which were:

*Measure of changes/quantity.* This provided the quantity of the occurred change and measured the area/s of change/s to provide statistical numbers, i.e., how much was/were the change/s?

Pre-classification approach results (Fig. 6.10) were generalized but very effective in relation to estimating the occurred change on the cultivated areas, especially when these areas were vegetated and not fallow. The total change in the whole study area (5,062,082 ha, 100 %) between 1975 and 2007 was about 600,967 ha (11.93 %), in which 238,646 ha (4.74 %) was changed from natural vegetated areas to bare areas, and 362,321 ha (7.19 %) changed from bare areas to cultivated areas (especially to irrigated agriculture). Areas recording no change were about 4,461,115 ha, 88.62 %. In comparison, the results of the three previously-mentioned approaches generally changed classes with those that resulted from applying the post-classification approach (see C6.C.2), but for the duration 1987-2007 the total change in the whole study area was about 5,027,722 ha, 99.32 % in which 170,454 ha, 3.36 % changed from natural vegetated areas to bare areas; 263,863 ha, 5.21 % changed from bare areas to cultivated areas; and areas recording no change were about 34,360 ha (0.68 %).

*Nature of changes/quality.* This explained the quantity of the occurred change and whether it was positive/gain or negative/loss. In addition, the nature of change determined what LULC-feature/s was/were changing and to what (Braumoh, 2004).

Based on the visual interpretation of the change map for the period 1975-2007, in addition to information obtained during field-work, secondary data and related previous literature, it can be shown that the land use which changed the most was agriculture, which increased largely because of the construction of irrigation projects among the Euphrates River and on account of a reduction in areas classified as bare. The most new agricultural lands were seen in the region near the Euphrates. This was obvious especially in the area of land which extends from the city of Arraqqqa and the Euphrates Dam in the south toward the Turkish border (including the Al-Balikh tributary) in the north. In addition, the area located along the south bank of Lake Al-Asad and the lands located along the southern side of the major irrigation canal, which runs from Lake Al-Asad towards the city of Aleppo, also experienced significant agricultural growth.

There were also changes in vegetation cover within the lands of the five agricultural stabilization zone (the pastures). Fig. 6.10 describes the nature of changes in LULC from 1975-2007. The result can be determined through three categories: LULC- no change, which remained unchanged, i.e., no loss and no gain (neutral/zero); LULC- Natural Vegetation to Bare Area change, where the natural vegetation class area decreased to bare area in 2007, i.e., loss and no gain; and the LULC- Bare Areas to Cultivated Areas category, where the cultivated class area increased in 2007 on account of changes to the bare area, i.e., gain and no loss.

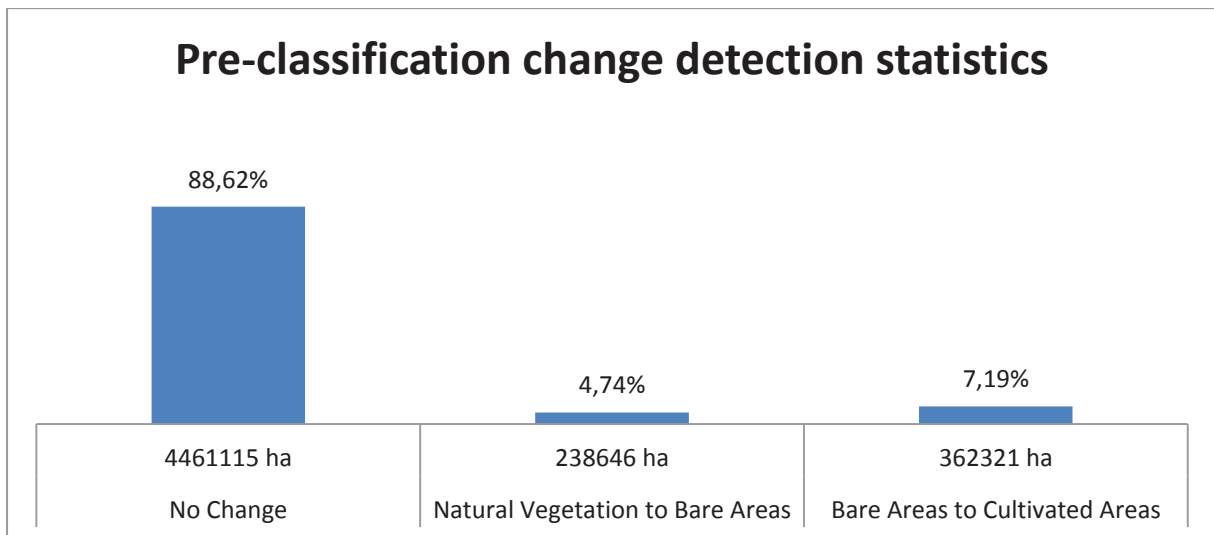


Fig. 6.10: Statistics of occurred changes in percentage and hectare, that resulted from applying the pre-classification approach using the data of LANDSAT-MSS from June-1975 and the data of LANDSAT-TM from August-2007

*Spatial distribution of changes/mapping.* This provided the clear location and extension of occurred change by mapping and visualizing the area/s of change/s to produce the thematic map/s, i.e., where was/were the change/s?

By differencing the raw data mosaic-image/LANDSAT-MSS-June-1975 (pixel gray values) of the initial comparison date from those of mosaic-image/LANDSAT-TM-August-2007, the distribution of the three general levels of LULC-changes of interest could be detected, calculated and mapped. ArcGIS 9.3 and ENVI 4.6 packages were used for this purpose. Fig. 6.11 visualizes the result of the changes.

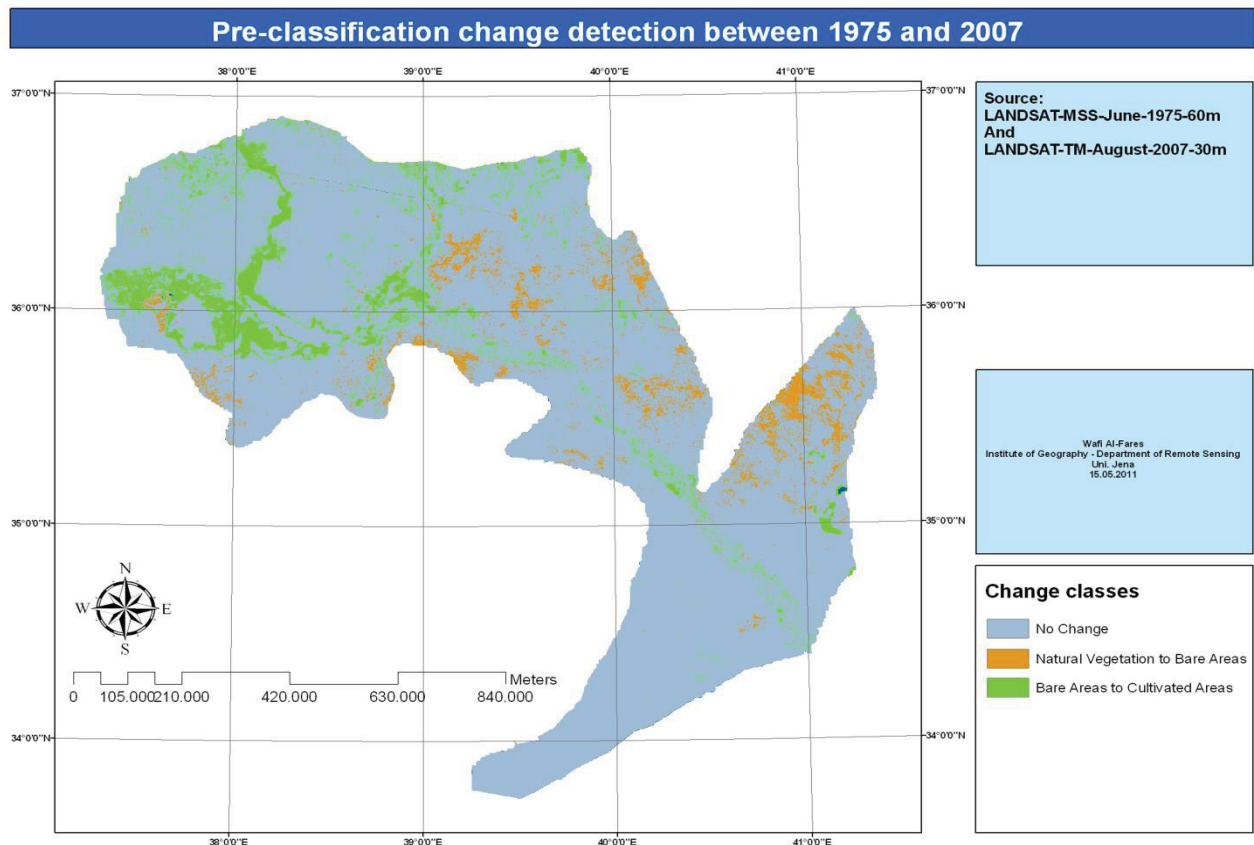


Fig. 6.11: The three wide major LULC-changes that resulted from applying the pre-classification change detection approach for the period (1975-2007)

*Evaluation of changes/accuracy.* This showed the accuracy of the produced change detection results by assessing the occurred errors which resulted from the adopted approach in change detection process and by using the general principle of the error matrix, i.e., How effective was the applied approach to detect the changes?

As the change classes are relatively general, it was possible to perform the accuracy visually using the remotely sensed data itself. Some 250, 200 and 150 testing points were automatically distributed (random-points) for the three resulted change classes respectively (i.e., no change, natural vegetation to bare areas, and bare areas to cultivated areas) over the resulted thematic map (Fig. 6.11). Then, the initial remotely sensed image, the final remotely sensed image and the resulted thematic map from the differencing process were geographically linked with each other. This was, of course, after the geographic registration (see C5.B.1). After that, came the manual step, where each point on the thematic map was compared to its land use/land cover in 1975 and again in 2007, using the visual interpretation of LANDSAT-MSS-June data and the LANDSAT-TM-August data. The point resulted change class (e.g., bare areas to cultivated) was found to be correct only when its use/s in both comparison dates (1975 and 2007) were compatible with the defined and resulted description of the change class. For example, it's the point resulted change class use in 1975 had to be as a bare area and then as a cultivated area in the year 2007. However, the thematic map that represented the change classes did not include all the possibilities of LULC-changes (e.g., cultivated areas to bare areas, etc.). Therefore, the class "other" was added for purposes of accuracy (i.e., the initial data), could be used to can represent the rest of the possibilities of the LULC-alternations between the two compared dates. The overall accuracy was 86 %. This method would be useful for assessment of the accuracy of change detection mapping, where it is almost impossible to gather ground and/or reference data for the relatively old dates.

Table 6.6: Accuracy assessment of pre-classification change detection approach results

Initial LANDSAT-MSS-data (1975)	Final LANDSAT-TM-data (2007)			Total/possible
	(1)	(2)	(3)	
No change (1)	230	21	7	258
Natural vegetation to bare areas (2)	13	155	4	172
Bare areas to cultivated areas (3)	3	8	132	143
Other (4)	4	16	7	27
<b>Total</b>	250	200	150	600
Overall pre-classification change detection accuracy = $230 + 155 + 132 / 600 = 86 \%$				

## 2. Post-classification results

*Measure of changes/quantity.* Post-classification approach results (Fig. 6.12, Fig. 6.13, Table 6.7, Table 6.8) were more obvious and detailed rather than those resulting from a pre-classification approach (see C6.C.1). The total change in the whole study area (5,062,082 ha, 100 %) between 1987 and 2007 was about 5,027,722 ha (99.32 %). Areas recording no changes were about 34,360 ha (0.68 %).

The greatest changes (Table 6.7, Fig. 6.12) were in the artificial surfaces classification with a total change of 83.16 %, in which 38.77 % was changed to cultivated areas and 35.08 % transformed to the bare areas class; natural vegetation with 68.33 %, where 42.95 % changed to cultivated areas and 24.00 % to bare areas; natural water-bodies with 21.45 %, where 13.34 % changed to cultivated areas; followed by cultivated areas with 17.86 %, of which about 6 % was changed to each of the other two classes, i.e., natural vegetation and bare areas. The bare areas class showed the most stability over time with 13.89 % change.

Three general trends in LULC-changes were found: negative values/loss, in which the represented classes were artificial surfaces (-64.81 %) and natural vegetation (-43.22 %); neutral value/stable, in which the represented class was bare areas (0.23 %); and positive values/gain, which included cultivated areas (+35.49 %) and natural water-bodies (+6.66%).

Table 6.7: LULC-change matrix (%) in the study area for 1987 and 2007

	Cultivated Areas	Natural Vegetation	Artificial Surfaces	Bare Areas	Natural Waterbodies	Class Total
Cultivated Areas	82.135	42.95	38.778	10.011	13.34	100
Natural Vegetation	6.59	31.667	4.556	2.775	0.041	100
Artificial Surfaces	1.945	0.019	16.831	0.641	2.86	100
Bare Areas	6.904	24.005	35.083	86.101	4.977	100
Natural Waterbodies	1.444	0.069	3.329	0.019	78.543	100
Class Changes	17.865	68.333	83.169	13.899	21.457	0
Image Difference	35.496	-43.228	-64.814	0.232	6.668	0

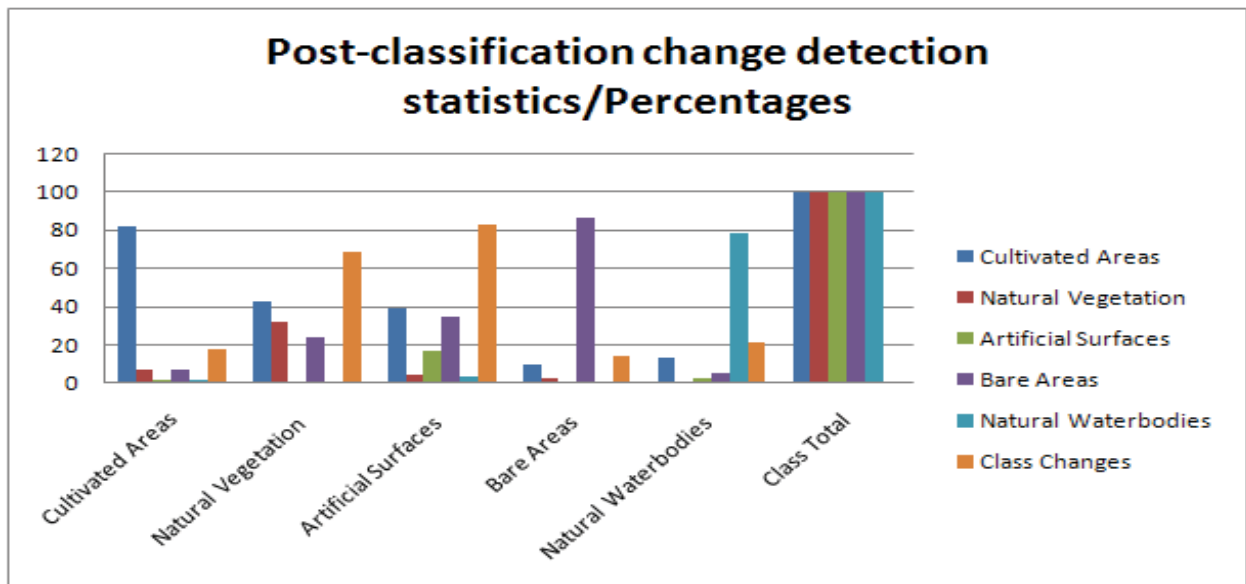


Fig. 6.12: Statistics of occurred changes in percentage which resulted from applying the post-classification approach using the data of LANDSAT-TM from May-1987 and the data of LANDSAT-TM from May-2007

Each LULC-class has three general trends (Table 6.8): 1) The stable trend, that represents the unchanged part of an individual class (e.g., cultivated areas: 1,080,987 ha) over the time period; 2) The positive trend (the horizontal direction in the change matrix), which represents the transform or gain from the other four LULC-classes (i.e., natural vegetation: 304,983 ha, artificial surfaces: 98,939 ha, bare areas: 263,863 ha, and the natural water-bodies: 13,703 ha) into an individual class such as cultivated lands. Therefore, the total areas of cultivation were 1,783,286 ha in 2007; and 3) The negative trend (the vertical direction in the change matrix), that represents the transformation or loss from an individual class (e.g., cultivated areas) into one or more of the other four LULC-classes (i.e., natural vegetation: 86,738 ha, artificial surfaces: 25,600 ha, bare areas: 90,864 ha, and natural water-bodies: 19,001 ha). Therefore, the total area of cultivation was 1,303,190 ha. The greatest difference was for the class of cultivated areas - 480,096 ha or +35.49%.

The state of the land use/land cover in 2007 was expressed in the following areas: cultivated (1,783,286 ha), natural vegetation (403,131 ha), artificial surfaces (89,772 ha), bare lands (2,641,953 ha), and natural water-bodies (109,580 ha).

Table 6.8: LULC-change matrix (hectares) in the study area for 1987 and 2007

	Cultivated Areas	Natural Vegetation	Artificial Surfaces	Bare Areas	Natural Waterbodies	Class Total
Cultivated Areas	1,080,987	304,983	98,939	263,863	13,703	1,783,286
Natural Vegetation	86,738	224,868	11,623	73,150	41	403,131
Artificial Surfaces	25,600	1,339	42,943	16,888	2,938	89,772
Bare Areas	90,864	170,454	89,510	2,269,485	5,112	2,641,953
Natural Waterbodies	19,001	486	8,493	503	80,687	109,580
Class Changes	235,129	485,222	212,196	366,344	22,043	0

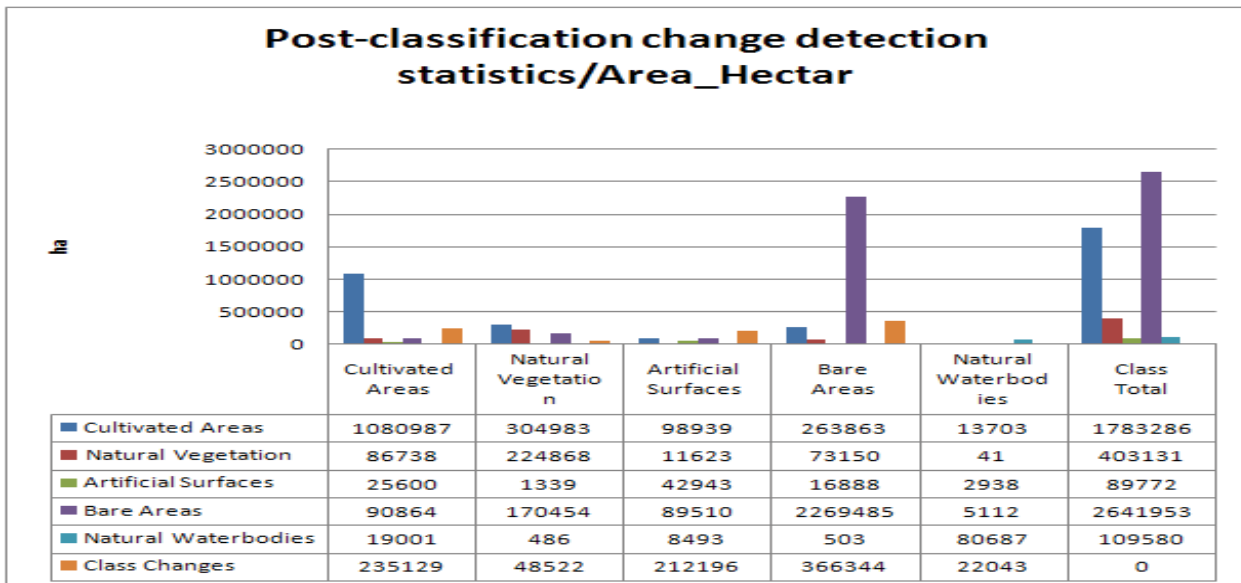


Fig. 6.13: Statistics of occurred changes in ha, that resulted from applying the post-classification approach using the data of LANDSAT-TM from May-1987 and the data of LANDSAT-TM from May-2007

*Nature of changes/quality.* For this purpose, the change matrix was generated (Table 6.7, Table 6.8) based on classified images from 1987 and 2007. It presented the nature of changes of the LULC-categories for the period 1987-2007. The results were defined by twentieth detailed combinations of the five general classes. Fig. 6.12 and Fig. 6.13 show the statistics describing the nature of LULC-changes for the period 1987-2007.

Results from the land cover change analysis, carried out from the post-classification approach, show that cultivated land increased from 1,080,987 ha in 1987 to 1,783,286 ha in 2007 on account of the transformed areas from natural vegetation, bare areas, artificial surfaces and natural waterbodies lands into managed terrestrial areas. The greatest mistake was in accounting the change value in artificial surfaces, especially based on the remotely sensed data obtained in 1987 (TM), since this approach was based on the classification results. These results were not efficient in classifying the artificial surfaces because the low spectral separability within the bare areas. However, what is important is that the artificial surfaces (especially the built-up areas) had little spectral mixture with the cultivated areas (especially fallow), since the greatest interest of this study is related to it. Also, it was possible to estimate the real artificial surfaces areas from the other two remotely sensed data gathered in 2005/ASTER-images fused with ETM+- images and 2007 (TM).

The change from cultivated to natural water-bodies can be explained, in addition to the errors in classification process that exist almost in every classified class. This was due to the changes in the water capacity (flooding) of the Euphrates in relation to the water allowed to enter to Syria from Turkey, and the natural conditions, such as the actual planted areas and the impacts of the climatic elements. It distributes nearly from the river-bed, especially in the upper-Euphrates (Fig. 6.14). The change from natural vegetation to cultivated areas can be explained because of the construc-

tion of the irrigation projects (e.g., the lands of Maskana-east and the 21,000 ha-project). This change-class was also found in the marginal lands northeast from Lake Al-Asad to the Al-Balikh surrounded areas, where some of these lands had been cultivated or sometimes left as uncultivated according to the availability of rains. The change into bare areas can interpreted as being due to the climatic factors (precipitation in particular), as most of these lands exist in the five agricultural stabilization zones (Al-Badia), i.e., to the east of the Al-Balikh River. The change from artificial surfaces to cultivated areas can be seen almost as a misclassification between the artificial surfaces (especially the dark appeared civilization areas) and the cultivated areas (the fallow on dark soils). The change into bare areas can be analyzed because of the misclassification between the dark appeared civilization areas (e.g., the cities) and the dark colored bare areas (e.g., the inactive volcanoes area in the east of Arraqa City), and the misclassification between the light appearing areas of artificial surfaces category (e.g., waste dumps and extraction sites) and the bare areas with light parent rocks or those that covered with shifting sands (e.g., dunes). The shift from bare areas to cultivated lands was because of the expansion in agriculture. Finally, the change of part of the water-bodies area into cultivated areas was because the misclassification of the TM-2007 final-data, where a dust-storm appeared over some river parts between the two cities of Arraqa and Deir Azzour, in addition to the drying of the swamps, which has left the river without some of its elbows (the abandoned elbows).

*Spatial distribution of changes/mapping.* This is illustrated by the thematic change map (Fig. 6.14) for the period 1987-2007. This thematic map was produced by overlaying the two LULC-classification results of the two dates, to locate, compute and map the spatial distribution of each change-type. The results were defined by twentieth detailed combinations of the five classified general classes, in addition to the class of (no change), i.e., it presents 21-classes of changes. Fig. 6.14 visualizes the results of the changes.

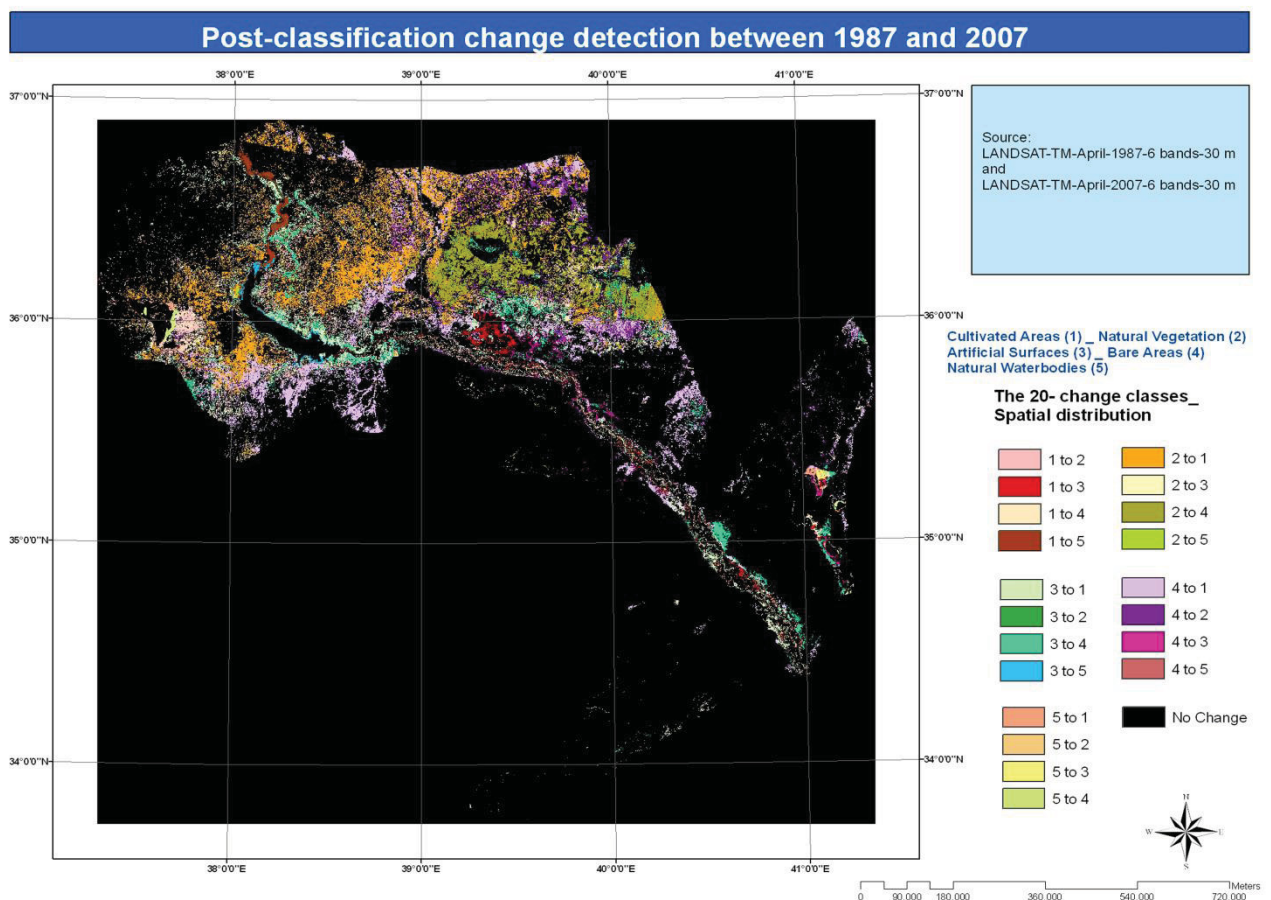


Fig. 6.14: The 21-detailed LULC-changes that resulted from applying the post-classification change detection approach for the period 1987-2007



*Evaluation of changes/accuracy.* Some 15 to 99 testing points for each change combination were distributed, i.e., 1,163 in total (Table 6.9), automatically (random-points), for the twentieth resulted change combinations classes, over the resulted thematic map (Fig. 6.14). The overall accuracy was 83 %, i.e., lesser than those resulted using the pre-classification approach (86 %) (see C6.C.1). There were two major reasons. The first was because of the misclassification of the five general LULC-classes of interest, especially between the artificial surfaces and the bare areas, and the second was due to the pre-classification approach being limited to only three wide general change possibilities in contrast to the post-classification approach, that had twentieth one change possibilities to be tested.

Table 6.9: Accuracy assessment of post-classification change detection approach results

Initial LANDSAT-TM-data (1987)	Final LANDSAT-TM-data (2007)																				Total/possible	
	12	13	14	15	21	23	24	25	31	32	34	35	41	42	43	45	51	52	53	54		N
<b>1 to 2</b>	49	0	1	0	2	1	1	0	0	1	3	0	0	0	2	0	0	0	0	2	62	
<b>1 to 3</b>	2	65	1	0	1	1	0	0	0	0	0	0	0	0	0	0	0	0	0	0	70	
<b>1 to 4</b>	0	0	53	0	0	3	0	0	0	0	0	2	3	0	0	0	1	0	0	1	63	
<b>1 to 5</b>	0	0	0	51	1	4	0	0	0	0	0	1	4	0	0	0	0	0	0	0	61	
<b>2 to 1</b>	1	2	0	3	87	0	0	0	0	0	0	0	0	2	0	2	0	0	0	2	99	
<b>2 to 3</b>	3	1	0	4	0	41	2	0	0	2	0	0	0	0	0	0	0	0	0	0	53	
<b>2 to 4</b>	0	3	0	1	0	1	79	0	0	0	0	0	0	0	0	0	0	0	0	0	84	
<b>2 to 5</b>	0	0	2	0	0	0	4	39	0	0	0	0	0	0	0	0	0	0	0	0	45	
<b>3 to 1</b>	0	0	0	0	0	0	0	0	40	0	0	0	0	0	0	0	0	0	0	0	40	
<b>3 to 2</b>	1	0	0	0	0	0	0	0	0	37	0	0	0	1	0	0	0	2	0	0	41	
<b>3 to 4</b>	0	0	0	0	0	0	0	0	0	0	85	1	0	0	0	0	0	0	3	0	89	
<b>3 to 5</b>	0	0	0	5	2	0	0	0	0	0	0	27	3	1	0	0	0	0	4	0	42	
<b>4 to 1</b>	4	0	0	0	3	0	2	0	0	0	0	1	66	1	1	0	0	0	0	0	78	
<b>4 to 2</b>	2	0	0	1	0	0	0	3	1	0	0	1	0	67	0	0	0	0	0	0	75	
<b>4 to 3</b>	0	0	0	0	0	0	0	4	1	0	2	2	0	0	25	0	0	2	0	0	36	
<b>4 to 5</b>	0	0	0	0	1	0	0	2	2	0	1	0	0	0	1	19	0	0	0	0	26	
<b>5 to 1</b>	0	0	0	2	0	0	0	1	0	0	0	0	2	0	0	2	17	0	0	0	24	
<b>5 to 2</b>	0	0	0	0	1	0	0	1	0	0	0	0	2	0	0	0	9	0	0	0	13	
<b>5 to 3</b>	0	3	0	0	0	3	0	0	0	0	0	0	1	3	0	0	0	2	8	0	20	
<b>5 to 4</b>	0	0	0	0	0	1	0	0	0	0	0	0	2	2	1	0	0	0	0	11	17	
<b>No Change</b>	3	0	1	0	1	0	0	0	0	0	2	0	0	2	0	1	0	0	1	0	102	
<b>Other</b>	0	1	2	3	0	0	2	0	1	0	2	0	2	1	0	1	2	0	3	0	23	
<b>Total</b>	65	75	60	70	99	55	90	50	45	40	95	35	85	80	30	25	20	15	15	15	99	1,163
Overall post-classification change detection accuracy = 49 + 65 + 53 + 51 + 87 + 41 + 79 + 39 + 40 + 37 + 85 + 27 + 66 + 67 + 25 + 19 + 17 + 9 + 8 + 11 + 91 / 1,163 = 83 %																						

## ***Chapter 7: Summary, concluding remarks and recommendations***

### **A. Summary**

The overall and general objective of this thesis is as a contribution to the use of remotely sensed data of LANDSAT: MSS, TM, and ETM+; and ASTER for agricultural purposes in the arid and semi-arid areas of the Euphrates River Basin (ERB) in Syria. The study area is located in the northeast of Syria. The geographical coordinates of the ERB are 36°49'N, 38°02'E at the Turkish border, and 34°29'N, 40°56'E at the Iraqi border. Its total area is about 50,335 km<sup>2</sup>. Starting in the 1970s, Syria began to utilize the water of Euphrates River in agriculture, reclaiming a large amount of uncultivated areas from the river. The main objective of this program was to increase the amount of cultivated areas in the basin, as Syria basically is an agricultural country. These irrigation projects during the past four decades produced a great deal of change in land use/land cover (LULC).

This thesis deals with four major emphases LULC-classification, LULC-change detection, irrigation mapping and irrigated agriculture classification of the Euphrates River Basin area in Syria. Four general LULC-classification products (see C6.A.1) have been generated for the years 1975, 1987, 2005 and 2007; also, two LULC-change detection maps (see C6.C) have been produced for the periods between 1975-2007 and 1987-2007. In addition, four thematic maps representing the development of the irrigation areas (see C5.A.2) in the last 37 years with the intervals 1975, 1987, 2005 and 2007 have also been produced. Finally, six detailed agricultural classes classification products (see C5.A.3) have been generated for the two major agricultural seasons in Syria, i.e., the winters (May data) and summers (August data) of 1987, 2005 and 2007.

To realize the objective of this study, eight scenes of LANDSAT-MSS obtained in June 1975 were chosen; 32 scenes of LANDSAT-TM obtained in May and August of the years 1987 and 2007; and 16 scenes of corrected LANDSAT-ETM+/SLC-OFF/ obtained in May and August 2005 which were fused with scenes of TERRA-ASTER obtained in May and August of 2005 in a bid to increase spectral resolution from three to six spectral bands.

Remote sensing techniques were approved and applied on the remotely sensed data (see C4.A) of 1975, 1987, 2005 and 2007 for the four major emphases (LULC-classification, LULC-change detection, irrigation mapping, and irrigated agriculture classification). There were no known determined adopted techniques that could be directly applied for the emphases. Therefore, it was necessary to set suitable methods that would be compatible with the used data, the thesis questions and the privacy of the study area environment. Most of the applied methods in this work were already recognized, some were modified and some were combined.

It is true that a lot of remotely sensed data and some processing programs are becoming more and more accessible to researchers at little or no cost, but remotely sensed data processing and interpretation techniques are still time consuming and not suitable for all regions of the Earth at the same level of accuracy. It has been shown in this study that the geometric, atmospheric and radiometric correction processes (see C5.B) are not always necessary for each image, each sensor data and each date. Geometric correction processes, especially for the geometric registration, were not difficult and were achieved at very high accuracies. However, atmospheric correction was impossible for the relatively old data (MSS-1975), where the weather parameters were difficult to obtain. Radiometric correction was applicable for all data, but this did not mean that it produced suitable results for the whole dataset. Therefore, when neither the raw data or the enhanced data after applying the atmospheric and/or the radiometric corrections gave good results (especially for use in mosaicing), then the data were processed and classified separately, i.e., each image alone. ATCOR-2 was used for atmospheric correction, while iMAD was used for radiometric correction. Both applications were relatively easy to use and required no additional external information. The-

se programs were found to give better results than those methods that are time consuming and needed more external data such as MFF and 6S (Chavez, 1996).

Where the results of the classifications were cartographic products, all spatial data were standardized, and were transformed and geometrically corrected to a general reference system: a UTM-projection of Zone 37 N with the international general ellipsoid/spheroid WGS84 and datum WGS84.

Geometric correction, geo-referencing and geometric registration formed the basis for mosaicing more than one image (see C5.B.5) for fusion of different remotely sensed data, i.e., the ASTER-data were fused with LANDSAT-ETM+-data (see C5.B.4) for detection of changes (see C5.L).

Precise mosaicing was very important for further remotely sensed data processing and interpretation (e.g., classification, change detection, etc.). The general algorithms of imagery mosaicing were not always able to produce a one mosaic-image with a consistent appearance in which the values of the histograms of each image were combined together in one mosaic-image. This gave an unsuitable presentation of the various LULC-features on the mosaic-image. In these situations, the MAD-technique was applied to satisfy a radiometric consistent mosaic. This was a comfortable relative radiometric calibration technique that built a data calibration with linear values as gain and offset coefficients as unnecessary. This technique had the robust advantage of the ability to create a scene comparison even though values were not available or wrong.

The international hierarchical classification scheme (LCCS) of FAO was followed as guide in the classification processes. This approach defined and determined the LULC-classes to be included in the classification/s. These classes were defined before starting each automated supervised classification procedure.

The classification of the remotely sensed data was based on the traditional pixel-based classification method. The results of classifications were always presented as thematic maps. The results of the various tested approaches and algorithms of classification on the various obtained remote sensing data were interpreted based on the accuracy assessment method.

In this study, several automated classification approaches (i.e., one-step, and multi-stage classification) and several algorithms (i.e., MLC, NN, and SVM) were tested on several remote sensing data (LANDSAT: MSS, and TM; TERRA: ASTER fused with corrected LANDSAT-ETM+/SLC-OFF/), to find the optimized approach and algorithm. The multi stage classification approach and the MLC-algorithm harvested the best results (see C5.G).

The classification of coarse resolution (spatial and spectral) data like LANDSAT-MSS in relation to its geographical location of ERB, was suitable to produce thematic maps of the five wide general classes for the whole large area of the ERB and to represent the spatial distribution of the one irrigated areas class. These data had not the ability to classify any more detailed classification level (e.g., agriculture). LANDSAT-TM data were more suitable for classifying the general classes and the irrigated areas. However, it was less suitable for classifying the detailed agricultural classes. Finally, the low spectral resolution ASTER-data of only three bands was less suitable in comparison to TM-data, although they had a higher spatial resolution, i.e., 15 m. However, after fusing them with the LANDSAT-ETM+/SLC-OFF/ corrected data to increase the spectral bands to six bands, these data harvested the best results. In general, the classification of the agricultural features using TM and ASTER-ETM+ data was very good over the State achieved irrigation projects (e.g., the 21,000 ha project, Maskana-East, etc.), where the individual planted fields were relatively large and thus classifiable in regard to the used remote sensing data, and the diversity in LULC-features was small. These were changed starting from the TM-data of 2007, where the fields became smaller and the diversity of planted agricultural types became more widespread. The diversity was acceptable over the State and farmer-cultivated irrigation areas (e.g., Maskana-West), where the private holdings were varied from small fields to very large fields. However, the classi-

fication results were unacceptable over the very old cultivated areas located on the Euphrates River banks, where the holdings were very small with great diversity in cultivated agricultural features. Therefore, this area requires remote sensing data with higher spatial and spectral resolution (e.g., IKONOS).

The classification of natural vegetation outside the irrigation areas in arid and semi-arid regions in Syria, especially in the fifth agricultural stabilization zone, was made difficult because of the dominant and variable soil signal (spectral response) (Huete et al., 1994). This was also true for the agricultural crops and trees (because of the relatively wide dimensions between the trees in relation to the spatial and spectral resolution of the used remotely sensed data), that were cultivated particularly in the third and fourth agricultural stabilization zones.

In this study, two approaches of change detection techniques were applied to almost all agricultural areas in the arid and semi-arid ERB-environment in Syria, to test the effectiveness of the two techniques in mapping the changes. The pre-classification change detection approach that was based on image differencing was very effective in mapping the change from bare areas to cultivated areas (the new irrigation projects) over the time period 1975-2007. The post-classification approach detected, mapped and defined 21 type of change. However, it offered a lower accuracy (83 %) rather than the first method (86 %), because it depended on the quality of already achieved classification and dealt with more types of change (21) rather than the first method (3). Therefore, it contradicted the assumption that this was the most accurate change detection approach (Mas, 1999). The two approaches were easy to interpret.

Based on the pre-classification change detection approach (see C6.C.1), there were three major trends of activities of land use/land cover: The first trend (no change) was stable and the most dominant with about 88.62 %. The second was negative, where as in most arid and semi-arid regions, the major cause of natural vegetation change to bare areas (4.74 %) was related to the climatic factor of precipitation, which is unstable and changes from one year to another. In addition the human factor of overgrazing must be taken into consideration. The largest area of natural vegetation exists in the fifth Agricultural Stable Zone (ASZ) which is made up of natural pastures. The third major driving force was positive because it accounted to a decrease in bare areas (7.19 %), where as in most developed countries, it was related to the activities of cultivation agriculture. These results were confirmed by applying the post-classification change detection approach (see C6.C.2), where the change value of natural vegetation was 68.33 %, in which 42.95 % was transformed to cultivated areas and 24 % transformed to bare areas, and the loss was at 43.22 %; the change value of cultivated areas was 17.86 %, and the gain was at 35.49 %. This was on account of the natural vegetation with 304,983 ha and bare areas with 263,863 ha. The change in bare areas was about 13.89 %, where 10.01 % transformed into cultivated areas, and the gain was only 0.23 %.

The major limitations of this study were the MSS-data of 1975 that were characterized by low spatial resolution of 60 \* 60 m and low spectral resolution of four bands. The corrected LANDSAT-ETM+/SLC-OFF/ data of 2005 that were fused with ASTER-data to increase their spectral resolution from three bands to six bands, were obtained after the applying a correction method from USGS. The time period lag between the remotely sensed data of the years 1975 and 1987, and the field-work in 2007 and 2009 limited the full usefulness of using the remotely sensed data, because it was very difficult to obtain the additional non-remotely sensed data (the ground reference data in particular), and the gathered ground reference data would only be partly suitable for some purposes. The study area was large with some locations inaccessible during field-work.

## **B. Concluding remarks**

The kernel of this study was whether, how and to what extent applying the various remotely sensed data that were used here, would be an effective approach to classify the historical and cur-

rent land use/land cover, to monitor the dynamics of land use/land cover during the last four decades, to map the development of the irrigation areas, and to classify the major strategic winter- and summer-irrigated agricultural crops in the study area of the ERB.

It is true that the development of remote sensing techniques focuses greatly on construction of new sensors with higher spatial and spectral resolution, but it is not possible to ignore the data of the older sensors (especially, the LANDSAT-mission) when the historical mapping of land use/land cover and monitoring of their dynamics are needed, although their low spatial and spectral resolution in comparison to the new sensors launched in the last decade (e.g., IKONOS) needs to be taken into consideration. These older sensors are still precious. To maintain the advantages of these sensors, researchers during the last five decades have developed new and more effective digital image processing and interpretation methods, to harvest more accurate results. Therefore, it is important to focus on the development of new and enhanced techniques that can translate the relationship between the general characteristics of the old acquired data and the specific characteristics of each individual environment such as the arid and semi-arid lands.

Regarding to field-work, this remains very important as a basis in most remote sensing applications, offering the training samples for supervised classification. It provides for evaluation the results of classification using accuracy assessment techniques. It is also useful to understand the specific characteristics of the environment of the study area.

The application of the various remote sensing techniques, which were adopted in this study, was not only related to the location of the study area, but also to various types of remotely sensed data (see C4.A).

These techniques were: extraction of the borders of the study area using the SRTM-data and ArcGIS-extensions (see C5.A); geometric correction based on GCPs, and/or geometric registration based on image to image method (see C5.B.1); atmospheric correction using the ATCOR-2 program (see C5.B.2); relative radiometric normalization using the MAD-concept (see C5.B.3); enhancing the spatial resolution of LANDSAT-ETM+ data from 30 m to 15 m using the Gram Schmidt Sharpening Technique to increase the spectral resolution of ASTER-data using the fusion-technique (see C5.B.4); mosaicing, subsetting and masking (see C5.B.5); training samples selection and evaluation (see C5.F); unsupervised classification (see C5.G.1.1); supervised classification using the three algorithms of classification (i.e., MLC, NN and SVM) with the two approaches of classification, i.e., the one stage and the multi stage classification approaches (see C5.G.1.2.1); post-classification processing (see C5.K); automated change detection mapping using the pre-classification approach (see C5.L.1) and the post-classification approach (see C5.L.2); and finally, the accuracy assessment techniques (see C5.M).

The new relative radiometric normalization method that was used in this study, was, after Canty et al. (2003), favored, where it can be applied automatically. It is consistent, constant, rapid, parameter free and sensor independent, and is enhanced by an orthogonal regression.

The aforementioned and used techniques in this study have various alternatives of sub-technique (e.g., radiometric normalization can be performed using more than one method, such as 6S, dark object method, histogram matching, etc.) and/or various parameters (e.g., SVM-algorithm of supervised classification can be used with various of parameters combinations). Thus, some of these alternatives were mentioned, discussed and compared to justify the final choice of each alternative technique and/or parameters that were used in this study.

This study proved that the use of multi-sensor (MSS-1975 and TM-2007) and multi-scale 60 m and 30 m data for change detection mapping is possible. Also, it is possible to use the multi-sensor ASTER-2005 and LANDSAT-ETM+ data for LULC-classification.

The available remotely sensed data of ASTER-sensor with low spectral resolution (three bands) and high spatial resolution (15 m) had given worse results with lower classification accuracy than those obtained after fusing with the data of LANDSAT-ETM+ to increase the spectral resolution.

New sensors (e.g., ASTER) offer higher accuracy rather than the old sensors (e.g., LANDSAT-MSS), but also bring new problems, such as the increasing time of processing because of the higher spatial resolution and the lower local coverage of each scene, and the increase of geometric errors because of the higher spatial resolution/pixel size.

Remotely sensed data spatial resolution/scale affects the level of useful information that can be extracted from the satellite imagery.

### **C. Recommendations/outlook**

Remote sensing techniques and data (LANDSAT and ASTER) were found to be very effective in the classification of land use/land cover and in the mapping of irrigation areas, and to detect and map changes that occurred over a number of years in the arid and semi-arid area of the Euphrates River Basin in Syria. However, these approaches were uneven for classification of agricultural crops, where their effectiveness were based on many factors, such as the used remotely sensed data type and its characteristics (e.g., spatial and spectral resolution, etc.), the agricultural holdings area and construction (e.g., the classification accuracy is very good where the large fields exist), and the crop type to be classified (e.g., the existing of wheat and barley together would make the spectral separation difficult that will impact the accuracy of classification). Here, more positive results may be realized by obtaining images at more times during the annual agricultural growing cycle.

The use of remote sensing techniques and data periodically to monitor and evaluate above ground surface natural resources can save time, effort and capital which are needed for traditional human-based ground surveys.

It is important to integrate the gathered human-based statistical records (agricultural statistics in particular) with the remote sensing techniques to interpret the relative old data of remote sensing that have no or insufficient compatible reference data. It is useful too, when a part of the study area is inaccessible.

The adoption of remote sensing techniques is an essential cartographical tool to map the general wide land use/land cover classes.

***Some demands include:*** The construction of user-friendly data archives with united data-formats as far as possible; the direction of more attention to the developed countries where there are many interesting topics to study using the remote sensing techniques. For instance, it is very difficult and time consuming to obtain remotely sensed data even if they are free of cost, and one requires a large amount of time to download one image because the slow Internet speed, in addition to a lack of digital image processing software.

***For further research:*** This study, like all studies, is an unfinished work because of the limitations of time, resources and finance. Therefore, the results included in this study are the best they can be, considering these limitations.

It would be interesting if the results of this study which are based on medium- to high- resolution optical remotely sensed data, were compared with those from resulting from the application of a very high resolution optical data (e.g., IKONOS), especially for agricultural purposes; the use of remotely sensed hyper-spectral data (e.g., Hyperion); and the application of remotely sensed RADAR-data (e.g., TerraSAR-X). In these cases, it would be necessary to apply new advanced digital analysis techniques, such as spectral un-mixing analysis.

Also, I am interested to link the results of this study and remote sensing techniques with GIS, for hydrologic study and regional water resources management of the Euphrates River Basin in Syria, and for agricultural water usage. I have collected a great deal of water data about the Euphrates, especially the water measurements at many measurement-stations along the river from the Syrian-Turkey borders to the Syrian-Iraqi borders over many decades.

This integration would be effective, because the classical applied approaches for estimating the hydraulic parameters are expensive and time consuming. Remote sensing can overcome these problems, by presenting a rapid and complete overview of the study area of interest. Here, weather satellites such as the NOAA-TIROS (National Oceanic and Atmospheric Administration-Television Infrared Observation Satellite), can provide us with some needed parameters (climatic parameters) which are essential for input in the hydraulic model. Evaporation or evapotranspiration (ET) is the most important and difficult to estimate in the hydraulic studies. Remote sensing techniques cannot measure it directly, but they suggest approaches based on LULC-features classification and climatic factors (e.g., solar radiation, temperature, humidity, surface albedo, etc.).

Also, for runoff measurement, techniques of remote sensing provide a source of input-data (watershed geometry, drainage networks, empirical flood peak, LULC-classes, etc.), and help to estimate equation coefficients and other model parameters.

## References

- Abou El-majd, I., & Tanton, T. (2002). *Remote sensing and GIS for irrigation water planning*. Proceedings of the GIS Research, 10<sup>th</sup> Annual Conference GISRU2002, Sheffield University, UK.
- Abuzar, M., McAllister, A., & Morris, M. (2001). Classification of seasonal images for monitoring irrigated crops in a salinity-affected area of Australia. *International Journal of Remote Sensing*, 22 (5), 717-726.
- Achard, F., Eva, H. D., Stibig, H. J., Mayaux, P., Gallego, J., Richards, T. (2002). Determination of deforestation rates of the world's humid tropical forests. *Science*, 297 (5583), 999-1002.
- ACSAD. (2001). *Surface water resources in the basins of the Euphrates and Tigris rivers*. Damascus-Syria, pp. 168.
- Adam, R., Adams, M., & Willens A. (1978). *Dry Lands: Man and Plants* (1st ed.). London: The Architectural Press Ltd.
- Adams, J. B., Smith, M. O., & Johnson, P. E. (1986). Spectral mixture modeling: A new analysis of rock and soil types at Viking Lander I site. *Journal of Geophysical Research*, 91 (B8), 8098-8112.
- Adams, J. B., Sabol, D. E., Kapos, V., Filho, R. A., Roberts, D. A., Smith, M. O., & Gillespie, A. R. (1995). Classification of multispectral images based on fractions of endmembers: Application to land cover change in the Brazilian Amazon. *Remote Sensing of Environment*, 52 (2), 137-154.
- Adeniyi, P. O., & Omojola, A. (1999). Landuse landcover change evaluation in Sokoto - Rima Basin of North Western Nigeria based on Archival of the Environment (AARSE) on Geoinformation Technology Applications for Resource and Environmental Management in Africa. *Resource and Environmental Management in Africa*, 143-172.
- Africover. (2003). Retrieved May 8, 2010, from <http://www.africover.org>
- Ahlquist, O., Keukelaar, J., & Oukbier, K. (2000). Rough classification and accuracy assessment. *International Journal of Geographical Information Science* 14 (5), 475-496.
- Ahmadi, H., & Mollazade, K. (2009). Application of remote sensing in the agricultural land-use assessment. *Journal of Theoretical and Applied Information Technology*, JATIT.
- Akkad, B. (2001). *Driving forces of land use change in Syria*. Damascus: Ministère de l'Agriculture et de la Réforme Agraire.
- Al-Ashram, M. (2001). Economy of water in the Arab countries and the world. *Al-Wahda Al-Arabiea- Studies* 84 (8), 217-226.
- Alberga, V. (2009). Similarity measures of remotely sensed multi-sensor images for change detection applications. *Remote Sensing*, 1 (3), 122-143.
- Albertz, J. (2009). *Einführung in die Fernerkundung: Grundlagen der Interpretation von Luft- und Satellitenbildern* (3. Aufl.). Darmstadt: Wiss. Buchges.
- Alcamo, J., Doll, P., Henrichs, T., Kaspar, F., Lehner, B., Rosch, T. (2003). Global estimates of water withdrawals and availability under current and future "business-as-usual" conditions. *Hydrologic Sciences Journal*, 48 (3), 339-348.
- Alilat, F., Loumi, S., & Sansal, B. (2006). Modified fuzzy ARTMAP and supervised fuzzy ART: Comparative study with multispectral classification. *International Journal of Computer Science*, 1 (3), 232-238.
- Al-Fares, W. (2007). *Wasserkonflikt zwischen Syrien und Türkei über das Wasser des Euphratesbecken und die Rolle, die das Südostanatolienprojekt auf diesem Konflikt spielt* (Diplomarbeit). Geographisches Institut zur George August Universität, Göttingen.
- Al-Khateeb, T. A. (2008). Land use classification utilizing Landsat thermal band based on wavelet transform. *Eng.&Tech.* 26 (11), 1411-1425.
- Allen, J. C., & Barnes, D. F. (1985). The causes of deforestation in developing countries. *Annals of the Association of American Geographers*, 75 (2), 163-84.



- Allen, J. D. (1990). A look at the remote sensing applications program of the National Agricultural Statistics Service. *Journal of Official Statistics*, 6 (4), 393-409.
- Allen, W. A., Gausman, H. W., Richardson, A. J., & Thomas, J. R. (1969). Interaction of isotropic light with a compact plant leaf. *Journal of the Optical Society of America*, 59 (10), 1376-1379.
- Allen, W. A., Gausman, H. W., & Richardson, A. J. (1973). Willstatter- Stoll theory of leaf reflectance evaluated by ray tracing. *Journal of the Optical Society of America*, 12 (10), 2448-2453.
- Al-Mansour, A. A. (2000). Das Wasser und die syrische Politik zu der Relation mit der Türkei. *Al-Wahda Al-Arabiea-Studien* 83 (1), 102-108.
- Alphan, H., Doygun, H., & Yüksel, I. (2009). Unlukaplan Post-classification comparison of land cover using multitemporal Landsat and ASTER imagery: The case of Kahramanmaraş, Turkey. *Environmental Monitoring Assessment*, 151 (1-4), 327-336.
- Al-Samman, N. (1991). War of the water from the Nile to the Euphrates: Transmission over the Syrian Ministry of Irrigation. *Al-Wahda Al-Arabiea-Studien* 74 (6), 124-140.
- Anderson, J. R., Hardy, E. E., Roach, J. T., & Witmer, R. E. (1976). *A land use and land cover classification system for use with remote sensor data*. Washington, DC: U.S. Government printing office.
- Aplin, P., Atkinson, P. M., & Curran, P. J. (1999 a). Fine spatial resolution simulated satellite sensor imagery for land cover mapping in the United Kingdom. *Remote Sensing of Environment*, 68 (3), 206-216.
- Aplin, P., Atkinson, P. M., & Curran, P. J. (1999 b). Per-field classification of land use using the forthcoming very fine spatial resolution satellite sensors: Problems and potential solutions. In P. M. Atkinson & N. J. Tate (Eds.), *Advances in Remote Sensing and GIS Analysis* (pp. 219-239). Chichester: Wiley.
- Aplin, P., & Atkinson, P. M. (2001). Sub-pixel land cover mapping for per-field classification. *International Journal of Remote Sensing*, 22 (14), 2853-2858.
- Aplin, P., & Smith, G. M. (2008). Advances in object-based image classification. In *ISPRS-International Archives of the Photogrammetry, Remote Sensing, and Spatial Information Sciences, Vol. XXXVII, Part B7* (p. 725-728). Beijing, China, July 3-11, 2008.
- Araus, J. L., Casadesus, J., & Bort, J. (2001). Recent tools for the screening of physiological traits determining yield. P. 59-77. In M.P. Reynolds J.I. Ortiz-Monasterio & A. McNab (Eds.), *Application of physiology in wheat breeding* (pp. 59-77). Mexico: CIMMYT.
- Ares, J., Bertiller, M., & del Valle, H. (2001). Functional and structural landscape indicators of intensification, resilience and resistance in agroecosystems in southern Argentina based on remotely sensed data. *Landscape Ecology*, 16 (3), 221-234.
- Arora, M. K., & Mathur, S. (2001). Multi-source classification using artificial neural network in a rugged terrain. *Geocarto International*, 16 (3), 37-44.
- Asati, P., & Asati, B. S. (2007). Potential application of remote sensing in management of agricultural resources in north eastern region. *ENVIS Bulletin: Himalayan Ecology*, 13 (2).
- Asner, G. P., Wessman, C. A., Bateson, C. A., & Privette, J. L. (2000). Impact of tissue, canopy, and landscape factors on the hyperspectral reflectance variability of arid ecosystems. *Remote Sensing of Environment*, 74 (1), 69-84.
- Atkinson, P. M., & Curran, P. J. (1995). Defining an optimal size of support for remote sensing investigation. *IEEE Transactions on Geoscience and Remote Sensing*, 33 (3), 768-776.
- Atkinson, P. M., Cutler, M. E. J., & Lewis, H. (1997). Mapping sub-pixel proportional land cover with AVHRR- imagery. *International Journal of Remote Sensing*, 18 (4), 917-935.
- Atkinson, P. M., & Tatnall, A. R. L. (1997). Introduction: Neural networks in remote sensing. *International Journal of Remote Sensing*, 18 (4), 699-709.
- Atkinson, P. M., & Aplin, P. (2004). Spatial variation in land cover and choice of spatial resolution for remote sensing. *International Journal of Remote Sensing*, 25 (18), 3687-3702.

- Aylward, B. (2000). *Economic analysis of land-use change in a watershed context*. Tech. Rep., World Commission on Dams, Kuala Lumpur, Malaysia.
- Baatz, M., Benz, U., Dehghani, S., Heynen, M., Höltje, A., Hofmann, P., Lingenfelder, I., Mimler, M., Sohlbach, M., Weber, M., & Willhauk, G. (2004). *eCognition User Guide 4*. München, Definiens Imaging GmbH.
- Badhwar, G. D. (1984). Classification of corn and soybeans using multitemporal thematic mapper data. *Remote Sensing of Environment* 16 (2), 175-181.
- Bagan, H., Jianwen, M., Qiqing, L., Xiuzhen, H., & Zhili, L. (2004). Land-use classification from ASTER data using wavelet fusion and self-organized neural networks. *Science in China Series D-Earth Sciences*, 47 (7), 651-658.
- Bagan, H., Qinxue, W., Masataka, W., Satoshi, K., & Yuhai, B. (2008). Land-cover classification using ASTER- multi-band combinations based on wavelet fusion and SOM- Neural Network. *Photogrammetric Engineering & Remote Sensing*, 74 (3), 333-342.
- Bagis, A. I. (1997). Turkey's Hydropolitics of the Euphrates-Tigris Basin. *International Journal of Water Resources Development*, 13 (4), 567-582.
- Ball, G. H., & Hall, D. J. (1965). *A novel method of data analysis and pattern classification* (Technical Report). Menlo Park, CA: Stanford Research Institute.
- Bannari, A., Morin, D., Bonn, F. & Huete, A. R. (1995). A review of vegetation indices. *Remote Sensing Reviews*, 13 (1-2), 95-120.
- Bannari, A., Khurshid, K. S., Staenz, K. & Schwarz, J. (2008). Potential of Hyperion EO-1 hyperspectral data for wheat crop chlorophyll content estimation. *Canadian Journal of Remote Sensing* 34 (S1), 139-157.
- Baraldi, A., & Parmiggiani, F. (1995). A neural network for unsupervised categorisation of multivalued input patterns: An application to satellite image clustering. *IEEE Transactions on Geoscience and Remote Sensing*, 33 (2), 305-316.
- Baret, F., & Guyot, G. (1991). Potentials and limits of vegetation indices for LAI and APAR assessment. *Remote Sensing of Environment*, 46 (2-3), 213-222.
- Bartholome, E., & Belward, A. S. (2005). GLC2000: A new approach to global land cover mapping from Earth observation data. *International Journal of Remote Sensing*, 26 (9-10), 1959-1977.
- Bastin, G. N., Pickup, G., & Pearce, G. (1995). Utility of AVHRR data for land degradation assessment: A case study. *International Journal of Remote Sensing*, 16 (4), 651-672.
- Bastin, L. (1997). Comparison of fuzzy c-means classification, linear mixture modelling and MLC probabilities as tools for unmixing coarse pixels. *International Journal of Remote Sensing*, 18 (17), 3629-3648.
- Bauer, M. E. (1975). The role of remote sensing in determining the distribution and yield of crops. In Brady & Staff B. G. (Eds.), *Advances in Agronomy*, 27 (pp. 271-304). New York: Academic Press, Inc.
- Bauer, M. E., Daughtry, C. S. T., Biehl, L.L., Kanemasu, E.T., & Hall, F.G. (1986). Field spectroscopy of agricultural crops. *IEEE Transactions on Geoscience and Remote Sensing*, 24 (1), 65-75.
- Bayraktar, H., & Bülent, B. (2007). *Monitoring irrigation areas using aster/terra images: Diyarbakir*. Proceedings of ASPRS Annual Conference Tampa "Identifying Geospatial Solutions". Florida, USA, May 7-11, 2007.
- Beaumont, P. (1996). Agricultural and environmental changes in the upper Euphrates catchment of Turkey and Syria and their political and economic implications. *Applied Geography*, 16 (2), 137-157.
- Beaumont, P., Blake, G. H., & Wagstaff, J. M. (1988). *The middle east: a geographical study*. 2nd ed., London: David Fulton Publishers.

- Benediktsson, J. A., Swain, P. H., & Ersoy, O. K. (1990). Neural network approaches versus statistical-methods in classification of multisource remote-sensing data. *IEEE Transactions on Geoscience and Remote Sensing*, 28 (4), 540-552.
- Benediktsson, J. A., & Kanellopoulos, I. (1999). Classification of multisource and hyperspectral data based on decision fusion. *IEEE Transactions on Geoscience and Remote Sensing*, 37 (3), 1367-1377.
- Benfield, S. L., Guzman, H. M., Mair, J. M., & Young, J. A. T. (2007). Mapping the distribution of coral reefs and associated sublittoral habitats in Pacific Panama: A comparison of optical satellite sensors and classification methodologies. *International Journal of Remote Sensing*, 28 (22), 5047-5070.
- Bennet, K. P., & Campbell, C. (2000). Support Vector Machines: Hype or hallelujah? *Special Interest Group on Knowledge Discovery and Data Mining*, 2 (2), 1-13.
- Benz, U. C., Hofmann, P., Willhauck, G., Lingenfelder, I., & Heynen, M. (2004). Multi-resolution, objectoriented fuzzy analysis of remote sensing data for GIS-ready information. *ISPRS Journal of Photogrammetry & Remote Sensing*, 58 (3-4), 239-258.
- Berberoglu, S., Lloyd, C. D., Atkinson, P. M., & Curran, P. J. (2000). The integration of spectral and texture information using neural networks for land cover mapping in the Mediterranean. *Computers and Geosciences* 26 (4), 385-396.
- Berberoglu, S., Curran, P. J., Lloyd, C. D., & Atkinson, P. M. (2007). Texture classification of Mediterranean land cover. *International Journal of Applied Earth Observation and Geoinformation*, 9 (3), 322-334.
- Berberoglu, S., & Akin, A. (2009). Assessing different remote sensing techniques to detect land use/cover changes in the eastern Mediterranean. *International Journal of Applied Earth Observation and Geoinformation*, 11 (1), 46-53.
- Berk, A., Bernstein, L. S., Anderson, G. P., Acharya, P. K., Robertson, D. C., Chetwynd, J. H., & Adler-Golden, S. M. (1998). MODTRAN Cloud and Multiple Scattering Upgrades with Application to AVIRIS. *Remote Sens. Environ.*, 65, 367-375.
- Bernstein, R. (1983). Image geometry and rectification. In R. N. Colwell (Eds.), *Manual of remote sensing*. Falls Church: American Society of Photogrammetry.
- Bezdek, J. C. (1981). *Pattern Recognition with Fuzzy Objective Function Algorithms*. New York: Plenum Press.
- Bianghi, E., Madella, P., Montesano, M. G., & Rampini, A. (1997). Fuzzy contextual classification of multisource remote sensing images. *IEEE Transactions on Geoscience and Remote Sensing*, 35 (2), 326-339.
- Bidwell, R. G. S. (1974). *Plant Physiology*. New York: MacMillan Publishing Company Inc.
- Bill, R. (1999). *Grundlagen der Geo-Informationssysteme, Band 1: Hardware, Software, Daten* (4. Aufl.); *Band 2: Analysen, Anwendungen und neue Entwicklungen* (2. Aufl.). Heidelberg: Wichmann.
- Billingsley, F. C. (1982). Modelling misregistration and related effects on multispectral classification. *Photogrammetric Engineering and Remote Sensing*, 48, 421 - 430.
- Binaghi, E., Brivio, P. A., Ghezzi, P., & Rampini, A. (1999). A fuzzy set accuracy assessment of soft classification. *Pattern Recognition Letters*, 20 (9), 935-948.
- Bishop, C. M. (1995). *Neural networks for pattern recognition*. Oxford University Press.
- Bishop, C. M. (2006). *Pattern recognition and machine learning* (1<sup>st</sup> ed). New York: Springer.
- Blackmer, T. M., Schepers, J. S., Varvel, G. E., & Walter-Shea, E. A. (1996). Nitrogen deficiency detection using reflected short wave radiation from irrigated corn canopies. *Agronomy Journal*, 88 (1), 1-5.
- Blaes X., Vanhalle, L., & Defourny, P. (2005). Efficiency of crop identification based on optical and SAR image time series. *Remote Sensing of Environment*, 96 (3-4), 352-365.

- Blaschke, T. (2000). Objektextraktion und regelbasierte Klassifikation von Fernerkundungsdaten: Neue Möglichkeiten für GIS-Anwender und Planer. In M. Schrenk (Hrsg.), *Computergestützte Raumplanung – Beiträge zum Symposium CORP 2000* (153-162). Wien.
- Blaschke, T. (2005). Towards a framework for change detection based on image objects. In S. Erasmí B. Cyffca & M. Kappas (Eds.), *Remote Sensing & GIS for Environmental Studies, (Göttinger Geographische Abhandlungen)* (113). Göttingen.
- Bloch, I. (1996). Information combination operators for data fusion: A comparative review with classification. *IEEE Transactions on Systems, Man, and Cybernetics*, 26 (1), 52–67.
- Bontemps, S., Bogaert, P., Titeux, N., & Defourny, P. (2008). An object-based change detection method accounting for temporal dependences in time series with medium to coarse spatial resolution. *Remote Sensing of Environment*, 112 (6), 3181–3191.
- Borak, J. S., & Strahler, A. H. (1999). Feature selection and land cover classification of a MODIS-like data set for semi-arid environment. *International Journal of Remote Sensing*, 20 (5), 919–938.
- Bosard, M., Feranec, J., & Otahel, J. (2000). *CORINE land cover technical guide* (Technical Report No. 40). Copenhagen, Denmark: European Environmental Agency.
- Boucher, O., Myhre, G., & Myhre, A. (2004). Direct human influence of irrigation on atmospheric water vapor and climate. *Climate Dynamics*, 22 (6-7), 597–603.
- Braimoh, A. K. (2004). *Modeling land-use change in the Volta Basin of Ghana* (Doctoral dissertation), Center for Research Development (ZEF), University of Bonn, Bonn: 159 p.
- Briassoulis, H. (2000). *Analysis of land-use change: Theoretical and modeling approaches*. Retrieved from West Virginia University, Regional Research Institute, Morgantown, book of regional science. The web <http://www.rri.wvu.edu/WebBook/Briassoulis/contents.htm>
- Brisco, B., & Brown, R. J. (1995). Multidate SAR/TM Synergism for crop classification in western Canada. *Photogrammetric Engineering & Remote Sensing*, 61 (8), 1009-1014.
- Brogaard, S., & Ólafsdóttir, R. (1997). *Ground-truths or ground-lies?* Retrieved from Lund University, Sweden, Electronic Reports in Physical Geography No. 1, Oct. 1997. The web <http://www.natgeo.lu.se/Publikationer/Lerpg/1/1Article.htm>
- Broge, N. H., & Mortensen, J. V. (2002). Deriving green crop area index and canopy chlorophyll density of winter wheat from spectral reflectance data. *Remote Sensing of Environment*, 81 (1), 45–57.
- Brooks, C. N., D. L., Schaub, R. B., Powell, N. H. F. French, R. A., Shuchman, Court, G., & Arbor, A. (2006). *Multi-temporal and multi-platform agricultural land cover classification in southeastern michigan*. Proceedings of ASPRS Annual Conference. Reno, Nevada, 1-5 May, 2006.
- Brown, D. G. (1998). Classification and boundary vagueness in mapping presettlement forest types. *International Journal of Geographical Information Science* 12 (2), 105-129.
- Bruzzone, L., & Carlin, L. (2006). A multilevel context-based system for classification of very high spatial resolution images. *IEEE Transactions on Geoscience and Remote Sensing*, 44 (9), 2587-2600.
- Bruzzone, L., & Serpico, S. B. (1997). An iterative technique for the detection of land-cover transitions in multitemporal remote-sensing images. *IEEE Transactions on Geoscience and Remote Sensing*, 35 (4), 858-867.
- Bruzzone, L., & Fernandez-Prieto, D. (1999). A technique for the selection of kernel-function parameters in RBF neural networks for classification of remote-sensing images. *IEEE Transactions on Geoscience and Remote Sensing*, 37 (2), 1179–1184.
- Bruzzone, L., Prieto, D. F., & Serpico, S. B. (1999). A neural-statistical approach to multitemporal and multisource remote-sensing image classification. *IEEE Transactions on Geoscience and Remote Sensing*, 37 (3), 1350-1359.
- Bruzzone, L., & Fernández-Prieto, D. (2000). Automatic analysis of the difference image for unsupervised change detection. *IEEE Transactions on Image Processing*, 38 (3), 1171-1182.

- Bruzzone, L., & Fernández-Prieto, D. (2002). *An adaptive semi-parametric and context-based approach to unsupervised change detection in multitemporal remote sensing images* (Technical Report). Also: Appeared on *IEEE Transactions on Image Processing*, 11 (4), 452-466.
- Bruzzone, L., Cossu, R., & Vernazza, G. (2004 a). Detection of land-cover transitions by combining multivariate classifiers. *Pattern Recognition Letters*, 25 (13), 1491-1500.
- Bruzzone, L., Marconcini, M., Wegmuller, U., & Wiesmann, A. (2004 b). An advanced system for the automatic classification of multitemporal SAR images. *IEEE Transactions on Geoscience and Remote Sensing*, 42 (6), 1321-1334.
- Bruzzone, L., & Marconcini, M. (2009). Toward the automatic updating of land cover maps by a domain-adaptation SVM classifier and a circular validation strategy. *IEEE Transactions on Geoscience and Remote Sensing*, 47 (4), 1108-1122.
- Burges, C. J. C. (1998). A tutorial on Support Vector Machines for pattern recognition. *Data Mining and Knowledge Discovery*, 2 (2), 121-167.
- Bürgi, M., Hersperger, A., & Schneeberger, N. (2004). Driving forces of landscape change - current and new directions. *Landscape Ecology*, 19 (8), 857-868.
- Burley, T. M. (1961). Land use or land utilization?. *Prof. Geographer*, 13 (6), 18-20.
- Campbell, B. C. (2002). *Introduction to remote sensing*. London & New York: Taylor & Francis.
- Campbell, J. B. (1981). Spatial correlation effects upon accuracy of supervised classification of land cover. *Photogrammetric Engineering and Remote Sensing*, 47 (3), 355-363.
- Camps-Valls, G., Gomez-Chova, L., Munoz-Mari, J., Vila-Frances, J., & Calpe-Maravilla, J. (2006). Composite kernels for hyperspectral image classification. *IEEE Geoscience and Remote Sensing Letters*, 3 (1), 93-97.
- Canty, M. J., Nielsen, A. A., & Schmidt, M. (2004). Automatic radiometric normalization of multitemporal satellite imagery. *Remote Sensing of Environment*, 91 (3-4), 441-451.
- Canty, M. J., & Nielsen, A. A. (2008). Automatic radiometric normalization of multitemporal satellite imagery with the iteratively re-weighted MAD transformation. *Remote Sensing of Environment*, 112 (3), 1025-1036.
- Canty, M. J. (2009). Boosting: A fast neural network for supervised land cover classification. *Computers & Geosciences*, 35 (6), 1280-1295.
- Canty, M. J. (2010). *Image analysis, classification and change detection in remote sensing, with algorithms for ENVI/IDL, second revised edition*. Taylor & Francis, CRC Press.
- Carfagna, E., & Javier Gallego, F. (2005). Using remote sensing for agricultural statistics. *International Statistical Review*, 73 (3), 389-404.
- Carleer, A. P., Debeir, O., & Wolff, E. (2005). Assessment of very high spatial resolution satellite image segmentations. *Photogrammetric Engineering and Remote Sensing*, 71 (11), 1285-1294.
- Carlotto, M. J. (1997). Detection and analysis of change in remotely sensed imagery with application to wide area surveillance. *IEEE Trans. on Image Processing*, 6 (1), 189-202.
- Carlotto, M. J. (1998). Spectral shape classification of Landsat Thematic Mapper imagery. *Photogrammetric Engineering & Remote Sensing*, 64 (9), 905-913.
- Carpenter, G. A., Gजा, M. N., Gopal, S., & Woodcock, C. E. (1997). ART neural networks for remote sensing: Vegetation classification from Landsat TM and terrain data. *IEEE Transactions on Geoscience and Remote Sensing*, 33 (2), 308-325.
- Castelli, V., Elvidge, D. C., Li, C. S., & Turek, J. J. (1999). Classification-based change detection: Theory and applications to the NALC data set. In R. S. Lunetta & C. D. Elvidge (Eds.), *Remote Sensing Change Detection Environmental Monitoring Methods and Applications* (Chapter 4: pp. 53-73). London: Taylor and Francis.
- Celik, T. (2010). change detection in satellite images using a genetic algorithm approach. *IEEE Geoscience and Remote Sensing Letters*, 7 (2), 386-390.

- Celik, T., & Kai-Kuang, M. (2010). Unsupervised change detection for satellite images using dual-tree complex wavelet transform. *IEEE Transactions on Geoscience and Remote Sensing*, 48 (3), 1199-1210.
- Celis, D., De Pauw, E., & Geerken, R. (2007 a). *Assessment of land cover and land use in Central and West Asia and North Africa (CWANA) using AVHRR and agroclimatic data* (part 1.: land cover/land use - base year 1993, p. 54). Aleppo, Syria: ICARDA.
- Celis, D., De Pauw, E., & Geerken, R. (2007 b). *Assessment of land cover and land use in Central and West Asia and North Africa (CWANA) using AVHRR and agroclimatic data* (part 2: hot spots of land cover change and drought vulnerability, p. 69). Aleppo, Syria: ICARDA.
- Central Bureau of Statistics/CBS. (Several Years). Statistical abstracts. Damascus, Syria: Ministry of Planning.
- Chan, J. C., Chan, K., & Yeh, A. G. (2001). Detecting the nature of change in an urban environment: A comparison of machine learning algorithms. *Photogrammetric Engineering and Remote Sensing*, 67 (2), 213–225.
- Chander, G., Markham, B. L., & Helder, D. L. (2009). Summary of current radiometric calibration coefficients for Landsat MSS, TM, ETM+, and EO-1 ALI sensors. *Remote Sensing of Environment*, 113 (5), 893–903.
- Chapelle, O., Vapnik, V., Bousquet, O., & Mukherjee, S. (2002). Choosing multiple parameters for support vector machines. *Machine Learning*, 46 (1-3), 131-159.
- Chavez, P. S. (1988). An improved dark-object subtraction technique for atmospheric scattering correction of multispectral data. *Remote Sensing of Environment*, 24 (3), 459- 479.
- Chavez, P. S., & Mackinnon, D. J. (1994). Automatic detection of vegetation changes in the southwestern United States using remotely sensed images. *Photogrammetric Engineering & Remote Sensing*, 60 (5), 571–583.
- Chavez, P. S. (1996). Image-based atmospheric corrections-revisited and improved. *Photogrammetric Engineering & Remote Sensing*, 62 (9), 1025- 1036.
- Chen, D. M., & Stow, D. A. (2002). The effect of training strategies on supervised classification at different spatial resolution. *Photogrammetric Engineering & Remote Sensing*, 68 (11), 1155–1162.
- Chen, D. M., Stow, D. A., & Gong, P. (2004 a). Examining the effect of spatial resolution and texture window size on classification accuracy: An urban environment case. *International Journal of Remote Sensing*, 25 (11), 2177-2192.
- Chen, J., Gong, P., He, C., Pu, R., & Shi, P. (2003). Land-use/land-cover change detection using improved change-vector analysis. *Photogrammetric Engineering & Remote Sensing*, 69 (4), 369– 379.
- Chen, Z., Zhou, Q., & Tang, H. (2004 b). The future agricultural applications' demanding on space-born remote sensing in China. In H. Tang (Ed), *Research on the agricultural resource utilization and regional sustainable development* (pp. 236-250). Beijing: China Outlook Press.
- Chen, Z., Li, S., Ren, J., Gong, P., Zhang, M., Wang, L., Xiao, S., & Jiang, D. (2008). Monitoring and management of agriculture with remote sensing. In S. Liang (Ed.), *Advances in land remote sensing - system, modelling, inversion and adaptation* (pp. 397-421). USA: Springer-Verlag, University of Maryland.
- Cheng, T. (2002). Fuzzy objects: Their changes and uncertainties. *Photogrammetric Engineering & Remote Sensing*, 68 (1), 41-49.
- Cheng, T., Molenaar, M., & Lin, H. (2001). Formalizing fuzzy objects from uncertain classification results. *International Journal of Geographical Information Science*, 15 (1), 27-42.
- Chust, G., Ducrot, D., & Pretus, J. L. L. (2004). Land cover discrimination potential of radar multitemporal series and optical multispectral images in a Mediterranean cultural landscape. *International Journal of Remote Sensing*, 25 (17), 3513-3528.

- Cihlar, J., Xiao, Q., Chen, J., Beaubien, J., Fung, K., & Latifovic, R. (1998). Classification by progressive generalization: A new automated methodology for remote sensing multispectral data. *International Journal of Remote Sensing*, 19 (14), 2685–2704.
- Cingolani, A. M., Renison, D., Zak, M. R., & Cabido, M. R. (2004). Mapping vegetation in a heterogeneous mountain rangeland: An alternative method to define and classify land-cover units. *Remote Sensing of Environment*, 92 (1), 84-97.
- Civco, D. L., Hurd, J. D., Wilson, E. H., Song, M., & Zhang, Z. (2002). *A comparison of land use and land cover change detection methods* (p. 12). Proceedings of ASPRS-ACSM Annual Conference and FIG XXII Congress, April 22-26, 2002, Washington D.C., USA.
- Clawson, M., & Stewart, C. L. (1965). *Land use information: A critical survey of U.S. statistics including possibilities for greater uniformity*. Baltimore, Md.: The Johns Hopkins Press for Resources for the Future, Inc.
- Cloutis, E. A., Connery, D. R., Major, D. J., & Dover, F. J. (1996). Airborne multi-spectral monitoring of agricultural crop status: Effect of time of year, crop type and crop condition parameter. *International Journal of Remote Sensing*, 17 (13), 2579-2601.
- Cohen, J. (1960). A coefficient of agreement for nominal scales. *Educational and Psychological Measurement*, 20 (1), 37-46.
- Collins, J. B., & Woodcock, C. E. (1996). An assessment of several linear change detection techniques for mapping forest mortality using multitemporal Landsat TM data. *Remote Sensing of Environment*, 56 (1), 66-77.
- Colwell, R. N. (1965). Spectrometric considerations involved in making rural land use studies with aerial photography. *Photogrammetria*, 20 (1), 15-33.
- Colwell, J. E., & Weber, F. P. (1981). *Forest change detection* (pp. 65-69). Proceedings of the 15th International Symposium on Remote Sensing of Environment, Ann Arbor, MI, May 16-20, 1981, Environmental Research Institute of Michigan, USA.
- Comber, A., Fisher, P., & Wadsworth, R. (2004). Integrating land-cover data with different ontologies: Identifying change from inconsistency. *International Journal of Geographical Information Science*, 18 (7), 691–708.
- Congalton, R. G. (1991). A review of assessing the accuracy of classifications of remotely sensed data. *Remote Sensing of Environment*, 37 (1), 35-46.
- Congalton, R. G., & Green, K. (1993). A practical look at the sources of confusion in error matrix generation. *Photogrammetric Engineering and Remote Sensing*, 59 (5), 641–644.
- Congalton, R. G., & Green, K. (1999). *Assessing the accuracy of remote sensed data: Principles and Practices* (1<sup>st</sup> ed). London: Lewis Publisher.
- Congalton, R. G., & Plourde, L. (2002). Quality assurance and accuracy assessment of information derived from remotely sensed data. In J. Bossler (Ed.), *manual of geospatial science and technology* (pp. 349-361). London: Taylor & Francis.
- Conrad, C., Fritsch, S., Zeidler, J., Rücker, G., & Dech, S. (2010). Per-field irrigated crop classification in arid central asia using SPOT and ASTER data, *Remote Sensing*, 2 (4), 1035-1056.
- Coppin, P., & Bauer, M. (1996). Digital change detection in forest ecosystems with remote sensing imagery. *Remote Sensing Reviews*, 13 (3-4), 207-234.
- Coppin, P., Jonckheere, I., Nackaerts, K., Muys, B., & Lambin, E. (2004). Digital change detection methods in ecosystem monitoring: A review. *International Journal of Remote Sensing*, 25 (9), 1565-1596.
- Cortijo, F. J., & De La Blanca, N. P. (1997). A comparative study of some non-parametric spectral classifiers: Application to problems with high-overlapping training sets. *International Journal of Remote Sensing*, 18 (6), 1259–1275.
- Cracknell, A. P. (1998). Synergy in remote sensing: What's in a pixel?. *International Journal of Remote Sensing*, 19 (11), 2025–2047.

- Craig, M. E. (2001). *The NASS cropland data layer program*. Proceedings of the Third Annual International Conference on Geospatial Information in Agriculture, November 5–7, 2001, Denver, Colorado, USA.
- Crapper, P. F. (1980). Errors incurred in estimating an area of uniform land cover using Landsat. *Photogrammetric Engineering and Remote Sensing*, 46 (10), 1295–1301.
- Crist, E. P., & Cicone, R. C. (1984). A physically based transformation of thematic mapper data: The TM tassled cap. *IEEE Transactions on Geoscience and Remote Sensing*, GE-22 (3), 256-263.
- Curlander, J. C., & McDonough, R. N. (1991). *Synthetic aperture radar system and signal processing*. New York: John Wiley and Sons Press.
- Curran, P. J. (1988). The semivariogram in remote sensing: An introduction. *Remote Sensing of Environment*, 24 (3), 493-507.
- Dai, X. L., & Khorram, S. (1999). Remotely sensed change detection based on artificial neural networks. *Photogrammetric Engineering and Remote Sensing*, 65 (10), 1187– 1194.
- De Colstoun, E. C. B., Story, M. H., Thompson, C., Commisso, K., Smith, T. G., & Irons, J. R. (2003). National park vegetation mapping using multitemporal Landsat 7 data and a decision tree classifier. *Remote Sensing of Environment*, 85 (3), 316-327.
- De Jong, S. M. (1994). Derivation of vegetative variables from a Landsat TM image for erosion modelling. *Earth Surface Processes and Landforms*, 19 (2), 165-178.
- De Jong, S. M., Van der Meer, F. D., & Clevers J. G. P. W. (2007). Basics of remote sensing. In S. M. De Jong & F. D. Van der Meer (Eds.), *Remote sensing image analysis: Including the spatial domain (Remote Sensing and Digital Image Processing)* (pp. 1-16). Dordrecht: Kluwer Academic Publishers.
- De Pauw, E., Oberle, A., & Zöbisch, M. (2004). *Land cover and land use in Syria: An overview*. Jointly published by Asian Institute of Technology (AIT), International Center for Agricultural Research in the Dry Areas (ICARDA) and the World Association of Soil and Water Conservation (WASWC).
- De Pauw, E. (2005). *Mapping the agricultural regions of Syria*. In Annual Report (2004), Natural Resource Management Program. Aleppo, Syria: ICARDA.
- Dean, A. M., & Smith, G. M. (2003). An evaluation of per-parcel land cover mapping using maximum likelihood class probabilities. *International Journal of Remote Sensing*, 24 (14), 2905–2920.
- Deaton, A., & Laroque, G. (1992). On the behavior of commodity prices. *Review of Economic Studies*, 59 (1), 1–23.
- Deer, P. (1998). *Digital change detection in remotely sensed imagery using fuzzy set theory* (Doctoral dissertation), Department of Geography and Department of Computer Science, University of Adelaide, Australia.
- Definiens AG (2004). *eCognition User Guide*. Retrieved May, 2006.
- DeFries, R. S., & Townshend, J. R. G. (1994). NDVI-derived land cover classifications at a global scale. *International Journal of Remote Sensing*, 15 (17), 3567–3586.
- DeFries, R. S., Hansen, M. C., Townshend, J. R. G., & Sohlberg, R. S. (1998). Global land cover classifications at 8 km spatial resolution: The use of training data derived from Landsat imagery in decision tree classifiers. *International Journal of Remote Sensing*, 19 (16), 3141–3168.
- DeFries, R. S., & Belward, A. S. (2000). Global and regional land cover characterization from satellite data: An introduction to the special issue. *International Journal of Remote Sensing*, 21 (6–7), 1083–1092.
- DeFries, R. S., & Chan, J. C. (2000). Multiple criteria for evaluating machine learning algorithms for land cover classification from satellite data. *Remote Sensing of Environment*, 74 (3), 503–515.



- Deguisse, J. C., McNairn, H., Staenz, K., & McGovern, M. (1998). *Spatial high resolution crop measurements with airborne hyperspectral remote sensing*. Proceedings of The 4th International Conference on Precision Agriculture, American Society of Agronomy/CSSA/SSSA, July 19-22, 1998, St Paul, USA.
- Del Frate, F., Ferrazzoli, P., & Schiavon, G. (2003). Retrieving soil moisture and agricultural variables by microwave radiometry using neural networks. *Remote Sensing of Environment*, 84 (2), 174 - 83.
- Del Frate, F., Schiavon, G., & Solimini, C. (2004). *Application of neural networks algorithms to QuickBird imagery for classification and change detection of urban areas* (pp. 1091-1094). Proceedings of International Geoscience And Remote Sensing Symposium, Anchorage, Alaska, September 20-24, 2004, Anchorage, Alaska, USA.
- Del Frate, F., Schiavon, G., Solimini, C. (2005). *Use of high resolution satellite data for change detection in urban areas*. Proceedings of ESA EUSC 2005 Conference: Image Information Mining – Theory and Application to Earth Observation, October, 2005, ESA/ESRIN, Frascati, Italy.
- Dheeravath, V., Thenkabail, P. S., Chandrakantha, G., Noojipady, P., Reddy, G. P. O., Biradar, C. M., Gummag, M. K., & Velpuri, M. (2010). Irrigated areas of India derived using MODIS 500 m time series for the years 2001-2003. *ISPRS Journal of Photogrammetry and Remote Sensing*, 65 (1), 42-59 .
- Di Gregorio, A. (1996). *FAO land cover classification: Adichotomous, modular, heirarchical approach* (pp.). Proceedings of the US Federal Geographic Data Committee Vegetation Subcommittee and Earth Cover Working Group, October 15–17, 1996, Washington, USA.
- Di Gregorio, A. (2005). *Land cover classification system LCCS: Classification concepts and user manual LCCS* (8<sup>th</sup> ed., part 1). Rome: Food & Agriculture Org.
- Dikshit, O., & Roy, D. P. (1996). An empirical investigation of image resampling effects upon the spectral and textural supervised classification of a high spatial resolution multispectral image. *Photogrammetric Engineering & Remote Sensing* 62 (9), 1085-1092.
- Directorate of Irrigation and Water Use (DIWU). (1993). *Water requirements for the agricultural plan 1993/94*. Damascus, Syria.
- Directorate of Irrigation and Water Use (DIWU). (2008). *Water requirements for the agricultural plan 2007/08*. Damascus, Syria.
- Donnay, J., Barnsley, M. J., & Longley, P. A. (2001). *Remote sensing and urban analysis*. New York: Taylor and Francis.
- Doraiswamy, P. C., Sinclair, T. R., Hollinger, S., Akhmedov, B., Stern, A., & Prueger, J. (2005). Application of MODIS derived parameters for regional crop yield assessment. *Remote Sensing of Environment*, 97 (2), 192–202.
- Draeger, W. (1976). *Monitoring irrigated land acreage using Landsat imagery: An application example*. USGS Open-file Report No. 76-630, USGS, Sioux Falls, S.D. 23 pp.
- Du, Y., Teillet, P. M., & Cihlar, J. (2002). Radiometric normalization of multitemporal high-resolution satellite images with quality control for land cover change detection. *Remote Sensing of Environment*, 82 (1), 123–134.
- Duda, R. O., Hart, P. E., & Stork, D. G. (2000). *Pattern classification* (2<sup>nd</sup> ed). Chichester, New York: John Wiley & Sons.
- Dungan, J. L. (2002). *Toward a comprehensive view of uncertainty in remote sensing analysis* (pp. 25-35). In G. M. Foody & P. M. Atkinson (Eds.), *Uncertainty in remote sensing and GIS*. Chichester: John Wiley & Sons.
- Eastman, J. R. (2006). *IDRISI Andes Tutorial*. Worcester: USA, Clark Labs.
- Eckhardt, D. W., Verdin, J. P., & Lyford, G. R. (1990). Automated update of an irrigated lands GIS using SPOT HRV imagery. *Photogrammetric Engineering & Remote Sensing*, 56 (11), 1515–1522.

- Egenhofer, M., & Frank, A. (1989). Object-oriented modelling in GIS: Inheritance and propagation. *Auto-Carto*, 9, 588–598.
- Elmahboub, W., Scarpace, F., & Smith, B. (2009). A highly accurate classification of TM data through correction of atmospheric effects. *Remote Sensing*, 1 (3), 278-299.
- Elvidge, C. D., & Lyon, R. J. P. (1985). Influence of rock-soil spectral variation on the assessment of green biomass. *Remote Sensing of Environment*, 17 (3), 265-269.
- Erb, R. B. (1980). The large area crop inventory experiment (LACIE); Methodology for area, yield and production estimation; Results and perspectives. In G. Frayssé (Ed.), *Remote Sensing Application in Agriculture and Hydrology* (pp. 502). Rotterdam: Balkema.
- Erbek, F. S., Ozkan, C., & Taberner, M. (2004). Comparison of maximum likelihood classification method with supervised artificial neural network algorithms for land use activities. *International Journal of Remote Sensing*, 25 (9), 1733–1748.
- ERDAS. (1999). *Field guide: Earth resources data analysis system*. Atlanta, Georgia: ERDAS Inc.
- Evans, M. I. (Eds.). (1994). *Important bird areas in the middle east. Bird life conservation series No.2., Bird life international*. Cambridge, U.K.
- Eve, M. D., & Merchant, J. W. (1998). *National survey of land cover mapping protocols used in the GAP analysis program. GAP land cover mapping protocols homepage center for advanced land management information technologies (CALMIT)*. Lincoln, NE: University of Nebraska–Lincoln. Retrieved August 05, 2010, from <http://www.calmit.unl.edu/gapmap/>.
- Everitt, J. H., Escobar, D. E., Cavazos, I., Noriega, J. R., & Davis, M. R. (1995). A three- camera multispectral digital video imaging system. *Journal of Remote Sensing of Environment*, 54 (3), 333-7.
- Fang, H. (1998). Rice crop area estimation of an administrative division in China using remote sensing. *International Journal of Remote Sensing*, 19 (17), 3411–3419.
- FAO. (1993 a). Land degradation in arid, semi-arid and dry sub-humid areas: *Rainfed and irrigated lands, rangelands and woodlands*. Text for FAO presentation at INCD, Nairobi, May 24-28, 1993, Rome: Italy.
- FAO. (1993 b). *Irrigation sub-sector review (mission report)*. Rome: Italy.
- FAO. (2009). Irrigation in the Middle East region in figures (AQUASTAT survey - 2008). In K. Frenken (Ed.), *FAO water reports* (p. 423). Rome: Italy.
- Farr, T. G., Rosen, P. A., Caro, E., Crippen, R., Duren, R., Hensley, ... Alsdorf, D. (2007). The shuttle radar topography mission. *Reviews of Geophysics*, 45 (RG2004), p. 33.
- Fauvel M., Chanussot, J., & Benediktsson, J. A. (2006 a). *A combined support vector machines classification based on decision fusion*. Proceedings of IEEE International Geoscience and Remote Sensing Symposium, IGARSS, July, 2006, Denver, USA.
- Fauvel, M., Chanussot, J., & Benediktsson, J. A. (2006 b). Decision fusion for the classification of urban remote sensing images. *IEEE Transactions on Geoscience and Remote Sensing*, 44 (10), 2828-2838.
- Feitosa, R. Q., Costa, G. A. O. P., Mota, G. L. A., Pakzad, K., & Costa, M. S. O. (2009). Cascade multitemporal classification based on fuzzy markov chains. *ISPRS Journal of Photogrammetry and Remote Sensing*, 64 (2), 159-170.
- Ferro, C. J. S., & Warner, T. A. (2002). Scale and texture in digital image classification. *Photogrammetric Engineering & Remote Sensing*, 68 (1), 51-63.
- Finn, J. T. (1993). Use of the average mutual information index in evaluating classification error and consistency. *International Journal of Geographical Information Systems*, 7 (4), 349–366.
- Fischer, M. M. (1996). *Computational neural networks: A new paradigm for spatial analysis* (pp. 297-314). Proceedings of First International Conference on Geocomputation, University of Leeds, UK.

- Fisher, P. (1997). The pixel: A snare and a delusion. *International Journal of Remote Sensing*, 18 (3), 679–685.
- Fitzgerald, G. J., Pinter, J., Hunsaker, D. J., & Clarke, T. R. (2005). Multiple shadow fractions in spectral mixture analysis of a cotton canopy. *Remote Sensing of Environment*, 97 (4), 526–539.
- Fitzpatrick-Lins, K. (1981). Comparison of sampling procedures and data analysis for a land-use and land-cover map. *Photogramm. Eng. Remote Sens.*, 47 (3), 343-351.
- Flanders, D., Hall-Beyer, M., & Pereverzoff, J. (2003). Preliminary evaluation of eCognition object-based software for cut block delineation and feature extraction. *Canadian Journal of Remote Sensing*, 29 (4), 441-452.
- Flygare, A. M. (1997). A comparison of contextual classification methods using Landsat TM. *International Journal of Remote Sensing*, 18 (18), 3835–3842.
- Foody, G. M. (1992). On the compensation for chance agreement in image classification accuracy assessment. *Photogrammetric Engineering and Remote Sensing*, 58 (10), 1459–1460.
- Foody, G. M., & Cox, D. P. (1994). Sub-pixel land cover composition estimation using a linear mixture model and fuzzy membership functions. *International Journal of Remote Sensing*, 15 (3), 619–631.
- Foody, G. M. (1995). Land cover classification by an artificial neural network with ancillary information. *International Journal of Geographical Information Systems*, 9 (5), 527-542.
- Foody, G. M. (1996). Approaches for the production and evaluation of fuzzy land cover classification from remotely-sensed data. *International Journal of Remote Sensing*, 17 (7), 1317–1340.
- Foody, G. M., & Arora, M. K. (1997). An evaluation of some factors affecting the accuracy of classification by an artificial neural network. *International Journal of Remote Sensing*, 18 (4), 799– 810.
- Foody, G. M. (1998). Sharpening fuzzy classification output to refine the representation of sub-pixel land cover distribution. *International Journal of Remote Sensing*, 19 (13), 2593–2599.
- Foody, G. M. (1999 a). Image classification with a neural network: From completely-crisp to fully-fuzzy situations. In P. M. Atkinson & N J. Tate (Eds.), *Advances in remote sensing and GIS analysis* (pp. 17-37). Chichester: Wiley.
- Foody, G.M. (1999 b). The signification of border training patterns in classification by a feedforward neural network using back propagation learning. *International Journal of Remote Sensing*, 20 (18), 3549–3562.
- Foody, G. M. (2002). Status of land cover classification accuracy assessment. *Remote Sensing of Environment*, 80 (1), 185-201.
- Foody, G. M. (2004 a). Supervised image classification by MLP and RBF neural networks with and without an exhaustively defined set of classes. *International Journal of Remote Sensing* 25 (15), 3091-3104.
- Foody, G. M. (2004 b). Thematic map comparison: Evaluating the statistical significance of differences in classification accuracy. *Photogrammetric Engineering and Remote Sensing*, 70 (5), 627–633.
- Foody, G. M., & Mathur, A. (2004 a). A relative evaluation of multiclass image classification by support vector machines. *IEEE Transactions on Geoscience and Remote Sensing*, 42 (6), 1335-1343.
- Foody, G. M., & Mathur, A. (2004 b). Toward intelligent training of supervised image classifications: Directing training data acquisition for SVM classification. *Remote Sensing of Environment*, 93 (1-2), 107–117.
- Foody, G. M., & Mathur, A. (2006). The use of small training sets containing mixed pixels for accurate hard image classification: Training on mixed spectral responses for classification by a SVM. *Remote Sensing of Environment*, 103 (2), 179–189.

- Foody, G. M., Mathur, A., Sanchez-Hernandez, C., & Boyd, D. S. (2006). Training set size requirements for the classification of a specific class. *Remote Sensing of Environment*, 104 (1), 1–14.
- Foti, T., Blaney, M., Li, X., & Smith, K. G. (1994). Classification system for the natural vegetation of Arkansas. *Proceedings Arkansas Academy of Science*, 48, 50 - 53.
- Franklin, J. (1995). Predictive vegetation mapping: Geographic modelling of biospatial patterns in relation to environmental gradients. *Progress in Physical Geography*, 19 (4), 474-499.
- Franklin, J., Phinn, S. R., Woodcock, C. E., & Rogan, J. (2003). Rationale and conceptual framework for classification approaches to assess forest resources and properties. In M. A. Wulder & S. E. Franklin (Eds.), *remote sensing of forest environments: Concepts and case studies* (pp. 279-300). Boston: Kluwer Academic Publishers.
- Franklin, S. E., Peddle, D. R., Dechka, J. A., & Stenhouse, G. B. (2002). Evidential reasoning with Landsat TM, DEM and GIS data for land cover classification in support of grizzly bear habitat mapping. *International Journal of Remote Sensing*, 23 (21), 4633–4652.
- French, A. N., Schmugge, T. J., Ritchie, J. C., Hsu, A., Jacob, F., & Ogawa, K. (2008). Detecting land cover change at the Jornada Experiment Range, New Mexico, with aster emissivities. *Remote Sensing of Environment*, 112, 1730-1748.
- Friedl, M. A., Mcgwire, K. C., & Mciver, D. K. (2001). An overview of uncertainty in optical remotely sensed data for ecological applications. In C. T. Hunsaker M. F. Goodchild M. A. Friedl & T. J. Case (Eds.), *spatial uncertainty in ecology: Implications for remote sensing and GIS applications* (pp. 258–283). New York: Springer.
- Friedl, M. A., McIver, D. K., Hodges, J. C. F., Zhang, X. Y., Muchoney, D., & Strahler, A. H. (2002). Global land cover mapping from MODIS: Algorithms and early results. *Remote Sensing of Environment*, 83 (1-2), 287–302.
- Frolking, S., Xiao, X., Zhuang, Y., Salas, W., & Li, C. (1999). Agricultural landuse in China: A comparison of area estimates from ground-based census and satellite-borne remote sensing. *Global Ecology and Biogeography*, 8 (5), 407–416.
- Fujisada, H. (1994). Overview of ASTER instrument on EOS-AM1 platform. *Proc. SPIE (The International Society for Optical Engineering)*, 2268, 14-36.
- Fujisada, H. (1995). Design and performance of ASTER instrument. *Proc. SPIE (The International Society for Optical Engineering)*, 2583, 16.
- Fukuda, S., & Hirose, H. (2001). *Support vector machine classification of land cover: Application to polarimetric SAR data* (pp. 187-189). Proceedings of IEEE International Geoscience and Remote Sensing Symposium IGARSS, July 9-13, 2001, Sydney.
- Fukunaga, K. (1990). *Introduction to statistical pattern recognition* (2<sup>nd</sup> ed.). Boston: Academic Press.
- Fuller, R., Smith, G., Sanderson, J., Hill, R., & Thomson, A. (2002). The UK land cover map 2000: Construction of a parcel-based vector map from satellite images. *Cartographic Journal*, 39 (1), 15–25.
- Fung, T. (1990). An assessment of TM imagery for land-cover change detection. *IEEE Transactions on Geoscience and Remote Sensing*, 28 (12), 681-684.
- Furby, S. L., & Campbell, N. A. (2001). Calibrating images from different dates to ``like-value`` digital counts. *Remote Sensing of Environment*, 77 (2), 186–196.
- Gallego, F. J. (2004). Remote sensing and land cover area estimation. *International Journal of Remote Sensing*, 25 (15), 3019–3047.
- Galvao, L. S., Ponzoni, F. J., Epiphanyo, J. C. N., Rundorff, B. F. T., & Formaggio, A. R. (2004). Sun and view angle effects on NDVI determination of land cover types in the Brazilian Amazon region with hyperspectral data. *International Journal of Remot. Remote Sensing* 25 (10), 1861-1879.
- Gao, B. C., & Goetz, A. F. H. (1992). *A linear spectral matching technique for retrieving equivalent water thickness and biochemical constituents of green vegetation* (pp. 35-37).

- Proceedings of the third Airborn Annual JPL Geosciences workshop (AVIRIS, TIMS and AIRSAR), Jet Propulsion Laboratory, Pasadena, CA.
- Gates, D. M., Keegan, H. J., Schleter, J. C., & Weidner, V. R. (1965). Spectral properties of plants. *Applied Optics*, 4 (1), 11–20.
- Gausman, H. W., Allen, W. A., & Cardenas, R. (1969). Reflectance of cotton leaves and their structure. *Remote Sensing Environment*, 1 (1), 19–22.
- Gausman, H. W., Allen, W. A., Cardenas, R., & Richardson, A. J. (1971). Effects of leaf nodal position on absorption and scattering coefficients and infinite reflectance of cotton leaves, *Gossypium hirsutum* L.1. *Agronomy Journal*, 63 (1), 87–91.
- Gausman, H. W. (1973). Reflectance, transmittance, and absorptance of light by subcellular particles of spinach (*Spinacia oleracea* L.) leaves. *Agronomy Journal*, 65 (4), 551–553.
- Gausman, H. W., & Allen, W. A. (1973). Optical parameters of leaves of 30 plant species. *Plant Physiology*, 52 (1), 57–62.
- Gausman, H. W. (1974). Leaf reflectance of near-infrared. *Photogrammetric Engineering*, 40 (2), 183–191.
- Gausman, H. W., Allen, W. A., & Escobar, D. E. (1974). Refractive-index of plant-cell walls. *Applied Optics*, 13 (1), 109–111.
- Gausman, H. W., & Hart, W. G. (1974). Reflectance of sooty mold fungus on citrus leaves over 2.5 to 40-micrometer wavelength interval. *Journal of Economic Entomology*, 67 (4), 479–480.
- Gausman, H. W., Gerbermann, A. H., & Wiegand, C. L. (1975). Use of ERTS-1 data to detect chlorotic grain-sorghum. *Photogrammetric Engineering & Remote Sensing*, 41 (2), 177–179.
- Gausman, H. W., Rodriguez, R. R., & Richardson, A. J. (1976). Infinite reflectance of dead compared with live vegetation. *Agronomy Journal*, 68 (2), 295–296.
- Gausman, H. W. (1977). Reflectance of leaf components. *Remote Sensing of Environment*, 6 (1), 1–9.
- Gausman, H. W., Menges, R. M., Richardson, A. J., Walter, H., Rodriguez, R. R., & Tamez, S. (1981). Optical-parameters of leaves of 7 weed species. *Weed Science*, 29 (1), 24–26.
- Geneletti, D., & Gorte, B. G. H. (2003). A method for object-oriented land cover classification combining Landsat TM data and aerial photographs. *International Journal of Remote Sensing*, 24 (6), 1273–1286.
- Gersar-Scet (1977). *Development of the lower Euphrates valley*. Technical Report, Zone 1. Ministry of Irrigation, Syrian Arab Republic, 266pp.
- Giacinto, G., & Roli, F. (1997). *Ensembles of neural networks for soft classification of remote sensing images* (pp. 166–170). Proceedings of the European Symposium on Intelligent Techniques, European Network for Fuzzy Logic and Uncertainty Modelling in Information Technology, Bari, Italy.
- Gilabert, M. A., Conese, C., & Maselli, F. (1994). An atmospheric correction method for the automatic retrieval of surface reflectance from TM images. *International Journal of Remote Sensing*, 15 (10), 2065–2086.
- Gitas, I. Z., Mitri, G. H., & Ventura, G. (2004). Object-based image classification for burned area mapping of Creus Cape Spain, using NOAA-AVHRR imagery. *Remote Sensing of Environment*, 92 (3), 409–413.
- Gitelson, A. A., Vina, A., Rundquist, D. C., Ciganda, V., & Arkebauer, T. J. (2005). Remote estimation of canopy chlorophyll content in crops. *Geophysical Research Letters*, 32, L08403.
- GOEDEB (The General Organization of Exploitation and Development of Euphrates Basin). (several years). *The annual statistical abstract*. Ministry of Irrigation, Planning Department (Statistics Division), Syria.
- Goetz, S. J., Prince, S. D., Thawley, M. M., Smith, A. J., Wright, R., & Weiner, M. (2000). *Applications of multi-temporal land cover information in the mid-Atlantic region: A RESAC*

- initiative* (pp. 1:357-359). Proceedings of the International Geoscience and Remote Sensing Symposium, July 24–28, 2000, Honolulu, Hawaii, USA.
- Gomez, C., Delacourt, C., Allemand, P., Ledru, P., & Wackerle, R. (2005). Using ASTER remote sensing data set for geological mapping, in Namibia. *Physics and Chemistry of the Earth*, 30 (1-3), 97–108.
- Gong, P., & Howarth, P. J. (1990). The use of structural information for improving land-cover classification accuracies at the ruralurban fringe. *Photogrammetric Engineering & Remote Sensing*, 56 (1), 67–73.
- Gong, P., & Howarth, P. J. (1992). Frequency-based contextual classification and gray-level vector reduction for land-use identification. *Photogrammetric Engineering and Remote Sensing*, 58 (4), 423–437.
- Gong, P., Marceau, G. J., & Howarth, P. J. (1992). A comparison of spatial feature extraction algorithms for land-use classification with SPOT HRV data. *Remote Sensing of Environment* 40 (2), 137-151.
- Gonzales-Alonso, F., Cuevas, J. M., Arbiol, R., & Baulies, X. (1998). Remote sensing and agricultural statistics: Crop area estimation in north-eastern Spain through diachronic Landsat TM and ground sample data. *International Journal of Remote Sensing*, 18 (2), 467–470.
- Gopal, S., & Woodcock, C. (1994). Theory and methods for accuracy assessment of thematic maps using fuzzy sets. *Photogrammetric Engineering and Remote Sensing*, 60 (2), 181–188.
- Gordon, L. J., Steffen, W., Jonsson, B. F., Folke, C., Falkenmark, M., & Johansen, A. (2005). Human modification of global water vapor flows from the land surface. *Proceedings of the National Academy of Sciences*, 102 (21), 7612–7617.
- Gorte, B. (1999). Supervised segmentation by region merging. In I. Kanellopoulos G. G. Wilkinson & T. Moons (Eds.), *machine vision and advanced image processing in remote Sensing* (pp. 329-335). Berlin: Springer.
- Green, K. (2006). Landsat in context: The land remote sensing business model. *Photogrammetric Engineering & Remote Sensing*, 72 (10), 1147–1153.
- Gross, J. E., Nemani, R. R., Turner, W., & Melton, F. (2006). Remote sensing for the national parks. *Park Science*, 24 (1), 30–36.
- Group on Earth Observation/GEO. (2010). *Best practices for crop area estimation with remote sensing*. Retrieved September 14, 2010, from [http://www.earthobservations.org/documents/cop/ag\\_gams/GEOSS%20best%20practices%20area%20estimation%20final.pdf](http://www.earthobservations.org/documents/cop/ag_gams/GEOSS%20best%20practices%20area%20estimation%20final.pdf)
- Gualtieri, J. A., & Crompton, R. F. (1998). *Support vector machines for hyperspectral remote sensing classification* (pp. 221-232). Proceedings of the of the SPIE, 27th AIPR Workshop: Advances in Computer Assisted Recognition, October 14-16, 1998, Washington, DC, USA.
- Guerschman, J. P., Paruelo, J. M., Di Bella, C., Giallorenzi, M. C., & Pacin, F. (2003). Land cover classification in the Argentine Pampas using multi-temporal landsat TM data. *International Journal of Remote Sensing*, 24 (17), 3381-3402.
- Guo, Q., Kelly, M., Gong, P., & Liu, D. (2007). An object-based classification approach in mapping tree mortality using high spatial resolution imagery. *GIScience & Remote Sensing*, 44 (1), 24–47.
- Gutman, G., Janetos, A. C., Justice, C. O., Moran, E. F., Mustard, J. F., & Rindfuss, R. R. (2004). *Land change science: Observing, monitoring and understanding trajectories of change on the Earth's surface*. Dordrecht: Kluwer Academic Publishers.
- Haack, B. N., & Slonecker, E. T. (1994). Merged spaceborne radar and thematic mapper digital data for locating villages in Sudan. *Photogrammetric Engineering & Remote Sensing*, 60 (10), 1253–1257.
- Haack, B. N., Herold, N. D., & Bechdol, M. A. (2000). Radar and optical data integration for land-use/land-cover mapping. *Photogrammetric Engineering & Remote Sensing*, 66 (6), 709–716.

- Haberäcker, P. (1995). *Praxis der digitalen Bildverarbeitung und Mustererkennung*. München: Hanser.
- Hadjimitsis, D. G., Clayton, C. R. I., & Hope, V. S. (2004). An assessment of the effectiveness of atmospheric correction algorithms through the remote sensing of some reservoirs. *International Journal of Remote Sensing*, 25 (18), 3651–3674.
- Hall, F. G., & Badhwar, G. D. (1987). Signature-extendable technology: Global space-based crop recognition. *IEEE Transactions on Geoscience and Remote Sensing*, 25 (1), 93–103.
- Hall, F. G., Strebel, D. E., Nickeson, J. E., & Goetz, S. J. (1991). Radiometric rectification: toward a common radiometric response among multirate, multisensor images. *Remote Sensing of Environment*, 35, 11–27.
- Halldorsson, G. H., Benediktsson, J. A., & Sveinsson, J. R. (2003). *Support vector machines in multisource classification* (pp. 2054-2056). Proceedings of IEEE International Geoscience and Remote Sensing Symposium IGARSS, July 21-25, 2003, Toulouse, France.
- Hansen, M., Defries, R., Townshend, J., & Solberg, R. (2000). Global land cover classification at 1 km spatial resolution using a classification tree approach. *International Journal of Remote Sensing*, 21 (6), 1331-1364.
- Hansen, M. C., DeFries, R. S., Townshend, J. R. G., Sohlberg, R., Dimiceli, C., & Carroll, M. (2002). Towards an operational MODIS continuous field of percent tree cover algorithm: Examples using AVHRR and MODIS data. *Remote Sensing of Environment*, 83 (1-2), 303-319.
- Hanuschak, G., Hale, R., Craig, M., Mueller, R., & Hart, G. (2001). *The new economics of remote sensing for agricultural statistics in the United States* (pp. XXII.1–XXII.10). Proceedings of the Conference on Agricultural and Environmental Statistical Applications in Rome (CAESAR), June 5–7, 2001, Rome, Italy.
- Haralick, R. M., Shanmugam, K., & Dinstein, I. (1973). Textural features for image classification. *IEEE Transactions on Systems, Man, and Cybernetics*, 3 (6), 610-621.
- Haralick, R. M., & Shapiro, L. G. (1985). Image segmentation techniques. *Computer Vision, Graphics and Image Processing*, 29 (1), 100-132.
- Haralick, R. M., & Shapiro, L. G. (1992). *Computer and robot vision* (Vol. I). Addison-Wesley, Reading.
- Hardin, P. J., & Shumway, J. M. (1997). Statistical significance and normalized confusion matrices. *Photogrammetric Engineering and Remote Sensing*, 63 (6), 735–740.
- Harris, P. M., & Ventura, S. J. (1995). The integration of geographic data with remotely sensed imagery to improve classification in an urban area. *Photogrammetric Engineering and Remote Sensing*, 61 (8), 993–998.
- Harrison, B. A., & Jupp, D. L. B. (1989). *Introduction to remotely sensed data*. CSIRO Publications.
- Hastie, T., Tibshirani, R., & Friedman, J. (2001). *The elements of statistical learning*. New York: Springer.
- Hatfield, J. L., Prueger, J. H., & Kustas, W. P. (2004). Remote sensing of dryland crops. In S. L. Ustin (Ed.), *remote sensing for natural resource management and environmental monitoring: Manual of remote sensing (3<sup>rd</sup> ed)* (pp. 531-568). Hoboken: John Wiley, NJ.
- Hay, G. J., Blaschke, T., Marceau, D. J., & Bouchard, A. (2003). A comparison of three image-object methods for the multiscale analysis of landscape structure. *ISPRS Journal of Photogrammetry & Remote Sensing*, 57 (5-6), 327-345.
- Hay, G. J., & Castilla, G. (2006). *Object-based image analysis: Strengths, weaknesses, opportunities and threats (SWOT)*. Proceedings of 1<sup>st</sup> International Conference on Object-based Image Analysis (OBIA), July 4-5, 2006, Salzburg University, Austria.
- Hay, G. J., & Castilla, G. (2008). Geographic object-based image analysis (GEOBIA): A new name for a new discipline. In T. Blaschke S. Lang & G. Hay (Eds.), *object-based image*

- analysis-spatial concepts for knowledge-driven remote sensing applications* (pp. 75-89). Berlin: Springer.
- Hazel, G. G. (2001). Object-level change detection in spectral imagery. *IEEE Transactions on Geoscience & Remote Sensing*, 39 (3), 553- 561.
- Heerman, P. D., & Khazenie, N. (1992). Classification of multispectral remote sensing data using a back propagation neural network. *IEEE Transactions on Geoscience and Remote Sensing*, 30 (1), 81-88.
- Heinl, M., Walde, J., Tappeiner, G., & Tappeiner, U. (2009). Classifiers vs. input variables: The drivers in image classification for land cover mapping. *International Journal of Applied Earth Observation and Geoinformation*, 11 (6), 423-430.
- Heller, R. C., & Johnson, K. A. (1979). Estimating irrigated land acreage from Landsat imagery. *Photogrammetric Engineering & Remote Sensing*, 45 (10), 1379-1386.
- Helmer, E. H., Ramos, O., López, T. DEL M., Quiñones, M., & Diaz, W. (2002). Mapping the forest type and land cover of Puerto Rico, a component of the Caribbean biodiversity hotspot. *Caribbean Journal of Science*, 38 (3-4), 165-183.
- Henderson, F. M., & Lewis, A. J. (1998). *Principles and applications of imaging radar. Manual of remote sensing 3rd edition, Vol.2*. American Society for Photogrammetry & Remote Sensing. Wiley & Sons, New York, 866 pp.
- Heo, J., & Fitzhugh, T. W. (2000). A standardized radiometric normalization method for change detection using remotely sensed imagery. *Photogrammetric Engineering and Remote Sensing*, 66 (2), 173-182.
- Hepner, G. F., Logan, T., Ritter, N., & Bryant, N. (1990). Artificial neural network classification using a minimal training set: Comparison to conventional supervised classification. *Photogrammetric Engineering and Remote Sensing*, 56 (4), 469-473.
- Hereher, M. E. (2009). Inventory of agricultural land area of Egypt using modis data. *Egypt. J. Remote Sensing & Space Sci.*, 12, 179-184.
- Herman, B., LaRocca, A. J., & Turner, R. E. (1993). Atmospheric Scattering. In W. L. Wolfe & G. J. Zissis (Eds.), *the infrared handbook* (pp. 4-76). Michigan: Environmental Research Institute of Michigan (ERIM), Ann Arbor.
- Herwitz, S. R., Johnson, L. F., Dunagan, S. E., Higgins, R. G., Sullivan, D. V., Zheng, J., Lobitz, B. M., Leung, J. G., Gallmeyer, B. A., & Aoyagi, M. (2004). Imaging from an unmanned aerial vehicle: Agricultural surveillance and decision support. *Computers and Electronics in Agriculture*, 44 (1), 49-61.
- Hildebrandt, G. (1996). *Fernerkundung und Luftbildmessung für Forstwirtschaft, Vegetationskartierung und Landschaftsökologie*. Heidelberg: Wichmann.
- Hill, J. D., Strommen, N. D., Sakamoto, C. M., & LeDuc, S. K. (1980). LACIE: An application of meteorology for United States and foreign wheat assessment. *Journal of Applied Meteorology*, 19 (10), 22-34.
- Hill, J. D. (2000). Assessment of semiarid lands: Monitoring dryland ecosystems through remote sensing. In R. Meyers (Ed.), *encyclopedia of analytical chemistry: Instrumentation and applications* (pp. 8769-8794). John Wiley and Sons.
- Hill, R. A. (1999). Image segmentation for humid tropical forest classification in Landsat TM data. *International Journal of Remote Sensing*, 20 (5), 1039-1044.
- Hillel, D. (1994). *Rivers of Eden: the struggle for water and the quest for peace in the Middle East*. Oxford University Press, New York, pp. 74-110.
- Hirata, M. K., Shinjo, N., Fujita, H., Gintzburger, H., Miyazaki, G., & Akira (2001). Vegetation classification by satellite image processing in a dry area of north-eastern Syria. *International Journal of Remote Sensing*, 22 (4), 507-516.
- Hobbs, T. J. (1995). The use of NOAA-AVHRR NDVI data to assess herbage production in the arid rangelands of central Australia. *International Journal of Remote Sensing*, 16 (7), 1289-1302.



- Hoffer, R. M. (1980). Computer-aided analysis techniques for mapping earth surface features. In G. Fraysse (Ed.), *remote sensing applications in agriculture and hydrology* (pp. 133-152). Netherlands: A A Balkema Publishers.
- Hoffer, R. M., & Johannsen, C. J. (1969). *Ecological potential in spectral signature analysis*. In: remote sensing in Ecology, P. L. Johnson (ed.), pp. 1-16. Athens: University of Georgia Press.
- Hoffmann, A. (2001). *Neue Ansätze zur Auswertung und Klassifizierung von sehr hochauflösenden Daten: Methoden der Segmentierung, der hierarchischen Klassifizierung und der per-Parcel-Methode mit Daten der digitalen Kamera HRSC-A und ihre Anwendbarkeit. HRSC-A und ihre Anwendbarkeit für die Aktualisierung topographischer Karten* (Doctoral dissertation, HU Berlin).
- Homer, C., Huang, C., Yang, L., Wylie, B., & Coan, M. (2004). Development of a 2001 national land-cover database for the United States. *Photogrammetric Engineering and Remote Sensing*, 70 (7), 829–840.
- Horwitz, H. M., Nalepka, R. F., Hyde, P. D., & Morgenstern, J. P. (1971). *Estimating the proportions of objects within a single resolution element of a multispectral scanner*. In: Seventh International Symposium on Remote Sensing of Environment, Ann Arbor, Michigan, Environmental Research Institute of Michigan, vol. 2: 1307-1320.
- Houghton, R. A., Hackler, J. L., & Lawrence, K. T. (1999). The US carbon budget: Contributions from land-use change. *Science*, 285 (5427), 574–578.
- Hsu, C. W., & Lin, C. J. (2002). A comparison of methods for multi-class support vector machines. *IEEE Transactions on Neural Networks*, 13 (2), 415-425.
- Huang, C., Davis, L. S., & Townshend, J. R. G. (2002). An assessment of support vector machines for land cover classification. *International Journal of Remote Sensing*, 23 (4), 725-749.
- Huang, H., Legarsky, J., & Othman, M. (2007). Land-cover classification using radarsat and Landsat imagery for St. Louis, Missouri. *Photogrammetric Engineering & Remote Sensing*, 73 (1), 037–043.
- Huang, Z., & Lees, B. G. (2004). Combining non-parametric models for multisource predictive forest mapping. *Photogrammetric Engineering and Remote Sensing*, 70 (4), 415–425.
- Hubert-Moy, L., Cotonnec, A., Le Du, L., Chardin, A., & Perez, P. (2001). A comparison of parametric classification procedures of remotely sensed data applied on different landscape units. *Remote Sensing of Environment*, 75 (2), 174–187.
- Huete, A. R., Post, D. F., & Jackson, R. D. (1984). Soil spectral effects on 4-space vegetation discrimination. *Remote Sensing of Environment*, 15 (2), 155-165.
- Huete, A. R., Jackson, R. D., & Post, D. F. (1985). Spectral response of a plant canopy with different soil backgrounds. *Remote Sensing of Environment*, 17 (1), 37-53.
- Huete, A. R., & Jackson, R. D. (1987). The suitability of spectral indices for evaluating vegetation characteristics on arid rangelands. *Remote Sensing of Environment*, 23 (2), 213-232.
- Huete, A. R. (1988). A soil-adjusted vegetation index (SAVI). *Remote Sensing of Environment*, 25 (3), 295-309.
- Huete, A., Justice, C., & Liu, H. (1994). Development of vegetation and soil indices for MODIS-EOS. *Remote Sensing of Environment* 29, 224–234.
- Huguenin, R. L., Karaska, M. A., Blaricom, D. V., & Jensen, J. R. (1997). Subpixel classification of bald cypress and tupelo gum trees in thematic mapper imagery. *Photogrammetric Engineering and Remote Sensing*, 63 (6), 717–725.
- Hunt, E. R., Cavigelli, M., Daughtry, C. S. T., McMurtrey, J., & Walthall, C. L. (2005). Evaluation of digital photography from model aircraft for remote sensing of crop biomass and nitrogen status. *Precision Agriculture*, 6 (4), 359-78.
- Hurcom, S. J., & Harrison, A. R. (1998). The NDVI and spectral decomposition for semi-arid vegetation abundance estimation. *International Journal of Remote Sensing*, 19 (16), 3109–3125.

- Im, J., & Jensen, J. R. (2005). Change detection using correlation analysis and decision tree classification. *Remote Sensing of Environment*, 99, 326-340.
- Im, J., Jensen, J. R., & Tullis, J. A. (2008). Object-based change detection using correlation analysis and image segmentation. *International Journal of Remote Sensing*, 29 (2), 399-423.
- Irons, J. R., Markham, B. L., Nelson, R. F., Toll, D. L., Williams, D. L., Latty, R. S. (1985). The effects of spatial resolution on the classification of thematic mapper data. *International Journal of Remote Sensing*, 6 (8), 1385– 1403.
- Irons, J. R., Weismiller, R. A. & Petersen, G. W. (1989). Soil reflectance. In G. Asrar (Ed.), *theory and applications of optical remote sensing* (pp. 66-106). New York: Wiley.
- Ito, Y., & Omatu, S. (1999). Extended LVQ neural network approach to land cover mapping. *IEEE Transactions on Geoscience and Remote Sensing*, 37 (1), 313–317.
- Jain, A. K., & Dubes, R. C. (1988). *Algorithms for clustering data*. Englewood Cliff: Prentice Hall College Div.
- Jain, A. K., Duin, R. P. W., & Mao, J. C. (2000). Statistical pattern recognition: A review. *IEEE Transactions on Pattern Analysis and Machine Intelligence*, 22 (1), 4-37.
- Janssen, L. L., & Van der Wel, F. J. M. (1994). Accuracy assessment of satellite derived land-cover data: A review. *Photogrammetric Engineering and Remote Sensing*, 60 (4), 419–426.
- Janssen, L. L. F., & Molenaar, M. (1995). Terrain objects, their dynamics and their monitoring by integration of GIS and remote sensing. *IEEE Transactions on Geoscience and Remote Sensing*, 33 (3), 749–758.
- Jensen, J. R., Cowen, D. J., Narumalani, S., Althausen, J. D., & Weatherbee, O. (1993). An evaluation of CoastWatch change detection protocol in South Carolina. *Photogrammetric Engineering and Remote Sensing*, 59 (6), 1039– 1046.
- Jensen, J. R. (2005). *Introductory digital image processing: A remote sensing perspective* (3<sup>rd</sup> ed.). New Jersey: Prentice Hall Series in Geographic Information Science.
- Jensen, J. R. (2007). *Remote sensing of the environment: An earth resource perspective* (2<sup>nd</sup> ed.). New Jersey: Pearson Prentice Hall.
- Jeon, B., & Landgrebe, D. A. (1999). Decision fusion approach for multitemporal classification. *IEEE Transactions on Geoscience and Remote Sensing*, 37 (3), 1227-1233.
- Jhung, Y., & Swain, P. H. (1996). Bayesian contextual classification based on modified M-estimates and markov random fields. *IEEE Transactions on Geoscience and Remote Sensing*, 34 (1), 67-75.
- Ji, C. Y. (2000). Land-use classification of remotely sensed data using Kohonen self-organizing feature map neural networks. *Photogrammetric Engineering & Remote Sensing*, 66 (12), 1451–1460.
- Jianwen, M., Bagan, H. (2005). Land-use classification using ASTER data and self-organized neural networks. *International Journal of Applied Earth Observation and Geoinformation*, 7 (3), 183–188.
- Jingan, S., Jiupai, N., Chaofu, W., & Deti, X. (2005). Land use change and its corresponding ecological responses: A review. *Journal of Geographical Sciences*, 15 (3), 305-328.
- Johnson, R. A., & Wichern, D. W. (1988). *Applied multivariate statistical analysis* (2<sup>nd</sup> Ed.). New Jersey: Prentice-Hall, Inc.
- Jordan, C. F. (1969). Derivation of leaf area index from quality of light on the forest floor. *Ecology*, 50 (4), 663–666.
- Ju, J., Gopal, S., & Kolaczyk, E. D. (2005). On the choice of spatial and categorical scale in remote sensing land cover classification. *Remote Sensing of Environment*, 96 (1), 62–77.
- Jurgens, C. (1997). The modified normalized difference vegetation index (mNDVI): A new index to determine frost damages in agriculture based on Landsat TM data. *International Journal of Remote Sensing*, 18 (17), 3583-3594.
- Justice, C. O., & Hiernaux, P. H. Y. (1986). Monitoring the grasslands of the Sahel using NOAA AVHRR data: Niger 1983. *International Journal of Remote Sensing*, 7 (11), 1475-1497.

- Justice, C. O., Wharton, S. W., & Holben, B. N. (1981). Application of digital terrain data to quantify and reduce the topographic effect on Landsat data. *International Journal of Remote Sensing*, 2 (3), 213-230.
- Kampouraki, M., Wood, G. A., & Brewer, T. R. (2008). Opportunities and limitations of object based image analysis for detecting urban impervious and vegetated surfaces using true-colour aerial photography. In T. Blaschke S. Lang & G. Hay (Eds.), *object-based image analysis-spatial concepts for knowledge-driven remote sensing applications* (pp. 555–569). Berlin: Springer.
- Kandrika, S., & Roy, P. S. (2008). Land use land cover classification of Orissa using multi-temporal IRS-P6 awifs data: A decision tree approach. *International Journal of Applied Earth Observation and Geoinformation*, 10 (2), 186–193.
- Kanellopoulos, I., Varfis, A., Wilkinson, G. G., & Mégier, J. (1992). Land-cover discrimination in SPOT HRV imagery using an artificial neural network: A 20-class experiment. *International Journal of Remote Sensing*, 13 (5), 917–924.
- Kanellopoulos, I., & Wilkinson, G. G. (1997). Strategies and best practice for neural network image classification. *International Journal of Remote Sensing*, 18 (4), 711–725.
- Kangarani, H. M. (2006). *Euphrates and Tigris watershed: Economic, social and institutional aspects of forest in an integrated watershed management* (working paper 81). Rome: FAO.
- Karen, C., Seto, K. C., & Liu, W. (2003). Comparing ARTMAP neural network with maximum likelihood for detecting urban change: The effect of class resolution. *Photogrammetric Engineering and Remote Sensing*, 69 (9), 981–990.
- Kartikeyan, B., Gopalakrishna, B., Kalubarme, M. H., & Majumder, K. L. (1994). Contextual techniques for classification of high and low resolution remote sensing data. *International Journal of Remote Sensing*, 15 (5), 1037–1051.
- Kartikeyan, B., Sarkar, A., & Majumder, K. L. (1998). A segmentation approach to classification of remote sensing imagery. *International Journal of Remote Sensing*, 19 (9), 1695–1709.
- Kasetkasem, T., & Varshney, P. K. (2002). Image change detection algorithm based on Markov random field models. *IEEE Transactions on Geoscience and Remote Sensing*, 40 (8), 1815-1823.
- Kattan, Z. (2008). Estimation of evaporation and irrigation return flow in arid zones using stable isotope ratios and chloride mass-balance analysis: case of the Euphrates River, Syria. *Journal of Arid Environments*, 72 (5), 730–747.
- Kaufman, Y. J. (1985). Atmospheric effect on the separability of field classes measured from satellites. *Remote Sensing of the Environment*, 18, 21–34.
- Kaufman, Y. J. (1989). The atmospheric effect on remote sensing and its correction. In G. Asrar (Eds.), *Optical Remote Sensing, Technology and Application* (chap. 9). N.Y.: John Wiley.
- Kaufman, Y. J., Tanre, D., Remer, L., Verniote, E. F., Chu, A., & Holben, B. N. (1997 a). Operational remote sensing of tropospheric aerosol over the land from EOS-MODIS. *Journal Geophysical Research*, 102 (14), 17051-17068.
- Kaufman, Y. J., Wald, A., Lorraine, L. A., Gao, B. C., Li, R. R., & Flynn, L. (1997 b). Remote sensing of aerosol over the continents with the aid of a 2.2  $\mu$ m channel. *IEEE Transactions on Geoscience and Remote Sensing*, 35 (5), 1286- 1298.
- Kaufman, Y. J., Karnieli, A., & Tanre, D. (2000). Detection of dust over deserts using satellite data in the solar wavelengths. *IEEE Transactions on Geoscience and Remote Sensing*, 38 (1), 525-531.
- Kavzoglu, T. (2001). *An Investigation of the design and use of feed-forward artificial neural networks in the classification of remotely sensed images* (Doctoral dissertation: The University of Nottingham, UK).
- Kennedy, R. E., Townsend, P. A., Gross, J. E., Cohen, W. B., Bolstad, P., Wang, Y. Q., & Adams, P. (2009). Remote sensing change detection tools for natural resource

- managers: Understanding concepts and tradeoffs in the design of landscape monitoring projects. *Remote Sensing of Environment*, 113 (7), 1382–1396.
- Keuchel, J., Naumann, S., Heiler, M., & Siegmund, A. (2003). Automatic land cover analysis for Tenerife by supervised classification using remotely sensed data. *Remote Sensing of Environment*, 86 (4), 530–541.
- Kheiry, M. A. (2003). *Monitoring and evaluation of vegetation cover changes in semi-arid areas: A case study of khartoum forest sub-sector, Sudan* (Master thesis: TUD, Germany).
- Kibaroglu, A. (2002). *Building a regime for the waters of the Euphrates-Tigris River Basin*. London: Kluwer Law International, New York: The Hague.
- Koeln, G., & Bissonnette, J. (2000). *Cross-correlation analysis: Mapping landcover change with a historic landcover database and a recent, single-date multispectral image*. Proceedings of ASPRS Annual Convention, Washington, D.C., 2000.
- Kohonen, T. (1989). *Self-organisation and associative memory*. New York: Springer.
- Kolm, K. E., & Case, H. L. (1984). The identification of irrigated crop types and estimation of acreages from Landsat imagery. *Photogrammetric Engineering and Remote Sensing*, 50 (10), 1479–1490.
- Kontoos, C., Wilkinson, G. G., Burrill, A., Goffredo, S., & Megier, J. (1993). An experimental system for the integration of GIS data in knowledge-based image analysis for remote sensing of agriculture. *International Journal of Geographical Information Systems*, 7 (3), 247–262.
- Korkutan, S. (2001). *The sources of conflict in the Euphrates-Tigris Basin and its strategic consequences in the Middle East* (Master's Thesis).
- Kulkarni, A. D., & Lulla, K. (1999). Fuzzy neural network models for supervised classification: Multispectral image analysis. *Geocarto International*, 14 (4), 42–50.
- Kumar, L., Schmidt, K., Dury, S., & Skidmore, A. (2001). Imaging spectrometry and vegetation science. In F. D. Van der Meer & S. M. De Jong (Eds.), *imaging spectrometry* (pp. 111-155). Dordrecht: Kluwer Academic Publishers.
- Kwarteng, A. Y., & Chavez, P. S. Jr. (1998). Change detection study of Kuwait city and environs using multitemporal Landsat Thematic Mapper data. *International Journal of Remote Sensing*, 19 (9), 1651–1661.
- Laba, M., Gregory, S. k., Braden, J., Ogurcak, D., Hill, E., Fegraus, E., Fiore, J., & Degloria, S. D. (2002). Conventional and fuzzy accuracy assessment of the New York gap analysis project land cover map. *Remote Sensing of Environment*, 81 (2-3), 443-455.
- Laliberte, A. S., Rango, A., Havstad, K. M., Paris, J. F., Beck, R. F., McNeely, R., & Gonzalez, A. L. (2004). Object-oriented image analysis for mapping shrub encroachment from 1937 to 2003 in southern New Mexico. *Remote Sensing of Environment*, 93 (1-2), 198-210.
- Laliberte, A. S., Fredrickson, E. L., & Rango, A. (2007). Combining decision trees with hierarchical object-oriented image analysis for mapping arid rangelands. *Photogrammetric Engineering & Remote Sensing*, 73 (2), 197-207.
- Lam, N. S.-N. (2008). Methodologies for mapping land cover/land use and its change. In S. Liang (Ed.), *advances in land remote sensing* (pp. 341–367). Springer.
- Lamb, D. W., & Brown, R. B. (2001). Remote sensing and mapping of weeds in crops. *Journal of Agricultural Engineering Research*, 78 (2), 117-125.
- Lambers, H., Stuart, F., C. III, & Pons, T. L. (1998). *Plant physiological ecology*. New York: Springer.
- Lambin, E. F., & Strahler, A. H. (1994). Change-vector analysis in multitemporal space: A tool to detect and categorize land-cover change processes using high temporal- resolution satellite data. *Remote Sensing of Environment*, 48 (2), 231-244.
- Lambin, E. F., & Ehrlich, D. (1997). Land-cover changes in sub-Saharan Africa (1982–1991): Application of a change index based on remotely sensed surface temperature and vegetation indices at a continental scale. *Remote Sensing of Environment*, 61 (2), 181-200.

- Lambin, E. F., Baulies, X., Bockstael, N., Fischer, G., Krug, T., Leemans, R., Moran, E. F., Rindfuss, R. R., Sato, Y., Skole, D., Turner, B. L. II, & Vogel, C. (1999). *Land-use and land-cover change (LUCC): Implementation strategy* (IGBP report no. 48, IHDP report no. 10). Stockholm, Bonn.
- Lambin, E. F., Geist, H. J., & Lepers, E. (2003). Dynamics of land-use and land-cover change in tropical regions. *Annual Review of Environment Resources*, 28, 205-241.
- Lambin, E. F., & Linderman, M. (2006). Time series of remote sensing data for land change science. *IEEE Transactions on geoscience and remote sensing*, 44 (7), 1926–1928.
- Landgrebe, D. A. (2003). *Signal theory methods in multispectral remote sensing*. Hoboken, NJ: John Wiley and Sons.
- Langford, M., & Bell, W. (1997). Land cover mapping in a tropical hillsides environment: A case study in the Cauca region of Colombia. *International Journal of Remote Sensing*, 18 (6), 1289-1306.
- Lardeux, C., Frison, P. L., Rudant, J. P., Souyris, J. C., Tison, C., & Stoll, B. (2006). *Use of the SVM classification with polarimetric SAR data for land use cartography*. Proceedings of International Geoscience And Remote Sensing Symposium IGARSS, Denver, USA, 2006.
- LaRocca, A. J. (1993). Atmospheric absorption. In W. L. Wolfe & G. J. Zissis (Eds.), *the infrared handbook* (pp. 5-132). Ann Arbor, Michigan: Environmental Research Institute of Michigan (ERIM).
- Lauer, D. T., Morain, S. A., & Salomonson, V. V. (1997). The Landsat program: It's origins, evolutions, and impacts. *Photogrammetric Engineering and Remote Sensing*, 63 (7), 831-38.
- Lechner, A. M., Stein, A., Jones, S. D., & Ferwerda, J. G. (2009). Remote sensing of small and linear features: Quantifying the effects of patch size and length, grid position and detectability on land cover mapping. *Remote Sensing of Environment*, 113 (10), 2194–2204.
- Lee, J., & Ersoy, O. K. (2007). Consensual and hierarchical classification of remotely sensed multispectral images. *IEEE Transactions on Geoscience and Remote Sensing*, 45 (9), 2953-2963.
- Lee, J. Y., & Warner, T. A. (2006). Segment based image classification. *International Journal of Remote Sensing*, 27 (16), 3403-3412.
- Leica Geosystems. (2005). *ERDAS IMAGINE 9.0*. Atlanta.
- Lesschen, J. P., Verburg, P. H., & Staal, S. J. (2005). *Statistical methods for analysing the spatial dimension of changes in land-use and farming systems*. Nairobi, Kenya: International Livestock Research Institute, LUCC Report Series, N. 7, p. 80.
- Liang, S., Fallah-Adl, H., Kalluri, S., JaJa, J., Kaufman, Y. J., & Townshend, J. R. G. (1997). An operational atmospheric correction algorithm for Landsat thematic mapper imagery over the land. *Journal Geophysical Research Atmospheres*, 102 (14), 17173-17186.
- Liang, S., Fang, H., & Chen, M. (2001). Atmospheric correction of Landsat ETM+ land surface imagery, part 1: Methods. *IEEE Transactions on Geoscience and Remote Sensing*, 39 (11), 2490-2498.
- Liang, S. (2004). Estimation of land surface biophysical variables. In G. A. Kong (Ed.), *qualitative remote sensing of land surfaces* (pp. 246-309). New York: Wiley Series in Remote Sensing, John Wiley & Sons.
- Lillesand, M. T., Kiefer, R. W., & Chipman, J. W. (2008). *Remote sensing and image interpretation* (6<sup>th</sup> ed.). Hoboken, NJ: John Wiley & Sons.
- Liu, D., Song, K., Townshend, J. R. G., & Gong, P. (2008). Using local transition probability models in Markov random fields for forest change detection. *Remote Sensing of Environment*, 112 (5), 2222–2231.
- Liu, D., & Xia, F. (2010). Assessing object-based classification: Advantages and limitations. *Remote Sensing Letters*, 1 (4), 187-194.

- Liu, J., Liu, M., Tian, H., Zhuang, D., Zhang, Z., Zhang, W., Tang, X., & Deng, X. (2005). Spatial and temporal patterns of China's cropland during 1990–2000: An analysis based on Landsat TM data. *Remote Sensing of Environment*, 98 (4), 442–456.
- Liu, J. G., & Mason, P. J. (2009). *Essential image processing and GIS for remote sensing*. UK: John Wiley & Sons Ltd.
- Liu, W., Gopal, S., & Woodcock, C. E. (2004 a). Uncertainty and confidence in land cover classification using a hybrid classifier approach. *Photogrammetric Engineering & Remote Sensing*, 70 (8), 963–971.
- Liu, W., Seto, K. C., Wu, E. Y., Gopal, S., & Woodcock, C. E. (2004 b). ART-MAP: A neural network approach to subpixel classification. *IEEE Transactions on Geoscience and Remote Sensing*, 42 (9), 1976–1983.
- Liu, W., & Wu, E. Y. (2005). Comparison of non-linear mixture models: Subpixel classification. *Remote Sensing of Environment*, 94 (2), 145–154.
- Liu, X., Li, X., & Zhang, X. (2010). Determining class proportions within a pixel using a new mixed-label analysis method. *IEEE Transactions on Geoscience and Remote Sensing*, 48 (4), 1882–1891.
- Liu, X.-H., Skidmore, A. K., & Van Oosten, H. (2002). Integration of classification methods for improvement of landcover map accuracy. *ISPRS Journal of Photogrammetry & Remote Sensing*, 56 (4), 257–268.
- Lloyd, C. D., Berberoglu, S., Curran, P. J., & Atkinson, P. M. (2004). A comparison of texture measures for the per-field classification of Mediterranean land cover. *International Journal of Remote Sensing*, 25 (19), 3943–3965.
- Lo, C. P., & Yeung, A. K. W. (2002). *Concepts and techniques of geographic information systems*. Upper Saddle River, NJ: Prentice-Hall.
- Lobo, A., Chic, O., & Casterad, A. (1996). Classification of Mediterranean crops with multisensor data: Per-pixel versus per-object statistics and image segmentation. *International Journal of Remote Sensing*, 17 (12), 2385–2400.
- Löffler, E. (1994). *Geographie und Fernerkundung: Eine Einführung in die geographische Interpretation von Luftbildern und modernen Fernerkundungsdaten* (2. Aufl.). Stuttgart: Teubner.
- Lohmann, P., Soergel, U., Tavakkoli, M., & Farghaly, D. (2008). *Multi-temporal classification for crop discrimination using Terra SAR-X spotlight images*. (Project paper: A pilot project of DLR TerraSAR Science proposal LAN0011).
- Lord, D., Desjardins, R. L., & Dube, P. A. (1985 a). Influence of wind on crop canopy reflectance measurements. *Remote Sensing of Environment*, 18 (2), 113–123.
- Lord, D., Desjardins, R. L., Dube, P. A., & Brach, E. J. (1985 b). Variations of crop canopy spectral reflectance measurements under changing sky conditions. *Photogrammetric Engineering and Remote Sensing*, 51 (6), 689–695.
- Los, S. O., Tucker, C. J., Anyamba, A., Cherlet, M., Collatz, G. J., Giglio, L., Hall, F. G., & Kendall, J. A. (2002). The biosphere: A global perspective. In A. Skidmore (Ed.), *environmental modelling with GIS and remote sensing* (pp. 70–96). CRC Press.
- Loveland T. R., Zhu, Z., Ohlen, D. O., Brown, J. F., Reed, B. C., & Yang, L. (1999). An analysis of the IGBP global land-cover characterization process. *Photogrammetric Engineering and Remote Sensing*, 65 (9), 1021–1032.
- Loveland, T. R., Reed, B. C., Brown, J. F., Ohlen, D. O., Zhu, Z., & Yang, L. (2000). Development of a global land cover characteristics database and IGBP DISCover from 1 km AVHRR data. *International Journal of Remote Sensing*, 21 (6–7), 1303–1330.
- Lu, D., Mausel, P., Brondizio, E., & Moran, E. (2003 a). Change detection techniques. *International Journal of Remote Sensing*, 25 (12), 2365–2407.
- Lu, D., Moran, E., & Batistella, M. (2003 b). Linear mixture model applied to Amazonian vegetation classification. *Remote Sensing of Environment*, 87 (4), 456–469.

- Lu, D., Mausel, P., Batistella, M., & Moran, E. (2004). Comparison of land-cover classification methods in the Brazilian amazon basin. *Photogrammetric Engineering and Remote Sensing*, 70 (6), 723–731.
- Lu, D., & Weng, Q. (2004). Spectral mixture analysis of the urban landscapes in Indianapolis with Landsat ETM+ imagery. *Photogrammetric Engineering and Remote Sensing*, 70 (9), 1053–1062.
- Lu, D., & Weng, Q. (2007). A survey of image classification methods and techniques for improving classification performance. *International Journal of Remote Sensing*, 28 (5), 823–870.
- Lu, L., Zhihao, Q., & Jingjing, L. (2008). *Mapping the irrigation area of winter wheat farmland in north China plain using modis remote sensing data* (Vol. XXXVII, Part: B4). Proceedings of The International Archives of the Photogrammetry, Remote Sensing and Spatial Information Sciences, Beijing, 2008.
- Lucas, R., Rowlands, A., Brown, A., Keyworth, S., & Bunting, P. (2007). Rule-based classification of multi-temporal satellite imagery for habitat and agricultural land cover mapping. *ISPRS Journal of Photogrammetry & Remote Sensing*, 62 (3), 165–185.
- Lunetta, R. S. (1999). Application, project, and analytical Approach. In Ross S. Lunetta & C. D. Elvidge (Eds.), *remote sensing change detection environmental monitoring methods and applications* (pp. 1-19). London: Taylor and Francis.
- Lunetta, R. S., & Elvidge, C. D. (2000). *Remote sensing change detection: Environmental monitoring methods and applications*. New York: Taylor and Francis.
- Lunetta, R. S., Ediriwickrema, J., Johnson, D. M., Lyon, J. G., & McKerrow, A. (2002). Impacts of vegetation dynamics on the identification of land-cover change in a biologically complex community in North Carolina, USA. *Remote Sensing of Environment*, 82 (2–3), 258–270.
- Lunetta, R. S., Johnson, D. M., Lyon, J. G., & Crotwell, J. (2004). Impacts of imagery temporal frequency on land-cover change detection monitoring. *Remote Sensing of Environment*, 89 (4), 444–454.
- Lunetta, R. S., Knight, J. F., Ediriwickrema, J., Lyon, J. G., & Worthy, L. D. (2006). Land-cover change detection using multi-temporal MODIS NDVI data. *Remote Sensing of Environment*, 105 (2), 142–154.
- Lyon, J. G., Yuan, D., Lunetta, R. S., & Elvidge, C. D. (1998). A change detection experiment using vegetation indices. *Photogrammetric Engineering and Remote Sensing*, 64 (2), 143–150.
- Ma, Z., & Redmond, R. L. (1995). Tau coefficients for accuracy assessment of classification of remote sensing data. *Photogrammetric Engineering and Remote Sensing*, 61 (4), 435–439.
- Ministry of Agriculture and Agrarian Reform (MAAR). (1993 a). *Annual plan for agricultural production 1993/94*. Damascus, Syria.
- Ministry of Agriculture and Agrarian Reform (MAAR). (1993 b). *Balance of land utilization for 1993*. Damascus, Syria.
- Ministry of Agriculture and Agrarian Reform (MAAR). (2008). *The distribution of irrigation projects in Euphrates River Basin*. Damascus, Syria.
- MacDonald, R. B., & Hall, F. G. (1980). Global crop forecasting. *Science*, 208 (4445), 670-679.
- MacLeod, R. D., & Congalton, R. G. (1998). A quantitative comparison of change detection algorithms for monitoring eelgrass from remotely sensed data. *Photogrammetric Engineering & Remote Sensing*, 64 (3), 207-216.
- Magnussen, S., Boudewyn, P., & Wulder, M. (2004). Contextual classification of Landsat TM images to forest inventory cover types. *International Journal of Remote Sensing*, 25 (12), 2421–2440.
- Mahmood, T., & Easson, G. (2006). *Comparing aster and Landsat-7 etm+ for change detection*. Proceedings of ASPRS Annual Conference, May 1-5, 2006, Reno, Nevada.

- Malpica, J. A., & Alonso, M. C. (2008). *A method for change detection with multi-temporal satellite images using the rx- algorithm* (Vol. XXXVII, Part: B7). Proceedings of The International Archives of the Photogrammetry, Remote Sensing and Spatial Information Sciences, Beijing, 2008.
- Mannan, B., Rot, J., & Ray, A. K. (1998). Fuzzy ARTMAP supervised classification of multispectral remotely-sensed images. *International Journal of Remote Sensing*, 19 (4), 767–774.
- Mannan, B., & Ray, A. K. (2003). Crisp and fuzzy competitive learning networks for supervised classification of multispectral IRS scenes. *International Journal of Remote Sensing*, 24 (17), 3491–3502.
- Marcal, A. R. S., Borges, J. S., Gomes, J. A., & Da Costa, J. F. P. (2005). Land cover update by supervised classification of segmented ASTER images. *International Journal of Remote Sensing*, 26 (7), 1347-1362.
- Marceau, D. J., Howarth, P., & Gratton, D. J. (1994 a). Remote sensing and the measurement of the geographical entities in a forested environment: 1. The scale and spatial aggregation problem. *Remote Sensing of Environment*, 49 (2), 93–104.
- Marceau, D. J., Gratton, D. J., Fourier, R. A., & Fortin, J. (1994 b). Remote sensing and the measurement of the geographical entities in a forested environment: 2. The optimal spatial resolution. *Remote Sensing of Environment*, 49 (2), 105–117.
- Markham, B. L., & Townshend, J. R. G. (1981). *Land cover classification accuracy as a function of sensor spatial resolution* (pp. 1075-1090). Proceedings of the 15<sup>th</sup> International Symposium on Remote Sensing of Environment, Ann Arbor, MI: Environmental Research Institute of Michigan.
- Markham, B. L., & Barker, J. L. (1987). Thematic mapper bandpass solar exoatmospheric irradiances. *International Journal of Remote Sensing*, 8 (3), 517–523.
- Martinez-Beltran, C., & Calera-Belmonte, A. (2001). Irrigated crop estimation using Landsat TM imagery in La Mancha, Spain. *Photogrammetric Engineering & Remote Sensing*, 67 (10), 1177–1184.
- Martínez-Casasnovas, J. A., Martí-in-Montero, A., & Casterad, M. A. (2005). Mapping multi-year cropping patterns in small irrigation districts from time-series analysis of Landsat TM images. *European Journal of Agronomy*, 23 (2), 159–169.
- Mas, J. F. (1999). Monitoring land-cover changes: A comparison of change detection techniques. *International Journal of Remote Sensing*, 20 (1), 139–152.
- Maselli, F., Conese, C., Petkov, L., & Gilabert, M. A. (1993). Environmental monitoring and crop forecasting in the Sahel through the use of NOAA NDVI data. A case study: Niger 1986-89. *International Journal of Remote Sensing*, 14 (18), 3471-3487.
- Maselli, F., Conese, C., & Petkov, L. (1994). Use of probability entropy for the estimation and graphical representation of the accuracy of maximum likelihood classifications. *ISPRS Journal of Photogrammetry and Remote Sensing*, 49 (2), 13–20.
- Maselli, F., Rodolfi, A., & Conese, C. (1996). Fuzzy classification of spatially degraded Thematic Mapper data for the estimation of sub-pixel components. *International Journal of Remote Sensing*, 17 (3), 537–551.
- Mather, P. M. (2004). *Computer processing of remotely-sensed images: An introduction* (3<sup>rd</sup> ed.). Chichester: John Wiley and Sons.
- Matinfar, H. R., Sarmadian, F., Alavi Panah, S. K., & Heck, R. J. (2007). Comparisons of object-oriented and pixel-based classification of land use/land cover types based on landsat7, Etm+ spectral bands (case study: arid region of Iran). *American-Eurasian J. Agric. & Environ. Sci.*, 2 (4), 448-456.
- Mausel, P. W., Kramber, W. J., & Lee, J. K. (1990). Optimum band selection for supervised classification of multispectral data. *Photogrammetric Engineering and Remote Sensing*, 56, 55–60.



- McCloy, K. R. (1995). *Resource management system: process and practice*. London: Taylor and Francis.
- McCloy, K. R., & Bøcher, P. K. (2007). Optimizing image resolution to maximize the accuracy of hard classification. *Photogrammetric Engineering & Remote Sensing*, 73 (8), 893–903.
- McCoy, R. M. (2005). *Field methods in remote sensing*. New York, NY: Guilford Press.
- McGovern, E. A., Holden, N. M., Ward, S. M., & Collins, J. F. (2002). The radiometric normalization of multitemporal Thematic Mapper imagery of the midlands of Ireland: A case study. *International Journal of Remote Sensing*, 23 (4), 751–766.
- McIver, D. K., Friedl, M. A. (2002). Using prior probabilities in decision-tree classification of remotely sensed data. *Remote Sensing of Environment*, 81 (2-3), 253–261.
- McLachlan, G. (1992). *Discriminant analysis and statistical pattern recognition*. New York: Wiley.
- McVicar, T. R., & Jupp, D. L. B. (1998). The current and potential operational uses of remote sensing to aid decisions on drought exceptional circumstances in Australia: A review. *Agricultural Systems*, 57 (3), 399-468.
- Meadows, M. E., & Hoffman, M. T. (2002). The nature, extent and causes of land degradation in South Africa: Legacy of the past, lessons for the future?. *Area*, 34 (4), 428-437.
- Medhavy, T. T., Sharma, T., Dubey, R. P., Hooda, R. S., Mothikumar, K. E., Yadav, M., Manchanda, M. L., Ruhai, D. S., Khera, A. P., & Jarwal, S. D. (1993). Crop classification accuracy as influenced by training strategy, data transformation and spatial resolution of data. *Journal of the Indian Society of Remote Sensing*, 21 (1), 21-28.
- Mehner, H., Fairbairn, D., Csaplovics, E., & Cutler, M. (2004). *Transferability of artificial neural networks for mapping land cover of regional areas with high spatial resolution imagery* (Vol. 35 (CD), pp. 6). Proceedings of XXth ISPRS Congress, Int. Arch. of Photogrammetry, Remote Sensing and Spatial Information Sciences, July 14-23, 2004, Istanbul, Turkey.
- Melgani, F., Serpico, S. B., & Vernazza, G. (2003). Fusion of multitemporal contextual information by neural networks for multisensor remote sensing image classification. *Integrated Computer-Aided Engineering*, 10 (1), 81-90.
- Melgani, F., & Bruzzone, L. (2004). Classification of hyperspectral remote sensing images with support vector machines. *IEEE Transactions on Geoscience and Remote Sensing*, 42 (8), 1778-1790.
- Melgani, F., & Bazi, Y. (2006). Markovian fusion approach to robust unsupervised change detection in remotely sensed imagery. *IEEE Geoscience and Remote Sensing Letters*, 3 (4), 457-461.
- Metternicht, G., Honey, F., Beeston, G., & Gonzalez, S. (2000). *Airborne videography for rapid assessment of vegetation conditions in agricultural landscapes*. Proceedings of the 10<sup>th</sup> Australasian Remote Sensing and Photogrammetry Conference, August 21-25, Adelaide, Australia.
- Meyer, W. B. (1995). Past and present land-use and land-cover in the U.S.A. *Consequences*, 1 (1), 24-33.
- Michelson, D. B., Liljeberg, B. M., & Pilesjo, P. (2000). Comparison of algorithms for classifying Swedish landcover using Landsat TM and ERS-1 SAR data. *Remote Sensing of Environment*, 71 (1), 1-15.
- Mickelson, Jr., John, G., Civco, D. L., Silander, Jr., & John, A. (1998). Responses of spectral indices to variations in vegetation cover and soil background. *Photogrammetric Engineering and Remote Sensing*, 64 (9), 915-921.
- Miguel-Ayanz, J. S., & Biging, G. S. (1997). Comparison of single-stage and multi-stage classification approaches for cover type mapping with TM and SPOT data. *Remote Sensing of Environment*, 59 (1), 92–104.
- Miski, & Shawaf (2003). *Aspects of groundwater resources management, protection and monitoring in Syria*. Rep. prepared for ACSAD, ACSAD-BGR, technical cooperation

- project management, protection and sustainable use of groundwater and soil resources in the Arab Region between BGR and ACSAD. Damascus, Syria: ACSAD.
- Mitri, G. H., & Gitas, I. Z. (2004). A performance evaluation of a burned area object-based classification model when applied to topographically and non-topographically corrected TM imagery. *International Journal of Remote Sensing*, 25 (14), 2863-2870.
- Molenaar, M., & Richardson, D. E. (1994). *Object hierarchies for linking aggregation levels in GIS* (vol. 30, pp. 610-617). Proceedings of International Archives of Photogrammetry and Remote Sensing, Athens, 1994.
- Möller, L., Lymburner, L., & Volk, M. (2007). The comparison index: A tool for assessing the accuracy of image segmentation. *International Journal of Applied Earth Observation and Geoinformation*, 9 (3), 311–321.
- Moran, M. S., Jackson, R. D., Slater, P. N., & Teillet, P. M. (1992). Evaluation of simplified procedures for retrieval of land surface reflectance factors from satellite sensor output. *Remote Sensing of Environment*, 41 (2-3), 169-184.
- Moran, M. S., Clarke, T. R., Inoue, Y., & Vidal, A. (1994). Estimating crop water deficit using the relationship between surface-air temperature and spectral vegetation index. *Remote Sensing of Environment*, 49 (3), 246-263.
- Moran, M. S. (2000). *New imaging sensor technologies suitable for agricultural management* (pp. 1-10). Aspects of Applied Biology, 60. Remote Sensing in Agriculture, June 26-28, Royal Agriculture College, Cirencester, U.K.
- Muchoney, D. M., & Haack, B. (1994). Change detection for monitoring forest defoliation. *Photogrammetric Engineering and Remote Sensing*, 60 (10), 1243-1251.
- Muchoney, D., Borak, J., Chi, H., Friedl, M., Gopal, S., Hodges, J., Morrow, N., & Strahler, A. (2000). Application of the MODIS global supervised classification model to vegetation and land cover mapping of central America. *International Journal of Remote Sensing*, 6 (6-7), 1115–1138.
- Müller, S. V., Walker, D. A., Nelson, F. E., Auerbach, N. A., Bockheim, J. G., Guyer, S., & Sherba, D. (1998). Accuracy assessment of a land-cover map of the Kuparuk river basin, Alaska: Considerations for remote regions. *Photogrammetric Engineering & Remote Sensing*, 64 (6), 619– 628.
- Mura, M. D., Benediktsson, J. A., Bovolo, F., & Bruzzone, L. (2008). An unsupervised technique based on morphological filters for change detection in very high resolution images. *IEEE Geoscience and Remote Sensing Letters*, 5 (3), 433-437.
- Murai, H., & Omatu, S. (1997). Remote sensing image analysis using a neural network and knowledge-based processing. *International Journal of Remote Sensing*, 18 (4), 811–828.
- Murdoch, D. A., Vos, R., Abdallah, A., Abdallah, M., Andrews, I., Al-Asaad, A., Van Beusekum, R., Hofland, R., Roth, T., Saveyn, B., Serra, G., & Wells, C. (2005). *A winter survey of Syrian wetlands* (final report of the Syrian wetland expedition, January – February 2004). Privately published, UK: London.
- Næsset, E. (1996). Use of the weighted kappa coefficient in classification error assessment of thematic maps. *International Journal of Geographical Information Systems*, 10 (5), 591-604.
- Nalepka, R. P., & Hyde, P. D. (1972). *Classifying unresolved objects from simulated space data*. In: Eighth International Symposium on Remote Sensing of Environment, Ann Arbor, MI: Environmental Research Institute of Michigan, vol. 2: 935-949.
- NASA. (2005). *Remote sensing*. Retrieved July 22, 2009, from <http://earthobservatory.nasa.gov/library/>.
- Nelson, G. C. (2002). Introduction to the special issue on spatial analysis for agricultural economists. *Agricultural Economics*, 27 (3), 197–200.
- Nelson, R. F. (1983). Detecting forest canopy change due to insect activity using Landsat MSS. *Photogrammetric Engineering & Remote Sensing*, 49, 1303-1314.

- Nielsen, A. A., Conradsen, K., & Simpson, J. J. (1998). Multivariate alteration detection (MAD) and MAF processing in multispectral, bitemporal image data: New approaches to change detection studies. *Remote Sensing of Environment*, 64 (1), 1-19.
- Nielsen, A. A. (2007). The regularized iteratively reweighted MAD method for change detection in multi- and hyperspectral data. *IEEE Transactions on Image Processing*, 16 (2), 463-478.
- Niemeyer, I., & Canty, M. J. (2001). *Object-oriented post-classification of change images* (pp. 100-108). Proceedings of the SPIE's International Symposium on Remote Sensing, Toulouse, France.
- Niemeyer, I., & Canty, M. J. (2003). *Pixel-based and object-oriented change detection analysis using high-resolution imagery*. Retrieved from [http://www.definiensimaging.com/documents/publications/esarda03\\_nieca.pdf](http://www.definiensimaging.com/documents/publications/esarda03_nieca.pdf)
- Nikolakopoulos, K. G., Kamaratakis, E. K., Chrysoulakis, N. (2006). SRTM vs ASTER elevation products. Comparison for two regions in Crete, Greece. *International Journal of Remote Sensing*, 27 (21), 4819-4838.
- Nilsson, N. J. (1965). *Learning machines*. New York: McGraw-Hill.
- Nordberg, M., & Evertson, J. (2003). Monitoring change in mountainous dry-heath vegetation at a regional scale using multitemporal Landsat TM data. *Ambio*, 32 (8), 502-509.
- Okin, G. S., Murray, B., & Schlesinger, W. H. (2001). Degradation of sandy arid shrubland environments: Observation, process modelling, and management implications. *Journal of Arid Environments*, 47 (2), 123-144.
- Okomato, K., & Fukuhara, M. (1996). Estimation of paddy field area using the area ratio of categories in each pixel of Landsat TM. *International Journal of Remote Sensing*, 17 (9), 1735-1749.
- Olsson, K. (1985). *Remote sensing for fuelwood resources and land degradation studies in Kordofan, the Sudan*. Meddelande från Lunds Universitets Geografiska Institution, Avhandlingar C.
- Olthof, I., King, D. J., & Lautenschlager, R. A. (2004). Mapping deciduous forest ice storm damage using Landsat and environmental data. *Remote Sensing of Environment*, 89 (4), 484-496.
- Ono, A., Sakuma, F., Arai, K., Yamaguchi, Y., Fujisada, H., Slater, P. N., Thome, K. L., Palluconi, F. D., & Kieffer, H. H. (1996). Pre-flight and in-flight calibration plan for ASTER. *Journal of Atmospheric and Oceanic Technology*, 13 (2), p. 321.
- Ozdogan, M., Salvucci, G. D., & Anderson, B. C. (2006). Examination of the Bouchet–Morton complementary relationship using a mesoscale climate model and observations under a progressive irrigation scenario. *Journal of Hydrometeorology*, 7 (2), 235-251.
- Ozdogan, M., & Woodcock, C. E. (2006). Resolution dependent errors in remote sensing of cultivated areas. *Remote Sensing of Environment*, 103 (2), 203-217.
- Ozdogan, M., Gutman, G. (2008). A new methodology to map irrigated areas using multi-temporal MODIS and ancillary data: An application example in the continental US. *Remote Sensing of Environment*, 112 (9), 3520-3537.
- Ozdogan, M. (2010). The spatial distribution of crop types from MODIS data: Temporal unmixing using independent component analysis. *Remote Sensing of Environment*, 114 (6), 1190-1204.
- Pacifici, F., Del Frate, F., Solimini, C., & Emery, W. J. (2007). An innovative neural-net method to detect temporal changes in high-resolution optical satellite imagery. *IEEE Transactions on Geoscience and Remote Sensing*, 45 (9), 2940-2952.
- Pal, M., & Mather, P. M. (2003). An assessment of the effectiveness of decision tree methods for land cover classification. *Remote Sensing of Environment*, 86 (4), 554-565.
- Pal, M., & Mather, P. M. (2004). Assessment of the effectiveness of support vector machines for hyperspectral data. *Future Generation Computer System*, 20 (7), 1215-1225.

- Pal, M. (2005). Random forest classifier for remote sensing classification. *International Journal of Remote Sensing*, 26 (1), 217-222.
- Pal, M., & Mather, P. M. (2005). Support vector machines for classification in remote sensing. *International Journal of Remote Sensing*, 26 (5), 1007–1011.
- Pal, M., & Mather, P. M. (2006). Some issues in the classification of DAIS hyperspectral data. *International Journal of Remote Sensing*, 27 (14), 2895-2916.
- Pal, N. R., & Pal, S. K. (1993). A review on image segmentation techniques. *Pattern Recognition*, 26 (9), 1277-1294.
- Palubinskas, G., Lucas, R. M., Foody, G. M., & Curran, P. J. (1995). An evaluation of fuzzy and texture-based classification approaches for mapping tropical forest classes from Landsat-TM data. *International Journal of Remote Sensing*, 16 (4), 747-759.
- Panigrahy, S., & Chakraborty, M. (1998). An integrated approach for potato crop intensification using temporal remote sensing data. *ISPRS Journal of Photogrammetry and Remote Sensing*, 53 (1), 54–60.
- Paola, J. D., & Schowengerdt, R. A. (1995 a). A detailed comparison of backpropagation neural network and maximumlikelihood. *IEEE Transactions on Geoscience and Remote Sensing*, 33 (4), 981-996.
- Paola, J. D., & Schowengerdt, R. A. (1995 b). A review and analysis of back propagation neural networks for classification of remotely sensed multispectral imagery. *International Journal of Remote Sensing*, 16 (16), 3033–3058.
- Pax-Lenney, M., Woodcock, C. E., Collins, J. B., & Hamdi, H. (1996). The status of agricultural lands in Egypt: The use of multitemporal NDVI features derived from Landsat TM. *Remote Sensing of Environment*, 56 (1), 8–20.
- Pax-Lenney, M., & Woodcock, C. E. (1997). The effect of spatial resolution on the ability to monitor the status of agricultural lands. *Remote Sensing of Environment* 61 (2), 210- 220.
- PCI. (2001). *Xspace help system* (softcopy, version 9.1). Ontario: Richmond Hill.
- Pedley, M. I., & Curran, P. J. (1991). Per-field classification: an example using SPOT HRV imagery. *International Journal of Remote Sensing*, 12 (11), 2181–2192.
- Pekkarinen, A. (2002). A method for the segmentation of very high spatial resolution images of forested landscapes. *International Journal of Remote Sensing*, 23 (14), 2817-2836.
- Peñuelas, J., Filella, I., Lloret, P., Munoz, F., & Vilajeliu, M. (1995). Reflectance assessment of mite effects on apple trees. *International Journal of Remote Sensing*, 16 (14), 2727-2733.
- Pervez, S., Brown, J. F., & Maxwell, S. (2008). *Evaluation of remote sensing-based irrigated area map for the conterminous united states*. Proceedings of Pecora 17: The Future of Land Imaging...Going Operational, November 18–20, 2008, Denver, Colorado, USA.
- Peynado, A., Gausman, H. W., Escobar, D. E., & Rodriguez, R. R. (1980). Detecting freeze damage to citrus leaves. *Hortscience*, 15, p. 435.
- Pilon, P. G., Howath, P. J., & Bullock, R. A. (1988). An enhanced classification approach to change detection in semi-arid environments. *Photogrammetric Engineering & Remote Sensing*, 54 (12), 1709-1716.
- Pinter, P. J., Zipoli, G., Maracchi, G., & Reginato, R. J. (1987). Influence of topography and sensor view angles on NIR/red ratio and greenness vegetation indices of wheat. *International Journal of Remote Sensing*, 8 (6), 953-957.
- Pinter, P. J., Ritchie, J. C., Hatfield, J. L., & Hart, G. F. (2003). The agricultural research service's remote sensing program: An example of interagency collaboration. *Photogrammetric Engineering and Remote Sensing*, 69 (6), 615–618.
- Platt, R. V., & Rapoza, L. (2008). An evaluation of an object-oriented paradigm for land use/land cover classification. *Professional Geographer*, 60 (1), 87-100.
- Palubinskas, G., Lucas, R. M., Foody, G. M., & Curran, P. J. (1995). An evaluation of fuzzy and texture-based classification approaches for mapping regenerating tropical forest classes from Landsat TM data. *International Journal of Remote Sensing*, 16 (4), 747-759

- Ponikarov, V. O. (1967). *The geology of Syria. Explanatory notes on the map of Syria, Scale: 1/500.000, part II, mineral deposits and underground water resources*. Moscow: Technoexport, 120 p.
- Potgieter, A. B., Apan, A., Hammer, G., & Dunn, P. (2010). Early-season crop area estimates for winter crops in NE Australia using MODIS satellite imagery. *ISPRS Journal of Photogrammetry and Remote Sensing*, 65 (4), 380-387.
- Powell, R. L., Matzke, N., De Souza Jr., C., Clark, M., Numata, I., Hess, L. L., & Roberts, D. A. (2004). Sources of error in accuracy assessment of thematic land-cover maps in the Brazilian Amazon. *Remote Sensing of Environment*, 90 (2), 221–234.
- Price, J. C. (2003). Comparing MODIS and ETM+ data for regional and global land classification. *Remote Sensing of Environment*, 86 (4), 491-499.
- Price, K. P., Egbert, S. L., Nellis, M. D., Lee, R. Y., & Boyce, R. (1997). Mapping land cover in a high plains agro-ecosystem using a multirate Landsat Thematic Mapper modeling approach. *Transactions of the Kansas Academy of Science*, 100 (1–2), 21–33.
- Qiu, F., & Jensen, J. R. (2004). Opening the black box of neural networks for remote sensing image classification. *International Journal of Remote Sensing*, 25 (9), 1749-1768.
- Qi, J., Chehbouni, A., Huete, A., Kerr, Y. H., & Sorooshian, S. (1994). A modified soil adjusted vegetation index. *Remote Sensing of Environment*, 48 (2), 119-126.
- Quarmby, N. A., Townshend, J. R. G., Settle, J. J., White, K. H., Milnes, M., Hindle, T. L., & Silleos, N. (1992). Linear mixture modeling applied to AVHRR data for crop area estimation. *International Journal of Remote Sensing*, 13 (3), 415–425.
- Radwan, W. (2006). *Water conflict between Syria and Turkey* (1<sup>st</sup> ed.). Beirut, Lebanon: Company of publications for distribution and publication.
- Rahman, Md. R., Hedayatul Islam, A. H. M., & Shareful Hassan, M. D. (2005). Change detection of winter crop coverage and the use of Landsat data with GIS. *The Journal of Geo-Environment*, 4, 1-13.
- Ram, B., & Kolarkar, A. S. (1993). Remote sensing application in monitoring land use changes in arid Rajasthan. *International Journal of Remote Sensing*, 14 (17), 3191–3200.
- Ram, K., & Chauhan, J. S. (2009). Application of remote sensing and GIS to assess land use changes in Jhunjhun district of arid Rajasthan. *Journal of the Indian Society of Remote Sensing*, 37 (4), 671-680.
- Ramachandra, T. V., & Kumar, U. (2004). *Geographic resources decision support system for land use, land cover dynamics analysis*. Proceedings of the FOSS/GRASS Users Conference, Bangkok, Thailand.
- Ranson, K. J., Daughtry, C. S. T., Biehl, L. L., & Bauer, M. E. (1985). Sun-view angle effects on reflectance factors of corn canopies. *Remote Sensing of Environment*, 18 (2), 147-161.
- Raptis, V. S., Vaughan, R. A., & Wright, G. G. (2003). The effect of scaling on land cover classification from satellite data. *Computers & Geosciences*, 29 (6), 705–714.
- Rashed, T., Weeks, J. R., Gadalla, M. S., & Hill, A. G. (2001). Revealing the anatomy of cities through spectral mixture analysis of multispectral satellite imagery: A case study of the Greater Cairo region, Egypt. *Geocarto International*, 16 (4), 5–15.
- Ray, T. W. (1995). *Remote monitoring of land degradation in arid/semiarid regions* (Doctoral dissertation, California Institute of Technology).
- Richards, J. (1986). *Remote sensing digital image analysis: an introduction*. New York, NY: Springer-Verlag.
- Richards, J. A., & Jia, X. (2003). *Remote sensing digital image analysis: An introduction* (3<sup>rd</sup> ed.). New York: Springer-Verlag.
- Richards, J. A. (2005). Analysis of remotely sensed data: The formative decades and the future. *IEEE Transactions on Geoscience and Remote Sensing*, 43 (3), 422-432.
- Richter, R. (1996 a). A spatially adaptive fast atmospheric correction algorithm. *International Journal of remote Sensing*, 17 (6), 1202-1214.

- Richter, R. (1996 b), Atmospheric correction of satellite data with haze removal including a haze/clear transition region. *Computers and Geosciences*, 22 (6), 675-681.
- Richter, R. (2011). *Atmospheric / topographic correction for satellite imagery: ATCOR-2/3 User Guide*. DLR IB 565-01/11, Germany: Wessling.
- Ricotta, C., & Avena, G. C. (1999). The influence of fuzzy set theory on the areal extent of thematic map classes. *International Journal of Remote Sensing*, 20 (1), 201–205.
- Ricotta, C., & Avena, G. C. (2002). Evaluating the degree of fuzziness of thematic maps with a generalized entropy function: A methodological outlook. *International Journal of Remote Sensing*, 23 (20), 4519–4523.
- Ricotta, C. (2004). Evaluation the classification accuracy of fuzzy thematic maps with a simple parametric measure. *International Journal of Remote Sensing*, 25 (11), 2169-2176.
- Ridd, M., & Liu, J. (1998). A comparison of four algorithms for change detection in an urban environment. *Remote Sensing of Environment*, 63 (2), 95-100.
- Riebsame, W. E., Meyer, W. B., & Turner, B. L. II. (1994). Modeling land-use and cover as part of global environmental change. *Climate Change*, 28 (1-2), 45-64.
- Ripley, B. (1996). *Pattern recognition and neural networks*. Cambridge: University Press.
- Roberts, D. A., Batista, G. T., Pereira, J. L. G., Waller, E. K., & Nelson, B. W. (1998 a). Change identification using multitemporal spectral mixture analysis: Applications in eastern Amazonia. In R. S. Lunetta & C. D. Elvidge (Eds.), *remote sensing change detection: Environmental monitoring methods and applications* (pp. 137–161). Chelsea, MI: Ann Arbor Press.
- Roberts, D. A., Gardner, M., Church, R., Ustin, S., Scheer, G., & Green, R. O. (1998 b). Mapping chaparral in the Santa Monica mountains using multiple endmember spectral mixture models. *Remote Sensing of Environment*, 65 (3), 267–279.
- Robin, A., Hégarat-Masclé, S. L., & Moisan, L. (2008). Unsupervised subpixelic classification using coarse-resolution time series and structural information. *IEEE Transactions on Geoscience and Remote Sensing*, 46 (5), 1359-1374.
- Robinson, C. J. (1981). The logic of multispectral classification and mapping of land. *Remote Sensing of Environment*, 11, 231-244.
- Rogan, J., Franklin, J., & Roberts, D. A. (2002). A comparison of methods for monitoring multitemporal vegetation change using Thematic Mapper imagery. *Remote Sensing of Environment*, 80, 143-156.
- Roli, F., Giacinto, G., & Vernazza, G. (1997). Comparison and combination of statistical and neural networks algorithms for remote-sensing image classification. In J. Austin I. Kanellopoulos F. Roli & G. Wilkinson (Eds.), *neurocomputation in remote sensing data analysis* (pp. 117-124). Berlin: Springer-Verlag.
- Rosenzweig, C., Strzepek, K. M., Major, D. C., Iglesias, A., Yates, D. N., McCluskey, A., & Hillel, D. (2004). Water resources for agriculture in a changing climate: International case studies. *Global Environmental Change Part A*, 14 (4), 345–360.
- Rumelhart, D. E., Hinton, G. E., & Williams, R. J. (1996). *Learning internal representation by error propagation. Parallel distributed processing: Explorations in the microstructure of cognition, volume 1: Foundations*. Cambridge, MA: The MIT Press.
- Rundquist, D. C., Hoffman, R. O., Carlson, M. P., and Cook, A. E. (1989). The Nebraska center-pivot inventory: An example of operational satellite remote sensing on a long-term basis. *Photogrammetric Engineering and Remote Sensing* 55 (1), 587–590.
- Salvato, P. J. (1973). *Iterative techniques to estimate signature vectors for mixture processing of multispectral data*. In: Symposium on Machine Processing of Remotely Sensed Data, IEEE, vol. 73CH0834-2GE: 3B:48-62.
- Satalino, G., Mattia, F., Le Toan, T., & Rinaldi, M. (2009). Wheat crop mapping by using ASAR AP data. *IEEE Transactions on Geoscience and Remote Sensing*, 47 (2), 527-530.

- Schaale, M., & Furrer, R. (1995). Land surface classification by neural networks. *International Journal of Remote Sensing*, 16 (16), 3003-3031.
- Solberg, A., Schistad, H., Jain, A. K., & Taxt, T. (1994). Fusion of multitemporal satellite images and GIS data for land-use classification. *IEEE Transactions in Geoscience and Remote Sensing*, 32 (4), 768-778.
- Schlerf, M., Hill, J., Bärtsch, S., & Atzberger, C. (2003). Einfluss der spektralen und räumlichen Auflösung von Fernerkundungsdaten bei der Nadelwaldklassifikation. *Photogrammetrie, Fernerkundung, Geoinformation*, 1, 27-34.
- Schmidt, H., & Karnieli, A. (2000). Remote sensing of the seasonal variability of vegetation in a semi-arid environment. *Journal of Arid Environments*, 45 (1), 43-59.
- Schmidt, M. (2003). Development of a fuzzy expert system for detailed land cover mapping in the Dra catchment (Morocco) using high resolution satellite images (Doctoral dissertation, Rheinischen Friedrich-Wilhelms-Universität Bonn, Mathematisch-Naturwissenschaftlichen Fakultät).
- Schölkopf, B., & Smola, A. (2002). *Learning with Kernels*. Cambridge, MA: MIT Press.
- Schott, J. R. (2007). *Remote sensing: The image chain approach*. USA: Oxford University Press.
- Schott, J. R., Salvaggio, C., & Volchok, W. J. (1988). Radiometric scene normalization using pseudo-invariant features. *Remote Sensing of Environment*, 26, 1-16.
- Schowengerdt, R. A. (1996). On the estimation of spatial-spectral mixing with classifier likelihood functions. *Pattern Recognition Letters*, 17 (13), 1379-1387.
- Schowengerdt, R. A. (2007). *Remote sensing models and methods for image processing*. New York: Academic Press.
- Schroeder, T. A., Cohen, W. B., Song, C., Canty, M. J., & Zhiqiang, Y. (2006). Radiometric calibration of Landsat data for characterization of early successional forest patterns in western Oregon. *Remote Sensing of Environment*, 103 (1), 16-26.
- Schultz, M. (2011). Land cover change detection of the Vu Gia Thu Bon river basin central Vietnam. (Master Thesis). Institute of Geography, University of Jena.
- Schurmann, J. (1996). *Pattern classification: A unified view of statistical and neural approaches*. New York, NY: John Wiley & Sons, 373 p.
- Sebal, D. J., & Bucklew, J. A. (2001). Support vector machines and the multiple hypothesis test problem. *IEEE Transactions on Signal Processing*, 49 (11), 2865-2872.
- Senay, G. B., Lyon, J. G., Ward, A. D., & Nokes, S. E. (2000). Using high spatial resolution multispectral data to classify corn and soybean crops. *Photogrammetric Engineering & Remote Sensing*, 66 (3), 319-327.
- Serpico, B., & Melgani, F. (2000). A fuzzy spatio-temporal contextual classifier for remote sensing images. In: Proc. of the IEEE-International Geoscience and Remote Sensing Symposium, IGARSS, Vol. 5, Hawaii, USA, 24-28 July, pp. 2438-2440.
- Serrano, L., Filella, I., & Peuelas, J. (2000). Remote sensing of biomass and yield of winter wheat under different nitrogen supplies. *Crop Science*, 40 (3), 723-731.
- Seto, K. C., & Liu, W. (2003). Comparing ARTMAP neural network with the maximum-likelihood classifier for detecting urban change. *Photogrammetric Engineering and Remote Sensing*, 69 (9), 981-990.
- Shahin, M. (1989). Review and assessment of water resources in the arab region. *Water International, journal of the International Water Resources Association*, 14.
- Shalan, M. A., Arora, M. K., & Ghosh, S. K. (2003). An evaluation of fuzzy classifications from IRS 1C LISS III imagery: A case study. *International Journal of Remote Sensing*, 24 (15), 3179-3186.
- Shaoqing, Z., & Lu, X. (2008). *The comparative study of three methods of remote sensing image change detection* (Vol. XXXVII. Part B7). Proceedings of the international archives of the photogrammetry, remote sensing and spatial information sciences, Beijing, 2008.

- Sharma, K. M. S., & Sarkar, A., (1998). A modified contextual classification technique for remote sensing data. *Photogrammetric Engineering and Remote Sensing*, 64 (4), 273–280.
- Shimabukuro, Y. E., Batista, G. T., Melio, E. M. K., Moreira, J. C., & Duarte, V. (1998). Using shade fraction image segmentation to evaluate deforestation in Landsat Thematic Mapper images of the Amazon region. *International Journal of Remote Sensing*, 19 (3), 535–541.
- Shimoni, M., Borghys, D., Heremans, R., Perneel, C., & Acheroy, M. (2009). Fusion of PolSAR and PolInSAR data for land cover classification. *International Journal of Applied Earth Observation and Geoinformation*, 11, 169–180.
- Siegel, B. S., & Goetz, A. F. H. (1977). Effect of vegetation on rock and soil type discrimination. *Photogrammetric Engineering and Remote Sensing*, 43 (2), 191–196.
- Singh, A. (1989). Review article: Digital change detection techniques using remotely-sensed data. *International Journal of Remote Sensing*, 10 (6), 989–1003.
- Skidmore, A. K. (1989). A comparison of techniques for calculating gradient and aspect from a gridded digital elevation model. *International Journal of Geographical Information Systems*, 3, 323–334.
- Skole, D. L., Chomentowski, W. H., Salas, W. A., & Nobre, A. D. (1994). Physical and human dimensions of deforestation in Amazonia. *BioScience*, 44 (5), 314-322.
- Slater, P. N. (1980). *Remote sensing: Optics and optical systems*. Massachusetts: Addison-Wesley Publishing Company, Reading.
- Smith, G. M., & Milton, E. G. (1999). The use of the empirical line method to calibrate remotely sensed data to reflectance. *International Journal of Remote Sensing*, 20 (13), 2653–2662.
- Smith, G. M., & Fuller, R. M. (2001). An integrated approach to land cover classification: An example in the Island of Jersey. *International Journal of Remote Sensing*, 22 (16), 3123-3142.
- Smith, J. H., & Ramey, D. B. (1982). *A crop area estimator based on changes in the temporal profile of a vegetative index* (495-498). Proceedings of the Survey Research Methods Section, American Statistical Association.
- Smith, J. H., Wickham, J. D., Stehman, S. V., & Yang, L. (2002). Impacts of patch size and land-cover heterogeneity on thematic image classification accuracy. *Photogrammetric Engineering & Remote Sensing*, 68 (1), 65-70.
- Smith, M. O., Ustin, S. L., Adams, J. B., & Gillespie, A. R. (1990 a). Vegetation in deserts: I. A regional measure of abundance from multispectral images. *Remote Sensing of Environment*, 31 (1), 31-26.
- Smith, M. O., Ustin, S. L., Adams, J. B., & Gillespie, A. R. (1990 b). Vegetation in deserts: II. Environmental influences on regional abundance. *Remote Sensing of Environment*, 31 (1), 27-52.
- Smits, P. C., Dellepiane, S. G., & Schowengerdt, R. A. (1999). Quality assessment of image classification algorithms for land-cover mapping: A review and a proposal for a costbased approach. *International Journal of Remote Sensing*, 20 (8), 1461–1486.
- Soares, J. J., Rennó, C. D., Formaggio, A. R., Da Costa Freitas, Y. C., & Frery, A. C. (1997). An investigation of the selection of texture features for crop discrimination using SAR imagery. *Remote Sensing of Environment*, 59 (2), 234-247.
- Sohl, T. L., Gallant, A. L., & Loveland, T. R. (2004). The characteristics and interpretability of land surface change and implications for project design. *Photogrammetric Engineering and Remote Sensing*, 70 (4), 439–448.
- Song, C., Woodcock, C. E., Seto, K. C., Lenney, M. P., & Macomber, S. A. (2001). Classification and change detection using Landsat TM data: When and how to correct atmospheric effect. *Remote Sensing of Environment*, 75 (2), 230–244.
- Song, M., Civco, D. L., & Hurd, J. D. (2005 a). A competitive pixel-object approach for land cover classification. *International Journal of Remote Sensing*, 26 (22), 4981-4997.



- Song, X., Fan, G. L., & Rao, M. (2005 b). Automatic CRP mapping using nonparametric Machine Learning approaches. *IEEE Transactions on Geoscience and Remote Sensing*, 43 (4), 888-897.
- South, S., Qi, J., & Lusch, D. P. (2004). Optimal classification methods for mapping agricultural tillage practices. *Remote Sensing of Environment*, 91 (1), 90-97.
- Spanner, M. A., Pierce, L. L., Peterson, D. L., Running, S. W. (1990). Remote sensing of temperate coniferous forest leaf area index: The influence of canopy closure, understory vegetation and background reflectance. *International Journal of Remote Sensing*, 11 (1), 95-111.
- Steele, B. M. (2000). Combining multiple classifiers: An application using spatial and remotely sensed information for land cover type mapping. *Remote Sensing of Environment*, 74 (3), 545-556.
- Stefan, S., & Itten, K. I. (1997). A physically-based model to correct atmospheric and illumination effects in optical satellite data of rugged terrain. *IEEE Transactions on Geoscience and Remote Sensing*, 35 (3), 708-717.
- Stefanov, W. L., Ramsey, M. S., & Christensen, P. R. (2001). Monitoring urban land cover change: An expert system approach to land cover classification of semiarid to arid urban centers. *Remote Sensing of Environment*, 77 (2), 173-185.
- Steffen, W., & Tyson, P. (Eds.). (2001). *Global change and the earth system: a planet under pressure*. The Global Environmental Change Programme, IGBP Science, Elsevier, Vol. 4, 32.
- Stehman, S. V., & Czaplewski, R. L. (1998). Design and analysis for thematic map accuracy assessment: Fundamental principles. *Remote Sensing of Environment*, 64 (3), 331-344.
- Stehman, S. V. (2004). A critical evaluation of the normalized error matrix in map accuracy assessment. *Photogrammetric Engineering and Remote Sensing*, 70 (6), 743-751.
- Stehman, S. V. (2005). Comparing estimators of gross change derived from complete coverage mapping versus statistical sampling of remotely sensed data. *Remote Sensing of Environment*, 96 (3-4), 466-474.
- Story, M., & Congalton, R. G. (1986). Accuracy assessment: A user's perspective. *Photogrammetric Engineering and Remote Sensing*, 52 (3), 397-399.
- Stow, D., Hamada, Y., Coulter, L., & Anguelova, Z. (2008). Monitoring shrubland habitat changes through object-based change identification with airborne multispectral imagery. *Remote Sensing of Environment*, 112 (3), 1051-1061.
- Strahler, A. H. (1980). The use of prior probabilities in maximum likelihood classification of remotely sensed data. *Remote Sensing of Environment*, 10 (2), 135-163.
- Stuckens, J., Coppin, P. R., & Bauer, M. E. (2000). Integrating contextual information with per-pixel classification for improved land cover classification. *Remote Sensing of Environment*, 71 (3), 282-296.
- Su, L. (2009). Optimizing support vector machine learning for semi-arid vegetation mapping by using clustering analysis. *ISPRS Journal of Photogrammetry and Remote Sensing*, 64 (4), 407-413.
- Sugiura, R., Noguchi, N., & Ishii, K. (2005). Remote-sensing technology for vegetation monitoring using an unmanned helicopter. *Biosystems Engineering*, 90 (4), 369-79.
- Sugumaran, R. (2001). Forest land cover classification using statistical and artificial neural network approaches applied to IRS LISS-III sensor. *Geocarto International*, 16 (2), 37-42.
- Suits, G. W. (1972). The calculation of the directional reflectance of a vegetative canopy. *Remote Sensing Environment*, 2, 117-125.
- Suliman, M. M. (2003). *Assessing and mapping land use/land cover change using remote sensing and GIS: A case study of El-Amud Al-Akhdar Settlement, southern Darfur-Sudan* (Master thesis, TUD, Germany).

- Swain, P. H., & Hauska, H. (1977). The decision tree classifier: Design and potential. *IEEE Transactions on Geoscience and Remote Sensing*, 15 (3), 142–147.
- Swain, P. H., & Davis, S. M. (Eds.). (1978). *Remote sensing: The quantitative approach*. New York: McGraw-Hill.
- Swain, P. H., Vardeman, S. B., & Tilton, J. C. (1981). Contextual classification of multispectral image data. *Pattern Recognition*, 13 (6), 429–441.
- Tanre, D., Deschamps, P. Y., Devaux, C., & Herman, M. (1988). Estimation of saharan aerosol optical thickness from blurring effects in thematic mapper data. *Journal of Geophysical Research*, 93 (12), 15955–15964.
- Tanre, D., & Legrand, M. (1991). On the satellite retrieval of Saharan dust optical thickness over land: Two different approaches. *Journal of Geophysical Research*, 96 (3), 5221–5227.
- Teillet, P. M., & Fedosejevs, G. (1995). On the dark target approach to atmospheric correction of remotely sensed data. *Canadian Journal of Remote Sensing*, 21 (4), 374–387.
- The General Authority for Meteorology. (2008). *Climatic data*. Damascus, Syria.
- The Syrian Ministry of Irrigation. (2005). *Reclamation and irrigation projects on the Euphrates River*. Report. Damascus, Syria.
- Theau, J., Peddle, D. R., & Duguay, C. R. (2005). Mapping lichen in a caribou habitat of northern Quebec, Canada, using an enhancement of classification method and spectral mixture analysis. *Remote Sensing of Environment*, 94 (2), 232–243.
- Thelin, G. P., & Heimes, F. J. (1987). *Mapping irrigated cropland from Landsat data for determination of water use from the high plains aquifer in parts of Colorado, Kansas, Nebraska, New Mexico, Oklahoma, south Dakota, Texas, and Wyoming* (USGS Professional Paper 1400-C). Washington: U.S. Government Printing Office.
- Thenkabail, P. S., Smith, R. B., & De Pauw, E. (2000). Hyperspectral vegetation indices and their relationships with agricultural crop characteristics. *Remote Sensing of Environment*, 71 (2), 158–182.
- Thenkabail, P. S., Smith, R. B., & De Pauw, E. (2002). Evaluation of narrowband and broadband vegetation indices for determining optimal hyperspectral wavebands for agricultural crop characterization. *Photogrammetric Engineering and Remote Sensing*, 68 (6), 607–621.
- Thiruvengadachari, S. (1981). Satellite sensing of irrigation patterns in semiarid areas: An Indian study. *Photogrammetric Engineering and Remote Sensing*, 47, 1493–1499.
- Thomas, N., Hendrix, C., & Congalton, R. G. (2003). A comparison of urban mapping methods using high-resolution digital imagery. *Photogrammetric Engineering and Remote Sensing*, 69 (9), 963–972.
- Tokola, T., Löfman, S., & Erkkilä, A. (1999). Relative calibration of multitemporal Landsat data for forest cover change detection. *Remote Sensing of Environment*, 68 (1), 1–11.
- Tompkins, S., Mustard, J. F., Pieters, C. M., Forsyth, D. W. (1997). Optimization of endmembers for spectral mixture analysis. *Remote Sensing of Environment*, 59 (3), 472–489.
- Tou, J., & Gonzalez, R. (1974). *Pattern recognition principles*. Reading, Massachusetts: Addison-Wesley.
- Toutin, T. (2004). Geometric processing of remote sensing images: Models, algorithms and methods. *International Journal of Remote Sensing*, 25 (10), 1893–1924.
- Townshend, J. R. G., & Justice, C. O. (1986). Analysis of dynamic of African vegetation using the NDVI. *International Journal of Remote Sensing*, 7 (11), 1124–1242.
- Townshend, J. R. G., Justice, C. O., & Gurney, C. (1992). The impact of misregistration on change detection. *IEEE Transactions on Geoscience and Remote Sensing*, 30 (5), 1054–1060.
- Townshend, J. R. G., & Justice, C. O. (1995). Spatial variability of images and the monitoring of changes in the normalized difference vegetation index. *International Journal of Remote Sensing*, 16 (12), 2187–2195.

- Townshend, J. R. G., Huang, C., Kalluri, S., DeFries, R., Liang, S., & Yank, K. (2000). Beware of per-pixel characterisation of land cover. *International Journal of Remote Sensing*, 21(4), 839–843.
- Tso, B., & Mather, P. M. (1999). Crop discrimination using multi-temporal SAR imagery. *International Journal of Remote Sensing*, 20 (12), 2443-2460.
- Tso, B., & Mather, P. M. (2009). *Classification methods for remotely sensed data* (2nd ed.). CRC Press, by Taylor & Francis Group, LLC.
- Tso, B. (1997). *An investigation of alternate strategies for incorporating spectral, textural, and contextual information in remote sensing image classification* (Doctoral dissertation, School of Geography, The University of Nottingham, UK.).
- Tucker, C. J. (1977). Asymptotic nature of grass canopy spectral reflectance. *Applied Optics*, 16 (5), 1151–1156.
- Tucker, C. J. (1979). Red and photographic infrared linear combinations for monitoring vegetation. *Remote Sensing of Environment*, 8 (2), 127–150.
- Tucker, C. J., Vanpraet, C., Boerwinkel, E., & Gaston, A. (1983). Satellite remote sensing of total dry matter production in the Senegalese Sahel. *Remote Sensing of Environment*, 13 (6), 461-474.
- Tucker, C. J. (1986). Maximum normalized difference vegetation index images for sub-Saharan Africa for 1983-1985. *International Journal of Remote Sensing*, 7 (11), 1383-1384.
- Tufte, L. (2003). Automatisierte Bestimmung von Bearbeitungsskalen für die Multiskalige Auswertung von hoch auflösenden Fernerkundungsdaten. *Photogrammetrie, Fernerkundung, Geoinformation*, 5, 383-394.
- Turner, B. L., Kasperson, R. E., Meyer, W. B., Dow, K., Golding, D., Kasperson, J. X., Mitchell, R. C., & Ratick, S. J. (1990). Two types of global environmental change: Definitional and spatial-scale issues in their human dimensions. *Global Environmental Change: Human and Policy Dimensions*, 1 (1), 14-22.
- Turner, B. L., Meyer, W. B., & Skole, D. L. (1994). Global land-use/land-cover change: Towards an integrated study. *Ambio* 23 (1), 91-95.
- Turner, B. L., Skole, D., Sanderson, S., Fischer, G., Fresco, L., & Leemans, R. (1995). *Land-use and land-cover change science/research plan* (IGBP report no. 35 & HDP report no. 7).
- Tutz, G. (2000). *Die Analyse kategorialer Daten: Anwendungsorientierte Einführung in Logit-Modellierung und kategoriale Regression*. München: Oldenbourg Wissenschaftsverlag.
- Udelhoven, Th., & Hill, J. (2009). Change detection in Syria's rangelands using long-term AVHRR data (1982–2004). In P. Aplin (Ed.), recent advances in remote sensing and geoinformation processing for land degradation assessment (pp. 117-132). ISPRS Series, Boca Raton, London: Taylor & Francis Group.
- Ulaby, F. T., Moore, R. K., & Fung, A. K. (1982). *Microwave remote sensing: Active and passive, from theory to applications* (vol. III). Massachusetts: Artech House.
- UNDP-FAO. (1966). *Etude des Ressources en Eaux Souterraines (République Arabe Syrienne)*. Rapport final, FAO/SF:17/SYR, p. 276.
- UNDP/FAO. (1994). *Improved management of water resources for agricultural use* (phase II). SYR/90/01. Damascus, Syria.
- USDA. (2004). *Census of agriculture* (vol. I). Geographic area series part 51, United States: Summary and state data. Washington, DC: U.S. Department of Agriculture.
- USGS. (2009). *USGS announcement: Opening the Landsat archive*. Retrieved January 5, from [http://landsat.usgs.gov/mission\\_headlines2009.php](http://landsat.usgs.gov/mission_headlines2009.php)
- Ustin, S. L., Smith, M. O., Jacquemoud, S., Verstraete, M., & Govaerts, Y. (1999). Geobotany: Vegetation mapping for the earth sciences. In A. N. Rencz (Ed.), *remote sensing for the earth sciences, manual of remote sensing* (pp. 189-248, vol. 3). New York: Wiley & Sons.

- Van der Linden, S., Waske, B., & Hostert, P. (2007). *Towards an optimized use of the spectral angle space*. Proceedings of the 5th workshop of the EARSeL SIG on Imaging Spectroscopy, Bruges, Belgium, 2007.
- Van der Wel, F., Van Der Gaag, L., & Gorthe, B. (1998). Visual exploration of uncertainty in remote sensing classification. *Computers & Geosciences*, 24 (4), 335–343.
- Van der Meer, F. D., & De Jong S. M. (Eds.). (2001). *Imaging spectrometry: Basic principles and prospective applications*. Bookseries remote sensing and digital image processing. Dordrecht: Kluwer Academic Publishers.
- Van der Meer, F. D., Schmidt, K. S., Bakker, W., & Bijker, W. (2002). New environmental remote sensing systems. In A. Skidmore (Ed.), *environmental modelling with GIS and remote sensing*. Taylor and Francis.
- Van Niel, T. G., & McVicar, T. R. (2000). *Assessing and improving positional accuracy and its effects on areal estimation at coleambally irrigation area* (technical report 101/00, p. 101). Cooperative Research Centre for Sustainable Rice Production.
- Van Niel, T. G., & McVicar, T. R. (2004 a). Determining temporal windows for crop discrimination with remote sensing: A case study in south-eastern Australia. *Computers and Electronics in Agriculture*, 45 (1-3), 91-108.
- Van Niel, T. G., & McVicar, T. R. (2004 b). Remote sensing of rice-based irrigated agriculture: A review. *Australian Journal of Agricultural Research*, 55 (2), 155-185.
- Van Oort, P. A. J. (2007). Interpreting the change detection error matrix. *Remote Sensing of Environment*, 108 (1), 1–8.
- Vapnik, V. N., & Chervonenkis, A. Y. (1971). On the uniform convergence of relative frequencies of events to their probabilities. *Theory of Probability and its Applications*, 16 (2), 264-280.
- Vapnik, V. N. (1995). *The nature of statistical learning theory*. New York: Springer-Verlag.
- Vapnik, V. N. (1998). *Statistical learning theory*. Chichester, New York: John Wiley & Sons.
- Vapnik, V. N. (1999). An overview of statistical learning theory. *IEEE Transactions of Neural Networks*, 10 (5), 988-999.
- Vermote, E., Tanre, D., Deuze, J. L., Herman, M., & Morcrette, J. J. (1997). Second simulation of the satellite signal in the solar spectrum, 6S: An overview. *IEEE Transactions on Geoscience and Remote Sensing*, 35 (3), 675–686.
- Velpuri, M., Thenkabail, P.S., Biradar, C.B., Gumma, M.K., Noojipady, P., Dheeravath, V., ...Cai, X. (2007). Methods for mapping irrigated areas using Landsat ETM+ 30 meter, SRTM 90 meter, and MODIS 500 meter time series data taking Krishna river basin, India.
- Vitousek, P. M. (1994). Beyond global warming: Ecology and global change. *Ecology*, 75 (7), 1861–1876.
- Vogelmann, J. E., Howard, S. M., Yang, L., Larson, C. R., Wylie, B. K., & Van Driel, J. N. (2001). Completion of the 1990's national land cover data set for the conterminous United States. *Photogrammetric Engineering and Remote Sensing*, 67, 650–662.
- Vörösmarty, C. J., Green, P., Salisbury, J., & Lammers, R. B. (2000). Globalwater resources: Vulnerability from climate change and population growth. *Science*, 289 (5477), 284–288.
- Vörösmarty, C. J., Douglas, E. M., Green, P. A., & Revenga, C. (2005). Geospatial indicators of emerging water stress: An application to Africa. *Ambio*, 34 (3), 230–236.
- Walter, V. (2004). Object-based classification of remote sensing data for change detection. *ISPRS Journal of Photogrammetry and Remote Sensing*, 58 (3-4), 225–238.
- Wang, F. (1993). A knowledge-based vision system for detecting land changes at urban fringes. *IEEE Transactions on Geoscience and Remote Sensing*, 31 (1), 136-145.
- Wang, L., Sousa, W. P., & Gong, P. (2004 b). Integration of object-based and pixel-based classification for mapping mangroves with IKONOS imagery. *International Journal of Remote Sensing*, 25 (24), 5655-5668.
- Wanjura, D. F., & Hatfield, J. L. (1986). Par and IR reflectance, transmittance, and absorptance of four crop canopies. *Transactions of the ASABE*, 29 (1), 143-150.

- Wardlow, B. D., Egbert, S. L., & Kastens, J. H. (2007). Analysis of time-series MODIS 250 m vegetation index data for crop classification in the U.S. Central Great Plains. *Remote Sensing of Environment*, 108 (3), 290–310.
- Wardlow, B. D., & Stephen, L. E. (2008). Large-area crop mapping using time-series MODIS 250 m NDVI data: An assessment for the U.S. Central Great Plains. *Remote Sensing of Environment*, 112 (3), 1096–1116.
- Warrender, C. E., & Augusteihn, M. F. (1999). Fusion of image classification using Bayesian techniques with Markov random fields. *International Journal of Remote Sensing*, 20 (10), 1987–2002.
- Watanachaturaporn, P., Arora, M. K., & Varshney, P. K. (2004). *Evaluation of factors affecting support vector machines for hyperspectral classification*. Proceedings of the ASPRS Annual Conference, May 23–28, Denver, Colorado, USA.
- Watanachaturaporn, P., Arora, M. K., & Varshney, P. K. (2006). *Sub-pixel land cover classification using support vector machines*. Proceedings of the ASPRS Annual Conference, May 1-5, 2006, Reno, Nevada, USA.
- Watanachaturaporn, P., Arora, M. K., & Varshney, P. K. (2008). Multisource classification using support vector machines: An empirical comparison with decision tree and neural network classifiers. *Photogrammetric Engineering & Remote Sensing*, 74 (2), 239–246.
- Weismiller, R. A., Kristoof, S. J., Scholz, D. K., Anuta, P. E., & Momen, S. A. (1977). Change detection in coastal zone environments. *Photogrammetric Engineering and Remote Sensing*, 43 (12), 1533-1539.
- Wellens, J. (1997). Rangeland vegetation dynamics and moisture availability in Tunisia: an investigation using satellite and meteorological data. *Journal of Biogeography*, 24, 845-855.
- Wessel, K. J., DeFries, R. S., Dempewolf, J., Anderson, L. O., Hansen, A. J., Powell, S. L., & Moran, E. F. (2004). Mapping regional land cover with MODIS data for biological conservation: Examples from the greater yellowstone ecosystem, USA and Para state, Brazil. *Remote Sensing of Environment*, 92 (1), 67-83.
- Wharton, S. W. (1982). A contextural classification method for recognizing land use patterns in high resolution remotely sensed data. *Pattern Recognition*, 15 (4), 317-324.
- Wiemker, D. (1997). *An iterative spectral-spatial bayesian labeling approach for unsupervised robust change detection on remotely sensed multispectral imagery* (pp. 263-270, vol. 1296). Proceedings of the 7th International Conference on Computer Analysis of Images and Patterns, G. Sommer K. Daniilidis & J. Pauli (Eds.), Lecture Notes in Computer Science. Heidelberg: Springer-Verlag.
- Wiens, J. A., Sutter, R. D., Anderson, M., & Blanchard, J. (2009). Selecting and conserving lands for biodiversity: The role of remote sensing. *Remote Sensing of Environment*, 113 (7), 1370–1381.
- Wilkinson, G. G. (2000). Processing and classification of satellite images. In *Encyclopaedia of Analytical Chemistry* (pp. 8679-8693), edited by R. A. Meyers. John Wiley and sons.
- Wilkinson, G. G. (2005). Results and implications of a study of fifteen years of satellite image classification experiments. *IEEE Transactions on Geoscience and Remote Sensing*, 43 (3), 433-440.
- Willhauck, G. (2000). Comparison of object oriented classification techniques and standard image analysis for the use of change detection between SPOT multispectral satellite images and aerial photos. *Analysis*, XXXIII, 214-222.
- Williams, D. L., Goward, S., & Arvidson, T. (2006). Landsat: Yesterday, today, and tomorrow. *Photogrammetric Engineering & Remote Sensing*, 72 (10), 1171–1178.
- Winston, P. (1975). Learning structural descriptions from examples. In P. Winston (Ed.), *The psychology of Computer Vision* (pp. 157-209). New York: Mc Graw Hill.
- Wirth, D. (1971). *Syrien: Eine geographische Landeskunde*. Darmstadt: Wissenschaftliche Buchgesellschaft.

- Wolberg, G. (1990). *Digital image warping*. Los Alamitos, CA: IEEE Computer Society Press, 318 p.
- Won, J. S., Kim, H. Y., & Ryu, J. H. (1999). *Coastal geomorphologic change detection using SAR and optical remote sensing data at the Nakdong river estuary, Korea* (pp. 6:2733-2735). Proceedings of the International Geoscience and Remote Sensing Symposium, 28 June-02 July, Hamburg, Germany.
- Woodcock, C. E., & Strahler, A. H. (1987). The factor of scale in remote sensing. *Remote Sensing of Environment*, 21 (3), 311-332.
- Woodcock, C. E. & Gopal, S. (2000). Fuzzy set theory and thematic maps: Accuracy assessment and area estimation. *International Journal of Geographical Information Science*, 14 (2), 153-172.
- Woodcock, C. E., Macomber, S. A., Pax-Lenney, M., & Cohen, W. B. (2001). Monitoring large areas for forest change using Landsat: Generalization across space, time and Landsat sensors. *Remote Sensing of Environment*, 78 (1-2), 194-203.
- Woodcock, C. E., Allen, A. A., Anderson, M., Belward, A. S., Bindschadler, R., Cohen, ... Wynne, R. (2008). Free access to Landsat imagery. *Science*, 320, 1011.
- Woolley, J. T. (1971). Reflectance and transmittance of light by leaves. *Plant Physiology*, 47 (5), 656-662.
- World Bank. (2001). *Syrian Arab Republic: Irrigation Sector Report*. Report 22602.
- Wu, S., Silvan-Cardenas, J., & Wang, L. (2007). Per-field urban land use classification based on tax parcel boundaries. *International Journal of Remote Sensing*, 28 (12), 2777-2800.
- Wulder, M. A., & Franklin, S. E. (2003). *Remote sensing of forest environments: concepts and case studies*. Kluwer Academic Publishers.
- Xiao, X., Liu, J., Zhuang, D., Froking, S., Boles, S., Xu, B. (2003). Uncertainties in estimates of cropland area in China: A comparison between an AVHRR-derived dataset and a Landsat TM-derived dataset. *Global and Planetary Change*, 37 (3-4), 297-306.
- Xiaomei, Y., & Ronqing, L. Q. Y. (1999). *Change detection based on remote sensing information model and its application to coastal line of Yellow River Delta*. China: Earth Observation Center, NASDA.
- Xu, B., & Gong, P. (2007). Land-use/land-cover classification with multispectral and hyperspectral EO-1 data. *Photogrammetric Engineering & Remote Sensing*, 73 (8), 955-965.
- Yamaguchi, Y., Tsu, H., & Fujisada, H. (1993). *Scientific basis of ASTER instrument design* (pp. 150-160). Proceedings of SPIE (The International Society for Optical Engineering).
- Yamaguchi, Y., Kahle, A. B., Tsu, H., Kawakami, T., & Pniel, M. (1998). Overview of advanced spaceborne thermal emission and reflection radiometer (ASTER). *IEEE Transactions on Geoscience and Remote Sensing*, 36 (4), 1062-1071.
- Yamaguchi, Y., Fujisada, H., Kudoh, M., Kawakami, T., Tsu, H., Kahle, A. B., & Pniel, M. (1999). ASTER instrument characterization and operation scenario. *Advances in Space Research*, 23 (8), 1415-1424.
- Yamamoto, T., Hanaizumi, H., & Chino, S. (2001). A change detection method for remotely sensed multispectral and multitemporal images using 3D segmentation. *IEEE Transactions on Geoscience and Remote Sensing*, 39 (5), 976-985.
- Yang, C., & Anderson, G. L. (1996). *Determining within-field management zones for grain sorghum using aerial videography* (pp. 606-611). Proceedings of the 26th Symposium on Remote Sensing of Environment, March 25-29, Vancouver, BC.
- Yang, X., & Lo, C. P. (2000). Relative radiometric normalization performance for change detection from multi-date satellite images. *Photogrammetric Engineering and Remote Sensing*, 66, 967-980.
- Yang, C.-M., Lee, Y.-J., Hong, K.-Y., & Hsu, F.-H. (2007). Estimation of forage production of Nilegrass using vegetation reflectance. *Crop Science*, 47 (4), 1647-1651.

- You, L., Wood, S., Wood-Sichra, U., & Chamberlin, J. (2004). Generating plausible crop distribution maps for sub-Saharan Africa using spatial allocation model. *Information Development*, 23 (2-3), 151-159.
- Yuan, F., Sawaya, K. E., Loeffelholz, B. C., & Bauer, M. E. (2005). Land cover classification and change analysis of the Twin Cities (Minnesota) metropolitan area by multitemporal Landsat remote sensing. *Remote Sensing of Environment*, 98 (2-3), 317-328.
- Yuan, H., Van der Wiele, C. F., & Khorram, S. (2009). An automated artificial neural network system for land use/land cover classification from Landsat TM imagery. *Remote Sensing*, 1 (3), 243-265.
- Yüksel, A., Abdullah, E. A., & Gundogan, R. (2008). Using ASTER imagery in land use/cover classification of Eastern Mediterranean landscapes according to CORINE land cover project. *Sensors*, 8 (2), 1237-1251.
- Zadeh, L. A. (1965). Fuzzy sets. *Information Control*, 8, 338-353.
- Zaitchik, B., Smith, R., & Hole, F. (2002). *Spatial analysis of agricultural land use changes in the Khabour river basin of northeastern Syria*. Proceedings of ISPRS Symposium Land Satellite Information. Denver, Colorado.
- Zhang, J., & Foody, G. M. (2001). Fully-fuzzy supervised classification of sub-urban land cover from remotely sensed imagery: Statistical neural network approaches. *International Journal of Remote Sensing*, 22 (4), 615-628.
- Zhang, J., & Kirby, R. P. (1999). Alternative criteria for defining fuzzy boundaries based on fuzzy classification of aerial photographs and satellite images. *Photogrammetric Engineering and Remote Sensing*, 65 (12), 1379-1387.
- Zhang, J., & Stuart, N. (2001). Fuzzy methods for categorical mapping with image-based land cover data. *International Journal of Geographical Information Science*, 15 (2), 175-195.
- Zhang, M., & Scofield, R. A. (1994). Artificial neural network techniques for estimating heavy convective rainfall and recognising cloud mergers. *International Journal of Remote Sensing*, 15 (16), 3241-3261.
- Zhang, N., Wang, M., & Wang, N. (2002). Precision agriculture: A worldwide overview. *Computers and Electronics in Agriculture*, 36 (2-3), 113-32.
- Zhang, Y. (2003). Spatial autocorrelation in remote sensing image analysis (a report, p. 43). Environmental Remote Sensing Laboratory, Electrical Engineering Department, University of Nebraska, Lincoln. Retrieved from [http://doppler.unl.edu/~rockee/Image\\_Report.pdf](http://doppler.unl.edu/~rockee/Image_Report.pdf).
- Zhou, Q., Robson, M., & Horn, G. (1998). *Comparisons between the results from different ground vegetation cover estimation methods in a rangeland environment*. Proceedings of the 9th Australasian Remote Sensing and Photogrammetry Conference, Sydney, Australia.
- Zhou, W. Q., Troy, A., & Grove, M. (2008). Object-based land cover classification and change analysis in the Baltimore metropolitan area using multitemporal high resolution remote sensing data. *Sensors*, 8 (3), 1613-1636.
- Zhu, G., & Blumberg, D. G. (2002). Classification using ASTER data and SVM algorithms: The case study of Beer Sheva, Palestina. *Remote Sensing of Environment*, 80, 233-240.
- Zhuang, X., Engel, B. A., Lozano-Garcia, D. F., Fernandez, R. N., & Johannsen, C. J. (1994). Optimisation of training data required for neuro-classification. *International Journal of Remote Sensing*, 15 (16), 3271-3277.
- Zhuang, X., Engel, B. A., Xiong, X., & Johannsen, C. J. (1995). Analysis of classification results of remotely sensed data and evaluation of classification algorithms. *Photogrammetric Engineering and Remote Sensing*, 61 (4), 427-433.

### Selbstständigkeitserklärung

Ich erkläre, dass ich die vorliegende Arbeit selbstständig und unter Verwendung der angegebenen Hilfsmittel, persönlichen Mitteilungen und Quellen angefertigt habe.

Jena, am 01.11.2012



## TABELLARISCHER LEBENS LAUF

### *Persönliche Daten*

Name, Vorname: Al-Fares, Wafi Marwan  
Geboren am: 24.01.1979 in Murik-Hama/Syrien  
Wohnhaft: Binswangerstr. 8, 07747 Jena,  
Telefon: 0176 24924408  
E-Mail: wa-no@hotmail.de



---

### *Schul- und Berufsausbildung*

- 04/2007 – 02/2012 Promotion an der Friedrich-Schiller-Universität Jena, Chemisch-Geowissenschaftliche Fakultät, Deutschland
- Institut für Geographie, Lehrstuhl für Fernerkundung
  - Promotionsthema: Historical land use/land cover classification and its change detection mapping using different remotely sensed data from LANDSAT (MSS, TM and ETM+) and Terra (ASTER) sensors: A case study of the Euphrates river basin in Syria with focus on agricultural irrigation projects
  - Prämierung durch das Ministerium für Hochschulwesen - Uni. Tishreen in Latakia – Syrien (04/2005-03/2011)
- 08.02.2012 Abschluss: doctor rerum naturalium (Dr. rer. Nat.) „cum laude“
- 04/2006 – 07/2007 Hochschulstudium an der Friedrich-Schiller-Universität Jena, Chemisch-Geowissenschaftliche Fakultät, Deutschland
- Zwei Aufbau-Semester am Institut für Geographie
  - Zulassung Promotion
- 04/2005 – 04/2007 Diplomstudium an der Georg-August-Universität Göttingen, Fakultät für Geowissenschaften und Geographie, Deutschland
- Geographisches Institut, Abteilung für Kartographie, GIS und Fernerkundung
  - Diplomarbeitsthema: Wasserkonflikt zwischen Syrien und Türkei über das Wasser des Euphratesbecken und die Rolle, die das Südostanatolienprojekt auf diesem Konflikt spielt
- 08.05.2007 Abschluss: Diplom-Geograph (Dipl.-Geogr.), Note 1,7 ++ Gut
- 09/1997 – 06/2001 Hochschulstudium an der Universität Aleppo, Fakultät für Geisteswissenschaften, Abteilung Geographie, Syrien
- Verleihung Universitätspreis (Aleppo-Universität-Preis für Academic Excellence) im Jahr 2000.
- 09.09.2001 Abschluss: Bakkalaureus/Bachelor in Geisteswissenschaften 4j, Geographie (Bachelor of Art in Geographics 4j), sehr Gut
- 09/1996 – 09/1997 Hochschulstudium an der Universität Aleppo, Fakultät für Naturwissenschaft,
- Abteilung: Mathematik, Physik, und Chemie

- Wechsel des Fachgebietes

09/1985 – 06/1996  
09.08.1996

Mustafa Abd Al-Kader, Murik-Hama, Syrien  
Abschluss: Abitur (wissenschaftlicher Zweig)

### ***Berufstätigkeit***

12/2008 – laufend

Freiberufliche Tätigkeit als Übersetzer, Deutschland

- Übersetzung Deutsch in Arabisch für verschiedene Kunden
- Übersetzung Englisch in Arabisch für verschiedene Kunden

04/2007 – 02/2008

Lehrtätigkeit an der Volkshochschule in Jena, Deutschland

- Kursleiter für Sprachkurs „Arabisch als Fremdsprache“
- Kursleitung für durchschnittlich acht Personen
- Zielgruppe: Anfänger und Fortgeschrittene

09/2003 – 06/2004

Dozententätigkeit am Hochschulministerium für Bildung, Tishreen Universität in Latakia, Syrien

- Dozententätigkeit in der Abteilung Geographie
- Fachbereich physische Geographie, Kartographie
- Zielgruppe: Studentinnen und Studenten des 6.-8. Semesters

09/2001 – 06/2003

Lehrtätigkeit am Ministerium für Bildung, an den Schulen der Al-eppo-Provinzen, Syrien

- Lehrtätigkeit im Bereich Geographie und Geschichte
- Zielgruppe: Schüler der 7.-12. Klasse

### ***Weiterbildungen***

02/2010 – 02/2010

MATLAB-Kurs

- Skript-basierte Extrapolation von Ökosysteminformationen mit MATLAB in Beispielen
- Friedrich-Schiller-Universität Jena, Institut für Geographie, Lehrstuhl Geoinformatik

10/2007 - 10/2007

IDL-Kurs

- Modulare Programmierung in der Fernerkundung mit IDL
- Einführung praktischer Beispiele aus der Fernerkundung in die modulare Programm-Entwicklung mit IDL
- Deutsches Zentrum für Luft- und Raumfahrt DLR e.V.

12/2004 – 03/2005

Sprachkurs „Deutsch“ (fortgeschrittene Stufe)

- Deutsche Sprachprüfung für den Hochschulzugang DSH am 04.04.2006
- Georg-August-Universität Göttingen, Seminar für Deutsche Philologie-Abteilung Interkulturelle Germanistik-Lektorat Deutsch als Fremdsprache, Göttingen-Deutschland

09/2003 – 06/2004

Sprachkurs „Deutsch“

- Zertifikat Deutsch ZD (Grundstufe)
- Goethe Institut Inter Nationes, Damaskus-Syrien

03/2000 – 05/2000

Informatik-Grundlagen

- Vorlesung und praktische Übungen
- Grundlagen Hardware und Software
- Windows und MS-Office

### ***Zusatzqualifikationen***

EDV Kenntnisse:

- Digitale Bildverarbeitung (ERDAS-Imagine, ENVI, PCI Geomatica, NEST-Toolbox, Adobe Photoshop, etc.)
- GIS (ESRI: ArcView GIS 3.x, und ArcGIS 7.x)
- Programmierung (Grundkenntnisse in IDL und MATLAB)
- Tabellenkalkulation (Microsoft Excel)
- Textverarbeitung (Microsoft Word)
- Präsentationsprogramme (Microsoft Powerpoint)

Sprachen:

- Gute bis sehr gute Deutschkenntnisse
- Gute Englischkenntnisse
- Arabische Sprache (Muttersprache)

### ***Sonstiges***

Wissenschaftliche Aktivitäten:

- Mitglied an der Deutschen Gesellschaft für Kartographie e.V. (2007-laufend)

Führerschein:

- Syrische Führerschein Klasse B
- Deutsche Führerschein Klasse B

Hobby:

- Sport (Fußball)
- Fach- und Allgemeinliteratur
- Reisen

Jena, 01.11.2012

